



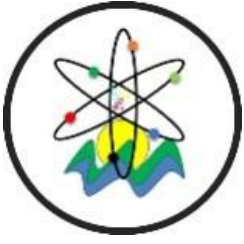
Black Sea Journal of Engineering and Science

Volume 7 | Issue 2



ISSN: 2619 - 8991


BS Journals



BLACK SEA JOURNAL OF ENGINEERING AND SCIENCE
(BSJ ENGIN SCI)


BS Journals

Black Sea Journal of Engineering and Science (BSJ Eng Sci) is a double-blind peer-reviewed, open-access international journal published electronically 6 times (January, March, May, July, September, and November) in a year by since January 2018. It publishes, in English and Turkish, full-length original research articles, innovative papers, conference papers, reviews, mini-reviews, rapid communications or technical note on advances in a wide range of scientific disciplines from all fields of engineering and science and from any source.

ISSN 2619 - 8991

Phone: +90 362 408 25 15

Fax: +90 362 408 25 15

Email: bsjsci@blackseapublishers.com

Web site: <http://dergipark.gov.tr/bsengineering>

Sort of publication: Periodically 6 times (January, March, May, July, September, and November) in a year

Publication date and place: March 15, 2024 - Samsun, TÜRKİYE

Publishing kind: Electronically

OWNER

Assoc. Prof. Dr. Uğur ŞEN

DIRECTOR IN CHARGE

Prof. Dr. Hasan ÖNDER

EDITOR BOARDS

EDITOR IN CHIEF

Prof. Dr. Hasan ÖNDER, Ondokuz Mayıs University, TÜRKİYE

Assoc. Prof. Dr. Uğur ŞEN, Ondokuz, Mayıs University, TÜRKİYE

SECTION EDITORS*

Prof. Dr. Ahmet UYANIK, Section Editor of Chemistry, Ondokuz Mayıs University, TÜRKİYE

Prof. Dr. Amila Sandaruwan RATNAYAKE, Section Editor of Geological Engineering, Uva Wellassa University, SRI LANKA

Prof. Dr. Berna KILIÇ, Section Editor of Fisheries Engineering, Ege University, TÜRKİYE

Prof. Dr. Çiğdem TAKMA, Section Editor of Statistics, Ege University, TÜRKİYE

Prof. Dr. Ertan BUYRUK, Section Editor of Mechanical Engineering, Sivas Cumhuriyet University, TÜRKİYE

Prof. Dr. Fahrul Zaman HUYOP, Section Editor of Biology, Universiti Teknologi Malaysia, MALAYSIA

Prof. Dr. Fauziatul FAJAROH, Section Editor of Chemical Engineering, Universitas Negeri Malang, INDONESIA

Prof. Dr. Fuad ALHAJOMAR, Section Editor of Electrical and Electronics Engineering, University of South Wales, UNITED KINGDOM

Prof. Dr. Gökhan CİVELEKOĞLU, Section Editor of Environmental Engineering, Akdeniz University, TÜRKİYE

Prof. Dr. Hasan TANAK, Section Editor of Physics, Amasya University, TÜRKİYE

Prof. Dr. Hasan TEMİZ, Section Editor of Food Engineering, Ondokuz Mayıs University, TÜRKİYE

Prof. Dr. Hojjat SADEGHİ-ALIABADI, Section Editor of Chemistry, Isfahan University, IRAN

Prof. Dr. İbrahim Özgür DENEME, Section Editor of Civil Engineering, Aksaray University, TÜRKİYE

Prof. Dr. İbrahim UĞUR, Section Editor of Mining Engineering, Süleyman Demirel University, TÜRKİYE

Prof. Dr. Jamrun EBBAH, Section Editor of Fisheries Engineering, Mindanao State University, PHILIPPINES

Prof. Dr. Messaoud SAIDANI, Section Editor of Civil Engineering, Coventry University, UNITED KINGDOM

Prof. Dr. Perarasu THANGAVELU, Section Editor of Aerospace Engineering, Anna University, INDIA

Prof. Dr. Sema PALAMUTCU, Section Editor of Textile Engineering, Pamukkale University, TÜRKİYE

Prof. Dr. Ümit Cafer YILDIZ, Section Editor of Forest Engineering, Karadeniz Technical University, TÜRKİYE

Assoc. Prof. Dr. Belgin KARABACAKOĞLU, Section Editor of Chemical Engineering, Eskişehir Osmangazi University, TÜRKİYE

Assoc. Prof. Dr. Bülent BOSTANCI, Section Editor of Geomatics Engineering, Erciyes University, TÜRKİYE

Assoc. Prof. Dr. Edit MİKÓ, Section Editor of Agricultural Engineering, University of Szeged, HUNGARY

Assoc. Prof. Dr. Ergün EKİCİ, Section Editor of Industrial Engineering, Çanakkale Onsekiz Mart University, TÜRKİYE

Assoc. Prof. Dr. Helal Uddin MOLLA, Section Editor of Physics, Rajshahi University of Engineering and Technology, BANGLADESH

Assoc. Prof. Dr. Kadyrbay CHEKİROV, Section Editor of Biology, Kyrgyz Turkish Manas University, KYRGYZSTAN

Assoc. Prof. Dr. Mehmet EBEOĞLUGİL, Section Editor of Metallurgical and Materials Engineering, Dokuz Eylül University, TÜRKİYE

Assoc. Prof. Dr. Nilüfer YURTAY, Section Editor of Computer Engineering, Sakarya University, TÜRKİYE

Assoc. Prof. Dr. Özgür Hakan AYDOĞMUŞ, Section Editor of Mathematics, Social Sciences University of Ankara, TÜRKİYE

Assoc. Prof. Dr. Rita ISMAİLOVA, Section Editor of Computer Engineering, Kyrgyz - Turkish Manas University, KYRGYZSTAN

Assoc. Prof. Dr. Samia Chehbi GAMOURA, Section Editor of Statistics, Strasbourg University, FRANCE

Assoc. Prof. Dr. Silvio DE OLIVEIRA JUNIOR, Section Editor of Mechanical Engineering, University of São Paulo, BRAZIL

Assoc. Prof. Dr. Sinan AKISKA, Section Editor of Geological Engineering, Ankara University, TÜRKİYE

Asst. Prof. Dr. Abdul JABBAR, Section Editor of Textile Engineering, National Textile University, PAKISTAN

Asst. Prof. Dr. Arsheed Ahmad RATHER, Section Editor of Forest Engineering, Annamalai University, INDIA

Asst. Prof. Dr. Ezenwanyi OCHULOR, Section Editor of Metallurgical and Materials Engineering, University Of Lagos, NIGERIA

Asst. Prof. Dr. Francis INEGBEDION, Section Editor of Industrial Engineering, University of Benin, NIGERIA

Asst. Prof. Dr. Haniyeh RASOULI PIROUZIAN, Section Editor of Food Engineering, Tabriz University, IRAN

Asst. Prof. Dr. Jun-wei LIM, Section Editor of Environmental Engineering, Universiti Teknologi Petronas, MALAYSIA

Asst. Prof. Dr. Mehmet GÜÇYETMEZ, Section Editor of Electrical and Electronics Engineering, Kırşehir Ahi Evran University, TÜRKİYE

Asst. Prof. Dr. Melahat CİHAN, Section Editor of Aerospace Engineering, Samsun University, TÜRKİYE

Asst. Prof. Dr. Muhammad GULİSTAN, Section Editor of Mathematics, Hazara University, PAKISTAN

Asst. Prof. Dr. Sedat KARADAVUT, Section Editor of Agricultural Engineering, Trakya University, TÜRKİYE

Asst. Prof. Dr. Seyedeh Narges SADATI, Section Editor of Mining Engineering, University of Mohaghegh Ardabili, IRAN

Asst. Prof. Dr. Xinyi WANG, Section Editor of Geomatics Engineering, Henan Polytechnic University, CHINA

* The ranking is arranged alphabetically within the academic title

EDITORIAL - ADVISORY BOARD*

Prof. Dr. Aglaia (Litsa) LIOPA-TSAKALIDI, Institute of Western Greece, GREECE

Prof. Dr. Ercan EFE, Kahramanmaraş Sutcu Imam University, TÜRKİYE

Prof. Dr. Mohammad Masood TARIQ, University of Balochistan, PAKISTAN

Prof. Dr. Mustafa Çağatay TUFAN, Ondokuz Mayıs University, TÜRKİYE

Prof. Dr. Özkan GÖRGÜLÜ, Ahi Evran University, TÜRKİYE

Assoc. Prof. Dr. Taner TUNÇ, Ondokuz Mayıs University, TÜRKİYE

Asst. Prof. Dr. Emil OMURZAK, Kyrgyz-Turkish Manas University, KYRGYZSTAN

Asst. Prof. Dr. Yılmaz KAYA, Ondokuz Mayıs University, TÜRKİYE

* The ranking is arranged alphabetically within the academic title

STATISTIC EDITOR

Prof. Dr. Mehmet TOPAL, Kastamonu University, TÜRKİYE

ENGLISH EDITOR

Asst. Prof. Dr. Betül ÖZCAN DOST, Ondokuz Mayıs University, TÜRKİYE

TURKISH EDITOR

Prof. Dr. Serkan ŞEN, Ondokuz Mayıs University, TÜRKİYE

REVIEWERS OF THE ISSUE*

Prof. Dr. Barış BİNAY, Gebze Technical University, Department of Bioengineering, Bioengineering, TÜRKİYE

Prof. Dr. Cahit GÜRER, Afyon Kocatepe University, Department of Civil Engineering, Transportation and Traffic, TÜRKİYE

Prof. Dr. İhsan BAKIRCI, Atatürk University, Department of Food Engineering, Dairy Technology, TÜRKİYE

Prof. Dr. Mehmet ŞAHİN, Gaziantep University, Department of Mathematics, Algebra and Number Theory, TÜRKİYE

Prof. Dr. Metin Hakan SEVERCAN, Niğde Ömer Halisdemir University, Department of Civil Engineering, Civil Engineering, TÜRKİYE

Prof. Dr. Niyazi ACER, İstanbul Arel University, Department of Anatomy, Information Systems Education, TÜRKİYE

Prof. Dr. Önder İDİL, Amasya University, Department of Mathematical Education, Mathematical Education, TÜRKİYE

Prof. Dr. Şeyda ZORER ÇELEBİ, Van Yüzüncü Yıl University, Department of Field Crop, Pasture-Meadow Forage Plants, TÜRKİYE

Prof. Dr. Vedat ORUÇ, Dicle University, Department of Machinery, Thermodynamics, TÜRKİYE

Prof. Dr. Yavuz AKBAŞ, Ege University, Department of Animal Science, Biometry, TÜRKİYE

Assoc. Prof. Dr. Adem EROL, Kahramanmaraş Sütçü İmam University, Department of Field Crops, Pasture-Meadow Forage Plants, TÜRKİYE

Assoc. Prof. Dr. Ahmet ATALAY, Atatürk University, Department of Civil Engineering, Transportation and Traffic, TÜRKİYE

Assoc. Prof. Dr. Ayla DEMİRCİ, Kırıkkale University, Department of Chemistry, Analytical Chemistry, TÜRKİYE

Assoc. Prof. Dr. Bahar MERYEMOĞLU, Çukurova University, Central Research Laboratory, Instrumental Methods, TÜRKİYE

Assoc. Prof. Dr. Banu KOÇ, Gaziantep University, Department of Gastronomy and Culinary Arts, Food Technology, TÜRKİYE

Assoc. Prof. Dr. Behcet İNAL, Siirt University, Department of Agricultural Biotechnology, Plant Biotechnology, TÜRKİYE

Assoc. Prof. Dr. Burak KURŞUN, Amasya University, Department of Machinery, Mechanical Engineering, TÜRKİYE

Assoc. Prof. Dr. Burhan ÖZTÜRK, Ordu University, Department of Horticulture, Pomology and Treatment, TÜRKİYE

Assoc. Prof. Dr. Elif TÜRKBOYLARI, Tekirdağ Namik Kemal University, Department of Green-House Technologies, Green-House Technologies, TÜRKİYE

Assoc. Prof. Dr. Ercan AYDOĞMUŞ, Fırat University, Department of Chemistry, Materials Science and Technologies, TÜRKİYE

Assoc. Prof. Dr. Erol ALVER, Hitit University, Department of Chemistry, Chemistry, TÜRKİYE

Assoc. Prof. Dr. Esra CENKÇİ, Akdeniz University, Department of Private Law, Commercial Law, TÜRKİYE

Assoc. Prof. Dr. Fadime ÖZDEMİR, Bilecik Şeyh Edebali University, Department of Molecular Biology and Genetics, Industrial Biotechnology, TÜRKİYE

Assoc. Prof. Dr. Fatma İnci ÖZDEMİR, Gebze Technical University, Department of Molecular Biology and Genetics, Molecular Biology, TÜRKİYE

Assoc. Prof. Dr. Firat KURT, Muş Alparslan University, Department of Plant Production and Technologies, Genomics and Transcriptomics, TÜRKİYE

Assoc. Prof. Dr. Fuat LULE, Adıyaman University, Department of Department of Machinery and Metal Technologies, Solar Energy Systems, TÜRKİYE

Assoc. Prof. Dr. Kemal Çağatay SELVİ, Ondokuz Mayıs University, Department of Agricultural Machinery, Agricultural Machines, TÜRKİYE

Assoc. Prof. Dr. Koray ÖZSOY, Isparta University of Applied Sciences, Department of Machinery and Metal Technologies, Optimization in Manufacturing, TÜRKİYE

Assoc. Prof. Dr. Mehmet HASKUL, Şırnak University, Department of Machinery, Mechanical Engineering, TÜRKİYE

Assoc. Prof. Dr. Muhammet Hüseyin ÇETİN, Konya Technical University, Department of Mechanical Engineering, Tribology, TÜRKİYE

Assoc. Prof. Dr. Mustafa RUSTEMOĞLU, Şırnak University, Department of Plant Protection, Plant Biotechnology, TÜRKİYE

Assoc. Prof. Dr. Özgül KARAGÜZEL, Recep Tayyip Erdoğan University, Department of Horticulture, Plant Tissue Culture, TÜRKİYE

Assoc. Prof. Dr. Sedat BOYACI, Kirşehir Ahi Evran University, Department of Biosystem Engineering, Agricultural Energy, TÜRKİYE

Assoc. Prof. Dr. Şerife ÇEVİK, Isparta University of Applied Sciences, Department of Food Processing, Food Technology, TÜRKİYE

Assoc. Prof. Dr. Vakkas ULUÇAY, Kilis 7 Aralık University, Department of Mathematics, Mathematics, TÜRKİYE

Assist. Prof. Dr. Ali CİNGÖZ, Tokat Gaziosmanpaşa University, Department of Food Engineering, Food Technology, TÜRKİYE

Assist. Prof. Dr. Alpaslan BAYRAKDAR, Iğdır University, Department of Medical Services and Techniques, Computational Chemistry, TÜRKİYE

Assist. Prof. Dr. Berivan YILMAZER POLAT, Munzur University, Department of Design and Architecture, Construction Materials, TÜRKİYE

Assist. Prof. Dr. Derya ÇEVİK TAŞDEMİR, Gaziantep University, Department of Management and Organization, Occupational Health and Safety, TÜRKİYE

Assist. Prof. Dr. Eda DAĞDEVİR, Kayseri University, Department of Electronic and Otomation, Biomedical Engineering, TÜRKİYE

Assist. Prof. Dr. Esra YAVUZ, Şırnak University, Department of Accounting and Tax, Biomerty, TÜRKİYE

Assist. Prof. Dr. Ferzat TURAN, Sakarya University of Applied Sciences, Department of Field Crop, Biomerty, TÜRKİYE

Assist. Prof. Dr. Güfte CANER AKIN, İstanbul Gelişim University of Applied Sciences, Department of Occupational Health and Safety, Occupational Health and Safety, TÜRKİYE

Assist. Prof. Dr. Kutlu ÇEVİK, Karamanoğlu Mehmetbey University, Department of Food Engineering, Oil Technology, TÜRKİYE

Assist. Prof. Dr. Onur DENİZHAN, Batman University, Department of Mechatronics, Machine Theory and Dynamics, TÜRKİYE

Assist. Prof. Dr. Ozan KILIÇKAYA, Afyonkarahisar Health Sciences University, Department of Pharmaceutical Technology, Genomics and Transcriptomics, TÜRKİYE

Assist. Prof. Dr. Rukiye AYDIN, Samsun University, Department of Basic Sciences, Analytical Chemistry, TÜRKİYE

Assist. Prof. Dr. Serhat UZAN, Batman University, Department of Chemistry, Physical Chemistry, TÜRKİYE

Assist. Prof. Dr. Timur Hakan BARAK, Acıbadem Mehmet Ali Aydınlar University, Department of Pharmacognasis, Pharmacognosy, TÜRKİYE

Assist. Prof. Dr. Uğur IŞIK, Artvin University, Department of Medical-Aromatic Plants, Catalysis and Mechanisms of Reactions, TÜRKİYE

Assist. Prof. Dr. Yaşar KARAGÖZ, Akdeniz University, Department of Forensic Medicine,
Forensic Medicine, TÜRKİYE

Dr. Burak GEDİK, Erzurum Technical University, Department of Civil Engineering, Reinforced
Concrete Buildings, TÜRKİYE

Dr. Ekrem TAÇGÜN, Adıyaman University, Department of Machinery, Mechanical Engineering,
TÜRKİYE

Dr. Hakan Can ALTUNAY, Ondokuz Mayıs University, Department of Computer Programming,
Information Security and Cryptology, TÜRKİYE

Dr. Merve ERCAN KALKAN, Kocaeli University, Department of Chemistry, Chemistry, TÜRKİYE

Dr. Rumeysa DİKİCİ, Alanya Alaaddin Keykubat University, Department of Anatomy Anatomy,
TÜRKİYE

* The ranking is arranged alphabetically within the academic title

Table of Contents

Research Articles

1. **A COMPARATIVE EVALUATION OF THE OUTLIER DETECTION METHODS**
Melis ÇELİK GÜNEY, Gökhan Tamer KAYAALP.....155-159
2. ***Streptomyces* sp. VYN22 SUŞUNUN TEKSTİL ATIK SULARINDA BOYAR MADDE GİDERİMİNE ETKİSİ**
Fadime ÖZDEMİR KOÇAK, Yeliz GENÇ BEKİROĞLU, Burcu YAMAN.....160-164
3. **PROTEIN HOMOLOGY MODELING IN THE LOW SEQUENCE SIMILARITY REGIME**
Sebnem ESSİZ.....165-174
4. **EXPRESSION AND CHARACTERIZATION OF A THERMOSTABLE A-GLUCURONIDASE FROM *Geobacillus kaustophilus***
Hilal TAŞDEMİR, Yunus ENSARİ.....175-183
5. **ÇOK KRİTERLİ KARAR VERME METODU AHP VE CBS TEKNOLOJİSİ KULLANILARAK SERA YER SEÇİMİ: AKSU İLÇESİ ÖRNEĞİ**
Eda BOSTANCI, Önder KABAŞ, Ercüment AKSOY.....184-195
6. **EFFECT OF FILLING RATIO-PATTERN PARAMETERS ON MECHANICAL PROPERTIES OF PLA FILAMENTS USED IN 3D PRINTING**
Fuat KARTAL, Arslan KAPTAN.....196-202
7. **EFFECT OF OHS CRITERIA ON SELECTION OF CONCRETE ADDITIVES IN MINE ORE CONSTRUCTION WORKS**
Tuğçe ORAL, Nuri BİNGÖL.....203-213
8. **AMNİYOTİK SIVIDA SÜKSİNİLASETONUN ELEKTROKİMYASAL DAVRANIŞI VE TAYİNİ**
Saadet Meral KARACAN, Behice YAVUZ ERDOĞAN, Atiye Nur ONAR.....214-212
9. **VOXEL-BASED MORPHOMETRY OF OPTIMISTIC AND PESSIMISTIC BRAINS: A DETAILED STUDY FOCUSING ON AGE RANGE AND GENDER**
Pınar OZEL.....223-236
10. **DETERMINATION OF THE KNOWLEDGE LEVEL OF THE TECHNICAL STAFF ABOUT ARBITRATION**
Hasan BAKIRCI, Ayten CANBAL.....237-245
11. **TRAVELLING WAVE SOLUTIONS FOR SOME TIME-FRACTIONAL NONLINEAR DIFFERENTIAL EQUATIONS**
Mustafa EKİCİ.....246-253
12. **CFD ANALYSIS OF PRESSURE DROP REDUCTION IN PEMFC FLOW CHANNELS WITH DISTINCT CROSS-SECTION SHAPES**
Mahmut KAPLAN.....254-260
13. **UTILIZING VBA IN MS EXCEL FOR SIMPLIFIED SOLUTIONS IN CHEMICAL ENGINEERING: SINGLE-EFFECT EVAPORATOR STUDY**
Muhammed Bora AKIN.....261-270

- 14. EFFECTS OF GEOMETRIC PARAMETERS OF PERFORATED DIFFUSER ON SOUND PRESSURE LEVEL SOURCED BY AIRFLOW**
Ahmet ERDOĞAN, İshak Gökhan AKSOY, Suat CANBAZOĞLU.....271-276
- 15. ANALYSIS OF THE ENERGY EFFICIENCY OF POULTRY HOUSES IN TÜRKİYE**
Asiye ASLAN.....277-297
- 16. 6 ŞUBAT 2023 TARİHLİ KAHRAMANMARAŞ DEPREMLERİ SONRASINDA BETONARME YAPILARIN İNCELENMESİ: MALATYA İLİ SAHA ÇALIŞMASI**
Enes EKİNCİ.....298-306
- 17. CAPS-SSR MARKIRLARI KULLANILARAK PAMUK KROMOZOM SUBSTİTÜSYON HATLARININ BELİRLENMESİ**
Adnan AYDIN, Mehmet KARACA.....307-315
- 18. DİYARBAKIR TOPLU TAŞIMA SİSTEMİNDE OTOBÜS KULLANIMININ İNCELENMESİ VE İYİLEŞTİRME ÖNERİLERİ**
Mehmet Yakup ÇEÇEN, Hümevra BOLAKAR TOSUN.....316-322
- 19. COĞRAFİ İŞARET SÜRECİNDE TÜRKİYE ODALAR VE BORSALAR BİRLİĞİNİN ROLÜ VE COĞRAFİ İŞARET MAĞAZASI ÖNERİSİ**
Tarık YÖRÜKOĞLU, Kenan Sinan DAYISOYLU, Tuğberk ANÇEL.....323-328
- 20. CONSERVING THE CRITICALLY ENDANGERED *Anacamptis Coriophora* L. IN TÜRKİYE THROUGH EX VITRO SEED GERMINATION**
Ines HARZLI, Yasemin ÖZDENER KÖMPE.....329-333
- 21. DETECTION OF BACTERIAL DIVERSITY OF VARIOUS HABITATS IN ÇORUM PROVINCE AND ITS CRIMINALISTICS CONTRIBUTION TO POSSIBLE CRIME SCENE STUDIES**
Esra BALCI, Demet TATAR, Aysel VEYISOGLU, Ali TOKATLI.....334-341
- 22. KATI YAĞ ALTERNATİFİ OLARAK ÇÖREKOTU YAĞI OLEJELİNİN KRAKER YAPIMINDA KULLANIM POTANSİYELİNİN ARAŞTIRILMASI**
Necla ÖZDEMİR ORHAN, Zeynep EROĞLU.....342-350
- 23. ORMAN GÜLÜ (*Rhododendron* ssp.) ÇELİKLERİNİN KÖKLENMELERİ ÜZERİNE FARKLI UYGULAMALARIN ETKİLERİ**
Bahadır ALTUN, Hüseyin ÇELİK.....351-358
- 24. A NEW SPECTROPHOTOMETRIC METHOD FOR DETERMINATION OF CARVEDILOL FROM TABLET**
Figen EREK, Işıl AYDIN.....359-364
- 25. THE EFFECTS OF DIFFERENT NITROGENOUS FERTILIZER SOURCES AND DOSES ON FOOTBALL FIELD GRASS PERFORMANCES**
Merve MARANGOZ, İbrahim HOSAFLIOĞLU.....365-373



A COMPARATIVE EVALUATION OF THE OUTLIER DETECTION METHODS

Melis ÇELİK GÜNEY^{1*}, Gökhan Tamer KAYAALP¹


¹Çukurova University, Faculty of Agriculture, Department of Animal Science, 01330, Adana, Türkiye


Abstract: In data mining, in order to calculate descriptive statistics and other statistical model parameters correctly, outliers should be identified and excluded from the data set before starting data analysis. This paper studied and compared the performance of model-based, density-based, clustering-based, angle-based, and isolation-based outlier detection methods used in data mining. ROC and AUC curves were used to compare the performances of outlier detection methods. A data set with a standard normal distribution and fit a logistic regression was simulated. To compare the methods, the data was modified by randomly adding 30 outliers to the data set. The iForest algorithm was found to have higher predictive power than Mahalanobis, LOF, k-means, and ABOD. In addition, outliers were found in a real data set with the iForest algorithm and deleted from the data set. Then, the data sets with outliers and without outliers were compared. The results showed that the model without outliers has a higher predictive ability.

Keywords: Outlier, LOF, iForest, ROC curve, Data mining

*Corresponding author: Çukurova University, Faculty of Agriculture, Department of Animal Science, 01330, Adana, Türkiye

E mail: celikm@cu.edu.tr (M. ÇELİK GÜNEY)

Melis ÇELİK GÜNEY  <https://orcid.org/0000-0002-6825-6884>

Gökhan Tamer KAYAALP  <https://orcid.org/0000-0003-2193-848X>

Received: November 22, 2023

Accepted: January 08, 2024

Published: March 15, 2024

Cite as: Çelik Güney M, Kayaalp GT. 2024. A comparative evaluation of the outlier detection methods. BSJ Eng Sci, 7(2): 155-159.

1. Introduction

The technique of simulating human intelligence with algorithms to create a new computer that can do the work that humans can do is defined as artificial intelligence (AI) (Bharadiya, 2023). Machine learning (ML) is a collection of algorithms that computers use to generate and refine predictions or behaviors based on data (Molnar, 2019). Logistic regression analysis, one of the machine learning methods, is used frequently in many fields.

In multi-category or ordinal scales, logistic regression forecasts the value of the dependent variable examines the connection between dependent and independent variables, and makes classification (Mertler and Vannatta, 2005).

Outliers are observations that are significantly different from other observations (Cebeci et al., 2022). These values may be due to incorrect entry of records, fraudulent behavior, humans or instruments error or a natural deviation in the population (Hodge and Austin, 2004). The frequent occurrence of outliers has increased interest in outlier detection methods in data mining.

Outlier detection methods are classified as univariate or multivariate; parametric, semi-parametric, and nonparametric; supervised, semi-supervised, and unsupervised. It is also classified as density-based, clustering-based, distance-based, and depth-based outlier detection methods (Ben-Gal, 2005; Gogoi et al., 2011; Yuçel Altay, 2014; Cebeci, 2020; Cebeci et al., 2022). Statistical-based, deviation-based, and subspace-

based outlier detection methods can also be added to this classification (Xu et al., 2018). There is also an isolation-based outlier detection method that has been actively used recently and has high performance (Liu et al., 2008). The aim of the study is to compare the performance of model-based method Mahalanobis distance, density-based method LOF, clustering-based method k-means, angle-based method ABOD, and isolation-based outlier detection method iForest used in data mining.

2. Materials and Methods

2.1. Dataset

The data set was generated a sample of size 3000 from a standard normal distribution using the R package. In this data set, there are 3 independent (X_1, X_2, X_3) and 1 dependent (Y) variable. The independent variables consist of continuous variables and the dependent variable consists of a binary variable containing 0 and 1 values. In order to compare the outlier detection methods, a total of 30 outliers, 10 in each independent variable, were randomly added to the data set and the data were modified.

The Asian rice (*Oryza sativa*) data obtained by Zhao et al. (2011) were used. From this data set, 282 observations were included in the analysis. From this data set, seed length (X_1), seed width (X_2), and seed volume (X_3) were used as independent variables and leaf pubescence (Y) was used as the dependent variable. The independent variables consist of continuous variables and the dependent variable is a categorical variable (no



pubescence: 0, pubescence: 1). The simulated and real data set split of training (70%) and test (30%) set.

2.2. Logistic Regression

Regression analysis is used to determine the relationship between dependent and independent variables. In this analysis, the dependent variable consists of continuous data. If the dependent variable is a categorical or ordinal, logistic regression analysis is needed. In logistic regression analysis, independent variables can be discrete, continuous or a mixture of these variables.

In binary logistic regression, one of the logistic regression model types, the dependent variable is two categories. The logistic regression model (Equation 1) is as follows.

$$\ln\left(\frac{\pi}{1-\pi}\right) = \beta_0 + \beta_1 X_1 + \dots + \beta_k X_k \quad (1)$$

where π is the likelihood of the event, β_0 is the constant term, β_k is the k th regression coefficient, X is the independent variable, and Y is the dependent variable (Juarto, 2023).

2.3. Outlier Detection Methods

2.3.1. Mahalanobis distance

Statistical methods (model-based methods) for outlier detection are divided into parametric methods and nonparametric methods (Han et al., 2012). In parametric methods, multivariate outlier detection using Mahalanobis distance (Equation 2) is performed as follows (Rousseeuw and Van Zomeren, 1990).

$$M = \sqrt{(x - \mu)\Sigma^{-1}(x - \mu)'} \quad (2)$$

Where M is Mahalanobis distance, x is vector of variables $x = (x_1, x_2, \dots, x_k)$, $\mu = (\mu_1, \mu_2, \dots, \mu_k)$ is vector of mean values, Σ is the covariance matrix (Leys et al., 2017).

If the squared Mahalanobis distances of each observation is greater than the quantile (e.g. 0.975 quantile) of the χ^2 distribution, these observations are outliers (Rousseeuw and Van Zomeren, 1990; Prykhodko et al., 2018; Cebeci, 2020).

The Mahalanobis distances were examined using the "Moutlier" function of the "chemometrics" package in R (Filzmoser and Varma, 2017).

2.3.2. Local outlier factor (LOF):

Proximity-based outlier detection methods are divided into density-based and distance-based outlier detection methods (Han et al., 2012). One of the density-based outlier detection algorithms is the LOF. This algorithm is based on k nearest neighbors (Breunig et al., 2000).

The distance between an object O and its nearest k neighbors is the k -distance of O , denoted by $dist_k(O)$, and the k -distance neighborhood of an object O (Equation 3) is as follows.

$$N_k(O) = \{O' | O' \in D, dist(O, O') \leq dist_k(O)\} \quad (3)$$

The reachable distance is defined as the maximum of k -distance of O' and the distance between O and O' , and its formula (Equation 4) is:

$$reachdist_k(O \leftarrow O') = \max\{dist_k(O), dist(O, O')\} \quad (4)$$

The local reachability density of object O (Equation 5) can be written as follows (Hofmann and Klinkenberg, 2014).

$$ldist_k(O) = \frac{\|N_k(O)\|}{\sum_{O' \in N_k(O)} reachdist_k(O \leftarrow O')} \quad (5)$$

The local outlier factor (LOF) of O can be written as follows (Equation 6).

$$LOF_k(O) = \frac{\sum_{O' \in N_k(O)} ldist_k(O')}{\|N_k(O)\| \cdot ldist_k(O)} \quad (6)$$

Observations that have a substantially lower density than their neighbors are identified as outliers (Cebeci, 2020).

The local outlier factors were examined using the "lof" function of the "Rlof" package in R (Hu et al., 2015).

2.3.3. k-means algorithm

Clustering-based outlier detection methods are divided into hierarchical and non-hierarchical clustering methods. In the k-means, which is one of the outlier detection methods with non-hierarchical clustering, the aim is to divide n objects into k number of clusters and to minimise the similarity between clusters and maximise the similarity within clusters (Yadav and Sharma, 2013; Deb and Dey, 2017).

Where k is no. of the cluster, D is a dataset containing n objects, the steps of the algorithm are given below (Kaya and Koymen, 2008; Han et al., 2012; Bertizlioglu and Ozgonenel, 2012).

1. Initially, to determine the cluster center, n objects are randomly selected from D to form the number k of clusters.
2. The average of each object is calculated and the center points are determined.
3. Based on the mean values, each object is grouped with the closest center point.
4. The new mean value of each data item is calculated.
5. Step 2 and 3 are repeated until k does not change.

In order to determine outliers with hierarchical clustering, after the 3rd step, the distances of each object are calculated by summing the squares of the deviations from the center of the cluster to which each object belongs and taking the square root. The objects with the maximum distance are considered outliers (Cebeci, 2020).

The distances of each object were examined using the "kmeans" function of the "Stats" package in R.

2.3.4. Angle-based outlier detection (ABOD)

In Angle-based outlier detection method, the variances of the angles between the difference vectors of the data objects are taken into account (Kriegel et al., 2008).

In dataset D , when one point $\vec{A} \in D$ ($\vec{A} = (A_1, A_2, \dots, A_n)$) and two other points $\vec{B}, \vec{C} \in D$ and $\vec{B}, \vec{C} \neq \vec{A}$, the Angle-Based Outlier Factor (ABOF) is calculated by Equation 7.

$$ABOF(\vec{A}) = Var_{\vec{B}, \vec{C} \in D} \left(\frac{(\overline{AB}, \overline{AC})}{\|\overline{AB}\|^2 \cdot \|\overline{AC}\|^2} \right) \quad (7)$$

where \overline{AB} is the difference vectors ($\vec{B} - \vec{A}$), $\|\overline{AB}\|$ is the Euclidean distance between \vec{A} and \vec{B} , $ABOF(\vec{A})$ is the

variance over the angles between the difference vectors of \vec{A} to all pairs of points in D weighted by the distance of the points (Kriegel et al., 2008). The ABOF values found by equation 7 are ranked and those that are smaller than the ABOF values of other observations are called outliers. The ABOFs were examined using the “abod” function of the “abodOutlier” package in R (Jimenez, 2015).

2.3.5. Isolation forest (iForest)

The iForest algorithm, which is one of the isolated-based outlier detection methods, used to calculate the anomaly score of a data point is based on the observation that the isolation tree (iTrees) structure is equivalent to binary search trees (BST). The anomaly score of a data point is calculated by Equations 8 and 9 (Liu et al., 2008; Negi, 2020).

$$c(m) = \begin{cases} 2H(m-1) - \frac{2(m-1)}{n}, & m > 2 \\ 1, & m = 2 \\ 0, & \text{otherwise} \end{cases} \quad (8)$$

$$s(x, m) = 2^{-\frac{E(h(x))}{c(m)}} \quad (9)$$

where s is anomaly score, h(x) is the path length of an x observation, E(h(x)) is the average of h(x) of the iTrees set, c(m) is average length of unsuccessful search in BST, H is a harmonic number, and n is the no. of external nodes.

The determination of whether or not the observations are outliers is based on the anomaly score. An observation is considered an outlier if its anomaly score is near 1; if it is near 0.5, it is not. The value is normal value if the anomaly score is much less than 0.5 (Liu et al., 2008).

The anomaly scores were examined using the “iForest” function of the “isofoR” package in R (Graves and Drozdov, 2019).

2.4. Comparison of the Performance of Methods

In this paper, the receiver operating characteristic (ROC) curve is used for measuring the performance of the outlier detection methods. The confusion matrix used when plotting the ROC curve is given in Table 1 (Sharma et al., 2022).

Table 1. Confusion matrix

	Actual Positive	Actual Negative
Predicted Positive	True Positive	False Positive
Predicted Negative	False Negative	True Negative

When plotting the ROC curve, the true positive rate (TPR) should be available in addition to the false positive rate (FPR). TPR and FPR are formulated in Equations 10 and 11 (Omar and Nassif, 2023).

$$TPR = \frac{\text{True Positive}}{\text{True Positive} + \text{False Negative}} \quad (10)$$

$$FPR = \frac{\text{False Positive}}{\text{False Positive} + \text{True Negative}} \quad (11)$$

The Area Under the Curve (AUC) is defined as the area

under the ROC curve and shows the percentage of correct classification of positive and negative results. A larger AUC value means better performance (Auslander et al., 2011). A lower FPR and a higher TPR are desired because of admirable predictive prowess (Hou et al., 2023).

3. Results and Discussion

In simulated data, the AUCs of the different methods were compared in Figure 1. The AUC of the iForest model was found to be higher than the Mahalanobis, LOF, k-means, and ABOD models. This demonstrated that the iForest model has higher predictive power compared to the other models. The AUC of the LOF model was found the second highest AUC. The iForest has higher predictive power than the LOF (Gao et al., 2019; Gnat, 2020; Negi, 2020; Kiruthika and Sowmyarani, 2020; Vijayakumar et al., 2020).

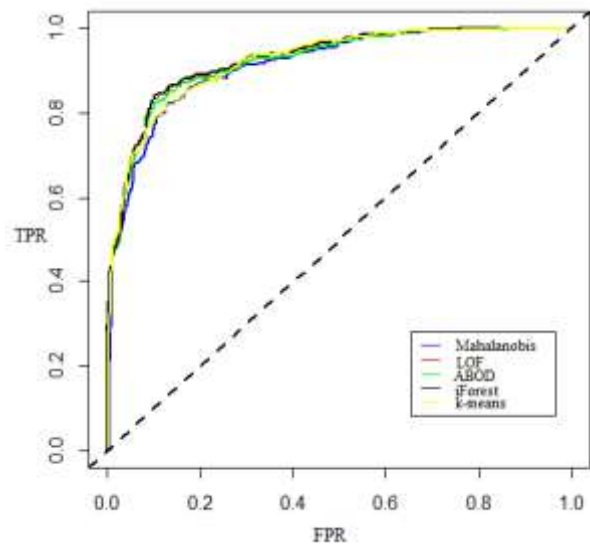


Figure 1. The ROC curve.

Since the iForest algorithm had higher predictive power than the other models, outliers were found using iForest in the real data. According to the outlier scores found by Equations 8 and 9, seven observations were identified as outliers and deleted from the data set. Then, the logistic models were developed for the data set with and without outliers and the ROC curves of these models were plotted in Figure 2.

In Figure 2, The AUC of without outliers and with outliers logistic regression models were 0.8526 and 0.7841. The AUC of the without outliers model was found to be higher than the outlier model. In other words, predictive modeling and classification are not reliable in the data set with outliers. Nurunnabi and West (2012) compared outlier and without outlier data sets and reported that the results of the outlier data set were not reliable in logistic regression analysis. Osborne and Amy (2004) reported that outliers significantly affect the analysis.

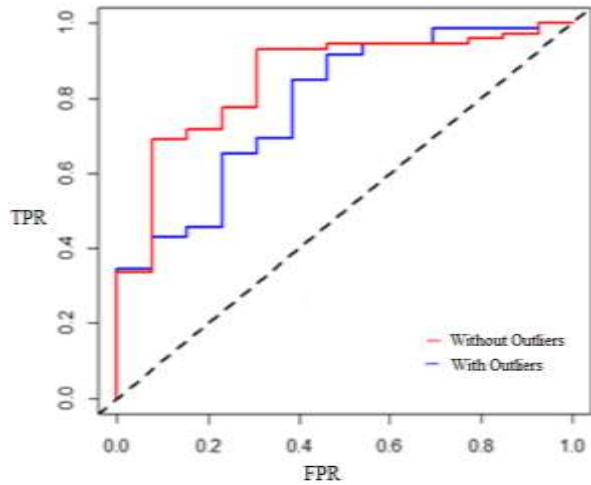


Figure 2. ROC curve of the data set with and without outliers.

4. Conclusion

In this study, the performances of Mahalanobis, LOF, k-means, ABOD, and iForest methods were compared. iForest algorithm was found to have a higher predictive power compared to the other methods. It is also concluded that outliers in logistic regression analysis affect the model considerably.

Author Contributions

The percentage of the author(s) contributions is presented below. All authors reviewed and approved the final version of the manuscript.

	M.Ç.G.	G.T.K.
C	50	50
D	50	50
S		100
DCP	100	
DAI	100	
L	100	
W	80	20
CR	20	80
SR	100	

C=Concept, D= design, S= supervision, DCP= data collection and/or processing, DAI= data analysis and/or interpretation, L= literature search, W= writing, CR= critical review, SR= submission and revision.

Conflict of Interest

The authors declared that there is no conflict of interest.

Ethical Consideration

Ethics committee approval was not required for this study because of there was no study on animals or humans. The authors confirm that the ethical policies of the journal, as noted on the journal's author guidelines page, have been adhered to.

Acknowledgements

We gratefully thank to Prof. Dr. Zeynel CEBECİ at the

Çukurova University for his contributions in this study.

We would like to thank Cukurova University Scientific Research Coordinatorship for supporting this study with project number FDK-2018 10287.

It was produced from the thesis titled "Comparative Examination of Outlier Detection Methods in Binary Logistics Regression Analysis" at Cukurova University Thesis no: 794371. <https://tez.yok.gov.tr/UlusalTezMerkezi/tezSorguSonucYeni.jsp>.

References

- Auslander B, Gupta KM, Aha DW. 2011. A comparative evaluation of anomaly detection algorithms for maritime video surveillance. Proceedings of the Society of Photographic Instrumentation Engineers Conference, June 15-17, Orlando, US, Vol. 8019, pp: 27-40.
- Bharadiya JP. 2023. A comparative study of business intelligence and artificial intelligence with big data analytics. American J Artific Intel, 7(1): 24-30.
- Ben-Gal I. 2005. Outlier detection. In Data Mining and Knowledge Discovery Handbook, Springer, Boston, US, pp: 288.
- Bertizlioglu IN, Ozgonenel O. 2012. Blackout detection using k-means clustering method. ELECO'2012 Electrical and Electronics Engineering Symposium, November 29-December 1, Bursa, Turkiye.
- Breunig MM, Kriegel HP, Ng RT, Sander J. 2000. LOF: Identifying Density-Based Local Outliers. In ACM Sigmod Record, 29(2): 93-104.
- Cebeci Z. 2020. Data preprocessing with R in data science. Nobel Academic Publishing, Ankara, Türkiye, opp: 552.
- Cebeci Z, Cebeci C, Tahtali Y, Bayyurt L. 2022. Two novel outlier detection approaches based on unsupervised possibilistic and fuzzy clustering. PeerJ Comp Sci, 8: e1060.
- Deb AB, Dey L. 2017. Outlier detection and removal algorithm in k-means and hierarchical clustering. World J Comp Appl Technol, 5(2): 24-29.
- Filzmoser P, Varmuza K. 2017. Chemometrics: Multivariate Statistical Analysis in Chemometrics. URL: <https://CRAN.R-project.org/package=chemometrics>. (accessed date: February 10, 2023).
- Gao R, Zhang T, Sun S, Liu Z. 2019. Research and improvement of isolation forest in detection of local anomaly points. J Physics: Conf Series, 1237(5): 1-6.
- Gnat S. 2020. Testing the effectiveness of outlier detecting methods in property classification. Real Estate Manag Valuat, 28(4): 81-92.
- Gogoi P, Bhattacharyya D, Borah B, Kalita JK. 2011. A survey of outlier detection methods in network anomaly identification. Comput J, 54(4): 570-588.
- Graves E, Drozdov I. 2019. Zelazny7/isofor: Isolation forest anomaly detection. URL: <https://github.com/Zelazny7/isofor>. (accessed date: February 01, 2023).
- Han J, Pei J, Pei J. 2012. Data mining: concepts and techniques, Third Edition. Morgan Kaufmann Publishers Elsevier, US, pp: 744.
- Hou S, Gao J, Wang C. 2023. Order acceptance choice modeling of crowd-sourced delivery services: a systematic comparative study. URL: <https://www.techrxiv.org/doi/full/10.36227/techrxiv.24139491.v1> (accessed date: February 23, 2023).

- Hodge V, Austin J. 2004. A survey of outlier detection methodologies. *Artific Intel Rev*, 22(2): 85-126.
- Hofmann M, Klinkenberg R. 2014. *RapidMiner: Data mining use cases and business analytics applications*. CRC Press, New York, US, pp: 528.
- Hu Y, Murray W, Australia YS. 2015. Rlof: R parallel implementation of local outlier factor (LOF). URL: <https://CRAN.R-project.org/package=Rlof> (accessed date: January 12, 2023).
- Jimenez J. 2015. abodOutlier: angle-based outlier detection. URL: <https://CRAN.R-project.org/package=abodOutlier> (accessed date: January 12, 2023).
- Juarta B. 2023. Breast Cancer classification using outlier detection and variance inflation factor. *Eng Math Comp Sci J*, 5(1): 17-23.
- Kaya H, Koymen K. 2008. Data mining concept and application areas. *Firat Univ Doğu Araşt Derg*, 6(2): 159-164.
- Kiruthika S, Sowmyarani CN. 2020. Credit card fraud detection using machine learning and deployment of model in public cloud as a web service. *Int J Recent Technol Eng*, 9(2): 548-552.
- Kriegel HP, Schubert M, Zimek A. 2008. Angle-based outlier detection in high-dimensional data. *Proceedings of the 14th ACM SIGKDD International Conference on Knowledge Discovery and Data Mining*, August 24-27, Las Vegas, US, pp: 444-452.
- Leys C, Klein O, Dominicy Y, Ley C. 2017. Detecting multivariate outliers: Use a robust variant of the Mahalanobis distance. *J Exp Soc Psychol*, 74: 150-156.
- Liu FT, Ting KM, Zhou ZH. 2008. Isolation forest. *Eighth IEEE International Conference on Data Mining*, December 15-19, Pisa, Italy, pp: 413-422.
- Mertler CA, Vannatta RA. 2005. *Advanced and multivariate statistical methods: practical application and interpretation*, 3rd edition. Glendale, Pyrczak Publishing, Los Angeles, US, pp: 234.
- Molnar C. 2019. Interpretable machine learning: a guide for making black box models explainable. URL: <https://christophm.github.io/interpretable-ml-book/> (accessed date: September 20, 2023).
- Negi SS. 2020. Early prediction of credit card fraud detection using isolation forest tree and local outlier factor machine learning algorithms. A Project Report of Capstone Project-2. Galgotias University, Uttar Pradesh, India, Act No: 14.
- Nurunnabi A, West G. 2012. Outlier detection in logistic regression: A quest for reliable knowledge from predictive modeling and classification. *IEEE 12th international conference on data mining workshops*, December 10, pp: 643-652.
- Omar AAC, Nassif AB. 2023. Lung cancer prediction using machine learning based feature selection: a comparative study. *Advances in Science and Engineering Technology International Conferences (ASET)*, February 20-23, pp: 1-6.
- Osborne JW, Amy O. 2004. The power of outliers (and why researchers should always check for them). *Pract Asses Res Eval*, 9(6): 1-12.
- Prykhodko S, Prykhodko N, Makarova L, Pukhalevych S. 2018. Application of the squared mahalanobis distance for detecting outliers in multivariate non-Gaussian data. *14th International Conference on Advanced Trends in Radioelectronics, Telecommunications and Computer Engineering (TCSET)*, February 20-24, Lviv-Slavske, Ukraine, pp: 962-965.
- Rousseeuw PJ, Van Zomeren BC. 1990. Unmasking multivariate outliers and leverage points. *J American Stat Assoc*, 85(411): 633-639.
- Sharma DK, Chatterjee M, Kaur G, Vavilala S. 2022. *Deep learning applications for disease diagnosis*. Academic Press, Cambridge, US, pp: 31-51.
- Vijayakumar V, Divya NS, Sarojini P, Sonika K. 2020. Isolation forest and local outlier factor for credit card fraud detection system. *Int J Eng Adv Technol*, 9(4): 261-265.
- Xu X, Liu H, Li L, Yao M. 2018. A comparison of outlier detection techniques for high-dimensional data. *Int J Comput Intel Syst*, 11(1): 652-662.
- Yadav J, Sharma M. 2013. A review of k-mean algorithm. *Int J Eng Trends Technol*, 4(7): 2972-2976.
- Yucel Altay S. 2014. Using of spatio-temporal data mining for trajectory outlier detection and interpretation in health care services. MS Thesis, Atatürk University, Graduate School of Natural and Applied Sciences, Erzurum, Türkiye, pp: 25-32.
- Zhao K, Tung CW, Eizenga GC, Wright MH, Ali ML, Price AH, Norton GJ, Islam MR, Reynolds A, Mezey J, McClung AM, Bustamante CD, McCouch SR. 2011. Genome-wide association mapping reveals a rich genetic architecture of complex traits in *Oryza sativa*. *Nature Commun*, 2(1): 467.



Streptomyces sp. VYN22 SUŞUNUN TEKSTİL ATIK SULARINDA BOYAR MADDE GİDERİMİNE ETKİSİ

Fadime ÖZDEMİR KOÇAK¹, Yeliz GENÇ BEKİROĞLU^{2*}, Burcu YAMAN¹

¹Bilecik Şeyh Edebali University, Faculty of Science, Department of Molecular Biology and Genetics, 11200, Bilecik, Türkiye

²Ondokuz Mayıs University, Bafra Vocation School, Department of Plant and Animal Production, 55400, Samsun, Türkiye

Özet: Tekstil endüstrisinde kullanılan boyalar ve boyar maddeler herhangi bir işlem görmeden sulara bırakıldıklarında toksik, kanserojen ve mutajenik etki göstererek çevre kirliliğine neden olmaktadır. Özellikle pigment boyar maddeler grubunda yer alan ve mikrobiyal bozunmaya karşı dirençli olan azo boyaların, tekstil kaynaklı atık suların bertarafı için biyoremediasyona dayalı çevre dostu yöntemler ilgi çekmektedir. Aktinobakteriler, doğada biyoremediasyon ve biyodegradasyon süreçlerine dahil olan ve organik madde ile karbon döngüsünde kilit rol oynayan bakterilerdir. Bu çalışmada, topraktan izole edilen Aktinobakteri izolatının 16S rRNA dizi analizleri ile tanımlanması ve *Streptomyces* sp. VYN22 olarak belirlenen bakterinin kullanılarak tekstil atıklarından azo boyaların boyar madde giderimi ile ortadan kaldırılması amaçlanmıştır. Bu izolatın 16S rRNA dizi analizlerine göre *Streptomyces bobili* tip türü ile %99,71 yakın akraba olduğu belirlenmiştir. Farklı pH'larda Colorsol Orange Deep tekstil boyası kullanılarak, *Streptomyces* sp. VYN22' nin canlı, kuru ve liyofilize formlarının 0-10 saatlerdeki boyar madde giderimleri spektrofotometrik ölçümlerle incelenmiştir. Çalışma sonunda bu bakterilerin pH 4, 6 ve 10'da boyar madde gideriminde yüksek sonuçlar verdiği gözlemlenmiştir.

Anahtar kelimeler: Aktinobakteri, Azo boya, Biyodegradasyon


Effect of *Streptomyces* sp. VYN22 Strain on Dyestuff Removal in Textile Wastewater


Abstract: Dyes and dyestuffs used in the textile industry cause environmental pollution by showing toxic, carcinogenic and mutagenic effects when they are released into water without any treatment. Environmentally friendly methods based on bioremediation for the disposal of azo dyes, which are especially in the pigment dyes group and resistant to microbial degradation, from textile wastewater are of interest. Actinobacteria are bacteria involved in bioremediation and biodegradation processes in nature and play a key role in the cycling of organic matter and carbon. In this study, it was aimed to identify an Actinobacterium isolate from soil by 16S rRNA sequence analysis and to eliminate azo dyes from textile wastes by dye removal using the bacterium identified as *Streptomyces* sp VYN22. According to 16S rRNA sequence analysis, this isolate was 99.71% closely related to *Streptomyces bobili* type strain. Using Colorsol Orange Deep textile dye at different pHs, the dyestuff removal of live, dry and lyophilized forms of *Streptomyces* sp VYN22 at 0-10 hours was investigated by spectrophotometric measurements. At the end of the study, it was observed that these bacteria gave high results in dyestuff removal at pH 4, 6 and 10.


Keywords: Actinobacteria, Azo dye, Biodegradation

*Sorumlu yazar (Corresponding author): Ondokuz Mayıs University, Bafra Vocation School, Department of Plant and Animal Production, 55400, Samsun, Türkiye

E mail: yeliz.bekiroglu@omu.edu.tr (Y. GENÇ BEKİROĞLU)

Fadime ÖZDEMİR KOÇAK  <https://orcid.org/0000-0002-8557-5166>

Yeliz GENÇ BEKİROĞLU  <https://orcid.org/0000-0003-0666-1857>

Burcu YAMAN  <https://orcid.org/0009-0005-6997-7404>

Gönderi: 06 Aralık 2023

Kabul: 15 Ocak 2024

Yayınlanma: 15 Mart 2024

Received: December 06, 2023

Accepted: January 15, 2024

Published: March 15, 2024

Cite as: Özdemir Koçak F, Genç Bekiroğlu Y, Yaman B. 2024. Effect of *Streptomyces* sp. VYN22 strain on dyestuff removal in textile wastewater. BSJ Eng Sci, 7(2): 160-164.

1. Giriş

Günümüzde hızla artan nüfusla birlikte, doğal kaynakların bilinçsizce kullanılması birçok çevre sorunu ve kirliliği beraberinde getirmektedir. Bu çevre sorunlarının başında ise alıcı ortama deşarj edilen ve organoklor bazlı pestisitlerden boyalarla ilişkili ağır metallere kadar birçok kirletici madde içeren endüstriyel atık sular gelmektedir. Atık su arıtımı, atık su deşarjından kaynaklı çevresel olumsuz etkilerin azaltılmasında önemli bir rol oynamaktadır (Ceretta ve ark., 2021).

Kimyasal strüktürü bakımından boyalar; azo, triaril methan, anthraquinon, heterosiklik ve ftalosiyanın boya olarak karakterize edilmektedir (Zhao ve Hardin, 2007). Azo boyalar ticari anlamda kullanılan sentetik boyaların en büyük grubunu temsil eder ve 3000'den fazla farklı

çeşidi ile tekstil, kağıt, gıda, kozmetik, ilaç endüstrilerinde yaygın olarak kullanılmaktadır (Maximo ve ark., 2003). Özellikle yapısında sülfö-, nitro- grupları ve halojenler bulunmayan azo boyalar yağlarda çözünme özellikleri bakımından aerobik çevre koşulları altında kalıcı olma eğilimindedirler (Kurbanova ve ark., 1998; Reiger ve ark., 2002).

Atık sulardan boyaların uzaklaştırılması için çeşitli fizikokimyasal yöntemler kullanılmaktadır. Bu yöntemlerin uygulanmasının, ekonomik olarak daha fazla enerji ve kimyasal gerektirmesi, inatçı azo boyaları veya organik metabolitlerini tamamen ortadan kaldıramaması ve önemli miktarda çamur oluşturması gibi doğal dezavantajları vardır. Ayrıca bu yöntemler ikincil kirlilik sorunlarına da neden olur ve karmaşık prosedürler içerir



(Forgacs ve ark., 2004). Mikroorganizmaların atık su ortamlarından boyaları ayrıştırma ve absorbe etme yeteneği uzun zamandır bilinmektedir ve buna bağlı olarak tekstil atık sularının arıtılması için biyoremediasyona dayalı teknolojilerin kullanımı ilgi çekmektedir (Chang ve Kuo, 2000; McMullan ve ark., 2001). Mikrobiyal veya enzimatik renk giderme süreci, fizikokimyasal arıtma yöntemlerine kıyasla su tüketimini azaltmaya yardımcı bir süreç olmasının yanı sıra, kullanılan biyolojik arıtım yöntemleri, tekstil endüstrisi için önerilen fiziksel ve kimyasal yöntemlere kıyasla daha az çamur üretmesi, maliyetinin düşük olması ve deşarj edilen ortamlar için daha az zararlı olması gibi özelliklerinden dolayı tekstil endüstrisinden kaynaklanan atık suların arıtılmasında ideal çözüm olarak kabul edilmektedir (Kocaer ve Alkan, 2002; Rai ve ark., 2005; Khehra ve ark., 2006).

Aktinobakteriler, özellikle ikincil bileşikler açısından çok sayıda biyoaktif molekül üretme kabiliyetleri nedeniyle tıbbi ve biyoteknoloji endüstrilerindeki paha biçilmez prokaryotlar olarak kabul edilmektedir (Gao ve Gupta, 2005; Çil ve ark., 2016; Özdemir Koçak ve ark., 2023). Aktinobakteriler, tüm mikrobiyal sekonder metabolitlerin %70'ini oluşturur ve bu özelliklerinden dolayı biyoaktif bileşiklerin en büyük üreticileri arasında yer almaktadırlar (Janardhan ve ark., 2014). Kirlenmiş topraklarda nitrojen fiksasyonu ve hidrokarbonlar gibi yüksek moleküler ağırlıklı bileşiklerin bozunması ile toprak ortamlarının biyolojik kontrolünü sağlamalarının yanı sıra, besin maddelerinin ve minerallerin mevcudiyetini iyileştirdiği, metabolitlerin üretimini arttırdığı ve bitki büyüme düzenleyicilerini teşvik ettiği de bilinmektedir (Radhika ve ark., 2011; Bhatti ve ark., 2017; Özdemir Koçak, 2019). Ayrıca, termofilik Aktinobakteriler DNA polimerazlar, pullulanazlar, amilazlar, ksilanazlar, lipazlar ve proteazlar gibi biyoteknolojik olarak önemli bazı enzimleri ürettikleri için endüstriyel öneme sahiptir (Mahajan ve Balachandran, 2017; Özdemir Koçak ve ark., 2023). Bu çalışmada da topraktan elde edilen *Streptomyces* suşunun 3 farklı formu kullanılarak Colorsol Deep Orange boyar maddesinin farklı pH'larda giderimi belirlenmiştir.

2. Materyal ve Yöntem

2.1. *Streptomyces* sp. Suşunun İzolasyonu

Avusturya (Viyana) bölgesi tarla toprağından yapılan izolasyon çalışmasında; dilüsyon plaka yöntemi uygulanarak farklı aktinobakteri izolatları elde edilmiştir (Özdemir Koçak, 2019). Steril kaplara alınan toprak örnekleri 15 gün süresince kurutulmuş ve steril havanda dövülerek 1 g örnek 9 ml ringer çözeltisine eklenmiştir. Oluşturulan bu ilk dilüsyon (10^{-1}) 55 °C'de su banyosunda 30 dk bekletilerek dekontaminasyon işlemine tabi tutulmuştur. İlk dilüsyondan sonra ringer çözeltisi içeren tüplerde seri sulandırma işlemi yapılmış, 10^{-5} ve 10^{-6} dilüsyonlar kullanılarak yayma plaka yöntemi ile önceden hazırlanmış nalidilik asit (4 µg/ml),

rifamycine (4 µg/ml) ve cyloheximide (50 µg/ml) ilaveli tripton yeast glukoz agar üzerine (TYGA) inoküle edilmiştir (Özdemir Koçak, 2019).

2.2. *Streptomyces* sp. VYN22 Suşunun 16S rRNA Gen Bölgesi Analizleri

Streptomyces sp. VYN22 suşunun DNA izolasyonu DNA İzolasyon Kiti (İnvitrogen, USA) kullanılarak yapılmıştır. DNA örneğinin varlığı agaroz jel elektroforezi kullanılarak kontrol edilmiştir.

Streptomyces sp. VYN22 suşunun 16S bölgesini çoğaltmak için 27f ve 1525r primerleri kullanılmıştır (Lane, 1991). PCR reaksiyonunda 50 µl ölçüdeki Hot Start Master Mix (25 µl), primerler (1 µl), DNA (1-2 µl) ve sudan (nükleaz içermeyen) oluşan bir reaksiyon karışımı hazırlanmıştır. PCR reaksiyon koşulları; ön denatürasyon (94 °C, 2 dk, 1 döngü), denatürasyon (94 °C, 1 dk, 35 döngü), bağlanma (55 °C, 2 dk, 35 döngü), uzama (72 °C, 3 dk, 35 döngü) ve son uzama (72 °C, 8 dk, 1 döngü) basamaklarından oluşmuştur.

16S rRNA gen bölgesinin dizi analizi MacroGen (Hollanda) firmasından hizmet alımı yapılarak gerçekleştirilmiştir. MacroGen firması tarafından 5 farklı primer (800r, MG3f, MG5f, 27f ve 1525r) kullanılarak 16S rRNA gen bölgesinin baz dizilimini ABI3730XL dizileme cihazı ile elde edilmiştir. ABI formatındaki dosyalar fasta formatına dönüştürüldükten sonra MEGAX programları kullanılarak karşılaştırmalı ve manuel olarak 5 farklı primerden elde edilen diziler birleştirilmiştir (Kumar ve ark., 2018). Birleştirilen diziler NCBI (National Center for Biotechnology Information) Blast ve ExTaxon Server programında analiz edilmiştir (Kim ve Chun, 2014). *Streptomyces* sp. VYN22 suşunun 16S rRNA gen bölgesi dizi analizleri MEGAX programı kullanılarak gerçekleştirilmiştir. Yine MEGAX programı kullanılarak 16S rRNA baz dizilerinin filogenetik soyağacı oluşturulmuştur. Neighbour-joining algoritması ve Jukes-Cantor uzaklık matriksi kullanılarak filogenetik soyağaçları elde edilmiştir (Jukes ve Cantor, 1969). Bootstrap analizleri 1000 tekrarlı olarak gerçekleştirilmiştir.

2.3. Biyosorpsiyon Deneyleri

Biyosorpsiyon deneylerinde kullanılacak olan izolatlar besiyeri isteklerine göre nutrient agar veya Luria-Bertani (LB) agar ortamında 30 °C'de 3-5 gün inkübe edildi. Suşlar 3 farklı formda kullanıldı. Canlı formda kullanılacak olanlar 0,1 OD'ye ayarlanıp giderim deneylerinde kullanıma hazır hale getirildi. Liyofilize form için besiyerinde büyütülen suşlar santrifüjlenerek -20 °C'de 24 saat bekletilip liyofilizatörde kurutuldu. Son olarak sıvı besiyerinde geliştirilen mikrobiyal kütle ortamdan uzaklaştırıldıktan sonra 70 °C 24 saat bekletilerek kurutulmuş hazır hale getirildi.

Biyosorpsiyon 250 ml'lik erlenlerde 100 ml saf su ve belirli konsantrasyonlarda Colorsol Deep Orange tekstil boyası içeren ortamlarda gerçekleştirildi. Optimal pH'ın belirlenmesi için 100 mg/L boya içeren saf su ortamının pH'sı 2, 4, 6, 8 ve 10 olacak şekilde ayarlandı. kuru örneklerden 0.015 g, liyofilize örneklerden 0.0075 g

alınarak 15 ml'lik cam tüplere aktarılmış, canlı form için ise mikroorganizma yoğunluğu 0,1 OD olarak ayarlanmıştır. Analizler için 2 saat ara ile 0- 10. saatlerde 2 ml örnek alınarak 470 nm dalga boyunda spektrofotometrik olarak ölçümleri yapıldı.

3. Bulgular

3.1. *Streptomyces* sp. Suşunun İzolasyonu

Toprak örneklerinden hazırlanan 10^{-5} ve 10^{-6} dilüsyonlar yayma plaka yöntemi ile antibiyotik ilaveli tripton yeast glukoz agar (TYGA) inoküle edilmiştir. *Streptomyces* izolatının miselyum ve sporları %25'lik steril gliserol çözelti içerisine transfer edilerek -20°C 'de stoklanmıştır. Bu izolatın isimlendirilmesinde izole edildiği lokasyonu temsilen (VYN: Viyana) ve tek koloni olarak elde edildiği izolat sayısı olan 22 kullanılmıştır.

3.2. *Streptomyces* sp. VYN22 Suşunun 16S rRNA Gen Bölgesi Analizleri

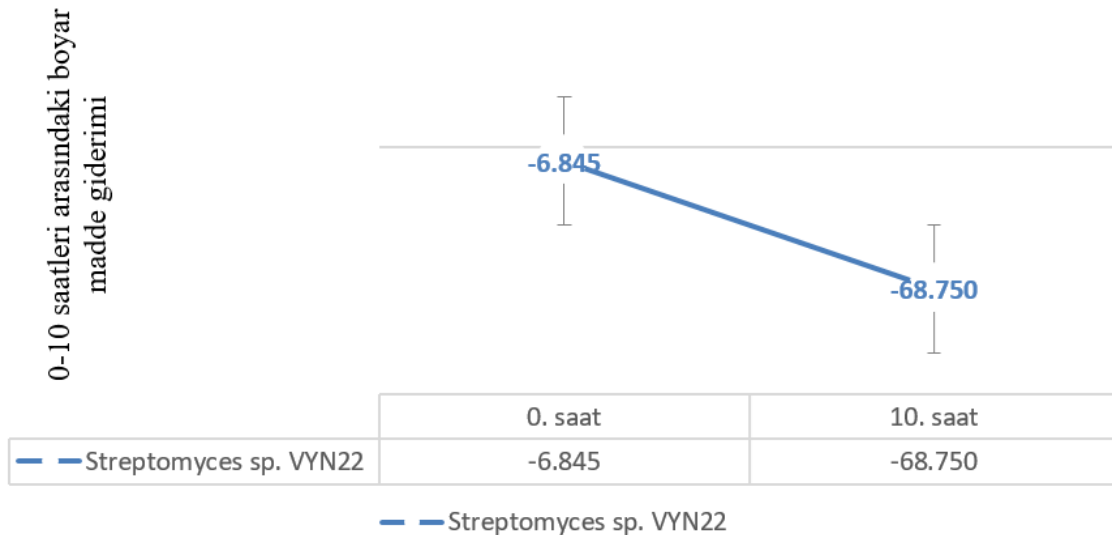
MEGAX programı kullanılarak gerçekleştirilen aligment işlemleri ve filogenetik analizler sonucunda *Streptomyces* cinsi ile ilişkili olduğu belirlenen VYN22 izolatının *Streptomyces bobili* tip türüne %99.71 benzer ve 4 nükleotit farklılığına sahip olduğu belirlenmiştir (Şekil 1). VYN22 izolatı daha sonra *Streptomyces phaeoluteigriseus* tip türü ile ilişkili olduğu tespit edilmiştir (%99.43 benzerlik; 8 nt farklılığı).

3.3. Biyosorbsiyon Deneyleri

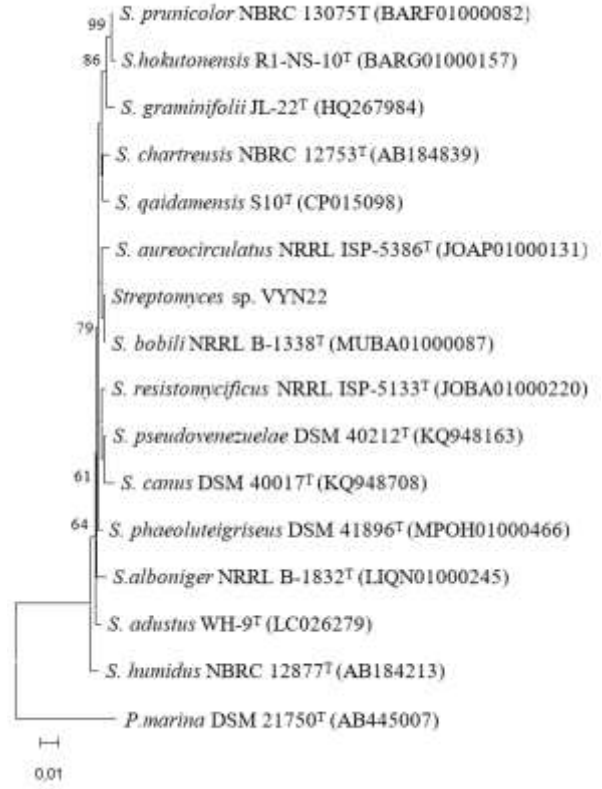
Analizler için 2 saat ara ile 0- 10. saatlerde alınan örneklerden elde edilen spektrofotometrik ölçüm sonuçları Tablo 1'de verilmektedir. Spektrofotometrik ölçümler sonrası *Streptomyces* sp. VYN22 suşunun biyosorbsiyon kapasitesi aşağıdaki eşitlik ile belirlendi ve boyar madde giderim yüzdeleri tespit edildi (eşitlik 1) (Hlihor ve ark., 2015).

$$\text{Boya Giderimi (\% BG)} = (\text{Co} - \text{Cf}) / \text{Co} \times 100 \quad (1)$$

Co: Başlangıç boya konsantrasyonu (mg/L), Cf: Belli bir zaman dilimindeki son boya konsantrasyonu (mg/L)



Şekil 2. pH 4'te (Colorsol Deep Orange M-S) *Streptomyces* sp. VYN22 kuru formunun 0-10 saatlerindeki boyar madde giderim değişiminde %61,9 boyar madde giderimi görülmüştür.



Şekil 1. *Streptomyces* sp. VYN22 suşu ile *Streptomyces* cinsine ait tip türlerinin 16S rRNA gen bölgesinin Neighbour-joining filogenetik soy ağacı. Dış grup olarak *P. marima* kullanılmıştır.

Absorbans ölçümlerine göre pH 2'de boyar madde giderim oranı oldukça düşüktür. pH 4'de *Streptomyces* sp. VYN22'nin canlı formunda %22,4, kuru formunda ise %61,9 boyar madde giderimi görülmüştür. pH 6'da kuru formunda %36,6 canlı formunda %17,5, pH 8'de kuru formunda %1,8, canlı formunda %9 ve son olarak pH 10'da kuru formunda %14,7, canlı formunda ise %11,3 boyar madde giderimi görülmüştür (Şekil 2).

Tablo 1. pH 2-4-6-8 ve 10'da Colorsol Deep Orange absorbans değerleri. (0-10 saatlik ölçüm) B. boya kons: Başlangıç boya konsantrasyonu

		pH 2	pH 4	pH 6	pH 8	pH 10
0. Saat	B. boya kons	0.636	0.552	0.596	0.607	0.693
	Kuru	0.458	0.336	0.442	0.448	0.568
	Canlı	0.367	0.388	0.445	0.466	0.459
	Liyofilize	0.465	0.375	0.442	0.492	0.506
2. Saat	B. boya kons	0.616	0.601	0.635	0.608	0.673
	Kuru	0.432	0.359	0.478	0.445	0.556
	Canlı	0.363	0.382	0.459	0.437	0.486
	Liyofilize	0.412	0.319	0.462	0.442	0.512
4. Saat	B. boya kons	0.630	0.561	0.624	0.458	0.733
	Kuru	0.436	0.497	0.518	0.433	0.518
	Canlı	0.366	0.408	0.740	0.478	0.484
	Liyofilize	0.367	0.378	0.431	0.432	0.502
6. Saat	B. boya kons	0.589	0.551	0.632	0.458	0.743
	Kuru	0.373	0.554	0.619	0.479	0.534
	Canlı	0.366	0.451	0.461	0.476	0.539
	Liyofilize	0.345	0.321	0.439	0.432	0.541
8. Saat	B. boya kons	0.567	0.558	0.641	0.468	0.748
	Kuru	0.364	0.578	0.632	0.468	0.589
	Canlı	0.364	0.462	0.522	0.516	0.614
	Liyofilize	0.339	0.313	0.442	0.439	0.539
10. Saat	B. boya kons	0.561	0.560	0.648	0.459	0.747
	Kuru	0.360	0.567	0.640	0.457	0.640
	Canlı	0.357	0.469	0.537	0.483	0.538
	Liyofilize	0.328	0.309	0.448	0.465	0.505

4. Tartışma ve Sonuç

Tekstil endüstrisinde yaygın olarak kullanılan azo boyalar herhangi bir işlem görmeden sulara bırakıldıklarında çevre kirliliğine neden olarak toksik, kanserojen ve mutajenik etki gösterdiği yapılan çalışmalarda belirtilmiştir (Bagewadi ve ark., 2011). Çoğu azo boyası bakteri hücreleri tarafından aerobik bozunmaya karşı dirençlidir, bu nedenle geçtiğimiz on yıllar boyunca biyolojik renk giderme süreci, azo boyları dönüştürmek, parçalamak veya mineralize etmek için alternatif bir yöntem olarak araştırılmaktadır (Chaubu ve ark., 2010).

Boyar maddelerin sulu ortamlardan giderimi için bakteri, maya, mantar, alg gibi değişik tipte mikroorganizmalar kullanılmaktadırlar (Kargı ve Ozmihçı, 2004). Koçak ve Evliya (2011) çalışmalarında Reaktif Black 5 boyar maddesinin renginin anaerobik ortamda *Bacillus subtilis* ile giderildiğini rapor etmiştir. Okur ve ark. (2020) *Candida tropicalis*'in azo boyar maddeye karşı dirençli olduğunu ve azo boyar maddeleri içeren endüstriyel atık suların biyolojik arıtımında kullanılabileceğini göstermişlerdir.

Bu çalışmada ise *Streptomyces* sp. VYN22 suşu kullanılarak Colorsol Deep Orange isimli azo boyanın biyolojik giderim oranları belirlenmiştir. Çalışmalar sonunda *Streptomyces* sp. VYN22'nin kuru ve canlı formunda pH 4, 6 ve 10'da yüksek boyar madde giderim oranları tespit edilmiştir.

Sonuç olarak yüksek pH'da daha fazla giderim

gerçekleştiği görülmüştür. Elde edilen bulgular, *Streptomyces* sp. VYN22 suşu ve Colorsol Deep Orange boyar maddesinin bulunduğu aerobik ortamda, inkübasyon süresince, boyar madde gideriminin sürekli azaldığını göstermektedir. Bu azalış, biyokimyasal olayların yürüdüğünü, boyar maddelerin biyokimyasal olarak parçalandıklarını ve parçalanan bileşiklerin deney suşu tarafından karbon ve enerji kaynağı olarak kullanıldığını göstermektedir.

Katkı Oranı Beyanı

Yazar(lar)ın katkı yüzdesi aşağıda verilmiştir. Tüm yazarlar makaleyi incelemiş ve onaylamıştır.

	F.Ö.K.	Y.G.B.	B.Y.
K	50	40	10
T	60	20	20
Y	60	20	20
VTI	50		50
VAY	50	50	
KT	30	30	40
YZ	30	70	
KI	50	50	
GR	30	70	
PY	80		20
FA	80	10	10

K= kavram, T= tasarım, Y= yönetim, VTI= veri toplama ve/veya işleme, VAY= veri analizi ve/veya yorumlama, KT= kaynak tarama, YZ= Yazım, KI= kritik inceleme, GR= gönderim ve revizyon, PY= proje yönetimi, FA= fon alımı.

Çatışma Beyanı

Yazarlar bu çalışmada hiçbir çıkar ilişkisi olmadığını beyan etmektedirler.

Etik Onay Beyanı

Bu araştırmada hayvanlar ve insanlar üzerinde herhangi bir çalışma yapılmadığı için etik kurul onayı alınmamıştır.

Destek ve Teşekkür Beyanı

Bu çalışma TÜBİTAK 2209-A proje kapsamında desteklenmiş olup. TÜBİTAK'a teşekkür ederiz.

Kaynaklar

Bagewadi ZK, Vernekar AG, Patil AY, Limaye AA, Jain VM. 2011. Biodegradation of industrially important textile dyes by actinomycetes isolated from activated sludge. *Biotechnol Bioinf Bioeng*, 1(3): 351-360.

Bhatti AA, Haq S, Bhat RA. 2017. Actinomycetes benefaction role in soil and plant health, *Microb Pathog*, 11: 458-467.

Ceretta MB, Necessian D, Wolski EA. 2021. Current Trends on Role of Biological Treatment in Integrated Treatment Technologies of Textile Wastewater. *Front Microbiol*, 12: 1-7.

Chang JS, Kuo TS. 2000. Kinetics of bacterial decolorization of azo dye with *Escherichia coli* NO3. *Bioresour Technol*, 75: 107-111.

Chaubha P, Indurkar H, Moghe S. 2010. Biodegradation and decolorisation of Direct Violet 51 and Tetracycline dye from isolated fungus (TYPE I). *Asiatic J Biotech Res*, 03: 220-226.

Çil E, Işık K, Koçak FÖ. 2016. Bazı toprak aktinomisetlerinin antimikrobiyal aktivite ve antibiyotik duyarlılıklarının incelenmesi. *Ordu Üniv Bil Tek Derg*, 6(2): 75-84.

Forgacs E, Cserhati T, Oros G. 2004. Removal of synthetic dyes from wastewaters: a review. *Environ Int*, 30(7): 953-971.

Gao B, Gupta RS. 2005. Conserved indels in protein sequences that are characteristic of the phylum Actinobacteria. *Int J Syst Evol Microbiol*, 55: 2401-2412.

Hlihor RM, Diaconu M, Leon F, Curteanu S. 2015. Experimental analysis and mathematical prediction of Cd (II) removal by biosorption using support vector machines and genetic algorithms. *New Biotech*, 32(3): 358-368.

Janardhan A, Kumar AP, Viswanath B, Saigopal DVR, Narasimha G. 2014. Production of bioactive compounds by Actinomycetes and their antioxidant properties. *Biotechnol Res Int*, 2014: 1-9.

Jukes TH, Cantor CR, 1969. Evolution of protein molecules. *Mammalian Protein Metabol*, 3: 21-132.

Kargı F, Ozmihçı S. 2004. Batch biological treatment of nitrogen deficient synthetic wastewater using *Azotobacter* supplemented activated sludge. *Bioresour Technol*, 94(2): 113-117.

Khehra MS, Saini HS, Sharma DK, Chadha BS, Chimni SS. 2006. Biodegradation of azo dye C.I. Acid Red 88 by an anoxic-aerobic sequential bioreactor. *Dyes Pigments*, 70: 1-7.

Kim M, Chun J. 2014. 16S rRNA gene-based identification of

bacteria and archaea using the EzTaxon server. *Methods Microbiol*, 41: 61-74.

Kocaer FO, Alkan U. 2002. Boyar madde içeren tekstil atık sularının arıtım alternatifleri. *Uludağ Üniv Müh Mim Fak Derg*, 7: 47-55.

Koçak G, Evliya H. 2011. *Bacillus subtilis* ile reaktif black 5 boyar maddesinin renk giderim kinetiğinin araştırılması. *Çukurova Üniv Fen Müh Bil Derg*, 26(1): 6-15.

Kumar S, Stecher G, Li M, Knyaz C, Tamura K. 2018. MEGA X: molecular evolutionary genetics analysis across computing platforms. *J Mol Biol*, 35(6): 1547.

Kurbanova R, Mirzaoğlu R, Ahmedova G, Şeker R, Özcan E. 1998. Boya ve tekstil kimyası ve teknolojisi. Selçuk Üniversitesi Fen-Edebiyat Fakültesi Yayınları, Konya, Türkiye, pp: 117-122.

Mahajan GB, Balachandran L. 2017. Sources of antibiotics: Hot springs. *Biochem Pharmacol*, 134: 35-41.

Maximo C, Amorim MTP, Costa-Ferreira M. 2003. Biotransformation of industrial reactive azo dyes by *Geotrichum* sp. CCM1 1019. *Enzyme Microb Tecol*, 32: 145-151.

McMullan G, Meehan C, Conneely A, Kirby N, Robinson T, Nigam P, Banat I, Marchant R, Smith W. 2001. Microbial decolourisation and degradation of textile dyes. *Appl Microbiol Biotechnol*, 56: 81-87.

Okur M, Saraçoğlu N, Aksu Z. 2020. Removal of metal-complex dye with *Candida tropicalis* from aqueous solutions: Growth and inhibition kinetics. *J Fac Eng Architect Gazi Univ*, 35(3):1399-1408.

Özdemir Koçak F, Tanir SGE, Cetin AK, Degirmenci L. 2023. Simultaneous evaluation of composting experiments and metagenome analyses to illuminate the effect of *Streptomyces* spp. on organic matter degradation. *World J Microbiol Biotechnol*, 39(3): 70.

Özdemir Koçak F. 2019. Identification of *Streptomyces* strains isolated from *Humulus lupulus* rhizosphere and determination of plant growth promotion potential of selected strains. *Turkish J Biol*, 43(6): 391-403.

Radhika S, Bharathi I, Radhakrishnan M, Balagurunathan R, Pharm J. 2011. Bioprospecting of fresh water actinobacteria: Isolation, characterization and antagonistic potential of selected actinobacteria. *J Pharm Res*, 4(8): 2584-2586.

Rai HS, Bhattacharyya MS, Singh J, Bansal TK, Vats P, Banerjee UC. 2005. Removal of dyes from the effluent of textile and dyestuff manufacturing industry: A review of emerging techniques with reference to biological treatment. *Crit Rev Environ Sci Technol*, 35: 219-238.

Reiger PG, Meir HM, Gerle M, Vogt U, Groth T, Knackmuss HJ. 2002. Xenobiotics in the environment: present and future strategies to obviate the problem of biological persistence. *J Biotechnol*, 94(1): 101-123.

Zhao X, Hardin IR. 2007. HPLC and spectrophotometric analysis of biodegradation of azo dyes by *Pleurotus ostreatus*. *Dyes Pigments*, 72(3): 322-325.



PROTEIN HOMOLOGY MODELING IN THE LOW SEQUENCE SIMILARITY REGIME

Sebnem ESSIZ^{1*}


¹Kadir Has University, Faculty of Engineering and Natural Sciences, Department of Molecular Biology and Genetics, 34083, İstanbul, Türkiye

Abstract: Predicting the 3-D structure of a protein from its sequence based on a template protein structure is still one of the most exact modeling techniques present today. However, template-based modeling is heavily dependent on the selection of a single template structure and the sequence alignment between target and template. Mainly when the target and template sequence identity is low, the error from the alignment introduces larger errors to the model structure. An iterative method to correct such alignment mistakes is used in this study with a benchmark set from CASP in the extremely low sequence-identity regime. This is a protocol developed and tested before and it evaluates the alignment quality by building rough 3-D models for each alignment. Then by using a genetic algorithm it iteratively creates a new set of alignments. Since the method evaluates models, not sequence alignments, structural features are automatically incorporated into the alignment protocol. In the current study, models from structural alignment have been built by Modeller program to show the maximum possible quality of the model that can be obtained from that template structure with the iterative modeling protocol. Then the results and correctly aligned segments from the iterative modeling protocol are analyzed. Finally, it has been shown that if a good local fragment assessment scoring function is developed, the correctly aligned segments exist in the pool of alignments created by the protocol. Thus, the improvement of modeling in the low sequence identity regime is conceivable.

Keywords: Homology modeling, Sequence-sequence alignment, Genetic algorithm, Molecular modeling, Structural alignment

*Corresponding author: Kadir Has University, Faculty of Engineering and Natural Sciences, Department of Molecular Biology and Genetics, 34083, İstanbul, Türkiye

E mail: sebnem.gokhan@khas.edu.tr (S. ESSIZ)

Sebnem ESSIZ  <https://orcid.org/0000-0002-5476-4722>

Received: December 09, 2023

Accepted: January 15, 2024

Published: March 15, 2024

Cite as: Essiz S. 2024. Protein homology modeling in the low sequence similarity regime. BSJ Eng Sci, 7(2): 165-174.

1. Introduction

The three-dimensional (3-D) structure of the protein dictates its biological function, consequently understanding protein structure at the molecular level is essential in terms of understanding the function and malfunctions of proteins. Experimental techniques such as X-ray crystallography, NMR spectroscopy, and Cryo-Electron Microscopy are golden standards for determining protein 3-D structure, however, they have certain limitations in terms of time, resolution, and size of the systems. Mainly NMR is limited in terms of the size of the protein, X-ray has limitations rooted in difficulties in the crystallization process under the natural physiological environment and cryo-EM has still limitations with the resolution of the maps. Due to these pitfalls, the number of protein structures resolved fell very behind the number of known unique sequences, namely protein structures in PDB Databank compared to distinct sequences obtained in UniProtKB are still 1000-fold smaller in numbers as of January 2023 (Nassar et al., 2021; Bertoline et al., 2023)

Consequently, to fill this large gap between known structures and sequences, computational studies have proven to be valuable for the prediction of protein structure (Pieper et al., 2006; Gromiha et al., 2018). In

general, there are two mainstream categories in computational protein structure prediction. The first one is free modeling and the second one is template-based modeling. Ab-initio modelling is free modeling and used when there is no known structure close to the unknown target sequence. As the name indicates, ab initio modeling uses first-principal forces which drives protein to go into their native state, namely physical forces, and the potential of chemical interactions in between particles are used to simulate the protein sequence into its folded state (Bonneau and Baker, 2001; Hardin et al., 2002; Pearce et al., 2022). The main advantage of the method is that since it is not dependent on the library of known structures, it can successfully predict novel folds; however, computation time and cost are the main drawbacks.

Template-based or comparative modeling, on the other hand, doesn't use physical or chemical interactions as an all-atom force field but a less-detailed knowledge or information-based driving forces. Threading and homology modeling is both template-based modeling and they require a similar known template structure to base the model target sequence on. In threading all possible 3-D structures are tried on the given unknown target sequence while in homology modeling a single 3-D



structure is picked based on sequence similarity. GenTHREADER (Jones, 1999) is one of the most widely used threading software which uses a fit function by trying a target sequence to all known folds that exist in the database. Hybrid methods in between ab-initio and threading methods also exist and these methods start modeling from known smaller structure fragments and they became one of the standard ways for protein structure prediction such as I-TASSER (Yang and Zhang, 2015), Robetta (Kim et al., 2004), Rosetta@home (Rohl et al., 2004), Quark (Xu and Zhang, 2012).

Swiss-Model (Guex and Peitsch, 1997) and Modeller (Webb and Sali, 2016) are examples of homology-based modeling which are dependent on the selection of a single template structure and the sequence alignment between target and template. After the alignment of the target and template sequences, they collect geometric restraints from the known template structure and impose those restraints on the model structure of the unknown target sequence's model.

Very recently there has been a breakthrough in the protein structure prediction area. In the critical assessment of protein competition, CASP 13 and CASP 14, artificial-intelligence-based programs AlphaFold and AlphaFold2 (Jumper et al., 2021a; Jumper et al., 2021b). AlphaFold and AlphaFold2 both use machine learning by training on the distance between amino acids of known structures in PDB databank. They then create distograms, which are like the histograms of the distribution of distances in the structure. Then they use neural networks for predicting distograms from multiple sequence alignment for the target sequence. They provided superb results compared to its competitors in recent CASP competitions. However, it is still a hybrid method in terms of machine learning from previously known structures and it inherits the problems of predicting loop segments, multi-subunit complexes, or different conformations of the proteins (Bertoline et al., 2023) Mainly using multiple sequence alignment and template structures is not a new technique, however, their training and neural network are very successful in terms of covering all the knowledge we have in the PDB databank. In general, when there is no close template structure like for the loop segments and disordered proteins, all methods still have limitations. However, it is widely known that structure is known to be conserved better than sequence (Sauder et al., 2000). Thus, if the structure information is somehow incorporated into the sequence alignment, then it has been shown to improve modeling in terms of the problems coming from sequence alignments. Again, please note that when the sequence identity between the target and template is above %30 percent, this alignment problem doesn't exist (Sauder et al., 2000).

Homology modeling as being still the most exact out of all these solutions suffers from sequence alignment errors when the target sequence is novel. As well as the AlphaFold, there have been many advances to correct

alignment errors such as PSI-BLAST in the past decades. They all benefit from aligning multiple sequences as a profile. This way it becomes possible to incorporate structural features from other sequences with structures into alignment substitution matrices. There are various profile-profile alignment methods with slight differences in the ways they create the profiles and alignments. (Wang and Dunbrack, 2004; Kahsay et al., 2005; Soding, 2005; Zhou and Zhou, 2005; Dunbrack, 2006).

Moulder is such a technique developed for correcting the alignment errors in modeling by Modeller (John and Sali, 2003). It is an iterative alignment and modeling approach. First, a reliable multi-sequence alignment profile is created with close homologs of the target sequence, which contains 25 different alignments for the target sequence-template construct. In normal homology modeling, a single best-scoring alignment is moved to the modeling step. In Moulder, the best 15 of the 25 alignments are selected and moved to the structural modeling step. The resulting 15 protein structures are then subjected to a simple model scoring. The main difference between the two steps is that sequence similarity is used to create the 25 alignments. After 15 model structures are created, GA341 structure scoring will be used which is a 3-D structure assessment score. Then, genetic algorithm moves, crossover and mutation operators are applied to these alignments to reach 300 different alignments. For the newly formed alignment population, protein structures are obtained using the rapid modeling technique. The evaluation of these alignments is performed by scoring the 3-D models. It has been supported by many studies that the structures of proteins are much better preserved than their sequences. In this respect, it is important to evaluate the 300 different alignments based on models. The resulting alignment of the 10 models with the best structure score forms the family alignments in the next iteration of the genetic algorithm. Moulder algorithm runs for multiple iterations until it reaches a certain number of alignments. This protocol has already been successfully implemented and its performance in the twilight zone, the area with low sequence similarity, is limited in terms of reaching to full potential improvement provided by template structures.

In the present work, the CASP8 benchmark set is used to show the model quality in terms of profile-profile alignment first. Then for the same targets, the models based on structure-structure alignment will be evaluated. For one of the hard targets, Moulder method will be tested. Then, the populations created by Moulder genetic algorithm step will be analyzed by comparing to the ideal structural alignment. This will help to show how independently the scoring and sampling parts of the resulting populations work and how this information can be used to eliminate alignment errors in homology modeling.

The genetic algorithm generally relies on advantageous features dominating the pool of sequences over time,

leading to the correct alignment. The important point here is that sampling alignments and scoring alignments cannot be considered in isolation from each other. The goal of this paper is to test and show, why Moulder, which uses a genetic algorithm for alignment, with a very low sequence similarity benchmark set is not getting the results guaranteed by templates. By analyzing this, the alignments created by the genetic algorithm will be tested in terms of the percentage of correct alignment segments. If the correct alignments exist in the population but not picked by scoring, it will be shown that if sampling and scoring algorithms can be separated, the modeling problems caused by errors in alignment can be solved by bringing correct alignment segments together.

2. Materials and Methods

2.1. MOULDER: An iterative Alignment Technique

The moves of Moulder below are directly adopted from previous studies (John and Sali, 2003; Eramian, 2008) with modified parameters to fit to the computer usage in terms of number of nodes available.

Step 1: Initial Alignment

In the modeling steps, there is a target unknown sequence and a known template structure.

First target and template sequences are obtained and then for each sequence, profiles are built by Modeller's `profile.build()` command with default parameters for global dynamic alignment and Uniprot-90 sequence database. Then these profiles are aligned by using Modeller's `Alignment.salign()` function with global dynamic scoring (Marti-Renom et al., 2004). In addition to the best alignment, 5 suboptimal alignments have been created in the alignment command by changing weight matrix values. Suboptimal alignments are created by shifting alignment parameters, in `Modeller.salign()` `n_subopt = 5`, `subopt_offset = 15` was used. In the low sequence identity range, the suboptimal alignments have been shown to include many correct segments, sometimes even more than the optimal alignment (Chen and Kihara, 2011)

Step 2: Initial Models from the alignment(s)

For the input alignment, Modeller's automodel class is used with default parameters. Optimization level is set to very fast and a total of 2500 models are obtained. The reason for creating this many models is to have a good quality assessment for the initial model.

Step 3: Distribute alignment(s) to 10 nodes and apply genetic algorithm.

For the initial round, there are only 6 parent alignments. After that, there are 100 alignments and nodes receive at least 2 different alignments. This way guarantees that crossover moves can be performed. On each node, child alignments are created by applying genetic algorithm operators to the alignments.

There are five different operators:

Single-point crossover: It requires two alignments as input. Each alignment is divided into two blocks and the

second part of the first alignment is swapped with the second part of the second alignment.

Double-point crossover: It requires two alignments as input. The alignments are divided into three blocks and the middle block of the first alignment is swapped with the middle block of the second alignment.

Gap Insertion: It requires a single alignment. A position is selected in the randomly picked location of the randomly selected sequence of the alignment and a random length of gaps is inserted into that sequence. To end meets, the same number of gaps are inserted at the end of the second sequence. A random number is selected from 1 to 7 for the number of gaps to be inserted.

Gap Deletion: A random gap position is selected in the first sequence, then a random amount of gap is deleted from the total length of that gap in that sequence. The same number of gaps are added to the random position of the second sequence. The amount of gap deleted is determined by a random number from 1 to the total number of gaps in the selected gap.

Gap Shift: A single gap is selected from one sequence, and it is shifted to a random position.

In the genetic move step, the weight of each move is as follows: Single-point crossover is chosen as %40, double-point cross-over is chosen as %20, gap insertion is chosen as %10, gap deletion is chosen as %10 and gap shift is set to %20.

After this step, a redundancy check is applied to the child alignments created from the parent alignments. This step is stopped when there are valid 2500 alignments in the pool of alignments.

Step 4: Model Building and picking 250 best alignments.

Like the initial alignment model, one rough modeling step is carried out, mainly again by using Modeller's automodel class. The restraints in the Modeller's automodel class were reduced to 10 Ångstrom from 14 Ångstrom. Model randomization is turned off. No molecular dynamics refinement has been carried out. And finally, the optimization cycle is reduced from 200 to 50. This way a very quick modeling step has been carried out.

Scoring function used in this step has the following Modeller scoring components:

1. Sequence identity
2. Percentage of gaps in the target/template alignment
3. Z-PAIR: C α - and C β -based Distance-Dependent
4. Z-SURFACE: C β -based Accessible Surface Score:
5. Z-COMBINED: Combined Distance and Surface Potential Score
6. GA341: Fold Assessment Score

Step 5: Model in detail and pick the best alignments.

For the best alignments, 3 models will be modeled for each alignment and evaluated by a more detailed scoring function namely DOPE, which is the Discrete Optimized Protein Energy score developed by Modeller. It is an atomistic, distance dependent scoring function developed by Modeller (Shen and Sali, 2006). It is a more detailed

scoring function than the ones present in Step 5.

Step 6: Pool and sort alignments.

Once each node has built 100 valid, non-redundant child alignments, the alignments are then ranked according to their DOPE scores. Please note that DOPE is not a 2-D sequence alignment score. Mainly alignments are evaluated from the 3-D models that have been created.

Moulder steps are summarized in Figure 1.

2.2. Benchmark Data Set

The targets of CASP 8, <https://predictioncenter.org/casp8/index.cgi> are downloaded from the template-based modeling class. The PDB structure of template structures is also obtained. The best templates with single chains are selected. The targets are selected from the low sequence identity range, sequence identity between target and template ranks from 1.99 % to 34.91 %. The target list with their corresponding sequence identities and sequence lengths are displayed in Table 1. The twilight

zone is defined as the zone of 20–35% sequence identity. Here the selected targets are even lower than twilight zone with low sequence identities to template structures.

2.3. Profile-Profile Alignment

Target and template sequences are obtained and then for each sequence profiles are built by Modeller’s profile.build() command with default parameters for global dynamic alignment and Uniprot-90 sequence database. Then these profiles are aligned by using Modeller’s Alignment.salign() function with global dynamic scoring (Marti-Renom et al., 2004).

2.4. Structure-Structure Alignment

For the target list in Table 2, both target and template structures are also downloaded. Modeller’s Alignment.salign() command with (0,3) 3D gap penalties are used for aligning two structures. Namely, this is the ideal test case. If both target and template structures were known, then the correct alignment would have been obtained.

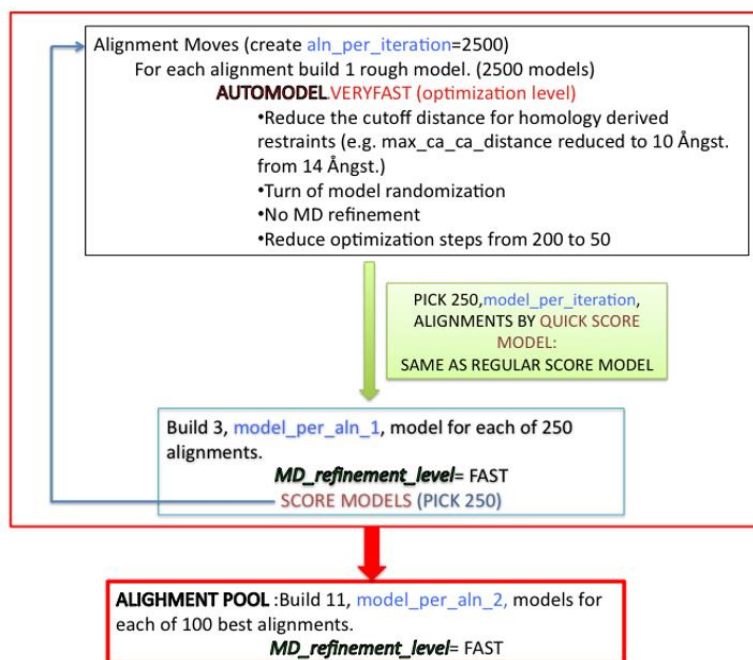


Figure 1. Schematic of the Moulder steps of one iteration.

Table 1. Target list

Target	Seq. Length	Seq. ID (%) ¹	Target	Seq. Length	Seq. ID (%) ¹
T0414-D1	127	7.09	T0490-D1	361	14.40
T0408-D1	98	17.35	T0494-D1	345	29.28
T0409-D1	62	4.84	T0497-D1	124	30.65
T0412-D1	166	16.27	T0501-D1	213	11.11
T0420-D1	168	17.26	T0501-D2	126	13.15
T0423-D1	143	32.87	T0502-D1	93	23.66
T0424-D1	175	21.71	T0503-D1	144	14.58
T0424-D2	84	25.00	T0504-D1	62	6.45
T0436-D1	405	16.05	T0504-D2	90	11.11
T0445-D2	107	7.48	T0505-D2	104	14.42
T0477-D1	106	34.91	T0506-D2	78	20.51
T0478-D1	126	9.52	T0507-D1	124	17.74
T0481-D1	135	12.59	T0509-D1	209	20.57

¹= The sequence identity is divided by the total length of the longer sequence.

Table 2. Comparison of models from profile-profile sequence and structure-structure alignments

Target	Profile-Profile Alignment					Structural Alignment		
	Seq. Length	Seq. Identity	Native Overlap	RMSD (Ångst)	Z-Dope	Native Overlap	RMSD (Ångst)	Z-Dope
T0414-D1	127	7.09	0.087	12.214	0.799	0.772	4.479	0.120
T0408-D1	98	17.35	0.878	3.572	-0.640	0.939	1.960	-0.463
T0409-D1	62	4.84	0.161	11.566	1.748	0.903	2.252	-0.465
T0412-D1	166	16.27	0.836	3.457	-0.618	0.880	3.066	-0.824
T0420-D1	168	17.26	0.637	12.557	0.573	0.946	2.064	-1.145
T0423-D1	143	32.87	0.958	2.095	-0.766	0.972	1.730	-0.967
T0424-D1	175	21.71	0.766	9.881	0.293	0.794	3.714	-0.415
T0424-D2	84	25.00	0.845	2.636	-0.693	0.988	1.776	-0.912
T0436-D1	405	16.05	0.691	6.997	-0.392	0.798	3.769	-0.541
T0445-D2	107	7.48	0.056	14.750	1.096	0.907	2.288	-0.749
T0477-D1	106	34.91	0.783	9.781	0.467	0.915	2.479	-0.104
T0478-D1	126	9.52	0.040	14.153	1.279	0.802	2.985	-1.247
T0481-D1	135	12.59	0.556	7.313	-1.066	0.815	3.380	-1.115
T0485-D1	207	16.43	0.647	7.923	-0.550	0.725	4.243	-0.792
T0490-D1	361	14.40	0.795	3.560	-0.184	0.850	2.631	-0.178
T0494-D1	345	29.28	0.812	4.188	-0.703	0.872	3.196	-0.947
T0497-D1	124	30.65	0.879	2.362	-1.227	0.960	1.991	-1.391
T0501-D1	213	11.11	0.643	11.347	0.330	0.831	10.418	0.015
T0501-D2	126	13.15	0.151	13.848	1.069	0.825	2.915	-0.517
T0502-D1	93	23.66	0.871	3.250	-0.523	0.968	2.255	-1.115
T0503-D1	144	14.58	0.729	7.931	0.815	0.861	4.240	0.384
T0504-D1	62	6.45	0.742	4.713	0.359	0.887	3.70	0.073
T0504-D2	90	11.11	0.111	10.972	0.901	0.750	8.830	0.894
T0505-D2	104	14.42	0.077	15.436	1.538	0.827	4.146	-1.195
T0506-D2	78	20.51	0.821	3.748	-0.396	0.936	2.228	-0.430
T0507-D1	124	17.74	0.105	11.870	0.746	0.847	2.537	-0.193
T0509-D1	209	20.57	0.828	3.274	-0.546	0.933	2.009	-1.114

Thus, structure alignment results will display how much template-based modeling can be improved if the errors from the sequence alignment are minimized (Sauder et al., 2000).

2.5. Model Assessment Parameters

Native overlap is the number of Cα atoms in the model within 3.5 Å of the corresponding atoms in the native structure divided by total number of Cα atoms. It is calculated after superposition of target and native structure. Root mean square displacement (RMSD) is proportional to the displacements of atom coordinates of the model structure from native structure by the following formula (Equation 1):

$$RMSD(x, y) = \sqrt{\frac{1}{n} \sum_{i=1}^n |x_i - y_i|^2} \quad (1)$$

In equation 1, x is the coordinates of model structure atoms, y is the coordinates of native structure atoms and i runs from 1 to number of atoms. It shows deviation from the ideal structure, while native overlap shows overlap with the ideal.

Finally, Z-Dope is the normalized DOPE scoring function. It is a distance-dependent statistical potential based on the separation between atoms and developed by MODELLER (Marti-Renom et al., 2004). Mainly Z-Dope is a statistical z-score that displays how your model's DOPE score is better than the average model. The more negative the Z-Dope the better the model quality is.

3. Results and Discussion

3.1. Comparison of Structure-Structure and Profile-Profile Alignments

In Table 2, model qualities are displayed for profile-

profile and structure-structure alignment results. Native overlap, RMSD, and Z-Dope score values are displayed. These are 3 different model assessment scores, explained in the Methods 2.5 section, used to evaluate the quality of the models. After models created based on profile-profile and structure-structure alignments, each model is compared to the native structure via these parameters. These are directly simple models from Modeller's automodel class, no iterations. In Figure 2, each of these parameters is plotted against the sequence identity between target and template. Mainly Figure 2 plots results tabulated in Table 2 according to sequence identity.

In Figure 2A, native overlap value of the models from profile-profile alignments is shown and in the low sequence identity regime, model quality is also low. When the sequence identity between target and template gets better than 15 %, the models are getting better both for profile-profile and structure-structure alignment in terms of native overlap. For the models that have very low model quality (shown in blue in Figure 2A), the native overlap values get directly above 0.6 from 0.1 when structural alignment is used. This means for this low-sequence identity regime, the template-based modeling can have much better results. However, due to the alignment errors, the models from profile-profile alignments have much lower native overlap values.

In Figure 2B, the model quality is displayed via RMSD values. Lower RMSD means the models are closer to the native structure. The model quality for profile-profile alignment is again very low in the low sequence identity, however, even for sequence identity greater than %15, there are problems with very high RMSD values for models from profile-profile alignments.

Z-Dope is a predictive scoring function, not a parameter for comparing a model to a native structure, unlike the first two parameters in Figure 2. It is the least predictive one for model assessment out of 3 parameters. Although structure-structure alignment results seem better than profile-profile alignment in Figure 2C, the predictive property of Z-Dope is still low for all models. Namely, it cannot differentiate between good models and bad models. Please note that in general, all the targets in the benchmark set are hard in terms of modeling. They all have sequence identity lower than %35, so even the structure conservation for better target and template pairs is low.

According to the results in Table 2, one of the worst profile-profile alignment results has been picked as a test case to analyze the results of Moulder. That target is T0409-D1 with a very low sequence identity of 4.84. According to profile-profile alignment results, the model's native overlap value is 0.161, RMSD is 11.566 Ångstrom and Z-Dope is 1.748.

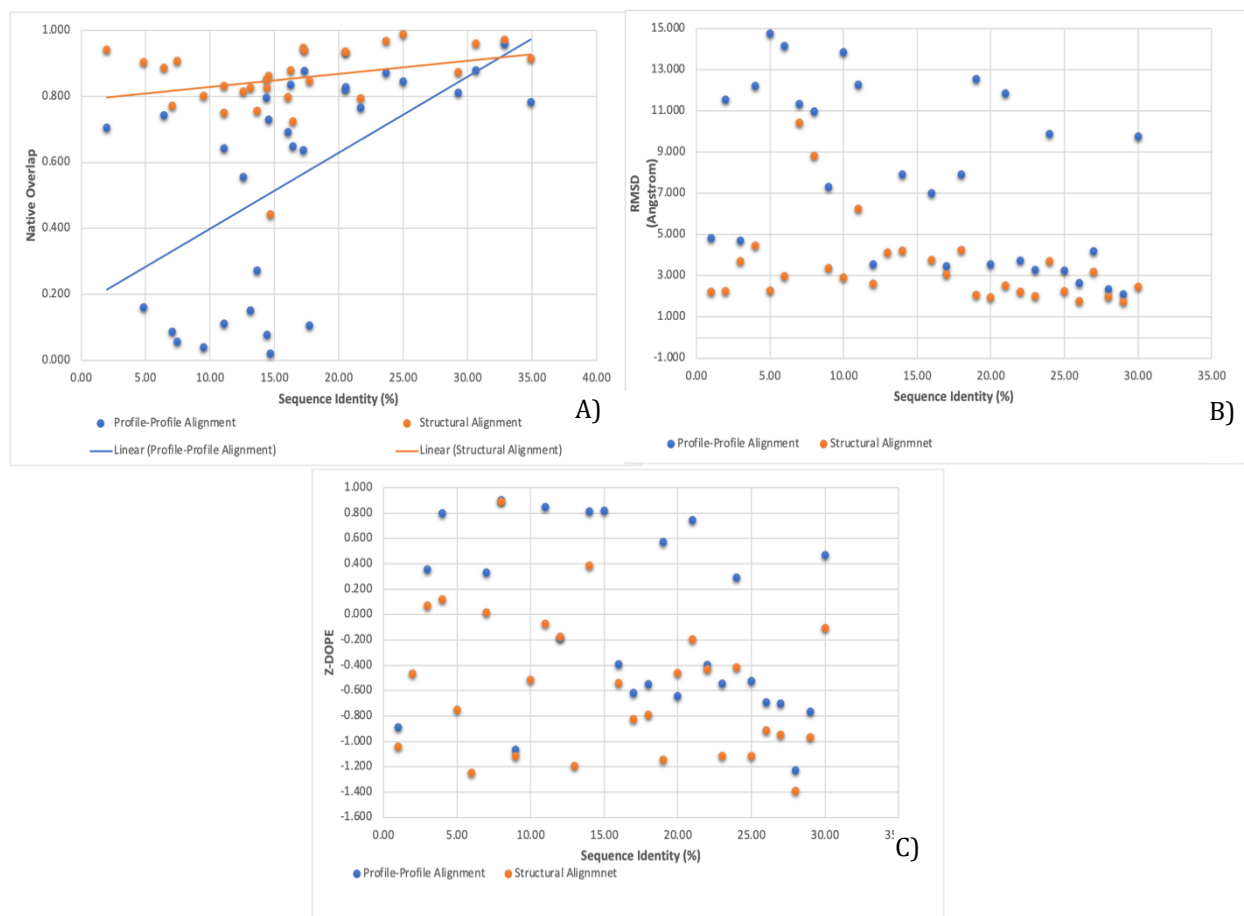


Figure 2. Benchmark set Model Quality A) Native overlap versus sequence identity B) RMSD versus sequence identity C) Z-Dope versus sequence identity.

Z-Dope is very positive and non-native like. However, when the model is built according to the structural alignment, the model has a native overlap of 0.903, a low RMSD of 2.252 Ångstrom. and finally, Z-Dope gets to a negative value. Now this target is selected for the analysis with Moulder since the low model quality comes from the errors in the sequence-sequence alignment. Thus, it has room for improvement. Overall, 30 Moulder iterations have been carried out for this target.

3.2. Analysis of the Genetic Algorithm Moves

During the iterations of Moulder the genetic algorithm moves have been analyzed for their weights. The single-point crossover is set to %40, double-point cross-over to %20, gap insertion to %10, gap deletion to %10, and gap shift is set to %20 in Moulder. In Figure 3, the moves for the initial 15 iterations are displayed. In the initial iterations number of gap deletions, gap shift, and gap insertions are higher than their expected weights because initially these mutation type changes are needed to create diverse alignment. Then the cross-overs get higher by adjusting to the final weights. Cross-overs are larger whole segment changes, thus the population needs gap moves to diverge from the starting alignment initially. The movement weights agree with the ones in Figure 3. Each color shows an iteration number starting from 1 to 15, and the y-axis is the number of moves.

3.3. Is the Correct Model in the Pool of Models?

In Figure 4A, best 100 alignments obtained after 30 iterations of Moulder are displayed. For T0409-D1, the profile-profile alignment results give 0.161 native overlap as the initial model quality. At the end of Moulder iterations, 100 best-scored alignments are obtained, and corresponding models are built by Modeller. The best model native overlap values get as better as 0.360 native overlap value.

In Figure 4B, the model picked at each iteration is shown with red lines, while the best model present in the pool of alignments at each iteration is shown with green lines. It is clear from the results in this low model quality, mainly because of the very low sequence identity, that the scoring function is not picking the best model present in

the pool of models. If the scoring function could have picked the model with the better native overlap value, the model quality would have reached to 0.46 range.

In Figure 4C, RMSD of the final models from the 30 iterations of Moulder is displayed. Again, the initial RMSD is 11.566 Ångstrom in Table 3, and the best model RMSD does not even reach 9.6 Ångstrom. However, when the best models versus best-scored models during each iteration are compared in Figure 4D, there is a model that has a RMSD as low as 5 Ångstrom at iteration 24. Namely that model is in the pool of models at the end of each iteration but not picked by the scoring function. If the alignment belonging to this model was picked by Moulder for the next iteration, there would have been an improvement. But RMSD value stays, the green line in Figure 5D, very flat during 30 iterations.

Here the aim is not to benchmark Moulder one more time. In the original method paper (John and Sali (2003), 19 hard modeling targets that shared 4-27% sequence identity with their template structures were used for benchmarking, and the average alignment accuracy increased from 37% to 45% relative to the initial alignment at the end of Moulder iterations. However here in Table 2, it is shown that the modeling accuracy can be improved more than this if the alignment incorporates structural information into the sequence alignment. Please see Figure 2A for the possible improvement of models when the sequences are aligned based on structure (orange points in Figure 2A). As shown in Figure 4, Moulder iterations are sampling better models than the models picked by scoring function in the iterations of Moulder. This result is very important in terms of the development of similar methods. All sampling methods by iterations can be separated into two parts. One of them is sampling the different alignments, while the second one is picking the best one when the native structure is unknown. Here since the native structures of CASP 8 benchmark set are known, it is shown that although better alignments exist, Z-Dope scoring function was not able to pick some of them.

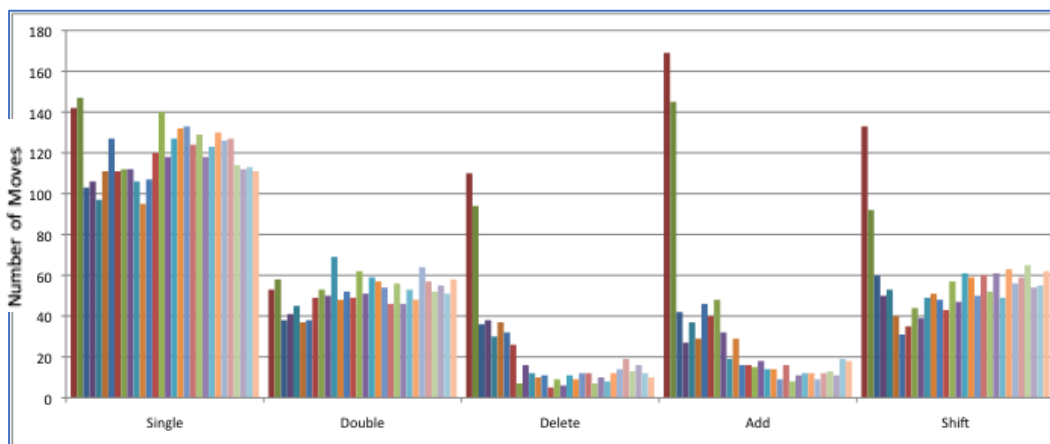


Figure 3. Genetic algorithm moves: The number of moves in each iteration is displayed with a different color. Single= Single-point cross-over, Double= Double-point cross over, Delete = Gap Delete, Add = Gap Insertion and Shift = Gap Shift.

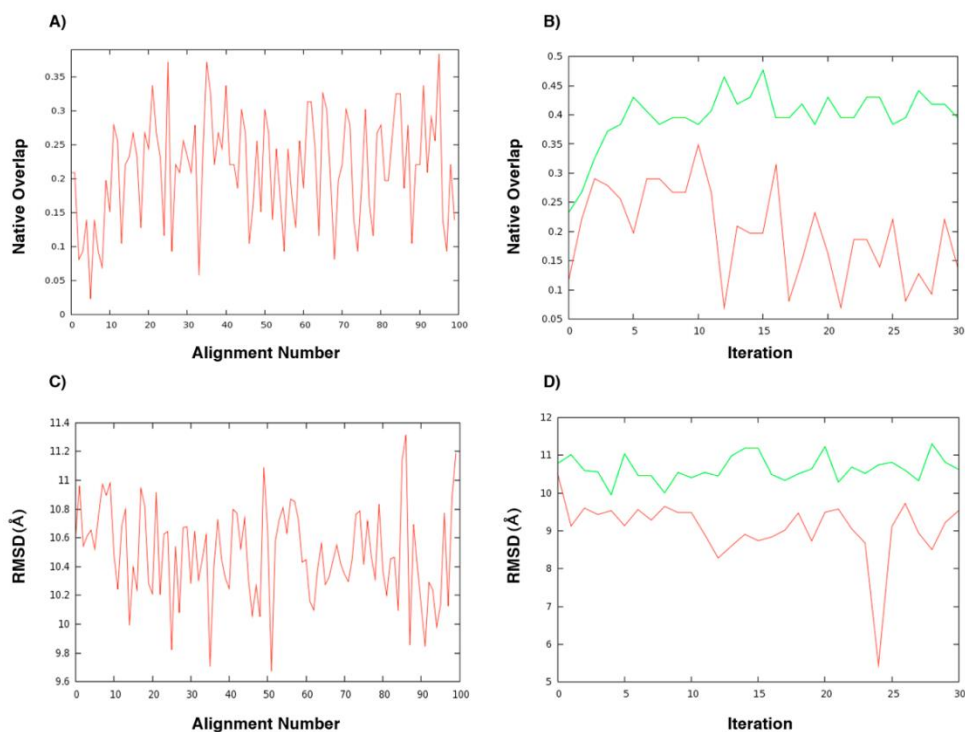


Figure 4. A) Native-overlap scores of models. B) Native overlap of models picked by DOPE (red), models with the best native overlap value (green). C) RMSD of models D) RMSD of models picked by DOPE (green), models with the best native overlap value (red).

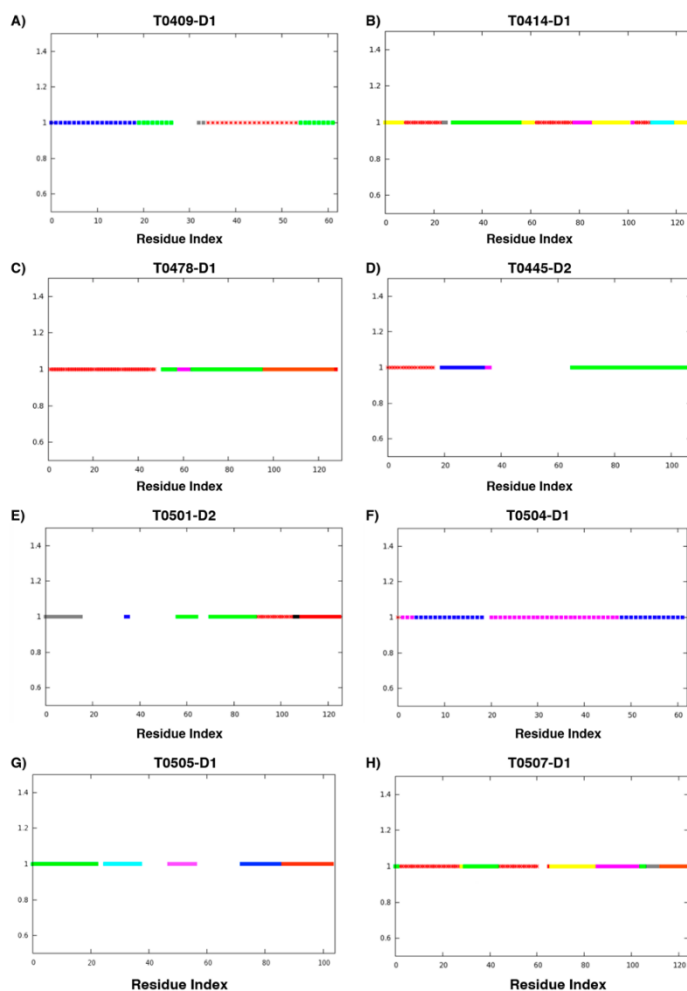


Figure 5. Coverage of suboptimal alignments. The red color shows the correctly alignment segments of the profile-profile alignment. The different colors show the correctly aligned segments from sub-optimal alignments.

3.4. Are Correct Alignment Segments in the Pool of Alignments?

The existence of correct alignment segments is checked by comparing the alignment segments to the structural alignment within the pool of suboptimal alignments. For this, the targets that have very low sequence identity and very low model quality from profile-profile alignments are selected in Table 2. Those targets are: T0409-D1, T0414-D1, T0445-D2, T0478-D1, T0501-D1, T0504-D2, T0505-D2 and T0507-D1. Their sequence identity ranges from 4.84 to 17.74. They all have very low native-overlap values with profile-profile alignments, but the models are getting much better when the modeling is done with structural alignment. That means they all have good template structures, however due to the alignment errors they are not modeled from the correct segment of the template.

To show the correctly aligned segments exist, all these targets are taken to the suboptimal alignment step. Namely, not only single best solution from dynamic programming alignment algorithm is considered, but all the additional suboptimal alignments are collected from Modeller's suboptimal algorithm. Figure 5 from A to H displays the results for different targets and the red dots shows the correctly aligned segments in the single optimal alignment. This is what is collected from a regular profile-profile alignment. Again, the alignments are compared to the structural alignment. The different colors in Figure 5 other than red, show the correct alignment segments in the pool of sub-optimal alignments. The number of suboptimal alignments obtained depends on the Modeller's dynamic programming alignment. For each target, the correctly aligned segments cover much more than the correctly aligned segments exist in the single optimal alignment. Thus, in the genetic algorithm moves such as single-point crossovers or double-point crossovers, if these segments can be evaluated by a more detailed and localized scoring function and brought together, the models will have a much higher number of correctly aligned positions.

4. Conclusion

In this work, one of the biggest challenges in homology modeling, modeling errors originated from alignment mistakes is evaluated with a benchmark set in the twilight zone, low sequence identity region of the template-based modeling. The profile-profile alignments produced low-quality models. When the structural features are incorporated into the alignment, the model qualities are improved. However, generally, when the target structure is not known which the standard is, incorporating structural features is not an easy task. The iterative modeling protocol, Moulder, tries to incorporate structural features by evaluating alignments with their 3-D models is used in this study. Its sampling method is shown to be successful, while scoring function used is not sufficient to pick the correct models or alignments segments. Finally, alignment of CASP 8 targets which has

extremely low sequence identity but good structural overlap with the template structures is analyzed in terms of suboptimal alignments. For each target, it has been shown that the correct alignment segments exist in the pool of sub-optimal alignments. Thus, if improved scoring functions to pick these fragments are developed, the sampling with genetic algorithm moves such as crossovers will be capable of bringing the correctly aligned segments together.

Finally, the importance of the model assessment scoring functions which are good in the local quality assessment is emphasized with the results here. If the reliability of different regions of a predicted structure is measured correctly, those segments can be brought together to form a single correct overall alignment.

Author Contributions

The percentage of the author contributions is presented below. The author reviewed and approved the final version of the manuscript.

	S.E.
C	100
D	100
S	100
DCP	100
DAI	100
L	100
W	100
CR	100
SR	100
PM	100
FA	100

C=Concept, D= design, S= supervision, DCP= data collection and/or processing, DAI= data analysis and/or interpretation, L= literature search, W= writing, CR= critical review, SR= submission and revision, PM= project management, FA= funding acquisition.

Conflict of Interest

The author declared that there is no conflict of interest.

Ethical Consideration

Ethics committee approval was not required for this study because of there was no study on animals or humans.

Acknowledgements

The author is thankful to Prof. Dr. Andrej Sali for technical discussions about the method, Dr. David Eramian for providing previous version of the software, and Dr. Burak Servili for the support in the preparation of the figures.

References

- Bertoline LMF, Lima AN, Krieger JE, Teixeira SK. 2023. Before and after AlphaFold2: An overview of protein structure prediction. *Front Bioinform*, 3: 1120370.
- Bonneau R, Baker D. 2001. Ab initio protein structure

- prediction: Progress and prospects. *Annu Rev Biophys Biomol Struct*, 30: 173-189.
- Chen H, Kihara D. 2011. Effect of using suboptimal alignments in template-based protein structure prediction. *Proteins: Structure, Function and Bioinformatics*, 79(1): 315-334.
- Dunbrack RLJ. 2006. Sequence comparison and protein structure prediction. *Curr Opin Struct Biol*, 16(3): 374-384.
- Eramian DD. 2008. Assessment and Prediction of Protein Structures. PhD thesis, University, University of California at San Francisco, San Francisco, pp: 252. URL: <https://escholarship.org/uc/item/3k41q2cq> (accessed date: June 12, 2023).
- Gromiha MM, Nagarajan R, Selvaraj S. 2018. Protein structural bioinformatics: An overview. In *Encyclopedia of Bioinformatics and Computational Biology: ABC of Bioinformatics*, 2: 445-459.
- Guex N, Peitsch MC. 1997. Swiss PDB Viewer - References. *Electrophoresis*, 18(15): 2714-2723.
- Hardin C, Pogorelov TV, Luthey-Schulten Z. 2002. Ab initio protein structure prediction. *Curr Opin Struct Biol*, 12(2): 176-181.
- John B, Sali A. 2003. Comparative protein structure modeling by iterative alignment, model building and model assessment. *Nucleic Acids Res*, 31(14): 3982-3992.
- Jones DT. 1999. GenTHREADER: An efficient and reliable protein fold recognition method for genomic sequences. *J Mol Biol*, 287(4): 797-815.
- Jumper J, Evans R, Pritzel A, Green T, Figurnov M, Ronneberger O, Tunyasuvunakool K, Bates R, Žídek A, Potapenko A, Bridgland A, Meyer C, Kohl SAA, Ballard AJ, Cowie A, Romera-Paredes B, Nikolov S, Jain R, Adler J, Hassabis D. 2021. Applying and improving AlphaFold at CASP14. *Prot Struct Funct Bioinform*, 89(12): 1711-1721.
- Jumper J, Evans R, Pritzel A, Green T, Figurnov M, Ronneberger O, Tunyasuvunakool K, Bates R, Žídek A, Potapenko A, Bridgland A, Meyer C, Kohl SAA, Ballard AJ, Cowie A, Romera-Paredes B, Nikolov S, Jain R, Adler J, Hassabis D. 2021. Highly accurate protein structure prediction with AlphaFold. *Nature*, 596: 583-589.
- Kahsay RY, Wang G, Gao G, Liao L, Dunbrack R. 2005. Quasi-consensus-based comparison of profile hidden Markov models for protein sequences. *Bioinformatics*, 21(10): 2287-2293.
- Kim DE, Chivian D, Baker D. 2004. Protein structure prediction and analysis using the Robetta server. *Nucleic Acids Res*, 32: W526-W531.
- Marti-Renom MA, Madhusudhan MS, Sali A. 2004. Alignment of protein sequences by their profiles. *Protein Sci*, 13(4): 1071-1087.
- Nassar R, Dignon GL, Razban RM, Dill KA. 2021. The Protein Folding Problem: The Role of Theory. *J Mol Biol*, 433(20): 167126.
- Pearce R, Li Y, Omenn GS, Zhang Y. 2022. Fast and accurate Ab Initio Protein structure prediction using deep learning potentials. *PLoS Comput Biol*, 18(9): e1010539.
- Pieper U, Webb BM, Dong GQ, Schneidman-Duhovny D, Fan H, Kim SJ, Khuri N, Spill YG, Weinkam P, Hammel M, Tainer JA, Nilges M, Sali A. 2006. MODBASE: a database of annotated comparative protein structure models and associated resources. *Nucleic Acids Res*, 34: D291-5.
- Rohl CA, Strauss CEM, Misura KMS, Baker D. 2004. Protein structure prediction using rosetta. *Meth Enzymol*, 383: 66-93.
- Sauder JM, Arthur JW, Dunbrack RLJ. 2000. Large-scale comparison of protein sequence alignment algorithms with structure alignments. *Proteins*, 40(1): 6-22.
- Shen MY, Sali A. 2006. Statistical potential for assessment and prediction of protein structures. *Protein Sci*, 15(11): 2507-2524.
- Soding J. 2005. Protein homology detection by HMM-HMM comparison. *Bioinformatics*, 21(7): 951-960.
- Wang G, Dunbrack RLJ. 2004. Scoring profile-to-profile sequence alignments. *Protein Sci*, 13(6): 1612-1626.
- Webb B, Sali A. 2016. Comparative protein structure modeling using MODELLER. *Curr Protoc Bioinformatics*, 20(54): 5.6.1-5.6.37.
- Xu D, Zhang Y. 2012. Ab initio protein structure assembly using continuous structure fragments and optimized knowledge-based force field. *Prot Struct Funct Bioinform*, 80(7): 1715-1735.
- Yang J, Zhang Y. 2015. I-TASSER server: New development for protein structure and function predictions. *Nucleic Acids Res*, 43(W1): W174-W181.
- Zhou H, Zhou Y. 2005. Fold recognition by combining sequence profiles derived from evolution and from depth-dependent structural alignment of fragments. *Proteins*, 58(2): 321-328.



EXPRESSION AND CHARACTERIZATION OF A THERMOSTABLE α -GLUCURONIDASE FROM *Geobacillus kaustophilus*

Hilal TAŞDEMİR¹, Yunus ENSARİ^{1*}


¹Kafkas University, Faculty of Engineering and Architecture, Bioengineering Department, 36000, Kars, Türkiye


Abstract: Fossil fuels are a crucial resource for the global economy, but they also contribute to greenhouse gas emissions and environmental pollution. Lignocellulosic biomass, which includes cellulose, hemicellulose, and lignin obtained from plants, is a promising alternative to fossil fuels. It can help address these problems while reducing environmental impact. Enzymatic pre-treatment is used to degrade lignocellulosic biomass into subunits. The degradation of the hemicellulose structure involves accessory enzymes of industrial importance, such as α -glucuronidase. α -glucuronidases (EC 3.2.1.139) catalyze the hydrolysis of the α -1,2-glycosidic bond between α -D-glucuronic acid (GlcA) or its 4-O-methyl ether form (MeGlcA) and D-xylose units in the structure of xylooligosaccharides. The aim of this study was cloning, heterologous expression and biochemical characterization of the α -glucuronidase enzyme from the thermophilic bacterium *Geobacillus kaustophilus*. With this aim, the codon optimized α -glucuronidase gene was cloned into pQE-30 vector, overexpressed in *E. coli* BL21 (DE3), and purified with nickel affinity chromatography. The biochemical characterization of the purified α -glucuronidase revealed that the enzyme has activity at elevated temperatures between 65-90 °C. Additionally, *Geobacillus kaustophilus* α -glucuronidase enzyme showed higher activity at acidic pH values from pH 4.0 to 6.5. This is the first study to report the gene cloning, recombinant expression and biochemical characterization of α -glucuronidase which could be used as accessory enzyme from a thermophilic bacterium *Geobacillus kaustophilus*.

Keywords: *Geobacillus kaustophilus*, α -glucuronidase, Thermostable enzymes, Lignocellulosic biomass, Hemicellulolytic enzymes

*Corresponding author: Kafkas University, Faculty of Engineering and Architecture, Bioengineering Department, 36000, Kars, Türkiye

E mail: yunusensari@kafkas.edu.tr (Y. ENSARİ)

Hilal TAŞDEMİR  <https://orcid.org/0000-0003-4404-3400>

Yunus ENSARİ  <https://orcid.org/0000-0002-4757-4197>

Received: December 19, 2023

Accepted: January 15, 2024

Published: March 15, 2024

Cite as: Taşdemir H, Ensari Y. 2024. Expression and characterization of a thermostable α -glucuronidase from *Geobacillus kaustophilus*. BSJ Eng Sci, 7(2): 175-183.

1. Introduction

Lignocellulosic biomass has gained popularity in recent years as a fuel for energy production due to the depletion of fossil fuels and climate change (Wang et al., 2021). Lignocellulosic biomass is the most abundant resource on our planet, with more than 40 million tons of non-food plant material produced each year. Together with forestry and agricultural wastes, this amounts to approximately 200 billion tons (Jaramillo et al., 2015). Numerous different agricultural goods are produced in significant amounts in the agricultural industry, and depending on the agricultural products, an equivalent quantity of agricultural waste is produced (Østby et al., 2020). The interest in this kind of waste is growing since it is employed in numerous sectors, including the culinary, chemical, and pharmaceutical industries. The development of novel bioproducts is made possible by the increased passion and interest in lignocellulosic biomass, a renewable biopolymer (Lee et al., 2014). Currently, the manufacture of bioethanol is the main application for lignocellulosic biomass, but it may also be used to make a variety of other products, including enzymes, food additives, pharmaceuticals, and cosmetic compounds (Jaramillo et al., 2015; Maitan-Alfenas et al., 2015; Arevalo-Gallegos et al., 2017).

The liberation of simple sugars in the lignocellulosic biomass structure is crucial for the production of high value-added products. However, this process is challenging due to the intricate nature of the biomass (Ezeilo et al., 2017). The hemicellulose chain of lignocellulose biomass consists of sugar molecules including xylose, galactose, and glucuronic acid which creates a significant obstacle for the direct hydrolysis of cellulose. Due to the structural diversity of xylans, the complex hydrolysis of xylan engages accessory enzymes such as, α -glucuronidases, α -L-arabinofuranosidases, acetyl xylan esterases, feruloyl esterases, and glucuronyl esterases, in addition to endoxylanases and β -xylosidases (Mohapatra and Manoj, 2019; Akkaya et al., 2023). Hardwoods, conifers, and many cereals contain xylan bonded to glucuronic acid or methyl-glucuronic acid (Yan et al., 2017). Therefore, to completely use glucuronoxylans, glucuronidases (E.C. 3.2.1.131), which remove bound glucuronic acid and its derivatives from xylan, are required (Wang et al., 2016). Glucuronidases belong to the families of glucoside hydrolases GH4, GH67, and GH115 (Rogowski et al., 2014; Wang et al., 2016). While some of them act only on short xylooligomers or small model molecules, others hydrolyze glucuronic acid from polymeric xylan (Adıgüzel, 2013; Chong et al.,



2015).

α -glucuronidases (EC 3.2.1.139) catalyze the hydrolysis of the α -1,2-glycosidic bond between α -D-glucuronic acid (GlcA) or its 4-O-methyl ether form (MeGlcA) and d-xylose units in the structure of xylooligosaccharides. The majority of α -glucuronidases that catalyze the hydrolysis of this linkage belong to the glycoside hydrolase 67 (GH67) family (Septiningrum et al., 2015). Glycoside hydrolases are grouped according to their amino-acid sequence similarity (Aalbers et al., 2015). The presence of 4-O-methylglucuronic acid moieties is one of the main factors affecting the adsorption of the xylan chain, and treatment of xylan with α -glucuronidase significantly increases the level of adsorption of xylan (Chimphango et al., 2016).

Considering that many industrial and biotechnological processes take place under very harsh conditions, extremophilic microorganisms living under extreme conditions such as high temperature, high pressure, low/high pH, etc. are a great source of new enzymes that can be used in such processes (Demirjian et al., 2001; Van den Burg, 2003). The discovery of enzymes capable of operating under extreme conditions has enabled the development of new industrial processes (Demirjian et al., 2001). Enzymes obtained from thermophilic organisms have many advantages in enzymatic hydrolysis of biomass (Yeoman et al., 2010). In general, thermostable enzymes have higher specific activity, so that the bioconversion process can be completed with a small amount of enzyme. They have high stability and can be used for a long time. In addition, better substrate solubility and enzyme penetration, as well as lower contamination, are achieved when conversion takes place at high temperatures (Turner et al., 2007; Yeoman et al., 2010).

In this study, we identified, cloned and expressed for the first time the α -glucuronidase enzyme encoded in the genome of the thermophilic bacterium *Geobacillus kaustophilus*. In addition, the biochemical characterization of the purified α -glucuronidase enzyme was performed.

2. Materials and Methods

2.1. Chemicals

All chemicals were purchased from Sigma-Aldrich, Merck, and Biobasic unless otherwise stated. Salt-free oligonucleotides were purchased from Sentebiolab (Ankara, Türkiye). Enzymes were purchased from ThermoFisher Scientific unless otherwise stated.

2.2. Cloning of the *Geobacillus kaustophilus* α -Glucuronidase Gene

The codon optimized *aguA* gene of the *Geobacillus kaustophilus* (Uniprot ID: A0A0D8BWB2) was amplified by PCR (94 °C for 3 min, 1 cycle; 94 °C for 60 s/55-65 °C for 60 s/72 °C for 180 s, 30 cycles; 72 °C for 10 min, 1 cycle) using the forward primer (5'-ATAGGTACCATGACGGCGGATACGAACC-3') and the reverse primer (5'-

CATAAGCTTTCACCGATAAATTTTCCGCCCG-3'). The amplified product was digested with *KpnI* and *HindIII* and then ligated with T4-DNA Ligase into pQE-30 plasmid vector. The ligation products were transformed into *E. coli* DH5 α and positive transformants were validated with colony PCR and sequencing.

2.3. Heterologous Expression of the *Geobacillus kaustophilus* α -Glucuronidase Enzyme

The pQE-30 plasmid harboring α -glucuronidase gene was transformed into *E. coli* BL21 (DE3). *E. coli* BL21 (DE3) was inoculated into LB media supplemented with ampicillin (100 μ g/mL) as pre-culture and cultivated overnight at 37 °C and 165 rpm. 0.5 mL of the pre-culture was inoculated into 50 mL of LB media supplemented with ampicillin (100 μ g/mL) and cultivated at 37 °C, 165 rpm until OD₆₀₀ reached 0.6-0.8. Protein expression was induced by the addition of 0.1 mM IPTG and 0.1 g/L Thiamine HCl. Then protein expression was carried out at 37 °C, 165 rpm for 24 h. Cells were harvested by centrifugation (4 °C, 3220 g, 30 min) and stored at -20 °C until further use.

2.4. Protein Purification and Quantification

The cell pellet was resuspended in four volumes of pH 7.5 phosphate buffer and lysed by sonication for 5 min (30 sec. on + 15 sec. off, 40% amplitude). The cell lysate containing α -glucuronidase enzyme was clarified by centrifugation (13680 g, 30 min, 4 °C). HisPur™ Ni-NTA Purification Kit was used to purify the His-tagged α -glucuronidase enzyme. The purified protein was dialyzed for 24 hours and then analyzed by SDS-PAGE and quantified using the Pierce™ BCA Protein Assay Kit.

2.5. Activity Measurement and Characterization of the *Geobacillus kaustophilus* α -Glucuronidase Enzyme

α -glucuronidase enzyme activity was measured via 4-nitrophenol based spectrophotometric assay. 56 μ l of phosphate buffer (50 mM, pH 7.5), 40 μ l of enzyme, and 4 μ l of 50 mM p-nitrophenyl- α -D-glucuronide were added to the reaction medium and incubated at 37 °C for 20 min. After incubation, 100 μ l of 1 M Na₂CO₃ was added to the reaction medium to stop the reaction and absorbance was recorded at 400 nm. A previously prepared 4-nitrophenol standard graph (0.01-0.1 mM) was used for the determination of enzyme activity. One unit of enzyme activity was defined as the conversion of 1 μ mol of substrate per minute. All measurements were performed in triplicate.

Optimal temperature, optimal pH and buffer were determined for further characterization of the *Geobacillus kaustophilus* α -glucuronidase enzyme. Additionally, effects of various chemicals were tested on enzyme activity. First, the optimal temperature was determined using the activity test explained above at various temperature between 40 and 90 °C. Then optimal pH and assay buffer was determined by testing 50 mM sodium acetate buffer (pH 4.0-6.0), 50 mM phosphate buffer (pH 6.0-7.5), 50 mM tris buffer (pH 7.5-9.0), and 50 mM glycine buffer (pH 9.0-10.0). Lastly, 10 mM of mM

SDS, EDTA, FeCl₃, MgCl₂, KCl, CaCl₂, MnCl₂, ethanol, DMSO, 2-Mercaptoethanol, DTT, sodium citrate, and CoCl₂ was included in the reaction mixture to determine the effect of various chemicals on α-glucuronidase enzyme activity.

3. Results and Discussion

3.1. Cloning of the *Geobacillus kaustophilus* α-Glucuronidase Gene

Geobacillus kaustophilus is a thermophilic, gram-positive bacterium that was first isolated from the Mariana Trench. It grows optimally between 55 °C and 65 °C and can tolerate temperatures between 37 °C and 75 °C. The bacterium can also grow in a pH range of 6 to 8, with optimal growth occurring between pH 6.2 and 7.5.

To express the *Geobacillus kaustophilus* α-glucuronidase enzyme heterologously in *E. coli*, the relevant gene codon was first optimized and synthesized as a synthetic gene by Genscript company. Subsequently, PCR was used to obtain copies of the gene and add restriction recognition sites for ligation to the pQE-30 expression vector. To determine the optimal annealing temperatures of the primers, gradient PCR was performed between 55 and 65 °C. The resulting PCR product was then analyzed on a 1% agarose gel (Figure 1). The α-glucuronidase gene yielded a 2040 bp. product through the PCR process at all tested temperatures, as shown in the figure.

The 2040 bp. gene fragment was digested with *KpnI* and *HindIII* and ligated into pQE-30 vector digested with the same restriction enzymes. The obtained plasmid construct was transformed into *E.coli* DH5α. Positive transformants were validated by colony PCR (Figure 2) and sequencing. The pQE-40 vector harboring the α-glucuronidase gene was transformed into *E. coli* BL21 (DE3) for heterologous expression.

3.2. Heterologous Expression and Purification of Recombinant α-glucuronidase Protein

Geobacillus kaustophilus α-glucuronidase enzyme was expressed in *E. coli* BL21 (DE3) and purified with His-Tag purification. Purified protein fractions were analyzed by SDS-PAGE (Figure 3) with a molecular mass of approximately 78.5 kDa. Purified protein fractions were combined and dialyzed to remove imidazole from enzyme solution. The concentration of the purified α-glucuronidase enzyme was determined using the Pierce BCA Protein Assay Kit after dialysis. A standard graph, containing bovine serum albumin (BSA) ranging from 0-2000 µg/mL, was used for protein quantification. The BCA analysis revealed that the concentration of the purified α-glucuronidase enzyme was 76.04 µg/mL.

3.3 Characterization of Recombinant *Geobacillus kaustophilus* α-glucuronidase Enzyme

The recombinant *Geobacillus kaustophilus* α-glucuronidase enzyme was characterized by determining the temperature, buffer, and pH value at which it showed optimum activity. Additionally, the effects of certain chemicals on enzyme activity were examined. The α-glucuronidase enzyme was characterized using a 4-nitrophenol (pNP) based colorimetric activity assay. The colorimetric activity determination utilized the pNP standard graph prepared at concentrations ranging from 0.001 mM to 0.1 mM. To characterize the α-glucuronidase enzyme, we incubated the enzymatic reaction at 40 °C for 20, 30, and 40 minutes to determine the optimal reaction time. We also tested two different buffers, phosphate and HEPES, for the reaction. Spectroscopic measurements were taken at 405 nm to determine the amount of pNP released, as shown in Figure 4. Based on the results, it was determined that the optimal conditions were achieved with a 30-minute incubation in phosphate buffer.

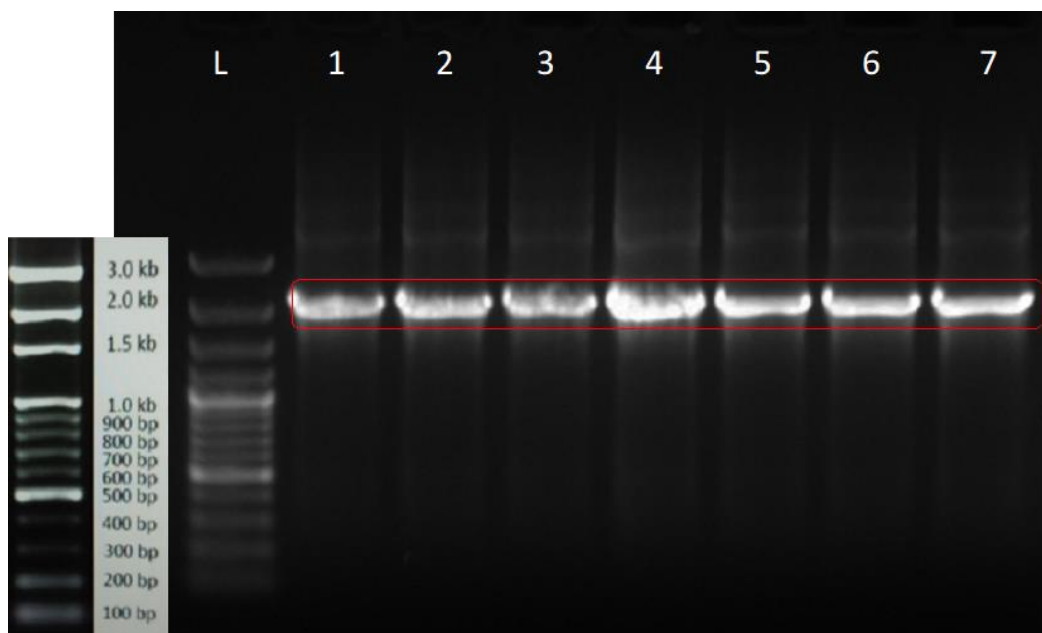


Figure 1. Agarose gel analysis of PCR performed for the amplification of α-glucuronidase gene. L: Molecular weight marker, 1: 55 °C, 2: 56.5 °C, 3: 57.6 °C, 4: 59 °C, 5: 60.7 °C, 6: 63.3 °C, 7: 64.7 °C.

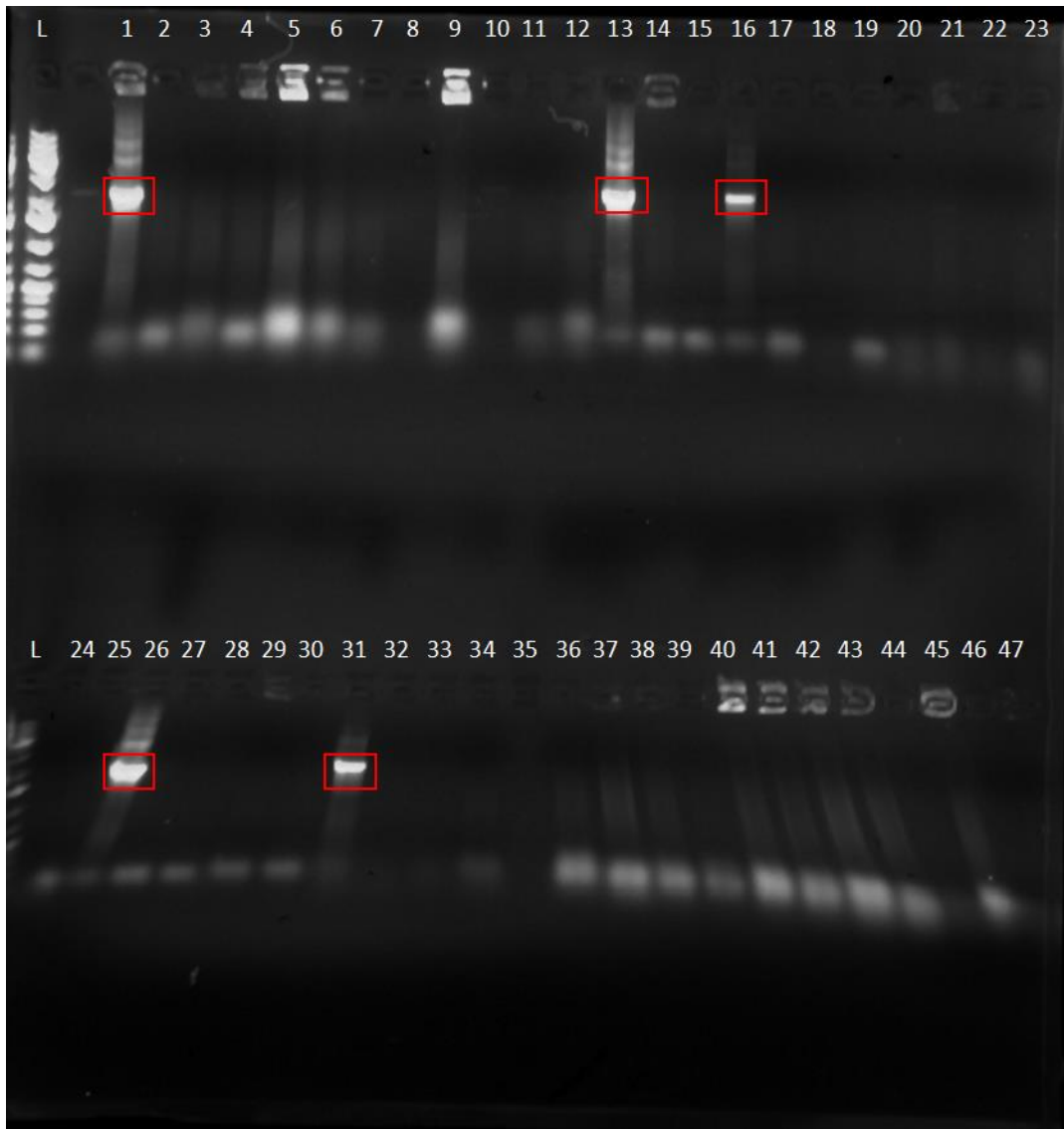


Figure 2. Agarose gel image of colony PCR analysis for α -glucuronidase gene. L: Molecular weight marker, 1-47: different colonies obtained after transformation. Red boxes show the positive clones with 2 kb DNA band.

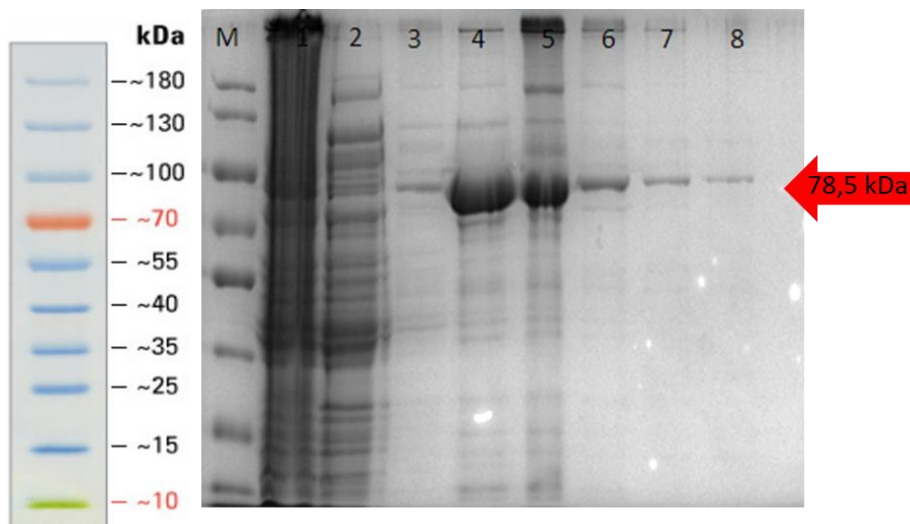


Figure 3. SDS-PAGE analysis of α -glucuronidase enzyme. M: Marker, 1: Cleared supernatant, 2: Flow-through (FT), 3: Wash Fraction, 4: Elution Fraction 1 (100 mM imidazole), 5: Elution Fraction 2 (200 mM imidazole), 6: Elution Fraction 3 (300 mM imidazole), 7: Elution Fraction 4 (400 mM imidazole), 8: Elution Fraction 5 (500 mM imidazole).

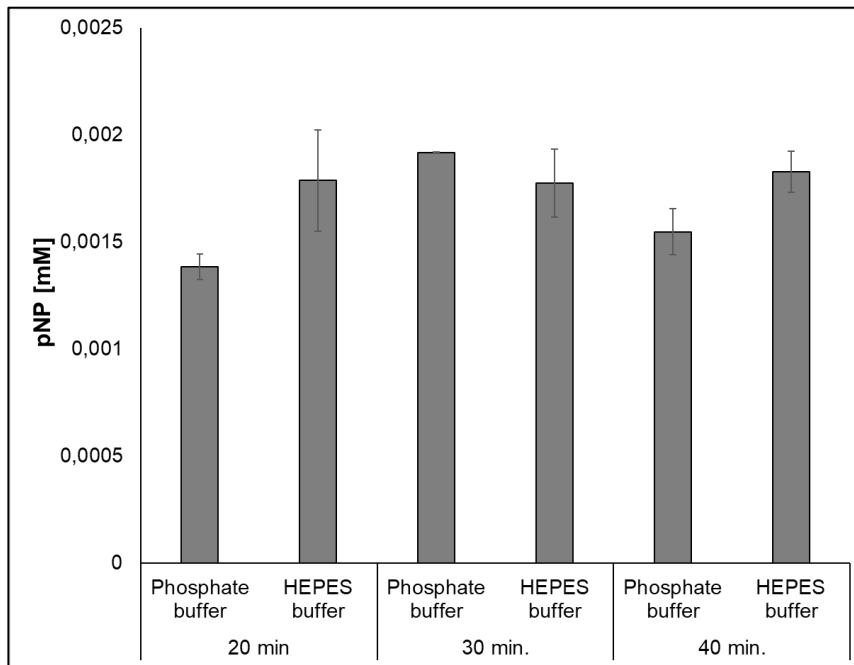


Figure 4. Determination of the appropriate incubation time for α -glucuronidase enzyme activity assay.

The results obtained after 30 minutes of incubation in phosphate buffer were the most consistent compared to other time periods and HEPES buffer. Therefore, 30 minutes of incubation in phosphate buffer was selected as the optimum reaction time, and subsequent biochemical characterization procedures were carried out. The standard deviation of the other results was higher than that obtained with 30 minutes of incubation in phosphate buffer.

The biochemical characterization of the recombinant α -glucuronidase enzyme began by determining its optimum temperature. Enzymatic activity was measured at various temperatures ranging from 40 °C to 90 °C, and the amount of pNP released at 405 nm was then measured spectrophotometrically. The temperature at which the highest enzymatic activity was measured is considered 100%, and the activity values obtained at other temperatures were proportioned accordingly (see Figure 5). The optimum activity of the α -glucuronidase enzyme was observed at 75 °C. Enzyme activity increased gradually from 45 ° and decreased slightly after 75 °C. The enzyme exhibited 66% activity at 70 °C and 40% activity at 65 °C when the activity observed at 75 °C was evaluated as 100%. Additionally, the enzyme activity remained around 10% at moderate temperatures (between 40-50 °C). At higher temperatures, the enzyme retained 93% of its activity at 80 °C and 90% at 85 °C, while exhibiting about 80% activity at 90 °C. The study's findings indicate that the enzyme is thermophilic, as expected, and exhibits low activity at mesophilic temperatures. Suresh and coworkers reported that the α -glucuronidase enzyme derived from *Thermotoga maritima*, a hyperthermophilic bacterial species, demonstrated the highest activity at 60 °C (Suresh et al., 2003). Similarly, Shao et al. (1995) found that the optimal

temperature for the enzyme was 60 °C in their study with α -glucuronidase enzyme obtained from *Thermoanaerobacterium sp.* Zaide and coworkers determined that the optimum temperature for *Bacillus stearothermophilus* α -glucuronidase enzyme activity was 75 °C (Zaide et al., 2001). In a similar study, the optimum temperature for *Geobacillus stearothermophilus* α -glucuronidase gene activity was found to be 65 °C (Dalia et al., 2004). In this study, we observed that the recombinantly produced *Geobacillus kaustaphilus* α -glucuronidase enzyme shares similar characteristics with those obtained from other thermophilic Bacillus species. Furthermore, it was found to have a higher operating temperature than *Thermotoga* and *Thermoanaerobacter* species, which are also thermophilic organisms described in the literature. Additionally, there are α -glucuronidase enzymes identified from mesophilic bacteria in the literature. The optimal activity of the α -glucuronidase enzyme obtained from a mixed culture was found to be within the range of 45 °C (Lee et al., 2012). Furthermore, the optimal operating temperature of the α -glucuronidase enzyme obtained from *Aspergillus fumigatus* was determined to be 37 °C (Rosa et al., 2013). After determining the optimal temperature for α -glucuronidase enzyme, we conducted enzyme activity tests using different buffer systems and pH values. The enzyme was tested using sodium acetate at pH 4 to 6, phosphate buffer at pH 6 to 7.5, tris buffer at pH 7.5 to 9, and glycine buffer at pH 9 to 10 to determine the pH value and buffer system that resulted in the highest enzyme activity. The pH value with the highest enzymatic activity was considered 100%, and the activity values obtained at other pH values were adjusted proportionally (see Figure 6).

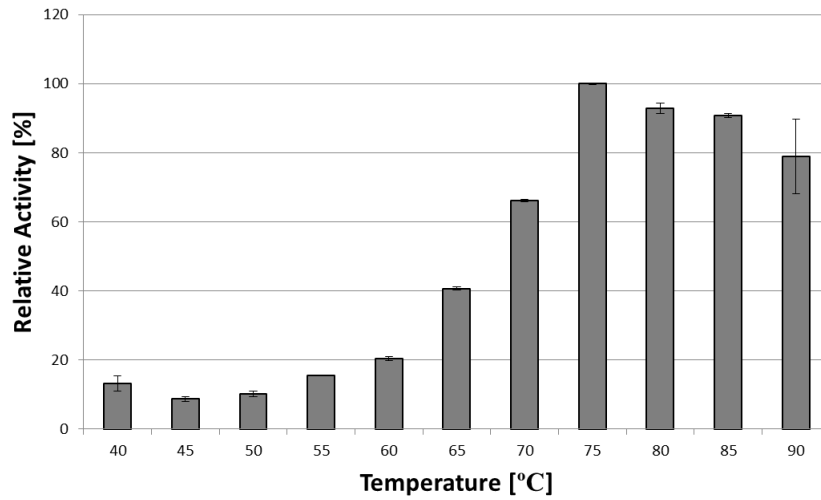


Figure 5. Effect of temperature on α -glucuronidase enzyme activity. The activity assay was performed in pH 7.5 phosphate buffer at various temperatures for 30 min.

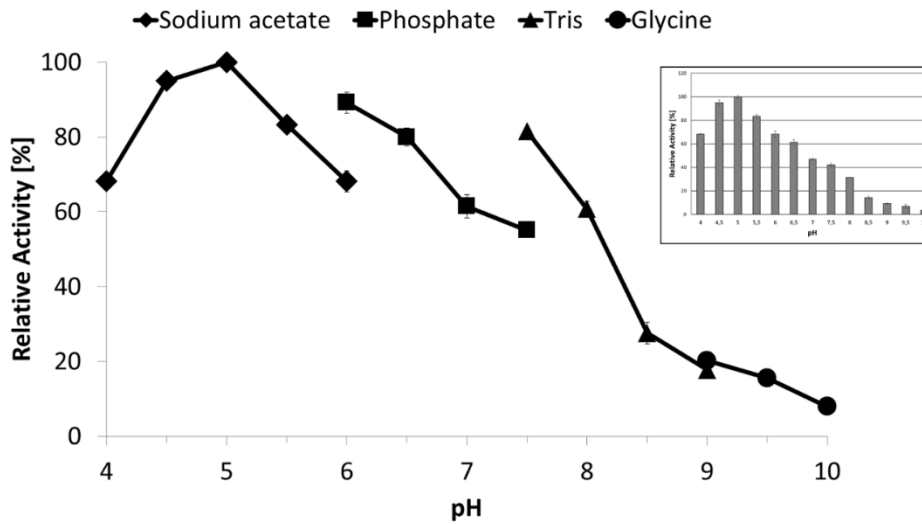


Figure 6. Effect of buffer and pH on α -glucuronidase enzyme activity. The activity was measured at 75 °C in various buffers of pH 4.0 – 10.0 for 30 min.

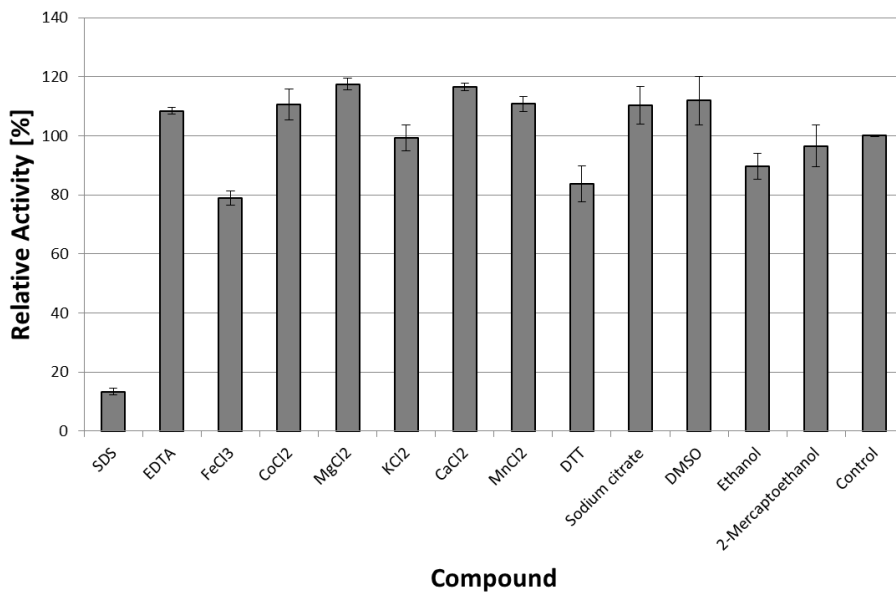


Figure 7. Effect of chemicals on α -glucuronidase enzyme activity. Chemical compounds were added to the reaction medium at final concentration of 0.1 mM.

The results indicate that the optimal pH value for the α -glucuronidase enzyme is pH 5.0, and it exhibits the highest activity in a sodium acetate buffer. The enzyme activity increased between pH 4.0 and 5.0 but started to decrease after pH 5.0. The α -glucuronidase enzyme from *Geobacillus kaustaphilus* showed the highest activity (over 80%) in mildly acidic conditions and about 50% activity at neutral pH values. In basic conditions, the α -glucuronidase enzyme lost most of its activity and exhibited about 10% activity. These findings indicate that the α -glucuronidase enzyme from *Geobacillus kaustaphilus* is both acidophilic and thermophilic. The optimal pH values for α -glucuronidase enzymes from *Aspergillus fumigatus*, *Thermotoga maritima*, and *Thermoanaerobacterium sp.* were determined to be 5.0, 7.5, and 7.5, respectively (Shao et al., 1995; Suresh et al., 2003; Rosa et al., 2013). According to Zaide et al. (2001) the optimal activity of the thermophilic *Bacillus stearothermophilus* α -glucuronidase enzyme was achieved in a phosphate buffer with a pH of 7.0. When comparing the results of this thesis study to other α -glucuronidase enzymes described in the literature, it was observed that enzymes described as thermophilic in the literature exhibited activity at neutral pH values. The α -glucuronidase enzyme produced in this study by recombinant *Geobacillus kaustaphilus* is both acidothermophilic and distinct from other thermophilic relatives in the literature. This acidophilic and thermophilic feature makes the *Geobacillus kaustaphilus* α -glucuronidase enzyme superior to its competitors, especially in industrial processes that occur under extreme conditions.

After determining the optimal operating temperature, pH value, and buffer for the α -glucuronidase enzyme, the aim was to evaluate the impact of different chemicals on enzyme activity. Under optimum conditions, the enzymatic reaction was carried out with the addition of SDS, EDTA, FeCl₃, CoCl₂, MgCl₂, KCl, CaCl₂, MnCl₂, DTT, sodium citrate, DMSO, ethanol, and 2-mercaptoethanol at a concentration of 0.1 mM. The amount of pNP released at 405 nm was measured spectrophotometrically. After the reaction, enzyme activity was measured and compared to a control reaction without any chemicals. The results, shown in Figure 7, indicate that MgCl₂ and CaCl₂ increased enzyme activity by approximately 20%. Conversely, FeCl₃, DTT, and ethanol partially inhibited enzyme activity, while SDS inhibited it by about 85%. No significant effect on enzyme activity was observed for any other chemicals. The addition of EDTA, CoCl₂, MgCl₂, CaCl₂, MnCl₂, sodium citrate, and DMSO positively affected α -glucuronidase activity. The highest increase in activity, approximately 117%, was observed with MgCl₂ and CaCl₂, while the increase in activity for the other chemicals remained around 110%. KCl and 2-mercaptoethanol did not show any effect. The addition of ethanol resulted in an activity of 90%, while the addition of DTT and FeCl₃ resulted in activities of 83% and 79%, respectively. Out of the 13 chemical compounds tested,

only SDS was found to be inhibitory, causing a dramatic decrease in enzyme activity to only 13% in a reaction medium containing 0.1 M SDS. The other chemicals did not cause any significant change. Zaide and coworkers also investigated the effect of FeCl₃, CoCl₂, MgCl₂, KCl, CaCl₂, BaCl₂, NiCl₂, HgCl₂, ZnCl₂, AgNO₃, and CuSO₄ on the activity of the *Bacillus stearothermophilus* α -glucuronidase enzyme. The enzyme activity was highly inhibited by HgCl₂, ZnCl₂, AgNO₃, and CuSO₄, while only FeCl₃ moderately increased it. The effect of other chemicals was not significant (Zaide et al., 2001).

4. Conclusion

The complete enzymatic hydrolysis of lignocellulose requires many cellulolytic and hemicellulolytic enzymes. While endoxylanase and β -xylosidase are primarily responsible for breaking down the hemicellulose structure, α -L-arabinofuranosidase, α -glucuronidase, α -galactosidase, acetylxylan esterase, and β -mannanase also play a role in its complete degradation. Glucuronic acid or its methyl ester is present in the lignocellulosic structure attached to xylan. During the hydrolysis of xylans, α -glucuronidases work alongside many other enzymes. α -glucuronidase enzymes are utilized in various industrial and biotechnological processes. Furthermore, this enzyme has applications in disease diagnosis and the food industry. In this study, the gene encoding α -glucuronidase enzyme in *Geobacillus kaustaphilus* was cloned into pQE-30 plasmid and successfully expressed in *E. coli* BL21 (DE3). The expressed enzyme was purified via nickel affinity chromatography and characterized biochemically. The purified enzyme showed the optimum activity at 75 °C and pH 5.0 in sodium acetate buffer. Furthermore, α -glucuronidase enzyme was inhibited in the presence of SDS, FeCl₃, DTT, and ethanol. On the other hand, EDTA, CoCl₂, MgCl₂, CaCl₂, MnCl₂, sodium citrate, and DMSO positively affected α -glucuronidase activity. In conclusion, the activity at high temperatures and mild acidic conditions shows the potential of the *Geobacillus kaustaphilus* α -glucuronidase enzyme in the lignocellulosic biomass degradation.

Author Contributions

The percentage of the author(s) contributions is presented below. All authors reviewed and approved the final version of the manuscript.

	H.T.	Y.A.
C	20	80
D	50	50
S		100
DCP	50	50
DAI	50	50
L	50	50
W	50	50
CR	20	80
SR	50	50
PM	50	50
FA		100

C=Concept, D= design, S= supervision, DCP= data collection and/or processing, DAI= data analysis and/or interpretation, L= literature search, W= writing, CR= critical review, SR= submission and revision, PM= project management, FA= funding acquisition.

Conflict of Interest

The authors declared that there is no conflict of interest.

Ethical Consideration

Ethics committee approval was not required for this study because of there was no study on animals or humans.

References

Aalbers F, Turkenburg JP, Davies GJ, Dijkhuizen L, Lammerts van Bueren A. 2015. Structural and functional characterization of a novel family GH115 4-O-methyl- α -glucuronidase with specificity for decorated arabinogalactans. *J Mol Biol*, 427(24): 3935-3946.

Adıgüzel AO. 2013. Biyoetanolin genel özellikleri ve üretimi için gerekli hammadde kaynakları. *Bitlis Eren Üniv Fen Bil Derg*, 2(2): 204-220.

Akkaya A, Ensari Y, Ozseker EE, Batur OO, Buyuran G, Evran S. 2023. Recombinant production and biochemical characterization of thermostable arabinofuranosidase from acidothermophilic alicyclobacillus acidocaldarius. *Protein J*, 42(4): 437-450.

Arevalo-Gallegos A, Ahmad Z, Asgher M, Parra-Saldivar R, Iqbal HMN. 2017. Lignocellulose: A sustainable material to produce value-added products with a zero waste approach-A review. *Int J Biol Macromol*, 99: 308-318.

Chimphango AFA, Görgens JF, van Zyl WH. 2016. In situ enzyme aided adsorption of soluble xylan biopolymers onto cellulosic material. *Carbohydr Polym*, 143: 172-178.

Chong SL, Derba-Maceluch M, Koutaniemi S, Gómez LD, McQueen-Mason SJ, Tenkanen M, Mellerowicz EJ. 2015. Active fungal GH115 α -glucuronidase produced in *Arabidopsis thaliana* affects only the UX1-reactive glucuronate decorations on native glucuronoxylans. *BMC Biotechnol*, 15(1): 56.

Dalia S, Gali G, Gil S, Yuval S. 2004. Effect of dimer dissociation on activity and thermostability of the α -glucuronidase from *geobacillus stearothermophilus*: Dissecting the different oligomeric forms of family 67 glycoside hydrolases. *J*

Bacteriol, 186(20): 6928-6937.

Demirjian DC, Morís-Varas F, Cassidy CS. 2001. Enzymes from extremophiles. *Curr Opin Chem Biol*, 5(2): 144-151.

Ezeilo UR, Zakaria II, Huyop F, Wahab RA. 2017. Enzymatic breakdown of lignocellulosic biomass: the role of glycosyl hydrolases and lytic polysaccharide monoxygenases. *Biotechnol. Biotechnol Equip*, 31(4): 647-662.

Jaramillo PMD, Gomes HAR, Monclaro AV, Silva COG, Filho EXF. 2015. Lignocellulose-degrading enzymes. *Fungal Biomolec*, 2015: 73-85.

Lee CC, Kibblewhite RE, Wagschal K, Li R, Robertson GH, Orts WJ. 2012. Isolation and characterization of a novel GH67 α -glucuronidase from a mixed culture. *J Ind Microbiol Biotechnol*, 39(8): 1245-1251.

Lee HV, Hamid SBA, Zain SK. 2014. Conversion of lignocellulosic biomass to nanocellulose: Structure and chemical process. *Sci World J*, 2014: 631013.

Maitan-Alfenas GP, Visser EM, Guimaraes VM. 2015. Enzymatic hydrolysis of lignocellulosic biomass: Converting food waste in valuable products. *Curr Opin Food Sci*, 1(1): 44-49.

Mohapatra SB, Manoj N. 2019. Structure of an α -glucuronidase in complex with Co²⁺ and citrate provides insights into the mechanism and substrate recognition in the family 4 glycosyl hydrolases. *Biochem Biophys Res Commun*, 518(2): 197-203.

Østby H, Hansen LD, Horn SJ, Eijsink VGH, Várnai A. 2020. Enzymatic processing of lignocellulosic biomass: principles, recent advances and perspectives. *J Ind Microbiol Biotechnol*, 47(9): 623-657.

Rogowski A, Baslé A, Farinas CS, Solovyova A, Mortimer JC, Dupree P, Gilbert HJ, Bolam DN. 2014. Evidence that GH115 α -glucuronidase activity, which is required to degrade plant biomass, is dependent on conformational flexibility. *J Biol Chem*, 289(1): 53-64.

Rosa L, Ravanal MC, Mardones W, Eyzaguirre J. 2013. Characterization of a recombinant α -glucuronidase from *Aspergillus fumigatus*. *Fungal Biol*, 117(5): 380-387.

Septeningrum K, Ohi H, Waeonukul R, Pason P, Tachaapaikoon C, Ratanakhanokchai K, Sermsathanaswadi J, Deng L, Prawitwong P, Kosugi A. 2015. The GH67 α -glucuronidase of *Paenibacillus curdlanolyticus* B-6 removes hexenuronic acid groups and facilitates biodegradation of the model xylooligosaccharide hexenuronosyl xylotriase. *Enzyme Microb Technol*, 71: 28-35.

Shao W, Obi S, Puls J, Wiegel J. 1995. Purification and Characterization of the (alpha)-Glucuronidase from *Thermoanaerobacterium* sp. Strain JW/SL-YS485, an Important Enzyme for the Utilization of Substituted Xylans. *Appl Environ Microbiol*, 61(3): 1077-1081.

Suresh C, Kitaoka M, Hayashi K. 2003. A thermostable non-xylanolytic α -glucuronidase of *Thermotoga maritima* MSB8. *Biosci Biotechnol Biochem*, 67(11): 2359-2364.

Turner P, Mamo G, Karlsson EN. 2007. Potential and utilization of thermophiles and thermostable enzymes in biorefining. *Microb Cell Fact*, 6(1): 9.

Van den Burg B. 2003. Extremophiles as a source for novel enzymes. *Curr Opin Microbiol*, 6(3): 213-218.

Wang F, Ouyang D, Zhou Z, Page SJ, Liu D, Zhao X. 2021. Lignocellulosic biomass as sustainable feedstock and materials for power generation and energy storage. *J Energy Chem*, 57: 247-280.

Wang W, Yan R, Nocek BP, Vuong TV, Di Leo R, Xu X, Cui H, Gatenholm P, Toriz G, Tenkanen M, Savchenko A, Master ER. 2016. Biochemical and structural characterization of a five-domain GH115 α -glucuronidase from the marine bacterium *Saccharophagus degradans* 2-40T*. *J Biol Chem*, 291(27):

- 14120-14133.
- Yan R, Vuong TV, Wang W, Master ER. 2017. Action of a GH115 α -glucuronidase from *Amphibacillus xylanus* at alkaline condition promotes release of 4-O-methylglucopyranosyluronic acid from glucuronoxylan and arabinoglucuronoxylan. *Enzyme Microb Technol*, 104: 22-28.
- Yeoman CJ, Han Y, Dodd D, Schroeder CM, Mackie RI, Cann IK. 2010. Chapter 1 - Thermostable Enzymes as Biocatalysts in the Biofuel Industry. In *Advances in Applied Microbiology*, Academic Press, London, UK, pp: 1-55.
- Zaide G, Shallom D, Shulami S, Zolotnitsky G, Golan G, Baasov T, Shoham G, Shoham Y. 2001. Biochemical characterization and identification of catalytic residues in alpha-glucuronidase from *Bacillus stearothermophilus* T-6. *Eur. J Biochem*, 268(10): 3006-3016.



ÇOK KRİTERLİ KARAR VERME METODU AHP VE CBS TEKNOLOJİSİ KULLANILARAK SERA YER SEÇİMİ: AKSU İLÇESİ ÖRNEĞİ

Eda BOSTANCI¹, Önder KABAŞ^{2*}, Ercüment AKSOY³

¹Antalya Metropolitan Municipality, 07310, Antalya, Türkiye

²Akdeniz University, Technical Sciences Vocational School, Department of Machinery, 07070, Antalya, Türkiye

³Akdeniz University, Technical Sciences Vocational School, Department of Geographical Informations Systems, 07070, Antalya, Türkiye

Özet: Yer seçimi birden çok faktörün ele alındığı karmaşık yapısı olan bir işlemdir. Bu çalışmanın amacı, uzaktan algılama (UA), coğrafi bilgi sistemleri (CBS) ve çok kriterli karar (ÇKK) metodu kullanılarak sera için uygun alanların belirlenmesidir. Çalışma alanı Türkiye'nin seracılık faaliyetlerinin yoğun olduğu bölge olması nedeniyle Antalya ili, Aksu ilçesi seçilmiştir. UA ve CBS veri toplama metodları ile on iki mevcut kriter (eğim, baki, su, yola yakınlık, nüfus yoğunluğuna yakınlık, toprak özellikleri, nem, yağış, sıcaklık, güneşlenme şiddeti, güneşlenme radyasyonu ve rüzgâr şiddeti), uygun alan seçimini gerçekleştirmek için kullanılmıştır. Kriterlerin ağırlıkları, analitik hiyerarşi süreci (AHP) matrisi ile elde edilmiştir. Tutarlılık oranı (CR) ve tutarlılık endeksi(CI) sırasıyla 0,067 ve 0,099 olarak elde edilmiştir. Çalışma alanı içinde farklı yasal ve yönetmelikler gereği seçim dışında kalması gereken alanlar çalışma alanından maskeleyme metodu ile dışarı çıkarılmıştır. Çalışma alanı uygun olmayan, az uygun, orta uygun, uygun, en uygun şeklinde beş sınıfa ayrılmıştır. Bu alanlar sırasıyla 136,51 ha, 751,61 ha, 155,04 ha, 216,41 ha, 411,71 ha'dır. Sera için en uygun alan, çalışma alanının %24.63'ünü kapsamaktadır. Çalışma metodu ile belirlenen sera yer seçimi ile yatırımcının altyapı, enerji ve pazar gibi zorunlu giderlerinin minimuma indirilmesi gerçekleştirilebilmektedir. Ayrıca yer belirleme için gerekli olan verilerin gelecekte güncellenebilir özellikte olması önerilen modelin gelecekte kullanılabilirliğini ve gelişebilirliğini artırmaktadır.

Anahtar kelimeler: Sera, Yer seçimi, CBS, Uzaktan algılama, AHP, Çok kriterli metod


Greenhouse Site Selection using Geographical Information Sand Multi-Criteria Method: The Case of Aksu


Abstract: Site selection is a complex process in which multiple factors are considered. This study aims to determine suitable areas for greenhouses by using remote sensing (RS), geographical information systems (GIS) and multi-criteria decision (MCD) methods. Aksu district of Antalya province was selected as the study area because it is the region where greenhouse activities are intensive in Türkiye. Twelve existing criteria (slope, aspect, proximity to water, road and population density, soil properties, humidity, precipitation, temperature, insolation intensity, insolation radiation and wind intensity) were used to select suitable areas for greenhouses with UA and GIS data collection methods. The criteria weights were obtained by the analytic hierarchy process (AHP) matrix. Consistency ratio (CR) and consistency index (CI) were obtained as 0.067 and 0.099 respectively. The areas within the study area that should be excluded from the selection due to different legal and regulatory requirements were excluded from the study area by masking method. The study area was classified into five classes as Absolutely Unsuitable, Unsuitable, Less Suitable, Suitable, Most Suitable. These areas are 136.51 ha, 751.61 ha, 155.04 ha, 216.41 ha, 411.71 ha respectively. The Most Suitable Area for Greenhouse covers 24.63% of the study area. With the greenhouse site selection determined by the study method, it is possible to minimum the mandatory expenses of the investor such as infrastructure, energy and market. In addition, the fact that the data required for location determination can be updated in the future increases the usability and developability of the proposed model in the future.


Keywords: Greenhouse, Site selection, GIS, Remote sensing, AHP, Multi criteria method

*Sorumlu yazar (Corresponding author): Akdeniz University, Technical Sciences Vocational School, Department of Machinery, 07070, Antalya, Türkiye

E mail: okabas@akdeniz.edu.tr (Ö. KABAŞ)

Eda BOSTANCI  <https://orcid.org/0000-0002-6579-7255>

Önder KABAŞ  <https://orcid.org/0000-0003-0703-4804>

Ercüment AKSOY  <https://orcid.org/0000-0001-7313-0891>

Gönderi: 03 Aralık 2023

Kabul: 20 Ocak 2024

Yayınlanma: 15 Mart 2024

Received: December 03, 2023

Accepted: January 20, 2024

Published: March 15, 2024

Cite as: Bostancı E, Kabaş Ö, Aksoy E. 2024. Greenhouse site selection using geographical information sand multi-criteria method: The case of Aksu. BSJ Eng Sci, 7(2): 184-195.

1. Giriş

Yıl içinde birden fazla üretim yapılması, mevsimlik ürünlerin her mevsim yetiştirilebilmesi ve üretim yapılabilmesi sonucu pazar fiyatlarında yükselmenin önüne geçilebilir. Bunlar seracılık faaliyetlerinin en belirgin avantajlarından biridir.

Günümüzde sera yer seçimi çok kriterli karar mekanizmaları, CBS ve uzaktan algılama teknolojisi

kullanılması ile yaygın olarak yapılmaktadır. Çevre ve politik, teknik ve sosyal sorunları barındıran kompleks bir yapı içeren çok kriterli karar problemi işletme yer seçimi sürecinde ortaya çıkmaktadır. Yüksel ve Yüksel (2012), Rezaeiniya ve ark. (2014) ve Rezaeiniya ve ark. (2012) tarafından yapılan çalışmalarda çok kriterli karar verme yöntemleri kullanmak suretiyle sera yapım yerlerinin belirlenmesi üzerine çalışmışlardır. Çalışmada



ANP ve COPRAS-G yöntemleri kullanılmıştır. Çalışma kapsamında kriterler arasındaki görecelik ağırlıkların belirlenmesi için ikili karşılaştırma metodu ve birbirine olan bağımlı ilişkiler vurgulanmıştır (Kouchaksaraei ve ark., 2015). Balaban ve Şen (1988) yaptıkları çalışmada topografik ve toprak koşulları, güneş ve hâkim rüzgârlar, işletmenin araziye göre konumu, çevresel etkiler, enerji ve su kaynakları ve yasal düzenlemeler gibi kriterlerin kurulacak bir örtü altı işletmesi için dikkat edilmesi gereken önemli kriterler olduğunu belirtmişlerdir. Öz (2017) yaptığı çalışmada solar radyasyon ve güneşlenme süresi kriterlerinin kullanımı ile örtü altı yetiştiricilik potansiyelini belirlenmiştir. Cemek (2005), seracılığın ekonomik olarak yapılabileceği yetiştirme dönemleri belirlenmiştir. Bu çalışma kapsamında iklim ve sayısal yükseklik modeli kullanılmıştır. Yetiştiricilik için gerekli olan iklimlendirme parametreleri CBS ile dezavantajlı ve avantajlı olarak ilçe ölçeğinde araştırılmıştır.

Kriter olarak fiziksel koşullar, çevresel koşullar, özel koşullar, iş gücü, hammadde, hükümet politikası ve sera tipi kullanılmıştır. Kazancın artırılması, maliyetlerin azaltılması ve işletmenin sürdürülebilirliği açısından işletme yerinin uygun seçilmesi çok önemli bir faktördür (Alkan, 1977; MEGEP, 2007).

Sera yer seçimi çalışmalarında, Analitik Hiyerarşi Süreci (AHP), basitliği, doğruluğu ve uzman görüşü etkisinin olması nedeniyle en yaygın olarak benimsenen ÇKK tekniklerinden biridir (Doğan, 2010; Akıncı ve ark., 2013; Ustaoglu ve ark., 2021).

UA ve CBS teknolojisi kullanılarak veriler elde edilmiştir. Çalışmaya dahil olmayacak alanların maskeleyme metodu uygulaması ile dışarıda tutulmuştur. Geriye kalan alanlara yoğunluk analizi, çok kriterli karar mekanizmaları vb. metodlar kullanılarak en uygun sera alanı yer seçimi işlemi gerçekleştirilmiştir.

2. Materyal ve Yöntem

2.1. Çalışma Alanı

Çalışma alanı, Türkiye'nin güneybatısında yer alan ve yaklaşık 445 km²'lik bir alanı kaplayan Aksu ilçesidir. Akdeniz ikliminin hâkim olduğu bölgede, yazları sıcak ve kurak, kışlar ise ılık ve yağışlı geçer. Türkiye'nin önemli bir turistik otel bölgesi olması yanı sıra önemli bir tarım bölgesidir. Bu özelliğiyle Ülke örtü altı tarımında önemli bir yere sahiptir (Eken ve ark., 2008). Çalışma alanı Şekil 1'de gösterilmiştir.

Tarım ve Orman bakanlığının 2020 yılı verileri ile Tablo 1 oluşturulmuş ve çalışma alanının ülke örtü altı tarım alanlarına önemli katkısı sayısal veriler ile elde edilmiştir. Veriler ışığında Antalya iline ait örtü altı alanları Türkiye'deki örtü altı alanlarının %39'unu oluşturmakta, bunu %83'ünü cam seralar, %54'ünü ise plastik seralar oluşturmaktadır. Çalışma alanı ülke örtü altı tarımı açısından önem arz etmesi nedeniyle tercih edilmiştir.



Şekil 1. Yer bulduru haritası.

Tablo 1. Örtü altı alan bilgi tablosu

Örtü altı alanlar (da)	Antalya	Türkiye	Antalya/Türkiye (%)
Toplam alan (da)	312,23	805,16	39
Cam sera (da)	66,74	80,78	83
Plastik sera (da)	218,01	401,80	54
Yüksek tünel (da)	14,29	104,26	14
Alçak tünel (da)	13,20	218,33	6

Uygun sera alanı yer seçimi konusunda literatür taraması yapılmıştır. Çalışma konusu ile ilgili ulusal ve uluslararası çalışmaların irdelenmesi sonucu ortak keşişim kriterleri belirlenmiştir. Bu çalışmada kullanılan referansları Tablo 2 'de gösterilmiştir.

2.2. Veri Seti

Bu çalışmada yol, akarsu, toprak özellikleri, nem, yağış, sıcaklık, güneşlenme şiddeti, güneşlenme radyasyonu, rüzgâr şiddeti, eğim, baki ve nüfus verileri olarak 12 adet veri kullanılmıştır. Meteorolojik veriler Meteoroloji Genel Müdürlüğü (MGM), yol verisi Open Street Map (OSM), akarsu verisi Devlet Su İşleri (DSİ), nüfus verisi Türkiye İstatistik Kurumu (TÜİK) veri kaynaklarından alınmıştır. Toprak özellikleri verisi Akdeniz Üniversitesi Ziraat Fakültesi Toprak Bilimi ve Bitki Besleme Bölümü'nden elde edilmiştir (Sarı ve ark., 2009). Baki ve eğim haritaları 30 metre çözünürlüğe sahip Sayısal Yükseklik Modeli (SYM) verisinden türetilmiştir. Çalışmada kullanılan verilerin tipi ve kaynakları ile bu veriler ile üretilen katmanların grup tablosu şeklinde gösterimi Tablo 3'de verilmiştir. Verinin adı, biçimi ve kaynağı gösterilmiştir. Bu bilgilere ek olarak veriler ile üretilen katmanlar kendi içinde Meteoroloji haritaları (nem, yağış, sıcaklık, güneşlenme şiddeti, güneşlenme radyasyonu, rüzgâr şiddeti), yakınlık haritaları (yola, suya ve nüfus yoğunluğuna) ve arazi özellik haritaları (toprak özellik, baki ve eğim) olacak 3 grup altında oluşturulmuştur. Yatırımcılar için ekonomik ve kazançlı sera temelli üretim için meteorolojik yakınlık ve arazi özellik kriterlerinin üretime pozitif katkı vermesi istenmektedir.

Tablo 2. Çalışma için belirlenen kriterler

Kriterler	Referanslar
Nem	Yüksel Türkboyları (2018), Mercan (2019), Paul ve ark. (2020).
Yağış	Demir ve ark. (2011), Erdoğan ve ark. (2015), Saltuk ve Artun (2018), Paul ve ark. (2020), Şahin ve Toroğlu (2020).
Sıcaklık	Cemek (2005), Öztekin ve ark. (2008), Ayrancı (2011), Demir ve ark. (2011), Marucci ve ark. (2014), Erdoğan ve ark. (2015), Kendirli (2015), Yüksel Türkboyları (2018), Saltuk ve Artun (2018), Selim ve ark. (2018), Paul ve ark. (2020), Şahin ve Toroğlu (2020).
Güneşlenme Şiddeti	Balaban ve Şen (1988), Kouchaksaraei ve ark., (2015), Kendirli (2015), Yüksel Türkboyları (2018).
Güneşlenme Radyasyonu	Cemek (2005), Kouchaksaraei ve ark., (2015), Öz (2017), Mercan (2019).
Rüzgâr Şiddeti	Balaban ve Şen (1988), Kouchaksaraei ve ark., 2015, Kendirli (2015), Saltuk ve Artun (2018), Mercan (2019).
Yola yakınlık	Kouchaksaraei ve ark., (2015), Mercan (2019), Ustaoglu ve ark. (2021),
Suya yakınlık	Balaban ve Şen (1988), Öztekin ve ark. (2008), Erdoğan ve ark. (2015), Kouchaksaraei ve ark., (2015), Saltuk ve Altun (2018), Mercan (2019), Şahin ve Toroğlu (2020), Ustaoglu ve ark. (2021)
Nüfus yoğunluğuna yakınlık	
Toprak özellikleri	Balaban ve Şen (1988), Demir ve ark. (2011), Akıncı ve ark. (2013), Delibaş ve ark. (2015), Erdoğan ve ark. (2015), Kouchaksaraei ve ark., (2015), Saltuk ve Artun (2018), Mercan (2019), Şahin ve Toroğlu (2020), Ustaoglu ve ark. (2021).
Baki	Balaban ve Şen (1988), Öztekin ve ark. (2008), Demir ve ark. (2011), Akıncı ve ark. (2013), Delibaş ve ark. (2015), Saltuk ve Artun (2018), Mercan (2019), Şahin ve Toroğlu (2020), Ustaoglu ve ark. (2021),
Eğim	Öztekin ve ark. (2008), Demir ve ark. (2011), Akıncı ve ark. (2013), Delibaş ve ark. (2015), Erdoğan ve ark. (2015), Selim ve ark. (2018), Saltuk ve Artun (2018), Mercan (2019), Şahin ve Toroğlu (2020), Ustaoglu ve ark. (2021).

Tablo 3. Kullanılan veri setleri

Veri ve katman bilgi tablosu		
Veri seti	Veri biçimi	Kaynak
Yollar	Vektör	(OSM 2022)
Akarsular	Vektör	(DSİ 2022)
Nüfus	Tablo	(TÜİK 2022)
Toprak özellikleri	Vektör	(DSİ 2022)
Sayısal yükseklik modeli	Raster	(OSM 2022)
Meteorolojik Veriler	Tablo	(MGM 2022)

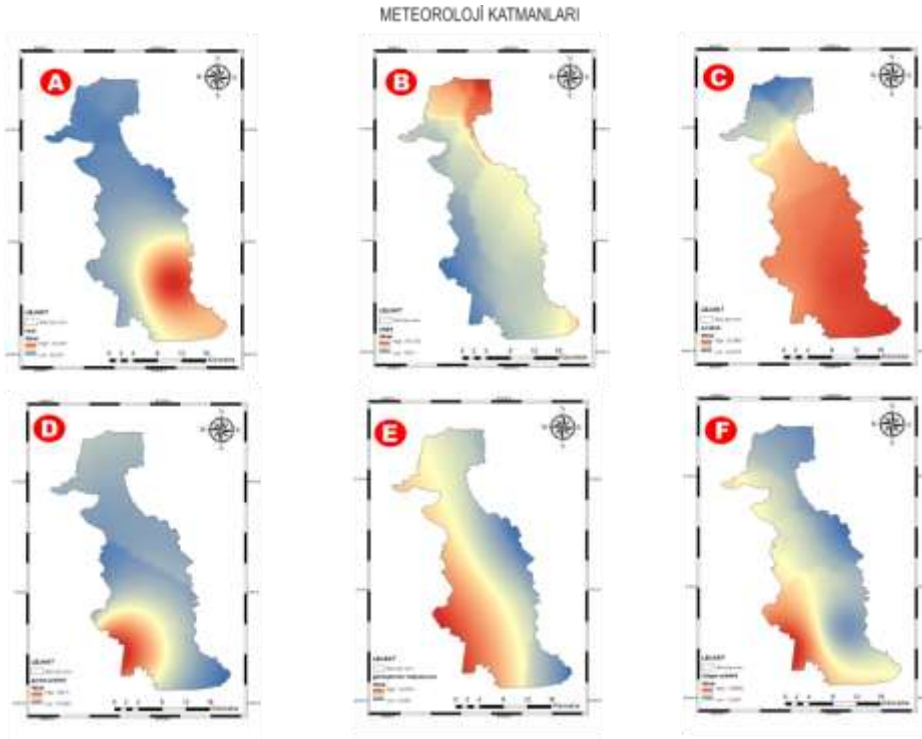
Çalışmada meteoroloji katmanı olarak nem, yağış, sıcaklık, güneşlenme şiddeti, güneşlenme radyasyonu, rüzgâr şiddeti kullanılmıştır. Yakınlık katmanı olarak yola yakınlık, suya yakınlık ve nüfus yoğunluğuna yakınlık kullanılmıştır. Arazi özellik katmanı olarak SYM verisinden baki ve eğim QGIS yazılımı kullanarak elde edilmiştir.

Bu çalışmada kriterlerin verilerinden yararlanılarak ön işlem çıktısı olarak haritalar oluşturulmuştur. Şekil 2’de meteoroloji haritaları, Şekil 3’de yakınlık haritaları, Şekil 4’de arazi özellik haritaları gösterilmiştir.

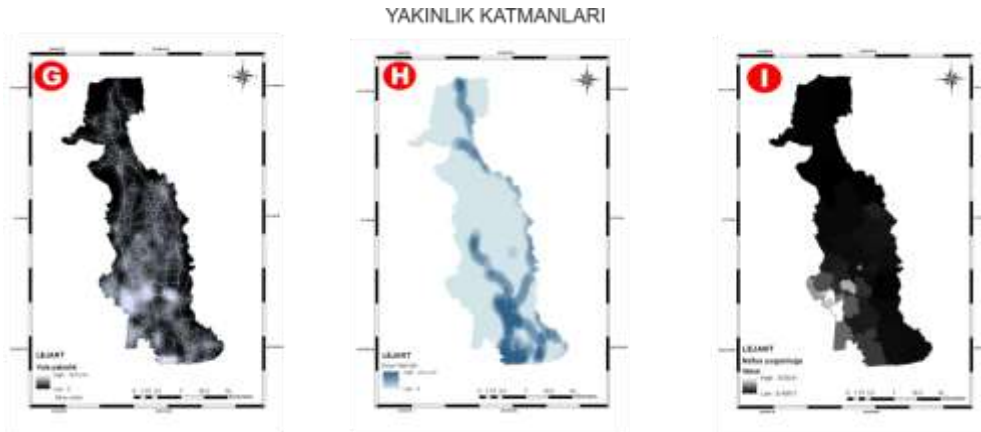
2.2.1. Meteoroloji haritaları

Çalışma alanı merkezinde bir adet meteoroloji istasyonu olması nedeniyle çalışma alanı çevresindeki meteoroloji istasyonlarını da kapsayacak bir alan belirlenmiştir. 100 istasyona ait 1926 yılı ile 2020 yılları arasındaki

ölçümlerin yıllık ortalama değerleri alınmıştır. Bu alan kullanılarak enterpolasyon haritaları üretilmiştir. Bu sayede enterpolasyon doğruluğu da artırılmıştır. İklim verileri üzerinde uygulanan Ters mesafe komşuluk benzerliği enterpolasyon Yöntemi (IDW, Inverse Distance Weighting) metodu ile yapılan enterpolasyon çalışmalarının diğer metotlara göre daha yüksek doğrulukta olduğu tespiti yapılmıştır (Jo ve ark., 2018). Bu nedenle çalışmada IDW metodu kullanılarak tüm meteorolojik kriterler için enterpolasyon işlemi yapılmıştır. Ters mesafe komşuluk benzerliği enterpolasyon yöntemi olarak bilinen IDW yöntemi, bilinmeyen noktaların bilinen noktalar ile arasındaki ters mesafe ilişkisinin ağırlıklandırılarak kestirilmesidir (Taylan ve Damçayırı, 2016; Göğsu ve Hastaoglu, 2019).



Şekil.2. Meteoroloji haritaları.



Şekil.3. Yakınlık haritaları.



Şekil.4. Arazi Özellik haritaları.

Nem haritası

Nem bitki beslenmesi ve sağlığı için önemli bir kriter olması nedeniyle çalışmada nem kriteri dahil edilmiştir (Topçu ve Kocaman, 2019). İstasyonlara ait nem verisi

içeren veri dosyası IDW metodu kullanılarak enterpolasyon işlemi gerçekleştirilmiştir. Nemin mekansal dağılım haritası Şekil 5.a'da gösterilmiştir. Çalışma alanında en düşük nem değeri %62,374 ve en

büyük değer ise %70,2167'dir.

Yağış haritası

Yağışlar, dolu, kar ve yağmur olarak sera yeri seçimine etki ederler. Dolu ve kar yağışı olan alanlarda, sera yapılırken dolu ve kar yükü de dikkate alınmalıdır ki bu da maliyeti artırıcı bir unsurdur. Ayrıca sürekli yağışlar sera içindeki ısı kaybının artmasına ve ışın eksikliğine sebep olur. Aşırı yağış alan bölgelerde ise toprakta mineral birikmeleri olacağından yağışın optimum düzeyde olması istenir (Şahin ve Toroğlu, 2020). Yağışın mekansal dağılım haritası Şekil 5.b'de gösterilmiştir.

Sıcaklık haritası

Sera içerisinde ortam sıcaklığı önemlidir. Yetiştirilmesi istenilen her bitkinin farklı sıcaklık gereksinimleri vardır (Filiz, 2001; Jo ve ark., 2018). Kışları ılıman iklim özelliği gösteren alanlar seçilmelidir; zira ısıtma maliyetleri daha düşüktür. Kış mevsiminde, özellikle gece saatlerinde sera ısıtılmalıdır ki bu da maliyeti artırıcı bir etmen olmaktadır. Ayrıca mikro iklim bölgeleri seraların kurulması için oldukça elverişlidir. Serada ısıtma masrafı ne kadar düşük olursa üreticinin kazancı da o oranda yüksek olmaktadır. Her istasyon için yıllık ortalama sıcaklıklar hesaplanmıştır. Şekil 5.c'de enterpolasyon sonucu elde edilen sıcaklık haritası verilmiştir. Buna göre alan içerisine düşen en düşük yıllık ortalama sıcaklık 20,28 °C, en yüksek yıllık ortalama sıcaklık 22,97 °C'dir.

Güneşlenme şiddeti haritası

Sera boyunca üniform ışık dağılımı bitkilerin gelişimi için çok önemlidir. Işıktan optimum düzeyde faydalanmak için hem seraların hem de bitki sıralarının doğu-batı yönünde düzenlenmesinin pozitif etkisi olması bölgesel bir özellik olarak tespit edilmiştir. Güneş bitki büyümesine katkı sağlamaktadır. Özellikle kış mevsiminde havaların neredeyse sürekli olarak bulutlu olduğu göz önüne alındığında, sera yeri seçiminde güneşlenme gün sayısının yüksek olduğu yerlerin çok önemli olduğu tespit edilmiştir. Şekil 5.d'de güneşlenme şiddeti haritası görülmektedir. Enterpolasyon yapıldıktan sonra çalışma alanında güneşlenme şiddetine ait en düşük değer 370,67 cal cm⁻², en yüksek değer 389,11 cal cm⁻² olmuştur.

Güneşlenme radyasyonu haritası

Güneşlenme radyasyonu bitki sağlığı ve verimlilik açısından diğer güneş parametresi gibi önemlidir (Öz, 2017). Şekil 5.e'deki oluşturulan haritaya göre en düşük güneşlenme radyasyonu değeri 2.55 kWh/m², en yüksek değer ise 3.65 kWh/m²'dir.

Rüzgâr şiddeti haritası

Sera kurulacak yerin seçimi yapılırken rüzgâr da etkili bir parametredir. Rüzgâr; sera içindeki sıcaklığın düşmesine neden olarak ısıtma giderinin artmasına sebep olur. Ayrıca doğal havalandırmaya etki eder ve seralarda fiziki hasarlara sebep olabilir. Bu durum maliyetin ve harcamaların artmasına neden olur. Bu nedenle sera kurulacak yerde rüzgâr haritalarının incelenmesi gereklidir. Soğuk ve kuvvetli rüzgârlardan etkilenemeyecek özellikte olmalıdır (MEGEP, 2007; Doğan, 2010). Rüzgâr şiddetinin artması tarımda

verimliliği olumsuz yönde etkilemektedir. Tercih edilmeyen bir özellik olduğundan 0'a doğru gidildikçe puan değeri artmalıdır. Bu nedenle maskeleme yapıldıktan sonra katmanın tersi (inverse) alınmıştır. Oluşturulan Şekil 5.f'de haritada en düşük rüzgâr şiddeti değeri 0,85 m s⁻¹, en yüksek 5,57 m s⁻¹ olarak bulunmuştur.

2.2.2. Yakınlık haritaları

IDW metodu CBS uygulamalarında mesafeye göre ağırlığın değişmesi işlemlerinde kullanılmaktadır. Bu çalışmada da aynı işlevi görmek için kullanılmıştır. Kritere yaklaştıkça ve uzaklaştıkça 0 ile 1 arasında piksel değerleri azalış veya artış olacak şekilde oluşturulmuştur.

Yola yakınlık haritası

Seralarda yetiştirilen ürünlerin hızlı bir şekilde tazeliğini koruyarak ürünlere zarar gelmeden tüketiciye ulaştırılması gerekir ki bu nedenden dolayı seranın yapıldığı yerin ulaşım yollarına yakın olması gerekmektedir (MEGEP 2007). Open Street Map tarafından paylaşılan Türkiye yol ağı haritası, Aksu ilçe sınırlarına göre düzenlenmiştir. Bu veri seti yolları içermektedir. Değerler 0 m ile 1673,34 m değeri arasındadır. Haritada piksel değeri yükseldikçe parlaklık artmaktadır. Şekil 5.g.'de yola yakınlık haritası ve yola yakınlık haritasının vektör yapıdaki yol ağlarıyla çakıştırılmış hali verilmiştir. Yola yakınlık katmanı oluşturulduktan sonra maskeleme işlemi ile oluşturulan yeni çalışma alanına göre düzenleme işlemi gerçekleştirilmiştir. Oluşturulan harita 0 ile 1 değerleri arasında normalize edilmiştir.

Suya yakınlık haritası

Serada yetiştirilecek olan bitkilerin su ihtiyaçlarını karşılamak, hava sıcaklığı yüksek olan ürünlerde sera içinin nemli kalmasını sağlamak veya serayı soğutabilmek için sera kurulacak yerlerde su bulunması gerekmektedir. Sera kurulumu yapılacak alanda yetiştirilecek bitkilerin besin ihtiyacını sağlamak için sulama suyuna ihtiyaç vardır. Bu nedenle oluşturulan haritada suya yakın yerler en yüksek puanı alacak şekilde işlem yapılmıştır. Suya yakınlık haritası Şekil 5.h'de verilmektedir.

Nüfus yoğunluğuna yakınlık haritası

Seracılık, tüm yıl boyunca iklim koşullarına bağlı kalmadan, birim alandan daha fazla ve kaliteli ürün almayı hedefleyen bir üretim biçimidir. Bundan dolayı sera kurulacak yerlerin büyük yerleşim yerlerine yakın olması istenir (TÜİK, 2022). Seraların nüfus yoğunluğunun çok olduğu yerlerde veya böyle yakın yerlerde konumlandırılması yol maliyetini düşürecek bir etkidir. Aynı zamanda sera kurulacak alanın yola yakın olması hem iş gücü tasarrufu sağlayacak hem de zaman kazandıracaktır. Bunun için nüfus yoğunluğuna ve yollara yakınlık önemli ve pozitif bir kriterdir (Ustaoglu ve ark., 2021).

İlk olarak TÜİK kurumundan elde edilen 2022 yılı mahalle nüfus verisinde her bir mahallenin nüfus değeri mahalle km² miktarına bölünerek mahalle nüfus yoğunluğu elde edilmiştir. Sonrasında vektör

formatındaki nüfus yoğunluğu haritası raster haritaya dönüştürülmüştür. Elde edilen mahalle yoğunluk değerlerinden yararlanarak GIS yazılımında mekansal nüfus yoğunluk haritaları oluşturulmuştur. Oluşturulan harita Şekil 5.i'de gösterilmiştir.

2.2.3. Arazi özelliği

Çalışma alanında arazi özellikleri bir grup olarak ele alınmıştır. Oluşan arazi grubu altında toprak, bakı ve eğim özellikleri bulunmaktadır.

Toprak özellikleri haritası

Tercih edilen sera toprağı, organik madde ve besin açısından zenginliğinin yanı sıra zararlılardan ve hastalıklardan arınmış, yüksek su tutma kapasitesi ve iyi geçirgenlik özelliğine sahip, pH 5-5,7 olan tuzsuz, taban suyu derinliği en az 2 m olan kumlu tınlı topraktır. Bu çalışmada kullanılan toprak özellikleri veri seti büyük toprak grubu sınıflandırmasını içermektedir. Veri seti Akdeniz Üniversitesi Ziraat Fakültesi Toprak Bilimi ve Bitki Besleme Bölümü tarafından yapılan detaylı toprak haritalarıdır. Bu kriterin çalışmada kullanılması çalışma özgünlüğünü artırmıştır (Dursun ve ark., 2008). Oluşturulan harita Şekil 5.a'da gösterilmiştir.

Çalışma bölgesi toprakları kırmızı Akdeniz toprakları /alüvyal topraklar, Kahverengi Orman toprakları/Alüvyal topraklar, Kırmızı Kahverengi Akdeniz toprakları, Kırmızı Akdeniz toprakları ve Kahverengi Orman topraklarından meydana gelmiştir. Toprak grupları uzmanların yardımıyla tarıma en elverişli toprak türleri en yüksek puanı alacak şekilde 0 ile 1 arasında puanlandırılmıştır (Tablo 4).

Tablo 4. Toprak grupları puanlama

Toprak Sınıfları	Puan
Alüvyal Topraklar	1
Kırmızı Akdeniz Toprakları + Alüvyal Topraklar	0,8
Kahverengi Orman Toprakları + Alüvyal Topraklar	0,7
Kırmızı Akdeniz Toprakları	0,6
Kırmızı Kahverengi Akdeniz Toprakları	0,3
Kahverengi Orman Toprakları	0,1

Bakı haritası

Bakı kriter verisi Terra-ASTER (Advanced Spaceborne Thermal Emission and Reflection Radiometer)'in 30 metrelik çözünürlükteki yükseklik verisi olan GDEM- V2 (Global Digital Elevation Model)'den elde edilmiştir. Elde edilen sayısal yükseklik model (SYM) verisi QGIS yazılımı ile bakı ve eğim kriterleri elde edilmiştir. SYM doğrudan kullanılmamaktadır, Bakı ve eğim kriterlerinin üretilmesi için kullanılmıştır.

Arazinin güneye, güneybatıya veya güneydoğuya bakan eğimi, arazinin güneşten daha fazla faydalanmasını sağlamaktadır. Kuzeye bakan arazi eğimlerinde seralar kurulmamalıdır. Kış mevsiminde seraların, en uygun biçimde ısıtma ihtiyacının karşılanabilmesi için işletme yönünün doğu-batı şeklinde planlanması gerekmektedir (Topçu ve Kocaman, 2019). Sera yeri seçiminde arazinin

güneye bakması önemlidir (Saltuk ve Artun, 2018). Arazinin güneye bakması, şiddetli rüzgârları engeller, gün ışığından sağlanacak verimi artırır (Alkan, 1977; Von, 2010). Bakı haritası 30 m çözünürlüklü SYM'den üretilmiştir. Üretilen harita yeniden sınıflandırılarak puanlandırması güneye bakan arazilere en yüksek, kuzeye bakan arazilere en düşük olacak şekilde yapılmıştır (Şekil 5.b). Her bir yön ayrı bir derecedir. En yüksek değer güney cephe iken, en düşük değer kuzey olarak ele alınmıştır. Bakı haritası cephe puanlaması Tablo 5'de verilmektedir.

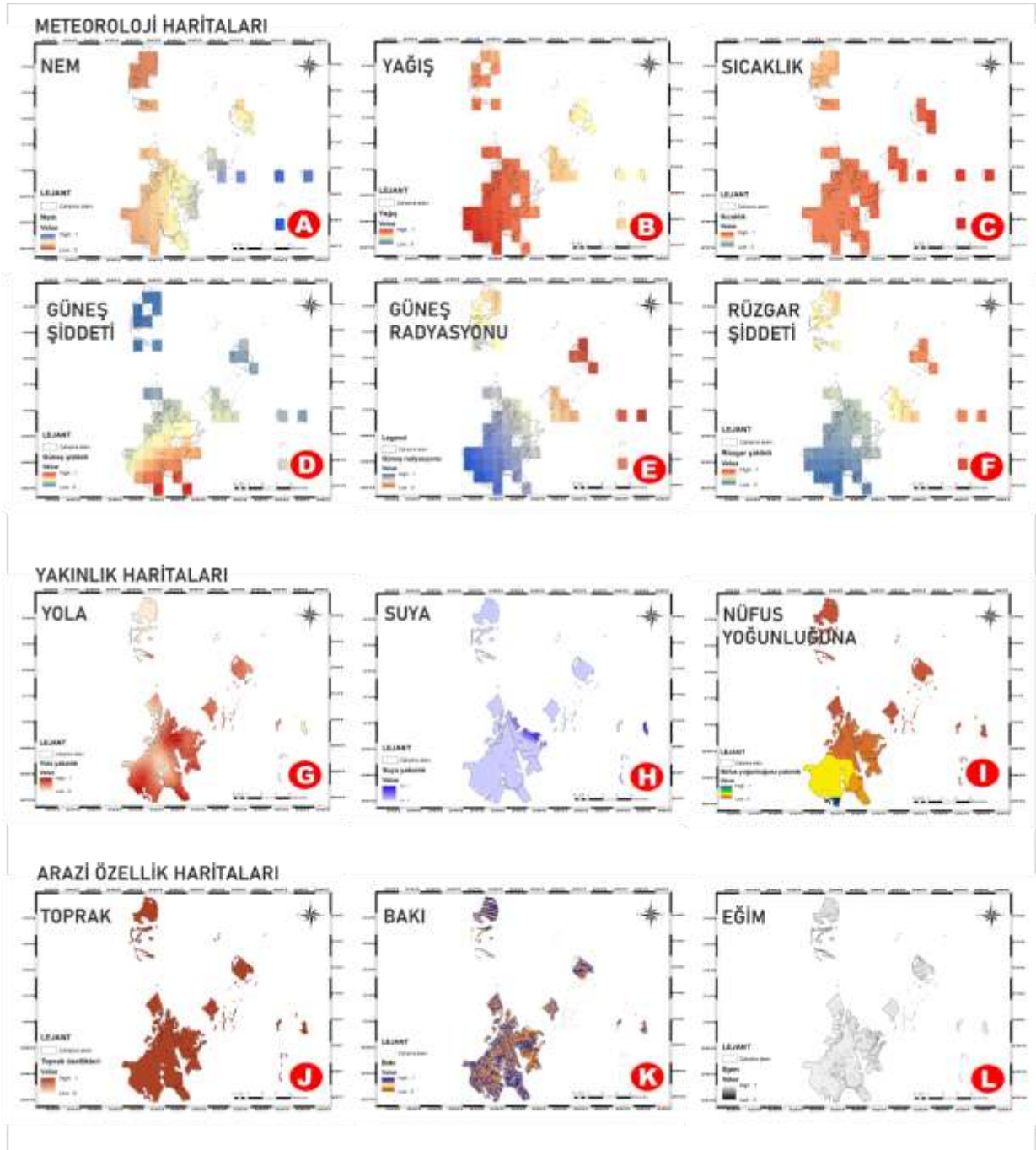
Tablo 5. Bakı cephesi puanlaması

Yönler	Açısal Aralık Değeri	Puan
Düz	-1	9
Kuzey	0-22,5	1
Kuzeydoğu	22,5-67,5	4
Doğu	67,5-112,5	6
Güneydoğu	112,5-157,5	8
Güney	157,5-202,5	10
Güneybatı	202,5-247,5	7
Batı	247,5-292,5	5
Kuzeybatı	292,5-337,5	4
Kuzey	337,5-360	2

Eğim haritası

Sera yapılacak sahanın %0,5-1,0° civarlarında hafif eğimli yapıda olması, hem karık sulaması hem de yüzey drenajı uygulanacak seralarda oldukça önemlidir. Yüksek eğim toprak kayması riskini artıracığından sera kurulacak alanlarda eğim değerinin düşük olması istenir (Şahin ve Toroğlu, 2020). Çalışma bölgesi eğim haritası Şekil 5.l'de verilmektedir.

Eğim haritası 30 metre çözünürlükteki SRTM verisinden elde edilmiştir. Tarım yapılacak bölgelerde arazi eğiminin az olmasına dikkat edilmelidir. Haritaya göre bölgede eğim 0° ile 236,96° arasında değişkenlik göstermektedir. Eğimin düştüğü yerlerde puanın artması istenmektedir. Maskeleme işlemleri yapıldıktan sonra ileri ki aşamalarda anlatılacağı üzere Ters Ağırlıklı Mesafe (IDW), Inverse Distance Weighted işlemi yapılarak katmanın tersi alınmıştır. Eğim az olması tüm tarımsal faaliyetler için pozitif katkı sağlamaktadır. Bu çalışmada da sera yer seçimi için avantaj sağlamaktadır. Çalışma bölgesi eğim haritası Şekil 5.l'de verilmektedir.



Şekil 5. Standartlaştırılmış Haritalar (a=Nem, b=Yağış, c=Sıcaklık, d=Güneşlenme şiddeti, e=Güneşlenme radyasyonu, f=Rüzgâr şiddeti, g=Yola yakınlık, h=Suya yakınlık, ı=Nüfus yoğunluğuna yakınlık, j=Toprak özelliği, k=Baki, l=Eğim).

2.3. Yöntem

Bu çalışmada, sera yer seçimi yöntemi olarak çok kriterli karar verme çalışmalarında yoğun olarak kullanılan AHP yöntemi seçilmiştir. İşlemlerde kullanılan kriterler sayısal haritalara dönüştürülmüşlerdir. Mesafe haritalama, yoğunluk haritalama, maskeleme, enterpolasyon işlemleri (Kriging), sınıflandırma gibi CBS işlemleri ile kriterler 30 m çözünürlüklü olacak şekilde sayısal haritaları oluşturulmuştur. Oluşturulan sayısal haritaların standardizasyonu gerektiği için yeniden ölçeklendirme ile piksel değerleri 0 ile 1 arasında olacak şekilde oluşturulmuştur. Çalışma ile önerilen yaklaşımın akış şeması Şekil 6'da verilmiştir.

2.3.1. Veri ön işleme

Çalışmada her bir kriter için sayısal harita üretilmiştir. Bu sayısal harita piksellerin bir araya gelmesinden meydana gelmektedir. Piksellerin değerleri 0 ile 1 değeri arasında gelecek şekilde yeniden ölçeklendirilmesi işlemi yapılmıştır. Bu işlem her bir kriter için oluşturulan sayısal haritaların standart hale getirilmesi için yapılmıştır. Piksel değerleri 1 değerine yaklaştıkça istenen yer olma niteliği artmaktadır. 0 değerine yaklaşması ise istenmeyen yer olmayı artıran bir özelliktir. AHP işlemi sonucu çıkan ağırlıklar standartlaştırılmış sayısal haritalar ile işleme tabi tutulacaklardır.



Şekil.6. Akış diyagramı.

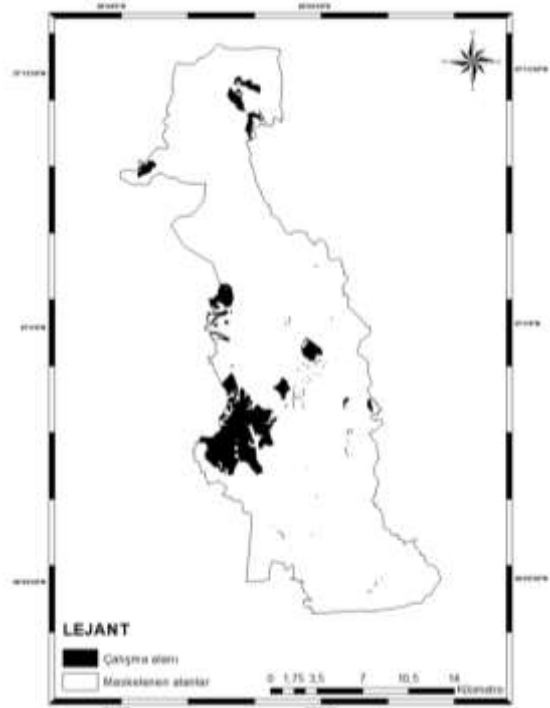
2.3.2. Maske (koruma alanları)

Maskeleme işlemi arkeolojik sit alanı, tabiat parkı, tabiat anıtı, akarsular ve tarımsal nitelikli alanları içeren çalışma alanı içerisinde bulunan kısımların çıkarılması için uygulanmıştır. Bu işlem ile yasa ve yönetmelikler ile koruma altında olan alanlar çalışmaya dahil edilmemiştir. Her bir maske katmanının maskeleme işlemi farklı yasa ve yönetmeliklerde ve farklı ölçütlerde olması nedeniyle her bir kriter için ayrı ayrı ele alınmış ve yapılmıştır. Vektör veri tipinde olan tampon poligon kriterleri 30 m çözünürlüklü raster veri tipine dönüştürülmüştür. Maskelenmesi gereken raster kriterlerin DN değeri 0, maskelenmeyen DN değeri ise 1 olacak şekilde CBS yazılımında oluşturulmuştur. Şekil 7'de yasa ve yönetmelikler ile korunan alanlar çalışmada maske olarak ele alınmıştır.

Bu alanların üretilen haritalardan çıkarılması işlemi yapılmıştır. Maske alanların açıklaması maddeler halinde verilmiştir (Resmi Gazete, 2004; Tomar, 2009; Resmi Gazete, 2014; Resmi Gazete, 2017; Resmi Gazete, 2022).

Tarımsal niteliği korunacak alanlar

Antalya Büyükşehir Belediyesi'nin 1/25000 ölçekli Çevre Düzeni Planı ile koruma altına alanlar tarımsal niteliği korunacak alanlar olarak alınmıştır.



Şekil.7. Maske haritası.

Kültür ve tabiat koruma alanları

2863 Sayılı Kültür ve Tabiat Varlıklarını Koruma Kanununda belirtilen arkeolojik sit alanı, tabiat parkı,

tabiat anıtı vb. doğal koruma alanları olarak alınmıştır.

Sulak koruma alanları

4 Nisan 2014 tarihli ve 28962 sayılı Resmî Gazete’de yayınlanan Sulak Alanların Korunması Yönetmeliğinde belirtilen alanlar sulak koruma alanları olarak alınmıştır.

2.3.3. Analytical hierarchy process (AHP)

Bu çalışmada, kriterlerin ağırlıklarının elde edilmesi için uzman görüşü etkisi nedeniyle çok kriterli karar verme çalışmalarında yaygın olarak kullanılan AHP metodu tercih edilmiştir. İkili karşılaştırma yapılarak her bir katmanın genel ağırlık değerleri bulunmuştur. Kriterler diğer kriterler ile 1 ve 9 arasında puanlama işlemine tabi tutulmuştur. AHP işlemleri için araştırmacıların ana referansı Saaty (1980) çalışmasıdır (Şahin ve Toroğlu, 2020).

Çalışmada yer seçimi için kriter olarak ele alınan tüm kriterlerin CBS yazılımı olan QGIS yazılımı kullanılarak birleştirilmiştir. Oluşturulan çalışma alanı içindeki tüm

kriterlerin maskeleme bölümünde üretilen maske katmanı ile çarpıtılmıştır. İşlem sonucu üretilen kriterler 0 ile 1 aralığında normalizasyonu yapılmıştır. İşlem sırasında dikkat edilmesi gereken husus, maske ile çıkarılan alanlardaki 0 ile 1 aralığının bozulması yeniden bir normalizasyon işlemi yapılması gerektiğidir. Bu nedenle maskeleme işlemi sonrasında yeni oluşan sayısal kriter haritaları 0 ile 1 aralığında normalize edilmiştir. AHP işlemi ile üretilen her bir kriterin ağırlığı Tablo 6’da gösterilmiştir. İşlemler sonucunda AHP matrisinin tutarlılığı kontrol işleminde tutarlılık oranı (CR) 0,067 ve tutarlılık endeksi (CI) 0,099 hesaplanmıştır. CR değerinin 0,1 değerinde düşük olması durumu AHP matris işleminin tutarlı olduğunu göstermektedir. Bu sonuç ile AHP işleminde elde edilen kriter ağırlıklarının çalışmada kullanılabilirliği sonucuna varılmıştır. CBS ve AHP işlemleri sonucunda belirlenen uygun sera alanları sayısal haritasında DN değerleri Tablo 6’da verilmiştir.

Tablo 6. AHP matris tablosu

	Nüfus	Yola Yakınlık	Eğitim	Toprak Özellikleri	Su Alanlarına Yakınlık	Yağış	Nem	Güneşlenme Şiddeti	Güneşlenme Radyasyonu	Bakı	Sıcaklık	Rüzgâr Şiddeti	Ağırlık (w)	
	A	B	C	D	E	F	G	H	I	J	K	L		
Nüfus	A	1	0,50	0,333	0,25	0,333	0,333	0,20	0,143	0,111	0,111	0,111	0,111	0,012504
Yola Yakınlık	B	2	1	0,50	0,333	0,25	0,20	0,143	0,143	0,125	0,111	0,111	0,111	0,016675
Eğitim	C	3	2	1	0,50	0,25	0,20	0,167	0,143	0,125	0,125	0,125	0,125	0,019684
Toprak Özellikleri	D	4	3	2	1	0,333	0,25	0,167	0,167	0,143	0,143	0,143	0,143	0,027119
Su Alanlarına Yakınlık	E	5	5	3	2	1	0,333	0,20	0,20	0,167	0,167	0,143	0,143	0,039570
Yağış	F	5	5	3	2	2	1	0,333	0,20	0,20	0,20	0,167	0,167	0,049463
Nem	G	5	5	3	2	2	1	1	0,50	0,333	0,333	0,20	0,20	0,059399
Güneşlenme Şiddeti	H	6	6	4	4	4	3	2	1	1	0,50	0,333	0,25	0,091544
Güneşlenme Radyasyonu	I	6	6	4	4	4	3	2	1	1	0,50	0,50	0,50	0,103023
Bakı	J	7	7	5	5	5	4	3	2	2	1	1	1	0,149545
Sıcaklık	K	8	8	6	6	6	5	4	3	3	2	1	1	0,189950
Rüzgâr Şiddeti	L	9	9	7	7	6	6	5	4	4	3	2	1	0,241524
Toplam		61	57,50	39,33	34,25	31,25	24,37	19,13	13,15	12,46	8,704	6,023	4,75	1

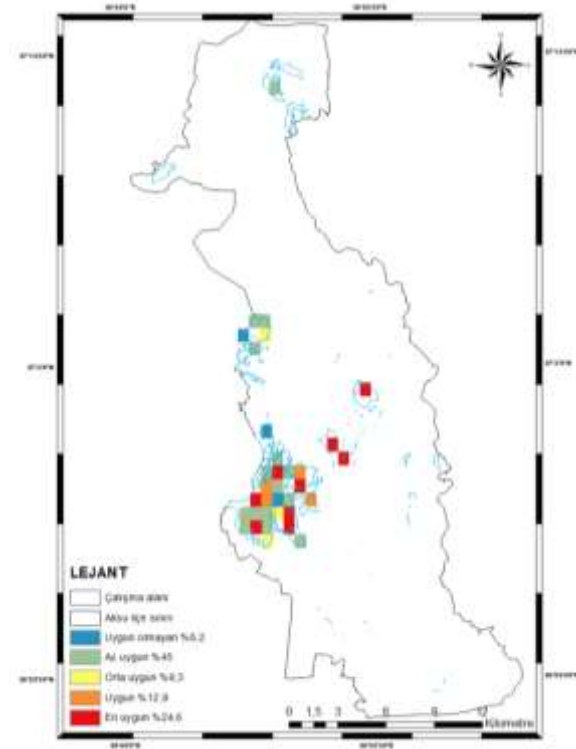
Çalışmada 12 adet kriter ele alınmıştır. Kriterler önem kriterine göre 1 ile 10 arasında bir değer verilmiştir. En düşük değer 1/9 iken en yüksek 9 puan verilmiştir. Eşit önem derecesinde değer 1’dir. Her bir katman için ağırlık değeri hesaplanmıştır. Bu hesaplamalarda RI değeri Tablo 7’den elde edilmiş ve L(max)=13,8, CI=0,099, CR=0,067 değerleri hesaplanmıştır. CR=0,067 değeri 0,1 değerinden küçük olması nedeniyle hesaplamalarımız doğru kabul edilmiştir.

QGIS yazılımındaki “Raster Calculator” aracı kullanılarak 0 ile 1 arasında normalleştirilen katmanların her biri, kendi ağırlık değeri ile çarpılarak toplanları alınmıştır (Denklem 1). Bu işlem ile uygunluk haritası elde edilmiştir (Şekil 8).

$$\begin{aligned}
 & \text{nüfus} * 0,012504 + \text{yola yakınlık} * 0,016675 + \text{eğitim} \\
 & * 0,019684 + \text{toprak özellikleri} * 0,027119 + \text{suya} \\
 & \text{yakınlık} * 0,039570 + \text{yağış} * 0,049463 + \text{nem} \\
 & * 0,059399 + \text{güneş şiddeti} * 0,091544 + \text{güneş} \\
 & \text{radyasyonu} * 0,103023 + \text{bakı} * 0,149545 + \text{sıcaklık} \\
 & * 0,189950 + \text{rüzgâr şiddeti} * 0,241524
 \end{aligned}
 \tag{1}$$

Tablo 7. Tesadüflük göstergesi

n	RI
1	0
2	0
3	0,58
4	0,9
5	1,12
6	1,24
7	1,32
8	1,41
9	1,45
10	1,49
11	1,51
12	1,48
13	1,56
14	1,57
15	1,59



Şekil 8. Analitik Hiyerarşi Süreci (AHP) sonucu uygunluk haritası.

3. Bulgular ve Tartışma

Ağırlıklandırma 0 ile 1 arasında yapılmıştır. Değerlerin 1'e yaklaşması önemli iken 0'a yaklaşması ise önemsiz olduğunu ifade etmektedir. Bu işlem ile Şekil 8'de verilen haritada renklendiren lejantdaki uygunluk durumları elde edilmiştir. AHP matris işlemi sonucunda elde edilen kriter sonucunda nüfus kriteri 0,013 değeri ile en düşük ağırlıktaki kriter iken rüzgar şiddeti 0,242 değeri ile en yüksek ağırlığa sahip kriter olarak tespit edilmiştir.

Tablo 8'e göre sonuç haritasında uygunluk sınıflarının tamamının kapladığı alan 1671,28 ha'dır. Kırmızı renk ile gösterilen alanlar sera yeri seçimine en uygun alanlar olup 411,71 ha alan ile sonuç haritasının %24,60'sını

kaplamaktadır. Turuncu ile gösterilen alanlar 216,42 ha ve %12,90'luk bir alan ile sera kurulumuna "uygun" alanları temsil etmektedir. Sera kurulumuna "orta uygun" alanlar sarı renk ile gösterilmektedir. Orta uygun alanlar 155,04 ha alan ile sonuç haritasının %9,3'ünü kaplamaktadır. Yeşil renkle ifade edilen alanlar sonuç haritasının en geniş alanını kaplamaktadır ve 751,61 ha alan büyüklüğünde olup toplam alanın %45'ini oluşturmaktadır. Bu alanlar sera kurulumu için "az uygun" sınıfındadır. Son sınıf olan "uygun olmayan" mavi alanlar ise sonuç haritasının %8,20'sini oluşturmakta ve 136,51 ha alan miktarına sahiptir.

Tablo 8. Sera yer uygunluk tablosu

Uygunluk Durumu	Alan (ha)	Oran (%)
Uygun olmayan	136.51	8.17
Az uygun	751.61	44.97
Orta uygun	155.04	9.28
Uygun	216.42	12.95
En uygun	411.71	24.63
Toplam	1671.28	100.00

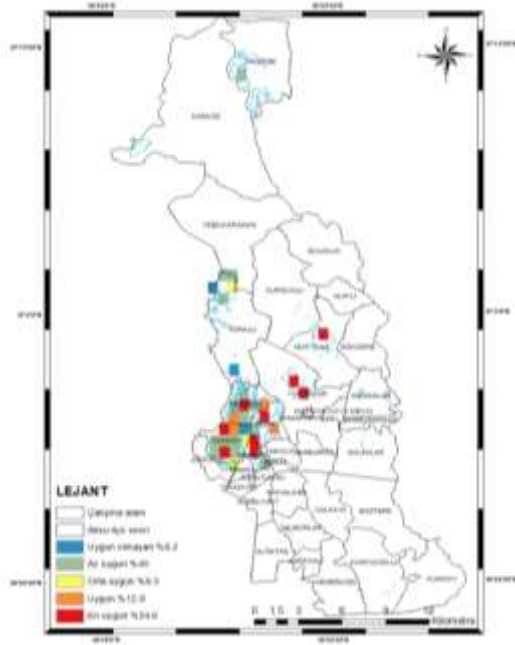
Çalışma alanı genel olarak Kırmızı Akdeniz toprakları ve Alüvyal topraklardan oluşmakta olup, Aksu ilçesinin kuzeydoğusunda kalan kısmını Kahverengi Orman toprakları, kuzeybatısında kalan kısmını ise Kırmızı Akdeniz toprakları oluşturmaktadır. Çalışma alanının kuzeydoğusunda kalan bölge AHP ile elde edilen sonuç haritasına göre uygun olmayan alanlar sınıfındadır. Kuzeybatı kriterlerin uygulanması sonucu uygun bulunmamış ve değerlendirme dışı bırakılmıştır.

3.1. Mahalle Ölçeğinde Değerlendirme

Mahalle ölçeğinde, çalışma alanı içerisinde sera kurulumuna en uygun alanlar Yurtpınar, Murtuna, Fettahlı, Fatih, Çamköy ve Hacılar Mahalleleri sınırları içerisinde kalmaktadır. Uygun olarak belirlenen alanlar Fettahlı, Çamköy ve Fatih Mahallesi sınırları içerisinde kalmaktadır. Orta uygun alanlar Pınarlı, Hacılar, Çamköy, Topallı ve Yeşilkaraman Mahalleleri içerisinde yer almaktadır. Az uygun alanlar Kayadibi, Yeşilkaraman, Topallı, Fettahlı, Fatih, Çamköy, Hacılar, Konak ve Soğucaksu Mahalleleri içerisinde yer almaktadır. Uygun olmayan alanlar ise Topallı, Fettahlı ve Çamköy Mahalleleri içerisinde yer almaktadır (Şekil 9). Bunun dışında çalışma alanı içerisinde AHP sonucunda veri üretilmeyen noktalarda bulunmaktadır. Bu alanlar tüm kriterler birlikte değerlendirildiğinde sera yeri seçimi için değerlendirme dışı kalan alanlardır.

4. Sonuç

Nüfusun artmasıyla besin ihtiyacı da artmakta bu da zamanla mevcut tarımsal faaliyetlerin yetersiz kalabileceği ihtimalini artırmaktadır. Sera tarımı her mevsim ürün alabilmeyi mümkün kılmaktadır (Ayrancı 2011). Özellikle mevsim bitkilerinin yıl içerisinde üretiminin devam ettirilmesine duyulan gereksinim, seracılık faaliyetlerinin önemini net olarak ortaya koymaktadır.



Şekil 9. Mahalle altlıklı Analitik Hiyerarşi Süreci (AHP) sonucu uygunluk haritası.

Mevsimsel üretim olmasının yanı sıra yıl boyu yapılan üretim, mevcut istihdam olanaklarını artırarak düzenli iş imkânı sağlamaktadır. Üretimde sağlanan süreklilik sayesinde ürünlerin pazarda uygun fiyata yer bulması sağlanmış olur. Nitekim sera alanlarının coğrafi ve beşerî unsurlar dikkate alınarak belirlenmesi birim alandan alınacak verimi maksimum değere çıkaracaktır.

İklim şartları ve topografik yapı arazi seçiminde önemli rol oynamaktadır. Çalışma için belirlenen kriterler yollara yakınlık, suya yakınlık, nüfus yoğunluğuna yakınlık, toprak özellikleri, eğim, nem, yağış, sıcaklık, güneşlenme şiddeti, güneşlenme radyasyonu ve rüzgâr şiddeti olarak belirlenmiştir. Bu kriterlerin yanı sıra seralarda ısınma kaynaklı enerji önemli bir gider kalemini oluşturmaktadır (Arcangeletti, 2014).

Sera alanı yer seçim çalışmasında birden çok kriterin ele alınması zorunluluğu bu tip çalışmaları zorlu hale getirmektedir. Bu çalışmada çok kriterli karar metodunda on iki adet kriter kullanılarak yer seçimi yapılmıştır. Çok kriterli metodlar içerisinde uzman görüşü etkisi ve yaygın kullanımı nedeniyle AHP seçilmiştir. Kriterler Uzaktan Algılama ve CBS araçları kullanılarak AHP işlemine hazır hale getirilmiştir.

Bu çalışma, örtü altı işletmeler için yapılmış olsa da çalışma kapsamı genişletilerek rahatlıkla farklı alanlarda uygulanabilir. Yetiştirilen ürün tipine, yetiştiği coğrafyaya göre belirlenecek benzer kriterler ile farklı bölgelerde kullanılabilir. Güneşlenme süresi, erozyon riski, arazi kullanım durumu, toprak tekstürü ve derinliği gibi katmanlar eklenerek çalışma kapsamı genişletilebilir. Çalışmada kriter olarak toprak özelliğinin kullanım ve bunun kullanılması sırasında hassas ve uzmanlar desteğinin alınması hem doğruluğu artırıcı hem de çalışmayı özgünleştirici bir özellik etki yaratmıştır.

Yer seçimi çalışmalarında yer seçim sonuçlarının alınması ve bunların nihai haritada gösterilmesi genel bir uygulama biçimi olduğu literatür çalışmalarında tespit edilmiştir. Bu çalışmada genel uygulamanın aksine sonuçlar elde edilmiş ve idari sınırlar olan mahalle sınırları içindeki uygun ve uygun olma oranları tespit edilmiştir. Yer seçimi sonrasında mahalle bazında bulgular elde edilmesi ile yerel halkın bilgilendirilmesi sağlanmıştır. Açıklamalar ve öneriler ışığında bu çalışmanın sera yeri seçiminde karar vericilere yol gösterici olacağı düşünülmektedir.

Katkı Oranı Beyanı

Yazar(lar)ın katkı yüzdesi aşağıda verilmiştir. Tüm yazarlar makaleyi incelemiş ve onaylamıştır.

	E.B.	Ö.K.	E.A.
K	30	40	30
T		50	50
Y		100	
VTI			100
VAY	40	30	30
KT	40	40	20
YZ	30	50	20
KI	20	40	40
GR	20	60	20

K= kavram, T= tasarım, Y= yönetim, VTI= veri toplama ve/veya işleme, VAY= veri analizi ve/veya yorumlama, KT= kaynak tarama, YZ= Yazım, KI= kritik inceleme, GR= gönderim ve revizyon.

Çatışma Beyanı

Yazarlar bu çalışmada hiçbir çıkar ilişkisi olmadığını beyan etmektedirler.

Etik Onay Beyanı

Bu araştırmada hayvanlar ve insanlar üzerinde herhangi bir çalışma yapılmadığı için etik kurul onayı alınmamıştır.

Kaynaklar

- Akıncı H, Özalp AY, Turgut B. 2013. Agricultural land use suitability analysis using GIS and AHP technique. *Comput Electr Agri*, 97: 71-82.
- Alkan Z. 1977. Sera planlama ve inşaa tekniği. Ege Üniversitesi Mühendislik Bilimleri Fakültesi Denizli Ön Lisans Yüksek Okulu, Denizli, Türkiye, pp: 205.
- Arcangeletti E. 2014. Mathematical modeling and GIS applications for greenhouse energy planning in Italy. *Appl Math Sci*, 8(132): 6651-6664.
- Ayrancı Y. 2011. Muğla yöresinde seraların iklimsel ihtiyaçlarının belirlenmesi. *Selçuk Tarım Gıda Bil Derg*, 25(1): 96-105.
- Balaban A, Şen E. 1988. Tarımsal yapılar. Ankara Üniversitesi Ziraat Fakültesi Yayınları, Ankara, Türkiye, pp: 845.
- Cemek B. 2005. Determination of indoor climate requirements of greenhouses in Samsun provinces with-GIS Assisted. *J Fac Agri*, 36(2): 179-186
- Delibaş L, Bağdatlı MC, Danışman A. 2015. Topoğrafya ve bazı toprak özelliklerinin coğrafi bilgi sistemleri (CBS) ortamında analiz edilerek ceviz yetiştiriciliğine uygun alanların

- belirlenmesi: Tekirdağ ili merkez köyleri örneği. *Gümüşhane Üniv Fen Bil Enst Derg*, 5(1): 50-59.
- Demir M, Yıldız ND, Bulut Y, Yılmaz S, Özer S. 2011. Alan kullanım planlamasında potansiyel tarım alanlarının ölçütlerinin coğrafi bilgi sistemleri (CBS) yöntemi ile belirlenmesi (Ispir örneği. *J Inst Sci Technol*, 1(3): 77-86.
- Doğan Ü. 2010. Kuruluş yeri seçimi. URL: http://kisi.deu.edu.tr//uzeyme.dogan/k_ulusyiserisecimi (erişim tarihi: 21 Ekim 2022).
- DSİ. 2022. DSİ Genel Müdürlüğü, Antalya, Türkiye.
- Dursun H, Dizdar M Y, Kırıştıoğlu Ş, Özcan İ, Hamurkar Y. 2008. Toprak ve arazi sınıflaması standartları teknik talimatı ve ilgili mevzuat. Tarım ve Köyişleri Bakanlığı Tarımsal Üretim ve Geliştirme Genel Müdürlüğü Yayını, Ankara, Türkiye, pp: 192.
- Eken M, Ceylan A, Taştekin AT, Şahin H, Şensoy S. 2008. *Klimatoloji II*. DMİ Yayınları, Ankara, Türkiye, pp: 184.
- Erdoğan Ö, Çabuk A, Memlük Y, Perçin H. 2015. Ekolojik alan kullanım kararlarına uygun tarım alanlarının AHP yöntemi kullanılarak Kütahya kenti örneğinde irdelenmesi. *Harita Teknoloji Derg*, 7(2): 1-16.
- Filiz M. 2001. Sera inşası ve iklimi. *Üniversite Kitapları Akademi Kitabevi*, İzmir, Türkiye, pp: 266.
- Gögsü S, Hastaoğlu KÖ. 2019. Ters mesafe ağırlıklı enterpolasyon yönteminde güç fonksiyonu etkisinin incelenmesi. *TMMOB Harita ve Kadastro Mühendisleri Odası*, 17. Türkiye Harita Bilimsel ve Teknik Kurultayı, Nisan 25-27, Ankara, Türkiye, pp: 1.
- Jo A, Ryu J, Chung H, Choi Y, Jeon S. 2018. Applicability of various interpolation approaches for high resolution spatial mapping of climate data in Korea. *J Environ Impact Asses*, 27(5): 447-474.
- Kendirli B. 2015. Sera ısıtma gereksiniminin tahmininde farklı yaklaşımların incelenmesi. *Ziraat Fak Derg*, 10(2): 125-134.
- Kouchaksaraei RH, Zolfani SH, Golabchi M. 2015. Glasshouse locating based on swara-copras approach. *Int J Strat Property Manag*, 19(2): 111-122.
- Marucci A, Cappuccini A, Petroselli A, Arcangeletti E. 2014. Mathematical modeling and GIS applications for greenhouse energy planning in Italy. *Appl Math Sci*, 8(132): 6651-6664.
- MEGEP. 2007. Bahçecilik, sera yapım tekniği. Millî Eğitim Bakanlığı, Mesleki Eğitim ve Öğretim Sisteminin Güçlendirilmesi Projesi, Ankara, Türkiye, pp: 43.
- Mercan Y. 2019. Aydın ili uygun örtü altı işletme yerlerinin coğrafi bilgi sistemi destekli çok ölçütlü karar analizi ile belirlenmesi. *Doktora Tezi*, Aydın Adnan Menderes Üniversitesi, Aydın, Türkiye, pp: 133.
- MGM. 2021. Meteorolojik veriler. Antalya Meteoroloji Müdürlüğü, URL: <https://mevbis.mgm.gov.tr> (erişim tarihi: 5 Mayıs 2021).
- OSM. 2022. URL: <https://www.openstreetmap.org/> (erişim tarihi: 19 Ağustos 2021).
- Öz H. 2017 Türkiye’de örtü altı yetiştiricilik potansiyelinin solar radyasyon ve güneşlenme süresi parametrelerine göre incelenmesi. *Süleyman Demirel Üniv Fen Bil Enst Derg*, 21(2): 509-513.
- Öztekin D, Susam T, Gerçekçioğlu R. 2008. Tokat Kazova arazilerinin şeftali yetiştiriciliğine uygunluklarının coğrafi bilgi sistemi yardımıyla belirlenmesi. *Tekirdağ Zir Fak Derg*, 5(2): 215-225.
- Paul M, Negahban-Azar M, Shirmohammadi A, Montas H. 2020. Assessment of agricultural land suitability for irrigation with reclaimed water using geospatial multi-criteria decision analysis. *Agri Water Manag*, 231: 105987.
- Resmî Gazete. 2004. Su kirliliği kontrolü yönetmeliği. Tarih: 31.12.2004, Sayı: 25687. URL: <https://www.mevzuat.gov.tr/mevzuat?MevzuatNo=7221&MevzuatTur=7&MevzuatTertip=5> (erişim tarihi: 22 Şubat 2022).
- Resmî Gazete. 2014. Sulak alanların korunması yönetmeliği. Tarih: 04.04.2014, Sayı:28962. URL: <https://www.resmigazete.gov.tr/eskiler/2014/04/20140404-11.htm> (erişim tarihi: 11 Eylül 2022).
- Resmî Gazete. 2017. İçme-kullanma suyu havzalarının korunmasına dair yönetmelik. Tarih: 28.10.2017, Sayı:30224. URL: <https://www.resmigazete.gov.tr/eskiler/2020/03/20200310-1.htm> (erişim tarihi: 18 Şubat 2021).
- Resmî Gazete. 2022. Korunan Alanların tespit, tescil ve onayına ilişkin usul ve esaslara dair yönetmelik. Tarih: 5.03.2022, Sayı: 31769. URL: <https://www.resmigazete.gov.tr/eskiler/2022/03/20220305-1.htm> (erişim tarihi: 22 Mayıs 2022).
- Rezaeiniya N, Ghadikolaei AS, Mehri-Tekme H, Rezaeiniya H. 2014. Fuzzy ANP approach for new application: Greenhouse location selection; a case in Iran. *J Math Comput Sci*, 8(1): 1-20.
- Rezaeiniya N, Zolfani SH, Zavadskas EK. 2012. Greenhouse locating based on anp-copras-g methods—an empirical study based on Iran. *Int J Strat Property Manag*, 16(2): 188-200.
- Saaty TL. 1980 *The analytic hierarchy process*. McGraw-Hill International, New York, US, pp: 287.
- Saltuk B, Artun O. 2018. Multi-criteria decision system for greenhouse site selection in lower euphrates basin using geographic information systems (GIS). *African J Agri Res*, 13(47): 2716-2724.
- Sarı M, Sonmez N, Altunbaş S. 2009. Aksu araştırma ve uygulama istasyonu topraklarının morfolojik, fiziksel ve kimyasal özellikleri. *Akdeniz Üniv Zir Fak Derg*, 22(2): 157-168.
- Selim S, Koc-San D, Selim C, San BT. 2018. Site selection for avocado cultivation Using GIS and multi-criteria decision analyses: Case study of Antalya, Turkey. *Comput Elect Agri*, 154: 450-459.
- Şahin M, Toroğlu E. 2020. Analitik hiyerarşi prosesi (AHP) kullanılarak Pınarbaşı ilçesi (Kayseri) arazilerinin tarımsal uygunluk derecelerinin belirlenmesi. *Türk Coğrafya Derg*, (75): 119-130.
- Taylan ED, Damçayırı D. 2016. Isparta bölgesi yağış değerlerinin IDW ve kriging enterpolasyon yöntemleri ile tahmini. *Teknik Dergi*, 27(3): 7551-7559.
- Tomar A. 2009. Toprak ve su kirliliği ve su havzalarının korunması. *TMMOB İzmir Kent Sempozyumu*, 8-10 Ocak, İzmir, Türkiye, pp: 333-345.
- Topçu T, Kocaman İ. 2019. Yalova ve Kocaeli illerindeki bitkisel üretim yapılarında ortaya çıkan yapısal başarısızlıklar üzerine bir araştırma. *Gaziosmanpaşa Bil Araş Derg*, 8(2): 66-75.
- TUİK. 2022. Türkiye İstatistik Kurumu. URL: <https://data.tuik.gov.tr/Kategori/> (erişim tarihi: 29 Eylül 2021).
- Ustaoglu E, Sisman S, Aydınoglu AC. 2021. Determining agricultural suitable land in peri-urban geography using GIS and multi criteria decision analysis (MCDA) techniques. *Ecol Model*, 455: 109610.
- Von Zabeltitz C. 2010. Integrated greenhouse systems for mild climates: Climate conditions, design, construction, maintenance, climate control. *Springer Science & Business Media*, new York, US, pp: 267.
- Yüksel A, Yüksel E. 2012. Sera yapım tekniği. *Hasad Yayıncılık Ltd. Şti*. İstanbul, Türkiye, pp: 272.
- Yüksel Türkoğlu EY, Yüksel AN. 2018. Use of solar panels in greenhouse soil disinfection. *Int Advan Res Eng J*, 2(2): 195-199.



EFFECT OF FILLING RATIO-PATTERN PARAMETERS ON MECHANICAL PROPERTIES OF PLA FILAMENTS USED IN 3D PRINTING

Fuat KARTAL^{1*}, Arslan KAPTAN²

¹Kastamonu University, Faculty of Engineering and Architecture, Department of Mechanical Engineering, 37150, Kastamonu, Türkiye

²Sivas Cumhuriyet University, Sivas Technical Sciences Vocational School, Department of Motor Vehicles and Transportation Technologies, 58140, Sivas, Türkiye


Abstract: This research primarily focuses on the mechanical properties of specimens produced using Polylactic Acid (PLA) through the Fused Deposition Modeling (FDM) technique, a method of 3D printing. Within the scope of this study, specimens were fabricated using various fill percentages and different infill patterns. The simultaneous effect of variable parameters on mechanical properties is a challenging task, and it is aimed to rank the importance of the parameters, model the process, and finally validate the models using tensile and bending experiments. The results show that samples with a Concentric pattern and 95% fill rate exhibited the highest tensile strength with an average of 48.67 MPa. In contrast, the Triangle pattern with 20% infill ratio showed the lowest tensile strength with an average of 14.15 MPa. When evaluating flexural strength values, the Concentric design with a 95% fill ratio stood out once again, recording an average peak value of 79.94 MPa. Meanwhile, the Honeycomb pattern at 20% infill ratio exhibited the lowest strength value measured with an average of 23.3 MPa. Scanning Electron Microscope images taken according to infill rates confirm each other with the voids formed and mechanical performance outputs. These findings underscore that the mechanical attributes of PLA specimens produced using 3D printing technology can significantly vary based on the chosen fill rate and pattern.

Keywords: Polylactic acid, Fused deposition modeling, 3D printer, Fill ratio, Fill pattern, ASTM D638

*Corresponding author: Kastamonu University, Faculty of Engineering and Architecture, Department of Mechanical Engineering, 37150, Kastamonu, Türkiye

E mail: fkartal@kastamonu.edu.tr (F. KARTAL)

Fuat KARTAL  <https://orcid.org/0000-0002-2567-9705>

Arslan KAPTAN  <https://orcid.org/0000-0002-2431-9329>

Received: November 09, 2023

Accepted: January 22, 2024

Published: March 15, 2024

Cite as: Kartal F, Kaptan A. 2024. Effect of filling ratio-pattern parameters on mechanical properties of PLA filaments used in 3D printing. BSJ Eng Sci, 7(2): 196-202.

1. Introduction

Fused deposition modeling (FDM) three dimensional (3D) printing is a type of additive manufacturing (AM) process that uses thermoplastic filaments to create objects layer by layer. FDM is one of the most widely used and affordable 3D printing technologies, suitable for rapid prototyping and various applications. FDM can print parts with complex geometries and internal cavities, thanks to the use of soluble support materials that can be dissolved after printing. FDM can print parts with different colors and materials, depending on the capabilities of the printer and the extruder. FDM can print parts with different levels of resolution and accuracy, depending on the nozzle size, layer height, infill density, and other parameters. The mechanical properties of PLA filaments in 3D printing are significantly influenced by the filling ratio and filling pattern parameters.

The filling ratio, often termed as infill percentage or density, denotes the material volume inside a 3D printed component. A higher filling ratio typically makes parts more robust and rigid, but it also lengthens the printing duration and uses more material.

On the other hand, the filling pattern, sometimes referred to as the infill or raster pattern, describes the internal geometry of the printed item. It plays a pivotal role in determining the part's strength, stiffness, and manner of failure. Various patterns like Concentric, Triangular, Honeycomb, Hilbert curve, and others, each offer distinct mechanical characteristics. For instance, parts printed with a Concentric pattern tend to have superior tensile strength when the pattern aligns with the stress direction, whereas triangular patterns excel in strength for lighter structures. Conversely, the Honeycomb pattern can reduce strength due to its spacious voids, but Hilbert curve patterns can enhance strength at high filling ratios. However, it's essential to remember that these effects are also modulated by other variables such as the part's orientation during printing, the thickness of each layer, nozzle dimensions, extrusion temperature, printing pace, and cooling speed, all of which impact the final quality and interplay between the printed lines and layers.

In their study, Dudescu and Racz (2017) examined the effects of different raster angles (0°, 30°, 45°, 90°), filling rates (20% to 100%) and patterns on the mechanical properties of 3D printed parts using ABS material. In



their study, Wittbrodt and Pearce (2015) evaluated the mechanical performances obtained from 3D printing of PLA materials of different colors at different processing temperatures. Özsoy et al. (2022) improved the temperature effect problem on the parts by detecting the correct coolant type at a rate of 95% through image processing and machine learning, using the FDM method to produce parts on a 3D printer. Özsoy and Aksoy (2022) created a user guide on the mechanical properties of 3D printed parts using image processing and real-time big data analysis. Benamira et al. (2023) investigated the effect of printing parameters on the mechanical and damage properties of 3D printed PLA. Kechagias et al. (2023) evaluated the process in which the mechanical response of PLA in 3D printing with the FDM method depends on many parameters. Kartal and Kaptan (2023) examined the effect of 3D printer nozzle diameter on the mechanical properties of PLA printed parts. Hamat et al. (2023) evaluated the effects of filament production parameters (extrusion temperature and rotation speed) on tensile strength. Bian et al. (2023) discussed the effect of the morphology and feed rate of FDM printed PLA on the mechanical properties at the time of exit from the nozzle during the hot extrusion process. Pandzic et al. (2019) focused on the effects of 3D printed samples with PLA material on the tensile strength depending on the filler type and ratio, while Lalegani Dezaki et al. (2021) focused on the effects of the filler pattern on surface roughness and tensile strength. Wu et al. (2015) comparatively examined the mechanical properties of layer thickness and raster angle in 3D printed materials. Moradi et al. (2021) have conducted experimental research on the mechanical characterization of 3D printed PLA produced by FDM.

In literature research, there does not appear to be a study that comprehensively examines the mechanical properties of parts printed with PLA materials according to 5 different filling percentages and 4 different filling patterns. This study aims to fill this knowledge gap by delving deep into the combined effect of fill rate and pattern on the mechanical behavior of PLA. Within this paper, detailed insights will be provided on the mechanical properties of PLA specimens produced using 3D printing techniques, with various fill rates (20%, 40%, 60%, 80%, and 95%) and infill patterns (Triangle,

Rectilinear, Honeycomb, and Concentric). Specifically, the tensile and flexural strength values will be thoroughly examined. The results are discussed to elucidate why the selection of printing parameters is so critical in determining the mechanical performance of the printed objects.

2. Materials and Methods

The filament properties and printing parameters used in this study are seen in Table 1. These parameters are the most commonly preferred values for manufacturing 3D printed parts with PLA material. Specimens were prepared taking into account various fill rates (20%, 40%, 60%, 80%, and 95%) and infill patterns (Triangle, Rectilinear, Honeycomb, and Concentric). A minimum of 5 samples were printed for each combination. Figure 1.a shows the sample printing on the Ender 3 S1 Pro printer, and Figure 1.b shows the tensile test of printed sample. Figure 1.c shows the broken samples at the end of the tensile test. For tensile tests, specimens were produced in accordance with ASTM D638 type IV standard dimensions, while for the flexural tests, they adhered to ASTM D790 standard sizes. Tensile tests were carried out using a universal testing machine with a capacity of 5 kN (Figure 1.b). Specimens were stretched at a constant rate of 5 mm/min. Flexural tests were conducted on the same testing machine under a three-point bending arrangement, where the loading rate was also set at 5 mm/min (Figure 1.d). All acquired data were analyzed using appropriate software to determine statistical parameters such as standard deviation and variance. Additionally, various graphs were generated to discern the impact of fill rate and pattern on mechanical properties.

Table 1. Specification of PLA filament and printing parameters

Specification	Units	Value
Density	g/cm ³	1.24
Melting temperature	°C	190-220
Bed temperature	°C	60
Nozzle temperature	°C	220
Printing speed	mm/s	60

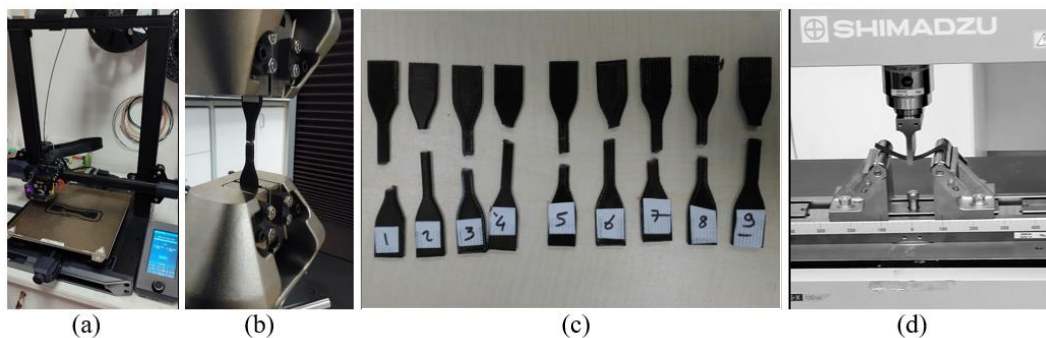


Figure 1. (a) PLA material samples printed using Ender 3 S1 pro printer (b) Tensile test (c) Broken tensile specimens (d) Flexural test.

3. Results

3.1. Tensile Characteristics

The tensile strength of various samples with different infill ratios and patterns was meticulously studied. The values given in the study are the average values obtained from 5 samples. The results for the 20% infill ratio indicate significant differences based on the pattern used. For instance, the Concentric pattern demonstrated the highest tensile strength at 19.88 MPa. In contrast, the Triangle pattern exhibited the lowest tensile strength, registering at 14.15 MPa. This can be attributed to the fact that the Triangle pattern contains more gaps compared to the Concentric pattern, which tends to be fuller and parallel to the fracture direction. Furthermore, the Rectilinear, Honeycomb, and Concentric patterns all showed a noticeable increase in tensile strength as the infill ratio increased, with the Concentric pattern achieving the highest tensile strength of 48.67 MPa at a 95% infill ratio. In comparing these findings with those of past studies, the trends identified by Pandzic et al. (2019) and Lalegani Dezaki et al. (2021) were somewhat consistent. They found that the Concentric pattern generally exhibited higher tensile and yield strengths, especially for PLA filaments with a 90% infill ratio. It should also be noted that the flexural strength results showcased the potency of each pattern at various infill ratios, highlighting the robustness of materials like the Concentric pattern, which reached a peak flexural strength of 79.94 MPa at a 95% infill ratio. In conclusion, the choice of infill pattern plays a pivotal role in determining both the tensile and flexural strengths of 3D printed objects, with the Concentric pattern consistently outperforming its counterparts at higher infill ratios.

According to Table 2 and Figure 2, the concentric pattern consistently showcases superior tensile strength, especially as infill ratios escalate, achieving its zenith at 48.67 MPa at 95% infill. This implies that for heightened tensile demands, the concentric pattern coupled with higher infill ratios might be the optimal choice. At the outset, with a 20% infill, the Triangle and Honeycomb patterns exhibit nearly identical tensile strengths, hovering around 14 MPa. However, as the infill ratio expands, their trajectories diverge. By 95% infill, the Honeycomb pattern registers a tensile strength of 36.63 MPa, outpacing the triangle pattern's 25.89 MPa. Notably, the Rectilinear pattern depicts a uniform ascent in tensile strength corresponding to rising infill percentages, denoting a predictable performance spectrum across diverse infill scales. To sum up, Table 2 underscores that both the choice of infill pattern and its proportion wield a substantial influence on the tensile strength of PLA samples, highlighting the necessity of judicious selection in tailoring 3D printed components to meet specific mechanical benchmarks. Additionally, the Rectilinear pattern steadily augments in tensile strength with each increment in infill percentage, indicating its stable and predictable response across varied infill gradations. Conclusively, the choice of infill design and proportion profoundly impacts the tensile strength of PLA specimens. A nuanced understanding of these nuances is imperative for customizing 3D printed items to distinct mechanical prerequisites, prompting an avenue for future research to unpack the foundational reasons behind these performance metrics and their practical connotations.

Table 2. The tensile strength of various samples with different infill ratios and patterns

Pattern	Tensile strength (MPa) according to infill ratio				
	20%	40%	60%	80%	95%
Triangle	14.15	17.32	19.24	23.35	25.89
Rectilinear	18.63	23.43	26.56	34.18	38.15
Honeycomb	14.68	22.63	26.25	30.84	36.63
Concentric	19.88	28.26	36.47	40.32	48.67

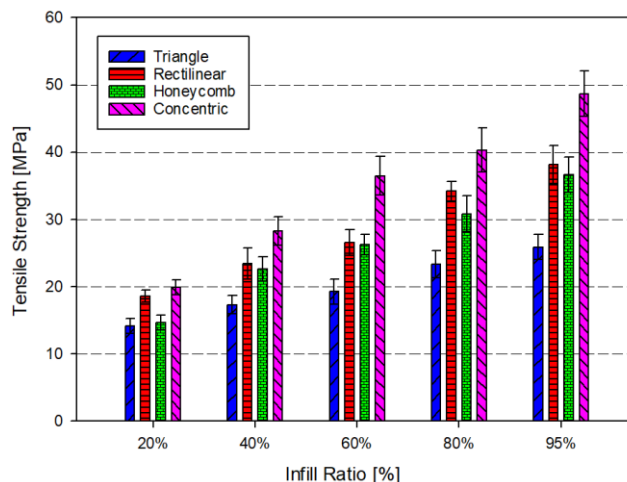


Figure 2. The tensile strength of various samples with different infill ratios and patterns.

3.2. Flexural Characteristics

The flexural test was conducted to further assess the mechanical properties of the samples, shedding light on their resistance to bending (Figure 1.d). Specimens with varying infill ratios and patterns were fixed at their ends, and a specific load was applied from their midpoints, providing insights into their load-displacement, flexural strength, and flexural strains. Analysis of the fractured sections clearly indicated that both the infill ratio and pattern significantly influence the mechanical performance of the samples. For the 20% infill ratio, the results, illustrated in Figure 3, align with observations from the tensile test. The Concentric pattern demonstrated superior resistance to flexural loads, outpacing other patterns in terms of its load-bearing capacity. Among the patterns studied, Concentric, Rectilinear, and Triangle achieved the highest flexural strength values, with the Concentric pattern being particularly outstanding, reaching 31.03 MPa at the 20% infill ratio. Conversely, even though the 3D Honeycomb pattern showed commendable resistance against tensile forces, it lagged in flexural strength, especially when compared to the other patterns. The Honeycomb's strength started at 23.3 MPa for the 20% infill ratio but improved considerably as the infill ratio increased. Notably, the Concentric pattern exhibited the highest flexural modulus, further emphasizing its exceptional mechanical properties. In summary, the choice of infill pattern and ratio is crucial in determining the flexural

strengths of 3D printed objects, with the Concentric pattern consistently proving to be the most formidable across multiple infill ratios. According to Table 3 and Figure 3, which delineates the flexural strength of various patterns at different infill percentages. Concentric pattern's dominance, the concentric pattern indisputably leads in flexural strength, especially as the infill percentage grows. Its strength peaks at a significant 79.94 MPa at 95% infill. This makes it evident that the concentric pattern, when paired with higher infill percentages, is superior in terms of flexural strength, potentially making it ideal for applications demanding higher bending resistance. Both the Triangle and Rectilinear patterns show an increase in flexural strength as infill percentage rises. However, the Rectilinear pattern significantly outperforms the Triangle pattern, especially at higher infill percentages, reaching 62.49 MPa at 95% infill compared to the Triangle's 39.22 MPa. Honeycomb's plateau, starting at a modest 23.3 MPa at 20% infill, the Honeycomb pattern sees a sharp increase as infill rises, but interestingly plateaus around the 51 MPa mark from 60% infill onwards. In conclusion, the infill pattern and its percentage crucially determine the flexural strength of PLA samples. Table 3 elucidates the need for careful consideration of these parameters when seeking to optimize the bending resistance of 3D printed materials for particular applications. Future research can explore the structural peculiarities of these patterns that contribute to such performance outcomes.

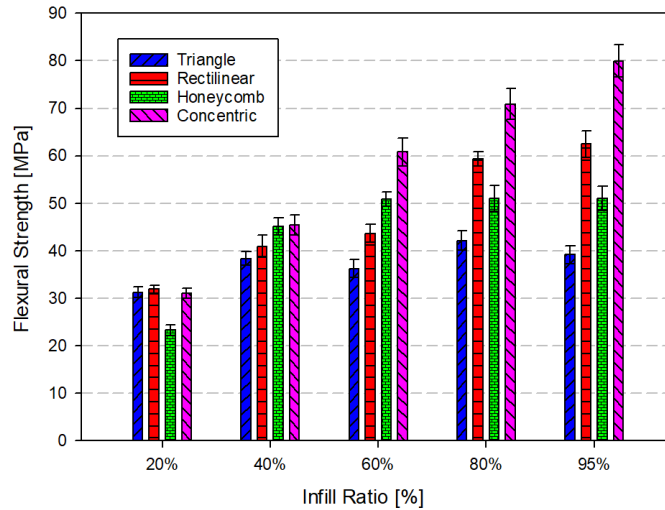


Figure 3. The flexural test properties of the samples.

Table 3. The flexural test properties of the samples

Pattern	Flexural strength (MPa) according to infill ratio				
	20%	40%	60%	80%	95%
Triangle	31.29	38.37	36.27	42.16	39.22
Rectilinear	31.88	40.97	43.68	59.29	62.49
Honeycomb	23.30	45.11	50.94	51.08	51.01
Concentric	31.03	45.50	60.79	70.90	79.94

3.3. Shore D Hardness

Shore D hardness values of the samples were measured with the PCE-D Shore D Durometer device as seen in Figure 4.a. The obtained hardness values are seen in Figure 4.b. Accordingly, the Triangular infill pattern offers hardness values ranging from approximately 85 to 105 Shore D for infill ratios from 20% to 95%, respectively. This reflects the Triangle pattern's tendency to provide high strength and impact resistance. It was observed that the hardness increased with the increase in the filling ratio. The rectilinear fill pattern offers good stability for general use. In this study, an increase from 84 Shore D at 20% infill to 104 Shore D at 95% infill was estimated. This is consistent with the hardness values of PLA reported in the literature, ranging from 77 to 81 Shore D (Mayén et al, 2022). Honeycomb filling pattern balances lightness and strength. In this study, an increase from 83 Shore D at 20% filling rate to 103 Shore D at 95% filling rate was achieved. The flexibility of the Honeycomb structure may result in lower hardness values. The Concentric filling pattern offers hardness values ranging from 82 Shore D at 20% filling rate to 102 Shore D at 95% filling rate. The flexible nature of this pattern may lead to lower hardness values. In the literature, it has been observed that the hardness generally increases as the filler density of PLA increases.

In their study, Şirin et al. (2023) based their studies on the values determined as 93.9, 99.9 and 102.6 Shore D for 30%, 50% and 70% filling densities, respectively.

3.4. Scanning Electron Microscope (SEM)

Figure 5.a shows the 3D printed structure with a 20% filling ratio. The large voids and gaps between the printed paths are clearly visible, which would contribute to a lower mechanical strength. This structure is less dense and would be more prone to fractures under stress due to the reduced material continuity. Figure 5.b shows the 3D printed structure with a 60% filling ratio. Compared to the 20% fill ratio, the paths are closer together, and there are fewer and smaller voids. This indicates a better layer adhesion and a potential for higher mechanical strength than the 20% fill ratio sample. However, it's still not as densely packed as a higher fill ratio would be, and thus, would have intermediate strength characteristics. Finally, Figure 5.c with a 95% fill ratio shows a very dense structure with minimal voids. The layers appear to be very tightly packed, which suggests excellent material continuity and strong layer-to-layer adhesion. This structure is expected to have the highest mechanical strength among the three, making it the most suitable for applications that require robust mechanical properties.

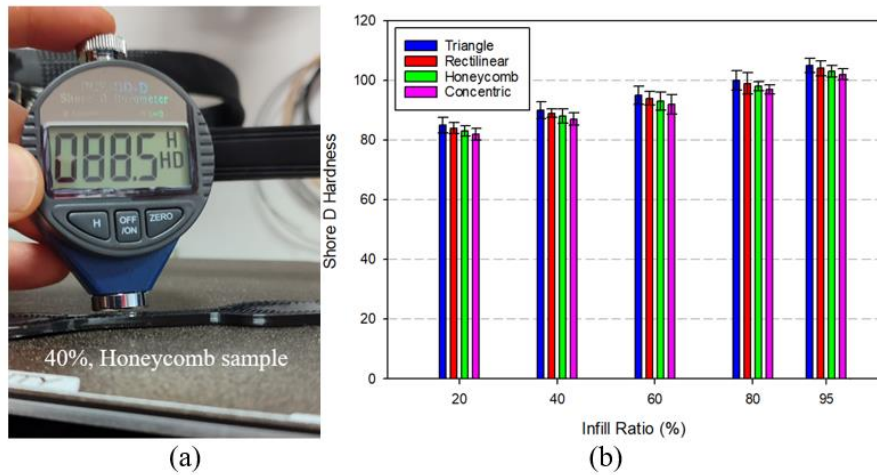


Figure 4. Shore D hardness variation according to filling ratio-pattern.

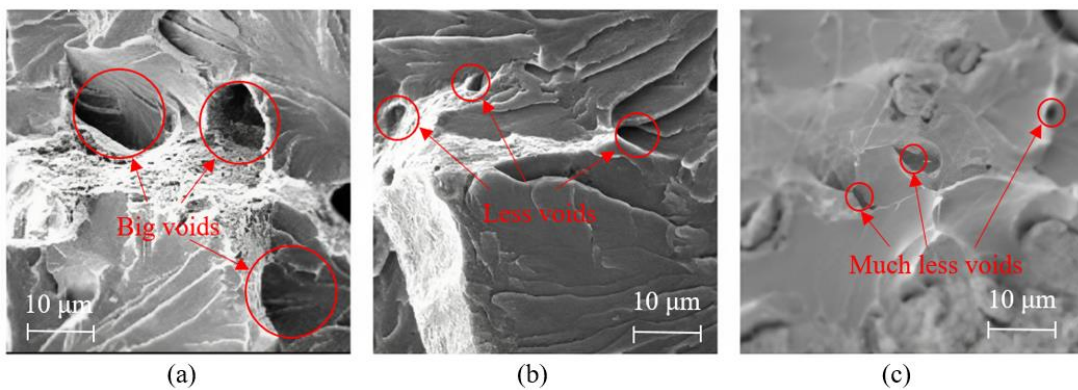


Figure 5. Scanning electron microscope views according to infill ratios of Concentric filling pattern, a) 20%, b.) 60%, c) 95%.

4. Discussion

An in-depth examination of tensile strengths across samples with varied infill patterns and ratios revealed insightful trends. The findings from the 20% infill samples highlighted discernible disparities based on patterns; with the Concentric pattern registering the highest tensile strength at 19.88 MPa, while the Triangle pattern lagged behind at 14.15 MPa. This difference could be attributed to the fuller, fracture-direction aligned nature of the Concentric pattern compared to the more gapped Triangle pattern. As infill percentages rose, the Rectilinear, Honeycomb, and Concentric patterns observed significant surges in tensile strength, culminating with the Concentric pattern's 48.67 MPa peak at 95% infill. Aligning with prior studies by Pandzic et al. (2019) and Lalegani Dezaki et al. (2021) the Concentric pattern, particularly with a 90% infill, was found to exhibit superior tensile and yield strengths for PLA filaments. Furthermore, the data from flexural tests underscored the pronounced strength variations across patterns at differing infill percentages. For instance, the Concentric pattern soared to a 79.94 MPa flexural strength at 95% infill. Collectively, these findings emphasize the pivotal role of infill pattern and ratio in determining tensile and flexural strengths in 3D printing. The insights drawn from Table 2 further accentuate the prominence of the Concentric pattern, especially at escalated infill percentages, for applications demanding enhanced tensile durability. Interestingly, while the Triangle and Honeycomb patterns started similarly at 20% infill, they diverged significantly at higher infill levels. This, combined with the consistent growth in the Rectilinear pattern, reaffirms the importance of strategic pattern and ratio selections in 3D printing to meet specific mechanical benchmarks. The flexural testing offered additional clarity on the mechanical prowess of the samples, specifically their bending resistance. When subjected to flexural stress, it became evident that both the infill pattern and ratio were crucial determinants of mechanical performance. The initial observations for the 20% infill, as depicted in Figure 3 echoed the trends seen in tensile tests, with the Concentric pattern emerging superior in terms of load-bearing capability. Notably, despite its tensile strength, the Honeycomb pattern underperformed in flexural strength when juxtaposed against its counterparts. However, as infill percentages increased, Honeycomb's strength saw improvements. The outstanding flexural modulus showcased by the Concentric pattern further underscores its mechanical robustness. Drawing from Table 3, the Concentric pattern's prowess, especially at higher infills, is evident. Conversely, the Honeycomb pattern's performance, though commendable, showcases a plateauing trend post the 60% infill mark. The data underscores the importance of the infill pattern and its ratio in optimizing the flexural performance of 3D printed objects. Potential avenues for future studies could involve dissecting the structural intricacies of these patterns to understand

their performance variations better. In Shore D hardness measurements, an increase in hardness values was observed in parallel with the increase in the filling ratio. On the other hand, changing the filling patterns was found to be less affected by the change in the hardness values of the samples. Overall, the SEM images visually support the idea that a higher fill ratio in 3D printing leads to a denser structure, better layer adhesion, and consequently, improved mechanical properties such as tensile strength. The 95% fill ratio with a Concentric pattern is likely to result in the most durable and structurally sound parts suitable for demanding applications.

5. Conclusion

The study presented a comprehensive investigation into the tensile and flexural strengths of 3D printed samples, focusing on varying infill patterns and ratios. The primary takeaways from this research are:

The choice of the infill pattern is paramount in determining both the tensile and flexural strengths of 3D printed objects. The Concentric pattern, in particular, exhibited consistent superior performance in both these categories, especially at higher infill ratios. At an initial 20% infill, while Triangle and Honeycomb patterns exhibited comparable tensile strengths, a clear divergence in their performance was observed as the infill ratio was increased. On the other hand, the Rectilinear pattern demonstrated a steady and predictable growth in tensile strength with rising infill percentages. Flexural tests revealed that, despite Honeycomb's promising tensile strength, it lagged in terms of flexural resistance, especially when juxtaposed against other patterns. However, its strength improved with higher infill ratios. The Concentric pattern, with its outstanding flexural modulus, highlighted its potential as a top choice for applications requiring strong resistance to bending. Aligning with prior studies, the Concentric pattern displayed superior tensile and yield strengths, especially for PLA filaments with higher infill ratios. These findings underscore the significance of strategic pattern and ratio selection in 3D printing to cater to specific mechanical requirements. There's a pronounced need for designers and engineers to be judicious in their selections, especially when aiming to optimize the mechanical properties of 3D printed components. The data suggests intriguing avenues for future research. A deep dive into the structural nuances of different patterns, coupled with real-world application testing, could offer more insights into optimizing 3D printed objects for various purposes.

In essence, this research provides valuable insights for stakeholders in the 3D printing realm. It emphasizes the profound impact of infill patterns and ratios on the mechanical strengths of printed objects, guiding future design decisions and paving the way for further exploration in the domain.

Author Contributions

The percentage of the author(s) contributions is presented below. All authors reviewed and approved the final version of the manuscript.

	F.K.	A.K.
C	50	50
D	80	20
S	25	75
DCP	70	30
DAI	40	60
L	50	50
W	80	20
CR	40	60
SR	65	35
PM	70	30
FA	90	10

C=Concept, D= design, S= supervision, DCP= data collection and/or processing, DAI= data analysis and/or interpretation, L= literature search, W= writing, CR= critical review, SR= submission and revision, PM= project management, FA= funding acquisition.

Conflict of Interest

The authors declared that there is no conflict of interest.

Ethical Consideration

Ethics committee approval was not required for this study because of there was no study on animals or humans.

Acknowledgements

We would like to thank Kastamonu University Scientific Research Coordinatorship for supporting this study with project number KÜBAP-01/2022-38.

References

Benamira M, Benhassin N, Ayad A, Dekhane A. 2023. Investigation of printing parameters effects on mechanical and failure properties of 3D printed PLA. *Eng Fail Anal*, 148: 107218.

Bian YH, Yu G, Zhao X, Li SX, He XL, Tian CX, Li ZY. 2023. Exit morphology and mechanical property of FDM printed PLA: influence of hot melt extrusion process. *Adv Manuf*, 11(1):

56-74.

Dudescu C, Racz L. 2017. Effects of raster orientation, infill rate and infill pattern on the mechanical properties of 3D printed materials. *ACTA Univ Cibiniensis*, 69(1): 23-30.

Hamat S, Ishak MR, Sapuan SM, Yidris N, Hussin MS, Abd Manan MS. 2023. Influence of filament fabrication parameter on tensile strength and filament size of 3D printing PLA-3D850. *Mater Today-Proc*, 74: 457-461.

Kartal F, Kaptan A. 2023. Investigating the Effect of Nozzle Diameter on Tensile Strength in 3D-Printed PLA Parts. *BSJ Eng Sci*, 6(3): 276-287.

Kechagias JD, Vidakis N, Petousis M, Mountakis N. 2023. A multi-parametric process evaluation of the mechanical response of PLA in FFF 3D printing. *Mater Manuf Proces*, 38(8): 941-953.

Lalegani Dezaki M, Ariffin MKAM, Serjouei A, Zolfagharian A, Hatami S, Bodaghi M. 2021. Influence of infill patterns generated by CAD and FDM 3D printer on surface roughness and tensile strength properties. *Appl Sci*, 11(16): 7272.

Mayén J, Gallegos-Melgar, ADC, Pereyra I, Poblano-Salas CA, Hernández-Hernández M, Betancourt-Cantera JA, Monroy MDA. 2022. Descriptive and inferential study of hardness, fatigue life, and crack propagation on PLA 3D-printed parts. *Mater Today Commun*, 32: 103948.

Moradi M, Aminzade A, Rahmatabadi D, Hakimi A. 2021. Experimental investigation on mechanical characterization of 3D printed PLA produced by fused deposition modeling (FDM). *Mater Res Express*, 8(3): 035304.

Özsoy K., Aksoy B. 2022. Real-time data analysis with artificial intelligence in parts manufactured by FDM printer using image processing method. *J Test Eval*, 50(1): 629-645.

Özsoy K., Aksoy B., Bayrakçı HC. 2022. Optimization of thermal modeling using machine learning techniques in fused deposition modeling 3-D printing. *J Test Eval*, 50(1): 613-628.

Pandzic A, Hodzic D, Milovanovic A. 2019. Effect of infill type and density on tensile properties of plamaterial for fdm process. *Ann DAAAM*, 30.

Şirin Ş, Aslan E, Akincioglu G. 2023. Effects of 3D-printed PLA material with different filling densities on coefficient of friction performance. *Rapid Prototyp J*, 29(1): 157-165.

Wittbrodt B, Pearce JM. 2015. The effects of PLA color on material properties of 3-D printed components. *Additive Manufact*, 8: 110-116.

Wu W, Geng P, Li G, Zhao D, Zhang H, Zhao J. 2015. Influence of layer thickness and raster angle on the mechanical properties of 3D-printed PEEK and a comparative mechanical study between PEEK and ABS. *Materials*, 8(9): 5834-5846.



EFFECT OF OHS CRITERIA ON SELECTION OF CONCRETE ADDITIVES IN MINE ORE CONSTRUCTION WORKS

Tuğçe ORAL^{1*}, Nuri BİNGÖL¹


¹Üsküdar University, Faculty of Health Science, Department of Occupational Health and Safety, İstanbul, Türkiye


Abstract: Construction, mining or tunneling projects in Türkiye are defined as workplaces in the very dangerous class due to their physical power needs. For this reason, metal ore mining, mining supporting service activities, sewage, external construction, special construction activities, construction and landscaping activities are the sectors where occupational accidents are most common. While determining the necessary materials or work equipment during the planning phase of the works in these sectors, making decisions by evaluating the effect of "occupational health and safety" will contribute to the reduction of accidents. This research consists of two parts. In the first part, accident frequency rates were calculated by using data related to metal ore mining, mining supporting service activities, sewerage, external structure, special construction activities, building and landscaping projects between 2012 and 2019. Thus, the relationship between occupational accidents experienced as of the adoption of the Occupational Health and Safety Law has been determined. In the second part, it is tried to gain a different perspective by adding occupational health and safety factor to the Analytical Hierarchy Process (AHP), which is one of the multi-criteria decision-making methods. As a result of the research, it has been determined that "occupational health and safety" criteria are given priority according to cost and engineering advantages in alternative product/material comparisons in mines or construction works.

Keywords: Analytical hierarchy process, Multi criteria decision making method, Occupational accident frequency rate, Occupational health and safety

*Corresponding author: Üsküdar University, Faculty of Health Science, Department of Occupational Health and Safety, İstanbul, Türkiye

E mail: tgcmylmz@gmail.com (T. ORAL)

Tuğçe ORAL  <https://orcid.org/0000-0003-1795-1550>

Nuri BİNGÖL  <https://orcid.org/0000-0001-6208-7277>

Received: December 10, 2023

Accepted: January 22, 2023

Published: March 15, 2024

Cite as: Oral T, Bingöl N. 2024. Effect of OHS criteria on selection of concrete additives in mine ore construction works. BSJ Eng Sci, 7(2): 203-213.

1. Introduction

Due to the usage of construction equipment and the requirement for physical strength, mining and tunnel projects are classified as very dangerous workplaces (Bayraktar et al., 2018; Bayrak, 2018). Türkiye's construction industry and mining companies both contribute to the nation's economy, with employment prospects rising by 10% annually. However, when the Social Security Institution (SSI) data for the years 2012 and 2019 are studied, the construction industry and mining businesses are found to have the greatest rates of occupational accidents (As one of the industries with a high rate of occupational accidents, metal mining, mining-related service activities, sewerage, outdoor structure construction, private construction, buildings, and landscaping activities should be investigated or methods developed to reduce occupational accidents in workplaces (Bingöl, 2010). The primary preventive measure to reduce occupational accidents is to determine an alternative working style or method. Among OHS practices, the first priority is to completely eliminate the situation that may cause a work accident. If the situation that may cause a work accident is caused by a material or equipment that must be used. It is necessary to investigate substitute methods or materials that provide occupational safety advantages. In short, the secondary

preventive measure to reduce occupational accidents is to determine an alternative working method or materials.

Occupational health and safety (OHS) is a scientific term that encompasses all systematic research into the effective integration and implementation of all essential workplace procedures. From this perspective, alternative techniques need to be investigated in cases where appropriate safety measures cannot be taken in the machines and equipment used to perform a task. In workplaces classified as very hazardous, it can sometimes be difficult to decide on the most advantageous method and material in terms of OHS. Generally, employers in this field only consider the engineering contribution and financial advantage they bring to the project when choosing the materials and equipment they will use on the construction site. OHS professionals, on the other hand, focus on the advantage of occupational health and safety in the selection of materials and equipment to be used. As a result, MCDM is an application that helps in selecting the most advantageous materials and methods by evaluating all the criteria together for a safe workplace idea.

In this research, the occupational accident statistics published by the SSI were used as a data source, and the occupational accident frequency rate was calculated



according to the occupational accidents experienced between 2012 and 2019. Secondly, the Analytical Hierarchy Process (AHP) method was applied to two different concrete reinforcement additives that are widely used in mines and the construction industry. Thus, while choosing between alternatives, priorities are listed among the criteria that affect the decision (Lyu et al, 2020; Banerjee et al, 2021). The original aspect of this research was to determine the ideal choice by adding the occupational health and safety contribution as a criterion while choosing the most suitable concrete reinforcement material among the alternatives. In addition, this research is a pioneering study emphasizing the inclusion of "Occupational Health and Safety Criteria" in all processes in material or equipment selection in similar sectors where occupational accident rates are high.

1.1 Sectors Where Macro Synthetic Fibers Are Used for 2012-2019

Occupational Health and Safety (OHS) is the umbrella term for all systematic research done to ensure that all relevant workplace procedures are effectively integrated and put into place. According to this viewpoint, substitution (alternative) solutions should be looked for when suitable safety precautions cannot be established in the apparatus and equipment used to carry out a job. Employers working on large-scale projects in these sectors only consider the engineering contribution and cost savings a piece of equipment or material will bring to the project when selecting it. It is important to take occupational health and safety into account when selecting the materials and equipment to be utilized. Consequently, the idea of a safe workplace in workplaces such as those involved in the extraction of metal ore, mining support services, sewage, the construction of non-building structures, special construction activities, etc., the likelihood of an employee developing a work accident or occupational disease is significant due to the work machinery employed, the erratic working environment, and the requirement for physical strength. As a result, these workplaces fall under the category of very dangerous (Tehlike Sınıfları Tebliği, 2012). The primary OHS procedures in extremely risky jobs;

- Vocational training, certification, and employee inspections ought to be done.
- To offer basic OHS training for at least 16 hours each year.
- One employee out of every 30 should receive emergency training, and one employee out of every 10 should receive first aid training.
- Emergency plans and risk assessment reports should be renewed every two years at the maximum (barring circumstances prescribed by law).

Establishing OHS committees and holding regular meetings each month, renewing employee health examinations on a regular basis each year, and assigning each employee an occupational safety specialist who will work for at least 40 minutes each month and a workplace doctor who will work for 15 minutes (Türk Tabipleri

Birliği, 2021).

Metal ore mining, mining support services, sewage, the construction of non-building structures, specialized construction activities, buildings, and landscaping activities were chosen as typical workplaces where two distinct concrete reinforcement materials may be used. When looking at Figure 1, it has been determined that between 2012 and 2019, in Türkiye, there were 973,192 workplaces and 10,636,427 workers in these industries (SGK, 2021). Examining the statistics in Figure 1, it can be seen that these industries support the economy of the nation by adding 9% additional jobs annually on average.

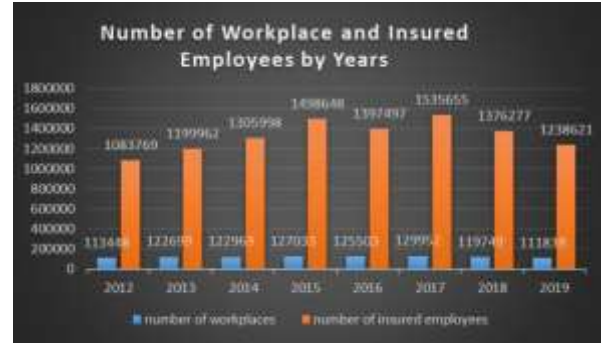


Figure 1. Number of workplace and insured employees between 2012 and 2019 (SGK, 2021).

When the data in Figure 2 in the years 2012 to 2019 with the adoption of the OHS Law is examined, it appears that 259,866 people had occupational accidents out of the 10,636,427 people employed in metal ore mining, mining support service activities, sewerage, construction of non-building structures, private construction activities, buildings, and landscaping activities (SGK, 2021). Even while this condition really offers employment prospects, it demonstrates that 2.44% of those who have been employed for seven years had experienced a workplace injury.

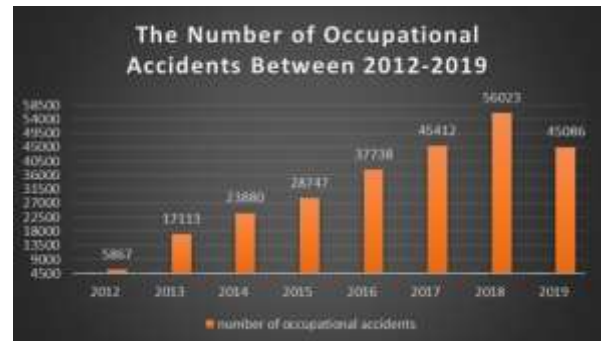


Figure 2. Number of occupational accidents in metal ore mining, mining support service activities, sewerage, construction of outdoor structures, special construction activities, buildings and landscaping activities between 2012 and 2019 (SGK, 2021).

As shown by the data in Figure 2, the fact that 24% of employees experience work-related accidents highlights the importance of occupational health and safety for the

industry. It's crucial that workplace safety and employee welfare continue to exist (Bilim ve Çelik, 2018). Employers should do a risk assessment pertaining to the use of tools and machinery needed for the job and look for alternatives for this reason. When making a decision, taking occupational health and safety into account will ensure business continuity. In terms of OHS, substitute methods encompass all the work done to reduce the effects of potentially harmful circumstances that may develop as a result of work that cannot be canceled in the course of a process. In a nutshell, the decrease of the success of alternative solutions makes it possible to reduce occupational accidents in various industries.

It is claimed that occupational accidents during the construction of outdoor constructions account for 8-15% of the project cost in his paper titled "Safety Risk Assessment Using Analytic Hierarchy Process (AHP) During Planning and Budgeting of Construction Projects" (Aminbakhsh et al, 2013; Soyalan, 2020). It is not just about occupational health and safety when it comes to occupational diseases or accidents, particularly in the construction industry. Occupational accidents also have an indirect impact on the nation's economy (Aminbakhsh et al, 2013). Occupational safety standards coordinated with the activity will therefore contribute to the project's success since mines and building projects are frequently seen as large-scale endeavors. OHS experts need to be involved from the planning stage of the project onward. Only engineering or cost advantage should not be taken into account during the planning phase when choosing the materials or work equipment to be utilized for the job in the absence of OHS professionals. Making the best decisions and including "occupational health and safety criteria" in the selection criteria will aid in preventing work accidents that might happen as the project progresses. Additionally, it will benefit the OHS procedures needed in the workplace. Macro synthetic fiber materials can be used as concrete reinforcement materials instead of conventional reinforcements in a specific area of work in metal ore mining, mining support service activities, sewerage, external structure construction, special construction activities, building, and landscaping projects. These concrete additives, which are polymer-based, ecologically friendly, and more useful compounds that can be utilized as an alternative to conventional reinforcements, have been introduced to the market as a result of evolving technology [14]. However, when it comes to strengthening reinforced concrete structures, traditional reinforcements are the first steel elements that come to mind. Macro Synthetic Fibers (MSF) and conventional reinforcements have similar engineering characteristics, but in some situations, it may be preferable to use one over the other (Dağdeviren and Tamer, 2001).

Özcan (2018) study claims that variations in engineering strength are brought on by the corrosion effect of traditional reinforcements along with the passage of time. MSFs should be prioritized in the use decisions

made for projects since they continue to function at their peak capacity even after being used (Dağdeviren and Tamer, 2001). Additionally, while comparing the two options, procedures like transporting, merging, and using conventional equipment necessitate the use of labor and professional expertise. In other words, workplace accidents or occupational diseases will inevitably occur whenever physical strength is successfully utilized in the workplace. The examination of each material's contribution to workplace health and safety when deciding between them would thus indirectly help the substitution approach in terms of OHS in these industries where both materials can be utilized interchangeably. Therefore, even a slight reduction in the number of work accidents that occur relative to the employment rate will be beneficial.

Enterprises frequently choose alternatives using Multi-Criteria Decision Method (MCDM) methodologies. In order to choose the best supplier, Dadeviren and Tamer identified four key criteria. Using these criteria, they used the AHP approach to establish the priorities of four vendors (Badri et al, 2011). In order to create and better organize the safety culture in a mining sector project, Badri, Nadeau, and Gbodossou used the MCDM method to identify OHS concerns (Bao et al, 2016). According to six primary criteria, Bao, Zhang, Li, Liu, and Shi used the fuzzy AHP technique to assess the societal benefits of the OHS management system in two separate mining operations in China and Switzerland (Bao et al, 2017). In order to guide the establishment of OHS management systems in mining firms, this study was conducted. According to six primary criteria, Bao et al. (2016) used the fuzzy AHP technique to assess the societal benefits of the OHS management system in two separate mining operations in China and Switzerland (Bao et al., 2017). The goal of this study is to guide the development of OHS management systems in mining businesses. For the prevention, efficient analysis, and ongoing improvement of occupational diseases in the mining industry, Bao et al. (2017) developed an FMEA-based technique (fault mode and impact analysis) and an enhanced AHP (analytical hierarchy process) model (Korkusuz et al, 2019). It has been demonstrated that this approach can be used to manage business processes. The level of OHS performance among hospitals was compared using the Korkusuz et al. (2019) study, which used AHP, Promethee, and GRA methodologies (Dağdeviren, 2008). By using MCDM techniques, a groundbreaking advancement in the field of OHS was made in the research, which incorporated "OHS Performance" as a criterion for evaluating hospital performance. Dağdeviren (2008) claimed that used the PROMETHEE approach to make the best choice and the AHP method to structure the criteria needed for the selection of appropriate equipment (Denizhan et al, 2017). This study's research topic is comparable to our own, but our study differs in that it takes occupational health and safety parameters into account while choosing the right

equipment.

However, there isn't a model study that highlights the importance of choosing the tools or supplies to use in the workplace while accounting for OHS contributions. In this study, "Occupational Health and Safety" has been incorporated as a selection factor along with the "Cost, Engineering, and Time Management Advantage" while choosing concrete reinforcement material by utilizing the AHP approach. This study's main goal is to increase public knowledge about the need to use OHS benefits as a selection factor when purchasing machinery or other items that will be used in workplaces. The use of MCDM techniques in workplace OHS procedures is the secondary goal. The third objective is to develop an efficient OHS infrastructure in the workplace by reducing the initial investment expenditures for OHS that companies avoid at the start of the job.

In this study, using the MCDM, in addition to the cost and engineering advantage of the proposed macro synthetic fiber material, the contribution of its use in OHS applications was added as a criterion. Thus, it was emphasized that enterprises can benefit from the AHP method by adding the OHS criterion in the selection of materials to be used to reduce investment costs in OHS applications.

The AHP method is one of the oldest and frequently used methods in various application areas. For this reason, in this article, this method was chosen among the MCDM methods and this method was used in the grading of the criteria.

2. Materials and Methods

In this investigation, two evaluations were conducted. First, for the industries covered by the Turkish Social Security Agency's research, the frequency of occupational accidents between 2012 and 2019 was estimated.

In the second, the decision-making factors were given priority using the AHP approach while deciding between the concrete reinforcement materials that are frequently utilized in these industries.

The AHP approach was chosen as the MCDM method because it has a wealth of literature applications and is one of the most effective criterion weighting methods (Dağdeviren, 2008). Denizhan et al. (2017), study used fuzzy AHP and AHP methods to choose the best provider out of two options and found that the application had no effect on the criteria's ranking (Aritan and Ataman, 2017). It was shown that in studies where two different options were evaluated, the results did not change in accordance with the fuzzy AHP approach; instead, the weight of the criteria with high relevance grew even more, and the weight of the criteria with low importance was reduced. Due to their difficulty in application, fuzzy numbers were not selected when choosing between conventional reinforcement and macro-synthetic fiber reinforcement material.

2.1. Accident Frequency Rate

The insured person's rate of occupational accidents

during working hours is expressed as a percentage (Yılmaz Oral and Ünal, 2020). For the years 2012 to 2019, occupational accident frequency rates were calculated using data on occupational accidents that the Turkish Social Security Agency had collected in the mining of metal ore, mining-related service activities, sewage, construction of non-building structures, private construction activities, and building and landscaping activities. As a result, it offers insight into how various industries approach workplace safety.

The Equation 1 is used to calculate the occupational accident frequency rate for each year (Kuruüzüm and Atsan, 2001).

$$KSO = TNWA / [(TWD - NWD) \times RDWT] \times 10.000 \quad (1)$$

TNWA= total number of work accidents, TWD= total working days, NWD= non-working day, RDWT= refers to the daily working time, expresses.

2.2. Analytical Hierarchy Process (AHP)

The AHP method, which was developed by Saaty in 1977, considers the main factors affecting the decision as the main decision criteria and divides them into sub-decision criteria that affect the main decision criteria (Lin and Kou, 2021). Briefly, the AHP method calculates the order of importance among the features that are effective in comparing the alternatives with each other (Keçek and Yıldırım, 2010). Thus, it provides a detailed comparison analysis for the right choice based on the opinions of people who have sufficient knowledge and equipment to solve the problem.

The AHP method is generally preferred for solving problems such as the most useful product or resource selection in projects, cost calculations, and employee performance evaluations (Saaty, 1987).

2.2.1. AHP method implementation stages

The four solution procedures that make up the AHP Method's solution are the construction of the hierarchical structure, the development of the comparison matrices, the development of the priority vector in light of the comparison matrices, and the determination of the consistency ratio.

In the initial phase of the study, a hierarchical structure is made with comparison standards developed using the opinions of specialists. In order to gather the required data sources for the problem's AHP method solution, comparison matrices are obtained using the AHP questionnaire forms. The priority vector, which is the next stage of the solution, is derived from the verbal responses provided by the survey respondents and converted into the numerical values shown in Table 1.

The meaning of a_{ij} value in the comparison matrix represents the comparison value between i diagonal criterion and j diagonal criterion and the comparison matrix representation created according to Table 1 is as given in (Equation 2). The value of the diagonal elements of the matrix is equal to 1 and the mutual values within the matrix are equal to $a_{ij} = 1 / a_{ji}$.

Table 1. Significance values and numerical correspondence of AHP method comparison criteria (Çetin, 2019)

Importance Values	Significance value definitions
1	Equally important
3	Moderately important
5	Strongly important
7	Very strongly important
9	Absolutely important
2,4,6,8	Intermediate values

$$A = \begin{bmatrix} a_{11} & a_{12} & \dots & a_{1n} \\ a_{21} & a_{22} & \dots & a_{2n} \\ \cdot & & & \cdot \\ \cdot & & & \cdot \\ \cdot & & & \cdot \\ a_{n1} & a_{n2} & \dots & a_{nn} \end{bmatrix} \quad (2)$$

The 'normalization' process (Equation 3) is carried out to produce the priority vector by dividing the total value of each row of the acquired comparison matrix by the sum of all rows. Row totals are divided by the total number of criteria weights in the priority vector to get the criteria weights.

$$b_{ij} = \frac{a_{ij}}{\sum_{i=1}^n a_{ij}} \quad (3)$$

Calculating the consistency ratio is necessary in order to analyze the comparable criteria for solving problems. It is required that the consistency ratio (CR) value be less than 0.10. The () value is determined by dividing the comparison matrix's row totals, which are derived by multiplying the matrix elements in each column of the decision matrix by the criterion weights. Reading from Table 2 yields the Random Consistency Index (RI) value, which is another parameter needed to calculate the CR value, and the n value is determined by how many criteria were considered. The consistency indicator (CI) value and the consistency rate (CR) value are calculated using the Equation (4), and a comparison of 0.10 is made.

$$CI = \frac{\lambda - n}{n - 1}, \quad CR = \frac{CI}{RI} \quad (4)$$

Table 2. RI Value Table (Çetin, 2019)

n	RI
1	0
2	0
3	0.52
4	0.89
5	1.11
6	1.25
7	1.35
8	1.4
9	1.45
10	1.49

If a consistency ratio is given, the criterion with the largest numerical value in relation to the outcome of the transaction is regarded as having the greatest influence

on the choice (Çetin, 2019).

Elements like the technical qualities and advantages of the alternatives are compared with the AHP technique and are grouped based on the judgments of the experts. The order of priority is established using the AHP approach, where each group value is used as a reference in the subheadings that are pulled from inside themselves. It makes decision-making more specific, particularly in circumstances where it is difficult to compare alternatives objectively.

3. Results

3.1. Occupational Accidents in Sectors Where Macro Synthetic Fibers Are Used

Data on occupational accidents that are specific to the industry for which the calculation of the occupational accident frequency rate is intended are needed, as well as details about daily working hours and weekends. Work is done six days a week in industries like mining for metal ore, providing mining support services, cleaning sewage, building buildings, landscaping, and creating outdoor constructions.

Table 3. Number of occupational accidents in 2012-2019 (SGK, 2021)

2012	5867
2013	17113
2014	23880
2015	28747
2016	37738
2017	45412
2018	56023
2019	45086

For the research's target industries, a total working day (TWD) of 45 hours per week was established. Weekends, paid time off, and public holidays are computed based on the calendar of the current year. The ranking is based on 10,000 hours as well, for clarity's sake. According to the number of work accidents listed in Table 3, occupational accident frequency data are derived for each year and are shown in Table 4.

Examining Table 4 and Figure 3, it can be seen that there is a linear increase in the likelihood of an occupational injury for insured individuals employed between 2012 and 2016. The increase in insured personnel by 138,158 over the prior year is assumed to be the cause of the fall in accident frequency rate in 2017. The significance of OHS practices is demonstrated by the increase in accident frequency over time. OHS's primary goal is to entirely eliminate work accidents, which unfortunately does not align with the existing scenario.

Table 4. Accident frequency rates by years

Years	2012	2013	2014	2015	2016	2017	2018	2019
TNWA	5867	17113	23990	28747	37738	45412	56023	45086
TWD-NWD	307	287	297	289	288	289	283	287
RDWT	7.5	7.5	7.5	7.5	7.5	7.5	7.5	7.5
Number of Employees	1083769	1199962	1305998	1498648	1397497	1535655	1376277	1238621
Time Calculation	10000	10000	10000	10000	10000	10000	10000	10000
AFR	0.04	0.13	0.18	0.22	0.29	0.14	0.19	0.17
Average Value	4%	13%	18%	22%	29%	14%	19%	17%

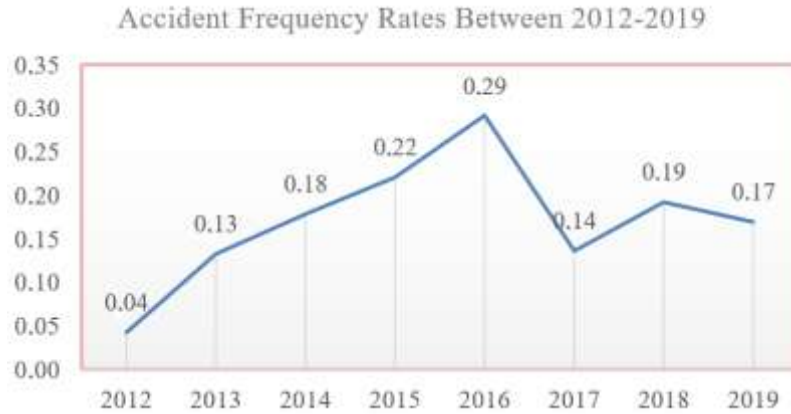


Figure 3. Number of occupational accidents in metal ore mining, mining support service activities, sewerage, construction of outdoor structures, special construction activities, buildings and landscaping activities between 2012-2019.

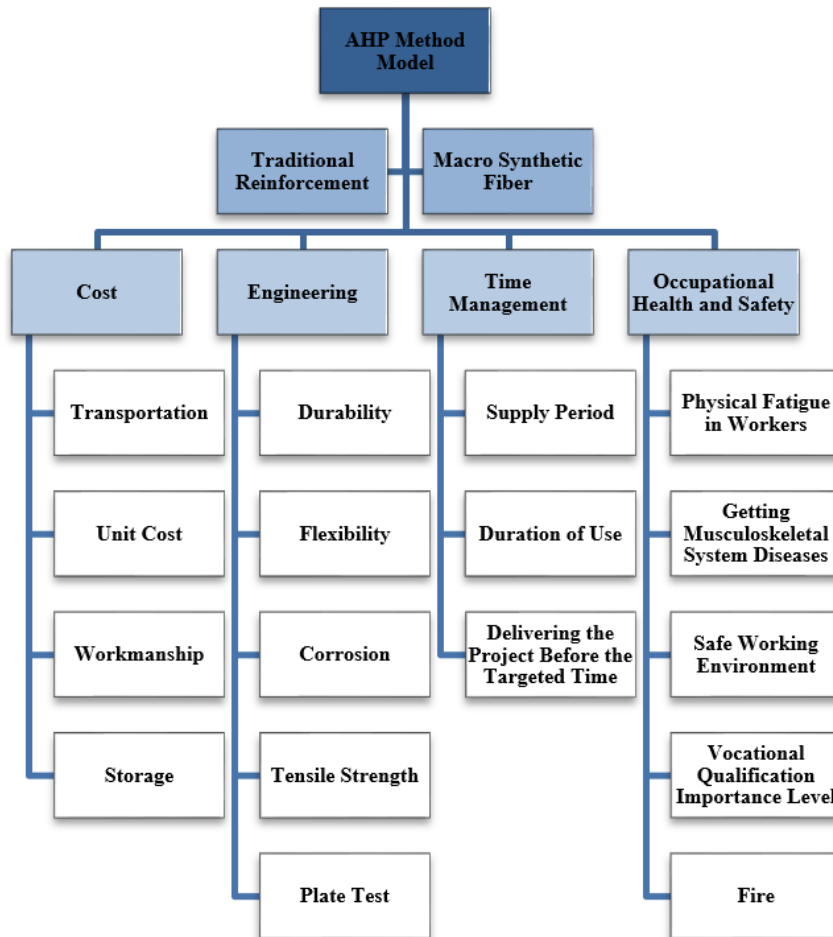


Figure 4. AHP method model.

3.2. AHP Method Application Results

The AHP technique used interviews with employers or expert engineers from 10 different businesses to determine the criteria. DM profiles consist of 10 experts in their fields, including employers or employers' representatives, site supervisors and expert civil engineers working in 10 different mining enterprises. The most important feature of these 10 people is; they have the authority to decide on the choice of alternative materials and the technical equipment to compare the products.

AHP questionnaires and major and sub-criteria were designed using the interviews with this expert panel (Figure 4). Also referred to as this expert team are the decision-makers. The evaluation of the questionnaire responses led to the calculation of the ranking of the selection criteria. On August 19, 2020, Uskudar University received the study's ethics committee's permission.

Table 5. Comparison matrix

Main Criteria	Cost	Engineering	Time Management	Occupational Health and Safety
Cost	1.0000	0.5213	0.9587	1.0000
Engineering	1.9184	1.0000	0.6834	0.7569
Time Management	1.0431	1.4633	1.0000	0.5444
Occupational Health and Safety	1.0000	1.3211	1.8369	1.0000

Table 6. Normalized comparison matrix

Main Criteria	Cost	Engineering	Time Management	Occupational Health and Safety
Cost	0.2016	0.1211	0.2140	0.3029
Engineering	0.3867	0.2323	0.1526	0.2293
Time Management	0.2102	0.3398	0.2233	0.1649
Occupational Health and Safety	0.2016	0.3068	0.4101	0.3029

Stage 4: Creating the priorities vector

The priority values of the main criteria of cost, engineering, occupational health and safety, time management, which are effective in determining the alternatives, were calculated and the values in Table 7 were obtained.

Table 7. Priority values

Main Criteria	Priority values
Cost	0.209894
Engineering	0.250191
Time Management	0.234561
Occupational Health and Safety	0.305354

When the values given in Table 7 are examined, it has been determined that the "Occupational Health and Safety" criterion is the most effective criterion in alternative selection, since it has the highest value.

Stage 5: Calculation of consistency analysis parameters

In order to calculate the consistency analysis parameters, the λ values of the main criteria were calculated as given in Table 8.

3.2.1. Evaluation of data with ahp method

Stage 1: Determination of decision criteria

Following interviews with key decision-makers, four main criteria—cost, engineering, time management, and occupational health and safety—and a total of 17 sub-criteria were established for comparing the two materials. The established major and sub-criteria were used to build the AHP questionnaire forms.

Stage 2: Developing criterion weights and binary comparison matrices

The AHP approach was used to transform the verbal data into their numerical equivalents and create comparison matrix values for the primary criteria listed in Table 5.

Stage 3: Normalized binary comparison matrices for key criteria

A single unit matrix was created by taking the geometric mean of the answers given by the survey participants, and the normalized comparison matrix is given in Table 6.

Table 8. Calculation of λ value

Main Criteria	Priority Matrix Total
Cost	4.147534
Engineering	4.173902
Time Management	4.202837
Occupational Health and Safety	4.180898
Lambda (λ)	4.176293087

Stage 6: Calculation of the CR value

CR = 0.06529 for main criteria. Since it satisfies the CR <0.1 rule, it is possible to mention that the results of the criteria weights obtained are consistent.

Stage 7: Creating the hierarchy

By providing the consistency analysis, the hierarchical ranking for the main criteria was calculated as Occupational Health and Safety 0.3053, Engineering 0.2501, Time Management 0.2345, Cost = 0.2098.

Stage 8: Determination of priority values for main criteria, sub-criteria and alternatives

In all calculations of the sub criteria, the CR <0.1 rule has been provided and the results obtained are given in Tables 9 and 10 below.

Table 9. Major criteria, sub-criteria and criteria weights of alternatives

Main Criteria	Criterion Weights	Sub Criteria	Criterion Weights	Alternatives	Priority Values
Cost	0.2098	Transportation	0.2208	Traditional Reinforcement	0.3640
				Macro Synthetic Fiber	0.6359
		Unit Cost	0.3245	Traditional Reinforcement	0.2311
				Macro Synthetic Fiber	0.7688
		Workmanship	0.3552	Traditional Reinforcement	0.4452
				Macro Synthetic Fiber	0.5547
		Storage	0.0993	Traditional Reinforcement	0.2984
				Macro Synthetic Fiber	0.7015
		Durability	0.1993	Traditional Reinforcement	0.1729
				Macro Synthetic Fiber	0.8270
Flexibility	0.1099	Traditional Reinforcement	0.1577		
		Macro Synthetic Fiber	0.8422		
Engineering	0.2501	Corrosion	0.2291	Traditional Reinforcement	0.8455
				Macro Synthetic Fiber	0.1544
		Tensile Strength	0.1651	Traditional Reinforcement	0.7594
				Macro Synthetic Fiber	0.2405
Plate Test	0.2964	Traditional Reinforcement	0.4577		
		Macro Synthetic Fiber	0.5422		

Table 10. Major criteria, sub-criteria and criteria weights of alternatives (more)

Main Criteria	Criteria Weights	Sub-Criteria	Criterion Weights	Alternatives	Priority Values
Time Management	0.2345	Supply Period	0.1936	Traditional Reinforcement	0.4452
				Macro Synthetic Fiber	0.5547
		Duration of Use	0.1365	Traditional Reinforcement	0.3815
				Macro Synthetic Fiber	0.6184
		Delivering the Project Before the Targeted Time	0.6697	Traditional Reinforcement	0.1078
				Macro Synthetic Fiber	0.8921
Occupational Health and Safety	0.3053	Physical Fatigue in Workers	0.1327	Traditional Reinforcement	0.5710
				Macro Synthetic Fiber	0.4289
		Getting Musculoskeletal System Diseases	0.2421	Traditional Reinforcement	0.8593
				Macro Synthetic Fiber	0.1406
		Safe Working Environment	0.3323	Traditional Reinforcement	0.4099
				Macro Synthetic Fiber	0.5900
		Vocational Qualification Importance Level	0.1145	Traditional Reinforcement	0.8785
				Macro Synthetic Fiber	0.1214
		Fire	0.1782	Traditional Reinforcement	0.3129
				Macro Synthetic Fiber	0.6870

The calculation's findings indicate that occupational health, with a weight value of 0.3053 before cost, engineering criteria, and safety, is the most crucial factor influencing the decision between the alternatives in projects involving dams, mine galleries and tunnel shotcrete projects, field concrete, and industrial floors where the use of both materials is common. The contribution that must be given in relation to OHS in the projects of the construction of dams, mine galleries and tunnel shotcrete, field concrete, and industrial floors has been emphasized in this place in comparison to the financial and engineering advantages of the employers.

4. Discussion

Construction of the mine or tunnel is associated with a high number of workplace accidents as work is done in the project area, and this is not just a problem in Türkiye, according to surveys of work accidents conducted throughout the world. 800 workplace accidents in Taiwan's construction sector were analyzed by Cheng et al. (2010) and Hola and Szostak (2017).

As a result of the analysis, he emphasized that occupational accidents occurring in small-scale construction projects are more common than in large-scale construction projects. As a result of this analysis, it

was emphasized that work accidents that occurred in small-scale construction projects were more common than in large-scale construction projects. In small-scale construction projects, they found that 41% of them were due to poor health and safety management. Hala and Szostak (2017), in Poland, 485 work accidents in the construction sector were examined, and the people who had a work accident were analyzed (Bayraktar et al., 2018). The study's findings revealed that 40% of workplace accidents were brought on by unsafe working conditions, and the significance of restrictive measures in accident prevention was underlined.

In their study "Statistical Analysis of Occupational Accidents in the Turkish Mining Sector," Bayraktar et al. (2018), also looked at the occupational accident data in the mining industry (Özcan et al., 2019). It was found that, despite having a safe workplace and giving employees training for the job, fatal occupational accidents have increased year over year. According to a report by Dede and Baltacı (2019) from which included 361 members of the construction industry, the workers were aware of the need for OHS training, but they expressed safety concerns about the tools and machinery they utilized.

In a study by Özcan et al. (2019), primary causes of occupational accidents in the construction industry were listed using the AHP technique, and the target-oriented starting point of the activities intended to minimize the accidents was established (Barriuso et al., 2020). According to the study's findings, "reasons arising from equipment and materials" were determined to be the top factors contributing to occupational accidents. It is obvious that using MCDM approaches to make decisions that take into account occupational health and safety criteria would help to prevent potential workplace accidents, particularly when choosing the materials or equipment to be utilized during the planning stage of projects.

According to a study conducted by Barriuso et al. (2020), with 250 workers in the Spanish construction industry, management must develop replacement methods in addition to employee safety training if workplace accidents are to be reduced (Bingöl, 2018). On the other side, Bingöl stated that employers or their representatives should be informed about occupational health and safety in order to help them avoid any hazards or dangers that may be present in the line of work they are in 2018 (Abukhashabah, 2020).

In a study conducted with 300 Saudi Arabian workers in the construction business Abukhashabah et al. (2020), it was attempted to identify the reasons for occupational accidents. According to the study, 82% of the participants were affected by a hazardous work environment, workers who lacked sufficient professional expertise, and workers who were unaware of occupational safety issues (Boyacı et al., 2021). Due to the extent of building projects, Abukhashabah et al. (2020), in their study, underlined the necessity of minimizing the circumstances

that result in accidents in these work zones (Boyacı et al., 2021).

Boyacı Çalış, Solmaz, and Kabak, introduced a new perspective to the Fine-Kinney approach, which is frequently used for assessing workplace risk (Kim and Park, 2021). By adding the "cost" aspect to the assessment, a multi-criteria determination was made. As a result, it did not just reduce the likelihood and severity of workplace accidents and their effects, but it also helped the employers understand the issue more realistically by including the potential costs. Kim and Park (2021) examined the effects of occupational accidents on employee performance and business image in corporate organizations. As listed above, the causes of occupational accidents in construction, mining, or tunnel projects were investigated, and the causes of the accidents were listed as lack of education, an unsafe working environment, or the machinery and equipment used. At the same time, it has been determined that occupational accidents are not only limited to negative effects on the health of employees but also cause sharp financial losses for enterprises.

The need to include "occupational health and safety" in the checklists created during the planning phase of the projects stands out as a result of the research's alternative perspective on the causes of occupational accidents in construction, mining, or tunnel projects. With the help of this illustrative study, it is clear that the materials are chosen with an eye toward improving occupational health and safety, in addition to employers' costs, time management, and engineering parameters. This is true even for the selection of concrete reinforcement admixture used in a specific area of construction, mining, or tunnel projects. To put it simply, occupational health and safety should be assessed holistically using additional criteria in these industries, where workplace accidents are quite common.

Occupational health and safety contributions will also be taken into consideration while researching the one that will provide the maximum benefit for the job in the procurement of materials or equipment included in the needs lists determined by evaluating from this point of view. In short, substitution methods will be developed to provide a safe working environment at the planning stage of the project.

5. Conclusion

In this study, "occupational health and safety" has been determined as the primary expectation in comparisons and selections between alternatives, even among concrete admixtures that will only be used in a certain part of the work in mines or construction works. Contrary to what is known, occupational health and safety have been calculated to have a higher priority than the first selection criteria that come to mind, such as cost, engineering, and time management.

The positive contribution to occupational health and safety should be considered a priority in the selection of

all necessary equipment and materials for the execution of the work in areas where occupational accidents are high and the probability of their occurrence is high.

As a result, while preparing business activity reports, which were created during the planning phase of metal ore mining, mining supporting service activities, sewerage, construction of non-building structures, special construction activities, buildings, and landscaping projects, necessary machinery, materials, etc., alternative lists of such equipment must be created. It is understood that making choices among the alternatives with the priority of "occupational health and safety" criteria will contribute to the creation of a safe working environment. With the inclusion of the OHS criteria in this study and a minimal expert team, it is at a level to direct other studies in terms of its applicability in a short time. The usage areas for working with this sample application model can be listed as follows:

- The main criteria remain the same in the selection of any material or equipment in the construction or mining sectors, and the sub-criteria are revised and implemented.
- In the root cause detection research of the work accident that occurred in a workplace with the AHP model,
- In choosing among the alternatives as a result of adapting the AHP model to different sectors,
- In making the ideal choice among the applicable methods to eliminate the hazards,
- In the future, comparisons can be made between different MCDM methods and concrete reinforcement materials in the same sector. In addition, a new study can be made by including the OHS criteria while choosing between more alternatives in the same sectors.

Author Contributions

The percentage of the author(s) contributions is presented below. All authors reviewed and approved the final version of the manuscript.

	T.O.	N.B.
C	50	50
D	50	50
S	50	50
DCP	50	50
DAI	50	50
L	50	50
W	50	50
CR	50	50
SR	50	50
PM	50	50
FA	50	50

C=Concept, D= design, S= supervision, DCP= data collection and/or processing, DAI= data analysis and/or interpretation, L= literature search, W= writing, CR= critical review, SR= submission and revision, PM= project management, FA= funding acquisition.

Conflict of Interest

The authors declared that there is no conflict of interest.

Ethical Consideration

This study was carried out with the approval of Üsküdar University Academic Ethics Committee (decision dated 19.08.2020)

Acknowledgements

This study was produced from a master's thesis.

References

- Abukhashabah E, Summan A, Balkhyour M. 2020. Occupational accidents and injures in construction industry in Jeddah city. Saudi J Biol Sci, 27(8): 1993-1998.
- Aminbakhsh S, Gündüz M, Sonmez R. 2013. Safety risk assessment using analytic hierarchy process (ahp) during planning and budgeting of construction projects. J Safety Res, 46: 99-105.
- Arıtan AE, Ataman M. 2017. Occupational accident analysis with accident rate calculations. Afyon Kocatepe Univ J Sci Eng, 17: 239-246.
- Badri A, Nadeau S, Gbodossou A. 2011. Integration of OHS into risk management in an open-pit mining proect in Quebec Canada. Minerals, 1(1): 3-29.
- Balçı B, Taçkın E, Balçı EÖ, Yerden A. 2013. Financial loss in labor accidents. İstanbul J Sci, 6: 66-83.
- Banerjee K, Kumar MS, Tilak LN. 2021. Delineation of potential groundwater zones using analytical hierarchy process (AHP) for Gautham Buddh Nagar District Uttar Pradesh India. Mater Today, 44: 4976-4983.
- Bao J, Johansson J, Zhang J. 2017. An occupational disease assessment of the mining industry's occupational health and safety management system based on FMEA and an improved AHP model. Sustainability, 9(1): 94.
- Bao J, Zhang J, Li F, Liu C, Shi S. 2016. Social benefits of the mine occupational health and safety management systems of mines in China and Sweden based on a fuzzy analytic hierarchy process: a comparative study. J Intell Fuzzy Syst, 31(6): 3113-3120.
- Barriuso AR, Escribano BM, Saiz Rodriguez A. 2020. The importance of preventive training actions for the reduction of workplace accidents within the Spanish construction sector. Safety Sci, 134: 105090.
- Bayrak S. 2018. General view of the construction industry in Turkey in terms of the concept of decent work. Work Society, 3(58): 1531-1554.
- Bayraktar B, Uyguçgil H, Konuk A. 2018. Statistical analysis of occupational accidents in the Turkish mining industry. Sci Mining J, 57: 85-90.
- Bilim A, Çelik O. 2018. General assessment of work accidents caused in construction sector in Turkey. Niğde Ömer Halisdemir Univ J Eng Sci, 7(2): 725-731.
- Bingöl N. 2018. The place and importance of education in reducing occupational accidents and occupational diseases in construction works. OHS Acad, 1(1): 24-49.
- Bingöl S. 2010. Occupational accident frequency and some effecting factors in work places of metal industry in Nilufer industrial zone. MSc Thesis, Uludag University, Faculty of Medicine, Department of Public Health, Bursa, Türkiye, pp: 80.
- Boyacı Çalış A, Solmaz M. B, Kabak M. 2021. A model proposal for occupational health and safety risk assessment based on

- multi- criteria hesitant fuzzy linguistic term sets: an application in plastics industry. *J Fac Eng Architect Gazi Univ*, 36: 1041-1053.
- Çetin A. 2019. Performance evaluation with fuzzy topsis and ahp methods: an application at Esenboğa airport. MSc Thesis Gazi University, Institute of Social Sciences, Ankara, Türkiye, pp: 122.
- Cheng CW, Leu SS, Lin CC, Fan C. 2010. Characteristic analysis of occupational accidents at small construction enterprises. *Safety Sci*, 48: 698-707.
- Dağdeviren M, Tamer E. 2001. The use of analytical hierarchy process and 0-1 goal programming methods in supplier selection. *J Gazi Univ Fac Eng Architect*, 16(1): 41-52.
- Dağdeviren M. 2008. Decision making in equipment selection: an integrated approach with AHP and PROMETHEE. *J Intell Manufact*, 19(4): 397-406.
- Dede T, Baltacı Y. 2019. Perceptibility of occupational safety regulations in the construction industry. *Duzce Univ J Sci Technol*, 7: 1087-1099.
- Denizhan B, Yalçın AY, Berber Ş. 2017. Green supplier selection application using analytical hierarchy process and fuzzy analytical hierarchy process methods. *Nevşehir Sci Technol J*, 6(1): 63-78.
- Hola B, Szostak M. 2017. An occupational profile of people injured in accidents at work in the police construction industry. *Procedia Eng*, 208: 43-51.
- Keçek G, Yıldırım E. 2010. Selection of enterprise resource planning (erp) system with analytical hierarchy process (ahp): an application in automotive industry. *Süleyman Demirel Univ Fac Econ Administ Sci J*, 15(1): 193-211.
- Kim KD, Park S. 2021. An analysis of the effects of occupational accidents on corporate management performance. *Safety Sci*, 138: 1-8.
- Korkusuz AY, İnan UH, Özdemir Y, Başlıgil H. 2019. Measuring occupational health and safety performance in the health sector with integrated multi-criteria decision-making methods. *J Gazi Univ Fac Eng Architect*, 35(1): 81-96.
- Kuruüzüm A, Atsan N. 2001. Analytical hierarchy method and its applications in the field of business. *Akdeniz FEAS J*, 1(1): 83-105.
- Lin C, Kou G. 2021. A heuristic method to rank the alternatives in the ahp synthesis. *Appl Soft Comput*, 100: 106916.
- Lyu HM, Zhou WH, Shen SL, Zhou AN. 2020. Inundation risk assessment of metro system using AHP and TFN-AHP in Shenzhen. *Sustain Cities Society*, 56: 102103.
- Özcan SG, Yıldızbaşı A, Eraslan E. 2019. Evaluation of construction firms with fuzzy group decision-making approach in the context of OHS. *J Indust Eng*, 30(3): 204-219.
- Özcan Z. 2018. Synthetic macro fibers in reinforced concrete elements experimental research of usability II. *International Symposium on Natural Hazards and Disaster Management*, May 04-06, Bursa, Türkiye, pp: 955-961.
- Saaty T. 1987. The analytic hierarchy process-what it is and how it is used. *Mat/D Model*, 9(3-5): 161-176.
- SGK. 2021. İş Kazası verileri. URL: <https://www.sgk.gov.tr/Istatistik/Yillik/fcd5e59b-6af9-4d90-a451-ee7500eb1cb4> (access date: November 10, 2021).
- Soyalan F. 2020. Investigation of the effects of macro synthetic fiber use on the behavior of concrete beams. MSc Thesis, İskenderun Technical University, Institute of Engineering and Science, İskenderun, Türkiye, pp: 119.
- Tehlike Sınıfları Tebliği. 2012. İş sağlığı ve güvenliğine ilişkin işyeri tehlike sınıfları tebliği. URL: <https://www.resmigazete.gov.tr/eskiler/2012/12/20121226-11.htm> (access date: March 01, 2021).
- Türk Tabipleri Birliği. 2021. URL: http://www.ttb.org.tr/mevzuat/index.php?option=com_content&view=article&id=923:-salii-ve-gueven-kanunu&Itemid=28 (access date: March 01, 2021).
- Yılmaz Oral T, Ünal A. 2020. Evaluation of occupational accident data of the travel industry between 2016-2018. *OHS Acad*, 3(2): 61-72.



AMNİYOTİK SIVIDA SÜKSİNİLASETONUN ELEKTROKİMYASAL DAVRANIŞI VE TAYİNİ

Saadet Meral KARACAN¹, Behice YAVUZ ERDOĞAN^{2*}, Atiye Nur ONAR³

¹Samsun Public Health Laboratory, 55060, Samsun, Türkiye

²Ondokuz Mayıs University, Terme Vocational School, Department of Food Processing, 55600, Samsun, Türkiye

³Ondokuz Mayıs University, Faculty of Science, Department of Chemistry, 55105, Samsun, Türkiye

Özet: Süksinilaseton (SA, 4,6 diketoheptanoik asit), kalıtsal hepatorenal tirozinemi tip I hastalığı için birincil tanı metabolitidir. Bu çalışma ile süksinilasetonun amniyon sıvısında voltametrik tayinini amaçlanmıştır. Voltametri için optimum koşullar belirlenmiştir. Destek elektrolit için 0,10 mol/L potasyum klorür kullanılmıştır. Çalışmada, asılı civa damlası (HMDE) çalışma elektrotu olarak seçilirken, referans elektrot Ag/AgCl (3M KCl), karşıt elektrot Pt olarak kullanılmıştır. Kalibrasyon için kare dalga voltametri kullanılmış, bu yöntem amniyotik sıvıya uygulandığında, süksinilaseton ekstraksiyon işleminin, metil ester oluşturduğu tespit edilmiştir. Süksinilaseton metil esteri, yapısız olarak süksinilasetondan farklı olduğu için elektrokimyasal davranışı tekrar çalışılmıştır. Voltametrik inceleme, süksinilaseton metil esterinin iki elektron transferi ile indirgeniğini göstermiştir. Doğrusallık aralığı $5,83 \times 10^{-5}$ – $3,25 \times 10^{-6}$ mol/L derişimleri arasındadır. Tespit limiti (LOD) ve tayin limiti (LOQ) sırasıyla $2,72 \times 10^{-7}$ mol/L ve $9,08 \times 10^{-7}$ mol/L olarak hesaplanmıştır. Amniyotik sıvı içindeki süksinilaseton metil esteri kare dalga voltametri ile analiz edilmiştir. Geri alınabilirlik %88,1 bulunmuştur.

Anahtar kelimeler: Süksinilaseton, Süksinilaseton metil ester, Voltametri


Electrochemical Behavior and Determination of Succinylacetone in Amniotic Fluid


Abstract: Succinylacetone (SA, 4,6 diketoheptanoic acid) is the primary diagnosis metabolite for hereditary hepatorenal tyrosinemia type I disease. In present research, voltammetric analysis of succinylacetone was aimed. The optimum conditions for voltammetry were determined. Optimum conditions for voltammetry were determined. Potassium chloride 0.10 mol/L was selected for the support electrolyte. For the experiments, hanging mercury drop (HMDE), Ag/AgCl (3M KCl) reference and Pt counter electrodes were used. Square wave voltammetry was used for calibration and when this method was applied to amniotic fluid, succinylacetone extraction process was found to form methyl ester. Since succinylacetone methyl ester has a different structure than succinylacetone, its electrochemical behavior was re-examined. Voltammetric data reveal that succinylacetone methyl ester is reduced by accepting two electrons. For calibration, concentrations in the range of 3.25×10^{-6} mol/L – 5.83×10^{-5} mol/L were used. From the calibration chart, the limit of detection (LOD) was found to be 2.72×10^{-7} mol/L and the limit of determination (LOQ) was 9.08×10^{-7} mol/L. Succinylacetone methyl ester in amniotic fluid was analyzed by square wave voltammetry. The recoverability was found to be 88.1%.


Keywords: Succinylacetone, Succinylacetone methyl ester, Voltammetry

*Sorumlu yazar (Corresponding author): Ondokuz Mayıs University, Terme Vocational School, Department of Food Processing, 55600, Samsun, Türkiye

E mail: berdogan@omu.edu.tr (B. YAVUZ ERDOĞAN)

Saadet Meral KARACAN  <https://orcid.org/0000-0001-6060-3231>

Behice YAVUZ ERDOĞAN  <https://orcid.org/0000-0003-4375-4323>

Atiye Nur ONAR  <https://orcid.org/0000-0001-8984-7758>

Gönderi: 02 Ocak 2024

Kabul: 01 Şubat 2024

Yayınlanma: 15 Mart 2024

Received: January 02, 2024

Accepted: February 01 2024

Published: March 15, 2024

Cite as: Karacan SM, Yavuz Erdoğan B, Onar AN. 2024. Electrochemical behavior and determination of succinylacetone in amniotic fluid. BSJ Eng Sci, 7(2): 214-222.

1. Giriş

Genetik hastalıkların pek çoğunun henüz tedavisi bulunmamaktadır. İnsanlar genetik bir rahatsızlık tehlikesi taşıyabilir. Fakat bu risk kimi ailelerde daha çoktur. Kalıtım uzmanları, yetişkin bireyler ve çocuklarda oluşabilecek kalıtsal rahatsızlık tehlikelerini saptayabilir (Anonim, 2010). Bugünlerde kalıtsal rahatsızlıkların önceden belirlenebilmesi, meydana gelebilecek kusurların önlenmesini, iyileşme şansı olmayan rahatsızlıklarda yaşam süresinin uzatılmasını ve yaşam kalitesinin artırılmasını sağlayabilmektedir.

Tirozin, hem bitkisel hem de hayvansal birçok proteinin yapısında olan, aynı zaman da karaciğerde parçalanmış bir aminoasittir. Tirozinemi, tirozin metabolizmasının

resesif, otozomal bir hastalık sınıfıdır. Bu hastalık grubunda; geçici tirozinemi, tirozinemi tip I, tirozinemi tip II, tirozinemi tip III bulunmaktadır.

Geçici tirozinemi, yeni doğmuş bebeklerde 4-hidroksifenilpiruvat dioksigenaz enziminin fizyolojik şekilde olgunlaşmaması halinde görülebilir. Tirozinemi tip I, fumarilasetoasetaz hidrolaz (FAH); tirozinemi tip II, tirozin aminotransferaz ve tirozinemi tip III ise 4-hidroksifenilpiruvat dioksigenaz eksikliğinde oluşmaktadır.

Tirozinemi tip I, akut veya kronik biçimde seyredebilir. Bu durum FAH enziminin miktarı ile yakında ilişkilidir. Hastalık ile oluşan klinik bulgular, büyüme güçlüğü, kusma, diyare, ateş, hepatit, ödem, karaciğer büyümesi



şeklinde emareler ve hatta ölümlü sonuçlanabilecek ileri boyutta karaciğer rahatsızlığı da olabilir (Macşai ve ark., 2001, Shinka ve ark., 2005).

Genetik ve bazı metabolik hastalıklar, aminoasitlerin takibi veya plazma, idrar, amniyon sıvısı gibi biyolojik ortamlarda organik asitlerin tayini ile belirlenebilir. Ceninin korunması ve fetal organların gelişiminde amniyon sıvısının rolü büyüktür. Genellikle otuzbeş üzeri ileri yaş hamileliklerinde yada cenin gelişiminde bir anormallik olursa, amniyon sıvısı incelenir (Tuma ve ark., 2006).

Tirosinemi tip I'in teşhisinde kullanılan tayin metodlarının çoğu gaz kromatografi (GC) ve sıvı kromatografi (LC) gibi kromatografik yöntemlerdir ve bu tekniklerde genellikle dedektör olarak kütle spektrometresi (MS) kullanılır. Klinik laboratuvarlarda çoğunlukla idrarda ve serumda süksinilaseton tayini için GC/MS kullanılmaktadır (Cry ve ark., 2006). Tandem kütle spektrometresi (MS/MS), yenidoğan taraması (NBS) uygulamaları için kurutulmuş kan lekelerinde kullanılır. LC-MS/MS, FIA-MS/MS veya genomik tarama da dahil olmak üzere diğer yöntemlerin yetersiz kaldığı durumlarda uygulanır (Michael ve ark., 2022). Bu tekniğin uygulanması için, örneklerdeki ön işlemler, türevlendirme, analiz süresi, çok fazla miktarda kimyasal kullanımları ve pahalı yöntemler olmalarıdır.

Elektrokimyasal yöntemler, hassasiyeti yüksek ve çok yönlü analitik tekniklerdir. Elektrokimyasal ölçümler iki boyutlu tekniklerdir. Niteliksel özellikler, termodinamik veya kinetik kontrolle belirlenebilir, niceliksel özellikler, ilgili akımın kütle taşıma süreci veya reaksiyon hızları tarafından kontrol edilir. Böylece, bileşikler seçici olarak elektrokimyasal yöntemlerle tespit edilir. Benzerlik nedeniyle elektrokimyasal ve biyolojik reaksiyonlarda, yükseltgenme/indirgenme mekanizmalarının elektrotta ve vücutta benzer prensipleri paylaşmaktadır. Biyolojik olarak önemli moleküller voltametri ile elektroanalitik olarak incelenirler. Voltametri doğruluğu ve kesinliği yüksek nispeten düşük maliyetli bir akım-voltaj tekniğidir. (Uslu ve Ar., 2004).

Bildiğimiz kadarıyla, süksinilaseton veya süksinilaseton metil esterini için HMDE ile uygulanan voltametrik ve elektrokimyasal davranışın sunulduğu bir yöntem literatürde yoktur. Bu çalışmada önce süksinilaseton çalışılmıştır. Sonra gerçek numune incelenmeye başlandığında görülmüştür ki, süksinilaseton ambiyotik sıvıda süksinilaseton metil esterine dönüşmektedir. Bunun üzerine voltametrik çalışmalarda başa dönülüp, süksinilaseton metil esterini üzerine yoğunlaşmıştır.

2. Materyal ve Yöntem

Elektrokimyasal ölçümler, Gamry Instruments (Reference600 Potentiostat/Galvanostat/ZRA, Warminster USA) ile üç elektrot içeren bir hücre kullanılarak yapılmıştır. Kullanılan elektrotlar: HMDE çalışma elektrodu, platin (Pt) tel karşıt elektrot ve Ag/AgCl (3M KCl) referans elektrotudur. İnfrared spektrumları, Bruker Vertex 80V marka infrared (IR)

spektroskopisi cihazı ile çekilmiştir. İnce tabaka için Silikagel F 25, çözelti pH'ı için Jenway 3040 iyon /pH metre, Eutech Instrument kombine cam elektrot kullanılmıştır. Ultra saf su için Millipore (Simplicity) marka saflaştırma sistemi kullanılmıştır.

Tüm kimyasallar analitik reaktif sınıfındadır. Süksinilaseton (SA) (Sigma), potasyum klorür, fosforik asit, sodyum hidroksit, metil alkol, XAD-4, petrol eteri, hidroklorik asit (Merck) kullanılmıştır.

Stok standart çözelti (1,70x10⁻³ mol/L) süksinilaseton tartılarak ve su ile seyreltilerek hazırlanmıştır. Standart çalışma çözeltileri stoktan seyreltilerek günlük olarak hazırlanmıştır. Tüm çözeltiler 0,45 µm membran filtreden (Millipore) süzülüş ve soğutucuda (4°C) tutulmuştur.

2.1. Örneklerin Hazırlanması

0,1 M, pH'ı 3,0 olan fosforik asit tamponu; H₃PO₄ kullanılarak hazırlanmış ve pH'ı sodyum hidroksit ile ayarlanmıştır. Tüm prosedürde ultra saf su kullanılmıştır. Ondokuzmayıs Üniversitesi Tıp Fakültesi Tıbbi Genetik Anabilim Dalı bünyesinde, alışagelmış çalışmalar için kullanılan, aynı zamanda genetik analizi tamamlanan amniyotik sıvılarda çalışılmıştır. Amniyotik ortamda süksinilaseton miktarını belirlemek için ön işlem olarak ekstraksiyon, tayin için voltametrik metod çalışmıştır. Amberlit XAD-4 (2,5 g) amniyotik sıvıdan süksinilaseton ekstrakte etmek için belirlenmiştir. Önce reçine üzerine 2 mL su, ardından 50 mM, pH'ı 2,0 olan 2 mL fosfat tamponu ve son olarak 2 mL metanol geçirerek aktive edilmiştir. Aktive olan XAD-4 ten 4 mL amniyotik sıvı, 12 mL, 50 mM pH'ı 2 olan fosfat tamponu geçirildikten sonra 12 mL metil alkol içine ekstrakt alınmıştır.

2.2. Esterleşme

Çalışma sırasında amniyotik sıvı içerisinde asidik ortamda metil alkol ile ester oluşumu tespit edilmiş. Çalışmaları ester ile devam ettirmek adına ester elde edilmiştir. Bu amaçla 1N HCl bulunan ortama süksinilaseton ve metanol (1:1:1) oranda eklenmiştir (Cerda ve ark., 2008). Reaksiyonun oluşum koşulları; 30 dk., 39 °C'lık su banyosunda bekletilerek gerçekleştirilmiştir. Ester oluşumu infrared spektrumları alınarak kanıtlanmıştır.

2.3. Elektrokimyasal Ölçümler

Civa elektrot ile kare dalga (SQW) ve dönüşümlü voltametri (CV) çalışılmıştır. Voltametrik hücre içerisine 10 mL ilave edilen destek elektrolit çözeltisinden 5 dakika boyunca azot gazı geçirilir. Destek elektrolit çözeltisinin voltamogramı alındıktan sonra voltametrik hücreye süksinilaseton stok çözeltisi eklenmiş ve 2 dakika azot gazı geçirildikten sonra tekrar voltamogram alınmıştır. Ancak yapılan çalışmalarda Ag/AgCl elektroduna karşı -1,684V potansiyelde süksinilaseton piki doğrudan amniyon sıvısı seyreltilerek kullanıldığında bu bölgeyi yayvan şekilde örten bir pik nedeni ile belirlenememiştir. Sonrasında ekstraksiyon yapılmış ve voltamogramı alınmıştır. Burada farklı bir pik gözlenmiştir. Konu üzerine araştırma yapıldığında görülmüştür ki süksinilaseton metil alkol ile süksinilaseton metil

esterine dönüşebilmektedir. Emin olmak için infrared (IR) spektrometri ve ince tabaka kromatografi (TLC) ile çalışılmış ve süksinilaseton metil esterinin süksinilasetondan farkı incelenmiştir. Tüm bunların sonrasında süksinilaseton için yapılan çalışmalar süksinilaseton metil esteri için güncellenmiştir.

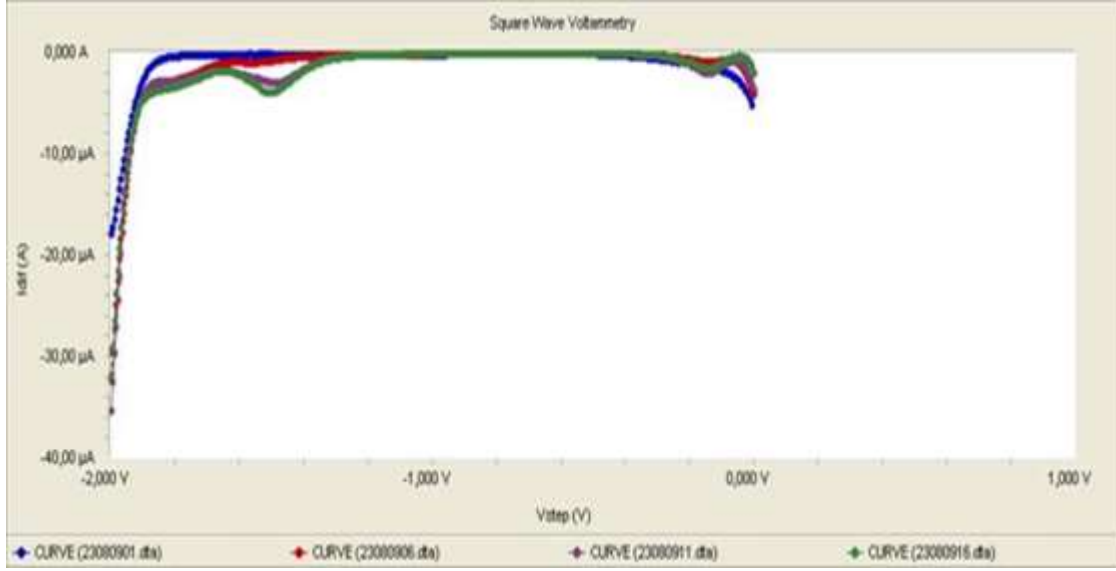
2.4. İnce Tabaka Çalışması

Süksinil aseton metil esterinin dönüşümünü izlemek için, süksinil aseton ve ekstraksiyon sonrası elde edilen ürün ince tabaka kromatografi ile incelenmiştir. Bu işlem için Silikagel F 25 marka, 60A⁰ partikül boyutuna sahip

silikajel ile kaplı ince tabaka plakaları ve yürütücü olarak, metil alkol ve petrol eteri (3:2) karıştırılarak kullanılmış ve deney sonrası lekeler UV(254 nm) ışığı ile tespit edilmiştir.

3. Bulgular ve Tartışma

Çalışmanın en başında süksinil aseton ile yöntem oluşturulup gerçek numunelere geçme aşamasında iken amniyon sıvısıyla direk çalışmanın mümkün olmadığı belirlenmiştir. Sonrasında ekstraksiyon yapılmış ve voltamogramı alınmıştır (Şekil 1).



Şekil 1. (0,1)M KCl çözeltisinde, amniyotik sıvıdan ekstrakte edilen süksinilaseton için kare dalga voltamogramı. 0,01 V, potansiyel adımı, 100 Hz, frekans; (-2,0 ve 0) V potansiyel aralığı.

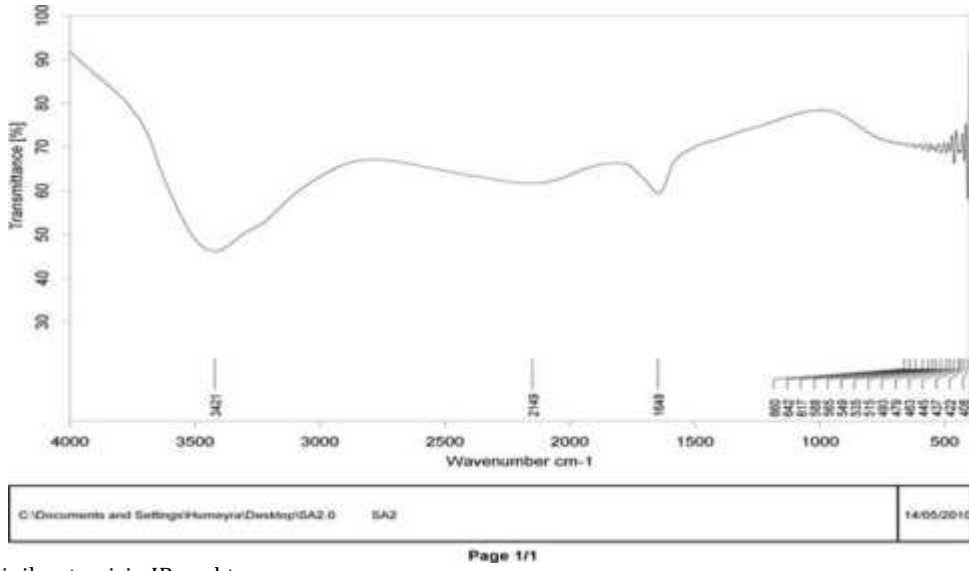
Burada farklı bir bölgede oluşan bir pik gözlenmiştir. Konu üzerine literatür araştırması yapıldığında görülmüştür ki süksinilaseton, asidik ortamda metil alkol ile süksinilaseton metil esterine dönüşebilmektedir. Bu dönüşümü daha iyi ortaya koyabilmek için, infrared spektrumu alınarak değerlendirilmiştir. Süksinilaseton ve yapılan süksinilaseton metil esteri için IR spektrumları Şekil 2 ve Şekil 3'de sunulmuştur. Süksinilaseton metil esteri olduğunu düşündüğümüz maddenin IR spektrumu süksinilasetona ait spektrumdan farklı şekilde 2953, 2842, 1109 ve 1016 cm⁻¹ de pikler vermiştir. IR spektrumundaki, 2953 cm⁻¹ ve 2842 cm⁻¹ deki pikler muhtemelen alifatik C-H fonksiyonel sınıfındadır. 2950 ve 2860 cm⁻¹ arası alifatik C-H alanıdır. 1641 ve 1648 cm⁻¹de görünen piklerin karbonil gruplarına ait olması muhtemeldir. Fakat ortamda çokça bulunan su IR absorpsiyonu yaptığı için pikler düşünülen daha küçük dalga sayılarında gelmiştir ve 1109 ve 1016 cm⁻¹de görünen pikler C-O-C (O=C-O-CH₃) grubunu temsil edebilir. Tüm bu veriler esterleşmenin meydana geldiğini düşündürmüştür.

Ayrıca, ince tabaka kromatografi ile süksinilasetonun ve süksinilaseton metil esteri arasındaki farklılık incelenmiştir (Şekil 4). Fotoğraftan anlaşıldığı üzere süksinilaseton, metanol ve petrol eteri, yürütücü faz ile

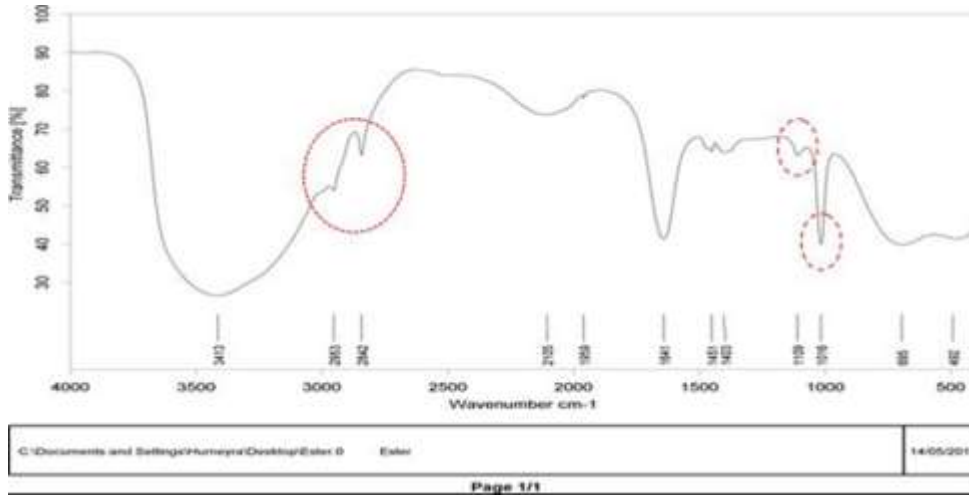
plaka üzerinde yol alırken süksinilasetonun metil esteri sabit kalmıştır. Sonuç süksinilasetonun ürüne (estere) dönüştüğünü göstermektedir. Tüm bunlardan sonra çalışmada yön süksinilaseton metil esterine çevrilmiştir.

Dönüşümlü voltametri yöntemiyle Süksinilaseton metil esteri çalışılmıştır. 0,1 M KCl içeren destek elektrolit, (-1,00V) – (-2,00V) potansiyel aralığında, 0,05V potansiyel adımında, 0,010 V potansiyel genişliğinde ve 50 Hz frekans ile uygulanmıştır. Voltamogramda Ag/AgCl'e karşı-1,723V potansiyelde bir indirgenme piki izlenmiştir. Yükseltgenme doğrultusunda herhangi bir pik bulunmadığı için, elektrokimyasal tepkimenin tersinir olmadığı sonucuna varılmıştır(Şekil 5). Bu yöntemdeki pik akımı ve pik potansiyel verileri kaydedilmiştir.

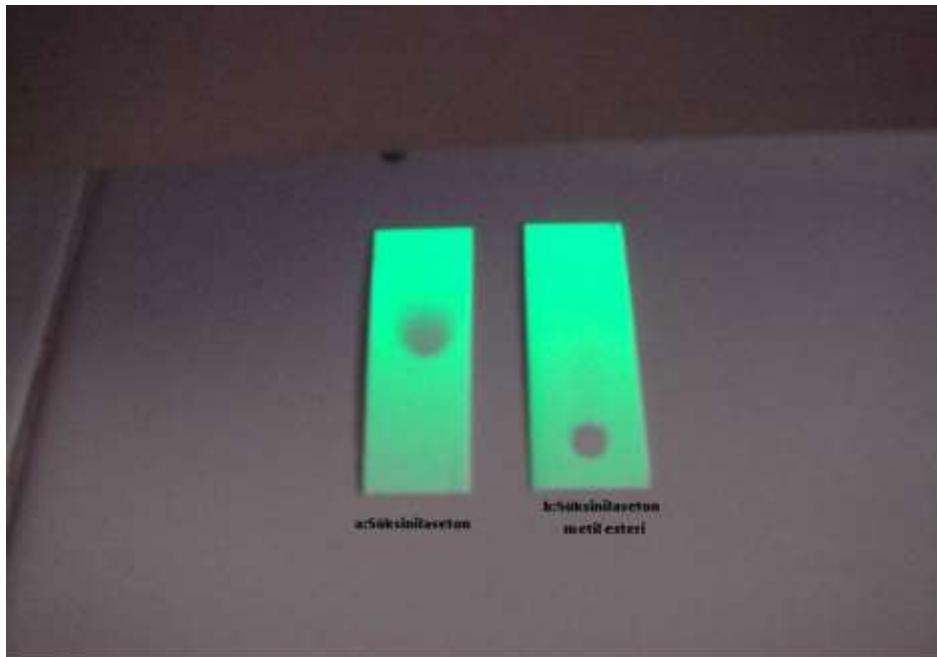
Akımın logaritmasına karşı tarama hızının logaritması grafiğe geçirildiğinde hazırlanan grafikteki eğri eğiminin 0,152 yani 0,5'ten küçük olduğu görülmüştür (Şekil 6). Bond ve arkadaşlarına göre bu eğim 0,5'ten büyük olması durumunda bileşiğin elektrot yüzeyinde adsorbe olduğu sonucuna varılır (Bond ve ark.,1980). Bu sebeple 1,95xE-05 M derişimde süksinilaseton metil esterinin indirgenme reaksiyonunun difüzyon kontrollü olduğu anlaşılmaktadır.



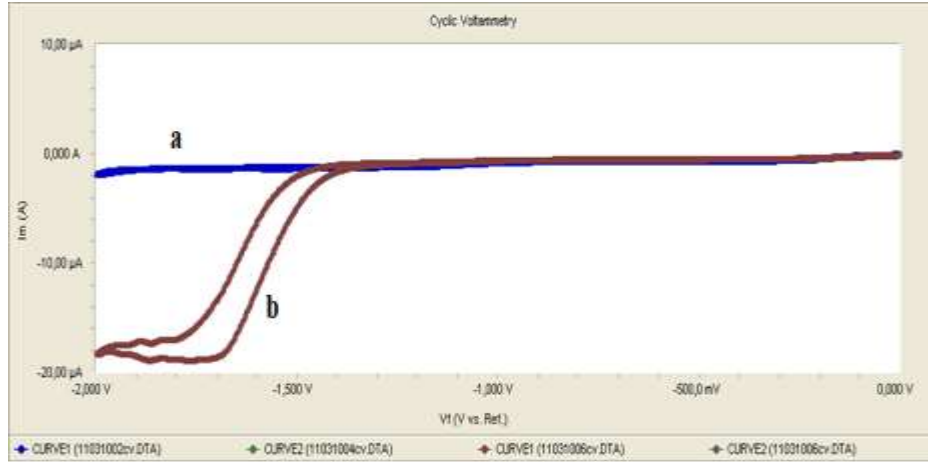
Şekil 2. Süksinilaseton için IR spektrumu.



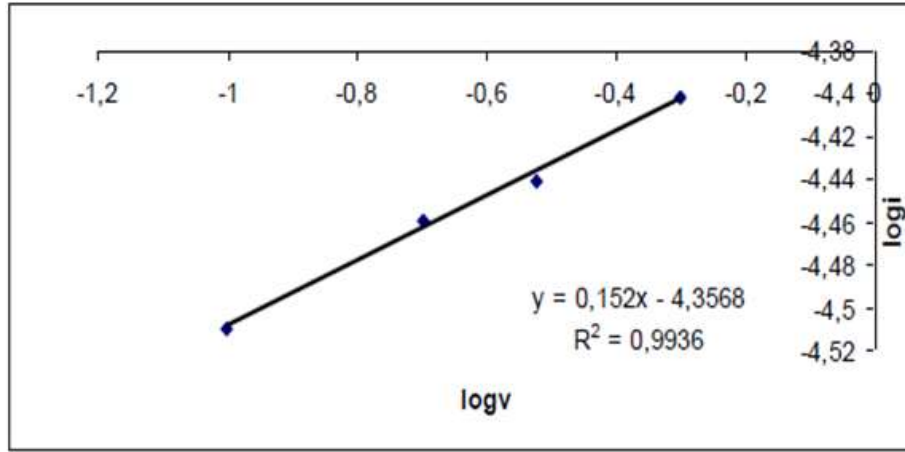
Şekil 3. Süksinilaseton metil esteri için IR spektrumu.



Şekil 4. Süksinilaseton ve süksinilaseton metil ester bileşiklerinin ince tabaka kromatografi plakaları üzerinde aldıkları yol. a) $4,57 \times 10^{-2}$ M süksinilaseton b) $2,28 \times 10^{-3}$ M süksinilaseton metil esteri.



Şekil 5. 1,95x10⁻⁵ M Süksinilaseton metil esterinin, 0,2 V tarama hızında dönüşümlü voltamogramı a) 0,1 M KCl çözeltisinde b) 0,1 M KCl çözeltisine 1,95x10⁻⁵ M süksinilaseton metil esterini ilavesi ile alınan dönüşümlü voltamogramlar.



Şekil 6. 1,95x10⁻⁵ M süksinilaseton metil esterinin, tarama hızı ve akımın logaritma grafiği.

Uslu ve arkadaşları, tarama hızı karekökü ile pik akımındaki doğrusal artışın, çalışılan CV de difüzyon kontrollü bir süreci gösterdiğini belirtmiştir (Uslu ve ark.,2004). Tarama hızının kareköküne karşı pik akım grafiği hazırlandığında pik için R²=0,8322 korelasyon katsayısı vermiştir (Şekil 7). Bu durumda difüzyon kontrolünü gösterir. Wang ve arkadaşları tarama hızının logaritmasının pik potansiyeline karşı grafiğe geçirildiğinde hazırlanan grafik doğru çıkmamışsa, bu durumda elektrokimyasal reaksiyonun difüzyon kontrollü olduğunu söylemişlerdir (Wang ve ark., 1986). Bu şekilde tarama hızının logaritmasının pik potansiyeline karşı hazırladığımız grafiğinde doğrusallık izlenmediği için Süksinilaseton metil esterinin indirgenme reaksiyonu difüzyon kontrollü olduğu sonucuna varılmıştır.

Tepkimede aktarılan elektron sayısını bulmak için akım örneklemeli polarografi ile çalışılmıştır. Destek elektrolit (0,1 M KCl) çözeltisi ve 1,05x10⁻⁴ M süksinilaseton metil esterini eklenerek akım örneklemeli polarografi çalışılmıştır. Bu yöntem ile alınan polarogramlar da süksinilaseton metil esterinin verdiği sınır akımı, id = 3,14x10⁻⁷ A ile yaklaşık -1,74 V potansiyelde izlenmiştir. Ardından, örneklemeli doğrusal tarama polarogramlarından elde

edilen veriler, potansiyele karşı log i/(id-i) grafiğini çizmek için kullanılmıştır. Bu grafikten elde edilen doğrunun eğimi 30,705 olarak bulunmuş ve eşitlik 1' de kullanılmıştır (Şekil 8).

$$m = \frac{nF}{22,303RT} \quad (1)$$

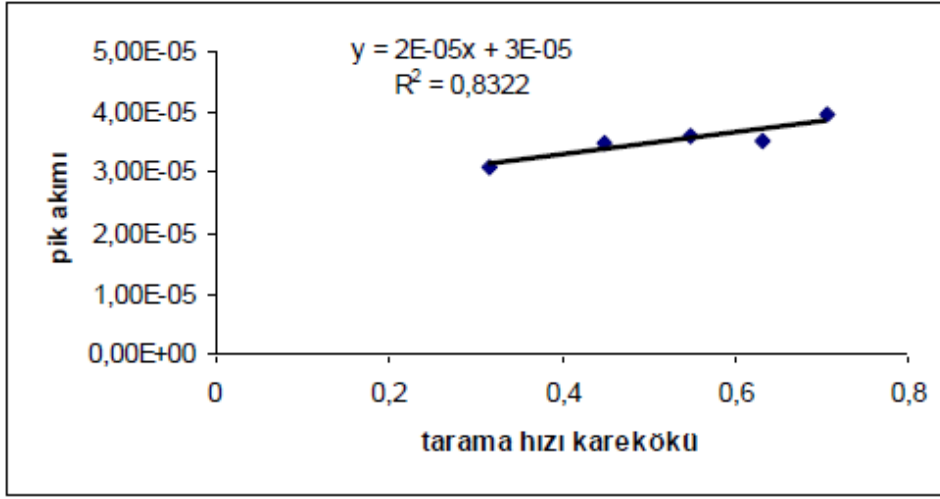
m: doğru eğimi;

R= ideal gaz sabiti (8,314 j/molK);

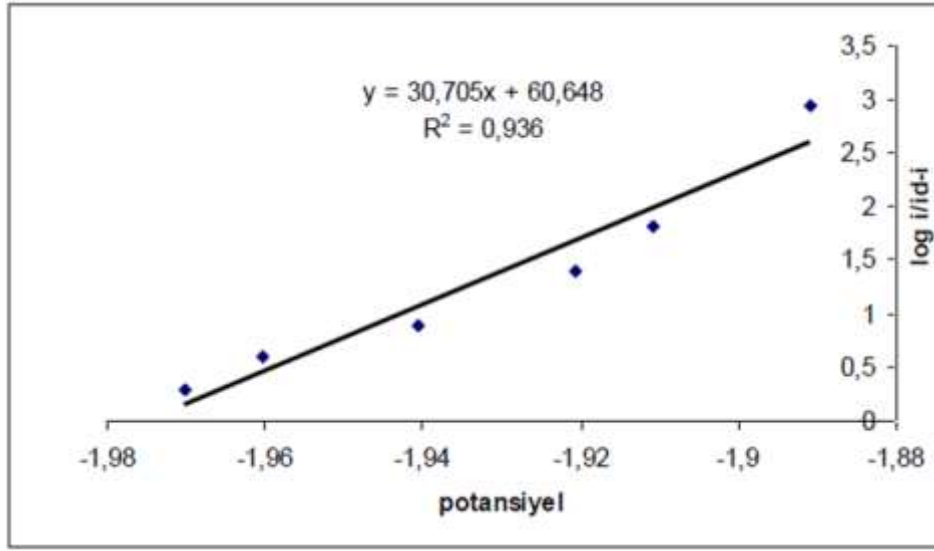
F= Faraday sabiti (96486); T: sıcaklık (K);

n: aktarılan elektron sayısı

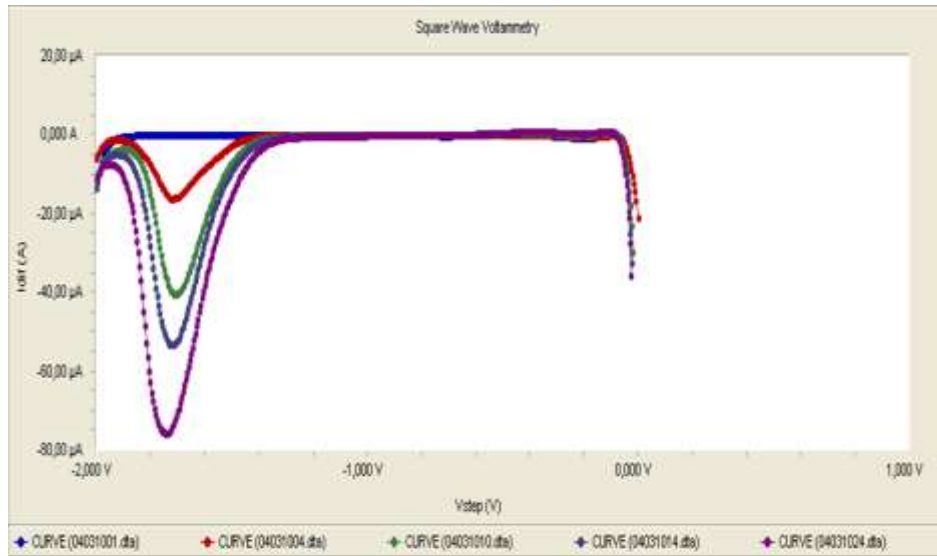
Eşitlik 1 de yapılan hesaplamalar sonrası n değeri 2 çıkar. Bu durum bize süksinilaseton metil esterinin elektrokimyasal reaksiyonda aktarılan elektron sayısının iki olduğunu vermektedir. Süksinilaseton metil esterinin kalibrasyon eğrisini hazırlamak için; süksinilaseton metil esterini kare dalga voltametri yöntemiyle 3,25x10⁻⁶ - 5,83x10⁻⁵ mol / L derişim aralığında çalışılmış, alınan voltamogramlar Şekil 9 ve Şekil 10' da sunulmuştur. Kalibrasyon eğrisi ile bulunan geçerlilik değerleri Tablo 1'de verilmiştir. Tabloya göre tespit sınırı (LOD) ve tayin sınırı (LOQ) değerleri sırasıyla 2,72x10⁻⁷ ve 9,08x10⁻⁷ M olarak bulunmuştur.



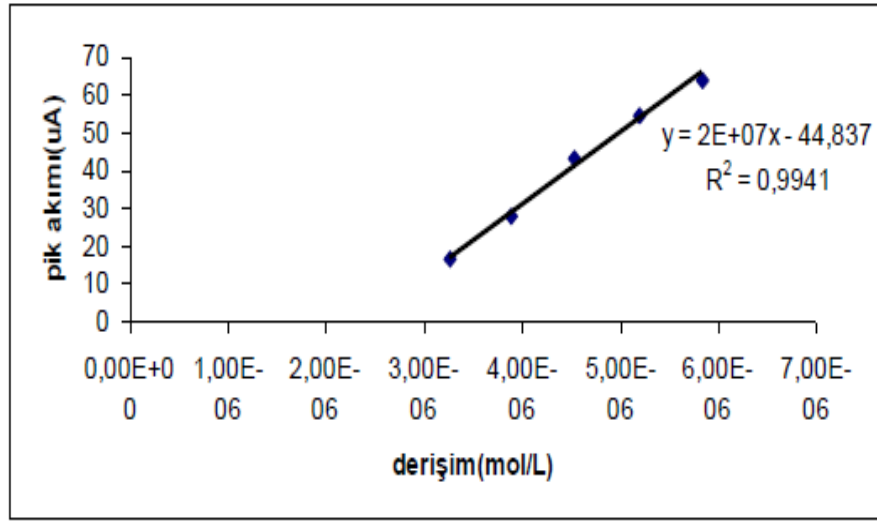
Şekil 7. 1,95x10⁻⁵ M süksinilaseton metil esterinin, tarama hızının kareköküne göre akım değerleri grafiği.



Şekil 8. 1,05x10⁻⁴ M süksinilaseton metil esterinin, tarama hızı; 0,05 V/s iken, potansiyele göre $\log i/(id-i)$ değişim grafiği.



Şekil 9. 0,1 M KCl çözeltisinde 3,25x10⁻⁶ – 5,83x10⁻⁵ M derişimleri arasında süksinilaseton metil esterinin kare dalga voltamogramları.



Şekil 10. Kare dalga voltametri ile 3,25x10⁻⁶ – 5,83x10⁻⁵ M derişim aralığındaki Süksinilaseton metil esteri için kalibrasyon eğrisi grafiğı.

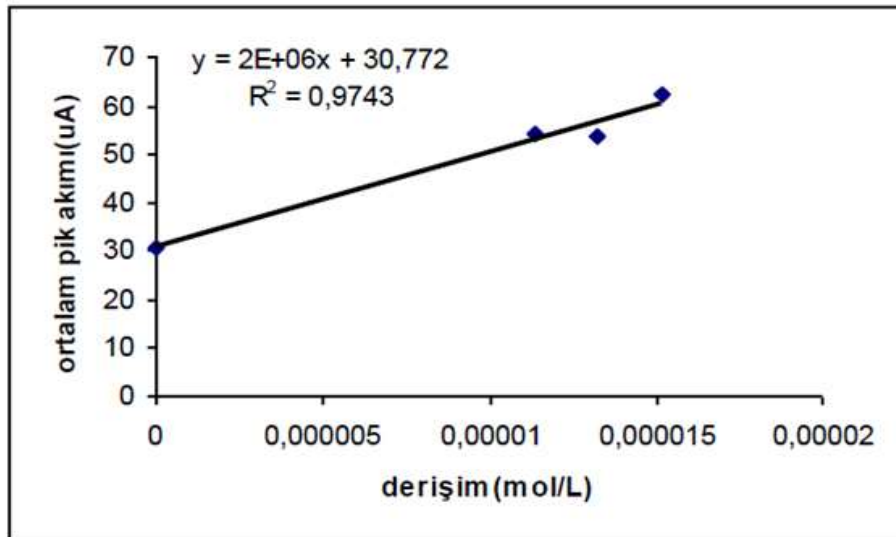
Tablo 1. Önerilen SQW yöntemi ile süksinilaseton metil esterinin doğrusal regresyon ve istatistiksel parametreleri

Parametre	Kare dalga voltametrik yöntem
Doğrusal Derişim Aralığı	3,25x10 ⁻⁶ – 5,83x10 ⁻⁵ M
Eğim	2,00x10 ⁷
Kesim Noktası	44,827
S _a *	3,90
S _b **	8,44x10 ⁻⁵
LOD	2,72x10 ⁻⁷
LOQ	9,08x10 ⁻⁷
Regresyon Katsayısı	0,9941

S_a* kesim noktasının standart sapması, S_b** eğimin standart sapması

Amniyon sıvısından süksinilaseton metil esterinin geri alınabilirliği için; Amniyotik sıvıya katılan süksinilaseton metil esterinin ve geri alınabilirlik değerlerini belirlemek

amacıyla standart ekleme yöntemi kullanılmıştır. Standart eklemede katılan süksinilaseton metil ester konsantrasyonları sırasıyla 1,13x10⁻⁵, 1,32x10⁻⁵ ve 1,52x10⁻⁵ mol/L olan çözeltilerdir. Kare dalga voltametri yöntemi sonucunda alınan voltamogramlardan elde edilen ortalama pik akımları - konsantrasyon grafiğı hazırlanmıştır. Bulunan doğrunun x ekseninden geçtiğı nokta amniyotik sıvıya eklenen süksinilaseton metil ester miktarının belirlenmesine olanak sağlamıştır (Şekil 11). Eklenen örneklerdeki süksinilaseton metil esterinin % geri alınabilirlik değerleri Tablo 2’de verilmiştir. Bu tabloya göre amniyon sıvılarında ise süksinilaseton metil esterinin geri alınabilirlik değeri ortalama %88,1 olarak bulunmuştur. Bu değerde yöntem validasyonunda bir kriter olarak kullanılan %80-120 aralığında yer almaktadır (Ermer ve ark., 2005). Süksinilaseton metil esteri, KCl destek elektrolit ortamında bir adet indirgenme piki vermektedir. Esterleşme mekanizması ve elektrot yüzeyinde gerçekleştiğı düşünölen mekanizma Şekil 12’de verilmiştir.

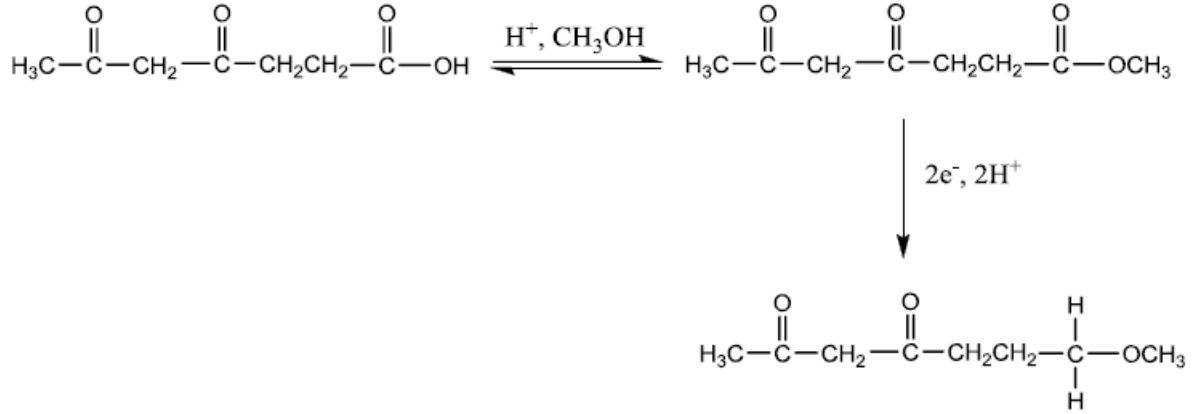


Şekil 11. Amniyon sıvısına eklenen süksinilaseton metil esteri miktarı ve geri alınabilirliğini tespit etmek için yapılan standart ekleme grafiğı.

Tablo 2. Eklenmiş örneklerdeki süksinilaseton metil esterinin % geri alınabilirlik değerleri*

Amniyon sıvısı	Eklenen süksinilaseton metil ester miktarı (M)	Geri alınan süksinilaseton metil ester miktarı (M)	% geri alınabilirlik
AS1	9,27xE-06	6,77x E-06	73,05(±0,99)
AS2	9,27x E-06	9,73 x E-06	104,96(±0,56)
AS3	9,27x E-06	8,63x E-06	88,76(±0,52)
AS4	9,27x E-06	7,94x E-06	85,63(±1,02)

*Her bir numune için üç kere ölçüm alınmıştır.



Şekil 12. Süksinilasetonun asidik ortamda metil alkol ile verdiği esterleşme tepkimesinin mekanizması.

4. Sonuç

Literatür araştırmalarında süksinilaseton ve süksinilaseton metil esterleri için amniyotik sıvıda civa elektrot ile elektrokimyasal davranışının açıklandığı bir çalışmaya rastlanmamıştır. Civa elektrotta ortaya çıkan indirgenme akımının difüzyon kontrollü olduğu elektrot yüzeyinde adsorplanmadığı açıklanmıştır. Süksinilasetonun amniyotik sıvıda esterleşme mekanizması verilmiştir. Önerilen voltametri yöntemi, süksinilaseton metil esterleri dolayısıyla süksinilaseton için amniyotik sıvıda kolaylıkla uygulanabilir. Önerilen analitik prosedür hem maliyet hem de zaman açısından basit ve ekonomiktir. Yöntemin geçerliliği ve geri alınabilirliği kabul edilebilir sınırlarda görünmektedir.

Katkı Oranı Beyanı

Yazar(lar)ın katkı yüzdesi aşağıda verilmiştir. Tüm yazarlar makaleyi incelemiş ve onaylamıştır.

	S.M.K.	B.Y.E.	A.N.O.
K	30	20	50
T		100	
Y		100	
VTI	90	10	
VAY	80	10	10
KT	60	40	
YZ		100	
KI		100	
GR		100	
PY	50	10	40
FA	50		50

K= kavram, T= tasarım, Y= yönetim, VTI= veri toplama ve/veya işleme, VAY= veri analizi ve/veya yorumlama, KT= kaynak tarama, YZ= Yazım, KI= kritik inceleme, GR= gönderim ve revizyon, PY= proje yönetimi, FA= fon alımı.

Çatışma Beyanı

Yazarlar bu çalışmada hiçbir çıkar ilişkisi olmadığını beyan etmektedirler.

Etik Onay Beyanı

Amniyotik sıvılar Ondokuzmayıs Üniversitesi Tıp Fakültesi Tıbbi Genetik Anabilim Dalı'ndan alınarak kullanılmış olup Ondokuz Mayıs Üniversitesi Klinik

Araştırma Etik Kurulundan etik kurul onayı alınmıştır (onay tarihi: 16 Nisan 2008, onay numarası: OMÜ Etik 2008/164).

Destek ve Teşekkür Beyanı

Bu çalışmanın Ondokuzmayıs Üniversitesinde OMÜ F-445 nolu proje kapsamında desteklenmiştir.

Kaynaklar

- Anonim. 2010. Prenantal Diagnosis. URL: <http://www.genetikbilimi.com/genbilim/prenantal.htm> (Erişim tarihi: 15 Haziran 2010).
- Bond AM. 1980. Modern Polarographic Methods in Analytical Chemistry. Marcel Dekker, New York, USA, pp: 196.
- Cerda B, Cherkasskiy A, Li Y. 2008. United States Patent Application Publication. Pub. No. US2008/0274563 A1.
- Cry D, Giguère R, Vilain, LB, Drouin R. 2006. A GC/MS validated method for the nanomolar range determination of succinylacetone in amniotic fluid and plasma: An analytical tool for tyrosinemia type I. *J Chromatogr B*, 832: 24-29.
- Ermer J, Miller JHM. 2005. Method validation in pharmaceutical analysis: A guide to best practice. In: Ermer J, Miller JHM editors. Wiley, VCH Verlag GmbH & Co. KGaA, Weinheim,

- Germany, pp: 200.
- Macsai MS, Schwartz TL, Hinkle D, Hummel MB, Mulhern MG, Rootman D. 2001. Tyrosinemia Type II: Nine Cases of Ocular Signs and Symptoms. *Am J Ophthalmol*, 132: 522-527.
- Michael HG, Khaja B, Alberto B, Hsiao-Jan C, Yin-Hsiu C, George D, Christine D, Roberto G, Amy H, Xinying H, Shu-Min K, Hamid K, Tracy K, Francyne K, Hsuan-Chieh L, Monica M, Adrienne M, Joseph O, Yin P, Enzo R, Andreas R, Nicolas SF, Coleman TT, Frédérick MV, Li-yun W, Dietrich M. 2022. Liquid chromatography–tandem mass spectrometry in newborn screening laboratories. *Int J Neonatal Screen*. 8,4: 62.
- Shinka T, Ohse M, Inoue Y, Kuhara T. 2005. Stability of 5-aminoevulenic acid on dried urine filter paper for a dignostic marker of tyrosinemia type I. *J Chromatogr B*, 823: 44–46.
- Tuma P, Samcova E, Anđelova K. 2006. Determination of free amino acids and related compounds in amniotic fluid by capillary electrophoresis with contactless conductivity detection. *J Chromatogr B*, 839:12-18.
- Uslu B, Ozkan SA. 2004. Anodic voltammetry of abacavir and its determination in pharmaceuticals and biological fluids *Electrochim Acta*, 49(25): 4321–4329.
- Wang J, Tuzhi P, Lin MS and Tapia T. 1986. Trace measurements of the antineoplastic agent methotrexate by adsorptive stripping voltammetry. *Talanta*, 33 (9): 707-712.



VOXEL-BASED MORPHOMETRY OF OPTIMISTIC AND PESSIMISTIC BRAINS: A DETAILED STUDY FOCUSING ON AGE RANGE AND GENDER

Pınar OZEL^{1*}


¹Istanbul University, Cerrahpasa, 34098, İstanbul, Türkiye

Abstract: The aim of the present study was to investigate brain volumes in pessimist and optimist participants. Therefore, in the present voxel-based morphometry research, it is investigated whether optimism has a corresponding counterpart in the structure of the brain. Thirty-two participants were screened via a publicly available dataset to test for this. The participants are divided into two groups: low optimists and high optimists, each with sixteen people. In comparison, a significant difference ($P < 0.05$) was not found between the groups we created as a result of statistical calculations; however, statistically significant results ($P < 0.001$) were obtained via a detailed VBM analysis in many brain regions, especially the thalamus, amygdala, left insula, superior frontal gyrus, and right cerebellum regions. These differences were identified and reported.

Keywords: Voxel based morphometry, Magnetic resonance imaging, Optimistic, Pessimistic

*Corresponding author: Istanbul University, Cerrahpasa, 34098, İstanbul, Türkiye

E mail: pozell@gmail.com (P. OZEL)

Pınar OZEL  <https://orcid.org/0000-0002-9688-6293>

Received: November 30, 2023

Accepted: February 02, 2024

Published: March 15, 2024

Cite as: Ozel P. 2024. Voxel-based morphometry of optimistic and pessimistic brains: A detailed study focusing on age range and gender. BSJ Eng Sci, 7(2): 223-236.

1. Introduction

Interpretations of events, whether pessimistic or optimistic, influence emotional reactions and cognitive processing. Optimism leads to positive outcomes and positive psychological adjustments, while pessimism leads to persistent anticipations and poorer outcomes (Levens and Gotlib, 2012).

Optimistic bias, prevalent across genders, ages, and countries, can lead to increased risk-taking and decreased preventative measures, while also calming the mind and alleviating stress, requiring education and awareness. Therefore, society must study and educate on how false optimism can damage our daily lives and self-esteem.

Brain morphometry refers to the scientific procedure of quantifying the dimensions, typically in terms of volume, of different structures within the brain. The assessment of macroscopic gray matter (GM) asymmetries with a high level of regional specificity is a crucial aspect in brain imaging methodologies, and Voxel Based Morphometry (VBM) stands out as one of the most significant approaches. VBM enables the differentiation of local GM concentration levels at the voxel level, facilitating comparisons between distinct groups or the right and left cerebral hemispheres. The VBM methodology encompasses the process of spatially normalizing structural magnetic resonance imaging (sMRI) scans obtained from all individuals to a standardized stereotactic space. Subsequently, the

process of segmentation is executed to partition the image into distinct regions representing GM and white matter (WM). The GM sections are then subjected to a smoothing operation in order to enhance the overall visual quality. Following the application of a smoothing technique to the GM images, voxelwise statistical tests are conducted in order to establish comparisons between the groups or between the right and left hemispheres (Whitwell, 2009; Ocklenburg and Güntürkün, 2018).

Neuroimaging technologies like functional magnetic resonance imaging (fMRI), MRI, and event-related potential (ERP) (Alessandri and De Pascalis, 2017) are being used to study optimism and pessimism. VBM and MRI are used to explore resting-state functional connectivity (RS-FC), often using a region of interest seed approach (Ran et al., 2017). Other resting-state metrics include fractional amplitude of low-frequency fluctuations (f-ALFF) and regional homogeneity (RegHom) (Jiang and Zuo, 2016), which measure brain connections and abnormally localized functioning (Egorova et al., 2017).

Studies show that optimism is correlated with GM in the orbitofrontal cortex (OFC), bilateral putamen, and thalamus, while the rostral anterior cingulate cortex (rACC) and the inferior frontal gyrus (IFG) are critical for self-referential processing and information suppression (Aberg, 2021). Ran et al. (2017) found that dispositional optimism is significantly linked to the strength of the RS-FC between the ventromedial prefrontal cortex (vmPFC)



and the middle temporal gyrus (mTG), and negatively associated with the RS-FC between the vmPFC and IFG. Yang et al. (2013) found that optimism is linked to increased gray matter volume (GMV) in the pulvinar/thalamus region, extending to the posterior part of the parahippocampal gyrus, suggesting that individuals with higher optimism may be more adept at emotion regulation. Dolcos et al. (2016) found a significant correlation between increased GMV in the left lateral OFC and optimism in healthy adults, highlighting the link between personality and brain characteristics. Lai et al. (2020) study found that increased bilateral putamen regional GM density significantly correlates with higher levels of optimism. Sharot et al. (2007) investigated that optimism is linked to increased activation in the amygdala and rACC, brain regions responsible for emotional salience, and that rACC activity is associated with trait optimism. Wang et al. (2018) utilized the f-ALFF technique to analyze optimism processes, revealing a correlation between optimism and spontaneous OFC activity and a relationship between the left supplementary motor cortex.

Lai et al. (2020) discovered a relation between increased optimism and higher GM density in the bilateral putamen, an area related to motivation processing. Carver et al. (2010)'s assertion suggests that motivation is strongly related to optimism, with bilateral putamen being responsible for optimistic individuals' motivation. Greater regional GM density correlates with higher optimism degrees.

Additionally, optimism was reported to be associated with higher GMV in the left lateral OFC (Dolcos et al., 2016), reduced f-ALFF in the right OFC, and connectivity seen between supplementary motor cortex and OFC (Wang et al., 2018). Research suggests that the OFC may protect healthy individuals from anxiety symptoms, with increased spontaneous activity linked to elevated anxiety levels in both patients and healthy individuals with anxiety disorders (Qiu et al., 2015).

The rACC's role in self-referential processing contributes to optimistic bias, as individuals rationalize favorable events based on positive self-imagination, which is linked to increased vmPFC activity, as suggested by (Sharot et al., 2007; Blair et al., 2013). Blair et al. (2013; 2017) discovered greater activation in the posterior cingulate cortex and vmPFC, essential for evaluating stimulus subjective value, but did not find a correlation with optimistic bias. They argued that biased subjective value within these regions contributes to optimism, but not to be optimistic bias generation.

Blair et al. (2013) found that participants were optimistic about both good and bad future events, overestimating milestones and underestimating heart attacks. Positive situations increased activity in the posterior cingulate cortex, vmPFC, and rACC, while negative situations decreased activity in the dorsomedial prefrontal cortex (dmPFC) and left insula activity.

Sharot et al. (2011) study used fMRI data to analyze

participants' likelihood of encountering 80 unfavorable scenarios. They found that 79% of participants modified their estimation when faced with a decreased likelihood of negative events. Activity in the left IFG, right cerebellum, and bilateral medial prefrontal cortex/superior frontal gyrus increased. When their initial likelihood estimates exceeded reality, activity within the proper IFG decreased.

The study by Sharot (2007) found a significant link between bilateral amygdala activity and rACC activity during positive future scenarios, while negative situations weaken this connection. A rise in rACC and amygdala activation is associated with optimism. Research has shown that negative self-information is not a necessary component of optimism bias, and participants' initial estimations may be updated when faced with actual probability (Sharot et al., 2007; Sharot, 2011; Ran et al., 2017). The IFG found that higher optimism scores lead to poorer outcomes when negative occurrences are greater than initial assessments. This indicates that the right IFG is crucial for rejecting unfavorable information and maintaining beliefs affecting well-being.

Overly optimistic individuals are more probably to disregard negative aspects of themselves. In their study, Kuzmanovic et al.'s study (Kuzmanovic et al., 2016) found that the ventral striatum partially omits negative information, contributing to individuals' optimism bias, as it's a part of the brain's reward system, causing individuals to disregard negative information. Ran et al.'s findings may imply that the mTG and inferior IFG, which are connected with emotion processing and regulation, are also involved in dispositional optimism (Ran et al., 2017).

Due to its interconnections to other limbic structures, the thalamus has formerly been connected with emotional processing (Bush et al., 2000; Davidson et al., 2000). Optimists are more likely to utilize reappraisal as an emotion-regulation approach and express more positive moods than pessimists (Yang et al., 2013). Reappraising experiences helps alleviate unpleasant emotions, as controlling emotions is crucial for maintaining a positive outlook, as evidenced by increased GMV in the thalamus in extremely o-individuals.

Is it able to conduct a methodical, objective, and scientific study of optimism and pessimism? Undoubtedly, although optimism and pessimism are applied uniquely and differentially in each individual's life and despite the subject's breadth, optimism research is quantitative in nature. Therefore, the possibility of qualitative differences in the brain volumes of optimistic and pessimistic people comes to mind. In addition, considering the gender difference, age distribution, and parameters such as the right and left lobes of the brain, it is a matter of curiosity whether these parameter differences have any effect on people's perspectives on life. Therefore, the aim of this study was to evaluate whether there was any difference by dividing people into

two groups, optimistic and pessimistic, and then dividing these groups into subgroups, such as male/female, age range, and right and left lobes of the brain. The outline of the study is designed as follows. First, the methods used in the study and the content of the dataset will be summarized in Section 2. Subsequently, the results are presented in Section 3. In Section 4, the results will be discussed, and in the fifth section, the current result and future works will be evaluated.

2. Materials and Methods

2.1. Dataset

The dataset known as the "Leipzig Study for Mind-Body-Emotion Interactions" (Lemon) consists of data from 227 individuals who were deemed healthy. These participants were divided into two groups: a youthful group consisting of 153 individuals with an average age of 25.1 years (ranging from 20 to 35 years), with 45 of them being female; and an elderly group consisting of 74 individuals with an average age of 67.6 years (ranging from 59 to 77 years), with 37 of them being female. The participants were recruited in a cross-sectional manner to investigate mind-body-emotion interactions in Leipzig, Germany, during the period from 2013 to 2015. All participants were subjected to testing at the "University Clinic Leipzig's Day Clinic for Cognitive Neurology" and the "Max Planck Institute for Human and Cognitive and Brain Sciences" (MPI CBS) located in Leipzig, Germany. The research adhered to the guidelines set forth in the Declaration of Helsinki, and its methodology was granted approval by the ethics committee of the medical faculty at the University of Leipzig (reference number 154/13-ff). The recruitment and exclusion criteria have been outlined in previous studies (Oligschläger et al., 2016; Mendes et al., 2017; Golchert et al., 2017a; Golchert et al., 2017b; Babayan et al., 2019). All of the data used in this study can be found on this website: http://fcon_1000.projects.nitrc.org/indi/retro/MPI_LEMON.html.

2.2. Participants

Since our focus in our study was to understand whether there is a difference between highly optimistic and less optimistic brain structures, we grouped our participants according to psychological assessment. Accordingly, the

Optimism Pessimism Questionnaire-Revised (LOT-R) test results given under the Psychological Assessment title of (Babayan et al., 2019) were suitable for our purpose. We conducted our study by choosing a narrower focus among all these broad parameters and participants and selected 32 individuals from the Lemon data set, equally distributed in the highly optimistic (H-optimistic) and low optimistic (L-optimistic) (pessimistic) groups.

Each group we formed thus consisted of 16 people. In each group, the number of men and women and the age distribution were equal. Namely, eight women (4 younger - 4 older) and eight men (4 young - 4 older) were selected. Therefore, comparisons were made according to subgroups as well as L-optimistic and H-optimistic groups. Figure 1 presents Group division representation. Subjects were nonsmoker and right-handed dominant, and their education level was generally Gymnasium, and as another lower percentage, Realschule. Furthermore, there was a participant whose education was Hauptschule. The age range had a different range for each group and is presented in Table 1. The participants were matched in psychopathology severity (e.g. HDRS). And the subjects have no SCID-diagnoses.

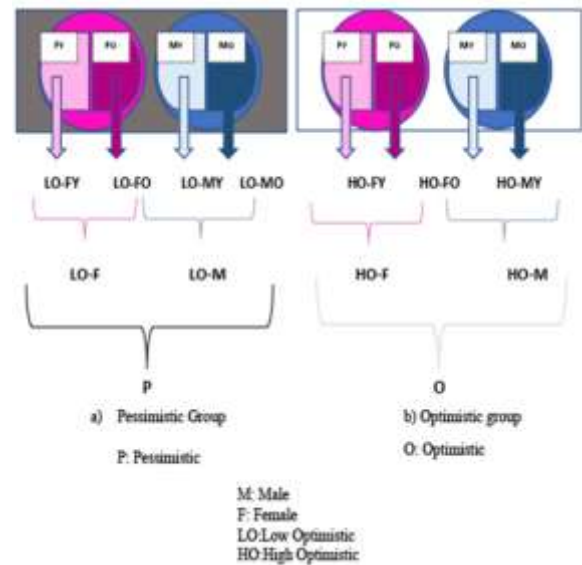


Figure 1. Group division representation.

Table 1. The demographic details of the participants

Participants	High Optimistic Group		Low Optimistic Group	
	Female-Old Male-Old	Female-Young Male-Young	Female-Old Male-Old	Female-Young Male-Young
Number	4 4	4 4	4 4	4 4
Age Range	65-75 60-75	20-30 20-30	60-70 60-75	20-30 30-30
Total Number (32)	8	8	8	8

2.3. Image Acquisition

The neuroimaging procedure was conducted using the 3 Tesla SIEMENS MAGNETOM Verio, manufactured by Siemens in Germany. The acquisition of T1-weighted 3D magnetization data was performed. The anatomical images in the sagittal plane were acquired using the Prepared Rapid Gradient Echo (MPPRAGE) sequence, with specific parameter settings. The sagittal acquisition orientation was used to obtain a 3D volume consisting of 176 slices. The repetition time (TR) was set to 5000 ms, while the echo time (TE) was 2.92 ms. Two inversion times (TI1 = 700 ms, TI2 = 2500 ms) and two flip angles (FA1 = 40°, FA2 = 50°) were employed. Prior to scanning, pre-scan normalization was performed. The echo spacing was set to 6.9 ms, with a bandwidth of 240 Hz/pixel. The field of view (FOV) was 256 mm, and the voxel size was 1 mm isotropic. A GRAPPA acceleration factor of 3 was applied, and the slice order was interleaved. The total duration of the scan was 8 minutes and 22 seconds.

2.4. Voxel Based Morphometry (VBM)

The estimation of the cerebrospinal fluid (CSF), WM, GM and total intracranial volume (TIV), was conducted using the VBM approach. The VBM technique is widely recognized for its efficacy in assessing the voxel-level differences between multiple groups by utilizing sMRI data (Ashburner, 2000). The VBM8-toolbox developed by (<http://dbm.neuro.uni-jena.de/vbm8/>) (the University of Jena) was employed in this study. The toolbox utilized in this study is derived from the SPM program, which can be accessed at the following URL: <http://www.fil.ion.ucl.ac.uk/spm/>. The SPM program itself is implemented in MATLAB. The utilization of a 3D T1-weighted sMRI image as input in the VBM8 toolbox allows for the consistent implementation of denoising, normalization, segmentation, and computation of CSF, WM, GM volumes by SPM. After performing segmentation, the normalized WM and GM images were

used for VBM analysis. The estimation of TIV was performed by aggregating the volumes of CSF, WM, GM. The volumes of these were subjected to Gaussian smoothing using a kernel size of [18.6 18.2 18.3 mm mm mm; 12.4 12.1. 12.2{voxels}], [1.5 1.5. 15. mm mm mm; 1.0 1.0 1.0{voxels}], [15.5 14.4 14.7 mm mm mm;10.3 9.6 9.8{voxels}] full width at half maximum (FWHM).

2.5. Statistical Approach

The smoothed and normalized adjusted nonlinear, white matter and gray images and cerebrospinal fluid images were employed for between-group comparisons. Absolute threshold masks of 0.05 were operated on the GM, WM, and CSF images. The statistical parametric maps were subjected to two thresholds: an uncorrected voxel-size threshold of P<0.001 and an expected voxel per cluster threshold (>50) for the purpose of eliminating counterfeit small clusters. The Mann-Whitney U test was calculated to compare the estimations of volumes between the H-optimistic and L-optimistic groups in MATLAB.

3. Results

No statistically significant differences were found in the volumes of TIV, WM, GM, and CSF between the groups categorized as H-optimistic and L-optimistic (P<0.05) (Figure 2 and Figure 3 and Table 9).

Furthermore, there were no significant differences observed in TIV, WM, GM, and CSF volumes within the brain for female and male participants, young and old participants, young female and male participants, or old female and male participants (P<0.05) (Tables 2-7). However, in the detailed analysis, many brain regions showed differences between groups when the low optimistic group was set as the default setting of <high optimistic on a scale of P<0.001 (Figure 4). Table 8 presents the regions of significantly different GM and WM and CSF volumes from the whole brain VBM analysis.

Table 2. Volume estimation (mean and standard deviation (SD)) of cerebrospinal fluid (CSF), white matter (WM), gray matter (GM), total intracranial volume (TIV), WM/TIV, and GM/TIV results for female participants

Brain Volumes	High Optimistic Group	Low Optimistic Group	P-value
	Mean ± SD	Mean ± SD	
(Absolute Volumes)			
CSF	255±64.38	274.25±76.69	0.46
WM	470.87±33.08	475.37±39.42	0.74
GM	470.75±54.26	635.5±66.6	0.10
TIV	1397.62±87.37	1387.75±67.96	0.84
(Relative Volumes)			
WM/TIV	33.68±0.86	34.22±1.7	0.57
GM/TIV	48.07±3.8	45.85±4.8	0.19
CSF/TIV	18.18±4.2	19.73±5.2	0.31



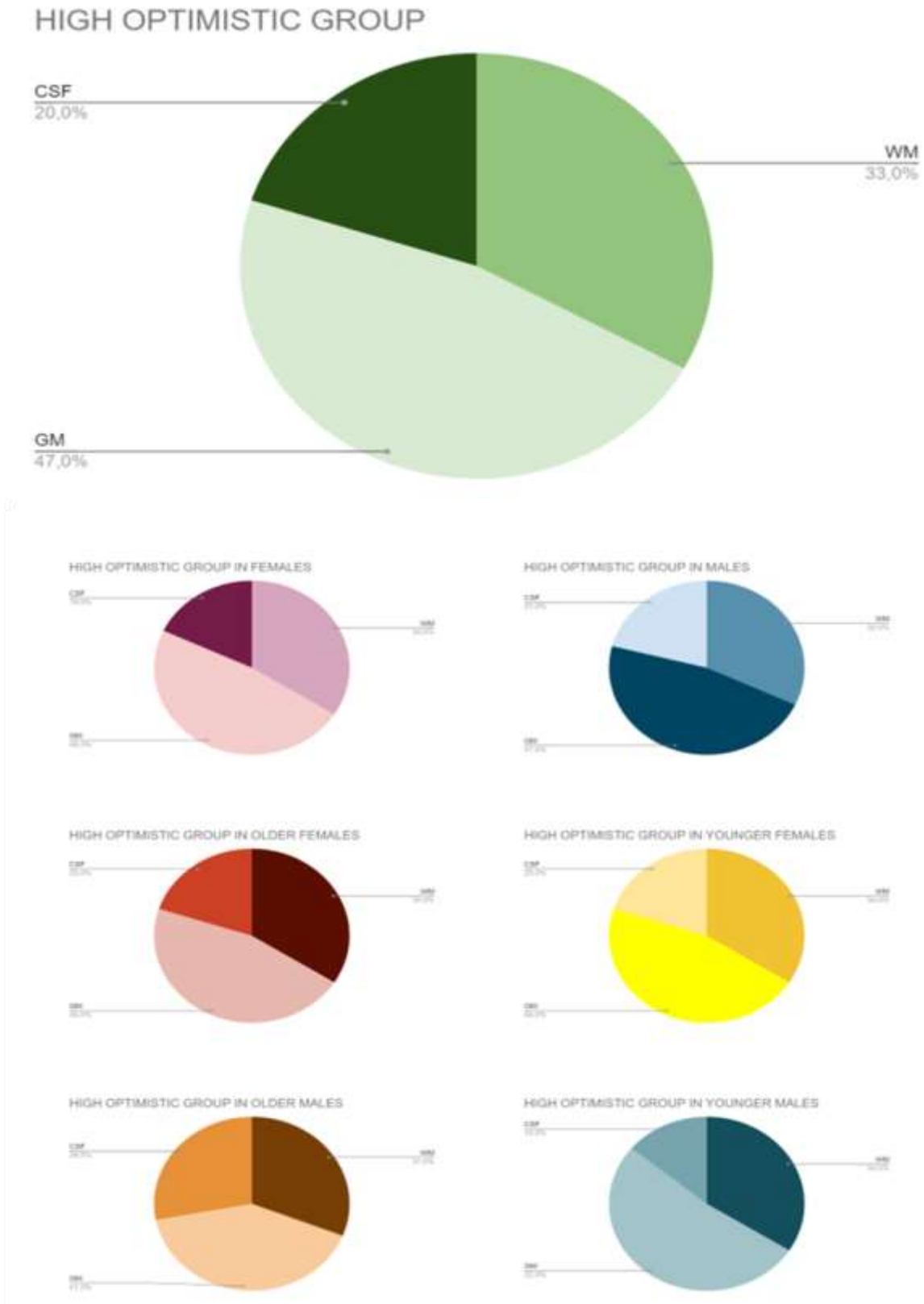


Figure 2. Percentage representation comparisons of highly optimistic groups for GM, WM, and CSF images.

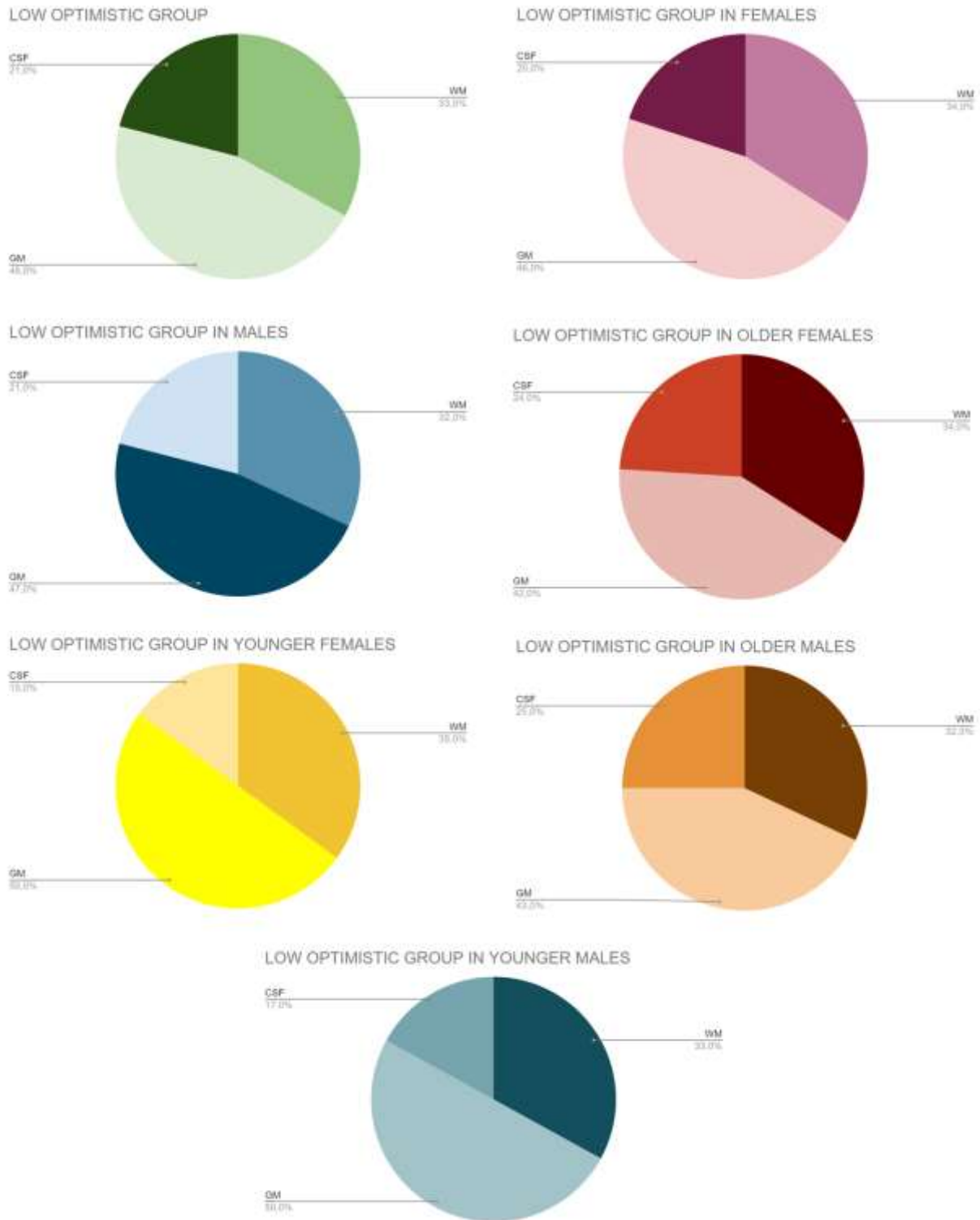


Figure 3. Percentage representation comparisons of low optimistic groups for GM, WM, and CSF images.

Table 3. Volume estimation (mean and standard deviation (SD)) of cerebrospinal fluid (CSF), white matter (WM), gray matter (GM), total intracranial volume (TIV), WM/TIV, and GM/TIV results for male participants

Brain Volumes	High Optimistic Group Mean \pm SD	Low Optimistic Group Mean \pm SD	P-value
(Absolute Volumes)			
CSF	315.12 \pm 114.60	329.87 \pm 80.95	0.44
WM	489.75 \pm 56.35	508.75 \pm 42.09	0.84
GM	706.625 \pm 131.24	728 \pm 80.82	0.46
TIV	1513.12 \pm 145.34	1568.12 \pm 86.89	0.38
(Relative Volumes)			
WM/TIV	32.37 \pm 1.8	34.42 \pm 1.7	0.94
GM/TIV	46.61 \pm 6.4	46.46 \pm 4.7	0.81
CSF/TIV	20.93 \pm 7.7	21.02 \pm 4.8	0.84

Table 4. Volume estimation (mean and standard deviation (SD)) of cerebrospinal fluid (CSF), white matter (WM), gray matter (GM), total intracranial volume (TIV), WM/TIV, and GM/TIV results for young female participants

Brain Volumes	High Optimistic Group Mean \pm SD	Low Optimistic Group Mean \pm SD	P-value
(Absolute Volumes)			
CSF	224.75 \pm 74.66	215.25 \pm 42.35	0.87
WM	469.25 \pm 49.58	480 \pm 4	0.62
GM	697.25 \pm 60.63	687 \pm 48.51	0.62
TIV	1392 \pm 132.48	1382.75 \pm 24.47	0.87
(Relative Volumes)			
WM/TIV	33.7 \pm 1.19	34.7 \pm 0.66	0.50
GM/TIV	50.22 \pm 3.65	49.67 \pm 3.22	1.00
CSF/TIV	16.05 \pm 4.66	15.57 \pm 3.05	0.87

Table 5. Volume estimation (mean and standard deviation (SD)) of cerebrospinal fluid (CSF), white matter (WM), gray matter (GM), total intracranial volume (TIV), WM/TIV, and GM/TIV results for young male participants

Brain Volumes	High Optimistic Group Mean \pm SD	Low Optimistic Group Mean \pm SD	P-value
(Absolute Volumes)			
CSF	241 \pm 37.7	269.75 \pm 39.39	0.12
WM	520.5 \pm 55.24	513.5 \pm 47.25	0.62
GM	811.25 \pm 97.03	795.75 \pm 52.77	0.87
TIV	1546.5 \pm 183.67	1579.75 \pm 102.44	0.87
(Relative Volumes)			
WM/TIV	33.72 \pm 0.51	32.5 \pm 1.82	0.37
GM/TIV	52.47 \pm 1.21	50.4 \pm 1.81	0.25
CSF/TIV	13.77 \pm 1.24	17.7 \pm 2.28	0.12

Table 6. Volume estimation (mean and standard deviation (SD)) of cerebrospinal fluid (CSF), white matter (WM), gray matter (GM), and total intracranial volume (TIV), WM/TIV, and GM/TIV results for old female participants

Brain Volumes	High Optimistic Group Mean \pm SD	Low Optimistic Group Mean \pm SD	P-value
(Absolute Volumes)			
CSF	285.25 \pm 40.70	333.25 \pm 51.44	0.25
WM	472.5 \pm 9.39	470.75 \pm 59.60	1.00
GM	644.25 \pm 36.36	584 \pm 27.54	0.12
TIV	1403.25 \pm 13.40	1392.75 \pm 100.55	0.87
(Relative Volumes)			
WM/TIV	33.67 \pm 0.57	33.72 \pm 2.38	0.87
GM/TIV	45.92 \pm 2.85	42.02 \pm 2.21	0.12
CSF/TIV	20.32 \pm 2.74	23.9 \pm 2.84	0.25

Table 7. Volume estimation (mean and standard deviation (SD)) of cerebrospinal fluid (CSF), white matter (WM), gray matter (GM), and total intracranial volume (TIV), WM/TIV, and GM/TIV results for old male participants

Brain Volumes	High Optimistic Group Mean \pm SD	Low Optimistic Group Mean \pm SD	P-value
(Absolute Volumes)			
CSF	416.25 \pm 44.19	390 \pm 64.04	0.87
WM	459 \pm 42.85	504 \pm 42.90	0.62
GM	602 \pm 39.85	660.25 \pm 14.79	0.12
TIV	1479.75 \pm 112.17	1556.5 \pm 82.24	0.37
(Relative Volumes)			
WM/TIV	31.02 \pm 1.56	32.35 \pm 1.93	0.62
GM/TIV	40.75 \pm 1.71	42.52 \pm 2.70	0.87
CSF/TIV	28.1 \pm 0.97	24.97 \pm 2.87	0.25

Table 8. The regions of significantly different gray and white matter and cerebrospinal fluid volumes from the whole brain VBM analysis (P<0.001 uncorrected)

LOW>HOG	Total Number of Voxels	z	T	MNI coordinate (x y z)	
Gray Matter	547254	3.91	3.16	18 -14 60	
			3.90	3.16	17 -39 42
			3.81	3.81	14 -39 44
White Matter	390919	4.18	4.92	-5 -81 -8	
		3.84	4.41	0 -68 18	
		3.27	3.62	11 -62 15	
		3.74	4.26	-5 -17 48	
		3.58	4.03	-35 29 42	
		3.42	3.82	-12 -33 51	
		3.27	3.62	-20 -47 60	
		3.26	3.60	29 44 21	
		3.17	3.49	-44 -21 36	
		3.13	3.43	-57 -15 -41	
Cerebrospinal Fluid	631691	3.09	3.39	-26 27 36	
		4.07	4.75	-39 30 45	
		3.67	4.17	47 -2 57	
		3.65	4.14	8 8 -21	
		3.60	4.07	-56 21 36	
		3.55	4.00	-60 -32 32	
		3.53	3.97	-9 29 50	
		3.49	3.91	50 -44 29	
		3.36	3.74	60 -38 42	
		3.33	3.69	54 -9 -5	
	3.69	-30 -95 14			
	3.26	3.61	68 -39 9		
	3.24	3.58	-53 -48 48		
	3.22	3.55	54 0 44		

3.1. Gray Matter Evaluations in terms of Anatomical Localization

In our study, the reference group is the group obtained by subtracting the low optimistic group from the high optimistic group. We evaluated our results first by grouping the participants into low-optimistic and high-optimistic groups with 16 subjects per group. Accordingly, when the low optimistic group was compared to the high optimistic group (P<0.001), there were significant differences in brain right hemisphere volumes. These regions: Right cerebral white matter,

Right OFuG, Right LiG, Right lateral ventricle, Right calcarine calcarine cortex, Right IOG.

When females in the L-optimistic group were compared to females in the H-optimistic group (P<0.001), no significant differences were found.

However, when males in the L-optimistic group were compared to males in the H-optimistic group (P<0.001), significant differences were found. These regions are the right cerebral white matter, right PrG, right SPF, right PCu, right PCgG, right MPrG, and right MPoG.

Table 9. Volume estimation (mean and standard deviation (SD)) of cerebrospinal fluid (CSF), white matter (WM), gray matter (GM), total intracranial volume (TIV), WM/TIV, and GM/TIV results

Brain Volumes	High Optimistic Group Mean \pm SD	Low Optimistic Group Mean \pm SD	P-value
(Absolute Volumes)			
CSF	285.06 \pm 95.01	302.06 \pm 81,41	0.2145
WM	480.31 \pm 45.69	492.06 \pm 42.99	0.5179
GM	688.69 \pm 98.77	681.75 \pm 85.83	0.6417
TIV	1455.37 \pm 130.30	1477.93 \pm 119.81	0.5349
(Relative Volumes)			
WM/TIV	33.03 \pm 1.52	33.32 \pm 1.90	0.6483
GM/TIV	47.34 \pm 5.15	46.15 \pm 4.62	0.2443
CSF/TIV	19.56 \pm 6.17	20.38 \pm 4.91	0.5014

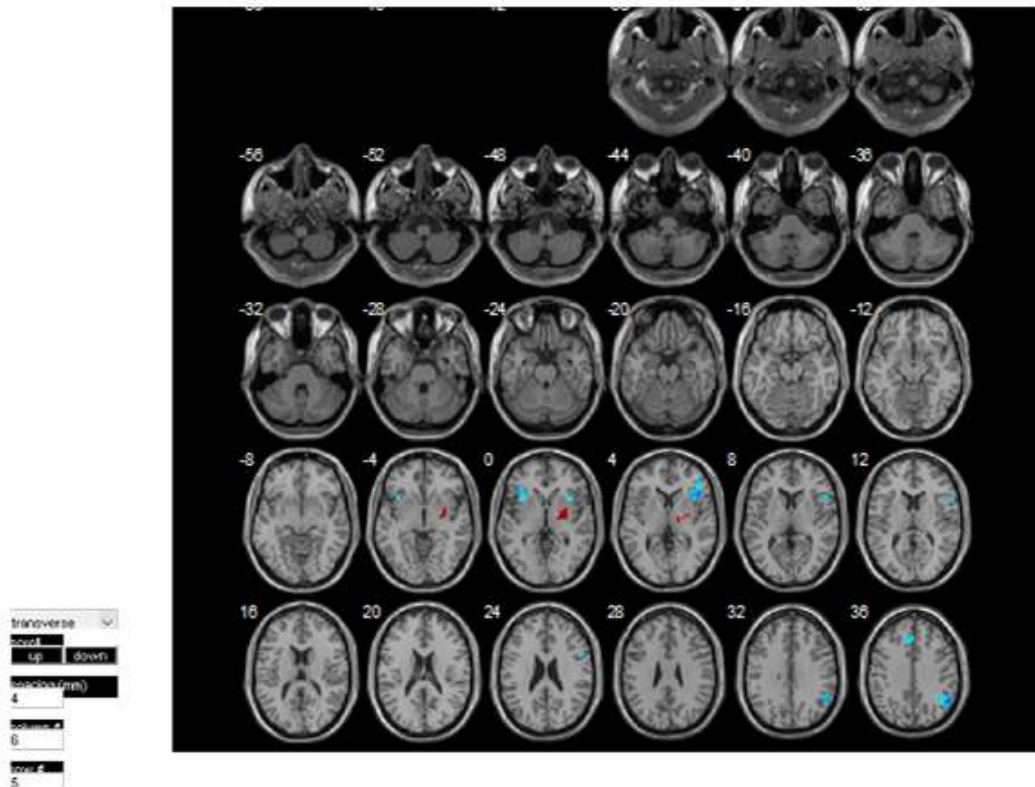
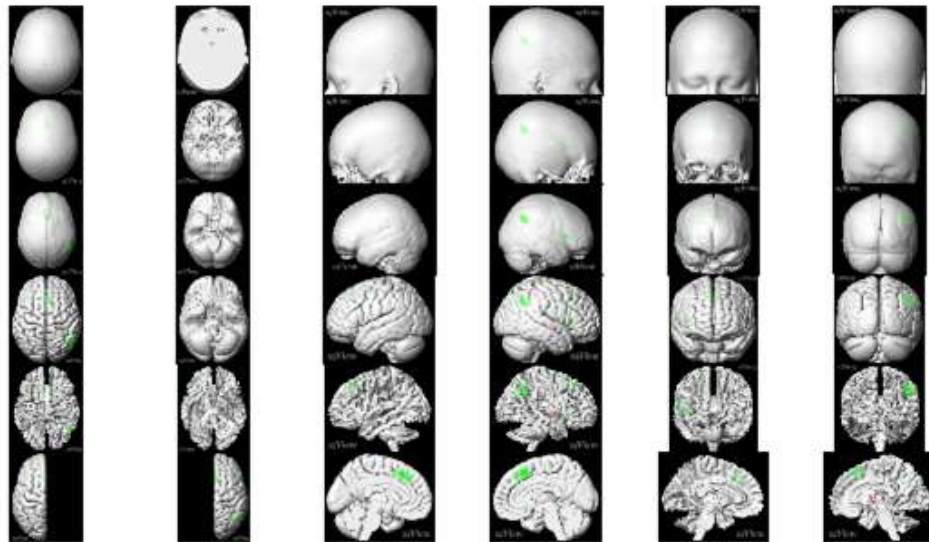


Figure 4. Render and Slice View of the GM images.

- When older females in the L-optimistic group were compared to older females in the H-optimistic group ($P < 0.001$), no significant differences were found.
- When younger females in the L-optimistic group are compared to younger females in the H-optimistic group ($P < 0.001$), significant differences are found. The regions under consideration include the Right SFG, Right MSFG, Right Cerebral White Matter, Right OFuG, Right LiG, Right Exterior of the Cerebellum, Right IOG, Right Palladium, Right Thalamus Proper, Right Amygdala, Left TrIFG, Left MFG, Left Cerebral White Matter, Left Ventral DC, Left Thalamus Proper, Brain Stem, 3rd Ventricle, CSF, Right Ventral DC, and 4th Ventricle.
- When older males in the L-optimistic group were compared to older males in the H-optimistic group ($P < 0.001$), significant differences were found. The aforementioned regions include the Left MOG, Left SOG, Left Cerebral White Matter, Left Occipital Pole, Left Cuneus. The regions of interest identified in our study include also the Left Ventral DC, Left Thalamus Proper, Left Pallidum, Right Thalamus Proper, Right Ventral DC, Left PCu, and Right PCu. The left PCgG, left MPoG, right PCgG, left MPrG, left MCgG, and right MCgG were observed. The MPrG, was also the focus of discussion. The regions of interest in this study include also the right cerebral white matter, left MTG, left ITG, left IOG, right PrG, right MPrG, right SFG, right SMC, left SOG, left MOG, left Calc, left Cun, left lateral ventricle, left cerebellum exterior, left OFuG, right MTG, right STG, right PCu, right SPL, left PCu, right TMP, right ITG, right FuG, right PHG, brain stem, right cerebellum exterior, right OFuG, right LiG, right IOG, and the fourth ventricle.
- When younger males in the L-optimistic group were compared to younger males in the H-optimistic group ($P < 0.001$), significant differences were found. The aforementioned regions encompass the Left Ventral DC, Left Thalamus Proper, Left Cerebral White Matter, and 3rd Ventricle. The left pallidum, right thalamus proper, right ventral DC, right FuG, right ITG, right cerebral white matter, right MPrG, and right PCgG, the right medial segment of the postcentral gyrus and the right precuneus in the posterior cingulate cortex, the right PrG, left MPrG, right MCgG, right PoG, and right MPrG were observed. The left OpIFG, left FO, and left TrIFG were examined in this study. The regions of interest in this study include also the right cerebral white matter, the right OFuG, and the right LiG. The regions of interest identified in the study include also the right lateral ventricle, the left IOG, left OFuG, left SPL, left AnG, right SOG, right MOG, right OCP, left FuG, left ITG, left PHG, right Cun, left cerebellum exterior, right IOG, right OFuG, right Calc, left Cun, left LiG, left MFG, left Calc, and left OCP.

3.2. White Matter Evaluations in terms of Anatomical Localization

Similarly, we evaluated our outcomes first by grouping the participants into low optimistic and high-optimistic groups with 16 subjects per group. Accordingly, when the pessimistic group was compared to the optimistic group ($P < 0.001$), there were significant differences in brain right and left hemisphere volumes. These regions are Left LiG Lingual gyrus, Left Cerebral White Matter, Left Calc calcarine cortex, Left Cerebellum Exterior, Cerebellar Vermal Lobules VI-VII, Left PCu, Left Cun cuneus, Right Cun cuneus, Right PCu, Right CALC, Right Cerebral White Matter, Right LiG, Left MCgG, Left SMC, Left MPrG, Right MCgG, Right MPrG, Right SMC, Left MFG, Left PCgG, Left MPoG, Left PrG, Left Pogyrus, Left MFG, Left PCgG, Right MFG, Left SFG, Left MPoG, Left MFG.

When females in the L-optimistic group were compared to females in the high optimistic group ($P < 0.001$), significant differences were found. The regions of interest in this study include the Left MPoG, Left PrG, Left Cerebral White Matter, Left SMG, Right Cerebral White Matter, Right Lateral Ventricle, Left Lateral Ventricle, Right Caudate, Right Accumbens Area, and Right SCA subcallosal area, 3rd Ventricle, Left Caudate, Right Ventral DC, Left SCA, and Right Thalamus Proper. The regions of interest in the brain include also the left accumbens area, right basal forebrain, right pallidum, left ventral DC, left PT, left STG, left CO, left PO, left PoG, left SMG, left TTG, left MTG, and left PO accumbens area. Additionally, the left PoG, left SMG, and left TTG was also of interest.

Moreover, when males in the L-optimistic group were compared to males in the H-optimistic group ($P < 0.001$), significant differences were found. The aforementioned regions encompass the Left Cerebral White Matter, Left SMC, and the Left MPrG. The left middle cingulate gyrus, right medial segment of the precentral gyrus, right middle cingulate gyrus, and right supplementary motor cortex were observed. The region of interest was also the calcaneus CALC. The right cuneus, right precuneus, and left precuneus were observed. The right LiG was also a region of interest in the brain. The left lingual gyrus, left cuneus, and left calcarine cortex were observed. The right cerebral white matter and right lateral ventricle were the anatomical structures under consideration. The SMC was observed as a region of the brain that plays a role in motor control. The central operculum located in the left cerebral hemisphere was examined. The left temporal pole of the middle temporal gyrus, the left OpIG, the left FO, the left STG, the left PrG, the left Alns, the left Cun, and the left OCP was seen. The regions of interest in this study include the right MFG, right SFG, left LiG, right LiG, left cerebellum exterior, right PrG, and right MFG. The right cuneus, right SPL, left SMG, left PoG, left PO, left SPL, left PoG, left PCu, and left MPoG were identified. In addition,

- When older females in the L-optimistic group were compared to older females in the H-optimistic group

($P < 0.001$), significant differences were found. The aforementioned regions include the Right Cerebral White Matter, Right Posterior Insula of the Planum Polare, Right ALNS, and Right PP. The right putamen, right vessel, right hippocampus, right inferior lateral ventricle, right putamen, and right amygdala were observed. The entorhinal area, also known as the Ent entorhinal area, was identified as a region of the brain. The left superior parietal lobule and left precuneus of the posterior cingulate cortex were examined. The white matter in the left cerebral hemisphere was seen. The following brain regions were identified: the SOG, the CUN, the ALNS, the FO, the OpIFG, the OpIFG, CO, and the ITG. The left FuG, the left cerebellum exterior, right MFG, right SFG, right ITG, and right FuG were the specific brain regions under consideration. The following brain regions were identified in the left hemisphere: the left putamen, left posterior insula of the parietal lobe, left anterior insula, left pallidum, left vessel, left hippocampus, left planum polare of the parietal lobe, left inferior lateral ventricle, left superior occipital gyrus, left angular gyrus, left amygdala, left fusiform gyrus, left lateral ventricle, left entorhinal area, left basal forebrain, left vessel, and left planum polare of the parietal lobe. In the right hemisphere, the identified regions were the right lateral ventricle, right caudate, right thalamus proper, right lateral ventricle, left middle occipital gyrus, right precentral gyrus, and right postcentral gyrus.

- When younger females in the L-optimistic group were compared to females in the younger H-optimistic group ($P < 0.001$), significant differences were found. These regions are Left Cerebral White Matter, Right Cerebral White Matter, Left MFG, Right SFG, Left CUN, Right CUN, Left CALC, Left STG, Left PT, Left MTG, Left TTG, Left MCgG, Right MCgG, Left SMC, Left AnG, Left MOG, Right FuG, Right ITG, Right Cerebellum Exterior, Right PHG, Right MSFG, Left MSFG, Left OFuG, Left CALC, Left IOG, Left OCP, Left LiG, Right Plns, Right PP, Right ALNS, Right TTG, Right CO, Right STG, Left STG, Left PT, Left PO, Left CO, Left PoG, Left SMG, Left SFG, Left MFG, Left PrG, Left ACgG, Left Hippocampus, Left Amygdala, Left Pallidum, Left Ventral DC, Left Putamen, Left Inf Lat Vent, Left Ent entorhinal area, Left vessel, Right ACgG, Right LiG, Left LiG, Right CALC, Left CALC, Right CUN, Left CUN.
- When older males in the L-optimistic group were compared to older males in the H-optimistic group ($P < 0.001$), significant differences were found. These regions are Left Cerebral White Matter, Right Cerebral White Matter, Right PCu, Left PCu, Left MPrG, Left PCgG, Left MPoG, Left MCgG, Left STG, Left MTG, Left PT planum temporale, Left TTG, Right MTG, Right SFG, Left CO, Left PP, Left OpIFG, Left FO frontal operculum, Left TMP, Left PrG, Left ALNS, Right PCgG, Right TMP, Left IOG, Left MOG, Left SMC,

Left MPrG, Right MCgG, Right SMC, Right MPrG, Left MTG, Left ITG, Left IOG, Right SPL, Right MSFG, Right ACgG, Left CALC, Left OpIFG, Left PrG Precentral gyrus, Right MPrG, Right MCgG, Right SMC, Left MPrG, Left SMC, Left MCgG, Right PCgG, Right TMP, Right ENT, Right ITG, Right FuG.

- When younger males in the L-optimistic group were compared to younger males in the H-optimistic group ($P < 0.001$), significant differences were found. These regions are Right Cun cuneus, Left Cun cuneus, Left Cerebral White Matter, Right Cerebral White Matter, Right Calc calcarine cortex, Left Calc calcarine cortex, Right PCu, Left PCu, Right LiG, Left LiG, Right FuG, Right ITG, Right ENT, Right PHG, Right TMP, Right Hippocampus, Right Amygdala, Right Inf Lat Vent, Cerebellar Vermal Lobules VI-VII, Cerebellar Vermal Lobules VIII-X, Left Cerebellum Exterior, Right Cerebellum Exterior, Left MFG, Left PrG, Right GRE, Left GRE, Right MORg, Right MFC, Left MFC, Right PORg, Right LORg, Right AORg, Right PrG, Right MFG, Left SMG, Left PoG, Left parietal operculum, Left SMC, Left MPrG, Left MCgG, Right MPrG, Right SMC, Right MCgG, Left OCP, Right CO, Right TTG, Right PP, Right Plns posterior insula, Right Alns anterior insula, Right PT.

3.3. Cerebrospinal Fluid Evaluations in terms of Anatomical Localization

Furthermore, we evaluated our outcomes by grouping the participants into low optimistic and high optimistic groups, with 16 subjects per group with cerebrospinal fluid. Accordingly, when the pessimistic group was compared to the optimistic group ($P < 0.001$), there were significant differences in brain right and left hemisphere volumes. These regions are the left MFG, right PrG precentral gyrus, left SMG, left cerebral white matter, right SMG, right cerebral white matter, left MOG, right STG, left SMG, right PrG, and right PoG.

By extension, when females in the L-optimistic group were compared to females in the H-optimistic group ($P < 0.001$), significant differences were found. These regions are the Left FuG fusiform gyrus, Left Cerebral White Matter, Right Cerebral White Matter, Left SOG, Left PoG postcentral gyrus, Left SMG, and Right GRE.

Moreover, when males in the L-optimistic group were compared to males in the H-optimistic group ($P < 0.001$), significant differences were found. These regions are the left cerebral white matter, right cerebral white matter, right MFG, right PrG, brain stem, right FuG, left MFG, left SPL, and left AnG. Additionally;

- When older females in the L-optimistic group were compared to older females in the H-optimistic group ($P < 0.001$), significant differences were found. These regions were the left cerebral white matter, right cerebral white matter, right PrG, left ITG, left GRE gyrus rectus, left SPL, right AORg, left PrG, right PCu, right ventral DC, and left MOG.
- When younger females in the L-optimistic group were compared to females in the younger H-

optimistic group ($P < 0.001$), significant differences were found. These regions were the left cerebral white matter, right cerebral white matter, right PT, left SMC, left LiG, left SMC, left SPL.

- When older males in the L-optimistic group were compared to older males in the H-optimistic group ($P < 0.001$), significant differences were found. These regions were the left cerebral white matter, right cerebral white matter, right MFG, right PoG, right caudate, left PrG precentral gyrus, right MSFG superior frontal gyrus medial segment, left PCu, left MSFG, left IOG, right TrIFG, left OFuG, and right SMG.
- When younger males in the L-optimistic group were compared to younger males in the H-optimistic group ($P < 0.001$), significant differences were found. These regions were the right cerebral white matter, right OrIFG, right OCP, right STG, and right STG, left AnG, right CO, right AnG, and right SMG.

4. Discussion

Significant differences in all of these regions in our study were found in the following comparisons: In GM evaluations in terms of anatomical locations, when younger females in the L-optimistic group were compared to younger females in the H-optimistic group, significant differences were found in the right and left thalamus proper. Similarly, when older males in the L-optimistic group were compared to older males in the H-optimistic group and younger males in the L-optimistic group were compared to younger males in the H-optimistic group, significant differences were found in these regions. Although we cannot detect an increasing GM according to our results, we can declare that we found a significant result in the statistical comparison between the H-optimistic and L-optimistic groups. In addition to the literature, we can state that we found almost a similar result in gender and age discrimination. In WM evaluations regarding anatomical locations, when females in the L-optimistic group were compared to females in the H-optimistic group, significant differences were found in the right and left thalamus proper. Additionally, when older females in the L-optimistic group were compared to older females in the H-optimistic group, significant differences were found in these regions. Since there is no WM study on optimism in the literature, we could not make an additional comment on this issue.

When we turn to GM evaluations in terms of anatomical locations, when younger females in the L-optimistic group are compared to younger females in the H-optimistic group, significant differences are found in the right amygdala. Similarly, in terms of anatomical locations, when older females in the L-optimistic group were compared to older females in the H-optimistic group, significant differences were found in the right and left amygdala. This comparison for younger females has only statistical significance in the left amygdala. This

comparison for younger males has only statistical significance in the right amygdala.

If we evaluate the results we found for "Insula," we see that we could not find a significant difference in any insula region in GM evaluations. However, when we looked at WM evaluations in terms of anatomical locations and when males in the L-optimistic group were compared to males in the H-optimistic group, statistical significance was found in the left Alns anterior insula. When older females in the L-optimistic group were compared to older females in the H-optimistic group, there was statistical significance in the right PLNS, right ALNS, left PLNS and left ALNS. Similarly, this comparison for older males only showed statistical significance in the left ALNS. Again, there was a significant difference in the right PLNS and right ALNS when comparing younger males.

What remains is to evaluate the SFG and right cerebellum regions, which are our intersection areas with the literature. Considering GM evaluations in terms of anatomical locations, males in the L-optimistic group were compared to males in the H-optimistic group, and significant differences were found in the right SFG. Similar results are valid for younger females as well. There was statistical significance in the right SFG and the right MSFG. This comparison for older males has only statistical significance in the right SFG. When we turn to WM evaluations regarding anatomical locations, there was a statistically significant difference in the right SFG in the H and L-optimistic group comparisons. This region shows a significant difference in males in the H- and L-optimistic groups and older females in the H- and L-optimistic groups. Concerning younger females, there was a statistically significant difference in the right SFG in addition to the left SFG. There was also a statistically significant difference in the right and left MSFG regions in this comparison. There was a statistically significant difference in the right SFG and right MSFG in older males. Furthermore, there was a statistically significant difference in the right cerebellum exterior when comparing younger females and older males in GM evaluations in terms of anatomical locations. Additionally, there was a statistically significant difference in the right cerebellum exterior between younger and older females and younger males in WM evaluations in terms of anatomical locations.

As a result of our detailed study, we can say that we found similar results to the literature. The most striking of these brain regions are the thalamus, amygdala, left insula, superior frontal gyrus, and right cerebellum, as mentioned in the literature. If we summarize what we found in the literature on optimism and our results, the studies in the following paragraphs are outstanding.

5. Conclusion

In summary, the study issue is quite dynamic, and future studies may lead to the establishment of more interconnections that create optimism. Based on the

findings described in this study, it is safe to conclude that optimism is not a product of a single brain region. Rather than that, the GM, WM, CSF volumes of specific locations are critical, as is functional connectivity between distinct parts in producing optimism.

Due to the numerous health advantages associated with optimism, this research further establishes the importance of optimism for nonclinical individuals. This research advances our understanding of optimism and the factors that underpin it. It is thus critical for the advancement of treatment and therapy aimed at enhancing individuals' well-being.

The antithesis of an optimistic perspective on life - a pessimistic perspective - is related to a variety of depressed symptoms and negative future expectations. Identifying potential disparities in optimism and determining whether it connects with depressive symptoms in nonclinical persons may aid in the avoidance of health problems such as anxiety and depressive symptoms.

Unfortunately, we could not control whether there was a significant difference regarding age between the H-optimistic group and the L-optimistic group since only the age range of the experiment participants was given in the LEMON dataset. Additionally, the study can be made more reliable by increasing the number of participants.

On the other hand, during our literature review, the results of increased and decreased activity in some brain regions in studies using fMRI provided satisfactory answers. We regret to inform you that we used anatomical MRI for the VBM study. Apart from this, some studies have also found information such as GM volume increase. Because of the VBM, we were only able to detect whether there was a significant difference rather than observing the volume increase or decrease.

In this study, we performed an analysis using only the participants grouped according to the LOT-R test performed before the experiment, but this study can be re-evaluated by considering the optimistic bias and by designing the videos to be watched.

The study's novelty is its detailed VBM analysis of brain structures in relation to optimism and pessimism, specifically focusing on regions such as the thalamus, amygdala, left insula, superior frontal gyrus, and right cerebellum. Detailed VBM analysis identified statistically significant structural brain differences associated with optimism levels across different genders and age ranges, despite the lack of significant differences in initial comparisons between low and high optimists. This aids in comprehending the neurobiological basis of optimism and pessimism.

Author Contributions

The percentage of the author contributions is presented below. The author reviewed and approved the final version of the manuscript.

	P.O.
C	100
D	100
S	100
DCP	100
DAI	100
L	100
W	100
CR	100
SR	100
PM	100
FA	100

C=Concept, D= design, S= supervision, DCP= data collection and/or processing, DAI= data analysis and/or interpretation, L= literature search, W= writing, CR= critical review, SR= submission and revision, PM= project management, FA= funding acquisition.

Conflict of Interest

The author declared that there is no conflict of interest.

Ethical Consideration

The research adhered to the guidelines set forth in the Declaration of Helsinki, and its methodology was granted approval by the ethics committee of the medical faculty at the University of Leipzig (reference number 154/13-ff). The recruitment and exclusion criteria have been outlined in previous studies (Oligschläger et al., 2016; Mendes et al., 2017; Golchert et al., 2017a; Golchert et al., 2017b; Babayan et al., 2019).

References

- Aberg E. 2021. Investigating the neural substrates and neural markers of optimism and optimism bias: a systematic review. *Högskolevägen: Högskolan of Skövde*, 2021: 1-29.
- Alessandri G, De Pascalis V. 2017. Double dissociation between the neural correlates of the general and specific factors of the Life Orientation Test-Revised. *Cognit Affect Behav Neurosci*, 17(5): 917-931.
- Ashburner J, Friston KJ. 2000. Voxel-based morphometry - the methods. *NeuroImage*, 11(6): 805-821.
- Ashburner JF. 2000. Voxel-based morphometry - the methods. *Neuroimage*, 11(6): 805-821.
- Babayan A, Erbey M, Kumral D, Reinelt RD, Reiter AMF, Röbbig J, Schaare LH, Uhlig M, Gaebler M, Villringer A. 2019. A Mind-brain-body dataset of MRI, EEG, cognition, emotion, and peripheral physiology in young and old adults. *Sci Data*, 6: 180308.
- Blair KS, Otero M, Teng C, Geraci M, Ernst M, Blair RJR, Grillon C, Pine DS. 2017. Reduced optimism and a heightened neural response to everyday worries is specific to Generalized Anxiety Disorder, and not seen in social anxiety. *Psychol Med*, 47(10): 1806-1815.
- Blair KS, Otero M, Teng C, Jabobs M, Odenheimer S, Pine DS, Blair RJR. 2013. Dissociable roles of ventromedial prefrontal cortex (vmPFC) and rostral anterior cingulate cortex (rACC)

- in value representation and optimistic bias. *NeuroImage*, 78: 103-110.
- Bush G, Luu P, Posner MI. 2000. Cognitive and emotional influences in anterior cingulate cortex. *Trends Cogn Sci*, 4(6): 215-222.
- Carver CS, Scheier MF, Segerstrom SC. 2010. Optimism. *Clin Psychol Rev*, 30(7): 879-889.
- Davidson RJ, Putnam KM, Larson CL. 2000. Dysfunction in the neural circuitry of emotion regulation: A possible prelude to violence. *Science*, 289(5479): 591-594.
- Dolcos S, Hu Y, Iordan AD, Moore M, Dolcos F. 2016. Optimism and the brain: Trait optimism mediates the protective role of the orbitofrontal cortex gray matter volume against anxiety. *Soc Cogn Affect Neurosci*, 11(2): 263-271.
- Egorova N, Veldsman M, Cumming T, Brodtmann A. 2017. Fractional amplitude of low-frequency fluctuations (fALFF) in post-stroke depression. *NeuroImage Clin*, 16: 116-124.
- Golchert J, Smallwood J, Jefferies E, Liem F, Huntenburg JM, Falkiewicz M, Lauckner ME, Oligschläger S, Villringer A, Margulies DS. 2017a. In need of constraint: Understanding the role of the cingulate cortex in the impulsive mind. *NeuroImage*, 146: 804-813.
- Golchert J, Smallwood J, Jefferies E, Seli P, Huntenburg JM, Liem F, Lauckner ME, Oligschläger S, Bernhardt CB, Villringer A, Margulies DS. 2017b. Individual variation in intentionality in the mind-wandering state is reflected in the integration of the default-mode, fronto-parietal, and limbic networks. *NeuroImage*, 146: 226-235.
- Jiang L, Zuo XN. 2016. Regional homogeneity: A multimodal, multiscale neuroimaging marker of the human connectome. *Neuroscientist*, 22(5): 486-505.
- Kuzmanovic B, Jefferson A, Vogeley K. 2016. The role of the neural reward circuitry in self-referential optimistic belief updates. *NeuroImage*, 133: 151-162.
- Lai H, Wang S, Zhao Y, Qiu C, Gong O. 2020. Neurostructural correlates of optimism: Gray matter density in the putamen predicts dispositional optimism in late adolescence. *Hum Brain Mapp*, 41(6): 1459-1471.
- Levens SM, Gotlib IH. 2012. The effects of optimism and pessimism on updating emotional information in working memory. *Cogn Emot*, 26(2): 341-350.
- Mendes N, Oligschläger S, Lauckner ME, Golchert J, Huntenburg JM, Falkiewicz M, Osoianu A. 2017. A functional connectome phenotyping dataset including cognitive state and personality measures. *bioRxiv*, 164764.
- Ocklenburg S, Güntürkün O. 2018. Chapter 9 - Structural Hemispheric Asymmetries. In *The Lateralized Brain: 1st Edition, the Neuroscience and Evolution of Hemispheric Asymmetries*. Academic Press, London, UK, pp: 239-262.
- Oligschläger S, Huntenburg JM, Golchert J, Lauckner ME, Bonnen TR, Margulies DS. 2016. Gradients of connectivity distance are anchored in primary cortex. *Brain Struct Funct*, 2016: 1-10.
- Qiu C, Feng Y, Meng Y, Liao W, Huang X, Lui S, Zhu C, Chen H, Gong Q, Zhang W. 2015. Analysis of altered baseline brain activity in drug-naive adult patients with social anxiety disorder using resting-state functional MRI. *Psychiatry Invest*, 12(3): 372.
- Ran Q, Yang J, Yang W, Wie D, Qiu J, Zhang D. 2017. The association between resting functional connectivity and dispositional optimism. *PLoS ONE*, 12(7): 1-13.
- Sharot T, Riccardi AM, Raio CM, Phelps EA. 2007. Neural mechanisms mediating optimism bias. *Nature*, 450(7166): 102-105.
- Sharot T. 2011. The optimism bias. *Curr Biol*, 21(23): R941-R945.
- Wang S, Zhao Y, Cheng B, Wang X, Yang X, Chen T, Suo X, Gong Q. 2018. The optimistic brain: Trait optimism mediates the influence of resting-state brain activity and connectivity on anxiety in late adolescence. *Hum Brain Mapp*, 39(10): 3943-3955.
- Whitwell JL. 2009. Voxel-based morphometry: An automated technique for assessing structural changes in the brain. *J Neurosci*, 29(31): 9661-9664.
- Yang J, Wie D, Wang K, Qiu J. 2013. Gray matter correlates of dispositional optimism: A voxel-based morphometry study. *Neurosci Lett*, 553(22): 201-205.



DETERMINATION OF THE KNOWLEDGE LEVEL OF THE TECHNICAL STAFF ABOUT ARBITRATION

Hasan BAKIRCI^{1,2*}, Ayten CANBAL¹

¹Istanbul Medipol University, Graduate School of Engineering and Natural Sciences, Department of Construction Management and Law, 34810, İstanbul, Türkiye


²Harran University, Hilvan Vocational School, Department of Construction, 63300, Şanlıurfa, Türkiye

Abstract: Türkiye has become one of the world's leading countries in the construction sector in the international arena. Today, the use of FIDIC and similar standard contracts is increasing in Turkish contractor companies. In parallel with this situation, it also becomes more common to prefer arbitration in the settlement of disputes in the international construction sector. In the literature, there is no actual publication about the knowledge level of technical staff on arbitration. By taking this deficiency into consideration, the purpose of this study is to measure the awareness of the groups working in the construction sector about the possibility of applying to arbitration as a result of the disputes that they encounter, by measuring the arbitration knowledge level of the technical staff. Accordingly, an empirical field work was conducted with a total of 100 (one hundred) technical staff working in the public and private sector transportation projects in Istanbul. The data collection tool that was used in the research is a questionnaire developed by the researchers and consisting of 25 questions. In the survey analysis, the data were analyzed with the SPSS 28 package program. In the study, a reliability test was conducted for each statement and the Mann-Whitney U test was used. As a result of the analysis, it has been determined that 84.4% of the participants do not follow up the actual developments in the field of arbitration in the world and in Türkiye, and do not have sufficient knowledge about arbitration. However, it has been determined that the arbitration knowledge level of the participants, who follow up the actual developments in the world and in Türkiye and have sufficient knowledge about arbitration, is high. In addition, it has been determined that 93.8% of the participants would like to participate an information training to be held on arbitration. To increase awareness about arbitration, it is necessary to introduce undergraduate-level arbitration courses for technical staff in engineering and architecture faculties at universities, and to organize periodic in-service training programs by the arbitration centers in our country.

Keywords: Arbitration, Construction law, Alternative dispute resolution ways, Knowledge level, Contract management

*Corresponding author: Harran University, Hilvan Vocational School, Department of Construction, 63300, Şanlıurfa, Türkiye

E mail: hasanbakirci@harran.edu.tr (H. BAKIRCI)

Hasan BAKIRCI  <https://orcid.org/0000-0002-8623-0880>

Ayten CANBAL  <https://orcid.org/0000-0002-8094-652X>

Received: November 22, 2023

Accepted: February 06, 2024

Published: March 15, 2024

Cite as: Bakirci H, Canbal A. 2024 Determination of the knowledge level of the technical staff about arbitration. BSJ Eng Sci, 7(2): 237-245.

1. Introduction

Türkiye is ranked Number Two after China in the list of the world's top 250 international contractors that has been published in 2022 by the "Engineering News Record" Magazine, which is recognized and approved by all authorities in the world. This situation demonstrates the active involvement of Turkish contractors in the construction sector in many countries around the world. During the implementation of construction projects, managing time, cost, and quality is crucial. Due to the complexity and scale of construction projects, disputes often arise among the parties involved in the management of these elements. Hence, the importance of choosing the right method for resolving disputes becomes evident in both domestic and international construction projects.

The disputes in the construction sector are one of the constant components of projects. The tools selected in the resolution process and the dispute resolution method can lead a successful project to failure and even change

the fate of a project. When literature research is conducted in this field, we conclude that there are many dispute resolution methods. By considering that the key to achieving easy and accurate results in the resolution of disputes is selection of the right solution, it can be stated that it is important for the parties to be aware of various dispute resolution methods and make a relevant assessment and take a decision accordingly.

Arbitration, as discussed and analyzed in this article, refers to the resolution of a dispute between two or more parties as a result of a legal process where an independent and impartial board considers the dispute and makes a binding decision accepted by all parties (Ossman et al., 2010). Pürselim (2021) defines arbitration as an agreement between the parties for the final and binding settlement of disputes that have arisen or may arise between two or more persons within the scope of the matters permitted by law to be resolved by arbitration, through independent persons called arbitrators instead of courts. Pekcanitez et al. (2017)



defines it as resolving disputes through a judicial process through impartial and independent arbitrators. The term Arbitration, as discussed in the field of private law, is commonly used in the construction sector and is defined as a dispute resolution method in international construction contracts. Arbitration currently represents a significant part of the dispute resolution dynamic of the construction sector. The increasing use of arbitration in the construction sector increases the necessity of this research. At this point, the important point is the ability to answer the question on the awareness of the managers, architects and engineers working in the sector at all levels of these opportunities and developments. Müngen and Kuruoğlu (2000) have emphasized in their study that technical staff are generally directed towards design and construction, but employers should now have knowledge in law and economics as well as their knowledge in architecture and engineering. In this article, which particularly deals with the Arbitration of Construction Disputes, it is aimed to measure the awareness of the groups working in the construction sector about the possibilities of making an application to Arbitration as a result of the disputes that they encounter in the sector.

There are many reasons for the parties to choose arbitration. Arbitration is faster than courts because the backlog in courts is very high. The arbitrators selected by the parties in arbitration are experts who know the subject of the dispute well. Arbitration awards are binding and enforceable. In addition, trade secrets are kept confidential in arbitration (Gürbüz, 2023).

Although mediation and arbitration, one of the Alternative Dispute Resolution Methods, are similar in appointing a neutral third party, in arbitration, the arbitrator makes a binding decision due to the judgment, while in mediation, the dispute is resolved without a judgment.

Arbitration is a commonly-used method for fast, impartial and reliable decisions on dispute resolution in many countries around the world. Today, arbitration centers are founded in every country in the world so that disputes can be resolved and decided in their own country (Akıncı, 2013). There are more than 200 arbitration centers in the world, and the number of the arbitration centers is increasing. The remarkable arbitration centers are the International Chamber of Commerce (ICC), the International Center for Settlement of Investment Disputes (ICSID), the Arbitration Institute of the Stockholm Chamber of Commerce (SCC), the World Intellectual Property Organization's Arbitration Court (WIPO), the United Nations Commission on International Trade Law (UNCITRAL) and the London Court of International Arbitration (LCIA), etc.

The arbitration centers in Türkiye are the Istanbul Arbitration Center (ISTAC), Union of Chambers and Commodity Exchanges of Türkiye (TOBB) Arbitration Court, Istanbul Chamber of Commerce Arbitration and Mediation Center (ITOTAM), Energy Disputes Arbitration

Center (EDAC) and Organization of Islamic Cooperation (OIC) Arbitration Center. When the data of the International Chamber of Commerce (ICC) are reviewed today, approximately 25.000 cases have been heard since its foundation. The disputes in approximately 20 fields such as construction, mining, energy, transportation, production, telecommunications, finance, manufacturing and sports have been resolved through arbitration. According to the 2019 data, construction and energy sectors account for 40% of the total number of arbitration cases, with 210 cases in construction sector and 140 cases in energy sector, and this ratio is increasing progressively (ICC, 2020).

An arbitration agreement must be prepared before the dispute arises between the parties. This agreement should include headings such as the number of arbitrators, how they will be appointed and their qualifications, the place of arbitration, the remedies to be applied before arbitration, arbitrator fee, arbitration costs, provisional legal protection measures, confidentiality, and the duration of arbitration. The proceedings start with the application of one of the parties. The selected arbitrators request a reply from the parties, and a decision is rendered after a hearing or a review of the file (Pekcanitez et al., 2017).

From 2019 to 2020, the average value of disputes worldwide has increased significantly to approximately 54.26 million USD, while the overall number of disputes has remained relatively same (Arcadis, 2022). The interests of the parties in the construction sector cause conflicts of interest and disagreements (Çevikbaş and Köksal, 2018). Thus, the construction sector is the leader in terms of the number of disputes (Gebken et al., 2005). Pekcanitez (2010) has emphasized in his study that there is a lack of information about arbitration in the public and that Arbitration is misunderstood. Alpkökin (2017), as a result of a survey conducted among 11 contractor and consultant company officials, found that the satisfaction level of the companies knowing arbitration was high. Dalmaz (2012) emphasized that the level of knowledge of construction companies that are members of the Turkish Contractors Association on arbitration should be determined.

When we today look at the reasons for preferring Arbitration in the world, these reasons are that disputes are resolved faster than the state jurisdiction and there is no publicity. Currently, the number of applications to arbitration is progressively increasing in the international arena due to its more positive aspects (Pekcanitez et al., 2017). In addition, the ability of the parties to determine the arbitration procedure within the framework of freedom of will in the dispute resolution process, to choose the place, language, applicable law, arbitrators, and arbitrators appointment procedure, and to complete the arbitration proceedings within the specified period make arbitration even more critical (Yılmazsoy, 2020).

2. Materials and Methods

The prepared survey form was designed to measure the level of knowledge among technical staff working in the construction sector transportation projects regarding their opportunities to resort to arbitration in case of disputes. A total of 100 technical staff (including civil engineers, architects, and other engineers) working in public and private sector transportation projects in Istanbul constitute the sample of the research. The sample size was confirmed to be sufficient by employing the Kirsh sampling formula (Kirsh, 1965). The reason for selecting technical staff in transportation projects is the longer duration and higher cost required for the construction of these projects.

Before the survey questions were prepared, a detailed literature review was conducted on Arbitration, and a questionnaire form with 25 questions was prepared according to the purpose of this study. Expert opinions were utilized for the scope validity of the survey, and the comprehensibility of the survey questions was assessed by academic professionals working in the field of arbitration, evaluating the measurement properties of each question. Experts rated the questions as 'appropriate, should be revised, and inappropriate,' thereby assigning a scoring to each question. Consequently, the calculated Content Validity Index (CVI) value was found to be above 0.80 for all items. This determined value was deemed suitable for content validity (Polit et al., 2007; Delgado Rico et al., 2012).

The questionnaire that was used as a data collection tool consists of 3 sections. The first section consists of optional questions asked to determine the demographic information of the participants. The second section was prepared based on a 3-point Likert scale (True, False, I do not know) to measure the arbitration knowledge level of the participants. The last section consists of 'Yes' and 'No' questions intended to enable the participants to determine the situation. Accordingly, the first 6 questions were created to obtain information about the demographic characteristics of the participants. The following 14 questions aim to measure the level of arbitration knowledge. The 5 questions in the last section aim to determine the relationship and status of technical staff with arbitration. In the second section which consists of 14 questions to determine the level of knowledge, each correct answer was accepted as 1 point, and a knowledge score of 0 to 14 was created for each participant of the survey. The knowledge levels of the participants were classified in five categories as 'Very Low', 'Low', 'Medium', 'Good' and 'Very Good' according to their answers. The calculated score ranges were obtained by dividing the total score by five. The answer of the participants, who marked the option "I do not know", was accepted as "Wrong".

The data regarding the knowledge level assessment criteria are provided in the Table 1. The questionnaire was applied to 100 technical staff completely optionally in face-to-face interviews and remotely. As 4 of the

participants filled the questions uniformly, they were not included into the analysis.

Table 1. Knowledge level assessment criteria

Factor Assessed	Score Range	Assessment Criteria
Arbitration Knowledge Level	$0 \leq x \leq 2$	Very Low
	$3 \leq x \leq 5$	Low
	$6 \leq x \leq 8$	Medium
	$9 \leq x \leq 11$	Good
	$12 \leq x \leq 14$	Very Good

Assessment of the data obtained in the research: The data obtained from the participants, who filled in the survey, were collected at the Web Page of the survey website, and when the survey application was completed, such data were transferred to the Statistical Package for The Social Sciences (SPSS) 28.0 package program, and the analyzes were continued through this program. To select the right statistical analysis and achieve consistent results in the research data, it was first tested whether the questions included into the questionnaire form were normally distributed. The kurtosis and skew values were examined for the normality distribution, and it was determined that the data groups in the study were not normally distributed, because the value indicated by George and Mallery (2019) was not between +2 and -2. However, Kolmogorov-Smirnov test is used if the sample size is equal to and above 29, and Shapiro-Wilk test is used if it is less than 29 (Kalaycı, 2006). For this reason, the significance value of the Kolmogorov-Smirnov test conducted in the research data group was tested as less than 0.05 ($0.00 < 0.05$), and it was determined that the research data groups were not normally distributed. Due to the abnormal distribution of the research data groups, the Mann-Whitney U test, which is known as the strongest test among the non-parametric tests (Baştürk, 2010), was applied in this study. The Mann Whitney U test assesses whether the rank is different between the two groups by comparing the medians of the two groups (Karagöz, 2016).

Before starting the survey application, a pilot study was conducted on a group of 25 individuals to test whether the survey items were understood correctly. Following the feedback from the group members and expert opinion; the survey study was finalized. Besides, reliability test was applied for each question included into the questionnaire form. The reliability test is defined as the consistency between the answers given to the survey questions by the participants. In other words, it demonstrates how accurately the questionnaire measures the answers. As a result of the reliability analysis, the Cronbach's Alpha (α) value was determined as 0.817. A value of $0.80 < \alpha < 1.00$ shows that the survey is highly reliable (Karagöz, 2016).

3. Results

The information about the demographic characteristics of the technical staff participating in the research is provided in the Table 2.

Table 2. Demographic characteristics of the participants

Characteristic	Category	n	%
Profession	Civil Engineer	57	59.4
	Architect	12	12.5
	Mechanical Engineer	3	3.1
	Electrical Electronics Engineer	6	6.3
	Other	18	18.8
Education	Associate Degree	3	3.1
	Bachelor's Degree	48	50.0
	Master's Degree	33	34.4
	Doctorate	12	12.5
Position in the Company	Project Manager	39	40.6
	Engineer	27	28.1
	Chief	12	12.5
	Other	18	18.8
Experience	Less than 5 years	30	31.3
	6-10 Years	21	21.9
	11-15 Years	15	15.6
	16-20 Years	6	6.3
	More than 20 years	24	25
Field of Activity of the Company	Construction	57	59.4
	Electrics Electronics Design	3	3.1
	Design	9	9.4
	Cost Planning	15	15.6
	Other	12	12.5
Working Area	Private Sector	81	84.4
	Public	15	15.6

When the professional status of the participants in the research is examined, it is observed that they are mostly civil engineers (59.4%) is. In terms of education, it is concluded that the majority of the participants (50%) have a bachelor's degree. Those that have postgraduate degrees account for 46.9% of the participants. In the research, the participants mostly consist of the individuals working in the position of project managers (40.6%). The lowest ratio among the overall participants is those individuals working in the position of chief (12.5%). It was determined that the majority of the participants have worked in the sector for less than 5 years (31.3%) and more than 20 years (25%). The majority of the participants (59.4%) work in the construction sector. This field of activity is followed by cost planning (15.6%). When the working area of the participants in the research is examined, it is observed that private sector (84.4%) is approximately 5 times higher than public sector (15.6%). When the relationship between profession and field of activity is examined, all

Architects, Electrical-Electronics Engineers and Mechanical Engineers work in private sector. The frequency analysis regarding the answers given to the statements in the arbitration knowledge level scale is provided in the Table 3.

When the answers given by the technical staff to the statements provided in the scale are examined to determine the arbitration knowledge level, it has been concluded that the statement "Arbitration is generally resolved faster than public jurisdiction." is the most correctly answered statement with a ratio of 84.4%. Among all statements, the statement with the highest number of wrong answers is "Arbitration award is final and binding. Also, it is not subject to appeal" with a ratio of 56.3%. The statement "Arbitration awards taken in the arbitration proceedings held abroad are also enforced (recognized) in Türkiye." received the highest number of I Do Not Know answers (50%).

The participants received a minimum of '0 points' and a maximum of '14 points' from the arbitration knowledge level test. 37% of the participants received a good or very good point. The knowledge level of the participants was classified as "very low", "low", "medium", "good" and "very good" according to the points that they received. The data about the knowledge level of the participants on arbitration is provided in the Figure 1.

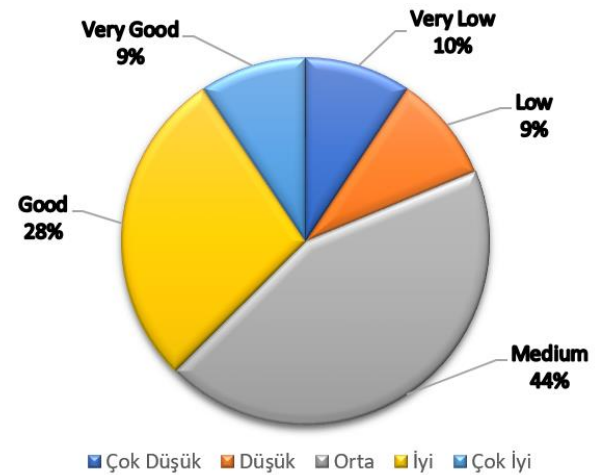


Figure 1. Arbitration knowledge level of participants.

The information about the determination of the situation by the technical staff participating in the research is provided in the Table 4.

Among the statements asked to the technical staff for the purpose of determination of the situation; the question "Would you consider participating in an arbitration information training?" received the highest number of Yes answers with a ratio of 93.8%. Among all statements, the highest "No" answer with a ratio of 84.4% was given for the questions "Do you follow up the actual developments about Arbitration in the world and in Türkiye?" and "Do you think that you have sufficient knowledge about arbitration?".

Table 3. Frequency analysis regarding the arbitration knowledge statements

	True		False		I do not know		\bar{X}	StdDev
	n	%	n	%	n	%		
1. Construction disputes are allowed to be resolved through arbitration by arbitrators instead of national courts.	66	68.8	3	3.1	27	28.1	1.59	0.901
2. Arbitration is generally resolved faster than public jurisdiction.	81	84.4	3	3.1	12	12.5	1.28	0.676
3. Arbitration award is final and binding. Also, it is not subject to appeal.	24	25	54	56.3	18	18.8	1.94	0.662
4. Arbitration is relatively less costly.	57	59.4	21	21.9	18	18.8	1.59	0.789
5. There is an Arbitration Center in Türkiye.	45	46.9	12	12.5	39	40.6	1.94	0.938
6. Arbitration process is confidential. (unless formal litigation is initiated in the future)	45	46.9	21	21.9	30	31.3	1.84	0.875
7. Parties may determine the process according to their own conditions.	60	62.5	6	6.3	30	31.3	1.69	0.921
8. During the arbitration process, parties may propose other solutions for settlement.	78	81.3	3	3.1	15	15.6	1.34	0.737
9. Arbitration proceedings including the hearings are not open to the public.	42	43.8	21	21.9	33	34.4	1.91	0.884
10. Personal data of the parties is protected against each other and against third parties.	75	78.1	3	3.1	18	18.8	1.41	0.789
11. Parties may select arbitrators.	42	43.8	24	25	30	31.3	1.88	0.861
12. Arbitration awards may be enforced like court orders.	66	68.8	0	0	30	31.3	1.63	0.932
13. Parties may agree on the venue of the arbitration, language of the arbitration and the arbitration rules and laws to be applied for the arbitration.	27	28.1	33	34.4	36	37.5	2.09	0.809
14. Arbitration awards taken in the arbitration proceedings held abroad are also enforced (recognized) in Türkiye.	39	40.6	9	9.4	48	50.0	2.09	0.952

Table 4. Frequency analysis of the statements about determination of the situation

	Yes		No		\bar{X}	StdDev
	n	%	n	%		
15. Do you follow up the actual developments about Arbitration in the world and in Türkiye?	15	15.6	81	84.4	0.16	0.365
16. Do you think that you have sufficient knowledge about arbitration?	15	15.6	81	84.4	0.16	0.365
17. Would you consider participating in an arbitration information training?	90	93.8	6	6.3	0.94	0.243
18. Would you add an arbitration clause in the contracts that you will make in your organization?	78	81.3	18	18.8	0.81	0.392
19. Did the contracts department in your company inform you about the arbitration process?	18	18.8	78	81.3	0.19	0.392

3.1. Test of the Difference in Terms of the Arbitration Knowledge Score of the Participants and the Status of Following up the Actual Developments About Arbitration

The Mann-Whitney U test results for the points received from the arbitration knowledge level scale of the participants who answered Yes or No to the statement “Do you follow up the actual developments about Arbitration in the world and in Türkiye?” are provided in

the Table 5.

H_0 : There is no difference between the Arbitration Knowledge Score of the Participants and the Status of Following up the Actual Developments about Arbitration.

H_1 : There is difference between the Arbitration Knowledge Score of the Participants and the Status of Following up the Actual Developments about Arbitration.

Table 5. Mann-Whitney test results between the statement S15 and the arbitration knowledge level

	Yes	No
n	15	81
Mean rank	70.70	44.39
Mean total	1060.50	3595.50
U value	274.50	
z	-3.558	
P	0.000	

Accordingly, it was determined that there is a significant difference between the points received from the arbitration knowledge level scale of the participants who answered Yes or No to the statement S15 ($z=-3.558$, $P<0.05$). For this reason, the H_1 hypothesis was accepted. When the mean rank is taken into consideration, it is concluded that the participants who answered Yes to the S15 statement have a higher arbitration knowledge level than those who answered No.

3.2. Test of the Difference between the Arbitration Knowledge Level Score of the Participants and the Answer Given to the Question Do You Think That You Have Sufficient Knowledge about Arbitration?

The Mann-Whitney U test results for the points received from the arbitration knowledge level scale of the participants who answered Yes or No to the statement “Do you think that you have sufficient knowledge about arbitration?” are provided in the Table 6.

H_0 : There is no difference between the Arbitration Knowledge Level Score of the Participants and the answer given to the question Do you think that you have sufficient knowledge about arbitration?

H_2 : There is difference between the Arbitration Knowledge Level Score of the Participants and the answer given to the question Do you think that you have sufficient knowledge about arbitration?

Table 6. Mann-Whitney test results between the statement S16 and the arbitration knowledge level

	Yes	No
n	15	81
Mean rank	74.30	43.72
Mean total	1114.50	3541.50
U value	220.50	
z	-4.136	
P	0.000	

Accordingly, it was determined that there is a significant difference between the points received from the arbitration knowledge level scale of the participants who answered Yes or No to the statement S16 ($z=-4.136$, $P<0.05$). For this reason, the H_2 hypothesis was accepted. When the mean rank is taken into consideration, it is concluded that the participants who answered Yes to the S16 statement have a higher arbitration knowledge level than those who answered No.

3.3. Test of the Difference between the Arbitration Knowledge Level Scale of the Participants and Their Demands to Receive Information Training on Arbitration

The Mann-Whitney U test results for the points received from the arbitration knowledge level scale of the participants who answered Yes or No to the statement “Would you consider participating in an arbitration information training?” are provided in the Table 7.

H_0 : There is no difference between the Arbitration Knowledge Level Scale of the Participants and their Demands to Receive Information Training on Arbitration.

H_3 : There is difference between the Arbitration Knowledge Level Scale of the Participants and their Demands to Receive Information Training on Arbitration.

Table 7. Mann-Whitney Test results between the statement S17 and the arbitration knowledge level

	Yes	No
n	90	6
Mean rank	47.95	56.75
Mean total	4315.50	340.50
U value	220.50	
z	-0.793	
P	0.428	

Accordingly, there is no difference between the points received from the arbitration knowledge level scale of the participants who answered Yes or No to the statement S17 ($z=-0.793$, $P>0.05$). For this reason, the H_0 hypothesis was accepted.

3.4. Test of the Difference between the Arbitration Knowledge Level Scale of the Participants and Their Actions of Adding an Arbitration Clause in the Contracts

The Mann-Whitney U test results for the points received from the arbitration knowledge level scale of the participants who answered Yes or No to the statement “Would you add an arbitration clause in the contracts that you will make in your organization?” are provided in the Table 8.

H_0 : There is no difference between the Arbitration Knowledge Level Scale of the Participants and their Actions of Adding an Arbitration Clause in the Contracts.

H_4 : There is difference between the Arbitration Knowledge Level Scale of the Participants and their Actions of Adding an Arbitration Clause in the Contracts.

Table 8. Mann-Whitney Test results between the statement S18 and the arbitration knowledge level

	Yes	No
n	78	18
Mean rank	50.23	41.00
Mean total	3918.00	738.00
U value	567.00	
z	-1.342	
P	0.180	

Accordingly, there is no difference between the points received from the arbitration knowledge level scale of the participants who answered Yes or No to the statement S18 ($z=-1.342$, $P>0.05$). For this reason, the H_0 hypothesis was accepted.

3.5. Test of the Difference between the Arbitration Knowledge Level Scale of the Participants and the Level of Providing Information by the Contracts Department in the Organization

The Mann-Whitney U test results for the points received from the arbitration knowledge level scale of the participants who answered Yes or No to the statement "Did the contracts department in your company inform you about the arbitration process?" are provided in the Table 9.

H_0 : There is no difference between the Arbitration Knowledge Level Scale of the Participants and the Level of Providing Information by the Contracts Department in the Organization.

H_5 : There is difference between the Arbitration Knowledge Level Scale of the Participants and the Level of Providing Information by the Contracts Department in the Organization.

Table 9. Mann-Whitney Test results between the statement S19 and the arbitration knowledge level

	Yes	No
n	18	78
Mean rank	68.50	43.88
Mean total	1233.00	3423
U value	342.00	
z	-3.579	
P	0.000	

Accordingly, it was determined that there is a significant difference between the points received from the arbitration knowledge level scale of the participants who answered Yes or No to the statement S19 ($z=-3.579$, $P<0.05$). For this reason, the H_5 hypothesis was accepted. When the mean rank is taken into consideration, it is concluded that the participants who answered Yes to the S19 statement have a higher arbitration knowledge level than those who answered No.

4. Discussion

The arbitration knowledge level of 63% of the technical staff participating in the research was very low, low, and medium. The main reason more than half of the participants' knowledge level was medium and below is the lack of courses such as construction law and contract management in undergraduate education at universities. Therefore, architects and engineers must include more legal courses in their education processes to raise awareness of dispute resolution methods. In addition, due to insufficient training and conferences on arbitration held by arbitration centers and professional chambers in Türkiye, the level of knowledge remains

moderate and below. Similarly, Müngen and Kuruoğlu (2000) emphasized in their study that the knowledge of the technical staff is oriented towards design and construction. Still, employers should now know law, economics, architecture, and engineering.

84.4% of the participants answered "No" to the questions "Do you follow the current developments in arbitration in the world and Türkiye?" and "Do you think you are sufficiently knowledgeable about arbitration?". The technical staff's score on the arbitration knowledge level supports these data. Due to the size and complexity of foreign-funded construction projects in Türkiye and the projects undertaken by Turkish contractors abroad, many disputes arise between the parties. In such comprehensive and international projects, the arbitration knowledge of technical staff comes to the fore. Technical staff who do not follow the current developments in arbitration and are not sufficiently knowledgeable in arbitration experience problems in the arbitration process due to insufficient construction law knowledge in the companies they work for. Similar to this result, Pekcanitez (2010), Arıcı (2012), İltar and Dikbaş (2011), and Daşdelen (2006) emphasized the lack of knowledge on arbitration in their studies. In addition, Pamuklu (2015) surveyed architects, engineers, lawyers, and academic staff with arbitration experience in Türkiye and found that 46.15% of the respondents had medium and low levels of arbitration knowledge. In the same survey, it was determined that only 5.88% of the participants had a medium level of knowledge, and the rest had a high and very high level of knowledge.

It was determined that the level of arbitration knowledge of the participants who follow the current developments in arbitration in the world and Türkiye, who consider themselves sufficiently knowledgeable about arbitration, and who are informed by the contract department is high. Technical staff who attend arbitration-related training and conferences better understand legal processes and can manage arbitration processes effectively.

When the participants were asked to evaluate themselves, 84.4% thought they did not have enough information about arbitration, and 93.84% stated that they would like to participate in information training on arbitration. We observe that the participant's responses to the self-assessment question align with the survey's general score evaluation results. It has been determined that even the respondents with a 'very good' score would like to receive more training on arbitration. This study is in parallel with the finding that 90% of the company lawyers interviewed in the study Mistelis (2004) would like to receive more training although they view themselves as knowledgeable about arbitration.

A relationship could not be established between the knowledge level of the participants and the actions of adding an arbitration clause in their contracts. However, when the knowledge level of the technical staff reaches a particular level through provision of the necessary

training, it will be possible to ensure that they will add an arbitration clause in the contracts. Currently, a significant relationship could not be established due to the lack of sufficient knowledge.

5. Conclusion

This study aims to measure the level of arbitration knowledge of technical staff working in public and private sector transport projects in Istanbul. Firstly, a questionnaire consisting of 25 questions was designed by making a detailed literature review on arbitration and taking expert opinion in this field. This study applied descriptive statistics, reliability analysis, and the Mann-Whitney U test.

It was examined whether there is a difference between the questions asked to determine the situation and the arbitration knowledge level questions. As a result of this examination, the hypotheses H_1 , H_2 and H_5 were accepted and the hypotheses H_3 and H_4 were rejected. The technical staff who keep up with current developments in arbitration and undergo informative training exhibit a higher level of arbitration knowledge. The majority of technical staff participating in the survey in transportation projects (63%) were classified with moderate, low, or very low levels of arbitration knowledge. In addition, 93.84% of the participants stated that they would like to attend an information training on arbitration.

Due to the limited number of studies regarding the arbitration knowledge level of the technical staff, the awareness of the technical staff working in the public and private sector transportation projects in Istanbul regarding arbitration was presented in this study, and attention was drawn to the necessity of introducing an Arbitration course at the undergraduate education level for technical staff at the engineering-architecture faculties of universities and the provision of professional trainings by the arbitration centers in our country. By increasing the awareness of technical staff in this manner regarding arbitration, it can enable the resolution of disputes in the construction sector through the mediation of arbitrators chosen by the parties involved, rather than resorting to the court, leading to a faster and more cost-effective resolution process. With the future studies, this study could be further improved by applying a questionnaire form to more participants, not only to the technical staff working in the transportation projects.

Author Contributions

The percentage of the author(s) contributions is presented below. All authors reviewed and approved the final version of the manuscript.

	H.B.	A.C.
C	60	40
D	60	40
S	40	60
DCP	70	30
DAI	60	40
L	60	40
W	60	40
CR	60	40
SR	100	
PM	60	40
FA	50	50

C=Concept, D= design, S= supervision, DCP= data collection and/or processing, DAI= data analysis and/or interpretation, L= literature search, W= writing, CR= critical review, SR= submission and revision, PM= project management, FA= funding acquisition.

Conflict of Interest

The authors declared that there is no conflict of interest.

Ethical Consideration

Ethics Committee Approval was obtained for the survey study included in this article with the decision No: 2022/193 in the session held at 13.30 on the date: 21.10.2022 of the Ethics Committee of Social Sciences and Humanities of Harran University.

References

- Akıncı Z. 2013. Neden İstanbul tahkim merkezi? Why center for arbitration in İstanbul?. *Yaşar Üniv E-Derg*, 8: 79-96.
- Alpkökin P. 2017. Türk inşaat sektöründe uyuşmazlık çözüm kurulu uygulamaları. *Karaelmas Fen Müh Derg*, 7(2), 674-683.
- Arcadis. 2022. Global construction disputes report. URL: <https://www.arcadis.com/en-gb/knowledge-hub/perspectives/global/global-construction-disputes-report> (erişim tarihi: 25 Eylül 2023).
- Arıcı Y. 2012. İnşaat sektöründe ADR (alternatif uyuşmazlık çözüm yolları) kullanımı ve seçim kriterlerinin kamu ve özel sektör açısından incelenmesi. Yüksek Lisans Tezi, İstanbul Teknik Üniversitesi, Fen Bilimleri Enstitüsü, İstanbul, Türkiye, pp: 137.
- Baştürk R. 2010. Nonparametrik istatistiksel yöntemler. Anı Yayınları, Ankara, Türkiye, pp: 240.
- Çevikbaş M. Köksal A. 2018. An investigation of litigation process in construction industry in Turkey. *Teknik Derg*, 29(6): 8715-8729.
- Dalmaz Ç. 2012. Uluslararası fidic sözleşmelerinde tahkim hususunun incelenmesi ve bir kavramsal model önerisi. Yüksek Lisans Tezi, Sakarya Üniversitesi, Fen Bilimleri Enstitüsü, Sakarya, Türkiye, pp: 114.
- Daşdelen A. 2006. Yapım yönetimi eğitiminde inşaat hukuku. Yüksek Lisans Tezi, İstanbul Teknik Üniversitesi, Fen Bilimleri Enstitüsü, İstanbul, Türkiye, pp: 132.
- Delgado Rico E, Carrtero Dios H, Ruch W. 2012. Content validity evidences in test development: An applied

- perspective. *Int J Clinic Health Psych*, 12: 449-459.
- Gebken RJ, Gibson GE, Groton JP. 2005. Dispute resolution transactional cost quantification: what does resolving a construction dispute really cost? *Proceedings of the Construction Research Congress*, April 5-7, California, US, pp: 1-10.
- George D, Mallery P. 2019. *IBM SPSS statistics 26 step by step: A simple guide and reference*, 16th ed. Routledge, New York, US, pp: 402.
- Gürbüz A. 2023. Spor tahkim mahkemesi'nin (cas) isminde yer alan "tahkim" ve "mahkeme" kavramlarının incelenmesi ve spor tahkim mahkemesi'nde uygulanan tahkim ile geleneksel tahkimin karşılaştırılması. *İstanbul Ticaret Üniv Sos Bil Derg*, 22(48): 921-941.
- ICC. 2020. ICC dispute resolution statistics. URL: https://library.iccwbo.org/content/dr/STATISTICAL_REPOR TS/SR_0042.htm?l1=Statistical+Reports (erişim tarihi: 20 Eylül 2023).
- İlter D, Dikbaş A. 2011. Uyuşmazlık çözüm yöntemi seçimi için bir karar verme yaklaşım, *İTÜ Derg/A Mimarlık*, 10(1): 165-176.
- Kalaycı Ş. 2006. SPSS uygulamalı çok değişkenli istatistik teknikleri. *Asil Yayın Dağıtım*, Ankara, Türkiye, pp: 426.
- Karagöz Y. 2016. *İstatistiksel analizler*. Nobel Yayıncılık, Ankara, Türkiye, pp: 1336.
- Kirsh L. 1965. *Survey sampling*. John Wiley and Sons, New York, US, pp: 664.
- Mistelis L. 2004. International arbitration-corporate attitudes and practices-12 perceptions tested: Myths, data and analysis research report. *American Rev Int Arbitrat*, 15: 525.
- Müngen U, Kuruoğlu M. 2000. İnşaat mühendisliğinde yapı işletmesi meslek içi eğitim ihtiyacı ve bir uygulama program örneği, 2.Yapı İşletmesi Kongresi, 15-17 Haziran, İzmir, Türkiye, pp: 259-270.
- Ossman G, Bayraktar ME, Cui Q. 2010. Consistency and reliability of construction arbitration decisions: empirical study. *J Manag Eng*, 26(2): 56-64.
- Pamuklu T. 2015. İnşaat projeleri ile ilgili tahkim yargılamalarında çapraz sorgu. Yüksek Lisans Tezi, İstanbul Teknik Üniversitesi, Fen Bilimleri Enstitüsü, İstanbul, Türkiye, pp: 143.
- Pekcanitez H, Korkmaz HT, Akkan M, Özkes M. 2017. Medeni usul hukuku. *On İki Levha Yayıncılık*, İstanbul, Türkiye, pp: 689.
- Pekcanitez H. 2010. İstanbul tahkim merkezi kanun taslağı, *Dokuz Eylül Üniv Hukuk Fak Derg*, 12: 635-655.
- Polit DF, Beck CT, Owen SV. 2007. Is the CVI an acceptable indicator of content validity? *Appraisal and recommendations*. *Res Nurs Health*, 30(4): 459-467.
- Purselim HS, 2021. Milletlerarası tahkim kanunu çerçevesinde kira sözleşmelerinin tahkime elverişliliği. *Marmara Üniv Hukuk Fak Hukuk Araş Derg*, 27(1): 496-512.
- Yılmazsoy E. 2020. Tahkim ve hakem sözleşmeleri. *Türkiye Adalet Akad Derg*, 1(41): 389-426.



TRAVELLING WAVE SOLUTIONS FOR SOME TIME-FRACTIONAL NONLINEAR DIFFERENTIAL EQUATIONS

Mustafa EKİCİ^{1*}


¹Çanakkale Onsekiz Mart University, Faculty of Education, Department of Mathematics and Science Education, 17100, Çanakkale, Türkiye

Abstract: This study employs the powerful generalized Kudryashov method to address the challenges posed by fractional differential equations in mathematical physics. The main objective is to obtain new exact solutions for three important equations: the (3+1)-dimensional time fractional Jimbo-Miwa equation, the (3+1)-dimensional time fractional modified KdV-Zakharov-Kuznetsov equation, and the (2+1)-dimensional time fractional Drinfeld-Sokolov-Satsuma-Hirota equation. The generalized Kudryashov method is highly versatile and effective in addressing nonlinear problems, making it a pivotal component in our research. Its adaptability makes it useful in diverse scientific disciplines. The method simplifies complex equations, improving our analytical capabilities and deepening our understanding of system dynamics. Additionally, we define fractional derivatives using the conformable fractional derivative framework, providing a strong foundation for our mathematical investigations. This paper examines the effectiveness of the generalized Kudryashov method in solving complex challenges presented by fractional differential equations and aims to provide guidance for future studies.

Keywords: Kudryashov method, Time-fractional Jimbo-Miwa equation, KdV-Zakharov-Kuznetsov equation, Drinfeld-Sokolov-Satsuma-Hirota equation, Conformable fractional derivative

*Corresponding author: Çanakkale Onsekiz Mart University, Faculty of Education, Department of Mathematics and Science Education, 17100, Çanakkale, Türkiye

E mail: mustafa.ekici@comu.edu.tr (M. EKİCİ)

Mustafa EKİCİ  <https://orcid.org/0000-0003-2494-8229>

Received: January 01, 2024

Accepted: February 06, 2024

Published: March 15, 2024

Cite as: Ekici M. 2024. Travelling wave solutions for some time-fractional nonlinear differential equations. BSJ Eng Sci, 7(2): 246-253.

1. Introduction

In the last decade, many complex real-world issues have been linked to nonlinear phenomena. Nonlinear processes are characterized by the sudden alteration of system properties in response to small changes, which poses significant challenges in control. The pursuit of precise solutions for nonlinear partial differential equations is essential for gaining insights into the underlying physical mechanisms in diverse fields, including fluid dynamics, viscoelasticity, and control theory, electrochemistry, acoustics, and system identification. Nonlinear fractional differential equations (NFDEs) are important in scientific research as they offer accurate solutions that capture a wide range of complex nonlinear physical phenomena. The use of these equations enhances our comprehension of complex systems and their nuanced behaviours. When combined with symmetry analysis, NFDEs provide an advanced understanding of complex systems, enabling more accurate predictions. The intersection of fractional differential equations (FDEs) and symmetry analysis is a significant area of research and application. Mathematicians and physicists have devoted significant effort to this research area, using symbolic computer programs such as Maple, Matlab, and Mathematica to simplify algebraic computations for exact solutions to

nonlinear partial differential equations. NFDEs have practical applications in various domains, such as modelling viscoelastic materials and understanding system identification processes. These equations can explain phenomena ranging from fluid dynamics to electrochemistry.

NFDEs are significant in modelling biological systems, financial analysis, and applications in fields ranging from economics to biology in the scientific landscape. The significance of these equations lies in their multifaceted applications, which have advanced our understanding of complex systems across various disciplines. In recent years, there has been noteworthy progress in developing diverse, potent, and efficient methods for accurately traversing fields, such as the (G'/G)-expansion method (Zhang et al., 2008; Unal and Ekici, 2021; Ekici and Unal, 2022), the exponential function method (He and Wu, 2006; Naher et al., 2012; Ekici and Unal, 2020), the generalized Riccati equation mapping method (Senol et al., 2021), the extended sinh-Gordon equation expansion method (Bulut et al., 2018), the unified method (Osman, 2019), the sinc-collocation method (Yang et al., 2023), the differential transformation method (Odibat and Momani, 2008; Ekici and Ayaz, 2017), the finite difference method (Tian et al., 2023), the homogeneous balance method (Wang et al., 1996), the homotopy analysis method (Arafa et al., 2011), the generalized



Kudryashov method (Kaplan et al., 2016; Ekici, 2023), etc.

The choice of the generalized Kudryashov method is motivated by its effectiveness in obtaining analytical solutions for complex nonlinear partial differential equations. This methodology is widely recognised as a powerful tool for solving nonlinear evolutionary equations and mathematical models. It is valued for its ability to generate precise solutions in a closed form. This capability aids in understanding the intricacies of nonlinear equations and allows for obtaining analytical solutions for particular problems. Additionally, the method is well-suited for parametric analyses and understanding various physical scenarios. This approach is considered highly effective in addressing fundamental challenges in mathematical physics and revealing the dynamics of complex systems (Jiang et al., 2023).

The KdV-Zakharov-Kuznetsov equations are nonlinear evolutionary equations with significant applications in fields such as plasma physics, magnetohydrodynamics, and quantum mechanics. They are used to model wave interactions, soliton formation, and other complex phenomena. The time-fractional modified KdV-Zakharov-Kuznetsov equation aims to expand this family by introducing a fractional dimension to encompass a broader spectrum of time. This framework enables a detailed analysis of systems that evolve over time, playing a crucial role in understanding nonlinear phenomena and modelling complex dynamics in various scientific domains.

The Jimbo-Miwa equation is a well-known model in the field of nonlinear partial differential equations. It is a generalization of the Korteweg-de Vries equation and is useful for studying solitons and analogous solutions in mathematical physics. The Jimbo-Miwa equation solutions include wave structures, such as solitons, which highlight its ability to model particular behaviours in physical systems. Nonlinear evolutionary equations are significant tools for comprehending wave interactions, energy transfer, and wave dissipation in mathematical physics, particularly in wave theory. The (3+1)-dimensional Jimbo-Miwa equation is a valuable tool that sheds light on the complexities of physical systems and enhances our understanding of specific phenomena.

The study is summarised as follows: Section 2 presents a brief explanation of the conformable fractional derivative and its properties. In Section 3, fundamental information is provided regarding the generalized Kudryashov method, a successful technique for solving partial differential equations of fractional order. In Section 4, the generalized Kudryashov method has been employed to obtain accurate analytical solutions for specific fractional partial differential equations. The conclusion thoroughly discusses our findings and proposes potential directions for future research.

2. Preliminaries

Here, we present a brief overview of the conformable fractional derivative and its main characteristics.

Definition 2.1. Let $\vartheta : \mathbb{R}^+ \cup \{0\} \rightarrow \mathbb{R}$ and $\alpha \in (0,1]$ are given. The definition of the conformable fractional derivative of the function ϑ with respect to order α is as follows (equation 1):

$$(F_\alpha \vartheta)(t) = \lim_{\varepsilon \rightarrow 0} \frac{\vartheta(t + \varepsilon t^{1-\alpha}) - \vartheta(t)}{\varepsilon} \quad (t > 0). \quad (1)$$

Theorem 2.1. Let $\alpha \in (0,1]$, $t > 0$ and ϑ, η be α -differentiable. The following properties can be written:

- $F_\alpha(a\vartheta + b\eta) = a(F_\alpha \vartheta) + b(F_\alpha \eta)$, for all $a, b \in \mathbb{R}$
- $F_\alpha(t^n) = nt^{n-\alpha}$ for all $n \in \mathbb{R}$
- $F_\alpha(\lambda) = 0$, for all constant functions $\vartheta(t) = \lambda$
- $F_\alpha(\vartheta\eta) = \vartheta(F_\alpha \eta) + \eta(F_\alpha \vartheta)$
- $F_\alpha\left(\frac{\vartheta}{\eta}\right) = \frac{\eta(F_\alpha \vartheta) - \vartheta(F_\alpha \eta)}{\eta^2}$
- If, in addition, ϑ is differentiable, then $(F_\alpha \vartheta)(t) = t^{1-\alpha} \frac{d\vartheta}{dt}$.

For a constant, the derivative of order α is zero (Abdeljawad, 2015; Ekici, 2023).

3. Methodology

The Kudryashov method is a well-established approach in mathematical physics, known for its effectiveness in solving nonlinear fractional differential equations. It is particularly strong in deriving analytical solutions for complex and nonlinear equations. Its adaptability and versatility make it a valuable tool for researchers dealing with equations that involve fractional derivatives. In comparison to alternative analytical methods, the Generalized Kudryashov method has demonstrated a higher degree of directness, a propensity for generating fewer trivial solutions, and a relative simplicity in symbolic calculations. Therefore, we suggest refining these methods to avoid extraneous solutions, which could lead to a significant reduction in the volume of symbolic calculations. The significance of the method in advancing our understanding of nonlinear phenomena across various scientific domains is highlighted by its ability to handle the complexities inherent in such equations. This research introduces the generalized Kudryashov method, which is useful in obtaining stable and explicit soliton solutions for FDEs. The methodology presents a general formulation for nonlinear evolution equations. The equation is represented as given in equation 2:

$$P(u, D_t^\alpha u, u_x, u_y, u_z, D_t^{2\alpha} u, D_t^\alpha u_x, D_t^\alpha u_y, D_t^\alpha u_z, \dots) = 0, \quad (2)$$

where α signifies the conformable fractional derivative, P is a polynomial involving the unknown function $u(x, y, z, t)$, its time-fractional derivatives and various ordinary derivatives. The generalized Kudryashov method stands as a comprehensive strategy for producing characteristic and wide-spectrum soliton solutions for NFDEs with respect to time variables

(Tuluze et al., 2014). The following steps are a summary of the generalized Kudryashov method:

Step 1: We apply the following transformation by introducing a new variable ξ (equation 3).

$$\xi = x + y + z + k \frac{t^\alpha}{\Gamma(1 + \alpha)}, \quad u(x, y, z, t) = q(\xi), \quad (3)$$

where k is nonzero constant. equation (2) undergoes a reduction to the following nonlinear ordinary differential equation (NODE) through the transformation defined in equation (3);

$$Q(q, kq', q', q', k^2q'', k(q')^2, k(q')^2, k(q')^2, \dots) = 0, \quad (4)$$

where Q is a polynomial involving q and its ordinary derivatives with respect to ξ . equation 4 is then integrated one or more times, with the constant of integration set to zero.

Step 2: The solution of equation 4 is conjectured to take the following form (equation 5):

$$q(\xi) = \frac{a_0 + \sum_{i=1}^m a_i U^i(\xi)}{b_0 + \sum_{j=1}^n b_j U^j(\xi)}. \quad (5)$$

Here; a_i, b_j denote the constants to be determined subsequently. Additionally,

$$U(\xi) = \frac{1}{1 + \lambda \exp(\xi)},$$

expresses the general solution for the equation 6,

$$U'(\xi) = U^2(\xi) - U(\xi), \quad (6)$$

where λ is a constant specifically representing the integration constant of the solution, and the prime notation denotes the first derivative with respect to ξ .

Step 3: The determination of the parameters m and n involves a systematic procedure of homogeneous balancing, with a specific emphasis on terms containing the highest-order derivatives and the highest-order nonlinear term in equation 4. The approach includes substituting the expression derived from equation 5 into equation 4, alongside equation 6. Setting each coefficient, including the various powers of $U(\xi)$, to zero leads to the formulation of a system of algebraic equations.

Step 4: When using mathematical software programs like Maple to solve algebraic equations, we can determine the values of the unknown constants $a_i (i = 0, 1, \dots, m)$, $b_j (j = 0, 1, \dots, n)$, k and λ . Following this determination, the substitution of these obtained values for a_i and b_j into equation 5 enables the effective derivation of the solution for the nonlinear evolution equation as formulated in equation 4.

4. Applications

This study applies the generalized Kudryashov method to address three prominent equations: the (3+1)-

dimensional time fractional modified KdV-Zakharov-Kuznetsov equation, the (3+1)-dimensional time fractional Jimbo-Miwa equation and the (2+1)-dimensional time fractional Drinfeld-Sokolov-Satsuma-Hirota equation. The goal is to unveil significant solutions and enhance our understanding of the underlying dynamics and behaviors described by these conformable time fractional differential equations.

4.1. The (3 + 1)-Dimensional Time Fractional mKdV-ZK equation

The (3+1)-dimensional time fractional mKdV-ZK equation's precise traveling wave solutions are investigated using the generalized Kudryashov method. The mKdV-ZK equation, first study by (Lazarus et al., 2008), later derive multiple-soliton solutions by (Rehman et al., 2022; Zhou et al., 2022) and investigate various traveling wave solutions by (Khater, 2022; Younas et al., 2023). The time-fractional mKdV-ZK equation is expressed as given in equation 7:

$$D_t^\alpha u + \delta u^2 u_x + u_{xxx} + u_{xyy} + u_{xzz} = 0, \quad (7)$$

where α represents the fractional derivative over the interval $[0,1]$ and $u(x, y, z, t)$ is a differentiable function (Mace and Hellberg, 2001; Alabedelhadi et al., 2023; Onder et al., 2023). The equation 7 is among the most vital integrable equations in nonlinear dynamics. It describes a wide range of nonlinear dispersive physical phenomena and has various applications in nonlinear sciences. Notably, it is crucial in modeling the conservative flow of the Liouville equation, the 2-dimensional gauge field theory of conformal field and the theory of quantum gravity among other areas.

Now we apply the method to the equation 7. Substituting equation 3 into equation 7 reduces to the nonlinear ODE

$$kq' + \delta q^2 q' + 3q''' = 0, \quad (8)$$

where $q' = \frac{dq}{d\xi}$. Integrating equation 8 once with respect to ξ , we get

$$kq + \frac{\delta S}{3} q^3 + 3q'' + c = 0, \quad (9)$$

where k is non-zero constant. Using the homogeneous balance method, that is balancing q'' and q^3 term in equation 9, we find $m = 3, n = 2$. Hence, from equation 5 we have

$$q(\xi) = \frac{a_0 + a_1 U(\xi) + a_2 U^2(\xi) + a_3 U^3(\xi)}{b_0 + b_1 U(\xi) + b_2 U^2(\xi)}. \quad (10)$$

Subsequently, we substitute equation 10 into equation 9 and organize all terms in a manner that each coefficient $U^i(\xi) (i = 0, 1, \dots, 9)$ equates to zero, resulting in a system of equations. Employing mathematical software, we can then solve these equations to deduce a set of solutions for $k, a_i (i = 0, 1, 2, 3), b_j (j = 0, 1, 2)$:

Case 1: Specifically, the obtained values for the constants are as follows:

$$a_0 = -\frac{a_3}{2}, a_1 = \frac{3a_3}{2}, a_2 = -\frac{3a_3}{2},$$

$$b_0 = \frac{b_2}{3}, b_1 = -b_2, k = \frac{27}{2}, \delta = -18 \left(\frac{b_2}{a_3}\right)^2.$$

Upon substituting these values into equation 10, the solution for equation 7 is obtained as:

$$q(\xi) = -\frac{3a_3[\lambda^3 e^{3\xi} - 1]}{2b_2[\lambda^2 e^{2\xi} - \lambda e^\xi + 1][1 + \lambda e^\xi]} \quad (11)$$

For the specific case where $\lambda = a_3 = b_2 = 1$ in equation 11, the solution simplifies to:

$$q(\xi) = -\frac{3}{2} \tanh\left(\frac{3\xi}{2}\right),$$

$$q(\xi) = -\frac{a_3(2b_1\lambda^3 e^{3\xi} + b_2\lambda^3 e^{3\xi} + 2b_1\lambda^2 e^{2\xi} + 3b_2\lambda^2 e^{2\xi} + 2b_1\lambda e^\xi + b_2\lambda e^\xi + 2b_1 + 3b_2)}{b_2(2b_1\lambda^2 e^{2\xi} - b_2\lambda^2 e^{2\xi} - 2b_2\lambda e^\xi - 2b_1 - 5b_2)(1 + \lambda e^\xi)} \quad (12)$$

For the specific case where $\lambda = b_1 = b_2 = a_3 = 1$ equation 12, the solution simplifies to:

$$q(\xi) = -\frac{3e^{3\xi} + 5e^{2\xi} + 3e^\xi + 5}{(e^{2\xi} - 2e^\xi - 7)(1 + e^\xi)}.$$

Here, ξ is defined as $\xi = x + y + z + \frac{6t^\alpha}{\Gamma(1+\alpha)}$.

Case 3:

$$q(\xi) = \frac{-\frac{b_0 a_3}{2b_2} + \frac{a_3(2b_0 - b_1)}{2b_2} U(\xi) + \frac{a_3(2b_1 - b_2)}{2b_2} U^2(\xi) + a_3 U^3(\xi)}{b_0 + b_1 U(\xi) + b_2 U^2(\xi)} \quad (13)$$

For the specific case where $\lambda = b_2 = a_3 = 1$ in equation 13, the solution simplifies to:

$$q(\xi) = -\frac{1}{2} \tanh(\xi/2),$$

where ξ is defined as $\xi = x + y + z + \frac{3t^\alpha}{2\Gamma(1+\alpha)}$.

Case 4:

$$a_0 = 0, \quad a_2 = -a_1 - a_3, \quad b_1 = -\frac{b_0(2a_1 + a_3)}{a_1},$$

$$b_2 = 2\frac{b_0 a_3}{a_1}, k = -3, \quad \delta = -72 \left(\frac{b_0}{a_1}\right)^2.$$

Upon substituting these values into equation 10, the solution for equation 7 is obtained as:

$$q(\xi) = \frac{a_1 U(\xi) + (-a_1 - a_3) U^2(\xi) + a_3 U^3(\xi)}{b_0 + \left(-\frac{b_0(2a_1 + a_3)}{a_1}\right) U(\xi) + \left(\frac{2b_0 a_3}{a_1}\right) U^2(\xi)} \quad (14)$$

For the specific case where $\lambda = b_0 = a_1 = 1$ in equation 14, the solution simplifies to:

$$q(\xi) = -\frac{1}{2} \operatorname{csch}(\xi),$$

where ξ is defined as $\xi = x + y + z - \frac{3t^\alpha}{\Gamma(1+\alpha)}$.

4.2. The (3+1)-Dimensional Time Fractional Jimbo-Miwa equation

Now, we intend to apply our methodology to the (3+1)-dimensional Jimbo-Miwa equation. Let us contemplate the (3+1)-dimensional Jimbo-Miwa equation (Roshid et al., 2014; Korkmaz, 2017),

$$u_{xxxy} + 3u_y u_{xx} + 3u_x u_{xy} + 2D_t^\alpha u_y - 3u_{xz} = 0. \quad (15)$$

We employ the generalized Kudryashov method to

where ξ is defined as $\xi = x + y + z + \frac{27t^\alpha}{2\Gamma(1+\alpha)}$.

Case 2:

$$a_0 = \frac{(2b_1 + b_2)a_3}{4b_2}, a_1 = -\frac{a_3 b_1}{b_2}, a_2 = \frac{(2b_1 - b_2)a_3}{2b_2},$$

$$b_0 = -\frac{2b_1 + b_2}{4}, k = 6, \quad \delta = -18 \left(\frac{b_2}{a_3}\right)^2.$$

Upon substituting these values into equation 10, the solution for equation 7 is obtained as:

$$a_0 = -\frac{b_0 a_3}{2b_2}, a_1 = \frac{a_3(2b_0 - b_1)}{2b_2}, a_2 = \frac{a_3(2b_1 - b_2)}{2b_2},$$

$$k = \frac{3}{2}, \quad \delta = -18 \left(\frac{b_2}{a_3}\right)^2.$$

Upon substituting these values into equation 10, the solution for equation 7 is obtained as:

equation 15. We apply the equation 3 to the equation 15, hence equation 15 reduces to the following nonlinear ODE

$$q^{(4)} + 6q'q'' - 2kq'' - 3q'' = 0 \quad (16)$$

where $q' = \frac{dq}{d\xi}$. Integrating equation 16 once with respect to ξ , we get

$$q''' + 3(q')^2 - 2kq' - 3q' = 0, \quad (17)$$

where k is a constant. Using the homogeneous balance method, that is balancing q''' and $(q')^2$ term in equation 16, we find $m = 3, n = 2$. Hence, from equation 5 we have

$$q(\xi) = \frac{a_0 + a_1 U(\xi) + a_2 U^2(\xi) + a_3 U^3(\xi)}{b_0 + b_1 U(\xi) + b_2 U^2(\xi)} \quad (18)$$

Next, we substitute equation 18 into equation 16 and the set of equations obtained by setting each coefficient of $U^i(\xi)$ ($i = 0, 1, \dots, 12$) to zero should be organized. These equations can then be solved using mathematical software to obtain a set of solutions for k, b_0, b_1, b_2, a_i ($i = 0, 1, 2, 3$):

Case 1: Specifically, the obtained values for the constants are as follows:

$$a_0 = \frac{a_2 b_0 + 2b_0 b_1}{b_2},$$

$$a_1 = \frac{a_2 b_1 - 2b_0 b_2 + 2b_1^2}{b_2},$$

$$a_3 = -2b_2, \quad k = -1.$$

Upon substituting these values into equation 18, the solution for equation 17 is obtained as:

$$q(\xi) = \frac{\frac{a_2 b_0 + 2b_0 b_1}{b_2} + \left(\frac{a_2 b_1 - 2b_0 b_2 + 2b_1^2}{b_2}\right) U(\xi) + a_2 U^2(\xi) - (2b_2) U^3(\xi)}{b_0 + b_1 U(\xi) + b_2 U^2(\xi)} \quad (19)$$

If we rearrange and simplify the equation 19, we obtain the following form

$$q(\xi) = \frac{\lambda a_2 e^\xi + 2\lambda b_1 e^\xi + a_2 + 2b_1 - 2b_2}{b_2(1 + \lambda e^\xi)},$$

where ξ is defined as $\xi = x + y + z - \frac{t^\alpha}{\Gamma(1+\alpha)}$. The solution function can be expressed in terms of hyperbolic functions by assigning specific values.

Case 2:

$$a_0 = -\frac{2a_2 b_1 + a_2 b_2 + 4b_1^2 + 4b_1 b_2 + b_2^2}{4b_2},$$

$$a_1 = \frac{b_1 a_2 + 2b_1^2 + b_1 b_2}{b_2},$$

$$a_3 = -2b_2, \quad b_0 = -\frac{1}{2}b_1 - \frac{1}{4}b_2, \quad k = \frac{1}{2}.$$

Upon substituting these values into equation 18, the solution for equation 15 is obtained as:

$$q(\xi) = -\frac{4b_2 U(\xi)^2 - (2a_2 + 4b_1 + 2b_2)U(\xi) + a_2 + b_2 + 2b_1}{(2U(\xi) - 1)b_2} \quad (20)$$

If we rearrange and simplify the equation 20, we obtain the following form

Case 4:

$$a_2 = -\frac{a_0^3 b_1^2 - 2a_0^2 a_1 b_0 b_1 - 4a_0^2 b_0^2 b_1 - 4a_0^2 b_0 b_1^2 + a_0 a_1^2 b_0^2 + 4a_0 a_1 b_0^3 + 6a_0 a_1 b_0^2 b_1}{4b_0^4}$$

$$+ \frac{4a_0 b_0^4 + 8a_0 b_0^3 b_1 + 4a_0 b_0^2 b_1^2 - 2a_1^2 b_0^3 - 4a_1 b_0^4 - 4a_1 b_0^3 b_1}{4b_0^4}$$

$$b_2 = -\frac{a_0^2 b_1^2 - 2a_0 a_1 b_0 b_1 - 4a_0 b_0^2 b_1 - 2a_0 b_0 b_1^2 + a_1^2 b_0^2 + 4a_1 b_0^3 + 2a_1 b_0^2 b_1 + 4b_0^4 + 4b_0^3 b_1}{4b_0^3},$$

$$k = -1, \quad a_3 = 0,$$

Upon substituting these values into equation 18, the solution for equation 15 is obtained as:

$$q(\xi) = \frac{2a_0 b_0^2 + (a_0^2 b_1 - a_0 a_1 b_0 - 2a_0 b_0^2 - 2a_0 b_0 b_1 + 2a_1 b_0^2)U(\xi)}{2b_0^3 + b_0(a_0 b_1 - a_1 b_0 - 2b_0^2)U(\xi)} \quad (22)$$

If we rearrange and simplify the equation 22, we obtain the following form

$$q(\xi) = \frac{2\lambda a_0 b_0^2 e^\xi + a_0^2 b_1 - a_0 a_1 b_0 - 2a_0 b_0 b_1 + 2a_1 b_0^2}{b_0(2\lambda b_0^2 e^\xi + a_0 b_1 - b_0 a_1)},$$

where ξ is defined as $\xi = x + y + z - \frac{t^\alpha}{\Gamma(1+\alpha)}$. The solution function can be expressed in terms of hyperbolic functions by assigning specific values.

4.3. The (2+1)-Dimensional Time-Fractional Drinfeld Sokolov Satsuma Hirota equation

We first consider the following Couple Boiti-Leon-Pempinelli equations system is of the form

$$\begin{cases} u_{ty} = (u^2 - u_x)_{xy} + 2v_{xxx} \\ v_t = v_{xx} + 2uv_x \end{cases} \quad (23)$$

The second considerable problem Drinfeld-Sokolov-Satsuma-Hirota (DSSH) equation which is widely used in mathematical physics in the form is given by (Ding and

$$q(\xi) = \frac{\lambda^2 e^{2\xi} (a_2 + 2b_1 + b_2) - (a_2 + 2b_1 - 3b_2)}{b_2(\lambda^2 e^{2\xi} - 1)},$$

where ξ is defined as $\xi = x + y + z + \frac{t^\alpha}{2\Gamma(1+\alpha)}$. The solution function can be expressed in terms of hyperbolic functions by assigning specific values.

Case 3:

$$a_0 = \frac{a_2}{3}, \quad a_1 = -a_2, a_3 = -2b_2, b_2 = 3b_0,$$

$$b_1 = -b_2, \quad k = 3.$$

Upon substituting these values into equation 18, the solution for equation 15 is obtained as:

$$q(\xi) = -\frac{a_2 + 3a_2 U(\xi) - 3a_2 U^2(\xi) + 18b_0 U^3(\xi)}{3b_0(1 - 3U(\xi) + 3U^2(\xi))} \quad (21)$$

If we rearrange and simplify the equation 21, we obtain the following form

$$q(\xi) = -\frac{\lambda^3 a_2 e^{3\xi} + a_2 - 18b_0}{3b_0(1 + \lambda e^\xi)(-\lambda^2 e^{2\xi} + \lambda e^\xi - 1)},$$

where ξ is defined as $\xi = x + y + z + \frac{3t^\alpha}{\Gamma(1+\alpha)}$. The solution function can be expressed in terms of hyperbolic functions by assigning specific values.

Feng, 2014; Ali et al., 2018).

$$u_{6x} - 9u_x u_{4x} - 18 u_{xx} u_{3x} + 18 u_x^2 u_{xx} - \frac{1}{2} D_t^{2\alpha} u + \frac{1}{2} D_t^\alpha u_{xxx} = 0.$$

By using the generalized Kudryashov method to solve equation 23. Substituting equation 3 into equation 23 reduces the to following nonlinear ODE

$$q^{(6)} - 9q' q^{(4)} - 18q'' q''' + 18(q')^2 q'' - \frac{1}{2} k^2 q'' - \frac{1}{2} k q^{(4)} = 0, \quad (24)$$

where $q' = \frac{dq}{d\xi}$. Integrating equation 24 once with respect to ξ , we get

$$q^{(5)} - 9q'q''' - \frac{9}{2}(q'')^2 + 6(q')^3 - \frac{1}{2}k^2q' - \frac{1}{2}kq'''' = 0, \quad (25)$$

where k is a constant. Using the homogeneous balance method, that is balancing $q^{(5)}$ and $(q')^3$ term in equation 25, we find $m = 2, n = 1$. Hence, from equation 5 we have

$$q(\xi) = \frac{a_0 + a_1U(\xi) + a_2U^2(\xi)}{b_0 + b_1U(\xi)}. \quad (26)$$

Next, we substitute equation 26 into equation 25 and the set of equations obtained by setting each coefficient of $U^i(\xi)$ ($i = 0, 1, \dots, 12$) to zero should be organized. These equations can then be solved using mathematical software to obtain a set of solutions for k, b_0, b_1, a_i ($i = 0, 1, 2$):

Case 1:

Specifically, the obtained values for the constants are as follows:

$$a_0 = \frac{a_1b_0 - 2b_0^2}{b_1}, \quad a_2 = 2b_1, \quad k = 1.$$

Upon substituting these values into equation 26, the solution for equation 23 is obtained as:

$$q(\xi) = \frac{\frac{a_1b_0 - 2b_0^2}{b_1} + a_1U(\xi) + 2b_1U^2(\xi)}{b_0 + b_1U(\xi)}. \quad (27)$$

If we rearrange and simplify the equation 27, we obtain the following form

$$q(\xi) = \frac{(\lambda a_1 - 2\lambda b_0)e^\xi + a_1 - 2b_0 + 2b_1}{b_1(1 + \lambda e^\xi)},$$

where ξ is defined as $\xi = x + y + \frac{t^\alpha}{\Gamma(1+\alpha)}$. The solution

$$q(\xi) = \frac{(\mp\sqrt{2}\lambda^2a_1 \mp 2\sqrt{2}\lambda^2b_1 - \lambda^2a_1 - 4\lambda^2b_1)e^{2\xi} + (\mp 2\sqrt{2}\lambda a_1 \mp 4\sqrt{2}\lambda b_1 - 8\lambda b_1)e^\xi \mp \sqrt{2}a_1 \mp 2\sqrt{2}b_1 + a_1}{b_1[\lambda(\mp\sqrt{2} - 1)e^\xi \mp \sqrt{2} + 1](1 + \lambda e^\xi)},$$

where ξ is defined as $\xi = x + y - \frac{2t^\alpha}{\Gamma(1+\alpha)}$. The solution function can be expressed in terms of hyperbolic functions by assigning specific values.

4. Conclusion

In the field of mathematical physics, obtaining analytical solutions for nonlinear differential equations is a significant challenge and a crucial step in advancing our comprehension of intricate physical phenomena. The research has achieved significant success by deriving analytical solutions for three challenging equations. These equations have contributed significantly to our understanding of physical phenomena due to their profound effects in mathematical physics. The efficacy of analytical methods in elucidating the latent dynamics inherent in complex time-fractional equations is underscored by our achievements. This provides valuable insights into their intrinsic behaviors and expands the boundaries of mathematical physics.

function can be expressed in terms of hyperbolic functions by assigning specific values.

Case 2:

$$a_0 = -\frac{a_1}{2}, \quad a_2 = 2b_1, \quad b_0 = -\frac{1}{2}b_1, k = 4.$$

Upon substituting these values into equation 26, the solution for equation 23 is obtained as:

$$q(\xi) = \frac{-a_1 + 2a_1U(\xi) + 4b_1U^2(\xi)}{b_1(-1 + 2U(\xi))}, \quad (28)$$

If we rearrange and simplify the equation 28, we obtain the following form

$$q(\xi) = \frac{\lambda^2a_1e^{2\xi} - a_1 - 4b_1}{b_1(\lambda^2e^{2\xi} - 1)},$$

where ξ is defined as $\xi = x + y + \frac{4t^\alpha}{\Gamma(1+\alpha)}$. The solution function can be expressed in terms of hyperbolic functions by assigning specific values.

Case 3:

$$a_0 = \frac{(\mp\sqrt{2} - 1)}{2}(a_1 + 2b_1) - b_1,$$

$$a_2 = 2b_1, b_0 = \frac{(\mp\sqrt{2} - 1)b_1}{2}, k = -2.$$

Upon substituting these values into equation 26, the solution for equation 23 is obtained as:

$$q(\xi) = \frac{\frac{(\mp\sqrt{2} - 1)}{2}(a_1 + 2b_1) - b_1 + a_1U(\xi) + 2b_1U^2(\xi)}{\frac{(\mp\sqrt{2} - 1)}{2}b_1 + b_1U(\xi)}, \quad (29)$$

If we rearrange and simplify the equation 29, we obtain the following form

This investigation has achieved significant success in uncovering multiple exact solutions, including novel hyperbolic solutions. These results serve as compelling evidence of the efficacy of the generalized Kudryashov method and hold the potential to advance our comprehension of nonlinear physical phenomena, offering insights into their underlying intricacies. Utilizing the potent nonlinear fractional transformation, commonly known as the fractional complex transformation, we adeptly transformed the intricate landscape of nonlinear fractional partial differential equations into more manageable ordinary differential equations with integer orders. The solutions for time-fractional nonlinear evolution equations can be elegantly articulated in the form of $U(\xi)$ polynomials.

In conclusion, this manuscript accentuates the efficacy of the generalized Kudryashov method in addressing intricate fractional differential equations. The obtained results not only broaden the array of available mathematical techniques but also deepen our

comprehension of nonlinear physical phenomena. Future research endeavors may explore more intricate fractional differential equations, leveraging advanced mathematical methodologies. This trajectory holds the promise of yielding further insights into the captivating realm of nonlinear dynamics, thereby contributing to the resolution of some of the most intricate problems in science. In our research, our main objective is not only to expand the array of mathematical methodologies but also to illuminate the complex dynamics inherent in nonlinear systems.

Author Contributions

The percentage of the author contributions is presented below. The author reviewed and approved the final version of the manuscript.

	M.E.
C	100
D	100
S	100
DCP	100
DAI	100
L	100
W	100
CR	100
SR	100
PM	100
FA	100

C=Concept, D= design, S= supervision, DCP= data collection and/or processing, DAI= data analysis and/or interpretation, L= literature search, W= writing, CR= critical review, SR= submission and revision, PM= project management, FA= funding acquisition.

Conflict of Interest

The author declared that there is no conflict of interest.

Ethical Consideration

Ethics committee approval was not required for this study because of there was no study on animals or humans.

References

Abdeljawad T. 2015. On conformable fractional calculus. *J Comput Appl Math*, 279: 57-66.

Alabedlhadhi M, Al-Omari S, Al-Smadi M, Alhazmi S. 2023. Traveling wave solutions for time-fractional mKdV-ZK equation of weakly nonlinear ion-acoustic waves in magnetized electron-positron plasma. *Symmetry*, 15(2): 361.

Ali HS, Miah MM, Akbar MA. 2018. Study of abundant explicit wave solutions of the Drinfeld-Sokolov-Satsuma-Hirota (DSSH) equation and the shallow water wave equation. *Propuls Power Res*, 7(4): 320-328.

Arafa AAM, Rida SZ, Mohamed H. 2011. Homotopy analysis method for solving biological population model. *Commun Theor Phys*, 56(5): 797.

Bulut H, Sulaiman TA, Baskonus HM. 2018. Dark, bright and other soliton solutions to the Heisenberg ferromagnetic spin chain equation. *Superlattices Microstruct*, 123: 12-19.

Ding S, Feng Q. 2014. New exact solutions for the DSSH equation. *Int J Appl Sci Res Rev*, 19(3): 194.

Ekici M, Ayaz F. 2017. Solution of model equation of completely passive natural convection by improved differential transform method. *Res Eng Struct Mater*, 3(1): 1-10.

Ekici M, Ünal M. 2020. Application of the exponential rational function method to some fractional soliton equations. *Emerging Applications of Differential equations and Game Theory*. IGI Global, Pennsylvania, US, pp: 13-32.

Ekici M, Ünal M. 2022. Application of the rational (G'/G)-expansion method for solving some coupled and combined wave equations. *Commun Fac Sci Univ*, 71(1): 116-132.

Ekici M. 2023. Exact solutions to some nonlinear time-fractional evolution equations using the generalized Kudryashov method in mathematical physics. *Symmetry*, 15(10): 1961.

He JH, Wu XH. 2006. Exp-function method for nonlinear wave equations. *Chaos Solit Fractals*, 30(3): 700-708.

Jiang X, Wang J, Wang W, Zhang H. 2023. A predictor-corrector compact difference scheme for a nonlinear fractional differential equation. *Fractal Fract*, 7(7): 521.

Kaplan M, Bekir A, Akbulut A. 2016. A generalized Kudryashov method to some nonlinear evolution equations in mathematical physics. *Nonlinear Dyn*, 85: 2843-2850.

Khater MM. 2022. Abundant stable and accurate solutions of the three-dimensional magnetized electron-positron plasma equations. *J Ocean Eng Sci*, (In Press, Corrected Proof). <https://doi.org/10.1016/j.joes.2022.03.001>.

Korkmaz A. 2017. Exact solutions to (3+ 1) conformable time fractional Jimbo-Miwa, Zakharov-Kuznetsov and modified Zakharov-Kuznetsov equations. *Commun Theor Phys*, 67(5): 479.

Lazarus IJ, Bharuthram R, Hellberg MA. 2008. Modified Korteweg-de Vries-Zakharov-Kuznetsov solitons in symmetric twotemperature electron-positron plasmas. *J Plasma Phys*, 74: 519-529.

Mace RL, Hellberg MA. 2001. The Korteweg-de Vries-Zakharov-Kuznetsov equation for electron-acoustic waves. *Phys Plasmas*, 8(6): 2649-2656.

Naher H, Abdullah FA, Akbar MA, Mohyud-Din ST. 2012. Some new solutions of the higher-order Sawada-Kotera equation via the exp-function method. *Middle-East J Sci Res*, 11(12): 1659-1667.

Odibat Z, Momani S. 2008. A generalized differential transform method for linear partial differential equations of fractional order. *Appl Math Lett*, 21(2): 194-199.

Onder I, Secer A, Bayram M. 2023. Soliton solutions of time-fractional modified Korteweg-de-Vries Zakharov-Kuznetsov equation and modulation instability analysis. *Phys Scr*, 99: 015213.

Osman MS. 2019. New analytical study of water waves described by coupled fractional variant Boussinesq equation in fluid dynamics. *Pramana*, 93(2): 26.

Rehman H, Seadawy AR, Younis M, Rizvi S, Anwar I, Baber M, Althobaiti A. 2022. Weakly nonlinear electron-acoustic waves in the fluid ions propagated via a (3+1)-dimensional generalized Korteweg-de-Vries-Zakharov-Kuznetsov equation in plasma physics. *Results Phys*, 33: 105069.

Roshid HO, Hoque MF, Alam MN, Akbar MA. 2014. New extended (G'/G)-expansion method and its application in the (3+ 1)-dimensional equation to find new exact traveling wave solutions. *J Comput Maths*, 2: 32-37.

Senol M, Az-Zobi E, Akinyemi L, Alleddawi A. 2021. Novel soliton solutions of the generalized (3+ 1)-dimensional conformable KP and KP-BBM equations. *Comput Sci Eng*,

- 1(1): 1-29.
- Tian Q, Yang X, Zhang H, Xu D. 2023. An implicit robust numerical scheme with graded meshes for the modified Burgers model with nonlocal dynamic properties. *Comput Appl Math*, 42(6): 246.
- Tuluçe Demiray S, Pandir Y, Bulut H. 2014. Generalized Kudryashov method for time-fractional differential equations. *Abstr Appl Anal*, 2014: 901540.
- Ünal M, Ekici M. 2021. The Double (G'/G, 1/G)-Expansion Method and Its Applications for Some Nonlinear Partial Differential equations. *J Sci Technol*, 11(1): 599-608.
- Wang M, Zhou Y, Li Z. 1996. Application of a homogeneous balance method to exact solutions of nonlinear equations in mathematical physics. *Phys Lett A*, 216(1-5): 67-75.
- Yang X, Wu L, Zhang H. 2023. A space-time spectral order sinc-collocation method for the fourth-order nonlocal heat model arising in viscoelasticity. *Appl Math Comput*, 457: 128192.
- Younas U, Ren J, Baber MZ, Yasin MW, Shahzad, T. 2023. Ion-acoustic wave structures in the fluid ions modeled by higher dimensional generalized Korteweg-de Vries-Zakharov-Kuznetsov equation. *J Ocean Eng Sci*, 8(6): 623-635.
- Zhang S, Tong JL, Wang W. 2008. A generalized (G'/G)-expansion method for the mKdV equation with variable coefficients. *Phys Lett A*, 372(13): 2254-2257.
- Zhou TY, Tian B, Zhang CR, Liu SH. 2022. Auto-Bäcklund transformations, bilinear forms, multiple-soliton, quasi-soliton and hybrid solutions of a (3+ 1)-dimensional modified Korteweg-de Vries-Zakharov-Kuznetsov equation in an electron-positron plasma. *Eur Phys J Plus*, 137: 912.



CFD ANALYSIS OF PRESSURE DROP REDUCTION IN PEMFC FLOW CHANNELS WITH DISTINCT CROSS-SECTION SHAPES

Mahmut KAPLAN^{1*}

¹Gaziantep University, Department of Machine and Metal Technology, 27600, Gaziantep, Türkiye

Abstract: Proton exchange membrane fuel cells (PEMFCs) have great potential to produce renewable, sustainable and clean energy and reduce air pollutants to mitigate climate change. PEMFCs consist of distinct parts including anode and cathode bipolar plates having flow channels, gas diffusion layers, catalyst layers, and membrane. The flow channel geometry influences the flow and pressure drop characteristics of the channel and cell performance. In this work, a three-dimensional (3D) CFD model is built employing SOLIDWORKS and ANSYS Workbench. The innovative configurations are generated by changing the half of 0.2 x 0.2 mm square channel to 0.3 x 0.1 mm, 0.3 x 0.15 mm, 0.3 x 0.2 mm and 0.3 x 0.25 mm rectangular section at the top. The results showed that increasing rectangular section height significantly reduced pressure drop at the anode and cathode with a slight decrease in the current density at 0.4 and 0.6 V. The new configuration with 0.2 x 0.1 mm half square section at the bottom and 0.3 x 0.25 mm rectangular section at the top decreases the current density, anode and cathode pressure drop of 11%, 69% and 58%, respectively in comparison to 0.2 x 0.2 mm flow channel at 0.4 V. Taking into account pressure loss along the flow channels, this configuration is a good option to improve the cell performance.

Keywords: PEMFC, CFD, Cross-sectional geometry, Current density, Pressure drop

*Corresponding author: Gaziantep University, Department of Machine and Metal Technology, 27600, Gaziantep, Türkiye

E mail: mahmutkaplan@gantep.edu.tr (M. KAPLAN)

Mahmut KAPLAN



<https://orcid.org/0000-0003-2675-9229>

Received: January 15, 2024

Accepted: February 15, 2024

Published: March 15, 2024

Cite as: Kaplan M. 2024. CFD analysis of pressure drop reduction in PEMFC flow channels with distinct cross-section shapes. *BSJ Eng Sci*, 7(2): 254-260.

1. Introduction

Fossil fuels like coal, natural gas and oil are the primary energy sources for the power production. But they are finite resources and burning of these fuels results in residual emissions which have the worst impact on the environment and our health. Therefore, researchers have been improving new technologies on producing alternative power sources. Fuel cells are the promising power sources because they are high power and quiet energy converters which transform the fuel chemical energy to clean electricity (Barbir, 2013). The PEM fuel cells (PEMFCs) have key advantages in comparison to other types of fuel cells thanks to low operating temperature, high energy density and having a wide power range (Wu, 2016). These advantages make PEMFC systems more suitable for distinct applications such as transportation, portable and backup power applications (Spiegel, 2008).

A PEMFC is a multi-part device comprises bipolar plates with gas channels and a membrane electrode assembly (MEA) containing a membrane, gas diffusion layers (GDLs), catalyst layers (CLs) at anode and cathode (Xing et al., 2019). The bipolar plate distributes hydrogen and oxygen along the channel. Hydrogen molecules are split into electrons and protons at the anode CL. Protons travel to the membrane whereas electrons move toward the cathode current collector by the electrical circuit. The

electricity, water and waste heat are produced by combining electrons with protons and oxygen molecules at the cathode CL.

The flow channels play a pivotal role in the enhancement of the cell performance. Their shapes affect the distributions of gas species at the reacting area. That is, the channel geometry determines the reactant supply to anode and cathode CL where the electrochemical reactions occur. Besides the geometrical alteration of the channels also impacts pressure drop throughout the channel.

Researchers have scrutinized the impacts of the geometric modification of the channel on the efficiency improvement of PEMFC. Cooper et al. (2017) examined the impact of the length-to-width ratio of channels with interdigitated flow fields on augmenting the PEMFC performance. It was observed that decreasing the aspect ratio (the channel length to width ratio) by reducing the channel length resulted in higher overall performance. Chowdhury et al. (2018) demonstrated that both channel and land widths were equally crucial to increase the current density and the flow channels having 1 mm channel and land widths could be best choice regarding pressure drop and current density in the channel. Carcadea et al. (2021) inspected the influence of the serpentine channel numbers (7, 11, and 14) and cross-sectional size on performance of PEMFC with a large active area. Their results illustrated that a rise in number



of serpentine channels or a decrease in the channel width to land width improved the cell performance, particularly at high current density. Kaplan (2021) scrutinized 15 case studies gained by altering the width and depth of the flow channel (0.2-1.6 mm) for 1 mm fixed depth and width. The results demonstrated that current density and velocity in the flow channel enhanced with reducing depth and width of the channel compared to base case having the channel cross-section of 1 x 1 mm (channel width x depth) at the cost of high pressure loss.

Brakni et al. (2024) assessed the impact of distinct flow field channels with constriction and widening sections at the middle of the channel on the PEMFC performance. They found that the configuration with a constricting hydraulic diameter of 50% showed better performance owing to this configuration enhancing fluid velocity and thus velocity distribution became more uniform at the disadvantage of higher pressure loss. Dong et al. (2023) improved a three-dimensional (3D) model to study the mass transport features and performance of the cell with novel two-block structures inside the channel at the cathode. Their findings revealed that the novel two-block structures augmented oxygen concentration thanks to convection influence of these structures and thus enhanced PEMFC performance with a slight increase in pressure drop.

The aim of the present study is to securitize the effect of the distinct flow channel cross-section shapes on the pressure drop in the flow channels and PEMFC performance. Previous research works were limited by the flow channels with square, rectangular, trapezoidal and stepped cross sections (Paulino et al., 2017). The present study describes the innovative channels with compound cross-section consisting of rectangular channels with a fixed cross-section (0.2 x 0.1 mm) at the bottom and larger cross-section at the top. Impact of this specific combination of cross-sections on current density, pressure, water and oxygen mass fraction distributions has not been addressed before.

2. Materials and Methods

In this work, a 3D geometric model is constructed employing SOLIDWORKS software and the structured mesh is generated using Sweep Method in ANSYS Meshing in Figure 1.

The model in Figure 1 consists of a membrane, anode and cathode current collectors, flow channels, GDLs and CLs. These parts are required for simulation of PEMFC using the Fuel Cell module (ANSYS Inc., 2018). Flow channel configurations with distinct cross-sections are obtained by fixing a half cross-section of 0.2 x 0.2 mm flow channel studied in previous published paper (Kaplan, 2023a) at the bottom combining with rectangular sections (0.3 x 0.1 mm, 0.3 x 0.15 mm, 0.3 x 0.2 mm and 0.3 x 0.25 mm) at the top in Figure 2.

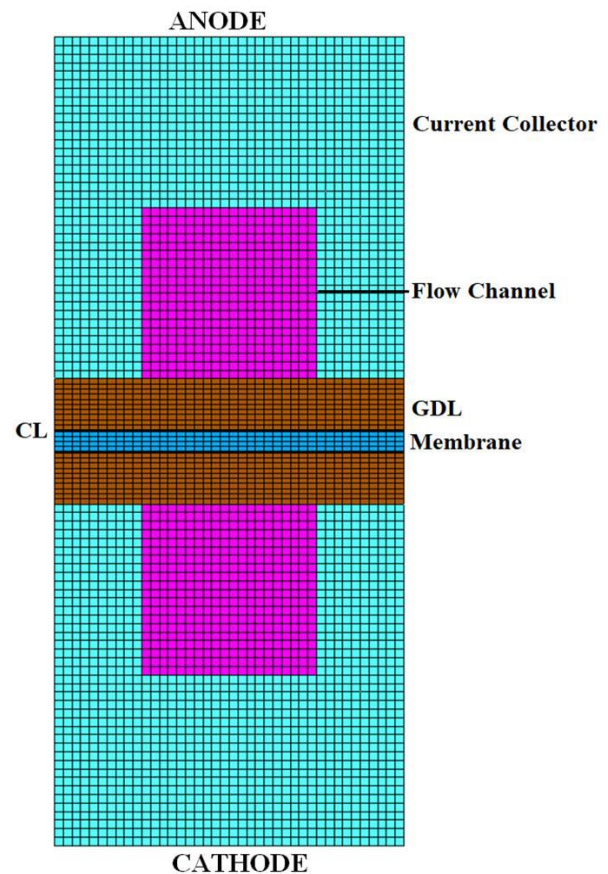


Figure 1. Grid structure and parts of PEMFC model.

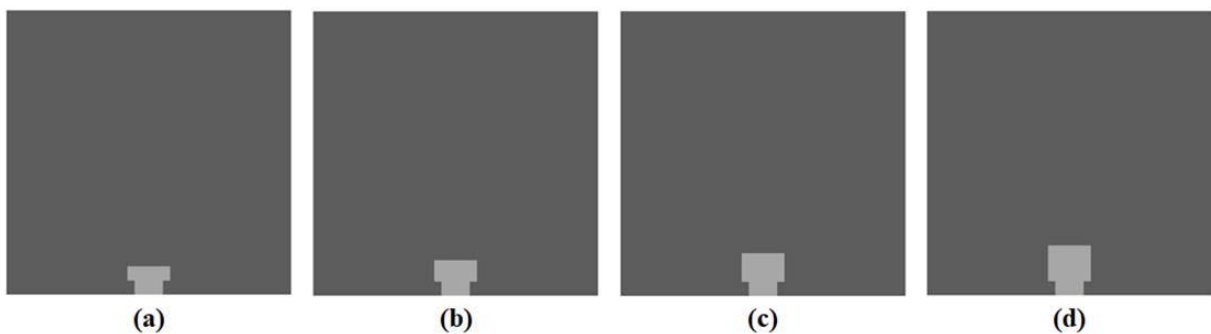


Figure 2. Configurations having a fixed half square section (0.2 x 0.1 mm) with rectangular sections: a) 0.3 x 0.1 mm, b) 0.3 x 0.15 mm, c) 0.3 x 0.2 mm and d) 0.3 x 0.25 mm.

The geometrical characteristics of the model utilized in the CFD analysis in Table 1 are based on Wang et al.'s experiment (2003).

The parameters and operating conditions employed in the CFD analysis are listed in Table 2.

The flow is considered steady state, incompressible and laminar. It is regarded that gas species behave like perfect gases. The MEA is supposed to be isotropic and homogenous porous media (Kaplan, 2023b).

The governing equations utilized in the PEMFC model are listed in Table 3.

Table 1. The geometrical features of the model

Parameter	Value
Cell length	70 mm
Cell width	2 mm
Channel height	1 mm
Channel width	1 mm
GDL thickness	300 μm
CL thickness	12.9 μm
Membrane thickness	108 μm

Table 2. Features and operating conditions used in the 3D CFD simulation

Parameter	Value
GDL and CL porosity (Kahveci and Taymaz, 2018)	0.5
GDL and CL viscous resistance (Kahveci and Taymaz, 2018)	$1 \times 10^{12} \text{ 1/m}^2$
CL surface/volume ratio	200000 1/m
Anodic and cathodic transfer coefficient at anode and cathode (Wang et al., 2003)	0.5 and 2
Reference exchange current density (anode and cathode)	4000 and 0.1 A/m^2
Anode inlet H_2 and H_2O mass fraction (Kaplan, 2022b)	0.2 and 0.8
Cathode inlet O_2 and H_2O mass fraction (Kaplan, 2022b)	0.2 and 0.1
Anode inlet mass flow rate (Kaplan, 2022a)	$5.40 \times 10^{-6} \text{ kg/s}$
Cathode inlet mass flow rate (Kaplan, 2022a)	$3.29 \times 10^{-5} \text{ kg/s}$
H_2O and H_2 reference diffusivity (Biyikoglu and Alpat, 2011)	$7.33 \times 10^{-5} \text{ m}^2/\text{s}$
O_2 and other species reference diffusivity	2.13×10^{-5} and $4.9 \times 10^{-5} \text{ m}^2/\text{s}$
Open-circuit cell voltage	0.94 V
The cell temperature	343 K

Table 3. The governing equations used in the PEMFC model

Equations	Mathematical expressions
Continuity	$\nabla(\rho\vec{u})=0$
Momentum	$\frac{1}{(\varepsilon)^2} \nabla(\rho\vec{u}\vec{u}) = -\nabla P + \nabla(\tau) + S_m$
Energy	$\nabla(\rho c_p \vec{u}T) = \nabla(k^{eff} \nabla T) + S_e$
Species	$\nabla(\vec{u}C_i) = \nabla(D_i^{eff} \nabla C_i) + S_i$
Charge	$\nabla(\sigma_{mem} \nabla \phi_{mem}) + R_{mem} = 0, \nabla(\sigma_{sol} \nabla \phi_{sol}) + R_{sol} = 0$

SIMPLE algorithm is utilized for a pressure velocity coupling in ANSYS Fluent. The gradient is computed by specifying Least Squares cell-based method. Second-order spatial discretization method is selected for pressure whereas the discretization scheme is second-order upwinding for momentum, density, energy and gases. The convergence criterion is set as 10^{-4} for the equations.

The fixed mass flow rates whose values given in Table 2 are specified the flow channel inlets at the anode and cathode. Atmospheric pressure is assigned for the flow channel outlet at the anode and cathode. All other faces are wall boundary conditions. Top faces of anode and cathode current collectors are determined as terminals. The potentials of anode and cathode terminals of 0 V and 0.39-0.92 V are selected respectively to verify the CFD model.

3. Results and Discussion

The PEMFC CFD model is validated using the current density measurements gained by Wang et al. (2003) in Figure 3.

As illustrated in Figure 3, the predicted results obtained by the PEMFC model are a well agreement with experiment, especially at lower and medium current densities whereas the model overprediction is found at higher current densities. This is probably due to the current model not regarding water (liquid) presence in the porous layers which causes a decrease in the porosity of the layers and augments species mass transfer resistance.

Figure 4 shows the estimated current densities for the configurations having a constant half square section (0.2 x 0.1 mm) at the bottom combining with different rectangular sections (0.3 x 0.1 mm, 0.3 x 0.15 mm, 0.3 x 0.2 mm and 0.3 x 0.25 mm) at the top for 0.4 and 0.6 V.

Figure 4 indicates that the current density slightly decreases with an increase of the height of rectangular section combining with a fixed half square section at the bottom for 0.4 and 0.6. It can be owing to the new configurations having higher land area near the GDLs in Figure 2 which contributes to minimize ohmic loses by reducing contact resistance between GDLs and bipolar plates. It is found that the land width is more sensitive than the rectangular section height for enhancing current

density. The narrow channel with higher land width provided a higher cell current density (Chowdhury et al., 2018). Therefore, the maximum current density of 2.82 A/cm² are gained with the configuration with 0.1 mm rectangular section height compared to a 0.2 x 0.2 square channel with current density of 2.92 A/cm².

Figure 5 illustrates the oxygen mass fraction contours in the cathode flow channel, GDL and CL at the middle of the cell length for configurations having a constant half square section with rectangular sections of 0.3 x 01 mm and 0.3 x 0.25 mm for 0.4 V.

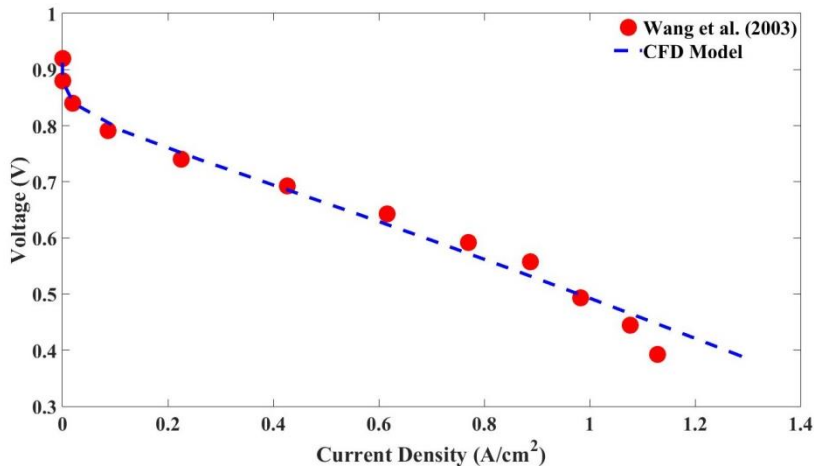


Figure 3. Validation of the PEMFC model with the measured data (Wang et al., 2003).

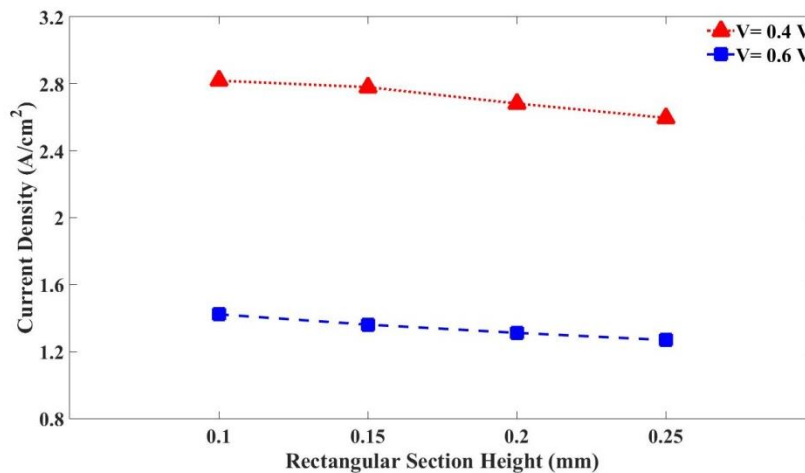


Figure 4. Change of current density as a function of height of a rectangular section at the top for 0.4 and 0.6 V.

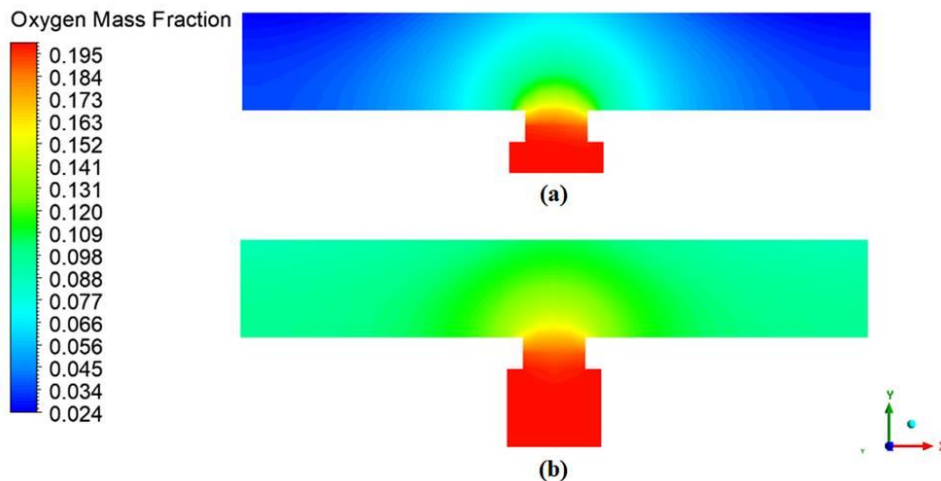


Figure 5. Contours of oxygen mass fraction in the cathode flow channel, GDL and CL at the midpoint of the cell length for channel configurations having a half square section with rectangular sections of (b) 0.3 x 0.1 mm and (c) 0.3 x 0.25 mm.

It is clear in Figure 5 that increasing the rectangular section height from 0.1 mm to 0.25 mm decreases consumption of oxygen in CL and GDL at 0.4 V. Since the channel with 0.1 mm rectangular section height produces higher current density in Figure 4, it consumes more oxygen for the reaction in the cathode CL as shown in Figure 5a compared to that having 0.25 mm rectangular section height in Figure 5b at 0.4 V.

Figure 6 demonstrates the water mass fraction contours in the cathode flow channel, GDL and CL at the middle of the cell length for configurations having a constant half square section with rectangular sections of 0.3 x 0.1 mm and 0.3 x 0.25 mm for 0.4 V.

It is apparent in Figure 6 that a rise in the rectangular section height from 0.1 mm to 0.25 mm reduces water production in CL and GDL at 0.4 V. 0.1 mm rectangular section height case generates more water in Figure 6a compared to the channel having 0.25 mm rectangular section height in Figure 6b owing to this configuration producing higher current density in Figure 4 at 0.4 V. sites. It is concluded that lower cross-sectional area results in a higher reaction rate and thus power density of the PEMFC.

Figure 7 illustrates the pressure contours at the cathode flow channel inlet and flow channel/GDL interface for configurations having a constant half square section with rectangular sections of 0.3 x 0.1 mm and 0.3 x 0.25 mm for 0.4 V.

It is seen that higher pressure distribution existed in the channel inlet section for both configurations shown in Figure 7a and 7b. The pressure diminishes gradually from the inlet towards the outlet because the gas mixture diffusion and frictional loss along the channel configurations. Larger rectangular section height in Figure 7b reduces pressure drop by decreasing friction. Chowdhury et al. (2018) provided similar results for flow channels having higher channel widths with a constant channel depth. Namely, pressure drop decreased with an increase in the flow channel size.

Table 4 indicates the current density and pressure drop results in the base (1 x 1 mm), square channel (0.2 x 0.2 mm) and innovative configurations having half square channel (0.2 x 0.1 mm) at the bottom with rectangular sections (0.3 x 0.1 mm, 0.3 x 0.15 mm, 0.3 x 0.2 mm and 0.3 x 0.25 mm) at the top for 0.4 V.

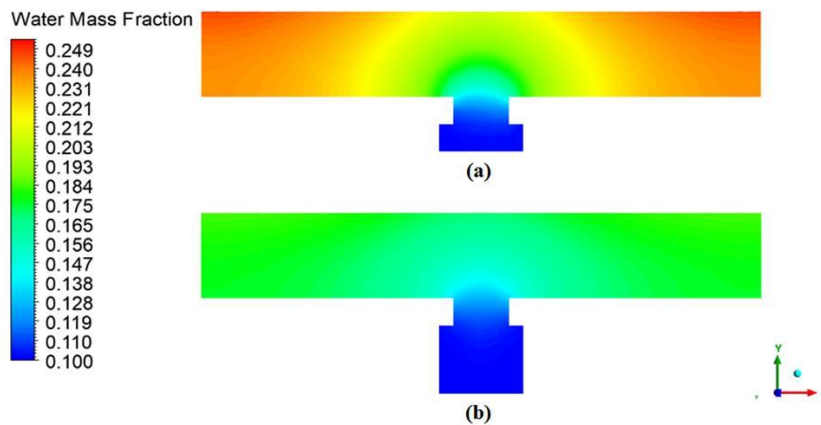


Figure 6. Contours of water mass fraction in the cathode flow channel, GDL and CL at the midpoint of the cell length for channel configurations having a half square section with rectangular sections of (b) 0.3 x 0.1 mm and (c) 0.3 x 0.25 mm.

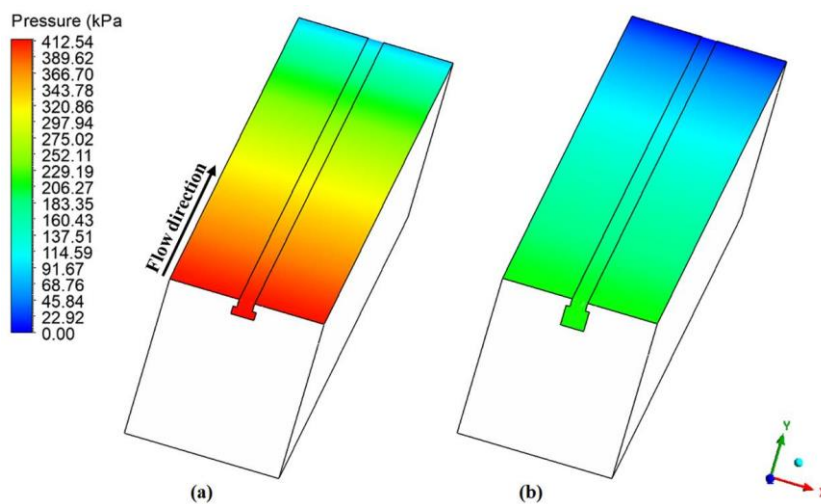


Figure 7. Contours of pressure at the cathode flow channel inlet and flow channel/GDL interface for channel configurations having a half square section with rectangular sections of (b) 0.3 x 0.1 mm and (c) 0.3 x 0.25 mm.

Table 4. Comparison of current density and pressure drop results for flow channel configurations (base, square and half square with different rectangular sections) for 0.4 V

Configurations	Current density (A/cm ²)	Pressure Drop	
		Anode (kPa)	Cathode (kPa)
Base (1 x 1 mm)	1.26	0.73	2.45
Square (0.2 x 0.2 m)	2.92	163.11	511.68
Half square with rectangular (0.3x 0.1 mm)	2.82	130.46	412.54
Half square with rectangular (0.3x 0.15 mm)	2.78	90.22	322.79
Half square with rectangular (0.3x 0.2 mm)	2.68	65.52	257.88
Half square with rectangular (0.3x 0.25 mm)	2.60	49.96	212.59

It is obvious in Table 4 that new configurations generated by modifying half square section at the top remarkably reduces the anode and cathode pressure drop with a slight decrease in the current density compared to 0.2 x 0.2 mm square channel. Besides the pressure drop at the cathode is much higher than that at the anode. This may be because of a mixture of gases in the channel at cathode being more complicated compared to that at the anode. The maximum current density is achieved with the configuration with 0.2 x 0.2 mm cross section channel but the cathode channel of this configuration produces the highest pressure drop of 511.68 kPa in Table 4. Higher pressure drop leads to the extra pumping work and thus reducing the cell efficiency. The configuration having 0.2 x 0.1 mm half square section with 0.3 x 0.25 mm rectangular section reduces current density, anode and cathode pressure drop by 11%, 69% and 58%, respectively in comparison to 0.2 x 0.2 channel at 0.4 V. Regarding to pressure drop and current density in the channels, this configuration is better option to improve PEMFC performance.

4. Conclusion

In the present study, a 3-D numerical model is improved and validated by the measured data (Wang et al., 2003) to examine the effect of changing half section of square flow channel at the top to distinct rectangular sections on pressure drop and PEMFC performance. The main findings are as follow:

- 0.2 x 0.2 mm square channel leads to considerably higher current density and pressure drop at the anode and cathode at 0.4 and 0.6 V.
- Innovative configurations produced by altering dimensions of half of square channel at the top remarkably reduce pressure in the anode and cathode flow channel with not considerably decreasing the current density.
- New configurations provide the higher land width dimensions near the GDL contributing to reducing contact resistance between GDL and bipolar plate and thus minimizing ohmic loses.
- A rise in the height of rectangular section at the top leads to increasing oxygen concentration and decreases water concentration at 0.4 V.
- Considering current density and pressure drop, the new configuration with the half square section (0.2

x 0.1 mm) at the bottom and the rectangular section (0.3x 0.25 mm) at the top is more efficient option with 11%, 69% and 58% reduction of the current density, anode and cathode pressure drop compared to 0.2 x 0.2 flow channel at 0.4 V.

These outcomes emphasize the significance of the flow channel cross-section shapes in the design of efficient fuel cell systems. Future work including the impact of distinct operating conditions and material properties on the cell performance which would improve the innovative configurations suggested in this study.

Author Contributions

The percentage of the author contributions is presented below. The author reviewed and approved the final version of the manuscript.

	M.K.
C	100
D	100
S	100
DCP	100
DAI	100
L	100
W	100
CR	100
SR	100
PM	100
FA	100

C=Concept, D= design, S= supervision, DCP= data collection and/or processing, DAI= data analysis and/or interpretation, L= literature search, W= writing, CR= critical review, SR= submission and revision, PM= project management, FA= funding acquisition.

Conflict of Interest

The author declared that there is no conflict of interest.

Ethical Consideration

Ethics committee approval was not required for this study because of there was no study on animals or humans.

References

ANSYS Inc. 2018. ANSYS Fluent 19.2 Advanced Add-On Modules, Canonsburg, PA, US.
 Barbir F. 2013. PEM fuel cells: theory and practice.

- Elsevier/Academic Press, London, UK, pp: 518.
- Biyikoglu A, Alpat CO. 2011. Parametric study of a single cell proton exchange membrane fuel cell for a bundle of straight gas channels. *Gazi Univ J Sci*, 24(4): 883-899.
- Brakni O, Kerkoub Y, Amrouche F, Mohammedi A, Ziari YK. 2024. CFD investigation of the effect of flow field channel design based on constriction and enlargement configurations on PEMFC performance. *Fuel*, 357: 129920.
- Carcadea E, Ismail MS, Ingham DB, Patularu L, Schitea D, Marinoiu A, Ebrasu DI, Mocanu D, Varlam M. 2021. Effects of geometrical dimensions of flow channels of a large-active-area PEM fuel cell: A CFD study. *Int J Hydrog Energy*, 46(25): 13572-13582.
- Chowdhury MZ, Genc O, Toros S. 2018. Numerical optimization of channel to land width ratio for PEM fuel cell. *Int J Hydrog Energy*, 43: 10798-10809.
- Cooper NJ, Santamaria AD, Becton MK, Park JW. 2017. Investigation of the performance improvement in decreasing aspect ratio interdigitated flow field PEMFCs. *Energy Convers Manag*, 136: 307-317.
- Dong Z, Qin Y, Zheng J, Qiaoyu G. 2023. Numerical investigation of novel block flow channel on mass transport characteristics and performance of PEMFC. *Int J Hydrog Energy*, 48: 26356-26374.
- Kahveci EE, Taymaz I. 2018. Assessment of single-serpentine PEM fuel cell model developed by computational fluid Dynamics. *Fuel*, 217: 51-58.
- Kaplan M. 2021. Numerical investigation of influence of cross-sectional dimensions of flow channels on PEM fuel cell performance. *J Energy Syst*, 5(2): 137-148.
- Kaplan M. 2022a. A numerical parametric study on the impacts of mass fractions of gas species on PEMFC performance. *Eng Technol Q Rev*, 5(2): 38-45.
- Kaplan M. 2022b. Three-dimensional CFD analysis of PEMFC with different membrane thicknesses. *Renew Energy Sustain Devel*, 8(2): 45-51.
- Kaplan M. 2023a. Performance improvement of PEMFC based on reducing size of the square flow channel: a 3D CFD approach. In: 3. International World Energy Conference Full Texts Book, December 4-5, Kayseri, Türkiye, pp: 700-707.
- Kaplan M. 2023b. Computational simulation study of the impact of isotropic GDL thermal conductivity on PEMFC characteristics. *Renew Energy Sustain Devel*, 9(2): 42-49.
- Paulino ALR, Cunha EF, Robalinho E, Linardi M, Korkischko I, Santiago EI. 2017. CFD Analysis of PEMFC Flow Channel Cross Sections. *Fuel Cells*, 17(1): 27-36.
- Spiegel C. 2008. PEM fuel cell modeling and simulation using Matlab. Elsevier/Academic Press, London, UK, pp: 440.
- Wang L, Husar A, Zhou T, Liu H. 2003. A parametric study of PEM fuel cell performances. *Int J Hydrog Energy*, 28(11): 1263-1272.
- Wu, HW. 2016. A review of recent development: transport and performance modeling of PEM fuel cells. *Appl Energy*, 165: 81-106.
- Xing L, Shi W, Su H, Xu Q, Das PK, Mao B, Keith S. 2019. Membrane electrode assemblies for PEM fuel cells: A review of functional graded design and optimization. *Energy*, 177: 445-464.



UTILIZING VBA IN MS EXCEL FOR SIMPLIFIED SOLUTIONS IN CHEMICAL ENGINEERING: SINGLE-EFFECT EVAPORATOR STUDY

Muhammed Bora AKIN^{1*}


¹Çankırı Karatekin University, Faculty of Engineering, Department of Chemical Engineering, 18200, Çankırı, Türkiye

Abstract: Solutions for an evaporator system involve equations that incorporate both mass and energy balances. Solving equations for a single-effect evaporator is simpler compared to those for multi-effect evaporator systems. However, due to the need for extensive analysis of diverse data from various sources, many prefer using simulation programs for convenience. These programs conduct calculations using their own data libraries, which contain thermodynamic and LLE-VLE data. To emulate the functionality of expensive a simulation program, an alternative interface was designed using Visual Basic for Applications (VBA) in MS Excel. In this study, we chose a single-effect evaporator system used for concentrating NaOH solution and solved its equations using a program created in VBA within MS Excel. Moreover, databases for saturated water and superheated steam data were developed within the MS Excel environment to facilitate the program. Ultimately, the program was employed to scrutinize the influence of selected parameters on other parameters, and the results were analyzed. This study serves as an illustration of how VBA in MS Excel can efficiently handle calculations pertaining to chemical engineering processes. By focusing on the single-effect evaporator, this study demonstrates how VBA in Excel can simplify and effectively conduct investigations into chemical engineering process calculations.

Keywords: Separation, Evaporation, Single-effect evaporator, Excel, Visual Basic for applications, VBA

*Corresponding author: Çankırı Karatekin University, Faculty of Engineering, Department of Chemical Engineering, 18200, Çankırı, Türkiye

E mail: mbakin@karatekin.edu.tr (M. B. AKIN)

Muhammed Bora AKIN  <https://orcid.org/0000-0003-3841-1633>

Received: December 08, 2023

Accepted: February 16, 2024

Published: March 15, 2024

Cite as: Akın MB. 2024. Utilizing VBA in MS Excel for simplified solutions in chemical engineering: Single-effect evaporator study. BSJ Eng Sci, 7(2): 261-270.

1. Introduction

The evaporator is a crucial device utilized across various industries, including paper, sugar, desalination, medicine, dairy, and food processing. These systems, engineered to meet specific process needs, are employed as either single-effect or multi-effect evaporators. Figure 1 illustrates a schematic representation of a single-effect evaporator.

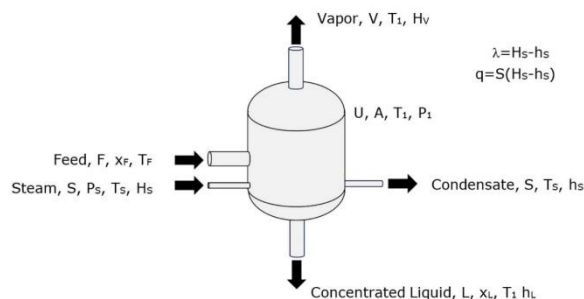


Figure 1. Scheme of an evaporator.

Various types of evaporators are utilized in different industries. An evaporator functions as a heat exchanger and is constructed from a material with a thermal conductivity coefficient, denoted as U . It is situated within a large enclosure to create a heat transfer area,

labeled A . The steam flow rate used for heating in the evaporator is represented by S . The pressure, temperature, and enthalpy values of this steam, are indicated as P_s , T_s , and H_s , respectively. This steam heats the feed flow (F), which has a concentration of x_F and a temperature of T_F . Water vapor transfers the heat load (q) to the feed, condenses, and exits the system with a saturated liquid enthalpy (h_F). Consequently, the feed reaches its boiling point (T_1), leading to the removal of the solvent in vapor form, with enthalpy H_v , from the upper part of the evaporator at a flow rate (V). This process results in a concentrated liquid stream (L), which sees an increase in concentration to x_L and possesses an enthalpy of h_L . A vacuum is applied in the vapor space at the top of the evaporator at pressure P_1 . This vacuum ensures that the product boils at lower temperatures, minimizing heat loss.

Calculations for the single-effect evaporator are divided into two parts: mass balance and heat balance calculations. The mass balance calculation starts with the feed flow rate (F), which is equal to the sum of the vapor flow rate (V) and the concentrated liquid flow rate (L) and it is written as given in Equation 1:

$$F = V + L \quad (1)$$



Total component mass balance is written as given in Equation 2:

$$F \cdot x_F = V \cdot y_V + L \cdot x_L \quad (2)$$

Since the component fraction in the vapor flow (V) in the equation $y_V=0$, it becomes Equation 3 (Çataltaş, 1963):

$$F \cdot x_F = L \cdot x_L \quad (3)$$

At this stage, the initial step involves solving Equation 3 using the available data. This culminates in the completion of the mass balance calculation through Equation 1, by employing the derived value of L. Subsequently, the heat balance calculation is initiated.

The comprehensive heat balance equation is formulated as given in Equation 4:

$$F \cdot h_F + S \cdot \lambda_S = V \cdot H_V + L \cdot h_L + Q_{lost} \quad (4)$$

In this scenario, the heat entering with the feed ($F \cdot h_F$) and the heat provided by steam heating ($S \cdot \lambda_S$) constitute the heat load in the vapor flow ($V \cdot H_V$) and the heat load in the concentrated liquid flow ($L \cdot h_L$). In this analysis, heat loss (Q_{lost}) in the system is neglected. The heat load in the exchanger is written as given in Equation 5:

$$q = U \cdot A \cdot \Delta T \quad (5)$$

Typically, the calculation of the heat exchanger area for the designed evaporator is performed using Equation 5. The calculations are then finalized by determining the steam economy using Equation 6 (Geankoplis, 1978; Geankoplis, 2003).

$$\text{Steam Economy} = V / S \quad (6)$$

In a study by Elmas (2017) in the literature, calculations for the evaporation of the NaOH solution used in the mercerization process applied to textiles were made using the approach described above. In the conducted study, in a process where the mass flow varies between 250 kg/h and 1000 kg/h, both single-effect and double-effect evaporators were used to increase the concentration of a 5% NaOH feed to 50% at a temperature of 50 °C, and the results have been analyzed. In another study, a more comprehensive but similar approach has been used to examine the optimum design and operating conditions of multi-effect evaporators used in tomato paste production. The study involves the development of a mathematical model by utilizing specific relationships for tomato concentration and a first-order degradation kinetics for lycopene. These calculations were carried out using Microsoft Excel. The findings indicate that increasing the capacity of the 5-effect evaporation system from 50 to 75 tons per hour results in an increase in lycopene yield from 95.25% to 96.27%. When examining the optimization from a total cost minimization perspective, it suggests an optimal configuration of 4 effects. However, when maximizing the Net Present Value while considering lycopene as a quality parameter, the optimal configuration is determined to be 3 effects (Simpson et al., 2008). In another study,

experimental data of the vacuum evaporation crystallization system are compared with the data obtained with the Aspen Plus simulation program. In the study at hand, both experimental and simulation results suggest that the crystallization of glycine solutions occurs at a slower rate compared to the evaporation of water. To illustrate, at a pressure of 40 mbar, while 60% of the feedwater has evaporated, only 40% of the glycine in the feed has undergone crystallization, resulting in 60% of uncrystallized glycine remaining in the feed solution. Additionally, the quantity of solid crystals produced through experimentation appears to be slightly higher than the forecasted output of the model generated by the Aspen program. According to the Aspen program model, it was anticipated that 50% of the glycine in the feed solutions would crystallize at an 80 mbar pressure, but experimental results indicate that glycine crystallized up to 60% (Said and Louhi-Kultanen, 2019).

Microsoft Visual Basic for Applications (VBA) allows users, even those without programming expertise, to record, create, and modify macros. This enables the automation of tasks within MS Office applications (Microsoft Inc., 2021).

A study highlights the significance of MS Excel in advancing Industry 4.0 in Germany. It presents four examples from chemical engineering where various programs interface with a chemical process simulator, with MS Excel playing a crucial role in most cases (Fricke and Schöneberger, 2015). The value of MS Excel and VBA in Chemical Engineering education was recognized earlier. In 2010, the Hong Kong University of Science and Technology (HKUST) began teaching Excel Visual Basic for Applications (VBA) programming in chemical engineering, focusing on enabling students to convert chemical engineering problems into functional programs (Wong and Barford, 2010). By 2016, Teppaitoon developed an Excel spreadsheet for numerical calculations in Liquid-Liquid extraction, using the 'TREND' function and mixing rule criteria for efficient problem-solving without the need for time-consuming graphing (Teppaitoon, 2016). This development underscored the need for Industry 4.0 chemical engineering students to acquire programming skills, as further emphasized in a subsequent study by Teles dos Santos, Vianna, and Le Roux (2018). Additionally, Argo et al. (2020) demonstrated an effective evaporator solution using Solid Works in conjunction with MS Excel. Similarly, Karic and Alic (2020) utilized Microsoft Excel with VBA to solve a mathematical model for integrating mechanical vapor compression into a single-effect evaporator (Karic and Alic, 2020).

Existing literature does not identify any graphical interface-based solutions for single-effect or multi-effect evaporator systems using a program. The programs developed in academic studies have evolved into paid services, continuing to support chemical and process engineering. This study aimed to solve a single-effect evaporator problem using a NaOH solution within MS

Excel, employing a graphical interface with VBA. It analyzed the effects of selected parameters on others and interpreted the results obtained.

2. Materials and Methods

A comprehensive heat and mass balance of a single-effect NaOH evaporator system has been integrated into an MS Excel program using VBA. The program's accuracy has been verified using example data from literature sources. Standard properties of water/steam and NaOH solutions have been obtained from relevant literature references.

2.1. Water/Steam Properties

The pressure, temperature, enthalpy, and heat values of water are utilized in the calculations within the evaporator system. Typically, the enthalpy and heat of vaporization are determined using pressure or temperature values. This determination often involves referencing tables or graphs of saturated and superheated water, which can require manual calculations. The data for this study, obtained from saturated water and superheated steam tables, were sourced from literature (Boles and Cengel, 2014; Geankoplis, 2003). These data were compiled into an MS Excel workbook named "Water", which is used during the evaporator calculations performed with the graphical interface.

2.2. NaOH Solution Properties

Boiling point elevation (BPE) occurs during the evaporation of NaOH solutions. The Duhring Diagram is used to determine the value of this increase. Additionally, enthalpy values are obtained using graphs that relate concentration and temperatures, which are essential in calculating the enthalpy of NaOH solutions. These data were sourced from the literature (Geankoplis, 2003; Kapuno, 2008) and compiled into an MS Excel workbook named "NaOH". The program then accesses the necessary data by referring to this workbook.

2.3. Program

The program works through a form, and a graphical interface is provided through the form. The known data on this form are given to the computer, and then the solution is reached by pressing the calculate button (Figure 2). The Calculate button activates the program related to the solution. The program was executed on a PC running MS Windows 10, equipped with 8 GB RAM and an Intel® Core™ i5-3470 CPU @ 3.20 GHz processor. During the solution process, water/steam data and NaOH solution data are calculated via interpolation in MS Excel files. These resulting data sets are then utilized in the calculation file. Additionally, at the end of the calculation, the calculated data are written into a separate file called "Report".

2.4. Single Effect NaOH Evaporator Case Study

In this case study, assuming an evaporation is used to concentrate 4536 kg/h of a 20% solution of NaOH in water entering at 60 °C to a product of 50% solid. The pressure of the saturated steam used is 172.4 kPa and the pressure in the vapor space of the evaporator is 11.7 kPa.

The thermal conductivity coefficient is 1560 W/m²·K. The requested calculation involves the steam used, the steam economy in kg vaporized/kg steam used, and the heating surface area in m² (Geankoplis, 2003). After entering the known data into the graphical interface created with VBA, the program is executed by pressing the "Calculate" button, which automatically performs the calculations. Additionally, parameters have been altered to observe their effects on the calculation. NaOH feed flowrate, NaOH feed concentration, steam pressure, vapor space pressure, thermal conductivity coefficient, concentrated liquid flow concentration, and NaOH feed temperature examined in the study. The parameters and range of values are listed in Table 1.

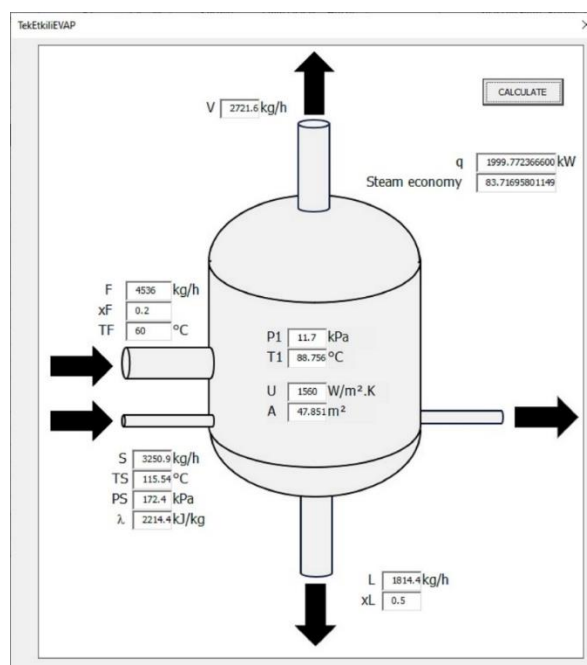


Figure 2. Graphical Interface Form in VBA workspace.

Table 1. Parameters and range of values in the study

Parameter	Set value	Value range in the study
NaOH feed flowrate, F (kg/h)	4536	1536-5536
NaOH feed concentration, x_F	0.2	0.01-0.49
Steam pressure, P_S (kPa)	172.2	75-400
Vapor space pressure, P_1 (kPa)	11.7	4-36
Thermal conductivity coefficient, U (W/m ² ·K)	1560	500-2500
Concentrated liquid flow concentration, x_L	0.5	0.3-0.659
NaOH feed temperature, T_F (°C)	60	10-100

3. Results and Discussion

To test programming and interface studies, a general example used in the field of Chemical Engineering was chosen. In solving this problem, the final result is the steam efficiency in the evaporator and the answer is

calculated as 83.6%. According to the example data, the calculated steam economy of the single-effect evaporator stands at 83.72% in the program. This result aligns closely with the outcome obtained using the calculation method outlined in (Geankoplis, 2003). Slight variations in the results are attributed to the precise calculation values used.

The effects resulting from changing each parameter, such as NaOH feed flow rate, F (kg/h), NaOH feed concentration, x_F , steam pressure, P_S (kPa), pressure in the vapor space, P_1 (kPa), thermal conductivity coefficient, U ($W/m^2 \cdot K$), and concentrated liquid flow concentration, x_L , are explained under separate headings below.

3.1. Effect of NaOH Feed Flowrate

The effect of the NaOH flow rate fed to the evaporator on the vapor flow rate and concentrated liquid flow rate, steam flow rate, transferred heat, and heat transfer area was investigated. During these calculations, the values of $x_F=0.2$, $T_F=60$ °C, $x_L=0.5$, $P_S=172.4$ kPa and $P_1=11.7$ kPa were kept constant, and the Feed (F) value has been changed between 1536 kg/h and 5536 kg/h.

Data illustrating the impact of the feed flow rate of NaOH on vapor flowrate, concentrated liquid flowrate, steam flowrate, transferred heat, and heat transfer area are graphically represented in Figure 3. As observed in Figure 3, an increasing trend in all these parameters is noted with the rise in NaOH feed flow rate. Furthermore, the fitted curves indicate that they all vary linearly.

3.2. Effect of NaOH Feed Concentration

The effect of the concentration of the NaOH feed to the evaporator on the vapor flow rate and concentrated liquid flow rate, enthalpy, transferred heat, heat transfer area and steam economy was examined. During these calculations, $F=4536$ kg/h, $T_F=60$ °C, $x_L=0.5$, $P_S=172.4$ kPa and $P_1=11.7$ kPa values were set and the concentration (x_F) value was changed between 0.01 and 0.49.

As a result of the calculations, the data showing the effect of the NaOH concentration fed to the evaporator on the vapor flow rate and concentrated liquid flow rate are given graphically in Figure 4. With increasing NaOH feed concentration, the vapor flow rate decreases, and the concentrated liquid flow rate increases linearly.

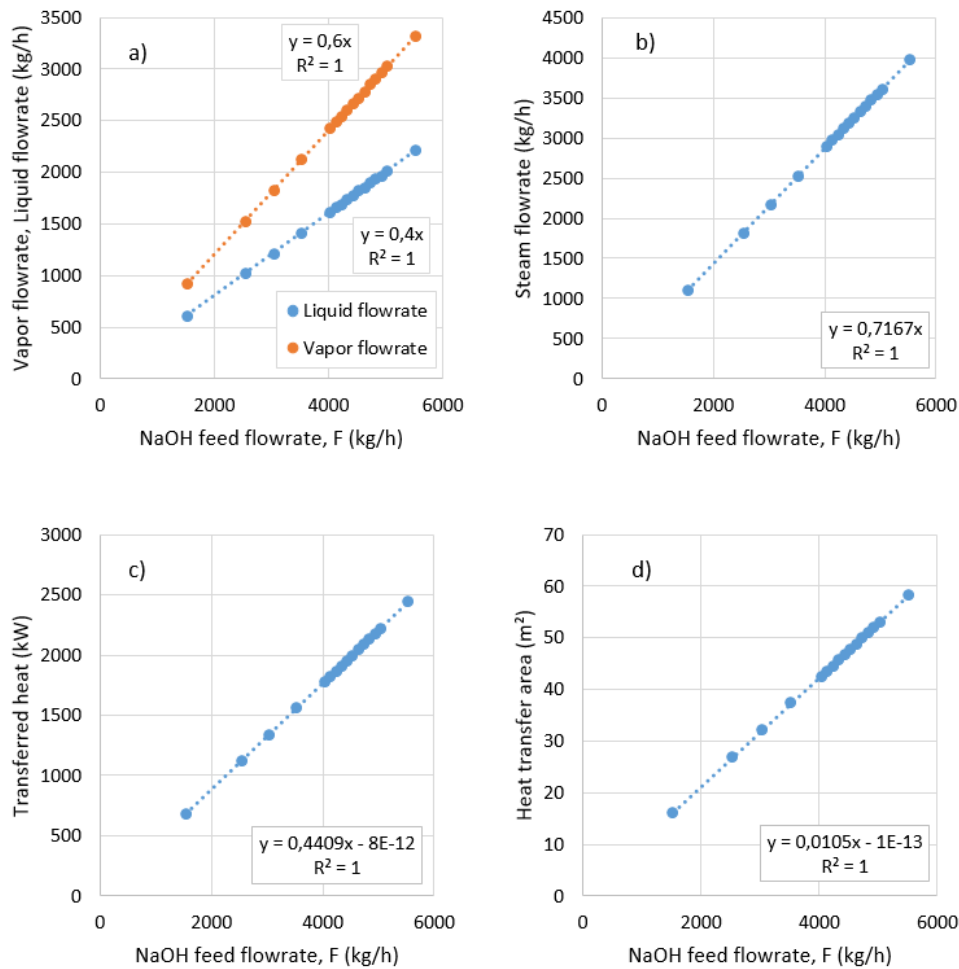


Figure 3. Effect of NaOH feed flowrate on (a) vapor and concentrated liquid flowrates, (b) steam flowrate, (c) transferred heat, and (d) heat transfer area.

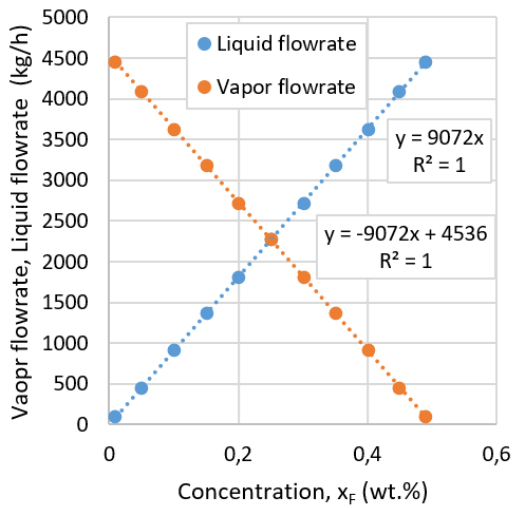
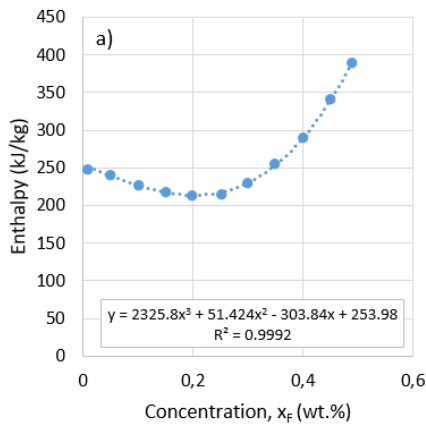


Figure 4. Effect of NaOH feed concentration on output flowrates.

In Figure 5a, data showing the effect of feed concentration on the enthalpy of the feed stream is given graphically. As a result, with increasing feed concentration, the enthalpy of the feed flow decreases first and but then it increases. The turning point is seen at $x_F=0.2$. With the curve fit, the suitability of a third-degree polynomial equation is revealed as $R^2 = 0.9992$. The increase in concentration of the NaOH feed flow causes the total transferred heat amount to decrease



(Figure 5b). It moves according to second-degree. The regression coefficient of fitted curve is 0.9999. The heat transfer area decreases with increasing feed concentration. The fitted curve is a second-degree polynomial equation with $R^2=0.9999$ (Figure 5c). The effect of feed concentration on steam economy is inversely proportional. Steam economy decreases with increasing feed concentration (Figure 5d). It has been determined that after $x_F = 0.4$, the decrease in steam economy reaches much higher values rapidly.

3.3. Effect of Steam Pressure

In the calculations made while investigating the effect of steam pressure, the values $F=4536$ kg/h, $x_F=0.2$ $T_F=60$ °C, $x_L=0.5$, and $P_1=11.7$ kPa were kept constant, and the steam pressure (P_s) value was changed between 75 kPa and 400 kPa. Figure 6a shows that the heat transfer area decreases with the increase in steam pressure. Under these conditions, the effect of using pressures higher than 125 kPa decreases on the heat transfer area. The effect of steam pressure on steam economy is appeared that steam economy decreases with increasing steam pressure (Figure 6b). It has been revealed that it can be modelled with a second-order equation, with an R^2 value of 0.9981. As the steam pressure increases, the steam flowrate increases. By the modelling for the data, the fitted curve fits a second order function and the R^2 is 0.9986 (Figure 6c).

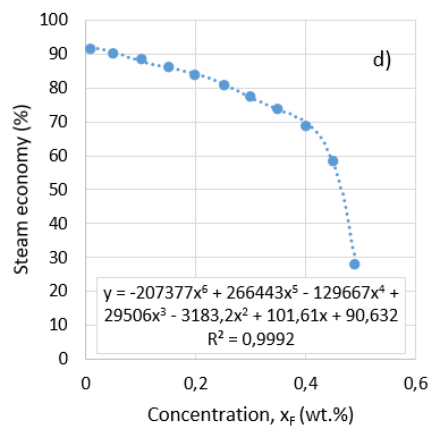
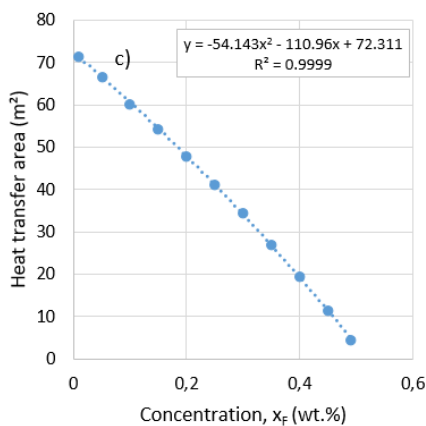
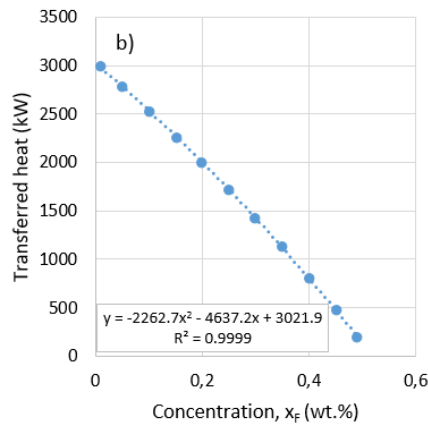


Figure 5. Effect of NaOH feed concentration on (a) enthalpy of concentrated liquid flow, (b) transferred heat, (c) heat transfer area, and (d) steam economy.

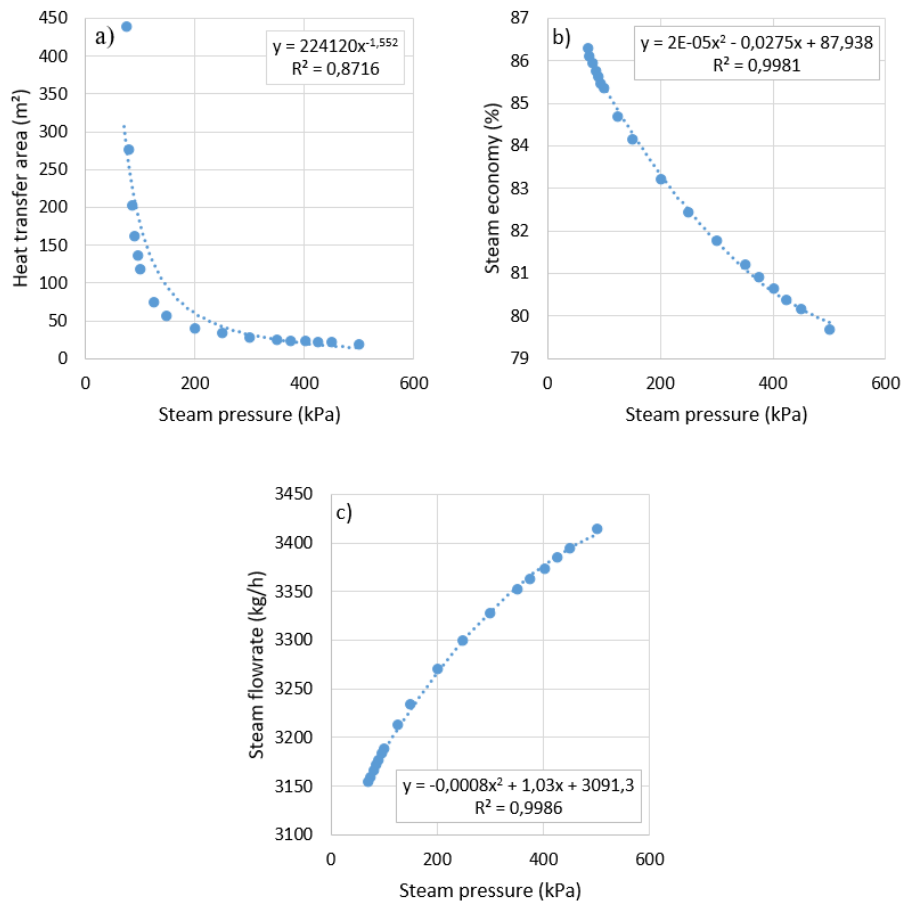


Figure 6. Effect of steam pressure on (a) heat transfer area, (b) steam economy, and (c) steam flowrate.

3.4. Effect of Pressure in the Vapor Space

In the series of calculations examining the effect of the pressure in the vapor space of the evaporator, the values $F=4536$ kg/h, $x_F=0.2$ $T_F=60$ °C, $x_L=0.5$, and $P_S=172.4$ kPa were kept constant, and the pressure (P_1) value increased from 4 kPa to 36 kPa (Figure 7).

It can be seen in Figure 7a that increasing the pressure in the vapor space of the evaporator causes the boiling point elevation to increase. When these data are modelled, an exponential function with an R^2 value of 0.9971 is obtained. The increase in vapor space pressure leads to an increase in the transferred heat. Additionally, the model suggested for the total transferred heat can be represented by an exponential function. The R^2 value of the function is 0.9979 (Figure 7b). Figure 7c shows that the heat transfer area increases with the increase in pressure in the vapor space of evaporator. After the pressure reaches 30 kPa, the increase in the heat transfer area accelerates. Another parameter examined is the variation in steam economy. As the pressure in the vapor space increases, steam economy decreases. It is observed that it can be modeled with a logarithmic function, where the R^2 value is obtained as 0.9990. The impact of pressure in the evaporator's vapor space on steam economy is presented in Figure 7d.

3.5. Effect of Thermal Conductivity Coefficient

While making calculations examining the effect of the thermal conductivity coefficient, U on the heat transfer

area, A , the values of $F=4536$ kg/h, $x_F=0.2$ $T_F=60$ °C, $x_L=0.5$, $P_S=172.4$ kPa and $P_1=11.7$ kPa are constant was kept, the coefficient (U) value was changed between 500 $W/m^2 \cdot K$ and 2500 $W/m^2 \cdot K$. The calculations in the study determine that with the increase in the thermal conductivity coefficient, the heat transfer area in the evaporator is exponentially related and decreases (Figure 8).

3.6. Effect of Concentrated Liquid Flow Concentration

In the calculations made while examining the effect of concentrated liquid flow concentration on heat transfer area, concentrated liquid flow rate, steam economy and steam flow rate, $F=4536$ kg/h, $x_F=0.2$ $T_F=60$ °C, $P_S=172.4$ kPa and $P_1=11.7$ kPa values were kept constant, and the x_L parameter was changed between 0.3 and 0.659. Increasing the concentrated liquid flow concentration causes the heat transfer area in the evaporator to increase (Figure 9a). Although the concentration (x_L) parameter shows an almost linear trend up to 0.5, this linearity breaks down after 0.6 and the heat transfer area increases more rapidly. With the increase in concentration of the concentrated liquid flow, the concentrated liquid flow rate and steam economy exhibit a decrease (Figure 9b and Figure 9c), in contrast, the vapor flow rate is observed to increase (Figure 9d). The behavior of these parameters aligns with second-order models.

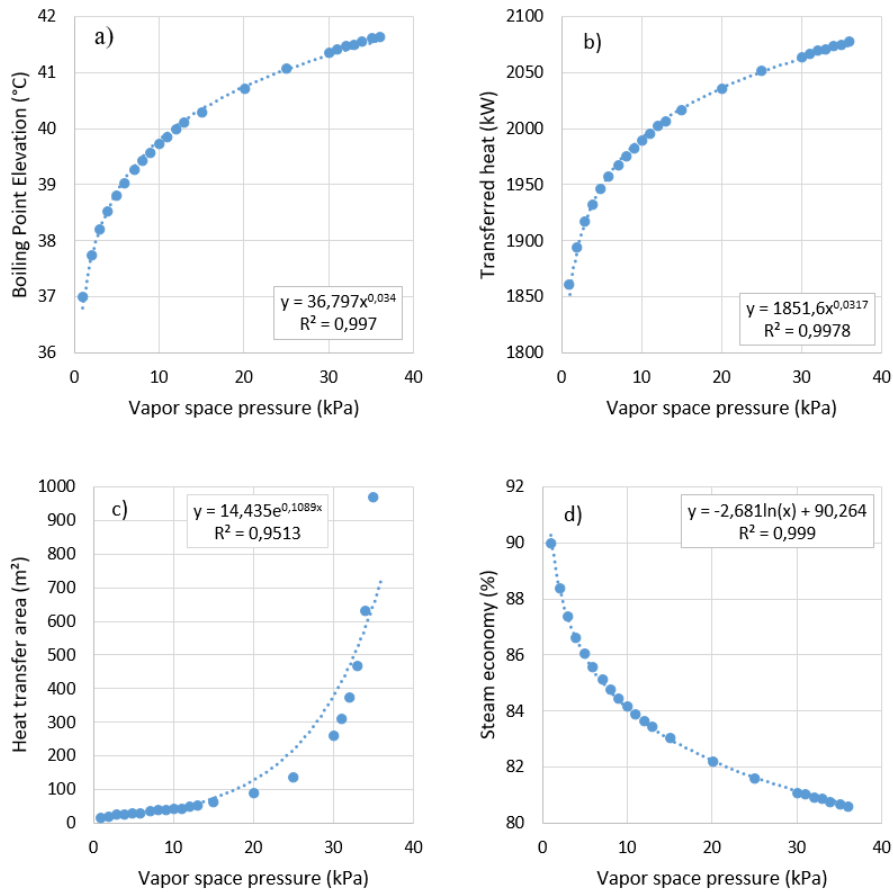


Figure 7. Effect of vapor space pressure on (a) BPE, (b) transferred heat, (c) heat transfer area, and (d) steam economy.

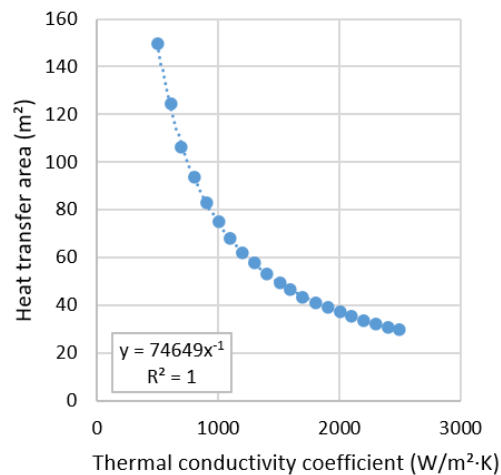


Figure 8. Effect of thermal conductivity coefficient on heat transfer area.

3.7. Effect of NaOH Feed Temperature

NaOH feed temperature changing affects the feed temperature, enthalpy, total transferred heat, heat transfer area, steam economy and work steam flow rate. During the calculations, the values of $F=4536$ kg/h, $x_F=0.2$, $x_L=0.5$, $P_S=172.4$ kPa and $P_1=11.7$ kPa were kept constant, and the temperature (T_F) parameter was changed between 10 °C and 100 °C. As the temperature increases, all parameters examined in the evaporator behave linearly. For all other parameters besides steam economy, the regression coefficient is found to be 1

($R^2=1$). Figure 10 displays the models with which they are compatible. As illustrated in the figure, with an increase in feed temperature, enthalpy and steam economy increase, while the transferred heat, heat transfer area, and steam flow rate decrease.

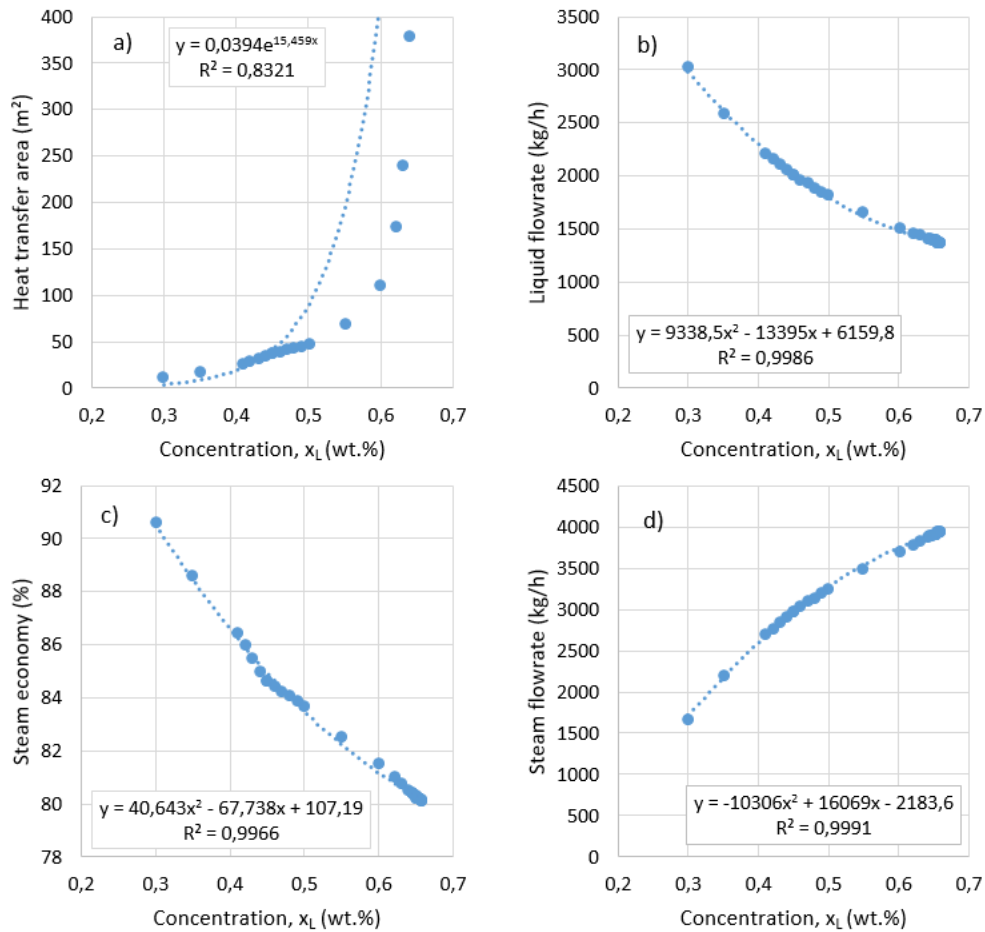


Figure 9. Effect of concentrated liquid flow concentration on (a) heat transfer area, (b) concentrated liquid flowrate, (c) steam economy, and (d) steam flowrate.

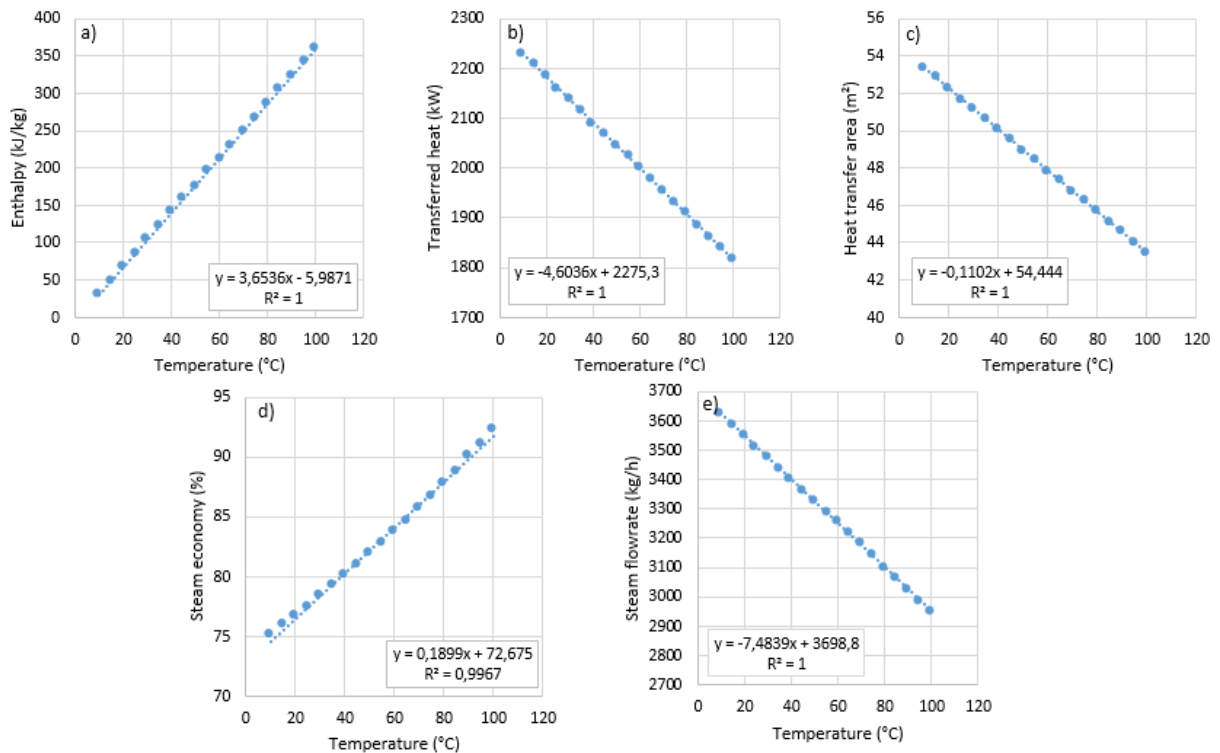


Figure 10. Effect of feed temperature on (a) enthalpy of concentrated liquid flow, (b) transferred heat, (c) heat transfer area, (d) steam economy, and (e) steam flowrate.

4. Conclusion

The most important result of the study is the ease of performing calculations for a single-effect evaporator using the graphical interface designed with VBA in the MS Excel program. This has enabled the calculation of missing data for NaOH solutions in a single-effect evaporator using known values, through the designed interface and the written program. Thanks to flexible programming, it is also possible to arrange designs for new solutions. Additionally, the effects of changing certain parameters on others were investigated using the calculations performed by the program, and the results are summarized below:

- The NaOH feed flow rate is directly proportional to the vapor flow rate, concentrated liquid flow rate, steam flow rate, total transferred heat, and heat transfer area.
- The NaOH feed concentration is inversely proportional to the vapor flow rate and directly proportional to the concentrated liquid flow rate.
- As the NaOH feed concentration increases, the feed enthalpy first decreases and then increases after reaching its lowest value of 0.2. This situation stems from enthalpy-concentration-temperature data in the literature.
- The NaOH feed concentration is inversely proportional to the total transferred heat, heat transfer area, and steam economy, and the steam economy drops rapidly after the value of 0.45.
- The steam pressure is directly proportional to the steam flow rate and inversely proportional to the heat transfer area and steam economy. It has been determined that the heat transfer area increases significantly, especially when the pressure is lower than 74.72 kPa.
- With the increase in pressure in the vapor space, the boiling point elevation, total transferred heat, and heat transfer area increase, especially after 25 kPa, the heat transfer area increases rapidly. The steam economy decreases with the increase in pressure.
- As expected, a relationship is given for the decrease in the heat transfer area with the increase in the thermal conductivity coefficient.
- With the increase in the concentration of the concentrated liquid flow, a decreasing effect is observed on the concentrated liquid flow rate and steam economy, while an increasing effect is seen on the heat transfer area and steam flow rate. Especially after the concentrated liquid concentration reaches 0.55, the heat transfer area increases rapidly.
- The feed flow temperature is directly proportional to the feed flow enthalpy and steam economy, and inversely proportional to the total transferred heat and heat transfer area.

Author Contributions

The percentage of the author contributions is presented below. The author reviewed and approved the final version of the manuscript.

	M.B.A.
C	100
D	100
S	100
DCP	100
DAI	100
L	100
W	100
CR	100
SR	100
PM	100
FA	100

C=Concept, D= design, S= supervision, DCP= data collection and/or processing, DAI= data analysis and/or interpretation, L= literature search, W= writing, CR= critical review, SR= submission and revision, PM= project management, FA= funding acquisition.

Conflict of Interest

The author declared that there is no conflict of interest.

Ethical Consideration

Ethics committee approval was not required for this study because of there was no study on animals or humans.

Acknowledgements

The author is grateful to Christie J. Geankoplis for the contributions to Chemical Engineering Science and Separation Technologies. Rest in peace.

References

- Argo BD, Angky Putranto W, Lestari A, Ramadhan F, Okatavian R. 2020. Multi effect evaporator design calculation for brown sugar production using computational fluid dynamics. *Int J Innov Technol Explor Eng*, 9(3S): 87-90. <https://doi.org/10.35940/ijtee.C1019.0193S20>.
- Boles MA, Cengel YA. 2014. *Thermodynamics: An engineering approach*. McGraw-Hill Education, New York, US, pp: 1024.
- Çataltas I. 1963. Tek tesirli evaporatörlerde kütle ve enerji bağıntıları. *Kimya Müh Derg*, 1(5): 31.
- dos Santos MT, Vianna AS, Le Roux GAC. 2018. Programming skills in the industry 4.0: Are chemical engineering students able to face new problems? *Educ Chem Eng*, 22: 69-76. <https://doi.org/10.1016/j.ece.2018.01.002>.
- Elmas ET. 2017. Evaporation plant for recycling of caustic soda. *Int J Eng Technol*, 3(3): 176-185.
- Fricke A, Schöneberger J. 2015. Industrie 4.0 with MS-Excel? *Chem Eng Transact*, 43: 1303-1308. <https://doi.org/10.3303/CET1543218>.
- Geankoplis CJ. 1978. *Transport processes and unit operations*. Allyn and Bacon Publishing, New York, USA, pp: 650.
- Geankoplis CJ. 2003. *Transport processes and separation process principles: (Includes Unit Operations)*. Upper Saddle River, NJ: Prentice Hall Professional Technical Reference, New York, USA, pp: 1026.

- Kapuno RR. 2008. Programming for chemical engineers using C, C++, and MATLAB? Jones & Bartlett Learning., New York, US,
- Karic E, Alic R. 2020. Simulation of a single-stage evaporator system integrated with a mechanical vapor compressor for concentrating the electrolytic system KNO₃ - H₂O. J Eng Proces Manag, 12(2): 50-56. <https://doi.org/10.7251/JEPM2002050K>.
- Microsoft Inc. 2021. VBA Programming in Office. Microsoft Inc. URL: <https://learn.microsoft.com/en-us/office/vba/api/overview/> (accessed date: August 2, 2022).
- Said A, Louhi-Kultanan M. 2019. Simulation and empirical studies of solvent evaporation rates in vacuum evaporation crystallization. Chem Eng Technol, 42(7): 1452-1457. <https://doi.org/10.1002/ceat.201800708>.
- Simpson R, Almonacid S, López D, Abakarov A. 2008. Optimum design and operating conditions of multiple effect evaporators: tomato paste. J Food Eng, 89(4): 488-497. <https://doi.org/10.1016/j.jfoodeng.2008.05.033>.
- Teppaitoon W. 2016. Solving L-L extraction problems with excel spreadsheet. Chem Eng Educ, 50(3): 169-175.
- Wong KWW, Barford JP. 2010. Teaching Excel VBA as a problem solving tool for chemical engineering core courses. Educ Chem Eng, 5(4): e72-77. <https://doi.org/10.1016/j.ece.2010.07.002>.



EFFECTS OF GEOMETRIC PARAMETERS OF PERFORATED DIFFUSER ON SOUND PRESSURE LEVEL SOURCED BY AIRFLOW

Ahmet ERDOĞAN^{1*}, İshak Gökhan AKSOY¹, Suat CANBAZOĞLU²

¹*Inönü University, Faculty of Engineering, Department of Mechanical Engineering, 44280, Malatya, Türkiye*


²*Retired scientist, Türkiye*


Abstract: This study investigates the aeroacoustic behaviors of a square truncated perforated diffuser under airflow, commonly used in Air Handling Units (AHUs). The design parameters are fundamentally taken into account to unveil the aeroacoustic performance of the diffuser. Initially, unsteady-state Computational Fluid Dynamics (CFD) simulations are conducted based on models that accurately represent the fluid domain of the chamber with the perforated diffuser in the ANSYS Fluent environment. Subsequently, the Ffowcs Williams and Hawkings (FW-H) method integrated into the software is employed to acquire time-dependent signals from microphones placed in three different locations within a perforated diffuser chamber. Finally, the results are converted to a frequency range of 0-1000 Hz using the Fast Fourier Transform (FFT) method, and the SPL values are obtained. The results show that the microphone location is crucially important to determine SPL and the porosity reduction from 0.55 to 0.35 can reduce SPL by approximately 30-40 dB. Variations in wall thickness of the diffuser fluctuated between 5-10 dB at each frequency value.


Keywords: Air handling units, Computational fluids dynamic, Perforated diffuser, Sound pressure level, Ansys fluent

*Corresponding author: Inönü University, Faculty of Engineering, Department of Mechanical Engineering, 44280, Malatya, Türkiye

E mail: ahmet.erdogan@inonu.edu.tr (A. ERDOĞAN)

Ahmet ERDOĞAN  <https://orcid.org/0000-0001-8349-0006>

İshak Gökhan AKSOY  <https://orcid.org/0000-0002-8798-5847>

Suat CANBAZOĞLU  <https://orcid.org/0000-0002-0166-4824>

Received: January 18, 2024

Accepted: February 19, 2024

Published: March 15, 2024

Cite as: Erdoğan A, Aksoy İG, Canbazoglu S. 2024. Effects of geometric parameters of perforated diffuser on sound pressure level sourced by airflow. *BSJ Eng Sci*, 7(2): 271-276.

1. Introduction

Air Handling Units (AHUs) are crucially important components of Heating, Ventilating, and Air Conditioning (HVAC) systems (Yu et al., 2014). An AHU typically conditions the air by adjusting temperature, humidity, and filtration. The cross-sectional area of fans employed in AHUs is less than the cross-sectional area of chambers situated adjacent to the HVAC equipment's fan, including heating/cooling coils, silencer (sound attenuator), filter, or heat recovery elements (Kamer et al., 2018). The air supplied by the fan is therefore partially in contact with the surfaces of other units. The operating efficiency of AHUs is significantly diminished by this situation. In order to address this issue, a chamber with a perforated diffuser is employed after the fan chamber (Erdoğan, 2017). When utilizing a chamber with a perforated diffuser, it becomes feasible to enhance operational efficiency by minimizing the overall pressure loss in the AHU (Bulut et al., 2011). This is achieved by ensuring a uniform passage of air across all the surfaces of the aforementioned units. Minimizing the total pressure loss in the AHU and achieving homogeneous airflow diffusion to the subsequent unit are crucial aspects for enhancing energy efficiency (Erdoğan and Daşkın, 2023). Figure 1 illustrates a schematic representation of an AHU equipped with a perforated diffuser. According to a market survey among manufacturers of AHUs, there is

insufficient information about the flow structure in chambers equipped with perforated diffusers.

Additionally, the perforated diffusers used in AHUs may cause significant noise (Yapanmış, 2016; Erdoğan, 2017). In many instances, this leads to health problems and, as such, is undesirable. Elevated noise levels can also indicate energy inefficiency and vibration problems. The noise generated by perforated diffusers is primarily a result of flow (aeroacoustic) issues. Yapanmış (2016) investigated the pre-emissive properties of perforated diffusers with square truncated pyramid and truncated cone geometries designed for AHUs. The study examined the effects of different geometrical parameters on sound transmission loss. However, it does not cover the aeroacoustic properties of perforated diffusers, focusing instead on their acoustic properties in a flow-free environment. Martinez-Lera et al. (2012) conducted a numerical flow study in an HVAC duct with a flapper inside and subsequently calculated the sound pressure level using the Ffowcs Williams-Hawkings (FW-H) approach in ANSYS-Fluent. Kaltenbacher et al. (2016) presented a novel computational scheme for simulating flow-induced sound in rotating systems. The method, they used, employs scale-resolving simulations with an arbitrary mesh interface, connecting rotating and stationary domains.



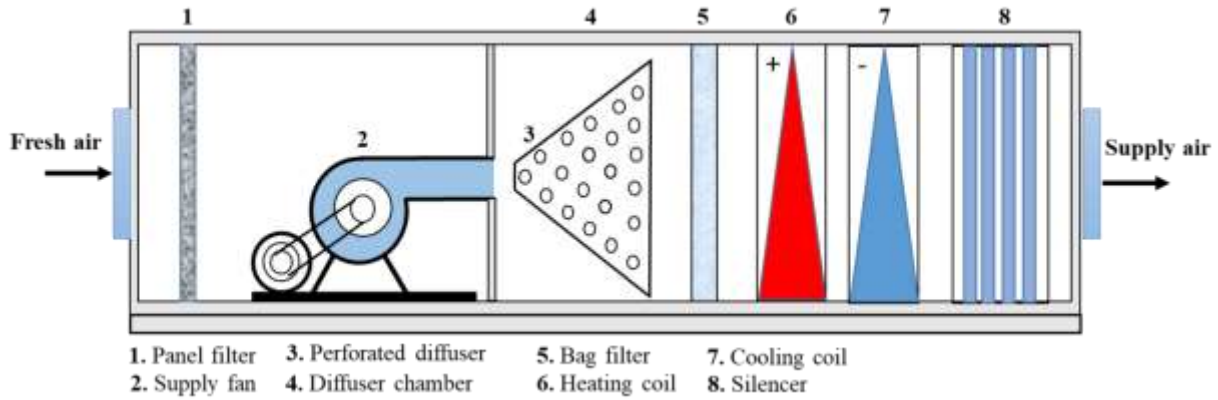


Figure 1. Schematic representation of an AHU with perforated diffuser.

The Finite-Element method, along with Nitsche type mortaring, was applied at the interface for solving. They demonstrated in the numerical computation of a side channel blower (Kaltenbacher et al., 2016). Kandekar et al. (2019) investigated flow-induced noise in the 400 Hz to 5000 Hz frequency range and discussed a Computational Aeroacoustics (CAA) approach for simulating. They validated through testing with good correlation between CFD predictions and measurements. Mikedis (2023) performed some numerical simulations on aeroacoustic characteristics in a HVAC duct by employing OpenFOAM CFD toolbox. The Direct Numerical Model (DNS) was used to solve the aeroacoustic simulations and the model was validated with experiments. Bezci numerically investigated the flow structure and aerodynamically induced noise in a centrifugal fan using $k-\epsilon$ and LES (Large Eddy Simulation) turbulence models under five different outlet pressure boundary conditions. Additionally, he determined the noise propagation from the flow in free space using the Ffowcs Williams-Hawkings (FW-H) approach (Bezci, 2009).

Numerous studies in the literature focus on the acoustic performance of silencers equipped with perforated surfaces, employed in diverse industrial applications. Ueda et al. (2002) observed the acoustic field of the resonator through measurements of instantaneous pressure and average velocity. They asserted that the phenomena responsible for sound wave generation and the acoustic resistance of the resonator are closely linked to the phase difference. Furthermore, the efficiency values were found to exhibit a connection at this juncture (Ueda et al., 2002). Emphasizing the significance of designing the grid structure inside the resonator to mitigate pressure fluctuations at the inlet, Zoccola highlighted that an incompatible design with the pressure fluctuation character could result in persistent oscillations. This could even lead to irregular vortex fields instead of periodic ones. Zoccola conducted velocity and sound measurements to establish the relationship between the excitation system, amplitude levels in the resonator, and grid configurations (Zoccola Jr, 2004). Morris et al. concentrated on the pressure

differential, oscillatory excitations, and secondary losses resulting from constrictions and expansions within the resonator flow field. They examined and discussed the interactions between the entire resonator and the expansion and constriction parts separately and in comparison (Morris et al., 2004).

2. Materials and Methods

The dimensions of the square truncated pyramid perforated diffuser chamber investigated in this study are shown in Figure 2. All geometric parameters considered in this study are given in Table 1.

Table 1. Variable geometric parameters and values

Parameters	Unit	Value
δ	[-]	0.35, 0.40, 0.45, 0.50, 0.55
α	[°]	50, 55, 60
t	[mm]	1, 2, 3
L_0	[mm]	0, 100, 200
Hole array type	[-]	Staggered, Straight
Diffuser surface type	[-]	Flat, convex, concave

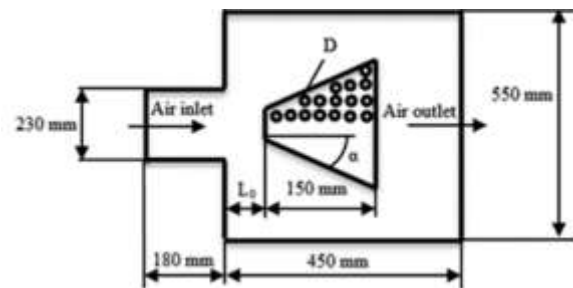


Figure 2. The dimensions of the square truncated pyramid perforated diffuser chamber.

In Table 1, ' t ' represents the plate thickness; ' δ ' indicates the porosity of the perforated diffuser, representing the ratio of the area of apertures to the total surface area of the perforated diffuser; ' α ' and ' L_0 ' denote the draft angle of the diffuser and the distance from air inlet to diffuser, respectively. Hole array types are illustrated in Figure 3.

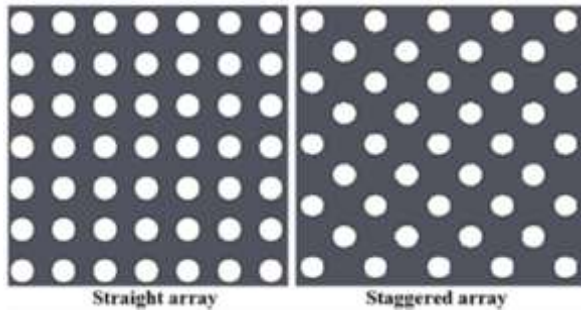


Figure 3. Hole array type.

Fluent within the ANSYS software package. Tetrahedral (four-faced) elements, recommended for relatively complex geometries, were employed as the mesh elements (Fluent, 2009). Throughout the surfaces of the perforated diffuser and in the flow domain, the maximum element size was set to 0.01 m, while on the surfaces of the perforated diffuser, it was determined to be 0.005 m. Figure 4 depicts the mesh structure of the CFD models.

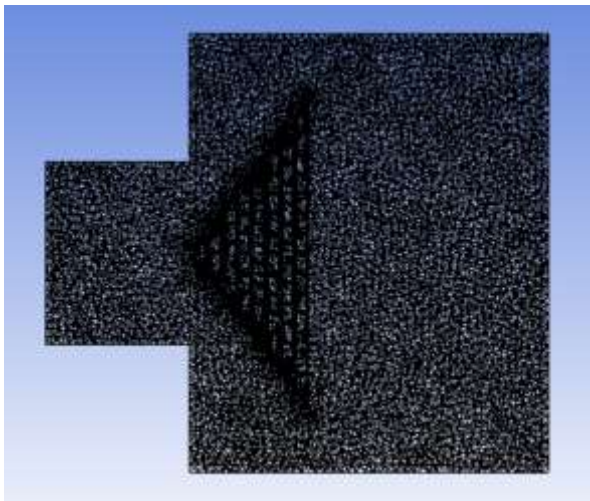


Figure 4. Mesh structure of the CFD models.

This study presents the sound pressure levels (SPL) in the chamber with a perforated diffuser in the frequency range of 0-1000 Hz, considering the geometric design parameters of the square truncated pyramid perforated diffuser. The numerical models, developed for aeroacoustic analyses, involved solving Equations 1-5, which represent mass (Equation 1), momentum (Equation 2), and the Standard k-ε turbulence model (Equation 3, 4) in the ANSYS-Fluent software (Fluent, 2009). The simulations were carried out with a time step of 0.0005 s and a total of 1000 time steps. The boundary conditions include a "velocity inlet" defined for the 230 mm x 230 mm air inlet section, and a "pressure outlet" defined for the 550 mm x 730 mm air outlet section. The air inlet velocity is assumed to be 16.2 m/s, while the average static pressure at the outlet section is assumed to be 100 Pa. Subsequently, employing the Fowcs Williams-Hawkings (FW-H) approach within the Ansys-Fluent program, based on the Lighthill acoustic analogy,

time-dependent acoustic signals were acquired from three microphones strategically placed within the chamber. The SPL values were then determined across frequencies using the Fast Fourier Transform (FFT) module in the CFD-Post section. The microphone positions placed inside the square truncated pyramid hole diffuser chamber, here presented as microphone 1-M1, microphone 2-M2, and microphone 3-M3, are shown in Figure 5.

$$\frac{\partial u_i}{\partial x_i} = 0 \quad (1)$$

$$\frac{\partial u_i u_j}{\partial x_j} = -\frac{\partial p}{\partial x_i} + \frac{\partial}{\partial x_j} \left[\mu \left(\frac{\partial u_i}{\partial x_j} + \frac{\partial u_j}{\partial x_i} \right) \right] - \frac{\partial}{\partial x_j} (\rho \overline{u_i' u_j'}) \quad (2)$$

where u and p are the velocity and pressure, respectively. $\overline{u_i' u_j'}$ states Reynolds stress.

$$\frac{\partial(\rho k)}{\partial t} + \frac{\partial(\rho k u_i)}{\partial x_i} = \frac{\partial}{\partial x_j} \left[\left(\mu + \frac{\mu_t}{\sigma_k} \right) \frac{\partial k}{\partial x_j} \right] + G_k - \rho \varepsilon \quad (3)$$

$$\frac{\partial(\rho \varepsilon)}{\partial t} + \frac{\partial(\rho \varepsilon u_i)}{\partial x_i} = \frac{\partial}{\partial x_j} \left[\left(\mu + \frac{\mu_t}{\sigma_\varepsilon} \right) \frac{\partial \varepsilon}{\partial x_j} \right] + C_{1\varepsilon} \frac{\varepsilon}{k} G_K - C_{2\varepsilon} \rho \frac{\varepsilon^2}{k} \quad (4)$$

In equation 3 and equation 4, the symbols k and ε represent turbulence kinetic energy and turbulence dissipation rate, respectively. The turbulent viscosity, denoted as μ_t , is expressed through the calculated Equation 5 presented below.

$$\mu_t = \rho C_\mu \frac{k^2}{\varepsilon} \quad (5)$$

The constants in these equations are assigned the following values, respectively: $\sigma_k=1$, $\sigma_\varepsilon=1.3$, $C_{1\varepsilon}=1.44$, $C_{2\varepsilon}=1.92$, and $C_\mu=0.09$ (Fluent, 2009).

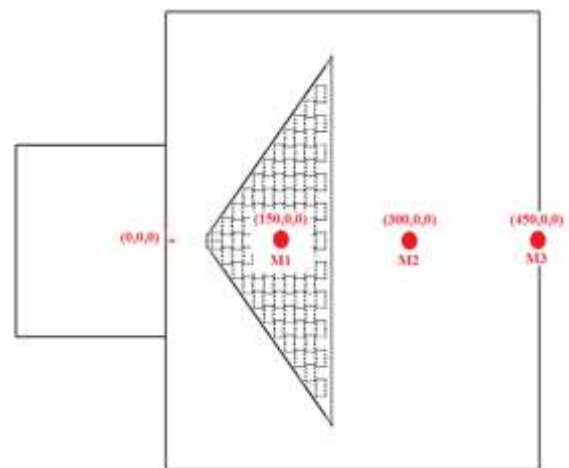


Figure 5. Microphone positions in chamber with perforated diffuser.

3. Results and Discussion

The CFD analyses conducted to investigate the impact of the geometrical design parameters of the square

truncated pyramid perforated diffuser on the SPL generated by the airflow within the chamber involved collecting data from microphones at three distinct locations across the frequency range of 0-1000 Hz. Figure 6 shows the porosity effect on the SPL. Upon analyzing Figure 5, it is noted that the variation in SPL with different porosity values differs depending on the position of the receiving microphone. Generally, however, the SPL within the chamber equipped with a perforated diffuser increases as the porosity value rises. Reducing the porosity value from 0.55 to 0.35 can result in a significant noise reduction in SPL, amounting to approximately 30-40 dB across nearly all frequency values. In the context of this flow model, it can be inferred that higher porosity values lead to increased SPL values due to the formation of more vortices in the flow domain. Figure 7 illustrates the impact of the diffuser draft angle on the SPL. According to Figure 7, a decrease

in SPL near the diffuser is observed as the draft angle increases. Specifically, signals from M1, positioned closest to the diffuser, consistently exhibit lower SPL values, except for certain frequency values observed in signals from M3, located farthest from the diffuser, for $\alpha=55^\circ$. Additionally, an increase in the draft angle induces greater fluctuations in SPL across various frequencies. The impact of the specified diffuser wall thickness values on the SPL is depicted in Figure 8. Upon analysis, it is noted that there is a decline in the SPL with an increase in the wall thickness parameter from 1 mm to 2 mm for signals received from M1, the microphone closest to the diffuser. However, in the case of signals received from microphones M2 and M3, it is observed that the SPL is higher at the intermediate value of 2 mm wall thickness compared to the values of 1 mm and 3 mm.

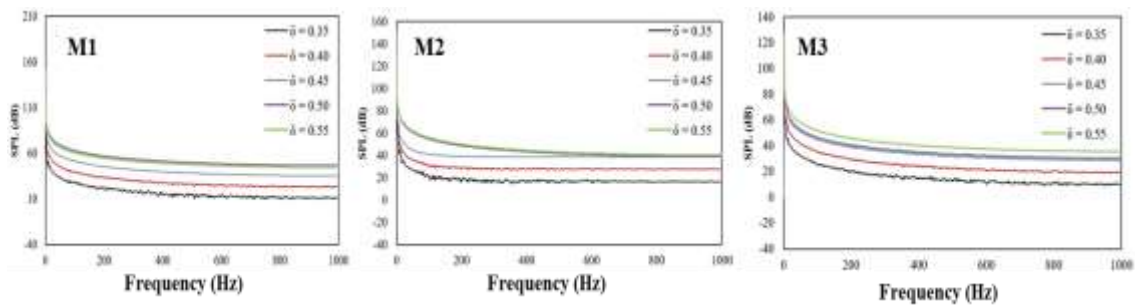


Figure 6. Porosity effect on SPL.

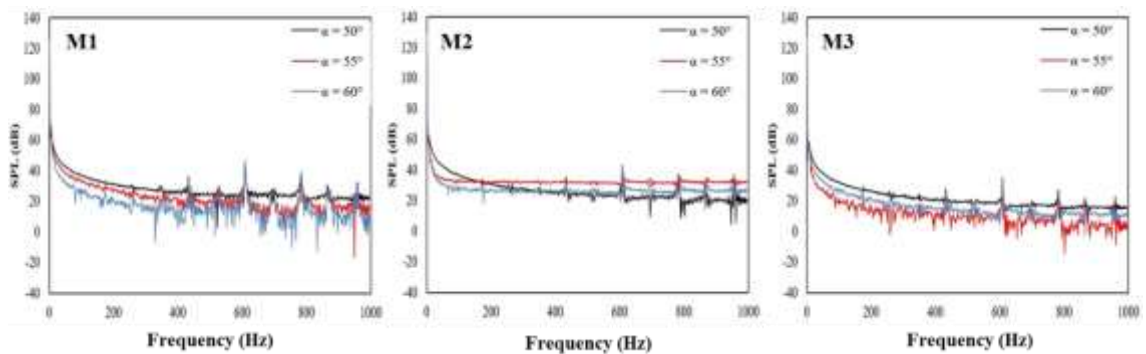


Figure 7. Draft angle effect on SPL.

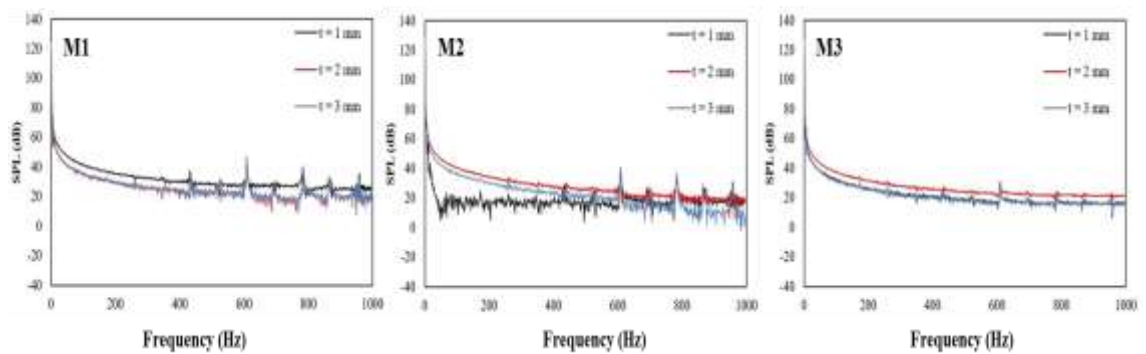


Figure 8. Diffuser thickness effect on SPL.

Figure 9 illustrates a graph depicting the variation in SPL with the position of the square truncated pyramid

perforated diffuser (L_0) within the chamber. Examination of this graph reveals a substantial correlation between

the diffuser position and the microphone position in the obtained signal values. Specifically, it is observed that the SPL is higher at $L_o=100$ mm in the signals received from the M1 receiver. This is attributed to the fact that the M1 microphone position is 50 mm inside the peak of the perforated diffuser, where the noise caused by the time-dependent vortical flow structure is more pronounced. Figure 10 gives the SPL values acquired for various hole array types and three different microphone positions. With the exception of some signal values obtained from

the M2 receiver at low frequencies, it is evident that the staggered array results in higher SPL than the straight placement type for all three microphone positions. Figure 11 presents the SPL values recorded from three distinct microphone positions when the surface type of the perforated diffuser is flat, convex, and concave. Based on the signals obtained from the microphone in all three positions, it can be concluded that the concave geometry induces more fluctuations in the SPL across different frequencies and results in a lower overall SPL.

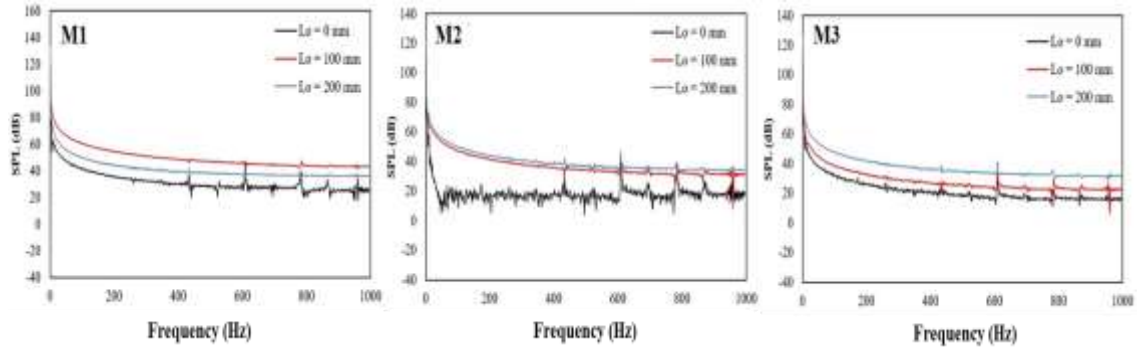


Figure 9. Diffuser locations effect on SPL.

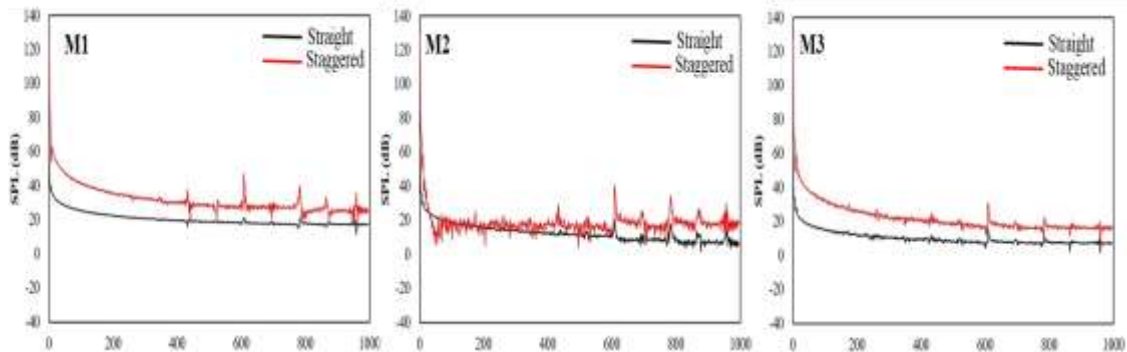


Figure 10. Hole array type effect on SPL.

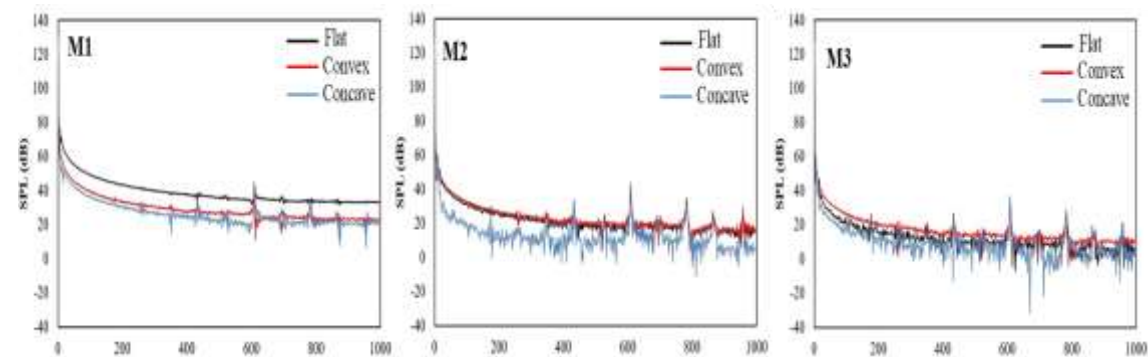


Figure 11. Diffuser surface type effect on SPL.

4. Conclusion

This study offers insights into how the geometric parameters of square truncated pyramid perforated diffusers, utilized in AHU, influence the SPL. Following CFD-based aeroacoustic analyses, SPL values were acquired within the frequency range of 0-1000 Hz for each geometric parameter value employed in the diffuser configuration.

- Low porosity value provides lower SPL values. A reduction in porosity from 0.55 to 0.35 can drastically reduce SPL by approximately 30-40 dB across almost all frequency ranges.
- While the SPL decreases with a reduction in the draft angle for the M2, a draft angle of 55° results in less noise, approximately 20 dB lower, compared to values obtained from microphones positioned (M3)

farther from the diffuser.

- Analyzing signals from the microphone in the downstream region of the diffuser revealed that the impact of wall thickness variation on SPL fluctuated at each frequency value, typically within a range of 5-10 dB.
- The placement of the diffuser within the chamber (L0) can influence the SPL by approximately 20 dB, regardless of the microphone's position. When the diffuser is positioned near the air inlet surface (L0=0), the lowest SPL is achieved downstream of the diffuser.
- The straight array results in a reduction in SPL of approximately 20 dB at all microphone positions compared to the staggered array.
- Analyzing signals from the microphone located downstream of the diffuser, it is observed that when the diffuser surface is flat, concave, or convex, there is a maximum difference of 5 dB in SPL across different frequencies.

As a future study, the fluid domain in these CFD models will be expanded to include the HVAC duct component. Consequently, the microphone positions will be relocated to align with the new model. Additionally, other AHU components, such as the heating/cooling coil, humidifier, and filter, will be integrated into the models. This expansion aims to yield more comprehensive results.

Author Contributions

The percentage of the author(s) contributions is presented below. All authors reviewed and approved the final version of the manuscript.

	A.E.	İ.G.A.	S.C.
C	40	30	30
D	60	20	20
S	60	20	20
DCP	80	10	10
DAI	60	20	20
L	50	25	25
W	50	25	25
CR	40	30	30
SR	80	10	10
PM	30	35	35
FA	20	40	40

C=Concept, D= design, S= supervision, DCP= data collection and/or processing, DAI= data analysis and/or interpretation, L= literature search, W= writing, CR= critical review, SR= submission and revision, PM= project management, FA= funding acquisition.

Conflict of Interest

The authors declared that there is no conflict of interest.

Ethical Consideration

Ethics committee approval was not required for this

study because of there was no study on animals or humans.

Acknowledgements

This study was supported by Turkish Scientific and Technological Research Council of Türkiye (Project No: 114M748).

References

- Bezci H. 2009. Aeroacoustic properties of a radial fan. PhD Thesis, İstanbul Technical University, Institute of Science and Technology, İstanbul, Türkiye, pp: 85.
- Bulut S, Unveren M, Arisoy, A, Boke, Y. 2011. Reducing internal losses in air handling units with CFD analysis method. TMMOB X. National Plumbing Engineering Congress and Exhibition, April 11-13, İzmir, Türkiye, pp: 291-326.
- Erdoğan A, Daşkın M. 2023. Comparing of CFD contours using image analysing method: A study on velocity distributions. *BSJ Eng Sci*, 6(4): 633-638.
- Erdoğan A. 2017. Investigation of airflow in empty chambers with perforated diffuser designed for air handling units in terms of flow and acoustic. PhD Thesis, İnönü University, Institute of Science, Malatya, Türkiye, pp: 115.
- Fluent A. 2009. 12.0 User's guide. Ansys Inc, 6: 552.
- Kaltenbacher M, Hüppe A, Reppenhagen A, Tautz M, Becker S, Kuehnel V. 2016. Computational aeroacoustics for HVAC systems utilizing a hybrid approach. *SAE Int J Passeng Cars Mech*, 9(3): 1047-1052.
- Kamer MS, Erdoğan A, Taçgün E, Sonmez K, Kaya A, Aksoy IG, Canbazoglu S. 2018. A performance analysis on pressure loss and airflow diffusion in a chamber with perforated V-profile diffuser designed for air handling units (AHUs). *J Appl Fluid Mech*, 11: 1089-1100.
- Kandekar A, Nagarhalli P, Dol Y, Thakur S, Gupta B, Jadhav T. 2019. HVAC system noise prediction through CFD simulation. *SAE Tech Pap*, 26: 210.
- Martinez-Lera P, Hallez R, Bériot H, Schram, C. 2012. Computation of sound in a simplified HVAC duct based on aerodynamic pressure. 18th AIAA/CEAS Aeroacoustic Conference (33rd AIAA Aeroacoustic Conference), June 4-6, Colorado, US, pp: 1-10.
- Mikedis K. 2023. Prediction of aerodynamically induced noise in automotive HVAC systems. Diploma Thesis, National Technical University, Athens School of Mechanical Engineering, Athens, Greece, pp: 93.
- Morris PJ, Boluriaan S, Shieh CM. 2004. Numerical simulation of minor losses due to a sudden contraction and expansion in high amplitude acoustic resonators. *Acta Acust United Acust*, 90: 393-409.
- Ueda Y, Biwa T, Mizutani U, Yazaki T. 2002. Acoustic field in a thermoacoustic Stirling engine having a looped tube and resonator. *Appl Phys Lett*, 81: 5252-5254.
- Yapanmış BE. 2016. Design of perforated diffuser as a pre-silencer. PhD Thesis, Mersin University, Institute of Science, Mersin, Türkiye, pp: 95.
- Yu Y, Woradechjumroen D, Yu, D. 2014. A review of fault detection and diagnosis methodologies on air-handling units. *Energy Build*, 82: 550-562.
- Zoccola Jr JP. 2004. Effect of opening obstructions on the flow-excited response of a Helmholtz resonator. *J Fluids Struct*, 19: 1005-1025.



ANALYSIS OF THE ENERGY EFFICIENCY OF POULTRY HOUSES IN TÜRKİYE

Asiye ASLAN^{1*}


¹Bandırma Onyedü Eylül University, Gönen Vocational School, 10900, Balıkesir, Türkiye

Abstract: Türkiye is an important producer, consumer and exporter in the poultry farming industry across the world. The poultry farming is one of the fastest growing sectors in the field of food and agriculture and has become one of the strongest sectors over time. Especially with the development of industrial sectors, the effective usage and management of energy, which is the most important issue of almost every business, has recently become an important structure in the building sector in Türkiye. This study examined optimum insulation layer thickness, energy savings, and emissions of CO₂ for the exterior walls and roofs of poultry farming facilities. The study used the degree day method, which is widely used in standard insulation calculations, in accordance with broiler production. As the equilibrium temperature, the desired temperature values of broilers for each week in the 6-week period were taken as the basis (31, 29, 25, 23.50, 22.50, 20.50°C). Life cycle cost analysis (LCCA) was applied to identify the optimal values of insulation thickness in the facilities. Accordingly, the optimum insulation layer thickness, savings amount, and payback period for the walls and roofs ranged between 0.043-0.270 m and 0.022-0.094 m, 7.53-164.65 \$/m² and 12.85-319.62 \$/m², 1.19-2.19 years and 1.18-1.99 years, respectively. It has been calculated that a 70-80% reduction in CO₂ emissions could be managed by applying the optimum insulation layer thickness.

Keywords: Poultry farms, Insulation, Energy saving, Life-cycle cost analysis

*Corresponding author: Bandırma Onyedü Eylül University, Gönen Vocational School, 10900, Balıkesir, Türkiye

E mail: aaslan@bandirma.edu.tr (A. ASLAN)

Asiye ASLAN  <https://orcid.org/0000-0002-1173-5008>

Received: December 15, 2023

Accepted: February 21, 2024

Published: March 15, 2024

Cite as: Aslan A. 2024. Analysis of the energy efficiency of poultry houses in Türkiye. *BSJ Eng Sci*, 7(2): 277-297.

1. Introduction

Energy efficiency is explained as the usage of lower rates of energy for performing the same task or achieving the same outcome. To achieve efficiency in terms of energy use, it is essential to use less energy for heating and cooling buildings and operating electronic devices. In addition, one of the most effortless and least costly methods to fight global climate change, raise the competitive power of firms and lower the cost of energy for consumers is energy efficiency. Energy efficiency also has a critical part in efforts to reach net zero carbon dioxide emissions by achieving decarbonization.

Another way of fighting against climate change is to use renewable energy resources instead of traditional energy resources and to create a significant effect on each aspect of energy policies of countries. Geothermal energy is a national, renewable, clean, and environmentally friendly underground resource. Türkiye is rich in terms of geothermal energy thanks to its geological and geographical location among world countries, and there are approximately 1,000 geothermal resources with varying temperatures spread across the country. 78% of geothermal resources are in West Anatolia Region, which is followed by Central Anatolia Region (9%), Marmara Region (7%), East Anatolia Region (5%), and other regions (Anonymous, 2023a).

Based on the size of livestock, poultry represents the greatest inventory of domesticated animals worldwide. Poultry has become the fastest growing component of global meat production in the early 21st century. Poultry production is economically important worldwide, for example, it is an industry of more than \$20 billion per year in the United States. In 2021, the global production rate of poultry meat was estimated as 137.8 million tons. As of 2020, the United States (22,705 million), China (19,500 million), Brazil (14,076 million), and the EU (13,769 million) were the largest producers of poultry meat. The vast majority of poultry meat production within the EU takes place in five states, among which Poland (19.2%) is the largest poultry producer. Consecutively, Germany (13.1%), France (12.8%), Spain (10.1%), and Italy (9.9%) follow Poland. In general, the worldwide production of poultry has grown steadily, with a rate of 1.32% over the previous decade (Gržinić et al., 2023).

Considering the number of broiler chickens in Türkiye by regions, the East Marmara and Aegean Regions had a collective portion of 59.8% in 2019. The region of East Marmara was the leader broiler producer in with a share of 33.5%, followed by the Aegean Region (26.3%) and the West Marmara (14.3%). More than half (56.4%) of the broilers in Türkiye were collected in five provinces in 2019. Manisa had the highest proportions of broiler



chickens at a rate of 12.6%, followed by Sakarya (12.6%), Balıkesir (11.6%), Bolu (10.8%), and Mersin (8.7%) (Anonymous, 2023b).

In this context, there are two significant factors affecting productivity in broiler farming: genetic composition and environmental conditions. Considering the environmental conditions, the most important factor is temperature (Aritürk et al., 1986). Several factors such as ensuring the poultry house to be least affected by cold in winter and hot in summer, preventing sudden indoor temperature changes and moisture condensation, and maintaining the appropriate indoor temperature should be considered when planning a good poultry house construction (Özdemir and Poyraz, 1997).

To increase efficiency and protect broiler chickens from the negative effects of climate, it is important to design and plan poultry houses according to proper rules and regulations. It is only possible with isolation to ensure the desired environmental conditions effectively in the poultry houses throughout the year (Özdemir and Poyraz, 1997). Insulation prevents losses of heat in winter and the accumulation of heat in summer. Economic benefits are achieved by reducing heating and cooling costs, allowing controlling sweating, condensation, and humidity. In addition, it is obligatory to reduce energy consumption in buildings and to obtain minimum values according to national regulations (Akpinar and Demir, 2018).

There are several studies about insulation in buildings. Annibaldi et al. (2019) presented a multidisciplinary approach to raise the performance of historic buildings in terms of energy utilization, allowing them to compare the optimized values of insulation thickness, which are found with the permeability parameters of walls in situ, and those in the relevant literature. This set of techniques involves an initial examination of the building envelope and an investigation of the insulation materials and thickness to identify the optimum combination between the building's energy performance and the investment cost. The methodology was implemented for a case study in Italy. The authors revealed that the specific usage of data in the relevant literature to organize an energy recovery plan of an existing historic building can cause substantial errors. Hou et al. (2022) calculated the optimum thickness for the exterior walls of rural traditional residences in the northeast of Sichuan hills using the degree-day method and the P1-P2 economic model. They also evaluated the energy savings and economic advantages according to the EnergyPlus and dynamic investment payback time model. As a result, they found that the optimum insulation layer thickness varied between 0.081 m and 0.144 m, considering the local climate and economic context. By using Mathcad software program, Malka et al. (2022) proposed removing the heating degree day limits for some materials used for insulation (EPS Graphite, EPS, GW and RW) and a set of different energy resources (electricity, diesel, natural gas, LPG and biomass). They considered

additional economic variables (i.e., inflation, interest rate, lifetime and present value factor) and properties of heating systems to determine the optimum insulation layer thickness, and applied the RETScreen Expert model for various types of structures in Albania. As a result, they stated that the overall heat transfer value (U) must equal or be smaller compared to 0.30 (W/m²K), and suggested that the proposed method could be implemented not only in Albania, but also in other parts of the world with comparable climate characteristics. Dombaycı et al. (2017) have examined optimum insulation layer thickness values for the exterior walls of homes in select cities in different climate zones of Türkiye. They applied a thermoeconomic method, considering inflation and interest rates with Life Cycle Cost Analysis (LCCA), and calculated maximum and minimum thicknesses for polystyrene and polyurethane insulation materials, respectively, for cold and hot climatic regions, thus obtained maximum and minimum savings amounts in these regions. Açıkkalp and Kandemir (2019) have presented an alternative technique to combine financial and environmental impacts in determining the optimum insulation layer thickness, which is known as the United Economic and Environmental Method (CEEM). They have made analyses for Bilecik province in Türkiye, using stone wool and glass wool insulation materials, compared their results with those of other methods, and calculated annual savings and energy savings. Ustaoglu et al. (2020) have conducted an energy analysis using various polyurethane insulation materials for various climate zones and fuels to determine energy performance in buildings. They have used coal, natural gas, liquefied petroleum gas (LPG), fuel oil, and electricity as fuels. Accordingly, they reported that polyurethane foam in which 3% paper mill sludge (PMS) was added had the most favorable thermal resistance values. Depending on the fuel used, they found that savings ranged from \$8.86 to \$54.6/m² with a thickness of 0.0245 m, and the payback period varied from 1.37 to 8.76 years.

In addition, some studies have also aimed to identify the energy needs and comfort conditions of poultry houses. Kapica et al. (2015) presented the simulation results of CO₂ reduction potential for poultry houses by replacing traditional heating system with hybrid sun-wind system. They calculated heat requirements for 2400 poultry houses and presented basic models for solar collectors, wind turbines and heat storage tanks in these houses. Their system was modelled in a MATLAB/Simulink environment by analyzing different settings of systems for climatic conditions specific to the Central Europe. As a result, they found that larger systems provided higher CO₂ reduction but their energy usage rates decreased. Yang et al. (2022) proposed a new pair of ventilation system by combining the advantages of exhaust air heat recovery system and perforated channel ventilation for poultry houses in China. As a result, they stated that a better interior can be created with improved ventilation

performance and low cost with a new double-channel ventilation system. Unlike traditional energy analysis approaches in Ghana, Akolgoa et al. (2022) analyzed environmental conditions and energy inputs in poultry houses using the Energyplus simulation and compared them using the artificial nervous system. They estimated the annual energy consumption and equipment use as 2,044 kWh and 1,452 kWh, respectively, and stated that the ANS model was applicable to the determination of energy consumption by poultry houses. Dağtekin (2012) aimed to meet the electrical energy need for a henhouse of 20,000 capacities by using photovoltaic solar energy system. By designing a PV system of 15 kW power, he made a techno-economic assessment of the system. The amount of energy to be generated in PV power plants, the cost of electricity, investment and business costs, and payback period were calculated. As a result of these calculations, payback period of the PV system was determined as 9.2 years, and electricity generation cost was found as 0.1100 TL/kWh. The efficiency of the system was calculated as 12.1% and CO₂ emission reduction rate as 20,259 kg/year. Özlü et al. (2017) investigated the use of paper industry waste as underlay in broiler facilities. In the study, 468 broilers with various genders were used. Underlay material consisted of rice hull, waste paper, and a mixture of the two in equal ratios. As a result, in week 6, the live weight of the group in which waste paper was used as underlay was determined to be about 60 g higher than the other groups. It was also determined that underlay type did not have any effect on factors such as living power and feed evaluation rate.

Despite the numerous studies conducted for buildings used for different purposes and especially for residential buildings, there exists limited research to determine the insulation thickness for energy efficiency in poultry houses. This study used the degree day method for the poultry farming sector and calculated the degree of day (DD) values for the insulation of poultry farming facilities considering the region's climate and temperatures. As the equilibrium temperature, the desired temperature values of broilers for each week in the 6-week period were taken as the basis (31, 29, 25, 23.50, 22.50, 20.50°C). The optimum insulation layer thickness of the exterior walls and roofs according to HDD and CDD numbers was calculated. This procedure was used as an alternate choice of method for building insulation accounts to achieve optimum results in poultry farming facilities. The calculations were made for all provinces with poultry farming facilities in Türkiye. There is no study that covers all cities with poultry farming facilities in Türkiye and deals with both the exterior walls and roofs of poultry farming facilities. The optimum insulation layer thicknesses are determined for Extruded Polystyrene and Expanded Polystyrene for the walls and sandwich panel for the roofs as insulation materials. This study used the meteorological data between 2018-2022 and considered natural gas, coal, fuel oil, LPG and electricity as fuel. In

addition, geothermal energy was evaluated as an alternative energy source in broiler facilities in cities where geothermal energy sources suitable for heating were available, and optimum insulation layer thickness was calculated and compared with other fuels. Energy savings, payback periods, and CO₂ emissions were calculated as a result of the use of insulation in poultry farming facilities. By conducting this study, it was aimed to make Türkiye gain an important place in the poultry farming sector worldwide.

2. Materials and Methods

2.1. HDD and CDD Calculation

The degree-day (DD) method is among the most preferred techniques to determine the energy needed for the heating or cooling of buildings (Eto, 1988; Büyükalaca et al., 2001). A reference temperature is used in calculating the degree-day number. The reference temperature for heating degree days is defined as the outside temperature at which the building's heating demand begins, and for cooling degree days, it is defined as the outside temperature at which the cooling demand begins. The degree-day number is calculated by subtracting the reference temperature from the daily temperature average and then adding the values for the designated time interval. In this study, HDD and CDD were determined using equations 1 and 2 (Christenson et al., 2006; De Rosa et al., 2014).

$$\text{For } T_{\text{out}} < T_{\text{base}},$$

$$\text{HDD} = \sum_{1}^n (T_{\text{base}} - T_{\text{out}}) \quad (1)$$

$$\text{For } T_{\text{base}} < T_{\text{out}},$$

$$\text{CDD} = \sum_{1}^n (T_{\text{out}} - T_{\text{base}}) \quad (2)$$

where, n is the total number of days specified for the period. T_{base} and T_{out} are the reference temperature and the average outside air temperature, respectively.

In broiler production, the production period in poultry houses is recommended as 41 or 42 days. In this study, 7 production periods per year were taken into account, considering 42 days of production and a 12-day break (Table 1). The temperature values required weekly by broilers during the 42-day process are the equilibrium temperature values recommended by the researchers and given in Table 2.

Table 1. Annual rotation dates of poultry production (Lindley and Whitaker, 1996; Matzarakis and Balafoutis, 2004).

Annual rotation	Dates	Number of days
Production Season 1	1 January - 11 February	42
Closed	12 February - 23 February	12
Production Season 2	24 February - 6 April	42
Closed	7 April - 18 April	12
Production Season 3	19 April - 30 May	42
Closed	31 May - 11 June	12
Production Season 4	12 June - 23 July	42
Closed	24 July - 4 August	12
Production Season 5	5 August - 15 September	42
Closed	16 September - 27 September	12
Production Season 6	28 September - 8 November	42
Closed	9 November - 20 November	12
Production Season 7	21 November - 31 December	42

Table 2. Basic temperatures according to weeks (Lindley and Whitaker, 1996; Matzarakis and Balafoutis, 2004).

Time	T _{base} (°C)
First week	31.00
Second week	29.00
Third week	25.00
Fourth week	23.50
Fifth week	22.50
Sixth Week	20.50

2.2. Optimum Insulation Layer Thickness on Walls and Roofs of Poultry Farms

The optimum insulation layer thicknesses of basic structure components vary according to financial criteria such as degree days, temperature, fuel, type of insulation material, inflation, and interest rates. In this study, the

life cycle cost analysis (LCCA) method covering these criteria was utilized when calculating the optimum insulation layer thicknesses of exterior walls and roofs in poultry houses (Şişman et al., 2007; Bolattürk, 2008).

Table 3 shows the structural properties of exterior walls and roof structure components in poultry farming facilities. Sheathing method, which is the most common and efficient technique for building insulation, was used on the exterior walls to surround the outer shell of the building, fully insulating the columns and beams. Poultry houses are mostly constructed using the cradle roof. It is important for the roof not to pour rain and to protect the interior from heat in sunny weather. The roof should be rain-proof and provide good isolation. Sandwich panel was applied as an insulation material on the roofs. Table 4 shows the parameters and economic variables that were used in the computations.

Table 3. Optimum insulated wall and ceiling constructions and U values

Building Component	Thickness (m)	Thermal Conductivity (W/mK)
Walls		
Interior plaster	0.02	0.87
Hollow brick	0.19	0.45
Insulation (XPS, EPS)	x_{opt}	0.032 - 0.035
Exterior plaster	0.03	1.4
$U = 1/(R_{ins}+0.637)$		
Roofs		
Roof construction	-	-
Roof covering (Particle board)	0.011	0.205
Waterproofing	0.002	0.19
Roof cover profile	-	-
Roof cover (Sandwich panel)	x_{opt}	0.023
$U = 1/(R_{ins}+0.329)$		

Table 4. Data and financial values (Anonymous, 2022a; Anonymous, 2022b; Anonymous, 2022c)

Fuel	Cost
Naturalgas	
$H_u=34.542 \times 10^6$ J/kg, $\eta=93\%$	0.2868 \$/kg
Coal	
$H_u=25.122 \times 10^6$ J/kg, $\eta=65\%$	0.1921 \$/kg
LPG	
46.442×10^6 J/kg, $\eta=88\%$	1.75 \$/kg
Fuel-Oil	
41.317×10^6 J/kg $\eta=80\%$	0.73 \$/kg
Geothermal energy	
36.000×10^6 J/kg $\eta=98\%$	0.4482 \$/kg
Electricity	
2.5 (COP)	0.1252 \$/kWh
Insulation material	Cost
Extruded polystyrene (XPS)	
($\lambda=0.032$ W/mK)	85 \$/m ³
Expanded polystyrene (EPS)	
($\lambda=0.035$ W/mK)	50 \$/m ³
Roof cover (Sandwich panel)	
($\lambda=0.023$ W/mK)	275 \$/m ³
Financial values	
Life (N)	10 years
PWF	8.11

2.3. Calculating the Heat Load

In buildings, heat losses are encountered either by heat transfer from the building's structural components or by leakage through doors and windows. The total heat transfer coefficient (U) of building components can be calculated as follows, considering the resistances and physical properties of the different layers of the structural component (equation 3);

$$U = \frac{1}{R_i + R_{sc} + R_{ins} + R_o} \quad (3)$$

where R_i and R_o represent the thermal resistances of the inner and outer surfaces, successively, R_{sc} is the total thermal resistance value of the uninsulated building component layers, and R_{ins} is the thermal resistance value of the insulation layer (equation 4).

$$R_{ins} = \frac{x}{\lambda} \quad (4)$$

In the equation, x (m) and λ (W/mK) are the thickness and thermal conductivity of the insulation material, respectively. If R_{sct} is the total heat resistance of the uninsulated building component, Eq (3) can be adjusted as follows (equation 5):

$$U = \frac{1}{R_{sct} + R_{ins}} \quad (5)$$

The unit surface heat loss of the building component is as follows (equation 6):

$$q = U\Delta T \quad (6)$$

Here, ΔT shows the difference between the fixed indoor

temperature and the changing temperature outside throughout the day. The heat loss per unit area in a year due to the degree-day values of the building component is as follows (equation 7):

$$q_A = 86400 \text{ DDU} \quad (7)$$

Here, DD is the degree-day value. In this case, the annual energy requirement for heating (E_A) and annual fuel consumption are as follows (equations 8 and 9).

$$E_A = \frac{86400 \text{ DD}}{\left(R_{sct} + \frac{x}{\lambda}\right) \eta_s} \quad (8)$$

$$m_{fA} = \frac{86400 \text{ DD}}{\left(R_{sct} + \frac{x}{\lambda}\right) H_u \eta_s} \quad (9)$$

The annual heating and cooling cost per unit area is shown below (equations 10 and 11).

$$C_{A,H} = \frac{86400 \text{ HDD} C_f}{\left(R_{sct} + \frac{x}{\lambda}\right) H_u \eta_s} \quad (10)$$

$$C_{A,C} = \frac{86400 \text{ CDD} C_f}{\left(R_{sct} + \frac{x}{\lambda}\right) \text{COP}} \quad (11)$$

In the equation, C_f (\$/kg) and H_u (J/kg; J/m³) refer to fuel cost and the lower heating value of the fuel, respectively. The value of the coefficient of performance (COP) for the cooling system was presumed to be equal to 2.5 (Bolattürk, 2008).

2.4. Optimum Insulation Layer Thickness Calculation

The LCCA technique was used to calculate the optimum insulation layer thickness values in this study. The total heating cost is calculated considering the life cycle and present worth factor (PWF) of N years. The present worth factor (PWF), which is found according to the inflation rate g and the interest rate i can be expressed as shown in the following (equation 12):

$$\begin{aligned} & i > g \text{ then,} \\ & r = \frac{i - g}{1 + g} \\ & i < g \text{ then,} \\ & r = \frac{g - i}{1 + i} \\ & \text{PWF} = \frac{(1 + r)^N - 1}{r(1 + r)^N} \end{aligned} \quad (12)$$

By considering the life cycle cost analysis (LCCA) of all system-related expenses, the total heating cost of the insulated building can be expressed as follows (equations 13 and 14):

$$C_t = C_A \text{PWF} + C_i x \quad (13)$$

or

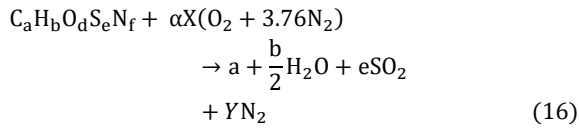
$$C_t = \frac{86400 \text{ HDD} C_f \text{PWF}}{\left(R_{sct} + \frac{x}{\lambda}\right) H_u \eta_s} + C_i x \quad (14)$$

In the equation, C_i (\$/m³) and x (m) refer to insulation material cost and insulation thickness, respectively. The optimum insulation layer thickness x_{opt} is found by the minimization of equation 15).

$$X_{opt} = 293.94 \left(\frac{DD C_f P W F \lambda}{H_u C_f \eta_s} \right)^{1/2} - \lambda R_{sct} \quad (15)$$

2.5.Environmental Analysis

The general chemical formula for combustion in fuels can be written as follows (equation 16).



X and Y can be calculated using the equilibrium formula for oxygen as shown below (equations 17 and 18):

$$X = a + \frac{b}{4} + e - \frac{d}{2} \quad (17)$$

$$Y = 3.76\alpha \left(a + \frac{b}{4} + e - \frac{d}{2} \right) + \frac{f}{2} \quad (18)$$

Equation 16) neglects CO and NOx emissions. The CO₂ emission value caused by the combustion of 1 kg of fuel can be determined as follows (equation 19):

$$M_{CO_2} = \frac{kCO_2}{M} \equiv kgCO_2/kgfuel \quad (19)$$

The total CO₂ emission can be calculated as shown below (equations 20 and 21).

$$M_{CO_2} = \frac{44a}{M} m_{fA} \quad (20)$$

$$M_{CO_2} = \frac{3801600 DD a}{M \eta_s H_u} \left(\frac{\lambda}{\lambda R_{wt} + x} \right) kg/year \quad (21)$$

The molar weight of the fuel, which is denoted by M, can be found using the equation below (equation 22):

$$M = 12a + b + 16d + 32e + 14f kg/kmol \quad (22)$$

3. Results and Discussion

More than half (56.4%) of poultry farming facilities in Türkiye are located in five provinces. Manisa and Sakarya have the highest number of facilities with a share of 12.6%, followed by Balıkesir (11.6%), Bolu (10.8%) and Mersin (8.7%). Figure 1 shows the all provinces with poultry farming facilities in Türkiye.

The present study calculated the optimum insulation layer thickness, energy saving values, and payback period for exterior walls and roofs of poultry farming facilities in Türkiye. For each region, values of heating and cooling degree days were calculated to provide an internal environment in accordance with broiler breeding. Table 5 presents the calculated HDD and CDD numbers. Figure 2 graphically shows the HDD and CDD according to the equilibrium temperatures in all cities.

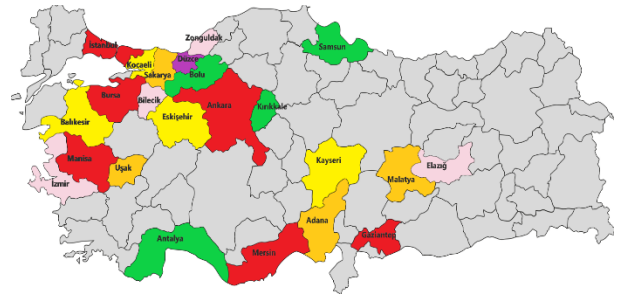


Figure 1. Cities where broilers are produced in Türkiye.

Table 5. HDD and CDD values for cities with poultry buildings in Türkiye

City	HDD	CDD	City	HDD	CDD
Adana	1871	416	İzmir	2089	343
Ankara	3485	89	Kayseri	3936	34
Antalya	1786	387	Kocaeli	2686	94
Balıkesir	3040	108	Malatya	3201	279
Bilecik	3436	27	Manisa	2504	320
Bolu	4146	2	Sakarya	2732	82
Bursa	2851	116	Samsun	2768	88
Elazığ	3318	238	Uşak	3455	66
Eskişehir	3686	25	Zonguldak	2950	30
Gaziantep	2808	350	Kırıkale	3366	120
Mersin	1680	420	Düzce	3096	38
İstanbul	2716	118			

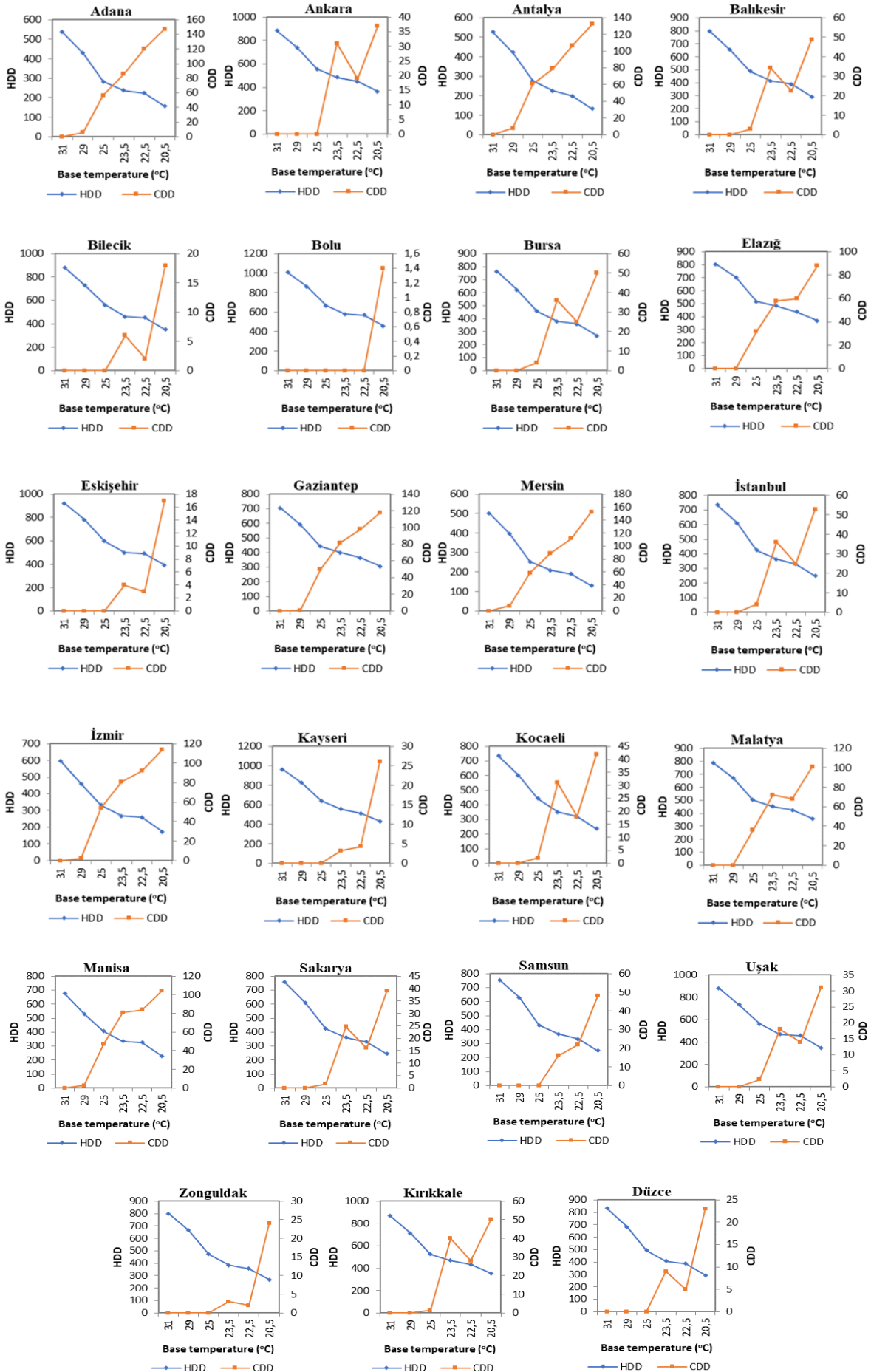


Figure 2. HDD and CDD values according to the equilibrium temperatures in all cities.

Tables 6, 7 and 8 show the values recorded at the optimum point for all provinces and the extent of energy savings and payback period calculated from the unit area in case of optimum insulation layer thickness with various insulation materials and fuel types on the exterior walls and roofs. Tables 6 and 7 present the values when XPS and EPS are used on the exterior walls, respectively; and Table 8 gives the values when sandwich panel is used on the roofs. The optimum insulation layer thickness varied according to varying types of fuel and insulation materials. As expected, the greatest amounts of savings and the shortest payback period in all tables were obtained for the same situation. In the tables, calculations for geothermal energy were done for provinces where there are geothermal resources suitable for heating. The highest savings amount was obtained in Bolu, which is the 4th province of Türkiye with the highest number of poultry farming facility. The lowest savings amount was obtained in Mersin, which is the 5th province of Türkiye with the highest number of poultry farming facility. The highest savings amount and the shortest payback period were obtained when EPS and LPG were used for heating, while the lowest savings amount and the longest payback period were obtained when XPS and natural gas used for heating. In addition, the highest savings amount and the shortest payback period were obtained when EPS insulation material was used for cooling. The payback period was found to be over 10 years for some provinces. In general, the order of savings by fuels was found to be LPG, fuel oil, geothermal energy, coal, and natural gas. Although geothermal energy was determined to be third in this order, it provides more advantages compared to other fuels in terms of the environmental dimension.

In case of heating in Manisa, Sakarya, Balıkesir, Bolu and Mersin, which are the first 5 provinces in Türkiye with the highest number of poultry farming facility, climatic conditions using natural gas fuel and XPS insulation materials on the walls, the optimum thickness values for the insulation materials were obtained as 0.056, 0.060, 0.064, 0.078 and 0.043 m, respectively. For the scenario of the usage of natural gas fuel and EPS on the walls for heating in the same provinces, the optimum insulation layer thickness results were obtained as 0.080, 0.090, 0.090, 0.110 and 0.060 m, respectively. When the case of the usage of natural gas fuel and sandwich panel on the roof in the same provinces was considered, the optimum insulation layer thicknesses were obtained as 0.029, 0.032, 0.039 and 0.022 m, respectively.

Figures 3, 4 and 5 show the effects of annual savings and payback periods on insulation thickness for varying energy resources (natural gas, coal, LPG, fuel oil and geothermal energy) in case of using XPS and EPS on the exterior walls and sandwich panels on the roof for different HDDs. When the fuels were compared, the highest amount of savings and the shortest payback period were obtained in case of using LPG due to its high cost.

Carbon dioxide has the highest greenhouse effect among gases. Fossil fuels are the most important source of carbon dioxide. It is important and necessary to apply optimum insulation layer thickness in buildings in reducing fuel consumption and emission values. Moreover, today, using clean and renewable energy resources such as geothermal energy and increasing the use of these resources is not a matter of preference but a necessity in terms of not creating irreversible environmental problems. Tables 9-11 present the fuel consumption and CO₂ emissions for all provinces with poultry farming facilities using optimum thickness insulation materials. Among the provinces, Bolu and Mersin had the highest and lowest fuel consumption and CO₂ emission values, respectively.

In case of using XPS insulation material on the walls, CO₂ emission amounts varied between 10.81-16.79 kg/m²-year for coal, 6.13-9.60 kg/m²-year for natural gas, 4.63-7.24 kg/m²-year for fuel oil and 2.51-3.93 kg/m²-year for LPG (Table 9). In case of using EPS insulation material on the walls, CO₂ emission amounts varied between 8.58-13.50 kg/m²-year for coal, 4.90-4.69 kg/m²-year for natural gas, 3.71-5.83 kg/m²-year for fuel oil and 2.01-3.16 kg/m²-year for LPG (Table 10). In case of using sandwich panel insulation material on the roof, CO₂ emission amounts varied between 16.52-25.60 kg/m²-year for coal, 9.30-14.58 kg/m²-year for natural gas, 7.04-11.15 kg/m²-year for fuel oil and 3.83-6.02 kg/m²-year for LPG (Table 11).

Figures 6, 7 and 8 show the annual fuel consumption and CO₂ emission values for heating according to insulation thickness in case of using XPS and EPS on the exterior walls and sandwich panels on the roof for different HDDs. As the insulation thickness rises, both annual consumption of fuel and emissions of CO₂ decline. Although the decline here varies slightly according to the type of insulation material, it becomes horizontal after a point. It has been observed that there can be a reduction of up to 70-80% in CO₂ emissions in case of insulation.

Table 6. Optimum insulation layer thickness, energy saving and payback period for XPS on walls

	Heating												Cooling												
	Natural gas				Coal				LPG				Fuel Oil				Geothermal Energy				Electricity				
	X _{opt} m	S \$/m ²	PP year	X _{opt} m	S \$/m ²	PP year	X _{opt} m	S \$/m ²	PP year	X _{opt} m	S \$/m ²	PP year	X _{opt} m	S \$/m ²	PP year	X _{opt} m	S \$/m ²	PP year	X _{opt} m	S \$/m ²	PP year	X _{opt} m	S \$/m ²	PP year	
Adana	0.046	8.83	2.08	0.056	13.01	1.86	0.125	65.20	1.35	0.084	29.47	1.54	0.059	14.4	1.81	0.042	7.26	2.21							
Ankara	0.070	19.83	1.73	0.084	28.32	1.59	0.178	130.62	1.26	0.122	61.05	1.39	0.088	31.2	1.56	0.008	<0	<0							
Antalya	0.044	8.25	2.13	0.054	12.20	1.90	0.122	61.76	1.36	0.082	27.80	1.56	-	-	-	0.040	6.51	2.30							
Balıkesir	0.064	16.80	1.78	0.077	24.10	1.63	0.165	112.58	1.27	0.113	52.34	1.41	0.081	26.5	1.60	0.011	<0	<0							
Bilecik	0.070	19.49	1.73	0.083	27.85	1.60	0.177	128.63	1.26	0.121	60.09	1.39	0.087	30.6	1.57	<0	<0	<0							
Bolu	0.078	24.33	1.67	0.093	34.59	1.55	0.196	157.40	1.24	0.135	73.98	1.36	0.098	38.0	1.52	<0	<0	<0							
Bursa	0.062	15.51	1.81	0.074	22.30	1.66	0.159	104.92	1.28	0.109	48.64	1.42	0.077	24.6	1.62	0.012	<0	<0							
Elazığ	0.068	18.69	1.74	0.081	26.73	1.61	0.173	123.85	1.26	0.119	57.78	1.40	0.085	29.4	1.57	0.027	2.64	3.49							
Eskişehir	0.073	21.20	1.71	0.087	30.22	1.58	0.184	138.76	1.25	0.126	64.98	1.38	0.091	33.2	1.55	<0	<0	<0							
Gaziantep	0.061	15.22	1.81	0.073	21.89	1.66	0.158	103.18	1.28	0.108	47.80	1.43	-	-	-	0.037	5.55	2.44							
Mersin	0.043	7.53	2.19	0.052	11.19	1.94	0.117	57.46	1.38	0.079	25.73	1.59	-	-	-	0.042	7.37	2.20							
İstanbul	0.060	14.59	1.83	0.071	21.02	1.67	0.155	99.45	1.29	0.105	46.00	1.44	-	-	-	0.013	<0	<0							
İzmir	0.050	10.32	1.99	0.060	15.07	1.79	0.133	74.04	1.33	0.090	33.73	1.51	0.063	16.7	1.75	0.036	5.37	2.47							
Kayseri	0.076	22.90	1.69	0.090	32.60	1.56	0.190	148.89	1.25	0.131	69.87	1.37	0.094	35.8	1.53	<0	<0	<0							
Kocaeli	0.059	14.38	1.84	0.071	20.74	1.68	0.154	98.23	1.29	0.105	45.41	1.44	0.075	22.9	1.64	0.009	<0	<0							
Malatya	0.066	17.89	1.76	0.079	25.62	1.62	0.170	119.11	1.27	0.116	55.49	1.40	-	-	-	0.030	3.70	2.91							
Manisa	0.056	13.14	1.87	0.068	19.01	1.71	0.148	90.86	1.30	0.100	41.85	1.45	0.071	21.0	1.67	0.034	4.77	2.59							
Sakarya	0.060	14.70	1.83	0.072	21.17	1.67	0.155	100.10	1.29	0.106	46.31	1.43	0.075	23.3	1.63	0.007	<0	<0							
Samsun	0.060	14.94	1.82	0.072	21.52	1.67	0.156	101.56	1.28	0.107	47.02	1.43	0.076	23.7	1.63	0.008	<0	<0							
Uşak	0.070	19.62	1.73	0.083	28.03	1.60	0.177	129.40	1.26	0.122	60.46	1.39	0.087	30.8	1.56	0.004	<0	<0							
Zonguldak	0.063	16.18	1.79	0.075	23.24	1.64	0.162	108.93	1.28	0.111	50.58	1.42	-	-	-	<0	<0	<0							
Kırıkkale	0.069	19.02	1.74	0.082	27.19	1.60	0.175	125.79	1.26	0.120	58.72	1.39	-	-	-	0.013	<0	<0							
Düzce	0.065	17.18	1.77	0.078	24.63	1.63	0.167	114.85	1.27	0.114	53.44	1.41	-	-	-	<0	<0	<0							

Table 7. Optimum insulation layer thickness, energy saving and payback period for EPS on walls

	Heating												Cooling												
	Natural gas				Coal				LPG				Fuel Oil			Geothermal Energy			Electricity						
	X _{opt} m	S \$/m ²	pp year	X _{opt} m	S \$/m ²	pp year	X _{opt} m	S \$/m ²	pp year	X _{opt} m	S \$/m ²	pp year	X _{opt} m	S \$/m ²	pp year	X _{opt} m	S \$/m ²	pp year	X _{opt} m	S \$/m ²	pp year				
Adana	0.024	15.06	1.89	0.028	21.81	1.72	0.061	135.04	1.26	0.042	63.03	1.40	0.030	24.11	1.68	0.022	17.12	1.82	0.022	17.12	1.68	0.022	17.12	1.82	
Ankara	0.035	33.67	1.57	0.041	47.35	1.48	0.086	265.99	1.19	0.060	127.28	1.29	0.043	51.96	1.45	0.006	<0	<0	0.006	<0	0.006	1.45	0.006	<0	<0
Antalya	0.023	14.08	1.93	0.028	20.46	1.75	0.059	128.14	1.27	0.041	59.65	1.41	-	-	-	0.021	15.51	1.87	0.021	15.51	-	0.021	15.51	1.87	
Balıkesir	0.032	28.54	1.62	0.038	40.31	1.51	0.080	229.88	1.21	0.055	109.57	1.31	0.040	44.28	1.49	0.007	0.03	320.48	0.007	0.03	1.49	0.007	0.03	320.48	
Bilecik	0.035	33.11	1.58	0.041	46.57	1.48	0.085	262.01	1.20	0.059	125.33	1.29	0.043	51.12	1.46	0.000	<0	<0	0.000	<0	1.46	0.000	<0	<0	<0
Bolu	0.039	41.30	1.53	0.046	57.81	1.44	0.094	319.62	1.18	0.066	153.59	1.27	0.048	63.37	1.42	<0	<0	<0	<0	<0	1.42	<0	<0	<0	<0
Bursa	0.031	26.36	1.65	0.037	37.31	1.53	0.077	214.55	1.21	0.053	102.04	1.31	0.039	41.02	1.50	0.008	0.47	18.50	0.008	0.47	1.50	0.008	0.47	18.50	
Elaçlı	0.034	31.75	1.59	0.040	44.70	1.49	0.084	252.44	1.20	0.058	120.63	1.29	0.042	49.08	1.46	0.015	7.24	2.46	0.015	7.24	1.46	0.015	7.24	2.46	
Eskişehir	0.036	35.99	1.56	0.043	50.53	1.46	0.089	282.30	1.19	0.062	135.28	1.28	0.045	55.43	1.44	0.000	<0	<0	0.000	<0	1.44	0.000	<0	<0	<0
Gaziantep	0.031	25.86	1.65	0.036	36.63	1.54	0.076	211.06	1.21	0.053	100.33	1.32	-	-	-	0.019	13.46	1.95	0.019	13.46	-	0.019	13.46	1.95	
Mersin	0.022	12.85	1.99	0.026	18.79	1.79	0.057	119.54	1.28	0.039	55.43	1.43	-	-	-	0.022	17.34	1.81	0.022	17.34	-	0.022	17.34	1.81	
İstanbul	0.030	24.80	1.67	0.036	35.18	1.55	0.075	203.60	1.22	0.052	96.67	1.32	-	-	-	0.008	0.58	15.22	0.008	0.58	-	0.008	0.58	15.22	
İzmir	0.025	17.57	1.81	0.030	25.26	1.66	0.065	152.73	1.25	0.044	71.71	1.37	0.032	27.87	1.62	0.019	13.07	1.96	0.019	13.07	1.62	0.019	13.07	1.96	
Kayseri	0.038	38.87	1.54	0.045	54.48	1.45	0.092	302.58	1.19	0.064	145.23	1.27	0.047	59.75	1.43	0.001	<0	<0	0.001	<0	1.43	0.001	<0	<0	<0
Kocaeli	0.030	24.46	1.67	0.035	34.70	1.55	0.075	201.16	1.22	0.051	95.47	1.32	0.037	38.17	1.52	0.006	<0	<0	0.006	<0	1.52	0.006	<0	<0	<0
Malatya	0.033	30.40	1.60	0.039	42.85	1.50	0.082	242.95	1.20	0.057	115.98	1.30	-	-	-	0.016	9.52	2.19	0.016	9.52	-	0.016	9.52	2.19	
Manisa	0.029	22.36	1.70	0.034	31.82	1.58	0.072	186.40	1.23	0.049	88.23	1.34	0.036	35.03	1.55	0.018	11.79	2.03	0.018	11.79	1.55	0.018	11.79	2.03	
Sakarya	0.030	24.99	1.66	0.036	35.43	1.55	0.075	204.90	1.22	0.052	97.30	1.32	0.038	38.97	1.52	0.005	<0	<0	0.005	<0	1.52	0.005	<0	<0	<0
Samsun	0.030	25.40	1.66	0.036	36.00	1.54	0.076	207.82	1.21	0.052	98.74	1.32	0.038	39.59	1.51	0.006	<0	<0	0.006	<0	1.51	0.006	<0	<0	<0
Uşak	0.035	33.33	1.58	0.041	46.87	1.48	0.086	263.56	1.20	0.059	126.09	1.29	0.043	51.45	1.45	0.004	<0	<0	0.004	<0	1.45	0.004	<0	<0	<0
Zonguldak	0.032	27.50	1.63	0.038	38.88	1.52	0.078	222.58	1.21	0.054	105.98	1.31	-	-	-	0.000	<0	<0	0.000	<0	-	0.000	<0	<0	<0
Kırıkkale	0.034	32.30	1.59	0.041	45.46	1.48	0.084	256.33	1.20	0.058	122.54	1.29	-	-	-	0.008	0.69	12.99	0.008	0.69	-	0.008	0.69	12.99	
Düzce	0.033	29.19	1.61	0.039	41.19	1.51	0.081	234.43	1.20	0.056	111.80	1.30	-	-	-	0.001	<0	<0	0.001	<0	-	0.001	<0	<0	<0

Table 8. Optimum insulation layer thickness, energy saving and payback period for SP on roofs

	Heating												Cooling													
	Natural gas				Coal				LPG				Fuel Oil				Geothermal Energy				Electricity					
	x_{opt} m	S \$/m ²	pp year	x_{opt} m	S \$/m ²	pp year	x_{opt} m	S \$/m ²	pp year	x_{opt} m	S \$/m ²	pp year	x_{opt} m	S \$/m ²	pp year	x_{opt} m	S \$/m ²	pp year	x_{opt} m	S \$/m ²	pp year	x_{opt} m	S \$/m ²	pp year		
Adana	0.024	15.06	1.89	0.028	21.81	1.72	0.061	135.04	1.26	0.042	63.03	1.40	0.030	24.11	1.68	0.022	17.12	1.82								
Ankara	0.035	33.67	1.57	0.041	47.35	1.48	0.086	265.99	1.19	0.060	127.28	1.29	0.043	51.96	1.45	0.006	<0	<0								
Antalya	0.023	14.08	1.93	0.028	20.46	1.75	0.059	128.14	1.27	0.041	59.65	1.41	-	-	-	0.021	15.51	1.87								
Balıkesir	0.032	28.54	1.62	0.038	40.31	1.51	0.080	229.88	1.21	0.055	109.57	1.31	0.040	44.28	1.49	0.007	0.03	320.48								
Bilecik	0.035	33.11	1.58	0.041	46.57	1.48	0.085	262.01	1.20	0.059	125.33	1.29	0.043	51.12	1.46	0.000	<0	<0								
Bolu	0.039	41.30	1.53	0.046	57.81	1.44	0.094	319.62	1.18	0.066	153.59	1.27	0.048	63.37	1.42	<0	<0	<0								
Bursa	0.031	26.36	1.65	0.037	37.31	1.53	0.077	214.55	1.21	0.053	102.04	1.31	0.039	41.02	1.50	0.008	0.47	18.50								
Elaçlı	0.034	31.75	1.59	0.040	44.70	1.49	0.084	252.44	1.20	0.058	120.63	1.29	0.042	49.08	1.46	0.015	7.24	2.46								
Eskişehir	0.036	35.99	1.56	0.043	50.53	1.46	0.089	282.30	1.19	0.062	135.28	1.28	0.045	55.43	1.44	0.000	<0	<0								
Gaziantep	0.031	25.86	1.65	0.036	36.63	1.54	0.076	211.06	1.21	0.053	100.33	1.32	-	-	-	0.019	13.46	1.95								
Mersin	0.022	12.85	1.99	0.026	18.79	1.79	0.057	119.54	1.28	0.039	55.43	1.43	-	-	-	0.022	17.34	1.81								
İstanbul	0.030	24.80	1.67	0.036	35.18	1.55	0.075	203.60	1.22	0.052	96.67	1.32	-	-	-	0.008	0.58	15.22								
İzmir	0.025	17.57	1.81	0.030	25.26	1.66	0.065	152.73	1.25	0.044	71.71	1.37	0.032	27.87	1.62	0.019	13.07	1.96								
Kayseri	0.038	38.87	1.54	0.045	54.48	1.45	0.092	302.58	1.19	0.064	145.23	1.27	0.047	59.75	1.43	0.001	<0	<0								
Kocaeli	0.030	24.46	1.67	0.035	34.70	1.55	0.075	201.16	1.22	0.051	95.47	1.32	0.037	38.17	1.52	0.006	<0	<0								
Malatya	0.033	30.40	1.60	0.039	42.85	1.50	0.082	242.95	1.20	0.057	115.98	1.30	-	-	-	0.016	9.52	2.19								
Manisa	0.029	22.36	1.70	0.034	31.82	1.58	0.072	186.40	1.23	0.049	88.23	1.34	0.036	35.03	1.55	0.018	11.79	2.03								
Sakarya	0.030	24.99	1.66	0.036	35.43	1.55	0.075	204.90	1.22	0.052	97.30	1.32	0.038	38.97	1.52	0.005	<0	<0								
Samsun	0.030	25.40	1.66	0.036	36.00	1.54	0.076	207.82	1.21	0.052	98.74	1.32	0.038	39.59	1.51	0.006	<0	<0								
Uşak	0.035	33.33	1.58	0.041	46.87	1.48	0.086	263.56	1.20	0.059	126.09	1.29	0.043	51.45	1.45	0.004	<0	<0								
Zonguldak	0.032	27.50	1.63	0.038	38.88	1.52	0.078	222.58	1.21	0.054	105.98	1.31	-	-	-	0.000	<0	<0								
Kırıkkale	0.034	32.30	1.59	0.041	45.46	1.48	0.084	256.33	1.20	0.058	122.54	1.29	-	-	-	0.008	0.69	12.99								
Düzce	0.033	29.19	1.61	0.039	41.19	1.51	0.081	234.43	1.20	0.056	111.80	1.30	-	-	-	0.001	<0	<0								

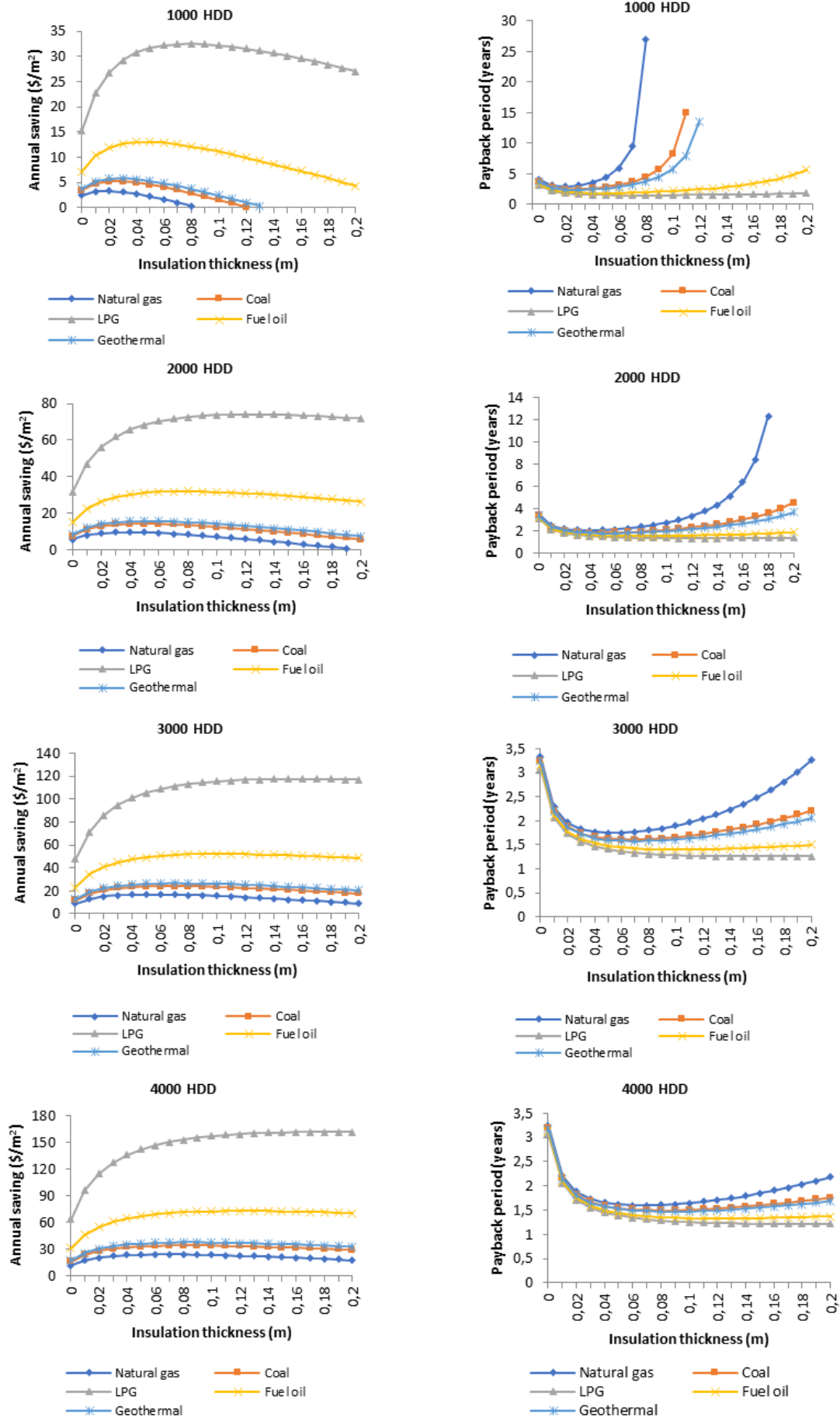


Figure 3. Energy saving and payback period for different HDD in walls (XPS).

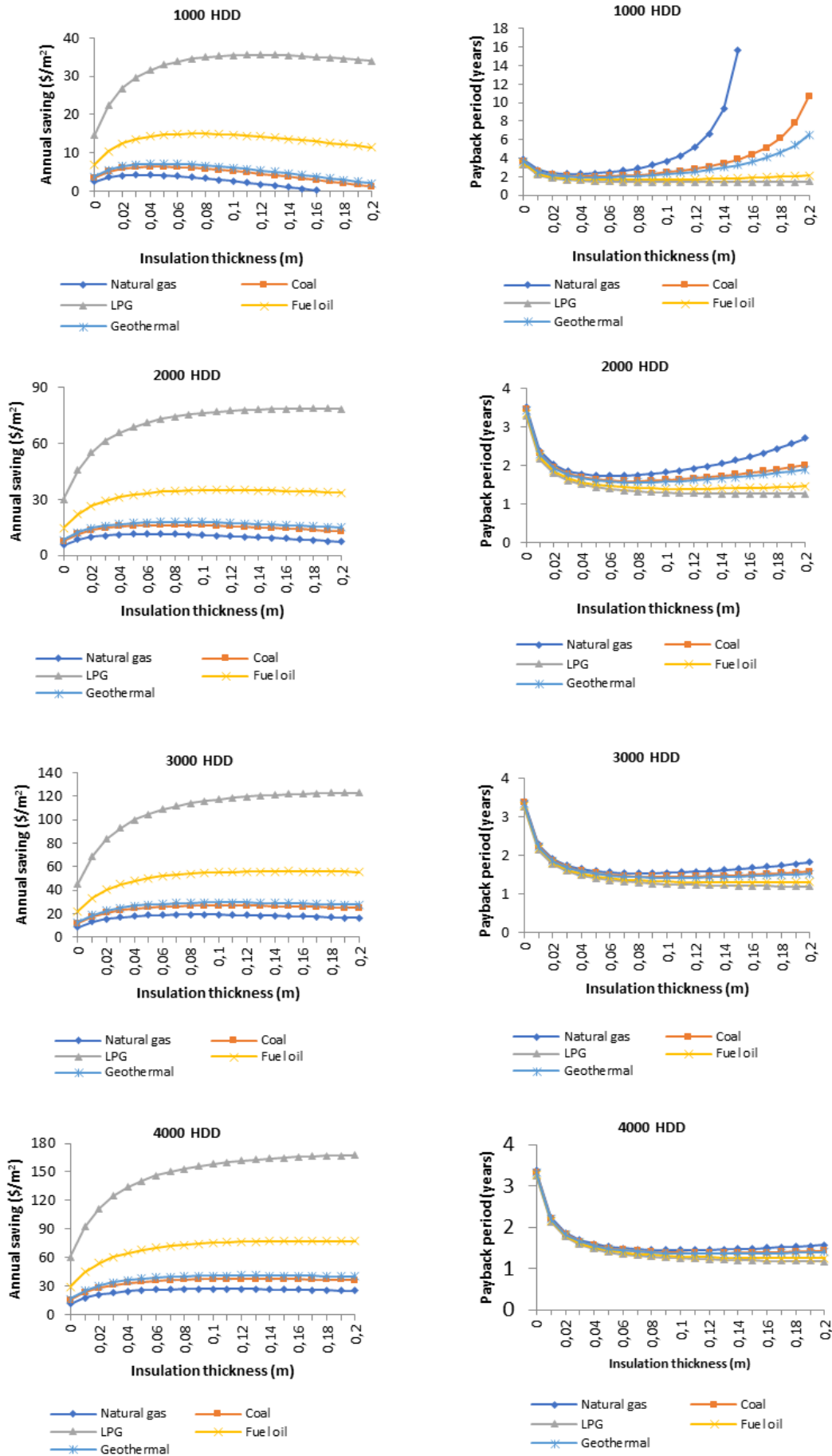


Figure 4. Energy saving and payback period for different HDD in walls (EPS).

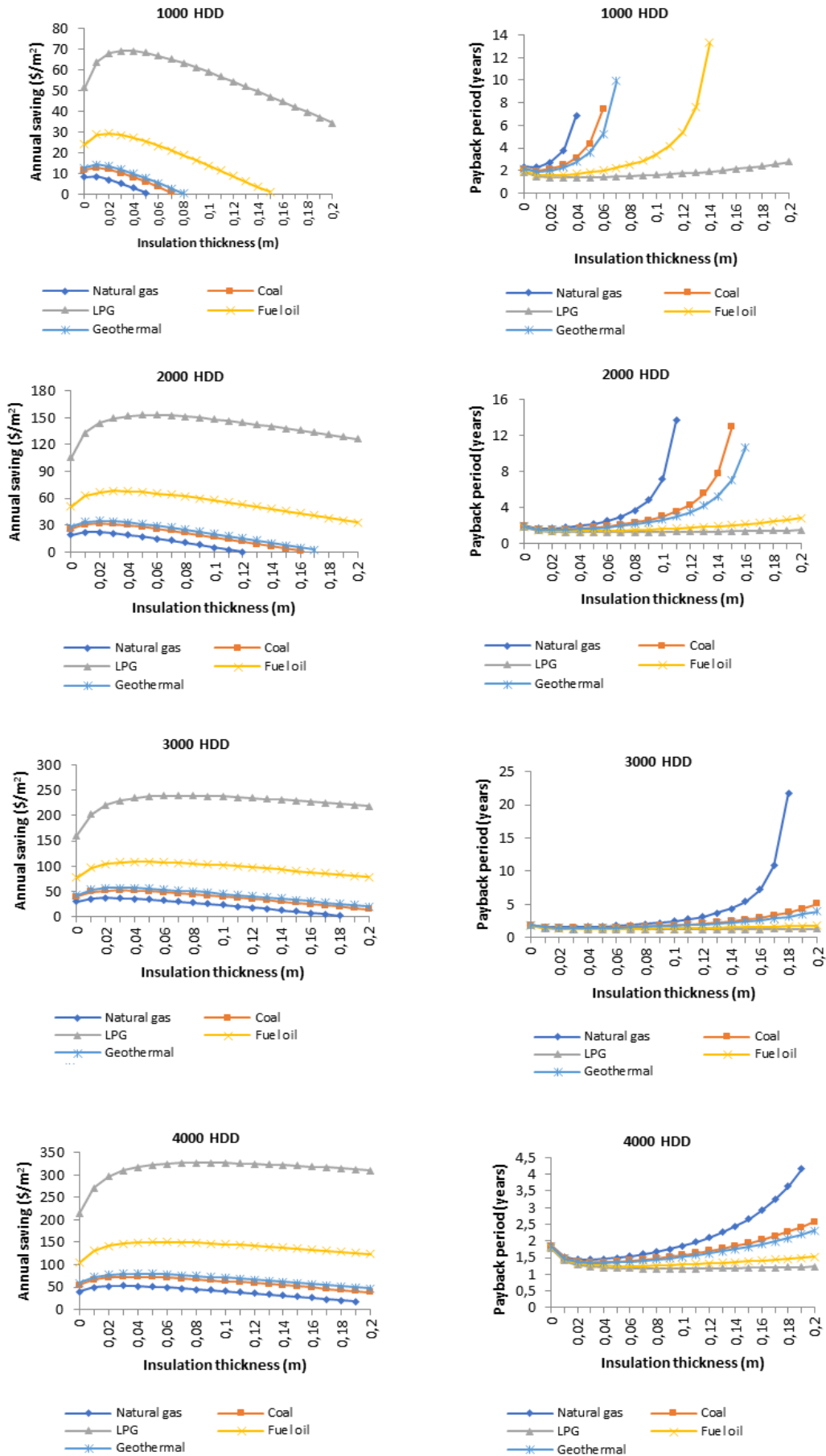


Figure 5. Energy saving and payback period for different HDD in roofs (SP).

Table 9. Fuel consumption and CO₂ amounts for XPS on walls

	Coal		Naturalgas		Fuel-Oil		LPG	
	m _{FA}	M _{CO2}	m _{FA}	M _{CO2}	m _{FA}	M _{CO2}	m _{FA}	M _{CO2}
	(kg/m ² year)	(kg/m ² year)	(kg/m ² year)	(kg/m ² year)	(kg/m ² year)	(kg/m ² year)	(kg/m ² year)	(kg/m ² year)
Adana	4.20	11.40	2.42	6.42	1.49	4.86	0.87	2.64
Ankara	5.70	15.48	3.31	8.78	2.04	6.64	1.18	3.60
Antalya	4.06	11.03	2.38	6.32	1.47	4.78	0.86	2.61
Balıkesir	5.34	14.49	3.10	8.20	1.92	6.23	1.11	3.38
Bilecik	5.68	15.41	3.30	8.75	2.03	6.60	1.18	3.59
Bolu	6.19	16.79	3.62	9.60	2.23	7.24	1.29	3.93
Bursa	5.16	14.02	3.01	7.98	1.85	6.03	1.07	3.26
Elazığ	5.54	15.03	3.23	8.55	2.00	6.51	1.16	3.52
Eskişehir	5.86	15.91	3.43	9.09	2.10	6.84	1.22	3.72
Gaziantep	5.14	13.96	3.00	7.96	1.84	5.98	1.07	3.24
Mersin	3.98	10.81	2.31	6.13	1.42	4.63	0.82	2.51
İstanbul	5.03	13.65	2.94	7.79	1.81	5.88	1.05	3.19
İzmir	4.40	11.93	2.59	6.86	1.59	5.18	0.92	2.79
Kayseri	6.03	16.38	3.55	9.40	2.17	7.06	1.26	3.84
Kocaeli	5.03	13.65	2.91	7.71	1.80	5.86	1.04	3.18
Malatya	5.45	14.79	3.18	8.44	1.96	6.37	1.14	3.46
Manisa	4.85	13.16	2.82	7.47	1.74	5.65	1.01	3.01
Sakarya	5.06	13.73	2.96	7.84	1.82	5.91	1.05	3.19
Samsun	5.07	13.76	2.96	7.84	1.83	5.95	1.06	3.22
Uşak	5.65	15.35	3.32	8.80	2.04	6.63	1.18	3.59
Zonguldak	5.23	14.20	3.08	8.15	1.89	6.14	1.09	3.32
Kırıkkale	5.62	15.25	3.27	8.67	2.02	6.56	1.17	3.55
Düzce	5.38	14.60	3.12	8.26	1.94	6.30	1.12	3.41

Table 10. Fuel consumption and CO₂ amounts for EPS on walls

	Coal		Naturalgas		Fuel-Oil		LPG	
	m _{FA}	M _{CO2}	m _{FA}	M _{CO2}	m _{FA}	M _{CO2}	m _{FA}	M _{CO2}
	(kg/m ² year)	(kg/m ² year)	(kg/m ² year)	(kg/m ² year)	(kg/m ² year)	(kg/m ² year)	(kg/m ² year)	(kg/m ² year)
Adana	3.35	9.10	1.95	5.16	1.20	3.90	0.70	2.12
Ankara	4.56	12.39	2.66	7.04	1.64	5.32	0.95	2.89
Antalya	3.26	8.85	1.90	5.04	1.18	3.83	0.68	2.07
Balıkesir	4.25	11.54	2.48	6.57	1.53	4.98	0.89	2.70
Bilecik	4.53	12.59	2.64	7.00	1.63	5.30	0.94	2.87
Bolu	4.97	13.50	2.90	7.69	1.79	5.83	1.04	3.16
Bursa	4.14	11.25	2.41	6.38	1.48	4.83	0.86	2.62
Elazığ	4.44	12.05	2.59	6.87	1.60	5.20	0.93	2.82
Eskişehir	4.69	12.74	2.74	7.27	1.69	5.49	0.98	2.98
Gaziantep	4.08	11.08	2.39	6.34	1.47	4.78	0.85	2.60
Mersin	3.16	8.58	1.85	4.90	1.14	3.71	0.66	2.01
İstanbul	4.04	10.97	2.36	6.25	1.45	4.71	0.84	2.55
İzmir	3.53	9.60	2.06	5.46	1.27	4.13	0.73	2.24
Kayseri	4.85	13.15	2.82	7.47	1.74	5.66	1.01	3.07
Kocaeli	4.00	10.85	2.33	6.18	1.44	4.68	0.83	2.54
Malatya	4.38	11.88	2.54	6.74	1.58	5.13	0.91	2.77
Manisa	3.88	10.54	2.26	5.98	1.39	4.52	0.80	2.45
Sakarya	4.03	10.95	2.35	6.22	1.45	4.73	0.84	2.56
Samsun	4.05	11.01	2.38	6.31	1.46	4.77	0.85	2.58
Uşak	4.56	12.37	2.65	7.04	1.63	5.31	0.94	2.88
Zonguldak	4.19	11.37	2.45	6.48	1.51	4.91	0.87	2.66
Kırıkkale	4.47	12.14	2.61	6.91	1.61	5.25	0.97	2.94
Düzce	4.30	11.67	2.50	6.63	1.55	5.04	0.90	2.73

Table 11. Fuel consumption and CO₂ amounts for SP on roofs

	Coal		Naturalgas		Fuel-Oil		LPG	
	m _{FA} (kg/m ² year)	M _{CO2} (kg/m ² year)	m _{FA} (kg/m ² year)	M _{CO2} (kg/m ² year)	m _{FA} (kg/m ² year)	M _{CO2} (kg/m ² year)	m _{FA} (kg/m ² year)	M _{CO2} (kg/m ² year)
Adana	6.40	17.36	3.78	10.02	2.31	7.52	1.34	4.08
Ankara	8.73	23.69	5.06	13.40	3.14	10.22	1.83	5.55
Antalya	6.28	17.05	3.61	9.56	2.25	7.33	1.30	3.95
Balıkesir	8.11	22.02	4.75	12.58	2.92	9.48	1.70	5.18
Bilecik	8.60	23.35	5.11	13.53	3.10	10.07	1.80	5.47
Bolu	9.43	25.60	5.50	14.58	3.43	11.15	1.98	6.02
Bursa	7.96	21.60	4.57	12.10	2.82	9.19	1.63	4.97
Elazığ	8.48	23.03	4.93	13.07	3.08	10.03	1.78	5.40
Eskişehir	9.04	24.55	5.23	13.85	3.23	10.49	1.87	5.69
Gaziantep	7.84	21.28	4.62	12.24	2.83	9.20	1.63	4.95
Mersin	6.09	16.52	3.51	9.30	2.16	7.04	1.26	3.83
İstanbul	7.76	21.06	4.47	11.83	2.78	9.05	1.68	5.10
İzmir	6.76	18.35	3.96	10.50	2.43	7.90	1.41	4.30
Kayseri	9.28	25.20	5.46	14.46	3.35	10.89	1.94	5.89
Kocaeli	7.67	20.83	4.54	12.02	2.75	8.95	1.60	4.85
Malatya	8.36	22.69	4.88	12.92	3.02	9.83	1.73	5.27
Manisa	7.51	20.37	4.35	11.52	2.66	8.64	1.54	4.70
Sakarya	7.81	21.19	4.49	11.90	2.80	9.10	1.60	4.88
Samsun	7.73	20.97	4.55	12.06	2.79	9.07	1.63	4.94
Uşak	8.65	23.48	5.14	13.61	3.12	10.13	1.18	5.50
Zonguldak	8.05	21.85	4.73	12.52	2.88	9.35	1.67	5.08
Kırıkkale	8.61	23.36	5.00	13.26	3.08	10.02	1.78	5.42
Düzce	8.26	26.43	4.84	12.81	2.97	9.66	1.71	5.21

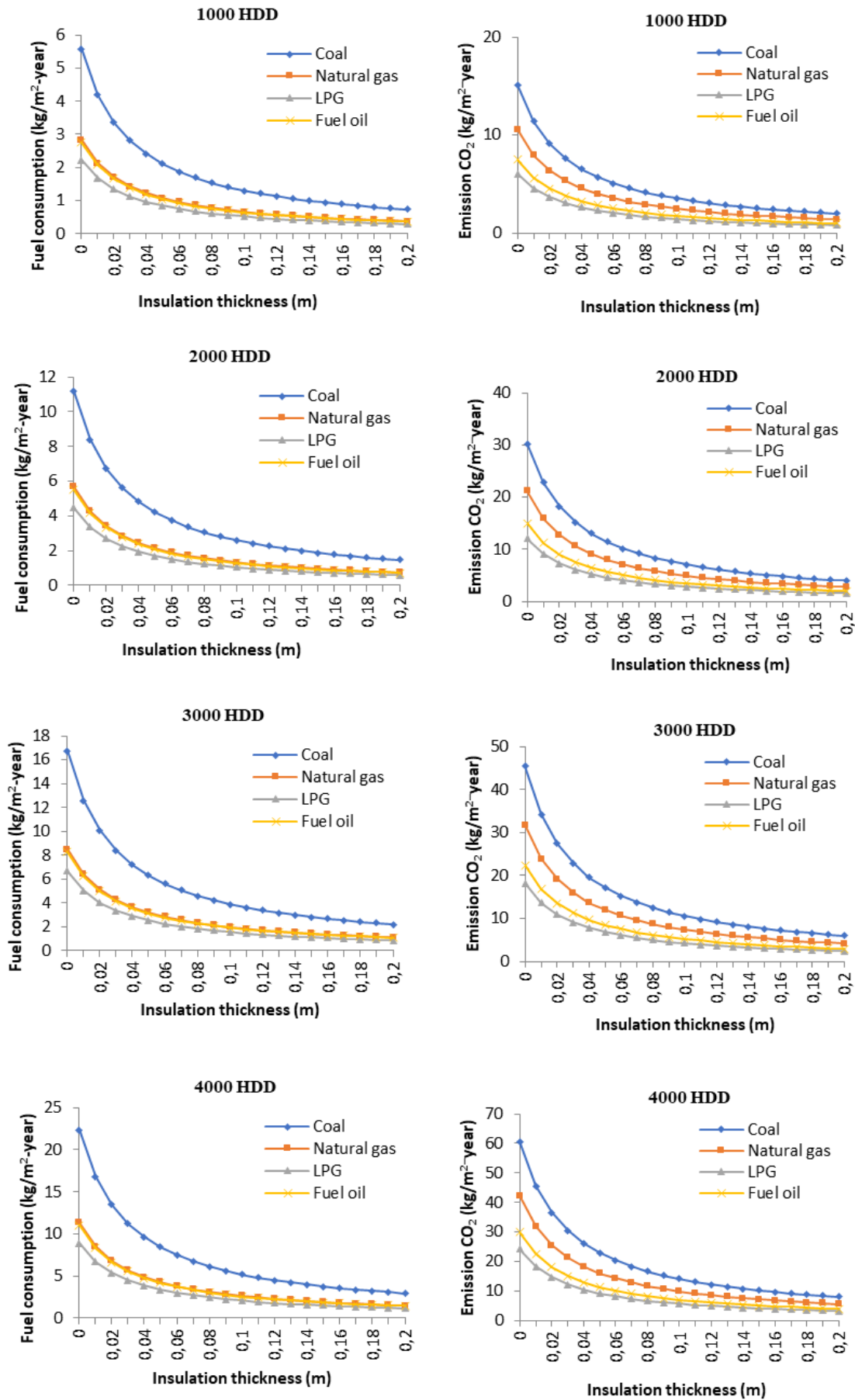


Figure 6. Fuel consumption and CO₂ emissions for different HDD in walls (XPS).

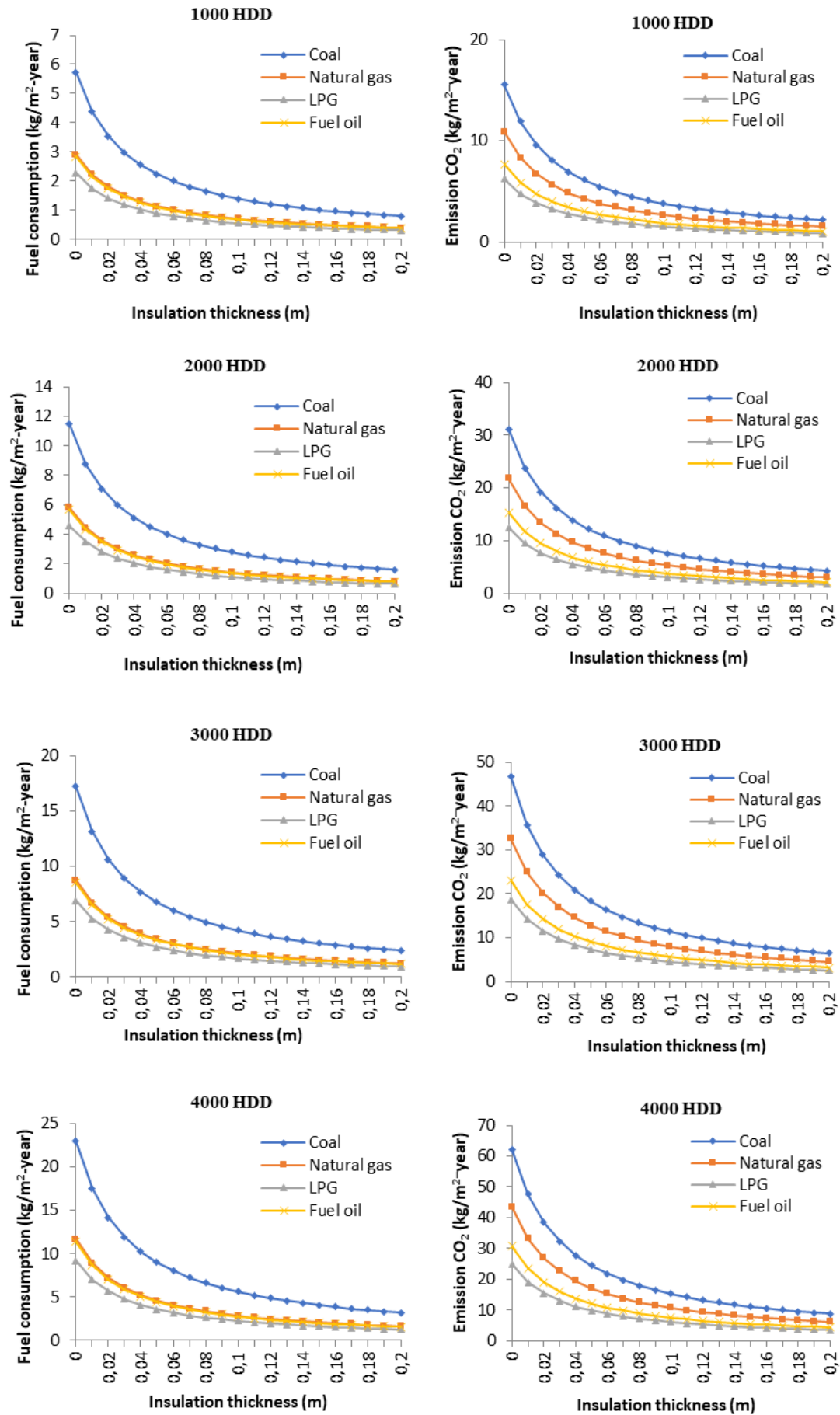


Figure 7. Fuel consumption and CO₂ emissions for different HDD in walls (EPS).

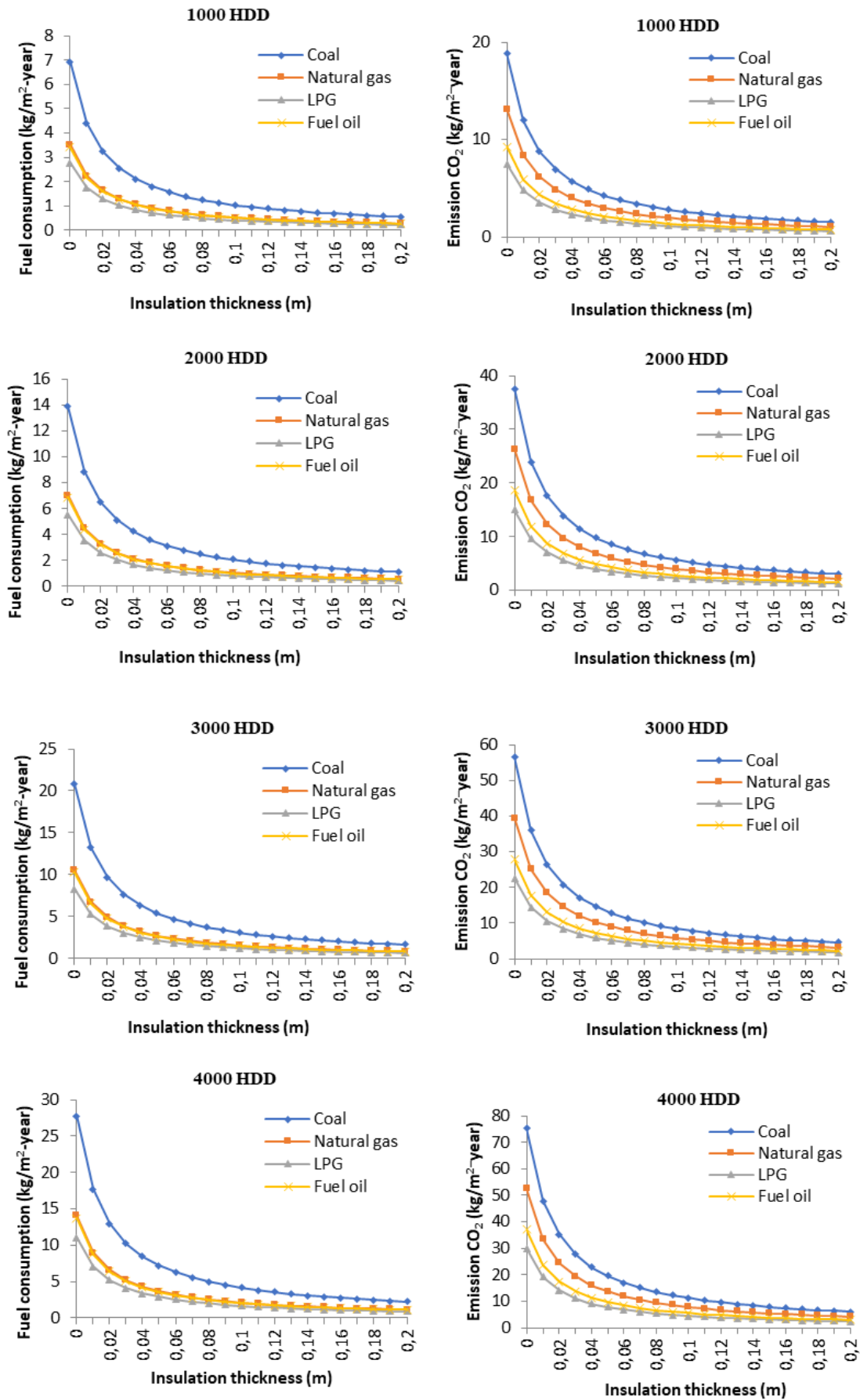


Figure 8. Fuel consumption and CO₂ emissions for different HDD in roofs (SP).

According to the Food and Agriculture Organization of the United Nations (FAO), global poultry meat production was estimated to be 137.8 million tons in 2021 (Gržinić et al., 2023). Türkiye ranks 10th in broiler meat production across the world. Europe produces about 18 million tons of broiler meat. In Europe, Türkiye ranks second in broiler meat production. There are a total of 11,056 enterprises in the poultry farming sector in Türkiye. There are 12,725 commercial poultry houses of these enterprises. It is estimated that the capacity utilization rate in existing enterprises and poultry houses is around 85-90% (Anonymous, 2023b).

Considering the number of poultry farming facilities by provinces in Türkiye, there are 1603 facilities in Manisa (12.6%) and Sakarya (12.6%), 1476 facilities in Balıkesir (11.6%), 1374 facilities in Bolu (10.8%) and 1007 facilities in Mersin (8.7%). In case of applying the optimum insulation layer thickness with XPS on the exterior walls by using natural gas, it was possible to save 13.14 \$/m² in Manisa, 14.70 \$/m² in Sakarya, 16.80 \$/m² in Balıkesir, 24.33 \$/m² in Bolu and 7.53 \$/m² in Mersin. In case of applying the optimum value for the insulation thickness parameter with sandwich panels on the roofs by using natural gas, it was possible to save 22.36 \$/m² in Manisa, 24.99 \$/m² in Sakarya, 28.54 \$/m² in Balıkesir, 41.30 \$/m² in Bolu and \$12.85 \$/m² in Mersin.

Assuming that poultry farming facilities comply with the relevant insulation standards and considering the floor area as 12x50 m and the wall height as 5 m; in Manisa, it was possible to save approximately 13 million dollars by applying exterior wall insulation with XPS, and 21 million dollars by applying sandwich panels on the roofs in all facilities. Considering that these figures are only obtained for just one province with 12.6% of the total facilities, the amount of savings to be achieved in case of applying insulation to poultry farming facilities throughout Türkiye will be very significant. In addition, there will be a significant reduction in CO₂ emissions as well.

4. Conclusions

In Türkiye, energy consumption increases in parallel with the population growth, and it is crucial to evaluate the potential for savings and reduce losses, especially in sectors with high energy consumption, in order to reduce energy expenditures. As is known, costs of heating and cooling are some of the greatest expense items for establishments in the poultry production sector. Thus, energy savings are of critical importance in poultry farming. The use of insulation systems in closed farm areas in recent years in the poultry farming sector also increases production quality and efficiency by providing suitable physical conditions. In this study, the optimum insulation layer thickness, energy savings, and payback period of the exterior walls of poultry farming facilities in the poultry sector in Türkiye were calculated to ensure efficient energy use in poultry farming facilities. The savings in walls and roofs through insulation vary

between 7.53-164.65 \$/m² and 12.85-319.62 \$/m², respectively, and the payback periods range from 1.19-2.19 years to 1.18-1.99 years, respectively. It is estimated that a 70-80% reduction in CO₂ emissions can be achieved in poultry farming facilities in Türkiye by applying the optimum insulation layer thickness.

Author Contributions

The percentage of the author contributions is presented below. The author reviewed and approved the final version of the manuscript.

	A.A.
C	100
D	100
S	100
DCP	100
DAI	100
L	100
W	100
CR	100
SR	100

C=Concept, D= design, S= supervision, DCP= data collection and/or processing, DAI= data analysis and/or interpretation, L= literature search, W= writing, CR= critical review, SR= submission and revision.

Conflict of Interest

The author declared that there is no conflict of interest.

Ethical Consideration

Ethics committee approval was not required for this study because of there was no study on animals or humans.

References

- Açıklalp E, Kandemir SY. 2019. A method for determining optimum insulation thickness: Combined economic and environmental method. *Therm Sci Eng Prog*, 11: 249-253.
- Akolgo GA, Uba F, Opoku R, Tweneboah-Koduah S, Alhassan ARM, Anokye EG, Jedaiah AOA, Nunoo E. 2022. Energy analysis of poultry housing in Ghana using artificial neural networks. *Sci Afr*, 17: 01313.
- Akpınar EK, Demir İH. 2018. Calculation of optimum insulation thickness and Energy savings for different climatic regions of Turkey. *J Sci Technol*, 13(2): 15-22.
- Annibaldi V, Cucchiella F, De Berardinis P, Rotilio M, Stornelli V. 2019. Environmental and economic benefits of optimal insulation thickness: A life-cycle cost analysis. *Renew Sust Energ Rev*, 116: 109441.
- Anonymous. 2022a. <http://www.canakkalegaz.com.tr/turkish> (accessed date: 10 December 2022).
- Anonymous. 2022b. <http://www.dosider.org>, Fuel prices (accessed date: 12 December 2022).
- Anonymous. 2022c. <http://www.izocam.com.tr>, Insulation Unit Prices (accessed date: 10 December 2022).
- Anonymous. 2023a. <https://www.mta.gov.tr> (accessed date:15 October 2023).
- Anonymous. 2023b. <https://arastirma.tarimorman.gov.tr/tepge> (accessed date: 10 October 2023).

- Arıtürk E, Ergün A, Yalçın S. 1986. The Relationship Between Poultry and Environmental Temperature. *Lalahan Zoot Arast Enst Derg*, 26(1-4): 42-52.
- Bolattürk A. 2008. Optimum insulation thicknesses for building walls with respect to cooling and heating degree-hours in the warmest zone of Turkey. *Build Environ*, 43(6): 1055-1064.
- Büyükalaca O, Bulut H, Yılmaz T. 2001. Analysis of variable-base heating and cooling degree-days for Turkey. *Appl Energy*, 69(4): 269-283.
- Christenson M, Manz H, Gyalistras D. 2006. Climate warming impact on degree-days and building energy demand in Switzerland. *Energy Convers Manag*, 47(6): 671-686.
- Dağtekin M. 2012. Tecno-ekonomik feasibility analysis of solar energy use in cooling of broiler poultry houses. *J Agric Fac ÇÜ*, 27(2): 11-20.
- De Rosa M, Bianco V, Scarpa F, Tagliafico LA. 2014. Heating and cooling building energy demand evaluation; a simplified model and a modified degree days approach. *Appl Energy*, 128: 217-229.
- Dombaycı ÖA, Atalay Ö, Acar ŞG, Ulu EY, Öztürk HK. 2017. Thermoeconomic method for determination of optimum insulation thickness of external walls for the houses: Case study for Turkey. *Sustain Energy Technol Assess*, 22: 1-8.
- Eto JH. 1988. On using degree-days to account for the effects of weather on annual energy use in office buildings. *Energy Build*, 12(2): 113-127.
- Gržinić G, Piotrowicz-Cieślak A, Klimkowicz-Pawlas A, Górny RL, Ławniczek-Wałczyk A, Piechowicz L, Olkowska E, Potrykus M, Tankiewicz M, Krupka M, Siebielec G, Wolska L. 2023. Intensive poultry farming: A review of the impact on the environment and human health. *Sci Total Environ*, 858: 160014.
- Hou J, Zhang T, Hou C, Fukuda H. 2022. A study on influencing factors of optimum insulation thickness of exterior walls for rural traditional dwellings in northeast of Sichuan hills, China. *Case Stud Constr Mater*, 16: 01033.
- Kapica J, Pawlak H, Ścibisz M. 2015. Carbon dioxide emission reduction by heating poultry houses from renewable energy sources in Central Europe. *Agric Syst*, 139: 238-249.
- Lindley JA, Whitaker JH. 1996. Agricultural buildings and structures. American Society of Agricultural Engineers (ASAE), USA, pp 636.
- Malka L, Kuriqi A, Haxhimusa A. 2022. Optimum insulation thickness design of exterior walls and overhauling cost to enhance the energy efficiency of Albanian's buildings stock. *J Clean Prod*, 381: 135160.
- Matzarakis A, Balafoutis C. 2004. Heating degree-days over Greece as an index of energy consumption. *Int J Climatol*, 24(14): 1817-1828.
- Özdemir E, Poyraz Ö. 1997. Insulation of poultry houses. *Lalahan Zoot. Arast. Enst. Derg*, 37(2): 91-108.
- Özlü S, Shiranjang R, Elibol O, Karaca A, Türkoğlu M. 2017. Effect of paper waste products as a litter material on broiler performance. *J Appl Poult Res*, 14(2): 12-17.
- Şişman N, Kahya E, Aras N, Aras H. 2007. Determination of optimum insulation thicknesses of the external walls and roof (ceiling) for Turkey's different degree-day regions. *Energy Policy*, 35(10): 5151-5155.
- Ustaoglu A, Kurtoğlu K, Yaras A. 2020. A comparative study of thermal and fuel performance of an energy-efficient building in different climate regions of Turkey. *Sustain Cities Soc*, 5: 102163.
- Yang Z, Tu Y, Ma H, Yang X, Liang C. 2022. Numerical simulation of a novel double-duct ventilation system in poultry buildings under the winter condition. *Build Environ*, 207: 108557.



6 ŞUBAT 2023 TARİHLİ KAHRAMANMARAŞ DEPREMLERİ SONRASINDA BETONARME YAPILARIN İNCELENMESİ: MALATYA İLİ SAHA ÇALIŞMASI

Enes EKİNCİ^{1*}

¹İnönü Üniversitesi, Mühendislik Fakültesi, İnşaat Mühendisliği Bölümü, 44280, Malatya, Türkiye

Özet: Bir deprem ülkesi olan Türkiye'de 6 Şubat 2023 tarihinde Doğu Anadolu Fay Hattı'nda meydana gelen iki büyük deprem sonrasında 50,000'i aşkın insanımız hayatını kaybetmiş ve insanlar birçok sosyo-ekonomik problemler ile karşı karşıya kalmıştır. Kahramanmaraş'a bağlı Pazarcık ve Elbistan'da Mw 7.7 ve Mw 7.6 büyüklüklerde meydana gelen iki büyük deprem ülkemiz yüzölçümünün yaklaşık %14'üne, nüfusunun ise yaklaşık %16,4'üne tekabül edecek şekilde 11 ilimizi doğrudan etkilemiştir. 2022 yılı verilerine göre, depremden etkilenen bu illerde konut sayısı yaklaşık 5,6 milyon civarında olup, yarım milyondan fazla binanın ise hasar gördüğü belirlenmiştir. Meydana gelen bu depremler bu denli yüksek bir etki alanına sahip olması nedeniyle asrın felaketi olarak nitelendirilmiştir. Bu çalışmada, depremlerin en çok etkilediği illerden birisi olan Malatya'da gerçekleştirilen saha araştırmasından elde edilen bulguların sunulması amaçlanmıştır. Yapılan incelemeler sonucunda; yıkılan, hasar alan veya hasar alması olası görülen yapılarda gözlenen en temel sorunlar; zemin taşıma gücü düşük olan bölgelerde gerçekleştirilen inşaa faaliyetleri, işçilik hataları, hatalı yapı tasarımları, bina yaşı, bitişik nizam imar planı (özellikle kat seviyelerinin farklı olması) ve oldukça düşük beton kalitesi olarak sıralanabilir.

Anahtar kelimeler: Kahramanmaraş depremleri, Deprem hasarları, Beton kalitesi, Pas payı


Examination of Reinforced Concrete Structures after the Kahramanmaraş Earthquakes of February 6, 2023: Field Study in Malatya Province

Abstract: In Türkiye, which is an earthquake country, after two major earthquakes occurred 9 hours apart on the Eastern Anatolian Fault Line on February 6, 2023, more than 50,000 people lost their lives and people have faced with many socio-economic problems. Two major earthquakes with magnitudes of Mw 7.7 and Mw 7.6, which occurred in Pazarcık and Elbistan in Kahramanmaraş, directly affected 11 cities, corresponding to approximately 14% of our country's surface area and approximately 16.4% of the total population. According to 2022 data, the number of residences in these cities affected by the earthquake is approximately 5.6 million, and it was determined that more than half a million buildings were damaged. These earthquakes have been described as the catastrophe of the century because they have such a high impact area. In this study, it was aimed to present the findings obtained from the field research carried out in Malatya, one of the provinces most affected by earthquakes. As a result of the investigations; the most basic problems observed in buildings that are destroyed, damaged or likely to be damaged are; construction activities carried out in areas with low soil bearing capacity, workmanship errors, faulty building designs, building age, adjacent zoning plan (especially different floor levels) and very low concrete quality

Keywords: Kahramanmaraş earthquakes, Earthquake damages, Concrete quality, Rust share

*Sorumlu yazar (Corresponding author): İnönü Üniversitesi, Mühendislik Fakültesi, İnşaat Mühendisliği Bölümü, 44280, Malatya, Türkiye

E mail: enes.ekinci@inonu.edu.tr (Enes EKİNCİ)

Enes EKİNCİ  <https://orcid.org/0000-0001-7669-887X>

Gönderi: 03 Ocak 2024

Kabul: 21 Şubat 2024

Yayınlanma: 15 Mart 2024

Received: January 03, 2024

Accepted: February 21, 2024

Published: March 15, 2024

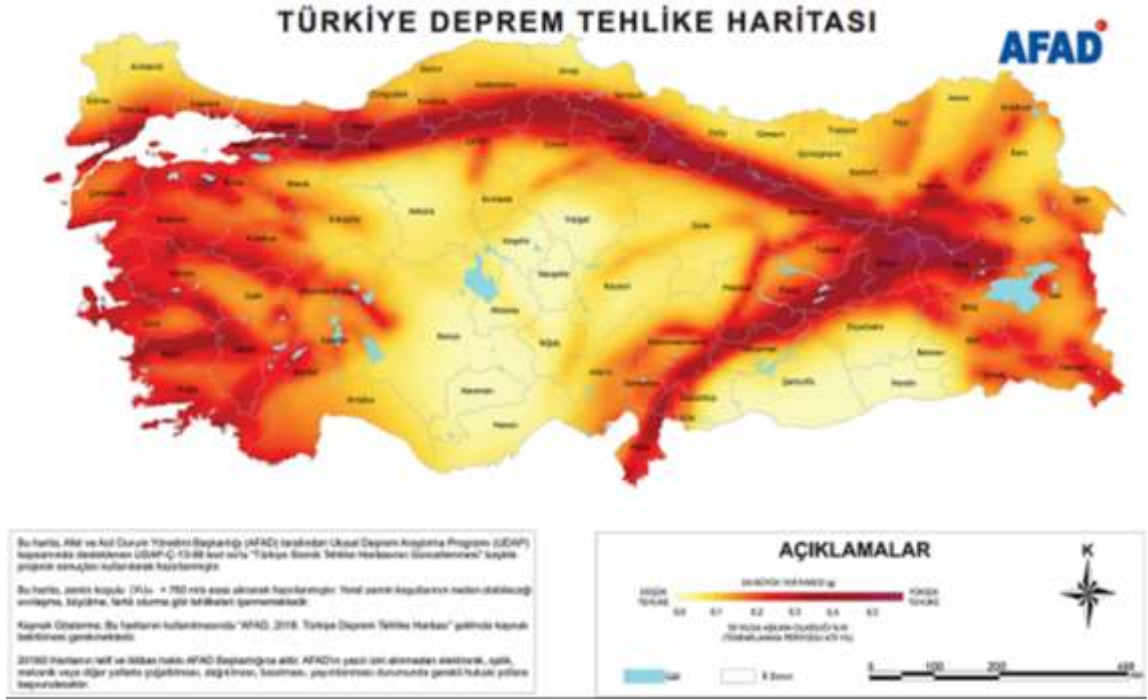
Cite as: Ekinci E. 2024. Examination of reinforced concrete structures after the Kahramanmaraş earthquakes of February 6, 2023: field study in Malatya province. BSJ Eng Sci, 7(2): 298-306.

1. Giriş

Türkiye'de 1900-2023 yılları arasında can kaybına veya hasara neden olan 269 deprem meydana gelmiştir. Yaşanan bu depremlerde can kaybı ve ağır hasar bakımından en büyük depremler sırasıyla 2023 Kahramanmaraş, 1939 Erzincan ve 1999 Gölcük merkezli Marmara depremleridir (T.C. Cumhurbaşkanlığı Strateji ve Bütçe Başkanlığı, 2023). Türkiye deprem haritası Şekil 1'de verilmiştir. Dünya üzerinde en aktif deprem bölgelerinden birinde yer alan Türkiye'de bulunan fay hatları çok şiddetli depremleri tetikleme potansiyeline

sahiptir. 6 Şubat 2023 tarihinde Kahramanmaraş ilinin Pazarcık ve Elbistan ilçelerinde meydana gelen Mw 7.7 ve Mw 7.6 büyüklüklerindeki depremler ülkemiz yüzölçümünün yaklaşık 110.000 km²'lik bir alanını doğrudan etkilemiştir (Mertol ve ark., 2023). Meydana gelen bu depremlerin yanı sıra, deprem afetinin ülkemiz için gelecekte de en önemli tehlikelerin başında geleceği gerçeği, depremden etkilenen yapılarda gözlenen hasar ve kusurların bilimsel yöntemlerle açıklanıp, gerekli önlemlerin alınması amacıyla yeni adımlar atılmasını gerektirmektedir.

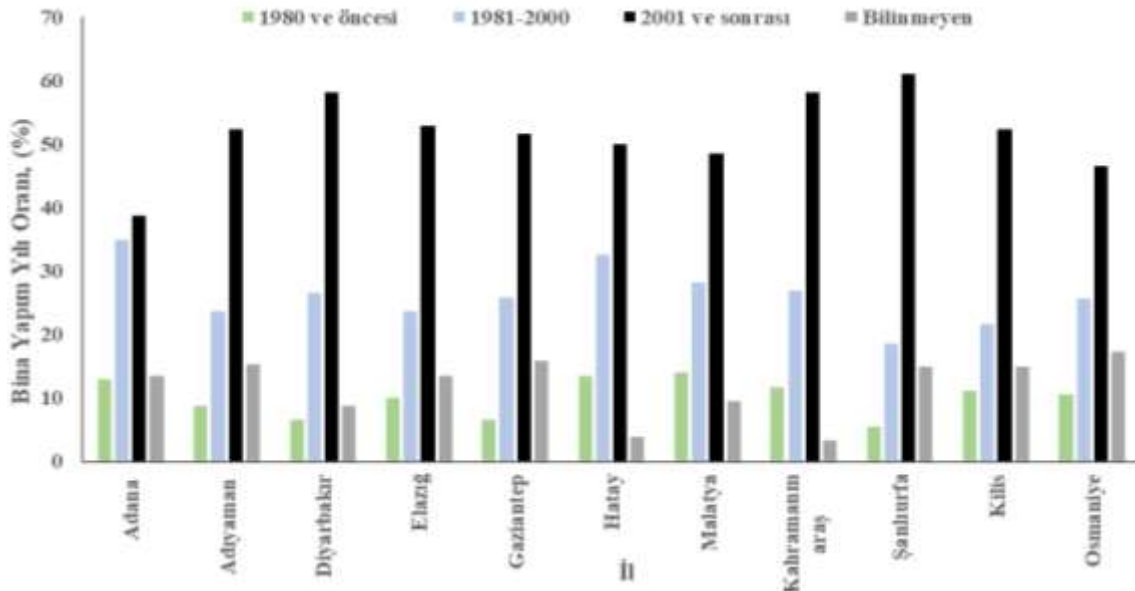




Şekil 1. Türkiye deprem tehlike haritası

İki milyonu aşkın yapının bulunduğu deprem bölgesinde, hasar oluşumu üzerinde büyük bir etkiye sahip olan mevcut yapı stoğunun incelenmesinde fayda görülmüştür. Şekil 2’de görüleceği üzere, afet bölgesinde bulunan illerde hane halkının kullanımında olan binaların yapım yılına göre dağılımları değişiklik göstermektedir. Ancak, bu illerin ortalamasına bakıldığında, hane halkının yaklaşık %10,12’sinin 1980 ve öncesinde inşa edilen yapılarda, %26,19’unun 1981-2000 arası inşa edilen yapılarda, %51,81’inin 2001 ve sonrası inşa edilen yapılarda ikamet ettiği gözlenirken, yapım yılının bilinmediği yapılarda ikamet oranının ise %11,89 oranında kaldığı belirlenmiştir. Afet bölgesinde bulunan, deprem performansı, yapım teknikleri ve

malzeme durabilitesi açısından daha yüksek performans beklenen ve gözlenen 2001 sonrası inşa edilen yapıların Türkiye ortalamasının (%47,4) üzerinde olmasının ise avantajlı bir durum olduğu gözlenmiştir. Bunun yanı sıra, yapım tarihi net olarak belirlenemeyen yapıların Türkiye ortalamasının (%9,1) üzerinde olmasının ise olumsuz bir durum olduğu söylenebilir. Yapının deprem performansı üzerinde oldukça büyük bir etkisi olan bina yaşının; yetersiz denetim uygulamaları, düşük malzeme kalitesi, durabilite problemleri, niteliksiz işçilik uygulamaları ve hatalı yapısal tasarımlardan dolayı meydana gelen olumsuzlukların bileşkesi şeklinde telafi edilmesi güç sonuçlara yol açtığı bilinmektedir.



Şekil 2. Afet bölgesinde bulunan illerde yapı inşa yılı istatistikleri, (TÜİK, 2021)

Bu çalışma, 6 Şubat 2023 tarihinde meydana gelen Kahramanmaraş depremleri sonrasında Malatya ilinde gerçekleştirilen detaylı gözlemsel analizlerin bulgularını sunmaktadır. Çalışma neticesinde elde edilen veriler, betonarme yapıların deprem performansının beklenen düzeyde olmasının ancak yüksek kalitede malzeme kullanımı, doğru bir yapısal tasarım süreci ve nitelikli işçilik faaliyetleri ile sağlanabileceğini ortaya koymuştur.

2. Materyal ve Yöntem

Bu çalışma, 6 Şubat Kahramanmaraş depremleri sonrasında Malatya ilinde meydana gelen hasar ve yıkımların incelenmesi, olası hasar nedenlerinin tartışılması ve bundan sonra dikkat edilmesi gereken hususların belirtilmesini kapsamaktadır. Bu bölümde, hasar alan ve/veya yıkılan yapılarda gözlenen hasar nedenleri sıralanmıştır.

2.1. Malzeme Özellikleri

2.2.1. Beton bileşenleri

Deprem sonrasında yıkılan ve ağır hasar alan yapılarda yapılan incelemeler sonucunda beton kalitesinin oldukça düşük olduğu belirlenmiştir. Kompozit bir yapı malzemesi olan betonun, ekonomik ömrü boyunca yıpratıcı dış etkenlere karşı dayanıklı olması gerekmektedir. Yapım yılı eski olan binalarda (2001 yılı öncesi) oldukça düşük beton basınç dayanımı değerleri elde edilmektedir. Çimento dozajının düşük olması, maksimum agrega tane çapının çok yüksek olması, daha iyi bir kalite-kontrol sistemine sahip olan hazır beton endüstrisinin kullanılmaması, su/çimento oranının yüksek tutulması gibi nedenlerden dolayı birçok hasar ve yıkımın gerçekleştiği belirlenmiştir. Beton basınç dayanımının yapıların deprem performansı üzerindeki önemli etkileri uzun süredir bilinmekte olup deprem bölgesinde inşa edilecek yapılarda kullanılması gereken minimum basınç dayanımı değerlerine farklı tarihlerde yayımlanan yönetmeliklerde yer verilmiştir. Tablo 1’de görüleceği gibi, farklı tarihlerde yürürlüğe giren yönetmeliklere (ABYYHY, 1975; ABYYHY,1998; DBYBHY, 2007; TBDY, 2018) göre:

Tablo 1. Farklı tarihlerdeki yönetmeliklerde yer alan beton basınç dayanımı sınır değerleri

Yönetmelik	Basınç Dayanımı, (MPa)	değerlerinden küçük olmamalıdır.
ABYYHY-1975,	18	
ABYYHY-1998	20	
DBYBHY-2007	20	
TBDY-2018,	25	

2000’li yılların başında Türkiye’de İstanbul, Ankara, İzmir başta olmak üzere birçok ilde elle beton dökümünün yasaklanmasını takiben, 2002 yılında yayımlanan Hazır Beton Standardı (TS EN 206-1, 2002) ve 2004 yılında ise hazır beton kullanımını zorunlu hale getiren genelge gibi girişimler bu tarih aralığının ülkemizdeki yapı stoğunun kalitesi açısından çok önemli

bir yere sahip olmasına neden olmaktadır. Modern bilimsel yöntemleri kullanması ve üniform bir üretim sağlaması açısından geleneksel yerindedöküm betonlardan oldukça avantajlı görülen hazır beton sisteminin kullanılmadığı yapılarda meydana gelen hasarların en önemli sebebinin beton kalitesinin düşük olmasından kaynaklandığı belirlenmiştir. Yapım yılı nispeten daha yeni olan yapılarda gözlenen en belirgin kusurların ise, beton dökümünde gözlenen segregasyon oluşumu ve betona uygulanan yetersiz kür işlemi olduğu belirlenmiştir. Şekil 3 (a)’da bir bina enkazında incelenen bir beton numunesi, Şekil 3 (b)’de ise ağır hasar alan bir binanın kolon örneği verilmiştir. Şekil 3 (b)’de görüleceği üzere, maksimum agrega tane çapının sınır değerlerin çok üzerinde olmasının beton ve donatı arasındaki aderansı olumsuz etkilediği belirlenmiştir.



Şekil 3. Yapı enkazından alınan ve maksimum agrega tane çapı yüksek olan beton örneği (a), Ağır hasar alan bir yapıda maksimum agrega tane çapının aderansı üzerindeki olumsuz etkisi (b).

Her ne kadar beton basınç dayanımına ait sınır değerler farklı tarihlerde yayımlanan yönetmeliklerde arttırılmış olsa da beton döküm işleminin uygun sıcaklıkta yapılması ve kür işleminin özenli bir şekilde gerçekleştirilmesi gerekmektedir. Örneğin, Şekil 4’te görüleceği üzere, incelenen natamam bir yapıda 27 Ocak 2023 tarihinde (meteorolojik verilere göre 3 gün süreyle hava sıcaklığının 5 °C’nin altında olduğu döneme denk gelmektedir) beton dökümü yapıldığı belirlenmiştir. TS 1248 standardına göre, günlük ortalama hava sıcaklığının ardı ardına 3 gün süreyle 5 °C’nin altında olduğu hava durumuna soğuk hava adı verilmektedir (TS 1248, 2012). Soğuk havada beton dökümünün taze ve sertleşmiş beton özelliklerine olumsuz etkilerini minimize etmek amacıyla priz hızlandırıcı, antifriz ve hava sürükleyici katkı maddelerinin kullanılması gibi birtakım önlemlerin alınması gerekmektedir.



Şekil 4. Soğuk havada beton dökülen ve kalıp söküm işlemi yapılmayan betonarme elemanlar

2.2.2. Segregasyon

Görülen en yaygın problemler arasında, betonun geçirimsizliğini önemli ölçüde etkileyen segregasyon oluşumları yer almaktadır. Yapılan gözlemsel incelemeler, özellikle, dar ve derin kalıplara beton dökümünün özensiz bir şekilde gerçekleştirildiğini, taze betonda serbest düşmeye maruz bırakılmak suretiyle ayrışmalar oluştuğu gözlenmiştir. Betonun geçirimsizliğini oldukça olumsuz etkileyen segregasyon oluşumun göz ardı edildiği yapım yılı yeni olan binalarda, ayrışmaya bağlı olarak kabuk atma şeklinde hasar oluşumlarının meydana geldiği tespit edilmiştir. Şekil 5, yapım yılı yeni olan yapılarda meydana gelen segregasyon oluşumunu göstermektedir.



Şekil 5. Yapılarda gözlenen segregasyon oluşumları

2.2.3. Pas payı mesafesi

Gözlemlenen tüm yapılardan gözlenen en önemli kusurlardan birisi de pas payı tabakasının yeterli olmamasıdır. Taşıyıcı elemanda kullanılan en dış donatının dış yüzeyinden en dış beton lifine kadar olan mesafe olarak adlandırılan pas payı (net beton örtüsü) kalınlığı gerek donatı korozyonunun engellenmesi gerekse beton ve donatının kenetlenmesinin üst düzeyde sağlanabilmesi amacıyla çok büyük bir öneme sahiptir. Bu asli görevlerin yanı sıra, donatıları olası yüksek sıcaklık etkilerinden korumak ve betonun ufalanmasını engellemek amacıyla kullanılan pas payı mesafesinin yönetmelikte belirtilen sınırlar içerisinde olması gerekmektedir. Pas payı mesafesinin yetersiz olması halinde yukarıda belirtilen sıkıntıların olması muhtemel iken, pas payı mesafesinin gereğinden fazla olarak kullanılmasının da çekirdek betonun boyutlarını azaltacağı ve taşıyıcı elemanların projelendirme aşamasında dikkate alınan tasarım değerlerini sağlayamayacağına altı çizilmelidir (Doğangün A, 2021). Şekil 6. pas payı kalınlığının yetersiz olduğu taşıyıcı sistem elemanlarını göstermektedir. Tasarım aşaması doğru bir şekilde yapılmış ve özenli bir işçilik ile üretilmiş betonarme elemanlarda, beton, çelik donatıları korozyondan koruyarak uzun bir performans sağlamaktadır. Çelik donatıların korozyondan korunması kimyasal açıdan betonun yüksek alkali özelliği sayesinde gerçekleşirken, fiziksel koruma ise pas payı tabakası oluşturmak suretiyle sağlanmaktadır. Yetersiz pas payı tabakası kullanılması halinde, çelik donatılar oldukça kısa bir sürede korozyona uğramaktadır. Bu durum, çelik donatılarda kesit kaybına, çelik donatıların taşıyıcı gücünü kaybetmelerine, beton ve çelik arasındaki aderans kabiliyetinin olumsuz etkilenmesine ve deprem kuvvetleri etkisiyle meydana gelecek kabuk atma oluşumlarına neden olmaktadır (Baradan ve ark., 2012). TS 500' de yer alan yeterli aderansın sağlanması ve donatının yıpratıcı çevresel etkilerden korunması amacıyla kullanılması gereken pas payı mesafeleri Tablo 2'de verilmiştir.

2.2.3. Donatı kusurları

6 Şubat Kahramanmaraş depremleri sonrasında Malatya ilinde gözlenen yıkım ve hasarların tümünde donatı kalitesi ve işçiliğinde önemli eksiklikler gözlenmiştir. Donatı montaj işleminde en sıkıntılı görülen noktalar ise; etriye bağ açılarının 90° olması, etriye aralıklarının çok fazla olması ve özellikle eski yapılarda düz yüzeyli donatıların kullanılması şeklinde sıralanabilir. Şekil 7 (a), 6 Şubat depremlerinden sonra Malatya ili sınırları içerisinde yer alan natamam bir binaya ait donatı işçiliği verilmiştir. Bahse konu bu işçilikte, etriye kancalarının 90° olduğu gözlenmektedir. Bu durum, olası bir yük altında donatıların burkulmasının ve betonun parçalanmasının daha kolay olacağı şeklinde açıklanabilir. Kesit içerisine yerleştirilen boyuna ve enine donatıların kenetlenmesi, yük aktarımının sağlanabilmesi ve beton ile aderansın sağlanabilmesi için donatıların düzgün bir şekilde bağlanması gerekmektedir. Şekil 7 (f),

etriye ve boyuna donatıların bağlanma işleminin özensiz yapıldığı bir yapıda beton dökümü sonrasında etriyenin

yer değiştirdiği ve sıklaştırma bölgesinde boyuna donatının burkulma boyunun arttığı gözlenmiştir.



Şekil 6. Pas payı mesafesi yetersiz olan elemanlar

Tablo 2. Gerekli görülen pas payı mesafesi, (TS 500, 2015)

Yapı Elemanı	Net Beton Örtüsü, (c _c)
Zemin ile doğrudan ilişkili olan elemanlar	≥ 50 mm
Hava koşullarına açık kolon ve kirişlerde	≥ 25 mm
Yapı içinde, dış etkilere açık olmayan kolon ve kirişlerde	≥ 20 mm
Perde duvar ve döşemelerde	≥ 15 mm
Kabuk ve katlanmış plaklarda	≥ 15 mm



Şekil 7. Donatı işçiliklerinde gözlenen kusurlar

2.2. Taşıyıcı Elemanlara Zarar Veren Montaj İşlemleri

Taşıyıcı sistem elemanları üzerinde gerçekleştirilen montaj işlemlerinin binaların hasar alma durumları üzerinde oldukça etkilidir. Herhangi bir denetim altında olmadan, sadece farklı mekanik ve elektriksel işlemlerin gerçekleştirilmesi amacıyla uygulanan bu işlemler binanın dayanım ve rijitlik özelliklerine oldukça zarar vermektedir. Taşıyıcı sistem elemanlarında oluşturulan bu boşluklar, boşluk çevresinde gerilme yığılmasının

oluşmasına ve bu bölgede oluşabilecek hasar boyutunu arttırmaya yönelik etki yapmaktadırlar. Şekil 8 (e)'de görüleceği üzere 10 katlı betonarme bir binanın ilk katında bulunan perde beton içerisinde unutulmuş/önemsenmeyen bir kalıp tahta parçasının çevresinde diyagonal çatlak oluşumlarına sebep olduğu gözlenmiştir. Betonarme sistem içerisinde bir boşluk olarak etki eden bu kalıp parçası meydana gelen gerilme yığılmaları nedeniyle çatlak oluşumuna neden olmuştur.



Şekil 8. Taşıyıcı sisteme zarar veren işlemler

2.3. Yapısal Hatalar

2.3.1. Bitişik nizam

Şekil 9 (a)'da bitişik nizam yapıda meydana gelen göçme durumu verilmiştir. Bitişik nizam yapılarda mutlak suretle bulunması gereken deprem derzinin bulunmaması ve bitişik olarak inşa edilmiş bu iki yapının döşeme seviyelerinin farklı olması çekiçleme etkisini ortaya çıkarmıştır. Döşeme seviyesinden yapıya etki eden deprem yükleri, döşeme seviyelerinin farklı olması durumunda, düşey taşıyıcı elemanlara etki etmektedir. Bitişik nizam olarak inşa edilecek yapılar için, TBDY (2018) Madde 4.9.3.2'de, "Bırakılacak minimum derz boşluğu, 6 m yüksekliğe kadar en az 30 mm olacak ve bu değere 6 m'den sonraki her 3 m'lik yükseklik için en az 10 mm eklenecektir" şeklinde ifade yer almaktadır.

Gerçekleştirilen saha çalışmaları sonrasında, birçok bitişik nizam yapının derz mesafesine uygun olmadığı gözlenmiştir. Pala ve Şaşmaz, (2019) tarafından yapılan bir çalışmada, döşeme seviyeleri farklı olan bitişik nizam olarak inşa edilmiş iki yapının farklı döşeme kalınlıklarına bağlı olarak meydana getirdikleri çarpışma kuvvetleri incelenmiştir. Elde edilen bulgular, döşeme kalınlıklarına ve derz mesafelerine bağlı olarak, döşemelerden diğer yapının kolonlarına etki eden maksimum çarpışma kuvvetinin farklı kotlarda olacağını göstermiştir. Şekil 8(b)'de, bitişik nizam imar planına göre inşa edilmiş ve hasar almış bir yapı verilmiştir.



Şekil 9. Bitişik nizam hasarları.

2.3.2. Kısa kolon

Şekil 10'da kısa kolon etkisi nedeniyle ağır hasar almış bir kesit verilmiştir. Yapım yılı 2021 olan bu binada hasarın oldukça rijit yüklemeye alan kısa kolon oluşumundan dolayı meydana geldiği belirlenmiştir. Belirli bir boy için tasarlanan kolonlarda, boyu kısaltacak herhangi bir etmen (arazide kot farkı olması, asma kat uygulaması, merdiven sahanlıkları, bant pencere yapılması, kolon boyunca devam etmeyen dolgu duvarların yapılması) nedeniyle bu kısa serbest boya beklenenden daha yüksek bir kesme gerilmesi gelmesi ve kolonun ağır hasar alması mümkün olabilmektedir. Meral, (2019) tarafından yapılan bir çalışmada, 2007 Deprem Yönetmeliği'ne göre tasarlanan ve hiçbir düzensizliği bulunmayan 4 ve 7 katlı iki bina modellenmiştir. 3-B yapı modellerinin her iki asal doğrultusunda 12 adet gerçek deprem ivme kaydı dikkate alınarak toplam 96 adet analiz yapılmıştır. Elde edilen sonuçlar, 4 ve 7 katlı kısa kolonlu modellerin zemin katında bulunan kolonlarda sırasıyla %40 ve %60 oranlarında göçme hasarı gözlemlendiği bildirilmiştir (Meral E, 2019).



Şekil 10. Kısa kolon hasarı

2.3.2. Yetersiz perde elemanı

Şekil 11'de arazi kot farkından dolayı yarım bodrum şeklinde tasarlanmış (bina girişi toprak üstü bodrumdan yapılmakta) ve perde oranının yetersiz olduğu bir yapıya ait hasar alan perde beton verilmiştir. Etriye kancasının 90° olması dışında, donatı sıkılaştırma işlemi, pas payı tabakası kalınlığı gibi detayların doğru bir şekilde gerçekleştirildiği bu yapıda, bodrum katta bulunan perde, deprem kuvveti etkisiyle mafsallaşmış ve yatay rijitliğini tamamen kaybetmiştir. Deprem kuvvetlerini bertaraf edebilmesi için mümkün olduğunca yapının en dış aksına yerleştirilmesi gerekmektedir. Ayrıca, yapının her iki deprem yönünde de $A_{perde}/A_{yapı} \geq 0.0015n$ ve $A_{perde}/A_{yapı} \geq 0.008$ koşulları, Malatya ilinde genel olarak, asansör boşluklarının etrafında perde imalatı yapılarak sağlanmaya çalışılmıştır. Bu durumun, yapıların deprem performansı üzerinde belirgin olumsuz etkilere yol açtığı gözlenmiştir. Öte yandan, genel bir kural olarak, yapı yüksekliğinin 1/6'sı kadarına tekabül eden kısmının yer seviyesinden aşağıda olması durumuna muhalefet eden bu yapıda taşıyıcı sistem ve zemin etkileşiminin tam olarak gerçekleşmemesi sonucu önemli bir hasar aldığı gözlenmiştir.



Şekil 11. Perde yetersizliğinden dolayı gözlenen hasar

2.3.3. Konsol durumu

Şekil 12'de yumuşak kat bulunan, bitişik nizam imar planına göre inşa edilmiş ve cephe boyunca konsolu bulunan ağır hasar alan bir yapı verilmiştir. Genel olarak, binalarda oturma alan kazanmak ve mimari kaygılar amacıyla yapılan konsol imalatından vazgeçmek gereklidir. Yapının rijitlik merkezi ile ağırlık merkezinin çakışmasını engelleyen, ağırlık merkezini konsola doğru kayması nedeniyle yapının deprem performansını olumsuz etkilemektedir. Diğer bir yandan, kapalı konsolların uç bölgesinde bulunan kolonları bağlayan kirişlerin mimari kaygılar nedeniyle konsol ucunda taşınması, yapının çerçeve davranışını bozmaktadır (6 Şubat 2023 Depremleri Sonrası Malatya Deprem Raporu ve Eylem Planı, 2023).



Şekil 12. Konsol durumu

3. Sonuç ve Tartışma

Bu çalışma, 6 Şubat 2023 tarihinde meydana gelen Kahramanmaraş depremleri sonrasında, Malatya'da meydana gelen hasar oluşumlarının detaylı gözlemsel analizini sunmaktadır. Çalışma neticesinde elde edilen bulgular aşağıdaki gibi sıralanabilir;

- İncelenen yapılarda oluşan hasarların nedenlerinin, kullanılan malzeme kalitesi, yapı tasarımı ve işçilik adı altında üç farklı perspektifte incelenmesi gerektiği belirlenmiştir.
- Dayanımı düşük beton kullanımı, nervüzsüz donatı kullanımı, etriye adımının fazla olması, etriye bağ açısının 135° olmaması, pas payı mesafesine dikkat edilmemesi ve beton yerleştirme ve sıkıştırma işlemlerine dikkat edilmemesi gibi işlemlerin, üretilen betonarme elemanların deprem performansı üzerinde olumsuz etkilere sahip olan başlıca etmenler olduğu gözlenmiştir. Yapıların uzun vadeli performansının sağlanabilmesinin temel şartının malzeme seçimi ve uygulamalarının doğru bir şekilde yapılmasına bağlı olduğunun altı çizilmiştir.
- Bir önceki maddede belirtilen hususların çoğunun doğru bir şekilde uygulandığı ve yapı denetim hizmeti almış yeni binalarda dahi, betona uygulanan kür işleminin yetersiz olması ve belirgin tasarım hataları sonucu hasar oluşumlarının daha kolay bir şekilde meydana geldiği belirlenmiştir.
- Malatya ili genelinde, yumuşak kat, bitişik nizam, bodrumu bulunmayan yüksek katlı bina sayısı, konsolların varlığı, perdelerin çoğunlukla asansör boşluğuna yapılması, asmolen döşeme kullanımı gibi faktörler ise binaların hasar alma durumları üzerinde dominant etki oluşturmuştur. TBDY 2018'de

düzensizlik adı altında yer alan birtakım durumlardan mümkün olduğunca kaçınılması, statik projeleri tamamlanan yeni yapım işlerinin alanında uzman kişilerce incelenmesi yoluyla bu tip hataların minimize edilmesi gerekmektedir.

- Yapılarda meydana gelen hasar oluşumlarının temelinde belirgin işçilik hataları olduğu gözlenmiştir. Yapım yılı yeni olan yapıların büyük çoğunluğunda, su basman üst kotu ile devam eden kolonun alt yüzeyinde donatı bükülmesine bağlı olarak kabuk atma oluşumları gözlenmiştir. Ayrıca, Malatya ili genelinde boğaz etriyesi kullanılan bir yapıya ise rastlanılmamıştır. Elde edilen gözlemler, yapı inşasında çalışacak kişilerin ciddi ve verimli bir eğitimden geçirilmesinin oldukça önemli ve faydalı olacağı kanısına varılmıştır.
- Hasar gören yapılarda ve henüz tamamlanmamış yapılarda gözlenen işçilik hatalarının yapıların deprem performansı üzerinde oldukça önemli olduğu gözlenmiştir. Her ne kadar yapı denetim faaliyetlerinin 2011 yılında ülke genelinde zorunlu hale getirilmiş olması daha iyi bir kontrol sistemini hayata geçirmiş olsa da yüklenicinin doğrudan denetim yapan şirketi seçemediği havuz sisteminin 2019 yılında hayata geçirilmesinin yeni yapılarda oluşacak olumsuz imalatları azaltma noktasında oldukça önemli bir yeri olduğu belirlenmiştir. Ancak, atılan bu olumlu adımlara rağmen, işçilik faaliyetlerinin tam anlamıyla denetlenmiş olduğu hiçbir yapı ile maalesef karşılaşmamıştır.
- Mevcut yönetmelik kriterlerini karşılamayan, hazır beton tekniğinden istifade etmemiş 2000 yılı öncesi yapıların deprem performanslarının belirlenmesi, teknik ve ekonomik bakımdan güçlendirilmesi uygun

olmayan yapılar için kentsel dönüşüm faaliyetlerinin hızlı bir şekilde uygulamaya konulması gerektiği belirlenmiştir.

Yaşanan depremler sonucunda meydana gelen hasarların oluşumunda birçok parametrenin varlığından bahsedilmelidir. Bina yaşı, malzeme özellikleri, kat sayısı, tasarım parametreleri, özensiz işçilik uygulamaları, yapısal düzensizlik durumları ve yapının oturduğu zemin karakteristikleri gibi ana faktörlerin yapıların deprem performansı üzerinde çok önemli bir yeri olduğu gözlenmiştir. Sonuç olarak, inşa edilecek herhangi bir yapının proje işlemlerinden başlayıp, teslimine kadar geçen sürede atılacak her türlü imalatın bilimsel verilere ve ilgili yönetmeliklere sonuna kadar bağlı kalınarak gerçekleştirilmesi gerektiği tespit edilmiştir.

Katkı Oranı Beyanı

Yazarın katkı yüzdesi aşağıda verilmiştir. Yazar makaleyi incelemiş ve onaylamıştır.

	E.E.
K	100
T	100
Y	100
VTI	100
VAY	100
KT	100
YZ	100
KI	100
GR	100
PY	100
FA	100

K= kavram, T= tasarım, Y= yönetim, VTI= veri toplama ve/veya işleme, VAY= veri analizi ve/veya yorumlama, KT= kaynak tarama, YZ= Yazım, KI= kritik inceleme, GR= gönderim ve revizyon, PY= proje yönetimi, FA= fon alımı.

Çatışma Beyanı

Yazar bu çalışmada hiçbir çıkar ilişkisi olmadığını beyan etmektedirler.

Etik Onay Beyanı

Bu çalışmada hayvanlar ve insanlar üzerinde herhangi bir çalışma yapılmadığı için etik kurul onayı

alınmamıştır.

Kaynaklar

- Baradan B, Türkel S, Yazıcı H, Ün H, Yiğiter H, Felekoğlu B, Tosun K, Aydın S, Yardımcı MY, Topal A, Öztürk AU. 2012. Beton. Dokuz Eylül Üniversitesi Mühendislik Fakültesi Yayınları, No:334, İzmir, Türkiye, ss: 591.
- Doğangün, A. 2021. Betonarme yapıların hesap ve tasarımı - Türkiye bina deprem yönetmeliği 'ne (TBDY2018) uygun. Birsen Yayınevi, İstanbul, Türkiye, 17. Baskı, ss: 52-53.
- Meral E. 2019. Betonarme binalarda kısa kolon etkilerinin araştırılması. Int J Eng Res Dev, 11(2): 515-527.
- Mertol HC, Tunç G, Akış T, Kantekin Y, Aydın İC. 2023. Investigation of RC buildings after 6 February 2023, Kahramanmaraş, Türkiye earthquakes. Buildings, 13 (7):1789.
- Pala M, Şaşmaz Z. 2019. Kat seviyeleri farklı bitişik nizam yapılarda kat kütlelerinin çarpışma kuvvetine etkisi. Adıyaman Üniv Müh Bil Der, 6(10): 47-63.
- T.C. Bayındırlık ve İskan Bakanlığı. 1975. Afet bölgelerinde yapılacak yapılar hakkında yönetmelik (ABYYHY-1975). <https://www.resmigazete.gov.tr/arsiv/15260.pdf> (erişim tarihi: 12 Aralık 2023).
- T.C. Bayındırlık ve İskan Bakanlığı. 1998. Afet bölgelerinde yapılacak yapılar hakkında yönetmelik (ABYYHY-1998). <https://www.resmigazete.gov.tr/eskiler/2006/03/20060306-3.htm> (erişim tarihi: 12 Aralık 2023).
- T.C. Bayındırlık ve İskan Bakanlığı. 2007. Deprem bölgelerinde yapılacak binalar hakkında yönetmelik (DBYBHY-2007). <https://www.resmigazete.gov.tr/eskiler/2007/03/20070306-3.htm> (erişim tarihi: 12 Aralık 2023).
- T.C. Cumhurbaşkanlığı Strateji ve Bütçe Başkanlığı. 2023. URL: <https://www.sbb.gov.tr/wp-content/uploads/2023/03/2023-Kahramanmaraş-ve-Hatay-Depremleri-Raporu.pdf> (erişim tarihi: 12 Aralık 2023).
- T.C. Çevre ve Şehircilik Bakanlığı. 2018. Türkiye Bina Deprem Yönetmeliği (TBDY-2018). <https://www.resmigazete.gov.tr/eskiler/2018/03/20180318-M1-2.htm> (erişim tarihi: 12 Aralık 2023).
- TS 1248. 2012. Betonun hazırlanması, dökümü ve bakım kuralları - Anormal hava şartlarında. Türk Standartları Enstitüsü, Ankara, Türkiye.
- TS 500. 2015. Betonarme yapıların tasarım ve yapım kuralları. Türk Standartları Enstitüsü, Ankara, Türkiye.
- TS EN 206-1. 2002. Beton- Bölüm 1: Özellik, performans, imalat, uygunluk. Türk Standartları Enstitüsü, Ankara, Türkiye.
- Türkiye İstatistik Kurumu (TÜİK). 2021. URL: <https://data.tuik.gov.tr/Bulten/Index?p=Bina-ve-Konut-Nitelikleri-Ara%C5%9Ft%C4%B1rmas%C4%B1-2021-45870&dil=1> (erişim tarihi: 12 Aralık 2023).



CAPS-SSR MARKIRLARI KULLANILARAK PAMUK KROMOZOM SUBSTİTÜSYON HATLARININ BELİRLENMESİ

Adnan AYDIN^{1*}, Mehmet KARACA²

¹Iğdır University, Faculty of Agriculture, Department of Agricultural Biotechnology, 76000, Iğdır, Türkiye

²Akdeniz University, Faculty of Agriculture, Department of Field Crops, 07000, Antalya, Türkiye

Özet: Pamuk (*Gossypium L.*) dünya genelinde tekstil endüstrisi için en önemli doğal lif kaynağı ve aynı zamanda önemli bir yağ bitkisidir. Pamuk lifleri tekstil için ana kaynak olmakla birlikte lifi, tohumu ve bitkisi ev izolasyon materyali olarak enerji tasarrufunda, proteince zengin hayvan yemi, yağı gıda olarak insan beslenmesinde, bitkisi ise altlık ve biyomateryal olarak ta değişik kullanım alanlarına sahiptir. Pamukta ıslah çalışmaları genellikle verim ve lif kaliteleri yönünden seçkin genotipler arasında yapılan melezlemeler ve daha önce geliştirilmiş çeşitlerden seleksiyon çalışmalarına dayanmaktadır. Ancak pamuk ıslah programları, kültür çeşitlerinde dar olan genetik çeşitlilikten olumsuz yönde etkilenmektedir. Bu durum araştırmacıları türler-arası melezleme ile introgresyona teşvik etmiştir. Türler-arası melezlemelerde kompleks antagonistik ilişkiler, farklı ploidi seviyelerinden dolayı sitogenetik farklılıklarla translokasyonlar ve inversiyonlar, kromozom yapısal farklılıkları, linkaj etkisi ile arzu edilmeyen tarımsal özelliklerin varlığı, rekombinasyonun azlığı, erken generasyonlarda introgresyonun kaybolması, kısırılık, Muller-Dobzhansky kompleksi nedeni ile ölümcül epistatik interaksiyonlar ve Mendel açılımının oluşmaması gibi nedenlerden dolayı sorunlar yaşanmaktadır. Kromozom substitüsyon hatlarının kullanılması ile yukarıda sözü edilen türler-arası melezlemelerdeki olumsuzluklar ortadan kaldırılabilir. Bu çalışmada 17 kromozom substitüsyon hattının tanımlanması için genik CAPS-SSR markırları kullanılmıştır. Toplamda 11 CAPS-SSR markırı ve 16 restriksiyon enzimi kullanılmıştır. Bu bağlamda 11 monomorfik olan SSR markırı CAPS-SSR yöntemi ile 9 polimorfik markır olarak tespit edilmiştir. Sonuç olarak CAPS-SSR markır yöntemi kullanılarak kromozom substitüsyon hatlarının kromozom lokasyonlarının tespit edilebileceği sonucuna varılmıştır.

Anahtar kelimeler: EST-SSR, -CAPS-SSR, CS-B, Pamuk


Determination of Cotton (*Gossypium L.*) Chromosome Substitution Lines Using CAPS-SSR Markers


Abstract: Cotton (*Gossypium L.*) is the most important natural fiber source for the textile industry worldwide and is also an important oil plant. Although cotton fibers are the main source for textiles, its fibers, seeds and plants are used in energy saving as home insulation materials, protein-rich animal feed, oil in human nutrition as food, and its plants as litter and biomaterial. Breeding studies in cotton are generally based on cross-breeding between distinguished genotypes in terms of yield and fiber quality and selection studies from previously developed varieties. However, cotton breeding programs are negatively affected by the narrow genetic diversity in cultivars. This situation has encouraged researchers to investigate introgression through interspecies hybridization. Complex antagonistic relationships in interspecies hybridizations, translocations, and inversions with cytogenetic differences due to different ploidy levels, chromosome structural differences, the presence of undesirable agricultural traits due to the linkage effect, lack of recombination, loss of introgression in early generations, sterility, lethal epistatic interactions due to the Muller-Dobzhansky complex and problems occur due to reasons such as Mendel expansion not occurring. By using chromosome substitution lines, the negativities in interspecies hybridizations mentioned above can be eliminated. In this study, genic CAPS-SSR markers were used to identify 17 chromosome substitution lines. A total of 11 CAPS-SSR markers and 16 restriction enzymes were used. In this context, 11 monomorphic SSR markers were converted to 9 polymorphic markers by the CAPS-SSR method. As a result, it was concluded that the chromosome locations of chromosome substitution lines can be determined by using the CAPS-SSR marker method.

Keywords: EST-SSR, -CAPS-SSR, CS-B, Cotton

*Sorumlu yazar (Corresponding author): Iğdır University, Faculty of Agriculture, Department of Agricultural Biotechnology, 76000, Iğdır, Türkiye

E mail: adnan.aydin@igdir.edu.tr (A. AYDIN)

Adnan AYDIN  <https://orcid.org/0000-0002-8284-3751>

Mehmet KARACA  <https://orcid.org/0000-0003-3219-9109>

Gönderi: 06 Şubat 2024

Kabul: 21 Şubat 2024

Yayınlanma: 15 Mart 2024

Received: February 06, 2024

Accepted: February 21, 2024

Published: March 15, 2024

Cite as: Aydın A, Karaca M. 2024. Determination of cotton (*Gossypium L.*) chromosome substitution lines using CAPS-SSR markers. BSJ Eng Sci, 7(2): 307-315.

1. Giriş

Tekstil sektörünün en önemli doğal hammaddesi olan pamuk (*Gossypium L.*), ticari olarak üretimi dünyanın sıcak enlemlerindeki alanlarda yoğunlaşmıştır. Pamuk üretimi, Kuzey yarımkürede 45°, Güney yarımkürede ise 32° enlemlerine kadar uzanmaktadır (Mert, 2007).

Ülkemizde bu enlem dereceleri arasında olduğundan pamuk üretimi yapan ülkeler arasında önemli bir yeri bulunmaktadır. Pamuk yaygın ve zorunlu kullanım alanıyla insanlık açısından, yarattığı katma değer ve istihdam olanaklarıyla da üretici ülkeler ve üretici aileler açısından büyük ekonomik öneme sahip bir üründür.



Pamuk işlenmesi açısından çırçır sanayisinin, lifi ile tekstil sanayisinin, tohumu ile yağ ve yem sanayisinin, linteri (hav) ile de kâğıt sanayisinin hammaddesi durumundadır. Dünyadaki nüfus artışı ve yaşam standardının yükselmesiyle pamuk lifine olan ihtiyacı da artırmaktadır (Aydın, 2023). Bundan dolayı dünya da ve ülkemizde pamuk bitkisinin önemini daha da ortaya çıkarmaktadır.

Pamuk bitkisinin *Malvaceae* ailesine ait yaklaşık 52 türü bulunmakta ve sitogenetik olarak 9 farklı genoma sahiptir (Viot ve Wendel, 2023). 52 tür içinde tetraploid ve diploid genom yapısına sahip türler bulunmaktadır. Dünya genelinde en çok kültürü yapılan pamuk türü de tetraploid kromozom ($n=26$) yapısına sahip olup bunlar yeni dünya pamukları olarak bilinen *Gossypium hirsutum* ve *Gossypium barbadense*'dir (Witt ve ark., 2020). Eski dünya pamukları olarak *Gossypium arberoum* ve *Gossypium herbaceum* diploid kromozom ($n=13$) yapısına sahiptirler. Diploid kromozom yapısına sahip eski dünya pamuklarının üretimi çok az düzeydedir. Dünyada ve ülkemizde en çok üretimi yapılan pamuk türü *G. hirsutum* türüne ait pamuk çeşitleridir. Bu türün çeşitleri *G. barbadense* türünün çeşitlerine göre daha verimli ve adaptasyon yetenekleri daha yüksektir. Fakat lif kalitesi (ince, uzun, sağlam) olarak ele alındığında *G. barbadense* türünün çeşitleri daha üstün gelmektedir. Bu tür verim düşüklüğü ve dar adaptasyon yeteneğine sahip olmasından dolayı ekim alanları sınırlıdır. Araştırmacılar *G. barbadense* çeşitleri ile *G. hirsutum* çeşitlerinin melezlenmesi ile hem yüksek verim hem de yüksek lif kalitesine sahip çeşitler geliştirmeyi amaçlamışlardır. *G. barbadense* türünde bulunan üstün lif özelliklerin aktarılmasına yönelik yapılan melezleme çalışmalarında istenmeyen geççilik, düşük verimlilik, küçük koza vb. özelliklerde aktarılmıştır. Bu sorunun çözümü içinde bütün bir genomun aktarılması yerine *G. barbadense*'nin bütün bir kromozom ve kromozom parçalarının *G. hirsutum* çeşitlerine aktarmaya yönelmişlerdir (Stelly ve ark., 2005). Buna yönelik yapılan ıslah çalışmaları ile *G. hirsutum* (Texas Marker-1)'e izogenik bir hata *G. barbadense* (Pima 3-79)'un kromozom çifti ya da kromozom çiftinin kolunu taşıyan disomik kromozom ikame (substitüsyon) hatları (CS-B) geliştirilmiştir (Liu ve ark., 2000).

Fenotip destekli markırlar, çevre şartlarından etkilenmediği, uzmanlık gerektirdiği ve yetersiz kaldıkları için araştırmacılar teşhislerin daha güvenilir yapılması için moleküler tabanlı markırlara yönelmişlerdir (Song ve ark., 2023). DNA moleküler markırları genom düzeyinde farklılıkları ortaya koyan ve DNA dizisinde özel bölge olarak tanımlanmaktadır (Lateef, 2015). DNA markırları direk gen üzerinde ise genik, doğrudan gen üzerinde değilse genomik markır olarak isimlendirilmektedirler. DNA moleküler markırlar organizmalarda kullanılan dokunun gelişim süresine bağlı olmadan her dokuda belirlenebildiği, değişim göstermediği, çevre şartlarından etkilenmediği, gen interaksiyonlarından (pleotropi, epistasi vb)

etkilenmediğinden kullanım alanları çok geniştir. Bundan dolayı moleküler markırlar fenotip tabanlı markırlardan daha avantajlı konumdadırlar (Arif ve ark., 2010; Lateef, 2015; Younis ve ark., 2020; Shah ve ark., 2023).

Kullanılan DNA markırları arasında en çok tercih edilen ise SSR olarak bilinen mikrosatellitlerdir. SSR markırlarının çok kullanılmasının nedenleri yüksek polimorfizme sahip olması, ko-dominant özellik göstermesi, tekrar edilebilir olması, uygulanmasının kolay ve ucuz olmasından kaynaklanmaktadır (Peng ve ark., 2021). Bu markır tekniğinin tek dezavantajı kullanılacak türün genom bilgisinin olması gerekmektedir. Günümüzde *in-silico* yöntemler ve veri tabanlarının kullanımının avantajları sayesinde geliştirilen primer çiftleri bir cinsin türleri arasında ve hatta yakın cinsler arasında aynı primerlerin çalıştığı rapor edilmektedir (Karaca ve ark., 2013, Preethi ve ark., 2020). *In-silico* yöntemlerle geliştirilen mikrosatellit markırlarının dezavantajı düşük polimorfizm göstermeleridir. SSR'ların *in-silico* veri tabanlarından geliştirilenlerde ve monomorfik markırların polimorfik markırlara dönüştürülmesinde kullanılan teknikse Cleaved Amplified Polymorphic Sequences (CAPS)-mikrosatellit yöntemidir. CAPS-mikrosatellit tekniğinde Expressed sequence tag (EST) tabanlı mikrosatellitlerde post-transkripsiyon olaylarından kaynaklanan çok büyük ve monomorfik mikrosatellit lokuslarının farklı restriksiyon enzimleri kullanılarak ortaya çıkan polimorfizme dayanan bir tekniktir. Bu teknik genelde ko-dominant markır üretmektedir. Ayrıca bu yöntem agaroz jel elektroforez ayırıştırma tekniğine uygun olması kullanımını da kolaylaştırır (İnce ve ark., 2009, İnce, 2010). Bu çalışmada monomorfik olarak bilinen 11 EST-SSR markırı 16 farklı restriksiyon enzimi ile kesilerek polimorfik özelliklerinin ortaya konması ve Pamuk kromozom substitüsyon hatlarının belirlenmesinde kullanılması amaçlanmıştır.

2. Materyal ve Yöntem

2.1. Bitki Materyali

Bu çalışmada Prof. Dr. Sukumar Saha (USDA/MSU, USA) tarafından tedarik edilen ve Stelly ve ark. (2005) tarafından geliştirilmiş olan 17 adet kromozom substitüsyon (CS-B) hattı kullanılmıştır. Bu genetik stoklar *G. barbadense* Pima 3-79'a (double haploid) ait 17 kromozom ya da kromozom kolu, TM-1'e (*G. hirsutum* L. Texas Marker-1) izogenik hat olan bir hatta aktarılmasıyla elde edilmiştir (Stelly ve ark., 2005). Her bir CS-B hattı *G. barbadense* Pima 3-79'dan bir çift kromozom, kromozom kısa kolu (Sh) veya kromozom uzun kolu (Lo) taşımaktadır. 17 CS-B, 1 TM-1 ve 1 Pima 3-79 olmak üzere toplamda 19 genotip üzerinde çalışılmıştır. Bitki materyaline ait örnekler Akdeniz Üniversitesi Ziraat Fakültesi Tarla Bitkileri Deneme Alanlarında yetiştirilerek yaprak örnekleri toplanmıştır.

2.2. DNA İzolasyonu

Bitkiler beşinci gerçek yapraklarını çıkardıktan sonra her bir bitki için steril şartlarda yaprak örnekleri toplanarak

DNA izolasyon işlemleri Karaca ve ark. (2005)'e göre gerçekleştirilmiştir.

2.3. DNA Kalite ve Miktarının Belirlenmesi

DNA kalite ve miktarının belirlenmesinde spektrofotometrik yaklaşım ile agaroz jel elektroforez yöntemi kullanılmıştır. Spektrofotometre ile ölçümde DNA örnekleri 25 kat seyreltilerek 200-300 nm arası tarama gerçekleştirilerek A₂₃₀, A₂₆₀ ve A₂₈₀ absorpsiyon değerleri ölçülmüştür.

2.4. Polimeraz Zincir Reaksiyonu (PZR)

Çalışmada kullanılan kimyasallar moleküler biyoloji grade olup Vivantis firmasından temin edilmiştir. PZR işlemlerinde GeneAmp System 9700 marka Termal Döngü Cihazından yararlanılmıştır. PZR işlemlerinde hacim 25 µL'ye ayarlanmış ve içerisinde 85 nanogram toplam genomik DNA, 0,5 µM kullanılan primer çifti, 10X buffer, 0,28 mM her bir dNTP, 2,5 mM MgCl₂ ve 1 ünite Taq DNA polimeraz (Vivantis) içeren solüsyonda gerçekleştirilmiştir. CAPS-SSR çalışmaları için Touch-Down PZR metodu uygulanmış ve ilk 10 döngü için her

döngüde 0,5 °C sıcaklık düşürülmüştür.

Ön denatürasyon için 4 dakika 94 °C, denatürasyon için 94 °C'de 20 saniye, primer bağlanma sıcaklığı 61 °C'de 30 saniye, 72 °C'de 1 dakika ve son olarak 72 °C'de 10 dakika olarak toplamda 40 döngüde gerçekleştirilmiştir.

2.5. CAPS-Mikrosatellit Analizleri

CAPS-mikrosatellit DNA markır tekniği polimorfizmin ortaya çıkarması yönünden RFLP ve SNP tekniklerinin her ikisinden de faydalanmaktadır. CAPS-mikrosatellit tekniği genik markırların elde edilmesinde kullanılabilirliği gibi genomik markırlarında elde edilmesinde kullanılabilir. Çalışmada kullanılan restriksiyon enzim isimleri, tanıma bölgeleri ve çalışma sıcaklıkları Tablo 1'de verilmiştir.

2.6. Primer Çiftleri

PZR çalışmalarında kullanılan primerin sekans ve motif bilgileri Tablo 2'de verilmiştir. Karaca ve Ince (2011) tarafından geliştirilen MK primerleri genomun ifade edilebilen kısmından geliştirilmiş markırlardır.

Tablo 1. Kullanılan restriksiyon enzimleri

No	Eim adı	Tanıma Bölgesi	Çalışma sıcaklığı	Ticari Kaynağı
1	<i>Hinf</i> I	5'...G [▼] ANTC...3' 3'...CTNA [▲] G...5'	37 °C	Bioron
2	<i>Cla</i> I	5'...AT [▼] CGAT...3' 3'...TAGC [▲] TA...5'	37 °C	Fermentas
3	<i>Rsa</i> I	5'...GT [▼] AC...3' 3'...CA [▲] TG...5'	37 °C	Fermentas
4	<i>EcoR</i> V	5'...GAT [▼] ATC...3' 3'...CTA [▲] TA G...5'	37 °C	Fermentas
5	<i>Hae</i> III	5'...GG [▼] CC...3' 3'...CC [▲] GG...5'	37 °C	Fermentas
6	<i>Hind</i> III	5'...A [▼] AGCTT...3' 3'...TTCGA [▲] A...5'	37 °C	Fermentas
7	<i>EcoR</i> I	5'... [▼] CCWGG...3' 3'...GGWCC [▲] ...5'	37 °C	Fermentas
8	<i>Aat</i> II	5'...GACGT [▼] C...3' 3'...C [▲] TGCAG...5'	37 °C	Fermentas
9	<i>Vsp</i> I	5'...AT [▼] TAAT...3' 3'...TAAT [▲] TA...5'	37 °C	Fermentas
10	<i>Hpa</i> II	5'...C [▼] CGG...3' 3'...GGC [▲] C...5'	37 °C	Fermentas
11	<i>BamH</i> I	5'...G [▼] GATCC...3' 3'...CCTAG [▲] G...5'	37 °C	Fermentas
12	<i>Hin6</i> I	5'...G [▼] CGC...3' 3'...CGC [▲] G...5'	37 °C	Fermentas
13	<i>Taq</i> I	5'...T [▼] CGA...3' 3'...AGC [▲] T...5'	65 °C	Fermentas
14	<i>Dra</i> I	5'...TTT [▼] AAA...3' 3'...AAA [▲] TTT...5'	37 °C	Fermentas
15	<i>Not</i> I	5'...GC [▼] GGCCGC...3' 3'...CGCCGG [▲] CG...5'	37 °C	Fermentas
16	<i>Nco</i> I	5'...C [▼] CATGG...3' 3'...GGTAC [▲] C...5'	37 °C	Fermentas

Tablo 2. Kullanılan primer çiftlerine ait bilgiler

Markır	Primer Sekans Dizisi (5'→3')	MOTİF
MK011	F:CCTCCTCGTTTCTTCACTGC R:CTTGTTCCATTTACCCAAAG	[TCT] ₁₂
MK048	F:TTTGGGCTTTCTTTTCTCTCTC R:AGACTTTGTGTCCCGCTCA	[CT] ₁₇
MK070	F:GAGACGGTGGTGATGATGG R:CCTTGTCAAGTGTCCGAGTTG	[AAG] ₁₆
MK095	F:AAACTGCAAACCCACACTC R:GGAGAGGCTATTCAGGGAGA	[CTT] ₅
MK098	F:TCACAAGAGGCTTTCAATGCT R:TTACACCTCCAGGCATCAA	[ATTT] ₅
MK101	F:TCATCATCATCCTCGTCTTGA R:TTATGGCCCAATCCTCTCAC	[CAT] ₁₅
MK105	F:CAAAGATGCCGAAAGAGAGG R:GTAAGATCGGCGGGTCATC	[CCG] ₁₂
MK114	F:ATGGTCATTCCGATGCTGTT R:CCAATGGTCCCTACATGACC	[CTG] ₅
MK158	F:CTTCCAGTTCCACCATAGCC R:ACCAAATCCAGGTTCCACAG	[AC] ₁₄
MK159	F:TTTGGGCTTTCTTTTCTCTCTC R:AGACTTTGTGTCCCGCTCA	[CT] ₁₇ [TCTCTT] ₄
MK173	F:GGGTCCACAGATACAGG R:GTCCAAAACCTGTCCATTAG	[TATG] ₉

2.7. CAPS-Mikrosatellit Markırlarının Belirlenmesi

CS-B'lerde kullanılan CAPS markırların belirlenmesinde 3 kriter üzerinde durulmuştur. Bu kriterler: 1) hem *G. hirsutum* hem de *G. barbadense* türünün çeşitlerinin DNA'larında amplikon üretmesi, 2) tekrar edilebilir markır ortaya koyması ve 3) agaroz jelde polimorfizmi net bir şekilde ortaya koymasındır.

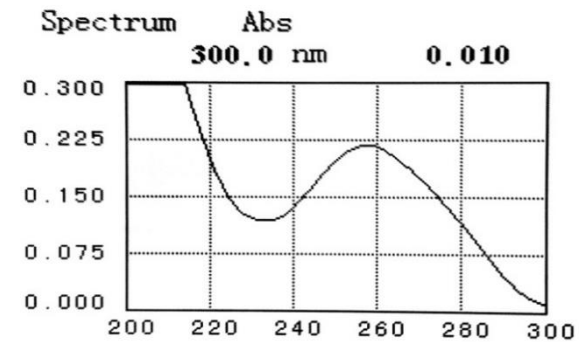
3. Bulgular ve Tartışma

3.1. DNA Kalite ve Miktarının Belirlenmesi

Toplam 19 bitkiye ait tohumlar tarla şartlarında ekilerek bitkilerden steril bir şekilde yaprak örnekleri toplanmıştır. Bitki yaprak örnekler toplanırken kaliteli DNA elde etmek amacıyla bitkinin strese girmediği sabah saatlerinde toplanmıştır. Çünkü bitki stres halinde yaprak örnekleri toplandığında polisakkarit ve fenolik bileşik miktarı fazlalaşır ve DNA izolasyonunu zorlaştırır (Karaca 2001, Aydın ve ark., 2018). Bitki yaprak dokuları -196 °C sıvı azot yardımı ile havan ve havaneli yardımıyla toz haline getirilerek DNA izolasyonu Karaca ve ark. (2005)'e göre gerçekleştirilmiştir. İzolasyonu gerçekleştirilen DNA'nın kalite ve miktarının belirlenmesinde spektrofotometrik yöntemde 25 kat seyreltilmiş olan toplam DNA'nın analizinde 200 nm ile 300 nm dalga boylarında tarama yapılmış ve A₂₃₀, A₂₆₀ ve A₂₈₀ değerleri tespit edilmiştir (Şekil 1).

Şekil 1'de spektrofotometre ile okunan değerler arasında restriksiyon enzim kullanımına uygun protein, polisakkarit ve fenolik bileşiklerden arındırılmış bir grafik çizmektedir. Saf DNA A₂₆₀/A₂₃₀ değeri yaklaşık 1,80 değerini vermesi gerekmektedir (Aydın ve ark., 2018). Tablo 3'te genomik DNA'ların spektrofotometre

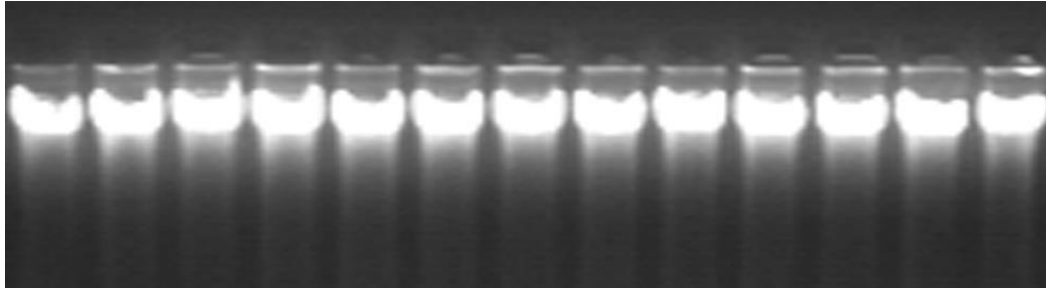
okumaları belirtilmiştir. Spektrofotometrik yöntemler ile DNA kalite ve miktarı belirlenmiş ve yapılan gözlemler sonucunda elde edilen DNA'ların hem protein hem de polisakkarit ve fenolik bileşiklerinden arındırıldığı tespit edilmiştir. Ayrıca elde edilen DNA miktarlarının da yeterli düzeyde olduğu saptanmıştır. Fakat spektrofotometrik yaklaşım ile elde edilen DNA'nın kırık olup olmadığı anlaşılamamaktadır (Karaca ve Ince, 2023). Bundan dolayı da agaroz jel elektroforez yöntemi ile bu tespit edilebilmektedir (İnce, 2010). Elde edilen DNA'ların kırık olup olmadığı anlaşılması için her bir örneğe ait 700 ng genomik DNA % 1'lik agaroz jelde 90 dk yürütülmüş ve elde edilen jel görüntüsünde DNA'nın kırık olmadığı tespit edilmiştir (Şekil 2).



Şekil 1. Spektrofotometre okuması ile genomik DNA'nın kalitesinin belirlenmesi

Tablo 3. İzolasyonu gerçekleştirilen genomik DNA spektrofotometre verileri ve genomik DNA miktarı

Materyal	A ₂₃₀	A ₂₆₀	A ₂₈₀	A _{260/280}	A _{260/230}	µg/mL
TM-1	0,124	0,241	0,132	1,82	1,93	601,3
Pima 3-79	0,149	0,321	0,173	1,85	2,15	801,3
B01	0,158	0,328	0,176	1,84	1,97	731,7
B02	0,185	0,400	0,215	1,86	2,09	906,7
B04	0,168	0,364	0,195	1,85	1,97	837,5
B05 Sh	0,155	0,324	0,174	1,84	1,98	737,9
B06	0,140	0,285	0,152	1,87	1,96	601,3
B07	0,157	0,325	0,175	1,81	1,91	718,8
B11 Sh	0,145	0,300	0,161	1,86	2,01	638,3
B12 Sh	0,176	0,375	0,201	1,84	1,99	831,3
B14 Sh	0,129	0,265	0,142	1,87	2,02	550,8
B15 Sh	0,110	0,208	0,113	1,83	1,87	454,2
B16	0,123	0,241	0,128	1,87	1,89	500,8
B17	0,127	0,251	0,134	1,87	1,97	522,1
B18	0,147	0,292	0,160	1,83	1,99	625,4
B22 Sh	0,129	0,262	0,142	1,83	1,94	577,9
B22 Lo	0,135	0,270	0,145	1,85	1,93	605,0
B25	0,143	0,270	0,145	1,85	1,86	545,8
B26 Lo	0,130	0,263	0,140	1,88	2,02	657,5

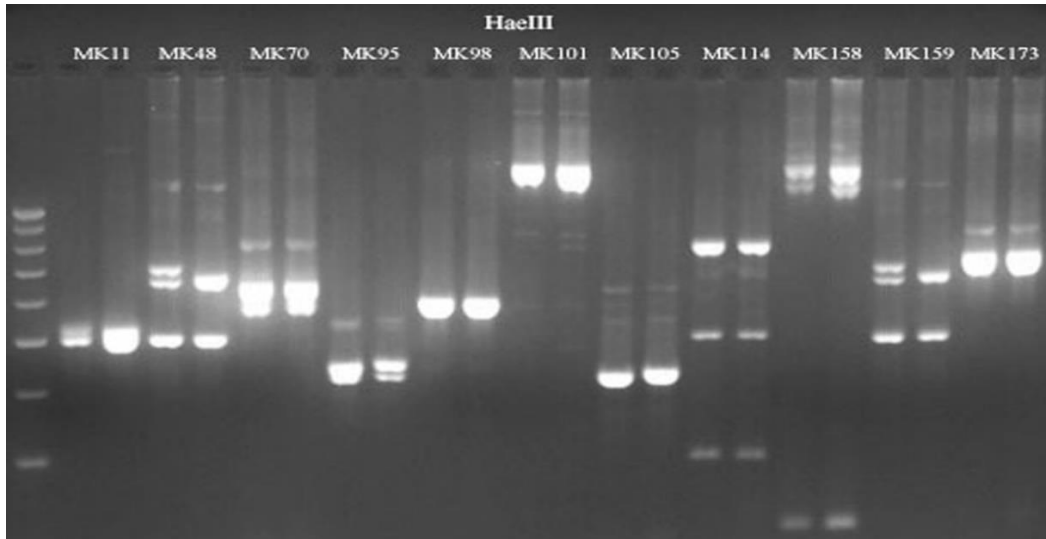


Şekil 2. Genomik DNA'nın agaroz jel elektroforez yöntemi ile belirlenmesi.

3.2. Polimeraz Zincir Reaksiyon Uygulamaları

Çalışmada 11 primer çifti TM-1 ve Pima 3-79 hattının genomik DNA'larından 8,5 µL kullanılarak (10 ng/µL stoktan) final hacmi 25 µL olacak reaksiyonda PZR içinde gerçekleştirilmiştir. 25 µL final hacim içinde 0,5 µM primer çifti konsantrasyonu, 10X *Taq* solüsyonundan 2,5 µL, her bir dNTP için 0,28 mM konsantrasyon, 2,5 mM MgCl₂ ve 1 ünite *Taq* DNA Polimeraz (Vivantis) enzimi

kullanılarak belirlenen primer ile PZR çalışmaları yapılmıştır. PZR'nin ürettiği ampliconlar jelde teyit edilerek her bir primer çiftinin ampliconları Tablo 1'de belirtilen restriksiyon enzimleri ile kullanım kılavuzuna göre işlem yapılarak gerçekleştirilmiştir. Şekil 3'te *Hae* III restriksiyon enziminin 11 MK primeri ile reaksiyonu sonucunda jel görüntüleri bulunmaktadır.



Şekil 3. *Hae* III restriksiyon enziminin 11 MK primeri ile PZR sonrası reaksiyonlarının agaroz jel elektroforez görüntüsü.

CAPS markırları ko-dominant bir markır tekniği olup özellikle 500 baz çifti (bc) üzerinde olan monomorfik markırları polimorfik markırlara dönüştüren bir markır yöntemidir (Matuszczak ve ark., 2020). Bu markır tekniği gen belirleme, genetik ilişkilerin ortaya konması, cinsiyet belirleme, organizmalarda biyotik ve abiyotik streslere karşı hassasiyeti ya da direnci belirlemede kullanılabilirler. Ayrıca uygulaması kolay ve çok maliyet gerektirmemektedir (Walkowiak ve ark., 2022;

Wang ve ark., 2023). CAPS markır tekniği bu çalışmada da kromozom substitüsyon hatlarının belirlenmesinde kullanılmıştır.

Yapılan gözlemler ve analizler sonucunda *Hae* III restriksiyon enzimi için polimorfik markırlara dönüşen pirimerler 17 CS-B hattında taranarak kromozom lokasyonlarının belirlenmesinde kullanılmıştır. Tablo 4'te her bir primer için hangi restriksiyon enziminde polimorfik olduğu belirtilmiştir.

Tablo 4. MK primerlerinin farklı restriksiyon enzim ile kesim sonuçları

Enzim/ Primer	MK Primer Çiftleri										
	MK 011	MK 048	MK 070	MK 095	MK 098	MK 101	MK 105	MK 114	MK 158	MK 159	MK 173
<i>Hinf</i> I	M	P	M	-	M	P	-	M	P	P	P
<i>Cla</i> I	-	-	-	-	M	-	-	M	-	-	-
<i>Rsa</i> I	P	P	-	-	M	P	-	-	M	P	P
<i>EcoR</i> V	-	-	M	-	M	-	-	M	M	-	-
<i>Hae</i> III	-	P	M	P	-	-	P	M	M	P	P
<i>Hind</i> III	-	-	M	-	M	-	-	-	M	M	-
<i>EcoR</i> I	-	-	-	-	-	M	-	-	M	M	-
<i>Aat</i> II	-	-	-	-	-	-	-	-	-	-	M
<i>Vsp</i> I	-	-	M	-	M	M	-	-	P	-	-
<i>Hpa</i> II	-	-	M	-	M	M	-	M	M	-	P
<i>BamH</i> I	-	-	-	-	-	-	-	-	M	-	-
<i>Hin6</i> I	-	-	M	-	-	-	-	M	M	-	-
<i>Taq</i> I			P	P							
<i>Dra</i> I			P	M	M						
<i>Not</i> I			-	P	-						
<i>Nco</i> I			-	-	-						

-= kesim bölgesinin olmadığı, M=: kesim bölgesinin olduğu ama monomorfik bant verdiği, P= kesim bölgesinin olduğu ve polimorfik bant olduğunu gösterir.

Kesim sonucunda tablo incelendiğinde MK098 primerinin kullanılan restriksiyon enzimleri arasında hiç birisi tarafından polimorfik bant oluşturmadığı gözlemlenmiştir. Bunun nedeni primerin hem *G. hirsutum* hem de *G. barbadense* için kullanılan hatların bu gen bölgesi için yüksek oranda benzerlik gösterdiği anlaşılmaktadır. MK158 primeri için ise *Hinf* I ve *Hae* III restriksiyon enzimleri tarafından polimorfik bantlar ortaya koyduğu tespit edilmiştir. *BamH* I, *Aat* II, *Not* I restriksiyon enzimleri sadece bir kesim bölgesi olduğu, *Nco* I restriksiyon enzimi için hiçbir primerde kesim bölgesinin olmadığı saptanmıştır. Primerler üzerinde en çok kesim bölgesine sahip restriksiyon enzimi *Hinf* I olarak tespit edilmiştir. Her bir primer ayrı ayrı incelendiğinde MK011 üzerinde 2, MK048 üzerinde 3, MK070 üzerinde 9, MK095 üzerinde 4, MK098 üzerinde 8, MK105 üzerinde 1, MK114 üzerinde 6, MK158 üzerinde 10, MK159 üzerinde 5 ve MK173 üzerinde 5 farklı restriksiyon enzim kesim bölgelerinin olduğu belirlenmiştir. Polimorfik primerlerin belirlenmesinde kullanılan restriksiyon enzimleri 11 MK primerinden 9 tane MK primerinde polimorfik olarak aday kullanılacak primerler olduğu belirlenmiştir. Elde edilen bilgiler değerlendirilerek TM-1, Pima 3-79 ve 17 disomik

kromozom substitüsyon hattında taramalar yapılmıştır.

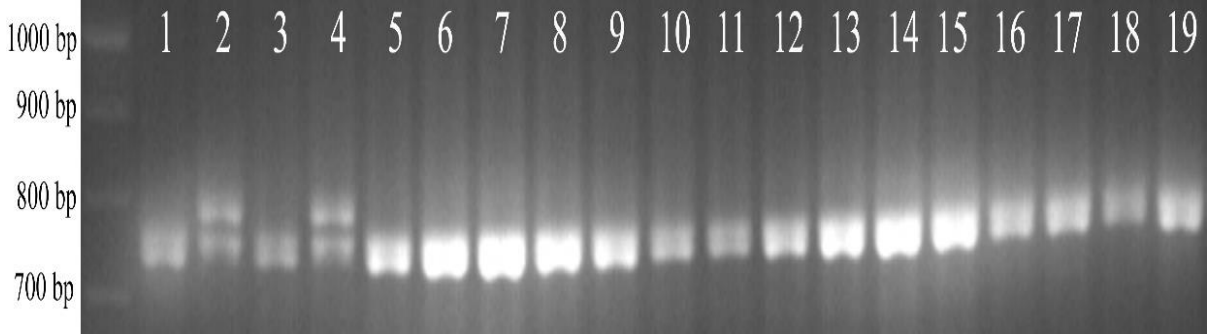
3.3. Polimorfik CAPS-Mikrosatellit Lokuslarının Tespiti

Son yıllarda kromozom substitüsyon hatlarının kullanımı genetik araç olarak çok fayda sağlamaktadır. Ayrıca ıslahçılar yeni çeşit geliştirme sürecindeki hem uzun süre hem de istenmeyen özelliklerin aktarılmasından dolayı bu sürece girmeyi pek istememektedir. Buna karşın kromozom substitüsyon hatlarının kullanımı ve sadece istenen lokusların aktarılması bu zahmeti azaltmaktadır (Saha ve ark., 2023). Kromozom substitüsyon hatlarının kullanım amaçlarından birisi de bitki büyümesindeki mikro-besin elementlerinin kromozom veya lokus düzeyinde ilişkileri incelenmiştir. Yapılan araştırmalarda kromozom substitüsyon hatlarında mikro-besin element düzeylerinde farklılıklar olduğu saptanmıştır (Bellaloui ve ark., 2020; Saha ve ark., 2023).

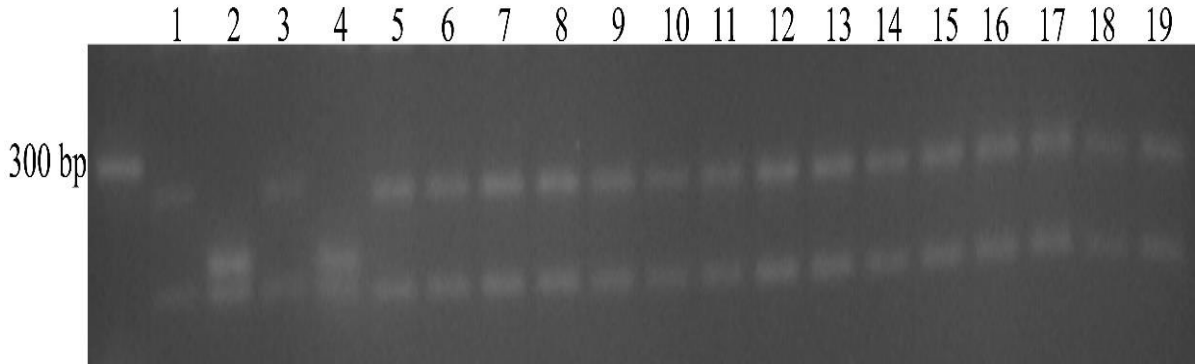
Yapılan taramalar sonucunda sadece CS-B02 nolu hat primerler tarafından tespit edilmiştir. CS-B02'nin belirlenmesinde daha önceki literatür çalışmalarında BNL1434 ve BNL3971 kodlu primerler bu hat üzerinde olduğu Gutierrez ve ark. (2009) tarafından rapor edilmiştir. Laboratuvar çalışmaları sonucunda birimizde mevcut bu primerler ile CS-B02 nolu

kromozom substitüsyon hattı teyit edilmiştir. Yapılan çalışmalar sonucunda MK070 primeri TM-1, Pima -79 ve 17 CS-B hattı PZR sonrası *Taq* I restriksiyon enzimi ile kesilmiş ve Şekil 4 ve 5'te de görüldüğü üzere CS-B02 nolu kromozom substitüsyon hattının *G. barbadense* türünün 2 nolu kromozomunu taşıdığı saptanmıştır. Aynı durumda MK048 primeri ve *Rsa* I restriksiyon enzimi kullanıldığında da CS-B02 nolu kromozom substitüsyon hattı teyit edilmektedir.

Kromozom substitüsyon hatlarının önemli özelliklerden biri niceliksel özellik lokusları ("Quantitative Trait Loci" QTL) çalışmalarında kullanımındır. Pamuk lif kalitesi ve diğer özelliklerden herhangi birinin QTL belirlenmesi yapılacak ıslah çalışmalarında da büyük önem arz etmektedir. Bundan dolayı pamuk kromozom substitüsyon hatlarının bu çalışmalarda kullanılması ve bu hatların belirlenmesi ıslah programları için çok önemlidir (Zhu et al. 2020).



Şekil 4. *Taq* I restriksiyon enzimin MK070 lokusu kullanılarak substitüsyon hatlarında analiz edilmesi (1: TM-1, 2: Pima 3-79, 3: CS-B01, 4: CS-B02, 5: CS-B04, 6: CS-B05Sh, 7: CS-B06, 8: CS-B07, 9: CS-B11Sh, 10: CS-B12Sh, 11: CS-B14Sh, 12: CS-B15Sh, 13: CS-B16, 14: CS-B17, 15: CS-B18, 16: CS-B22Sh, 17: CS-B22Lo, 18: CS-B25, 19: CS-B26Lo).



Şekil 5. *Rsa* I restriksiyon enzimin MK048 lokusu kullanılarak substitüsyon hatlarında analiz edilmesi (1: TM-1, 2: Pima 3-79, 3: CS-B01, 4: CS-B02, 5: CS-B04, 6: CS-B05Sh, 7: CS-B06, 8: CS-B07, 9: CS-B11Sh, 10: CS-B12Sh, 11: CS-B14Sh, 12: CS-B15Sh, 13: CS-B16, 14: CS-B17, 15: CS-B18, 16: CS-B22Sh, 17: CS-B22Lo, 18: CS-B25, 19: CS-B26Lo).

4. Sonuç

Çalışma kapsamında CAPS-mikrosatellit analizleri için MK primer çiftleri ile taranan TM-1 ve Pima 3-79 hatları arasında monomorfik ve 500 baz çiftinden büyük ampikon oluşturan MK011, MK048, MK070, MK095, MK098, MK101, MK105, MK114, MK158, MK159 ve MK173 lokusları kullanılmıştır. PZR ürünleri 16 farklı restriksiyon endonükleaz enzimi ile taranmıştır. Bu tarama sonucunda MK098 ve MK114 nolu primerler hariç diğer primerlerin polimorfik markırlara dönüştüğü tespit edilmiştir. Kullanılan restriksiyon enzimlerinden *Nco* I çalışmada kullanılan primerlerin oluşturmuş olduğu gen bölgelerinde herhangi bir kesim bölgesinin olmadığı analizler sonucunda ortaya konulmuştur. Kullanılan restriksiyon enzimlerinden *Rsa* I ve *Taq* I sırasıyla MK048 ve MK070 nolu primerlerin CS-B02 nolu pamuk kromozom substitüsyon hattını teyit ettiği tespit edilmiştir. Sonuç olarak ülkemiz pamuk ıslahı için önemli

olan pamuk kromozom substitüsyon hatlarının teyit edilmesi büyük önem arz etmektedir. Ayrıca EST-SSR markırları her ne kadar monomorfik olsalar da CAPS yöntemi ile polimorfik markırlara dönüştürülebileceği bu çalışma ile ortaya konulmuştur. Ülkemiz pamuk ıslahı için bu tür moleküler yaklaşımların daha yüksek bütçe ve iş hacmi ile araştırılması ve ıslah çalışmalarına katkı sağlamaları gerekmektedir.

Katkı Oranı Beyanı

Yazar(lar)ın katkı yüzdesi aşağıda verilmiştir. Tüm yazarlar makaleyi incelemiş ve onaylamıştır.

	A.A.	M.K
K	50	50
T	100	
Y		100
VTI	50	50
VAY	50	50
KT	50	50
YZ	50	50
KI	50	50
GR	50	50
PY	50	50
FA	50	50

K= kavram, T= tasarım, Y= yönetim, VTI= veri toplama ve/veya işleme, VAY= veri analizi ve/veya yorumlama, KT= kaynak tarama, YZ= Yazım, KI= kritik inceleme, GR= gönderim ve revizyon, PY= proje yönetimi, FA= fon alımı.

Çatışma Beyanı

Yazarlar bu çalışmada hiçbir çıkar ilişkisi olmadığını beyan etmektedirler.

Etik Onay Beyanı

Bu araştırmada hayvanlar ve insanlar üzerinde herhangi bir çalışma yapılmadığı için etik kurul onayı alınmamıştır.

Teşekkür ve Bilgilendirme

Bu çalışma Adnan Aydın'ın yüksek lisans çalışmasının bir parçasıdır. Çalışmanın mali bütçesi Akdeniz Üniversitesi BAP koordinasyonu tarafından 2011.02.0121.052 nolu proje tarafından karşılanmıştır.

Kaynaklar

Arif IA, Bakir MA, Khan HA, Al Farhan AH, Al Homaidan AA, Bahkali AH, Shobrak M. 2010. A brief review of molecular techniques to assess plant diversity. *Inter J Molec Sci*, 11(5): 2079-2096.

Aydin A, Ince A. G, Uygur Gocer E, Karaca M. 2018. Single cotton seed DNA extraction without the use of enzymes and liquid nitrogen. *Fresen Environ Bullet*, 27(10): 6722-6726.

Aydin A. 2023. Determination of genetic diversity of some upland and Sea Island cotton genotypes using high-resolution capillary electrophoresis gel. *Agron*, 13(9): 2407.

Bellaloui N, Saha S, Tonos JL, Scheffler JA, Jenkins JN, McCarty JC, Stelly DM. 2020. Effects of interspecific chromosome substitution in upland cotton on cottonseed micronutrients. *Plants*, 9(9): 1081.

Gutiérrez OA, Stelly DM, Saha S, Jenkins JN, McCarty JC, Raska DA, Scheffler BE. 2009. Integrative placement and orientation of non-redundant SSR loci in cotton linkage groups by deficiency analysis. *Molec Breeding* 23: 693-707.

Ince AG, Karaca M, Onus, AN. 2009. An in silico analysis of ginger expressed sequence tags for microsatellites. *AJT CAM*, 6: 340-341

Ince AG. 2010. Doku/Organ spesifik mikrosatellit dna gen içeriklerinin capsicum cdna kütüphanelerinde in silico ve in vitro yaklaşımlarla belirlenmesi. Doktora Tezi Akdeniz Üniversitesi, Antalya, Türkiye, ss: 135.

Karaca M. 2001. Characterization of cynodon spp. and gossypium spp. genomes using molecular and cytological techniques. PhD thesis, Dissertation University of Mississippi, Mississippi, USA, pp: 201.

Karaca M, Ince AG, Aydın A, Ay ST. 2013. Cross-genera transferable e-microsatellite markers for 12 genera of the *Lamiaceae* family. *J Sci Food Agri*, 93(8): 1869-1879.

Karaca M, Ince AG, Elmasulu SY, Onus AN, Turgut K. 2005. Coisolation of genomic and organelle DNAs from 15 genera and 31 species of plants. *Analytical Biochem*, 343(2): 353-355.

Karaca M, Ince AG. 2011. New non-redundant microsatellite and CAPS-microsatellite markers for cotton (*Gossypium L.*). *Turkish J Field Crops*, 16(2): 172-178.

Karaca M, Ince AG. 2023. A DNA extraction method for nondestructive testing and evaluation of cotton seeds (*Gossypium L.*). *Biochem Genet*, doi.org/10.1007/s10528-023-10496-5.

Lateef DD. 2015. DNA marker technologies in plants and applications for crop improvements. *J BioSci Med*, 3(5): 1-7.

Liu L, Saha S, Stelly D, Burr B, Cantrell R. G. 2000. Chromosomal assignment of microsatellite loci in cotton. *J Heredity*, 91(4): 326-332.

Matuszczak M, Spasibionek S, Gacek K, Bartkowiak-Broda I. 2020. Cleaved amplified polymorphic sequences (CAPS) marker for identification of two mutant alleles of the rapeseed *BnaA.FAD2* gene. *Molec Biol Reports*, 47(10): 7607-7621.

Mert M. 2007. Pamuk tarımının temelleri. TMMOB Ziraat Mühendisleri Odası, Ankara, Türkiye, ss: 282.

Peng J, Shi C, Wang D, Li S, Zhao X, Duan A, He C. 2021. Genetic diversity and population structure of the medicinal plant *Docynia delavayi* (Franch.) Schneid revealed by transcriptome-based SSR markers. *J Applied Res Med Arom Plant*, 21: 100294.

Preethi P, Rahman S, Naganeeswaran S, Sabana AA, Gangaraj KP, Jerard BA, Rajesh MK. 2020. Development of EST-SSR markers for genetic diversity analysis in coconut (*Cocos nucifera L.*). *Molec Biol Reports*, 47: 9385-9397.

Saha S, Tewolde H, Jenkins J. N, McCarty J. C, Stelly D. M. 2023. Chromosome substitution lines with improved essential mineral nutrients and fiber quality traits in Upland cotton. *Genet Resour Crop Evolut*, 2023: 1-15.

Shah RA, Bakshi P, Jasrotia A, Itoo H, Padder BA, Gupta R, Dolkar D. 2023. Morphological to molecular markers: Plant genetic diversity studies in Walnut (*Juglans regia L.*)—A Review. *Erwerbs-Obstbau*, 2023: 1-13.

Song L, Wang R, Yang X, Zhang A, Liu D. 2023. Molecular markers and their applications in marker-assisted selection (MAS) in bread wheat (*Triticum aestivum L.*). *Agri*, 13(3): 642.

Stelly D. M, Saha S, Raska D. A, Jenkins J. N, McCarty J. C, Gutierrez O. 2005. Registration of 17 germplasm lines of upland cotton (*Gossypium hirsutum*) each with a different pair of *G. barbadense* chromosome or chromosome arms substituted for the respective *G. hirsutum* chromosome or chromosome arms. *Crop Sci* 45 2663-2665.

Viot CR, Wendel JF. 2023. Evolution of the cotton genus *Gossypium* and its domestication in the Americas. *Critical Rev Plant Sci*, 42(1): 1-33.

Walkowiak M, Matuszczak M, Spasibionek S, Liersch A, Mikołajczyk K. 2022. Cleaved amplified polymorphic sequences (CAPS) markers for characterization of the LuFAD3A gene from various flax (*Linum usitatissimum L.*)

- cultivars. *Agronomy*, 12(6): 1432.
- Wang Y, Hu X, Fu L, Wu X, Niu Z, Liu M, Ru Z. 2023. Cleaved amplified polymorphic sequence (CAP) marker development and haplotype geographic distribution of TaBOR1. 2 associated with grain number in common wheat in China. *Cereal Res Commun*, 51(2): 463-470.
- Witt TW, Ulloa M, Schwartz RC, Ritchie GL. 2020. Response to deficit irrigation of morphological yield and fiber quality traits of upland (*Gossypium hirsutum* L.) and Pima (*G. barbadense* L.) cotton in the Texas High Plains. *Field Crops Res*, 249: 107759.
- Younis A, Ramzan F, Ramzan Y, Zulfiqar F, Ahsan M, Lim K. B. 2020. Molecular markers improve abiotic stress tolerance in crops: a review. *Plants* 9(10) 1374.
- Zhu D, Li X, Wang Z, You C, Nie X, Sun J, Lin Z. 2020. Genetic dissection of an allotetraploid interspecific CSSLs guides interspecific genetics and breeding in cotton. *BMC Genom*, 21(1): 1-16.



DİYARBAKIR TOPLU TAŞIMA SİSTEMİNDE OTOBÜS KULLANIMININ İNCELENMESİ VE İYİLEŞTİRME ÖNERİLERİ

Mehmet Yakup ÇEÇEN¹, Hümeysra BOLAKAR TOSUN^{1*}

¹Aksaray University, Faculty of Engineering, Department of Civil Engineering, 68100, Aksaray, Türkiye

Özet: Kent içi ulaşım sorunları gün geçtikçe artan hızla çözüm önerileri üretilmesi gereken önemli bir konudur. Bu hususta sürdürülebilir bir ulaşım çözüm önerisi politikası belirlemek şehirler için elzem olmuştur. Çünkü sürdürülebilir bir ağı oluşturulmaması ve buna paralel kent içi trafik sıkışıklığının etkisiyle araç içinde geçirilen süre, şehirlerde önemli ölçüde artmaktadır. Bu durum hem ekonomik hem de psikolojik açıdan olumsuz sonuçlara yol açmaktadır. Bu çalışma geleceğe yönelik ulaşım alanındaki sıkıntıları ortadan kaldırmak ve yenilikçi çözüm önerileri sunabilmeyi hedeflemektedir. Bu sebeplerden ötürü Diyarbakır il genelinde yapılan çalışmalarda kentin genel yapısına uygun, sürdürülebilir ve gelişmiş bir toplu taşıma sisteminin kurulması için kamu Diyarbakır Büyükşehir Belediyesinden alınan veriler ile istatistiksel analizler yapılmış, sorunlar tespit edilmiş ve geleceğe yönelik tahminlerde bulunulmuştur. Çalışma neticesinde elde edilen bulgulara göre çözüm önerileri sunulmuş ve belirlenmesi gereken politikalar hakkında değerlendirmeler yapılmıştır.

Anahtar kelimeler: Kent içi ulaşım, Toplu taşıma, Sürdürülebilir ulaşım

Examination of Bus Usage in Diyarbakır Public Transportation System and Improvement Suggestions

Abstract: Urban transportation problems are an important issue that needs to be produced with increasing speed day by day. In this regard, it has become essential for cities to determine a sustainable transportation solution proposal policy. Because the time spent in the vehicle increases significantly in cities due to the lack of a sustainable network and the parallel effect of urban traffic congestion. This situation leads to negative consequences both economically and psychologically. This study aims to eliminate the problems in the field of transportation for the future and offer innovative solutions. For these reasons, in the studies carried out throughout Diyarbakır province, statistical analyzes were made with data received from public institutions and organizations, problems were identified and predictions were made for the future in order to establish a sustainable and developed public transportation system suitable for the general structure of the city. Based on the findings obtained as a result of the study, solution suggestions were presented and evaluations were made about the policies that should be determined.

Keywords: Urban transportation, Public transportation, Sustainable transportation

*Sorumlu yazar (Corresponding author): Aksaray University, Faculty of Engineering, Department of Civil Engineering, 68100, Aksaray, Türkiye

E mail: bolakarmehmet@gmail.com (H. BOLAKAR TOSUN)

Mehmet Yakup ÇEÇEN



<https://orcid.org/0000-0002-1303-3456>

Hümeysra BOLAKAR TOSUN



<https://orcid.org/0000-0002-6710-2277>

Gönderi: 03 Ocak 2024

Kabul: 21 Şubat 2024

Yayınlanma: 15 Mart 2024

Received: January 03, 2024

Accepted: February 23, 2024

Published: March 15, 2024

Cite as: Çeçen MY, Bolakar Tosun H. 2024. Examination of bus usage in Diyarbakır public transportation system and improvement suggestions. BSJ Eng Sci, 7(2): 316-322.

1. Giriş

Ulaşım genel ve öz bir tanımla, fayda sağlamak amacıyla kişilerin ve eşyaların yer değiştirmesi anlamına gelmektedir (Ayaz ve Bakan, 2022). Ulaşımın ekonomik, emniyetli, hızlı, konforlu ve elverişli gibi koşulları yerine getirmesi için çağdaş ve ideal bir ulaşım sistemi kurulmalıdır. Çağdaş ve ideal bir ulaşım sisteminin kurulması için ise sürdürülebilir bir ulaşım planlamasının yapılması gerekmektedir (Uçar ve Eryiğit, 2020). Sanayileşmenin getirdiği kent merkezlerinin sayısının artması ve araç sayısının artması, trafikte altyapı eksikliği, çevre kirliliği ve enerji ihtiyacının artması gibi sorunlara neden olmuştur. Bu durum kent yöneticilerini toplu taşıma sistemlerinin verimliliğinin artırılması ve verimliliğinin artırılması yönünde çözüm arayışlarına yöneltmiştir (Atalay ve Biricik, 2021). Toplu taşıma sistemlerinden otobüs kullanımının bazı girdileri

ve çıktıları vardır. Sistemin girdileri hat uzunlukları, hat üzerindeki araç sayısı gibi değişkenlerdir. Sistemin çıktıları taşınan yolcu sayısı ve yakıt tüketimidir. Hatların verimli çalışıp çalışmadığını belirlemek için değişkenle birlikte değerlendirilmelidir. Kaynakların en iyi şekilde kullanılması verimlilik olarak tanımlanmaktadır (Karlaftis ve Tsamboulas, 2012). Toplu taşıma sistemlerini doğru kullanmak çevre, sağlık ve ekonomi için oldukça önemlidir. Bu yüzden, toplu taşıma operasyonunun doğru değerlendirilmesi, analiz edilmesi ve çözümlenmesi, mevcut önemli sorunları planlama açısından yararlıdır (Atalay ve Biricik, 2022). Şehir içi toplu taşıma hizmetleri son yıllarda çoğunlukla kamu tarafından sunulmaktadır. Ancak toplu taşıma sistemlerinin sosyal çıktılarına sıkça vurgu yapılması, sistemin dolaylı olarak ekonomik boyutuna etkisi olduğunun kanıtıdır (Güner, 2017). Toplu taşıma



sistemlerinin performansı, kamusal ihtiyaçların daha ekonomik ve verimli bir şekilde karşılanabilmesi açısından büyük önem taşımaktadır. (Güner, ve ark., 2017). Toplu taşımaya ilişkin mevcut değerlendirmeler, kentler üzerindeki etkilerinin diğer ulaşım araçlarından farklı olduğunu ortaya koymaktadır. Özel araç kullanımına nazaran toplu otobüs kullanımı özellikle büyük şehirlerdeki hava kirliliğinin azaltılmasına yardımcı olmaktadır. Hava kirliliğinin yanısıra maliyet unsuru da otobüs kullanımını önemli kılmaktadır. Glaeser ve ark. (1992) toplu taşımının kentsel eşitsizlik üzerindeki etkisini vurgulamışlardır. Bir yandan, arabaya dayalı hareketlilik çok pahalı olduğundan, toplu taşımının iyi olduğu Amerikan şehirlerinde yoksulların hareketliliği daha yüksek olduğunu belirtmişlerdir. Sürdürülebilir bir ulaşım planlaması ile karayolu ulaşımı, toplu taşıma, bisiklet yolları ve yaya yolları gibi farklı ulaşım modüllerinin birbiri ile uyumlu çalışması sonucuna varılmakta ve bu sayede kent içi ulaşımında başarılı bir sonuca ulaşılmaktadır. Bu başarılı sonuçla beraber kent içi ulaşımında stres, zaman kaybı ve kaygı azalırken, kent genelinde daha sürdürülebilir bir ulaşım sağlanmış olmaktadır (Ağaoğlu ve ark., 2021).

Kapsamlı ve sürdürülebilir bir amaç doğrultusunda, bilimsel çalışmalara konu olan kent içi ulaşım planlamalarında toplu taşıma sistemlerine özellikle önem verilmektedir. Toplu taşıma sistemlerinde otobüs kullanımı, birçok avantajıyla gelecekteki kentsel ulaşım için umut vericidir. Öncelikle merkezi bir sistemdir, kontrol edilir ve istek üzerine dinamik araç paylaşımı sağlayabilir. İkinci olarak, özel arabalar ve taksilere oranla fiyat çok daha düşüktür ve son olarak, trafik paylaşımını iyileştirmede otobüs kullanımı kapasitesi çok daha büyüktür (Zhu, ve ark., 2016). Bunlara ek olarak toplu taşıma da otobüs kullanımı, kentlerde yapılan ulaşımlarda kent içi trafik sıkışıklığını ortadan kaldırmakta enerji ve zamandan tasarruf sağlamakta, doğaya ve çevreye daha az zarar vermekte ve stres ve kaygıyı azaltmaktadır. Bu sebeplerden ötürü kent içi ulaşımında ve kent içi ulaşım sorunlarının ortadan kaldırılmasında yapılacak en önemli adım toplu taşıma sistemlerinin geliştirilmesi ve özendirilmesidir (Akbulut, 2016).

Kent içi ulaşım sorunlarının ekonomi, toplum ve çevre üzerindeki olumsuz etkileri (Ağaoğlu ve Başdemir, 2019):

1. Trafik sıkışıklığına bağlı olarak zaman, yakıt gibi ekonomik kayıplar,
2. Maddi ve ölümlü kazalar sonucu oluşan ekonomik ve manevi kayıplar,
3. Trafikte meydana gelen tartışma ve kavgaların yarattığı stres ve olumsuz hissiyatlar,
4. Petrol ve türevi yenilenemeyen enerji kaynaklarının tüketimiyle oluşan riskler,
5. Sera gazlarının oluşumu, asit yağmurları ve iklim değişimleri,
6. Trafik kaynaklı gürültü, görsel kirlilik ve fiziki tehlikelerdir.

Kent içi ulaşım sorunlarından meydana gelen bu olumsuz etkilerin ortadan kaldırılması için yapılan bilimsel çalışmalarda da belirtildiği üzere sürdürülebilir ulaşım planlamaları yapılmalı ve bu bağlamda toplu taşımaya özellikle önem verilmeli, geliştirilmeli ve özendirilmelidir. Toplu taşıma sistemlerinin özendirilmesinde ise çekme ve itme politikalarının izlenmesi önem arz etmektedir (Altuntaş ve Eyigün, 2021).

Çekme politikaları, yolcuların kent içi ulaşımında otomobil yerine toplu taşıma sistemlerini tercih etmelerini sağlamak üzere uygulanan ve asıl amacı toplu taşıma kullanımını arttırıp, mevcut sistemlerin hizmet kalitesini arttırmak olan strateji ve uygulamalar bütünüdür. Çekme politikalarının başarıya ulaşabilmesi için toplu taşımaya olan güvenin sağlanması ve toplu taşıma sistemlerinin geliştirilip insanların kaliteli bir sistem varlığına inanması gerekmektedir (Cirit, 2014).

Çekme politikaları kapsamında (Koç, 2019):

1. Otobüs sistemleri,
2. Metrobüs sistemleri,
3. Metro sistemleri,
4. Hafif raylı sistemler ve tramvay sistemleri,
5. Bisiklet sistemleri,
6. Yaya ve yürüme sistemleri yer almaktadır.

Tüm bu sistemlerin kentlerin yapısına uygun olarak inşa edilmesi ve birbirleri ile entegre edilmiş olarak çalışması durumunda, çekme politikaları amacına ulaşmış olmaktadır. Amacına ulaşmış bu politikalar sonucu kent içi ulaşım sorunları çözülmüş olup kent içi trafik yoğunluğunu rahatlatmış olmaktadır.

İtme politikalarının asıl amacı; yolcuların otomobil kullanımını azaltmak ve yolcuları toplu taşıma sistemlerine itmektir. Bu sayede kent içi trafik yoğunluğunu en aza indirip, yakıt tasarrufu sağlamaktır (Uğurlar, 2019).

İtme politikaları kapsamında (Aydın ve Aydın, 2017):

1. Yol ücretlendirme,
2. Trafik yavaşlatma,
3. Yakıt/taşıt vergilerinin düzenlenmesi
4. Park et-bin uygulamaları yer almaktadır.

Kent içi ulaşım, insanların günlük yaşamlarını sürdürebilmeleri için gerekli olan iş, eğitim, sağlık hizmetleri gibi temel ihtiyacı karşılayan kritik bir role sahiptir. Fakat bilim ve sanayinin gelişimiyle beraber hızla artan nüfus ve mobilite, kent içi ulaşım sistemlerini olumsuz etkileyecek çeşitli temel sorunları da beraberinde getirmektedir (Akbulut, 2016).

Kent içi ulaşımın temel sorunları şu şekilde sıralanabilir (Acar, 2004):

1. Trafik sıkışıklığı ve yoğunluk,
2. Nüfus artışı,
3. Özel araç kullanımının artması,
4. Yetersiz toplu taşıma hizmetleri,
5. Ulaşım altyapı eksiklikleri,
6. Otopark yetersizliği,
7. Bisiklet ve yaya yollarının eksiklikleri,
8. Akıllı ulaşım sistemlerinin eksiklikleri,

9. Eğitim eksikliği ve trafik kurallarına uymama. Genel bir özetle bilim ve sanayinin gelişimiyle beraber kentlere yoğun bir göç yaşanmıştır. Bu nüfus yoğunluğu ile kentlerde trafik ve ulaşım sorunları baş göstermiştir (Adıgüzel ve ark., 2015). Bu sorunların çözülmemesi durumunda oluşacak negatif etkileri toplum, çevre ve ekonomi üzerinde şiddetli bir biçimde görmemiz kaçınılmaz olmaktadır. Bu sebeplerden dolayı merkezi ve yerel yönetimlerin, şehrin yapısına uygun kapsamlı ulaşım planlarının yapılması gerekmektedir (Aliefendioğlu ve Bostancı, 2018). Yapılacak ulaşım planlamalarında 'sürdürülebilirlik' ana fikir olmalı ve toplu ulaşımın geliştirilip kullanılması üzerinde şiddetle durulmalıdır (İlgazi, 2018). Bu kapsamda Diyarbakır ilinin toplu ulaşım bilgilerini analiz edip çözümü için sürdürülebilir fikirler ortaya çıkarmak başlıca amacımız olmuştur.

2. Materyal ve Yöntem

Bu çalışmanın amacı Diyarbakır ili otobüs kullanım istatistiklerinin incelenerek durum tespiti yapmaktır. Çalışmada, kullanım türü, hatlar detayında aylık olarak otobüs kullanım değişimleri derinlemesine incelenmiştir. Ortalama, standart sapma, basıklık ve çarpıklık gibi tanımlayıcı istatistiksel hesaplamalar ile betimleme yapılmıştır (Pallant, 2017). Araştırmanın anlam düzeyi $P < 0,05$ olarak belirlenmiştir. Araştırmada toplanan veriler istatistiksel paket programı (SPSS 20.0) aracılığıyla analiz edilip sonuçlar yorumlanmıştır. Hat, bilet türü, aylar bazında karşılaştırma testleri yapılarak otobüs kullanımı detaylıca analiz edilmiştir. Son olarak elde edilen sonuçlar %95 güven düzeyinde değerlendirilmiştir.

Diyarbakır Büyükşehir Belediyesi Ulaşım Daire Başkanlığından alınan veriler ile:

- En yoğun ve sessiz hatlar,
- En yüksek ve en düşük sefer sayıları,
- Tam, öğrenci, indirimli ve serbest gibi kart tipi yolcu sayıları,
- Kart tipine göre genel hasılat verileri,
- Ocak-Aralık ayları arası 12 aylık yolcu verileri

istatistiği gibi analizler yapılmış olup bu analizler sonucu bilimsel çıkarımlar yapılmıştır.

3. Bulgular ve Tartışma

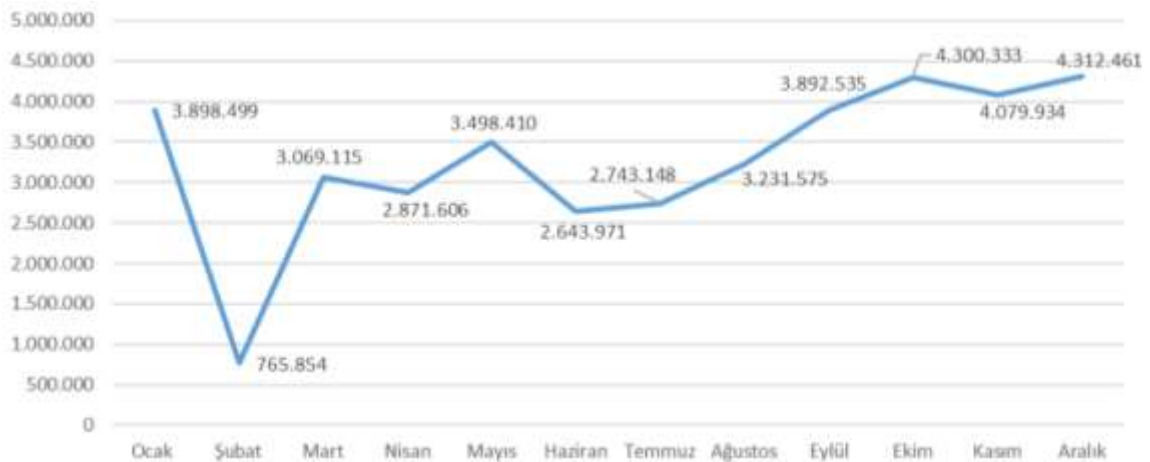
Şekil 1 tüm hatların, toplam yolcu sayılarını aylık olarak göstermektedir.

Şekil 1, Diyarbakır ilinde 01.07.2022 ile 01.07.2023 tarihleri arasında aylara göre yolcu sayısı ve bu yolcu sayılarının getirdiği hasılatı göstermektedir. Normal binişler, tüm aylarda en yüksek yolcu sayısı ve hasılatı sahiptir. En yüksek yolcu sayısı Ekim ayında 2935997, en düşük yolcu sayısı ise Şubat ayında 477207'dir. Hasılat da benzer bir dağılım göstermektedir. Tablo 1 hatların aylara göre sefer sayılarını göstermektedir (DUAP, 2023).

Tablo 1. Aylara göre sefer sayıları

	n	%
Ocak	525	8,1
Şubat	463	7,2
Mart	581	9,0
Nisan	574	8,9
Mayıs	617	9,5
Haziran	616	9,5
Temmuz	518	8,0
Ağustos	531	8,2
Eylül	523	8,1
Ekim	513	7,9
Kasım	498	7,7
Aralık	516	8,0

Tablo 1, Diyarbakır ilinde 01.07.2022 ile 01.07.2023 tarihleri arasında düzenlenen aylık sefer sayısını ve bu sefer sayılarının toplam sefer sayısına oranını göstermektedir. Analiz edildiğinde, bu bir yıllık dönemde toplam 6,484 sefer düzenlendiği görülmektedir. Aylık ortalama sefer sayısı 540,33 olarak hesaplanmıştır. Mayıs ve Haziran ayları, her biri %9,5 oranında ve sırasıyla 617 ve 616 sefer ile en yoğun aylar olarak öne çıkmaktadır. Diğer yandan, Şubat ayı 463 sefer ve %7,2 oranı ile en sessiz ay olarak dikkat çekmektedir.



Şekil1. Hatların aylık olarak toplam yolcu sayısı.

Yaz aylarında (Haziran, Temmuz, Ağustos) toplam 1,663 sefer düzenlenmiştir. Kış aylarında (Aralık, Ocak, Şubat) ise toplam 1504 sefer düzenlenmiştir. Bu durum, yaz aylarında kış aylarına göre daha fazla sefer düzenlendiğini gösterir. Tablo 2 kart tipine göre kullanım oranlarını göstermektedir.

Tablo 2. Yolculuk için kullanılan kart tipine göre sefer sayısı

	n	%
Ücretsiz	1555	24,0
Tamkart	900	13,9
Öğrenci	897	13,9
İndirimli	890	13,7
Kt_230	789	12,2
Sınırlı Ücretsiz Kt49	766	11,8
Emv	295	4,6
Adliye Personel	271	4,2
Diğer	112	1,7

Diğer:

- 2 Binişlik UL Kart
- Sürücü Harcama (İlçe Araçları)
- Sürücü_Harcama_Kartı
- Adliye 500 TL
- KT_0
- Belediye Bonuslu Sürücü Kartı 1.50 TL
- BAYİ KARTI
- Aylık belirli sayıda biniş hk.
- KT_32

Tablo 2, Diyarbakır ilinde 01.07.2022 ile 01.07.2023 tarihleri arasında yolculuk için kullanılan kart tipine göre kullanım sayısını ve bu kullanım sayılarının toplam kullanım sayısına oranını göstermektedir.

Ücretsiz kart tipi, 1555 sefer ile en yüksek sefer sayısına sahiptir ve toplam sefer sayısının %24,0'ını oluşturmaktadır. Bu, ücretsiz kart tipinin oldukça yaygın olarak kullanıldığını göstermektedir.

Tamkart ve Öğrenci kart tipleri, sırasıyla 900 ve 897 sefer ile diğer yüksek sefer sayılarına sahip kart tipleridir. Bu kart tipleri toplam sefer sayısının sırasıyla %13,9 ve %13,9'unu oluşturmaktadır.

Diğer kart tipi, 112 sefer ile en düşük sefer sayısına sahiptir ve toplam sefer sayısının %1,7'sini oluşturmaktadır. Bu kart tipi altında 2 Binişlik UL Kart, Sürücü Harcama (İlçe Araçları), Sürücü_Harcama_Kartı, Adliye 500 TL, KT_0, Belediye Bonuslu Sürücü Kartı 1.50 TL, BAYİ KARTI ve Aylık belirli sayıda biniş hk. gibi çeşitli alt kategoriler bulunmaktadır. Tablo 3 kart tipine göre yolcu sayısı ve hasılat oranlarını göstermektedir.

Tablo 3, Diyarbakır ilinde 01.07.2022 ile 01.07.2023 tarihleri arasında düzenlenen sefer başına yolcu sayısı ve bu yolcu sayılarının getirdiği hasılatı göstermektedir. Normal binişler, toplam 25568179 adet biniş ve 118375461 TL hasılat ile en büyük paya sahiptir. Bu, toplam yolcu sayısının %63,1'ini ve toplam hasılatın %78,8'ini oluşturmaktadır. Ardışık binişler, toplam

5258750 adet biniş ve 29520550 TL hasılat ile ikinci en büyük paya sahiptir. Bu, toplam yolcu sayısının %13,0'ini ve toplam hasılatın %19,6'sını oluşturmaktadır.

Ücretsiz binişler, toplam 8297581 adet biniş ile üçüncü en büyük paya sahiptir. Bu, toplam yolcu sayısının %20,5'ini oluşturmaktadır. Aktarma binişler, toplam 1134545 adet biniş ve 2446734 TL hasılat ile dördüncü en büyük paya sahiptir. Bu, toplam yolcu sayısının %2,8'ini ve toplam hasılatın %1,6'sını oluşturmaktadır. Abonman binişler, toplam 211111 adet biniş ve 17993 TL hasılat ile en düşük paya sahiptir. Bu, toplam yolcu sayısının %0,5'ini ve toplam hasılatın %0,01'ini oluşturmaktadır. Tablo 4 yolcuların kullandığı kart tipi dağılımını göstermektedir.

Tablo 3. Yolcu sayısı istatistikleri ve hasılat oranları

	Tüm Hatlar için Toplan Kullanılan Sefer Sayısı	Hasılat TL
Normal Biniş Adet	6475	25568179
Normal Biniş Tutar	6475	118375461
Ardışık Biniş Adet	6475	5258750
Ardışık Biniş Tutar	6475	29520550
Ücretsiz Biniş Adet	6475	8297581
Aktarma Biniş Adet	6475	1134545
Aktarma Biniş Tutar	6475	2446734
Abonman Biniş Adet	6475	211111
Abonman Biniş Tutar	6475	17993
Genel Toplam Biniş Adet	6475	40470170
Genel Toplam Biniş Tutar	6475	150360738

Tablo 4, Diyarbakır ilinde 01.07.2022 ile 01.07.2023 tarihleri arasında aylara göre yolcuların kullandığı kart tipi dağılımını göstermektedir. Ücretsiz kart kullanımı tüm aylarda en yüksek orana sahiptir. Ocak ve Ağustos aylarında ücretsiz kart kullanım oranı %25,6 ile en yüksektir. Mart ayında ise %22,5 ile en düşüktür. Tamkart, Öğrenci ve İndirimli Kart Kullanımı: Tamkart, Öğrenci ve İndirimli kart kullanım oranları birbirine oldukça yakındır. Bu kart tiplerinin kullanım oranları tüm aylarda %13 ile %15 arasında değişmektedir. Kt_230 ve Sınırlı Ücretsiz Kt49 Kart Kullanımı: Kt_230 ve Sınırlı Ücretsiz Kt49 kart kullanım oranları da birbirine oldukça yakındır. Bu kart tiplerinin kullanım oranları tüm aylarda %10 ile %13 arasında değişmektedir. Emv kart kullanımı Mart, Nisan ve Mayıs aylarında %10 ile %13 arasında bir orana sahiptir. Ancak diğer aylarda kullanım oranı %0'dır. Adliye Personel kart kullanım oranı tüm aylarda %2 ile %5 arasında değişmektedir. Diğer kart kullanımı ise Mart, Nisan, Mayıs ve Kasım aylarında %0,3 ile %1,9 arasında bir orana sahiptir. Ki Kare testi, kart tipi kullanım oranlarının aylar arasında anlamlı bir farklılık gösterip göstermediğini test etmek için kullanılmıştır.

Tablo 4. Aylara göre yolcuların kullandığı kart tipi dağılımı

	Ücretsiz	Tamkart	Öğrenci	İndirimli	Kt_230	Kt_49	Emv	Adliye	Diğer
Ocak	25,5	14,7	14,5	14,5	12,8	12,8	0,0	4,8	0,6
Şubat	25,3	15,8	15,8	15,1	11,7	11,0	2,2	2,8	0,4
Mart	22,5	13,4	13,4	13,4	11,5	11,7	10,2	3,4	0,3
Nisan	22,3	13,4	13,4	13,2	11,7	11,0	10,5	4,2	0,3
Mayıs	21,6	13,1	13,3	13,3	11,5	10,2	12,5	3,9	0,6
Haziran	21,1	13,3	13,3	13,1	11,0	10,2	13,0	3,6	1,3
Temmuz	24,3	14,1	13,5	13,5	11,6	12,4	1,7	4,6	4,2
Ağustos	25,6	13,6	13,6	13,6	12,6	12,6	0,0	4,5	4,0
Eylül	25,2	13,6	13,6	13,6	12,8	11,9	0,0	4,6	4,8
Ekim	25,0	14,0	14,0	13,8	13,3	13,1	0,0	4,9	1,9
Kasım	25,3	14,3	14,3	14,3	13,5	12,9	0,0	4,0	1,6
Aralık	26,0	14,1	14,1	14,0	12,8	13,0	0,0	5,0	1,0

Ki Kare test sonucu 540,335 ve P değeri 0,000 olarak bulunmuştur. Bu, kart tipi kullanım oranlarının aylar arasında anlamlı bir farklılık gösterdiğini ifade etmektedir. Ek Tablo 5 hatların aylık olarak taşıdığı yolcu sayılarını göstermektedir.

Ek Tablo 5'e göre, her ayın en yoğun kullanılan hatları sıralanmıştır. Bu hatlar, genellikle şehrin en önemli bölgelerinden geçen, yoğun trafiğe sahip bölgeleri kapsayan veya çok sayıda durak içeren hatlardır.

3.1. Ocak

En yoğun hatlar: A3, A7, E1, AZ, A1, CE2, E2, Z1, E8, C5.
Ocak ayında, A3 ve A7 hatları öne çıkıyor. Bu, kış aylarında bu hatların yoğun kullanıldığını gösterir. Şehir merkezine veya önemli noktalara ulaşım sağlayan bu hatlar, kış aylarında insanların daha fazla toplu taşıma kullanmasına neden olabilir.

3.2. Şubat

En yoğun hatlar: A7, C5, Z1, E2, A3, AZ, A1, CE2, E1, Z6.
Şubat ayında da A7 hattı öne çıkıyor. Bu, kış aylarında bu hattın popülerliğinin devam ettiğini gösterir. Şubat ayında C5 ve Z1 hatları da yoğun kullanılıyor, bu da bu hatların önemli bir ulaşım alternatifi olduğunu gösterir.

3.3. Mart

En yoğun hatlar: A7, A3, AZ, E1, C5, A1, CE2, Z1, E8, Z5.
Mart ayında A7 ve A3 hatları yine öne çıkıyor. Bu, bu hatların bahar aylarında da popüler olduğunu gösterir. Mart ayında Z5 hattının da yoğun kullanıldığını görüyoruz, bu da bu hattın önemli bir ulaşım alternatifi olduğunu gösterir.

3.4. Nisan

En yoğun hatlar: A3, A7, AZ, E1, A1, CE2, E2, E8, Z1, B8.
Nisan ayında A3 ve A7 hatları yine öne çıkıyor. Bu, bahar aylarında bu hatların popülerliğinin devam ettiğini gösterir. Nisan ayında B8 hattının da yoğun kullanıldığını görüyoruz, bu da bu hattın önemli bir ulaşım alternatifi olduğunu gösterir.

3.5. Mayıs

En yoğun hatlar: AZ, A7, E1, A1, CE2, E8, Z5, A2, A3, B8.
Mayıs ayında AZ hattı en öne çıkıyor. Bu, ilkbahar ve yaz aylarının başında bu hattın popülerliğinin arttığını gösterir. A2 ve B8 hatları da yoğun kullanılıyor, bu da bu hatların önemli bir ulaşım alternatifi olduğunu gösterir.

3.6. Haziran

En yoğun hatlar: A3, E1, A1, CE2, E8, Z5, AZ, A7, A2, B8.
Haziran ayında, A3 ve E1 hatları öne çıkıyor. Bu, yaz aylarının başlangıcında bu hatların yoğun kullanıldığını gösterir. A3, E1 ve A1 hatları şehir merkezine veya önemli noktalara ulaşım sağladığı için, yaz aylarında bu hatlar üzerindeki yoğunluk artabilir.

3.7. Temmuz

En yoğun hatlar: A3, E1, AZ, A1, E8, Z5, B8, A7, A2, C5.
Temmuz ayında, A3 ve E1 hatları yine en yoğun hatlar arasında yer alıyor. Yaz aylarında şehir içi ulaşımın daha yoğun olduğu görülüyor. A1, AZ ve E8 hatları da önemli bir rol oynuyor.

3.8. Ağustos

En yoğun hatlar: A3, AZ, E1, A1, E8, Z5, A7, B8, A2, C5.
Ağustos ayında, A3 ve AZ hatları öne çıkıyor. Yaz aylarında bu hatların yoğun kullanılması, insanların tatil dönemlerinde şehir içinde daha fazla seyahat ettiğini gösterir. E8 ve Z5 hatları da yoğun kullanılan hatlar arasında yer alıyor.

3.9. Eylül

En yoğun hatlar: A3, A7, E1, AZ, A1, E8, Z1, Z5, B8, C5.
Eylül ayında, A3 ve A7 hatları yine en yoğun hatlar arasında yer alıyor. Yaz aylarının sona ermesiyle birlikte, şehir içi ulaşımın hala yoğun olduğu görülüyor. E1, AZ ve A1 hatları da önemli bir rol oynuyor.

3.10. Ekim

En yoğun hatlar: A7, A3, AZ, E1, A1, E8, Z1, Z5, B8, C5.
Ekim ayında, A7 ve A3 hatları en yoğun hatlar arasında yer alıyor. Sonbaharın başlangıcında bu hatların yoğun kullanılması, insanların hava koşulları nedeniyle daha fazla toplu taşıma kullanmaya başladığını gösterir. E1, AZ ve A1 hatları da önemli bir rol oynuyor.

3.11. Kasım

En yoğun hatlar: A7, A3, AZ, E1, A1, E8, Z1, C5, Z5, B8.
Kasım ayında, A7 ve A3 hatları yine en yoğun hatlar arasında yer alıyor. Sonbaharın devamında bu hatların yoğun kullanılması, insanların soğuk hava koşullarında daha fazla toplu taşıma kullanmaya devam ettiğini gösterir. E1, AZ ve A1 hatları da önemli bir rol oynuyor.

3.12. Aralık

En yoğun hatlar: A7, A3, AZ, E1, A1, CE2, E8, Z5, C5, Z1.

Aralık ayında, A7 ve A3 hatları yine en yoğun hatlar arasında yer alıyor. Kış aylarının başlangıcında bu hatların yoğun kullanılması, insanların soğuk hava koşullarında daha fazla toplu taşıma kullanmaya devam ettiğini gösterir. E1, AZ ve A1 hatları da önemli bir rol oynuyor.

Çalışmada görüldüğü üzere bir hat için ortalama talep çok yüksek olabilmektedir. Fakat bu hatta ait talep yılın farklı aylarında ve mevsimlerinde büyük dalgalanmalar oluşturuyorsa, bu güzergahta inşa edilecek yeni bir otobüs hattı yatırımı yılın bazı dönemlerinde, işletme maliyetinden daha düşük bir maliyetle çalışmasını neden olabilir (Özsuysal, ve ark., 2011). Aylara göre daha dengeli bir dağılım için belirlenebilecek politikalar, verimliliği en etkin kılacak ve ülke ekonomisine büyük oranda katkı sağlayacaktır.

4. Sonuç

Çalışma sonuçları incelendiğinde, belli güzergahlarda ve belli aylarda yolcu sayısı önemli ölçüde fazlalık göstermiştir. Bu artışla beraber belirli zamanlarda trafik yoğunluğu aşırı artmış ve otobüsle seyahat elverişliliğini yitirmiştir. Bu sonuçlar ışığında bir dizi önlemler alınması ve iyileştirmelerin yapılması kaçınılmaz bir son olmuştur. Bunun için alınabilecek önlemler şu şekilde sıralanabilir:

- Sefer sayısının dağılımına bakıldığında, bazı hatlarda çok daha fazla sefer düzenlendiği, bazı hatlarda ise oldukça az sefer düzenlendiği görülmektedir. Bu durum, hatlardaki talep yoğunluğunun farklılık gösterdiğini ve bazı hatlarda sefer sayısının artırılması gerekebileceğini göstermektedir.
- A3, A7, AZ, E1 ve A1 hatları şehir içi ulaşımda sürekli olarak yoğun kullanılan hatlardır. Bu hatlar şehir merkezi ve önemli noktalara ulaşım sağladığı için, yıl boyunca yoğun kullanılmaktadır. Bu yoğun kullanımdan dolayı yukarıda belirtilen hat güzergahına ek otobüs seferleri ve bu hatları rahatlatacak yeni güzergahlar-seferler eklenmelidir.
- Aylık toplam biniş sayılarına bakıldığında, en yoğun kullanımın kış aylarında olduğunu görmekteyiz. Bunun başlıca sebepleri; yağışlı havalarda toplu ulaşım ile seyahat ve üniversite öğrencilerinin sınav dönemlerinin olmasıdır. Bu analiz verisine göre kış aylarında ek seferler ile yolcuların ulaşımı rahatlatılmalıdır.
- Aylık toplam biniş sayılarına bakıldığında, en sakin ayların ise yaz aylarında olduğu görülmektedir. Bunun başlıca sebepleri; güneşli havalarda vatandaşların yaya ulaşımını kullanmaları ve üniversitenin kapalı olmasında kaynaklanmaktadır. Bu analiz sonucuna göre seferlerin azaltılması ekonomik tasarruf ve trafik yoğunluğunun azaltılması noktasında faydalı olacaktır.
- Emv binişleri yani kredi kartı ile temassız seyahatin oranlarına bakıldığında çok düşük kaldığı

görülmektedir. Bu analiz sonucuna göre yerel yönetimlerinin bu hususu reklam ve afişlerle vatandaşlara tanıtmasının önemli olacağı düşünülmektedir.

Katkı Oranı Beyanı

Yazar(lar)ın katkı yüzdesi aşağıda verilmiştir. Tüm yazarlar makaleyi incelemiş ve onaylamıştır.

	M.Y.Ç.	H.B.T.
K	90	10
T		100
Y	100	
VTI	100	
VAY	100	
KT	80	20
YZ	80	20
KI	80	20
GR	80	20
PY	80	20
FA	80	20

K= kavram, T= tasarım, Y= yönetim, VTI= veri toplama ve/veya işleme, VAY= veri analizi ve/veya yorumlama, KT= kaynak tarama, YZ= Yazım, KI= kritik inceleme, GR= gönderim ve revizyon, PY= proje yönetimi, FA= fon alımı.

Çatışma Beyanı

Yazarlar bu çalışmada hiçbir çıkar ilişkisi olmadığını beyan etmektedirler.

Etik Onay Beyanı

Bu çalışmada hayvanlar ve insanlar üzerinde herhangi bir çalışma yapılmadığı için etik kurul onayı alınmamıştır.

Destek ve Teşekkür Beyanı

Makale verileri Diyarbakır Büyükşehir Belediyesinden alınmıştır.

Kaynaklar

- Acar İH. 2004. Kent içi ulaşımda sorunlar ve çözümler. Türkiye Müh Hab, 429: 33-36.
- Adigüzel F, Toroğlu E, Kaya Ö. 2015. Kentsel gelişme ile ulaşım ilişkisi: Adana örneği. Turkish Stud, 10(6): 27-46.
- Ağaoğlu MN, Başdemir H. 2019. Şehir içi ulaşım sorunları ve çözüm önerileri. Gaziosmanpaşa Bil Araş Derg, 8(1): 27-36.
- Ağaoğlu MN, Korkmaz F, Alakara EH. 2021. Sürdürülebilir ulaşım ve bisiklet yollarının planlanması: Sivas Cumhuriyet Üniversitesi yerleşkesi örneği. Gaziosmanpaşa Bil Araş Derg, 10(2): 140-155.
- Akbulut F. 2016. Kentsel ulaşım hizmetlerinin planlanması ve yönetiminde sürdürülebilir politika önerileri. Kastamonu Üniv İİBF Derg, 11(1): 336-355.
- Aliefendioğlu Y, Bostancı S. 2018. Yerel yönetimlerde raylı sistem yatırımlarının yapılabilirliği: Ankara Büyükşehir Belediyesi Batıkent-Sincan-Törekent metro hattı örneği. Sos Bil Derg, 5(21): 117-142.
- Altuntaş S, Eyigün Y. 2021. Sürdürülebilir kent içi ulaşım politikaları raylı sistemler örneği. İstanbul Ticaret Üniv Teknoloji Uyg Bil Derg, 3(2): 217-233.
- Atalay A, Bircik Ö. 2021. Determination of operational efficiency

- in urban public transport lines. *Civil Eng Beyond Limits*, 2(1): 16-20.
- Atalay A, Bircik ÖF. 2022. Determining the effectiveness of the bus lines in urban transportation using data envelopment analysis. *J Transport Logist*, 7(1): 37-54.
- Ayaz Ö, Bakan, S. 2022. Türkiye'deki ulaştırma sektörünün sosyo-ekonomi politikası. *Akad İzdüşüm Derg*, 7(1): 22-46.
- Aydın M, Aydın Gl. 2017. Kentiçi ulaşım hizmetleri ve dışsalılık: Çanakkale örneği. *IJOPEC Publication*, Ankara, Türkiye, pp: 49.
- Cirit F. 2014. Sürdürülebilir kent içi ulaşım politikaları ve toplu taşıma sistemlerinin karşılaştırılması. *İktisadi Sektörler ve Koordinasyon Genel Müdürlüğü Yayınları*, Yayın no: 2891, Ankara, Türkiye, pp: 210.
- DUAP. 2023. Diyarbakır Büyükşehir Belediyesi, Ulaşım Daire Başkanlığı.
- Glaeser EL, Kallal HD, Scheinkman JA, Shleifer A. 1992. Growth in cities. *J Political Econ*, 100(6): 1126-1152.
- Güner S, Taşkın K, Gürler G. 2017. Şehir içi toplu taşıma hatlarının hizmet etkinliğinin veri zarflama analizi ile ölçülmesi: Özel ve kamu işletmelerinin karşılaştırılması. *İşlet Bil Derg*, 5(3): 127-145.
- Güner S. 2017. Operational efficiency and service quality analysis in public transportation systems. *J Transport Logist*, 2(2): 33-48.
- İlgazi B. 2018. Kentsel yaşam kalitesinin sosyal çevre boyutu Sarıyer örneği. Yüksek Lisans Tezi, İstanbul Sabahattin Zaim Üniversitesi, Fen Bilimleri Enstitüsü, Mimarlık Anabilim Dalı, İstanbul, Türkiye, pp: 91.
- Karlaftis MG, Tsamboulas D. 2012. Efficiency measurement in public transport: are findings specification sensitive? *Transport Res Part A*. 46: 392-402. <https://doi.org/10.1016/j.tra.2011.10.005>.
- Koç B. 2019. Bütünleşik ulaşım planlamasında bisikletin yeri: akkent mahallesi (Gaziantep) örneği. Doktora Tezi, Necmettin Erbakan Üniversitesi, Fen Bilimleri Enstitüsü, Şehir ve Bölge Planlama Ana Bilim Dalı, Konya, Türkiye, pp: 145.
- Özaysal M, Tanyel S, Alver Y. 2011. BRT sisteminin İzmir'de uygulanabilirliği üzerine bir değerlendirme. *Dokuz Eylül Üniv Denizcilik Fak Derg*, 3(1): 19-33.
- Pallant J. 2017. SPSS kullanma kılavuzu: SPSS ile adım adım veri analizi. Anı Yayıncılık, İstanbul, Türkiye, pp: 178.
- Uçar A, Eryiğit BH. 2020. Vatandaşların belediyelerin ürettiği kentsel hizmetlere erişebilirliğinin değerlendirilmesi: Karaman Belediyesi örneği. *Paradoks: J Econ Sociol Polit*, 16(2): 175-188.
- Uğurlar A. 2019. Kentsel ulaşımında özel araç odaklı düzenlemelere eleştirel bir bakış. *OPUS Int J Soc Res*, 13(19): 1976-2014.
- Zhu M, Liu XY, Tang F, Qiu M, Shen R, Shu W, Wu MY. 2016. Public vehicles for future urban transportation. *IEEE Transact Intell Transport Syst*, 17(12): 3344-3353.



COĞRAFİ İŞARET SÜRECİNDE TÜRKİYE ODALAR VE BORSALAR BİRLİĞİNİN ROLÜ VE COĞRAFİ İŞARET MAĞAZASI ÖNERİSİ

Tarık YÖRÜKOĞLU^{1*}, Kenan Sinan DAYISOYLU¹, Tuğberk ANÇEL²

¹Kahramanmaraş Sütçü İmam University, Faculty of Engineering and Architecture, Department of Food Engineering, 46040, Kahramanmaraş, Türkiye

²Kahramanmaraş Sütçü İmam University, Technical Sciences Vocational School, Department of Food Processing, 46040, Kahramanmaraş, Türkiye

Özet: Coğrafi işaretler sadece bir ürünün kökenini belirtmekle kalmayıp aynı zamanda ürünün kalitesi, üretim yöntemleri ve kültürel bağlamı hakkında önemli bilgiler de sunmaktadır. Bu noktada, Türkiye'de coğrafi işaretlerin tescili ve yönetimi konusunda önemli bir role sahip olan Türkiye Odalar Borsalar Birliği (TOBB), ülkenin zengin kültürel ve doğal mirasının korunması ve ekonomik değerinin artırılması noktasında stratejik bir konumda bulunmaktadır. TOBB'un, Türkiye genelindeki odalar ve borsaların çatı kuruluşu olarak, coğrafi işaretlerin tanımlanması, tescili, korunması ve yönetimi gibi konularda çeşitli sorumluluklar üstlendiği görülmektedir. Bu çalışma üç ana bölümden oluşmuştur; ilk bölümde coğrafi işaretler kavramına dair kapsamlı bir literatür taraması yapılmış, ikinci bölümde, 1 Ocak 2024 tarihine kadar coğrafi işaret başvurusunda bulunan ve tescil alan kurum ve kuruluşlar genel bir bakış açısıyla incelenmiş ve TOBB'un bu süreçteki rolü detaylandırılmıştır. Son bölümde ise, TOBB bünyesinde coğrafi işaretli ürünlerin tanıtımını ve ekonomik değerini artıracak Coğrafi İşaretler Mağazası (CİM) adıyla bir yapı oluşturulması yönünde öneride bulunulmuştur.

Anahtar kelimeler: Coğrafi işaret, Odalar, Borsalar, Coğrafi işaret mağazası


The Role of Turkish Chambers and Commodity Exchanges in the Geographical Indication Process and Geographical Indication Store Suggestion


Abstract: Geographical indications not only indicate the origin of a product, but also provide important information about the product's quality, production methods and cultural context. At this point, the Union of Chambers and Commodity Exchanges of Türkiye (TOBB), which has an important role in the registration and management of geographical indications in Türkiye, is in a strategic position to protect the country's rich cultural and natural heritage and increase its economic value. It is seen that TOBB, as the umbrella organization of the chambers and commodity exchanges across Türkiye, undertakes various responsibilities in matters such as the definition, registration, protection and management of geographical indications. This study consists of three main parts; In the first part, a comprehensive literature review was made on the concept of geographical indications, and in the second part, the institutions and organizations that applied for and registered geographical indications until January 1, 2024 were examined from a general perspective and TOBB's role in this process was detailed. In the last section, a suggestion was made to create a structure called Geographical Indications Store (CIM) within TOBB, which will increase the promotion and economic value of geographically indicated products.


Keywords: Geographical indications, Chambers, Commodity exchanges, Geographical indications store

*Sorumlu yazar (Corresponding author): Kahramanmaraş Sütçü İmam University, Faculty of Engineering and Architecture, Department of Food Engineering, 46040, Kahramanmaraş, Türkiye

E mail: tarikyorukoglu@ksu.edu.tr (T. YÖRÜKOĞLU)

Tarık YÖRÜKOĞLU  <https://orcid.org/0000-0001-8507-708X>

Kenan Sinan DAYISOYLU  <https://orcid.org/0000-0002-0673-3526>

Tuğberk ANÇEL  <https://orcid.org/0000-0003-1446-567X>

Gönderi: 12 Ocak 2024

Kabul: 25 Şubat 2024

Yayınlanma: 15 Mart 2024

Received: January 12, 2024

Accepted: February 25, 2024

Published: March 15, 2024

Cite as: Yörükoğlu T, Dayısoylu KS, Ançel T. 2024. The role of Turkish chambers and commodity exchanges in the geographical indication process and geographical indication store suggestion. *BSJ Eng Sci*, 7(2): 323-328.

1. Giriş

Coğrafi işaret; menşe, mahreç veya geleneksel ürün işareti olarak tanımlanan ve tescil edilen önemli sınai mülkiyet haklarıdır. Küresel ekonominin hızla dönüştüğü bu dönemde, yerel ürünlerin kimliklerini koruma ve onlara değer katma amacıyla kullanılan coğrafi işaretler; ürünlerin kalitesini, kökenini ve özgünlüğünü tescilleyerek bölgesel kalkınmayı destekler. Bu çalışmada, Türkiye'deki coğrafi işaret tescilinin ve bu alanda yapılan başvuruların istatistiksel bir analizi sunulmuştur. Coğrafi işaret tesciline sahip kurum ve

kuruluşların dağılımı, özellikle coğrafi işaret sürecinde TOBB'un durumu hakkında detaylı bir inceleme yapılmış; başvuru ve tescil süreçlerinde öne çıkan eğilimler, bu süreçlerin yerel ekonomilerle ve ürün çeşitliliğine etkisi değerlendirilmiştir. Son bölümde ise TOBB bünyesinde coğrafi işaretli ürünlerin tanıtımını ve ekonomik değerini artıracak bir platform olması tasarlanan coğrafi işaret mağazaları (CİM) hakkında bilgi paylaşılmıştır. Avrupa Birliği (AB) tarım politikasında coğrafi işaretler, yerel ürünlerin tanıtımı ve korunması açısından önemli bir rol oynar. Bu işaretler, belirli bir coğrafi bölgeyle



ilişkilendirilen ve bu bölgenin özgün özelliklerini, tarihini ve üretim yöntemlerini yansıtan ürünleri tanımlar. Coğrafi işaretler sayesinde tüketicilere ürünlerin kökeni ve üretim metotları hakkında güvenilir bilgiler sağlanırken, üreticilere de ürünlerinin özgünlüğünü ve kalitesini koruyarak daha yüksek gelir elde etme fırsatı sunulur (Balaban, 2016).

Bu sistem, yerel üretim tekniklerinin ve geleneklerin korunmasına ve kültürel mirasın yaşatılmasına katkıda bulunmaktadır. Ayrıca coğrafi işaretler sayesinde, üreticiler kaliteye odaklanarak rekabet güçlerini artırabilir ve uluslararası pazarlarda daha iyi bir konuma

gelebilirler. Böylelikle, AB'nin coğrafi işaret sistemi hem yerel ekonomileri desteklemekte hem de tüketiciler için kalite ve güvenilirlik anlamına gelmektedir (Marangoz ve Akyıldız, 2006; Balaban, 2016).

Coğrafi işaret, farklılığını üretildiği bölgeden alan ve o bölge ile özdeşleşen ürünler olup menşe, mahreç veya geleneksel ürün işareti olarak tescil edilen sınai mülkiyet hakları olup yerel değerlerin sürdürülebilir bir şekilde korunmasına, bu değerlerin gelecek nesillere aktarılmasına, bölge ve kırsal ekonominin gelişmesine yardımcı olurlar (Karadaş ve ark., 2023).



Şekil 1. Türk patent ve marka kurumu coğrafi işaretler; menşe, mahreç ve geleneksel ürünler amblemleri.

Ürüne katma değer sağlayan coğrafi işaret bölgesel kalkınma, ürün kalitesinin korunması, üretici gelirinin artırılması, tüketicilerin kalitesini ve kökenini bildikleri ürünleri tüketebilmeleri açısından önemlidir (Güler ve Saner, 2018). Coğrafi işaret, ayırt edici özelliği ile öne çıkan ve bulunduğu bölge ile özdeşleşen ürünlere verilen bir tescil süreci olup sadece tarım ürünleri ile sınırlı olmayıp insan eliyle yapılan ürünleri de kapsamaktadır. Yani coğrafi işaretlerin kapsamına doğal ürünler, tarım, maden, el sanatları ve sanayi ürünleri de girebilmektedir (Oraman, 2015). Avrupa Birliği (AB) 2081/92 sayılı tüzüğü'nün bir uyarlaması olan 555 sayılı Kanun Hükmünde Kararname (KHK), 6769 sayılı Sınai Mülkiyet Kanunu'nun 10 Ocak 2017 tarihinde yürürlüğe girmesi ile coğrafi işaretlerle ilgili yeni bir döneme geçilmiştir. 1995-2017 yıllarına kadar mahreç ve menşe tanımı kullanılırken, 2017'de kabul edilen yeni kanunla beraber bu tanımlar mahreç, menşe ve geleneksel ürünler olmak üzere üç kategoride (Şekil 1) değerlendirilmeye başlanmıştır (Anonim 1992; Anonim 2017).

6769 Sayılı kanuna göre coğrafi işaret tescili için, ürünün tek bir üreticisi olan gerçek veya tüzel kişilerin, tüketici derneklerinin, konu ve coğrafi yöre ile ilgili kamu kuruluşlarının başvuruda bulunabileceği belirtilmiştir. Türk Patent ve Marka Kurumunun (TPMK) coğrafi işaretlerle ilgili sayfası incelendiğinde hem gerçek kişilerin hem de tüzel kişilerin coğrafi işaret başvuruları ve aldıkları tescilli ürünleri görülmektedir (TPMK, 2024a).

Coğrafi işaret tescilinin temel amacı, ürünlerin kalitesini ve kökenini belirginleştirmek ve bu özelliklerin sürdürülebilirliğini sağlamaktır. Tescil aynı zamanda, yerel üreticilerin koruma altına alınan isimlerden öncelikli olarak faydalanmalarını, ürünlerin kalitesinin korunmasını ve tüketicilere güvenilir bilgi sunarak

bilinçli tercih yapmalarına yardımcı olacak bir rehber oluşturmayı hedeflemektedir (Tanrıku, 2007).

Coğrafi işaret tesciline sahip ürünler, tüketicilerin gözünde "yüksek kaliteli ve güvenilir ürün" algısı yaratmaktadır. Bu durum, coğrafi işaret tescilli ürünlerin tescilsiz ürünlere kıyasla daha pahalı satılmasına karşın tüketicilerin yine de coğrafi işaret tescilli ürünleri tercih etmelerine neden olmaktadır. Bu da üreticiler için önemli bir gelir artışı sağlamaktadır. Ayrıca coğrafi işaretlemenin kolektif bir hakkı ifade etmesi; üretici birliklerini daha aktif bir işlerliğe kavuşturmakta, küçük çaplı işletme olmanın dezavantajından dolayı üreticinin pazar karşısında güçsüz kalması engellenmekte ve ortak pazarlama faaliyetleri sayesinde maliyetler ciddi oranda azalmaktadır (Özsoy, 2015).

Coğrafi işaret koruması, tüketiciler açısından tescilli ürüne karşı prestij ve güven sağlayan; üreticiler açısından ise piyasadaki rakiplerinden farklılaşmasına aracı olan bir mekanizma olarak işlev görmektedir. Coğrafi İşaretleme Sisteminin temel fonksiyonları şu şekilde özetlenebilir: Köken Belirtme Fonksiyonu, Kalite Fonksiyonu, Yatırım veya Reklam Fonksiyonu, Kültür Koruma Fonksiyonları (Rovamo, 2006; Bagade ve Metha, 2014).

Globalleşen dünyada ticaretin tüketici merkezli kalite gereksinimleri ve ürün talepleri artmakta; bu gibi gelişmeler, Avrupa ve Türkiye'deki özellikle tarım sektörünü yeni zorluklarla karşı karşıya bırakmaktadır. Değişimler sadece tarımsal pazarı değil, aynı zamanda kırsal alanlardaki yerel ekonomileri de etkilemektedir. Bu nedenle, yerel ekonomileri canlandırmak ve küreselleşmenin olumsuz etkilerini, özellikle küçük işletmeler üzerindeki etkilerini en aza indirmek için yeni stratejiler geliştirmek hayati önem taşımaktadır. Coğrafi işaretin bu sorunlara yönelik geliştirilebilecek

stratejiler arasında önemli bir rolü olduğu düşünülmektedir (Kan ve Gülçubuk, 2008).

Coğrafi işaretin önemini artıran faktörlerden bir diğeri ise içerdikleri anlam ve küreselleşmeye karşı yerel hareketleri teşvik ederek kırsal kalkınma aracı olarak işlev görmeleridir. Dolayısıyla coğrafi işaretlerin yerele ve böylece kırsal kalkınmaya sağladıkları avantajlar beş ana başlık altında sınıflandırılabilir. Bunlar: Coğrafi işaretler üretici ve tüketicileri haksız rekabete karşı korur, coğrafi işaretler tüketiciyi yönlendirir, kaliteli beslenmesini sağlar, coğrafi işaretler katma değer ve istihdam yaratır, coğrafi işaretler gerçek kırsal kalkınma araçlarıdır, coğrafi işaretler turizmi geliştirir (Rangnekar, 2004; Kop ve ark., 2006; Kan, 2007; Tekelioğlu, 2019).

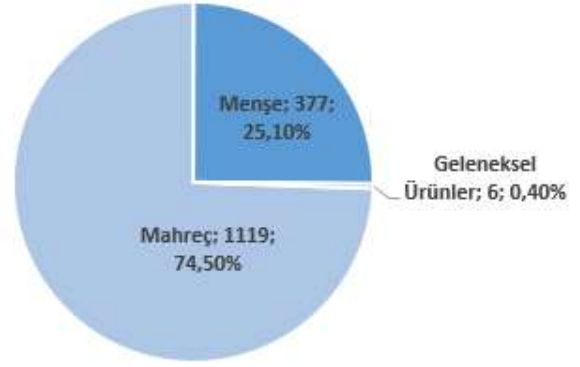
Kolektif üretim, doğası gereği işbirlikçi bir yönetim yapısını gerektirir; bu da coğrafi işarete sahip tedarik zincirlerinin belirli organizasyonel güçlendirmelere ihtiyaç duyduğunu gösterir. Coğrafi işaret kullanacak üretici sınıfların belirlenmesi, ürün kalitesi, üretim aşamalarını denetleyecek kurumların kurulması ve coğrafi işaretlerin yetkisiz kişiler tarafından veya kötüye kullanılması durumlarında müdahale edebilecek otoritelerin tahsis edilmesi önemlidir. Daha etkili ve etik bir coğrafi işaret kullanımını sağlamak için daha özgün ve uyarlanabilir bir platform üzerinde durulmalıdır. Bu platform; teknolojik uygulamalarıyla birlikte gelişmeyi, üretici sınıflar arasında sürekli iyileşme kültürünü teşvik etmeyi ve coğrafi işaret kullanımının şeffaf ve sorumlu olmasını desteklemeyi içermektedir. Ayrıca standartlara uyumu teşvik etmek ve kötüye kullanımı caydırmak için teşvikler ve cezalar sistemi oluşturulabilir (Gökova, 2007).

2. Coğrafi İşaret Sürecinde Ülkemizdeki Kurumların Durumu

2024 yılı Ocak ayına kadar TPMK'nin coğrafi işaret tescilli almış olan ürünleri incelendiğinde toplamda 1493 farklı kurum ve kuruluş ile 9 gerçek veya tüzel kişiye ait ürünlerin bu tescilli aldığı görülmektedir. Bu tescillerin içerisinde 1119 tanesi (%74,5) mahreç işareti, 377 tanesi (%25,1) menşe işareti ve sadece 6 tanesi (%0,4) geleneksel ürün kategorisinde yer almaktadır (Şekil 2). Bu dağılımda, mahreç işaretli ürünler en yüksek paya sahipken geleneksel ürünlerin en düşük payı aldığı görülmektedir. Geleneksel ürünlerin bu kadar az tescile sahip olmasının nedeni, bu tanının 2017 yılında yürürlüğe giren 6769 Sayılı Sınai Mülkiyet Kanunu ile getirilmiş olmasından kaynaklanmaktadır.

Şekil 3 incelendiğinde, Türkiye'deki yöresel ve/veya kültürel ürünleri en fazla tescil eden şehir 102 ürünle Gaziantep'tir. Bu ili sırasıyla 72 tescille Konya, 50 tescille ile Diyarbakır, 48 tescille ile Afyonkarahisar, 47 tescille Şanlıurfa ve 46 tescille Malatya takip etmektedir. Türkiye'nin tüm illerinin en az birden fazla coğrafi işarete sahip olduğu görülmektedir. Bu durum, Türkiye'nin coğrafi işaret açısından ne kadar zengin bir çeşitliliğe sahip olduğunu çok daha net göz önüne sermektedir.

Tescilli Coğrafi İşaret Dağılımı



Şekil 2. 01.01.2024 tarihine kadar tescil edilmiş ürünlerin coğrafi işaret dağılımı.

COĞRAFI İŞARET TESCİL SAYISI TÜRKİYE HARİTASI

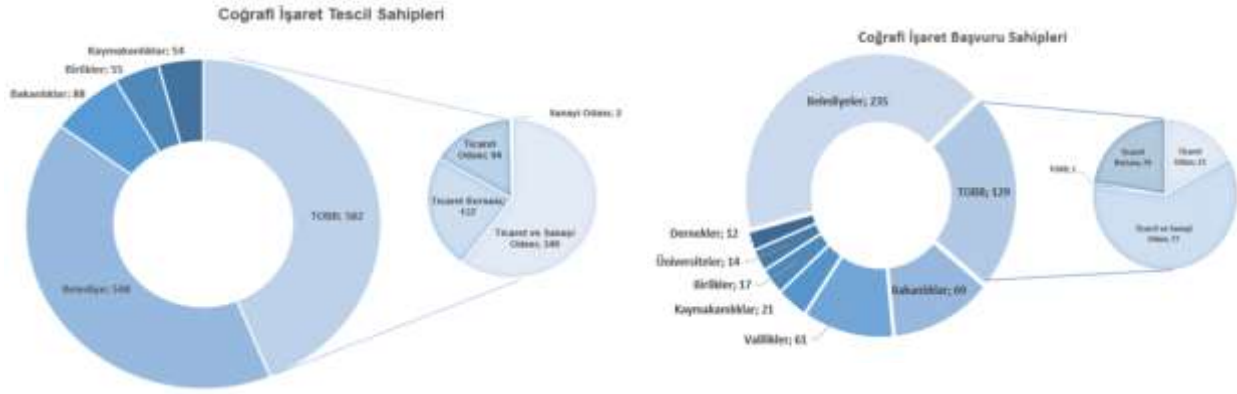


Şekil 3. Coğrafi işaret tescil sayılarının il bazında gösterilmesi.

Coğrafi işaret tescili alan kurumlar arasında yapılan detaylı incelemede (Şekil 4), TOBB'un 582 tescille en fazla coğrafi işarete sahip kuruluş konumunda olduğu görülmektedir. Bunu 548 tescille belediyeler takip etmektedir. Bakanlıklar 88 tescille üçüncü sırada yer alırken, birlikler 55 ve kaymakamlıklar 54 tescille dördüncü ve beşinci sırayı paylaşmaktadır. Ayrıca vakıflar 37, ziraat odaları 36, dernekler 23, valilikler 22 ve kooperatifler 21 tescille diğer önemli coğrafi işaret sahipleri arasında bulunmaktadır (TPMK, 2024a). Bu dağılım, TOBB'un coğrafi işaretlerin korunması ve geliştirilmesi konusunda ne kadar önemli bir rol oynadığını göstermektedir. Ayrıca belediyeler ve bakanlıklar gibi yerel ve merkezi yönetim organlarının da bu alanda aktif olduğunu ve coğrafi işaretlerin gelişimine katkıda bulduklarını ortaya koymaktadır.

Aşağıda Şekil 4'te coğrafi işaret tesciline sahip kurum ve kuruluşlar, Şekil 5'de ise coğrafi işaret başvurusu yapmış kurum ve kuruluşlar verilmiştir.

01.01.2024 tarihine kadar olan mevcut coğrafi işaret başvuruları incelendiğinde ise Belediyeler 235 adet, TOBB 129 adet, Bakanlıklar (Milli Eğitim Müdürlükleri, Turizm İl Müdürlükleri, Tarım ve Orman İl Müdürlükleri) 69 adet, Valilikler 61 adet, Kaymakamlıklar 21 adet, Birlikler 17 adet, Üniversiteler 14 adet, Dernekler 12, Ziraat Odaları 10 adet başvuru yapmıştır (Şekil 5) (TPMK, 2024b).

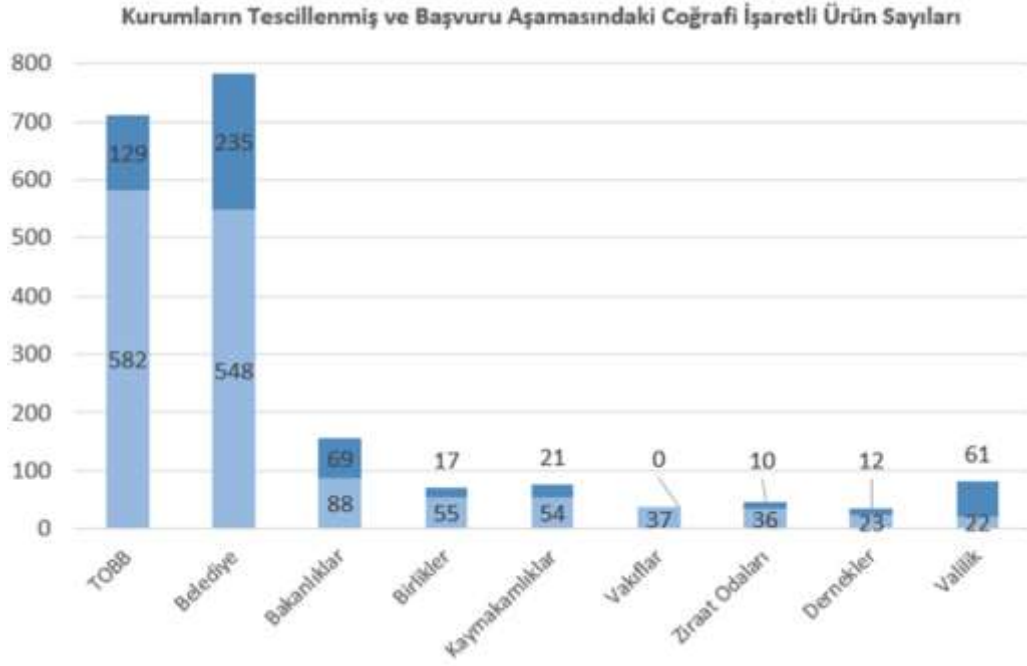


Şekil 4. Coğrafi işaret tesciline sahip kurum ve kuruluşlar.

Şekil -5: 01.01.2024 Tarihine Kadar Coğrafi İşaret Başvurusu Yapmış Kurumlar.

Kurumların tescillenmiş ve başvuru aşamasındaki coğrafi işaretli ürün sayılarına bakıldığında (Şekil 6) belediyeler ve TOBB'un ön plana çıktığı görülmektedir. TOBB hala bünyesinde en fazla tescilli ürüne sahip kurum olurken belediyeler başvuru sayısı açısından en önde yer

almaktadır. Bu iki kurumun toplam başvuru ve tescilli coğrafi işaretli ürün sayıları toplam başvuru ve tescilli ürün sayılarının yaklaşık olarak %70'lik kısmını oluşturmaktadır.



Şekil 6. Tescillenmiş ve başvuru aşamasında olan coğrafi işaretlerin kurumlar bazında dağılımları.

3. Coğrafi İşaret Sürecinde Türkiye Odalar ve Borsalar Birliğinin Rolü

TOBB, Türkiye genelindeki odaları ve borsaları bir araya getiren, 5174 Sayılı Türkiye Odalar ve Borsalar Birliği ile Odalar ve Borsalar Kanunu ile görevlerini yürüten bir çatı kuruluş (Anonim, 2004) olup ülkedeki ticaret ve sanayi faaliyetlerini destekleyerek ekonomik kalkınmayı teşvik etmektedir. Coğrafi işaretlerle ilgili olarak TOBB'un önemi büyüktür, çünkü bu işaretler, ülkedeki çeşitli bölgelerin özgün ürünlerinin korunmasına ve pazarlanmasına yardımcı olmaktadır. TOBB, odalar ve borsalar arasında koordinasyonu sağlamak, coğrafi

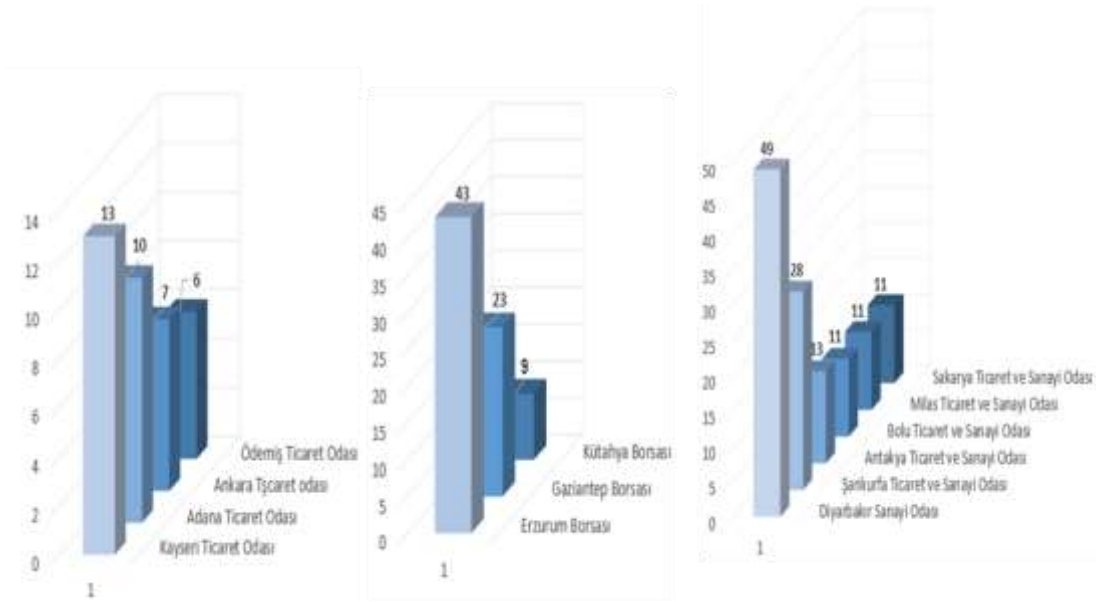
işaretleri etkin bir şekilde yönetmek ve korumak, ülke ekonomisine katkı sağlamak yoluyla Türkiye'nin kültürel ve ekonomik zenginliğine sürdürülebilir bir yaklaşım sunmaktadır.

Ayrıca TOBB'un ülke genelindeki odalar ve borsalar arasında iletişimi güçlendirmesi ve bilgi paylaşımını teşvik etmesi, coğrafi işaretlerin daha etkin bir şekilde kullanılmasına imkân sağlamaktadır. Bu sayede, coğrafi işaretli ürünlerin ekonomik değeri artmakta ve ülkedeki yerel üreticilerin rekabet avantajı elde etmeleri mümkün olmaktadır.

Oda ve borsaların sahip olduğu tescillenmiş coğrafi işaretler incelendiğinde, en fazla 438 adet ürün ile

mahreç işareti bulunduğu, bunu sırasıyla 129 adet ürünle menşe işareti ve 3 adet geleneksel ürün adının takip ettiği görülmektedir. Başvuru aşamasında ise bu durum şu şekildedir: Ticaret ve sanayi odaları 77 adet, borsalar 29 adet ve ticaret odaları ise 22 adet başvuru yapmıştır. Son olarak, geleneksel ürün kategorisinde ise başvuru sayısı birdir. TPMK veri tabanında, coğrafi işaret başvurularının menşe veya mahreç işareti olup olmadığı gösterilmediği için değerlendirme kurum adı üzerinden yapılmak zorunda kalmıştır. 02.05.2023 tarihinde TOBB, "Türk Kahvesi" için TPMK'ye geleneksel ürünler kategorisinde doğrudan başvuru yapmıştır. Bu başvuru, TOBB'un kendi başına bir ürün için doğrudan başvurusunu yaptığı yegâne bir ürün durumundadır. Oda ve borsaların mevcut tescilli coğrafi işaretleri

incelendiğinde (Şekil 7) en fazla tescile sahip olan kurum Diyarbakır Ticaret ve Sanayi Odası olup toplamda 49 adet coğrafi işaretli ürüne sahiptir. Erzurum Ticaret Borsası, 43 adet coğrafi işaret ile ikinci sıradadır. Üçüncü sırayı ise 28 adet coğrafi işaret ile Şanlıurfa Ticaret ve Sanayi Odası almaktadır. TOBB bünyesindeki yapılar içinde Ticaret ve Sanayi Odalarının ülke genelinde coğrafi işaretli ürünlerin tescilinde önemli bir katkı sağladığına dair mevcut bulgunun Ticaret ve Sanayi Odalarının hem il genelinde hem de ilçelerde hizmet veriyor olmalarından kaynaklandığı değerlendirilmektedir. Örneğin, Milas Ticaret ve Sanayi Odası'nın (Muğla iline bağlı bir ilçe) 11 adet tescilli coğrafi işaretli ürüne sahip olması, bu durumu daha net bir şekilde ortaya koymaktadır (TPMK, 2024a).



Şekil 7: Oda ve borsaların sahip olduğu tescilli coğrafi işaretli ürün sayısı.

4. Sonuç ve Öneriler

Coğrafi İşaretler Mağazası önerisi, TOBB liderliğindeki bir iş birliği modeliyle, yerel üreticilerin güçlenmesini, coğrafi işaretlerin daha etkili bir şekilde kullanılmasını ve ülkemizin kültürel mirasının sürdürülebilir bir şekilde korunmasını sağlamaya yönelik olarak getirilmiştir. Bu bağlamda CİM, tüm illerinin geleneksel ve özgün ürünlerini bir araya getirerek coğrafi işaretle tescillenmiş ürünleri tanıtmak ve pazar şanslarını arttırmak amacı ile başta İstanbul, Ankara ve İzmir olmak üzere büyükşehirlerde açılması planlanan bir konsept platformdur. CİM coğrafi işaretlerle korunan ve belirli bir coğrafi bölgeye özgü niteliklere sahip tarım ürünleri, el sanatları, yöresel lezzetleri ve benzeri ürünleri içerecektir.

TOBB, CİM'de yer alacak coğrafi işaret tescilli ürünlerin yönetimini optimize etmek ve üreticilere etkili destek sağlamak üzere stratejik bir model benimseyecektir. Bu çerçevede, Oda ve Borsalar, coğrafi işaret tescilli ürünleri üreten firmalarla sözleşmeler imzalayarak, bu firmalara kullanım hakkı tanıyan bir protokol oluşturacaklardır.

Söz konusu protokoller, coğrafi işaret tescilli ürünlerin üretimine dair belirlenen standartları, kalite kriterlerini ve diğer spesifikasyonları içerecektir. Belirlenen şartlar, coğrafi işaret tesciline uygunluğu denetlemek ve ürünlerin kalitesini güvence altına almak üzere titiz bir denetim sürecini içerecektir. Oda ve Borsalar, bu süreçte üretici firmalara destek olmak ve denetim süreçlerini etkin bir biçimde yönetmek adına kalite kontrol analizlerini gerçekleştirecek özel komisyonlar ve ekipler kuracaklardır. Bu analizler; ürünlerin fiziksel, kimyasal ve organoleptik özelliklerini objektif bir şekilde ele alarak coğrafi işaret tescil sürecinde tanımlanmış üretim standartlarına ve Türk Gıda Kodeksinin belirlemiş olduğu mevzuatlara uygunluğunu değerlendirecektir. Elde edilen veriler, üretici firmalarla paylaşılacak ve geri bildirimlerle üretim süreçleri sürekli olarak iyileştirilecektir. Bu süreç, coğrafi işaretli ürünlerin sürdürülebilir kalitesini ve ayırt ediciliğini korurken aynı zamanda yerel ekonomilere de katma değer sağlayacaktır.

CİM'lerde satışa sunulan ürünlerin daha yüksek katma

değere sahip olması üreticilerin bu mağazalara ürün verme konusunda daha istekli olmalarını teşvik edecektir. Yüksek kaliteli ürünler ve coğrafi işaret tescili, üreticilerin marka değerini artırarak yerel ekonomilere ve kültürel mirasa katkı sağlamalarını destekleyecektir. Bu da CİM'lerin hem tüketiciler hem de üreticiler için önemli bir ticaret platformu olmasını sağlayacaktır.

Üretici firmaların ürünleri, kalite kontrol ve coğrafi işaret uygunluğu analizlerini başarıyla tamamladıktan sonra, CİM'lerde satışa sunulacaktır. Bu ürünler, daha yüksek katma değerli ve özgün niteliklere sahip olacak, bu da yerel üreticileri CİM'lere ürün sunma konusunda daha fazla teşvik edecektir. Bu stratejik model, coğrafi işaretli ürünlerin toplumdaki gıda güvenliği olgusuna farklı bir bakış açısı getirmek, yerel ekonomilere katma değer kazandırmak ve tüketicilere nitelikli ve çeşitli ürünler sunmak amacıyla uygulanacaktır.

Son olarak, CİM'ler, aynı zamanda dijital pazarlarda da varlık göstererek online satış kanallarıyla tüketicilere ulaşacak ve coğrafi işaretli ürünleri daha geniş bir kitleye tanıttıkları inovatif yöntemlere öncülük edecektir. Böylece, yerel üreticiler sadece fiziki mekanlarda değil, aynı zamanda dijital pazarlarda da tüketici katmanlarıyla buluşabileceklerdir.

Katkı Oranı Beyanı

Yazar(lar)ın katkı yüzdesi aşağıda verilmiştir. Tüm yazarlar makaleyi incelemiş ve onaylamıştır.

	T.Y.	K.S.D	T.A.
K	50	25	25
T	100		
Y	50	25	25
VTI	80	10	10
VAY	100		
KT	50		50
YZ	50	25	25
KI	20	40	40
GR	40	30	30
PY	40	30	30
FA	40	30	30

K= kavram, T= tasarım, Y= yönetim, VTI= veri toplama ve/veya işleme, VAY= veri analizi ve/veya yorumlama, KT= kaynak tarama, YZ= Yazım, KI= kritik inceleme, GR= gönderim ve revizyon, PY= proje yönetimi, FA= fon alımı.

Çatışma Beyanı

Yazarlar bu çalışmada hiçbir çıkar ilişkisi olmadığını beyan etmektedirler.

Etik Onay Beyanı

Bu çalışmada hayvanlar ve insanlar üzerinde herhangi bir çalışma yapılmadığı için etik kurul onayı alınmamıştır.

Kaynaklar

Anonim. 1992. Council Regulation (EEC) No. 2081/92 on the protection of geographical indications and designations of

origin for agricultural products and foodstuffs. FAO, URL: <https://www.fao.org/faolex/results/details/en/c/LEX-FAOC019440/> (erişim tarihi: 10 Ocak 2024).

Anonim. 2004. Türkiye odalar ve borsalar birliği ile odalar ve borsalar kanunu. 01.06.2004 tarih ve 25479 Sayılı Resmi Gazete, URL: <https://www.resmigazete.gov.tr/eskiler/2004/06/20040601.html> (erişim tarihi: 10 Ocak 2024).

Anonim. 2017. Sınai mülkiyet kanunu. 2. Kitap coğrafi işaretler ve geleneksel ürün adı, 10 Ocak 2017 tarih ve 29944 sayılı Resmi Gazete, URL: <https://www.mevzuat.gov.tr/MevzuatMetin/1.5.6769.pdf> (erişim tarihi: 10 Ocak 2024).

Bagade SB, Metha DB. 2014. Geographical indications in India: hitherto and challenges. Res J Pharm Biol Chem Sci, 5(2): 1225-1239.

Balaban ST. 2016. Ekonomik açıdan coğrafi işaretler. FMR, 1: 57-62.

Gökova U. 2007. Coğrafi işaretler ve coğrafi işaretlerin ekonomik etkileri: Türkiye örneği. Atatürk Üniv İktis İdar Bil Derg, 21(2): 141-160.

Güler D, Saner G. 2018. Türkiye'de hayvansal gıdaların coğrafi işaret korumalarının Avrupa birliği çerçevesinde değerlendirilmesi. Tar Bil Araş Derg, 11(1): 50-55.

Kan M, Gülçubuk B. 2008. Kırsal ekonominin canlanmasında ve yerel sahiplenmede coğrafi işaretler. Uludağ Üniv Zir Fak Derg, 22(2): 57-66.

Kan M. 2007. Kırsal kalkınmada coğrafi işaretler ve bazı ülkelerden uygulama örnekleri. Doktora Tezi, Ankara Üniversitesi, Fen Bilimleri Enstitüsü, Ankara, Türkiye, pp:378.

Karadaş Ö, Yılmaz E, Yılmaz İ, Geçgel U. 2023. Trakya bölgesinde coğrafi işaretleme çalışmaları ve bölge ekonomisine katkısı. Giriş Kalk Derg, 17(2): 180-189.

Kop van de P, Sautier D, Gerz A. 2006. Origin based products. Lessons for propoor market development. Royal Tropical Institute - CIRAD, Bulletin The Netherland and France, pp: 372.

Marangoz M, Akyıldız M. 2006. Doğal ve kültürel mirasın korunması açısından coğrafi işaretlerin önemi ve buldan bezi örneği. Buldan Sempozyumu, 23-24 Kasım 2006, Denizli, Türkiye, ss: 1.

Oraman Y. 2015. Türkiye'de coğrafi işaretli ürünler. Balkan Near East J Soc Sci, 1(1): 76-85.

Özsoy T. 2015. Coğrafi işaretlemenin katma değer oluşturmada bir araç olarak kullanımı. Çukurova Üniv Sos Bil Enst Derg, 24(2): 31-46.

Rangnekar D. 2004. The socio-economics of geographical indications, A Review of Empirical Evidence from Europe, UNCTAD-ICTSD Project on IPRs and Sustainable Development, Issue Paper No.8, Bern, Switzerland, pp: 123.

Rovamo O. 2006. Monopolising Names? The protection of geographical indications in the European Community. MSc Thesis, University of Helsinki, Faculty of Law, Helsinki, Finland, pp: 80.

Tanrıkulu M. 2007. Türkiye'de coğrafi işaretlerin tespiti ve tescil edilmesinin önemi. J Int Soc Sci Educ, 1(2): 173-184.

Tekelioğlu Y. 2019. Coğrafi işaretler ve türkiye uygulamaları. J Ufuk Üniv Sos Bil Enst, 8(15): 47-75.

TPMK. 2024a. Türk patent ve marka kurumu coğrafi işaret tescil sahipleri. URL: <https://ci.turkpatent.gov.tr/Statistics/RegistrationOwners> (erişim tarihi: 10 Ocak 2024).

TPMK. 2024b. Türk patent ve marka kurumu coğrafi işaretli ürünler veri tabanı. URL: <https://ci.turkpatent.gov.tr/veri-tabani> (erişim tarihi: 10 Ocak 2024).



CONSERVING THE CRITICALLY ENDANGERED *Anacamptis Coriophora* L. IN TÜRKİYE THROUGH *EX VITRO* SEED GERMINATION

Ines HARZLI*1, Yasemin ÖZDENER KÖMPE¹


¹Ondokuz Mayıs University, Faculty of Science, Department of Biology, 55270, Samsun, Türkiye


Abstract: *Anacamptis coriophora* (Orchidaceae) is a highly endangered orchid in Türkiye due to its excessive collection and the continuing deterioration of its habitat. In this study, the cultivation conditions of *A. coriophora* were determined. A sterile soil mixture was filled into jars and the fungal isolate (previously isolated from *A. coriophora* roots), Ceratobasidiaceae MG762693 was inoculated in separate glass jars, producing fungal compost when hyphae were developed. This fungal compost was then filled into pots where *A. coriophora* seed packs (0.001 g) were placed and subsequently moistened with sterile liquid nutrient medium. After 45 days of germination, fifty seedlings of approximately equal size were transferred directly to a natural environment and after 6 months of development the measuring of the tubers was done. The phenological process was then monitored until flowering. After 45 days, germination and developmental stages rates were determined from the seed packs in the pots inoculated with the Ceratobasidiaceae MG762693 fungal isolate and 64.3% germination and 11.75% leaf-rooted seedlings (stage 4) occurred. Plants flowered in June the following year, and the seeds ripened in July. The largest tuber in adult individuals was about 3 times the weight of first-year tubers. Each individual formed 2 or 3 tubers, thus increasing the number of tubers approximately 2.5 times in 2 years. In this study, *ex vitro* symbiotic seedlings were planted in the natural environment and a small population was formed in a 2-year period. The results revealed that orchids can be grown on a large scale with this method, both economically and for conservation and reintroduction.

Keywords: Orchidaceae, Orchid cultivation, Seed germination, Symbiotic

*Corresponding author: Ondokuz Mayıs University, Faculty of Science, Department of Biology, 55270, Samsun, Türkiye

E mail: inesharзли9@gmail.com (I. HARZLI)

Ines HARZLI  <https://orcid.org/0000-0003-4009-2993>

Yasemin ÖZDENER KÖMPE  <https://orcid.org/0000-0003-1649-4298>

Received: September 23, 2023

Accepted: February 26, 2024

Published: March 15, 2024

Cite as: Harzlı I, Özdener Kömpe Y. 2024. Conserving the critically endangered *Anacamptis coriophora* L. in Türkiye through *ex vitro* seed germination. BSJ Eng Sci, 7(2): 329-333.

1. Introduction

The Orchidaceae family ranks among the world's largest, comprising more than 27,000 species (Zhang et al., 2018). Orchids are able to grow in diverse climates and ecosystems, spanning from sea level to temperate and tropical mountains (Oktalira et al., 2019; Steinfort et al., 2010). Orchids have both terrestrial and epiphytic growth habits and produce a large number of tiny seeds (Pujasatria et al., 2020). Orchids hold a prominent place in the list of endangered plant species in certain countries like Türkiye (León-Yáñez et al., 2011; Qin et al., 2017). Nevertheless, despite many orchid species being familiar in biodiverse tropical countries, the number of threatened orchid species is expected to be higher in national and international registries during the few coming years (Joppa et al., 2011a, b).

Tubers of Euroasian orchids are over-harvested, especially in Türkiye, Greece, Iran, and some Middle Eastern countries for the salep beverage and ice cream additive production. The harvesting of these orchids is so extreme that all orchid species are now protected by law, but unfortunately, the illegal collection continues extensively (Ghorbani et al., 2014; Kreziou et al., 2016;

Sezik, 2002). In the last 30 years, orchids and the related ecosystem have become more vulnerable to extinction, especially due to the extreme pressure brought on by human activities. The fragmentation and destruction of habitats, fires, and a decrease in pollinators have caused serious losses in orchid populations and diversity (Sosa and Platas, 1998; Hopper, 2000; Coats and Dixon, 2007). Therefore, orchids face a risky future due to habitat loss caused by human activities and climate change. Both *in vitro* asymbiotic and symbiotic methods have been used to successfully achieve seed germination and seedling development for Euroasian temperate orchids (Eşitgen et al., 2005; Çığ et al., 2018; Fatahi et al., 2022). However, these methods are expensive and time-consuming for the germination and seedling development processes. The difficulty of adapting seedlings to the natural environment complicates the applicability of these methods. All tuberous orchids, especially *Anacamptis* species, are collected from nature to meet this demand. A sustainable production model can be an effective solution to both industrial demands and especially, the conservation and reintroduction efforts of endemic and severely threatened orchid species. *Ex vitro* symbiotic



seedling production of some tropical and temperate orchids and then the formation of mature plants by easily adapting these seedlings to the natural environment (Quay 1995; Aewsakul et al., 2013; Kömpe and Mutlu 2021; Kömpe et al., 2022; Deniz et al., 2022) is very promising for their mass production. The genus *Anacamptis* (Orchidaceae) consists of about 34–35 species and hybrids in Europe, west-northwest Asia, and the Mediterranean. All species of this genus have underground tubers (Govaerts et al., 2017). Otherwise, even the most common orchids will face the threat of extinction shortly, and unfortunately, orchids in Türkiye will only be kept in cemeteries (Löki et al., 2015). Although protocols for mass production were suggested in studies on the *in vitro* asymbiotic germination and seedling development of this species, it could not be transferred from the laboratory to the field (Bektaş et al., 2013; Gümüő and Ellialtıođlu 2012).

In light of this information, the aim of this research are to make mass production of *A. coriophora* seeds from Türkiye and to determine the morphological characteristics of the tubers formed.

2. Materials and Methods

2.1. Plant Materials

In this research, *Anacamptis coriophora* seeds were collected from the capsules of adult plants formed by natural pollination around Bolu–Abant lake (Black Sea Region, Türkiye). The seeds were collected from mature capsules, kept at room temperature for a few days to dry, and stored at 4 °C until used in germination tests.

2.2. Fungal Inocula

Ceratobasidiaceae MG762693, a fungal isolate that was isolated from the roots of *A. coriophora* in a previous study (Mutlu and Kömpe 2020) was tested in this study to investigate seed germination and seedling development. The fungal isolate was inoculated into PDA (Potato Dextrose Agar) medium, incubated in the dark at 25 °C for 5 days and activated.

2.3. Ex Vitro Symbiotic Seed Germination

For *ex vitro* symbiotic seed germination, after collecting the soil from *A. coriophora* habitat, the soil mixture was prepared (2:1 soil: perlite), filled in glass jars, and sterilized in an autoclave (121 °C, 1.5 Atm). The fungal isolate was inoculated first into the jars containing a sterile soil mixture and incubated at 25 °C in the dark for 15 days. When fungal hyphae developed, this compost

was filled into sterile pots (20×31×15 cm), and 6 seed packs were buried in each pot and six repetitions were made for germination tests.

The soil mixtures in the pots were moistened with a modified oat medium once a week. After two months of incubation, the germination and development stages in the seed packs were evaluated.

For the control group, the soil mixture was put in the pots without fungus-inoculated compost. Six seed packs were embedded in each pot.

Development was assessed according to the following stages by modifying Clements et al. (1986):

0: Ungerminated seed

1: Protocorm

2: Leaf primordium

3: First leaf

4: Developed leaves and/or roots

2.4. The Seedling Plantation

After 50 seedlings (reaching stages 1-2 and stages 3-4) were planted in a natural field at a distance of 50-60 m from the main habitat of *A. coriophora* adult plants, the phenological process was followed and evaluated from the seedling stage to the flowering adult stage. From the seedlings transferred to nature, the formation rate, sizes and weights of the tubers were measured. All of the tubers were buried in the ground again after their measurements were taken and the flowering process was followed. The number of tubers in adult plants at the flowering stage and tuber sizes were determined.

2.5. Statistical Analysis

The rates of seeds at germination and seedling development stages were compared against the control group (without fungal inoculation). The rate of germination and seedling growth were evaluated by using one-way ANOVA. Statistical significance was set at P<0.05. Differences among the means were compared with the Duncan test. All the statistical analyses were performed using SPSS software 25.0 (SPSS Inc., Chicago, USA).

3. Results and Discussion

Ceratobasidiaceae (Access Number MG762693), which is an earlier isolate from *A. coriophora* roots, promoted germination and seedling development. 64.3 % of the seeds germinated and developed. 14.06 % and 11.75 % of the seeds reached stages S3 and S4, respectively. (Table 1, Figure 1A).

Table 1. Germination and development of *Anacamptis coriophora* seeds with Ceratobasidiaceae (±: Standard deviation)

	Developmental Stages (%)					Germination (%)
	S0	S1	S2	S3	S4	
Control	100.00 ± 0.00	0.00 ± 0.00	0.00 ± 0.00	0.00 ± 0.00	0.00 ± 0.00	0.00 ± 0.00
Ceratobasidiaceae MG762693	35.92 ± 10,72	14.23 ± 5.6	24.01 ± 7.74	14.06 ± 4.65	11.75 ± 3.03	64.30 ± 10.71



Figure 1. A: Seedlings that develop 45 days after seeds sowing , B: Seedlings transferred to nature, C: Flowering plants after 2 years of growth, D: The tubers of the mature individual of *A. coriophora*. (The arrow shows the previous (old) tuber).

The results of this research conducted on the relationship between orchid seed germination and mycorrhizal fungi showed varying effectiveness of the different isolates on orchid seed germination. In some orchids, different fungi are effective at the germination and development stages, while in some species, a certain type of fungus supports both germination and development (Wang et al., 2011; Zhang et al., 2020; Kömpe et al., 2021). In addition, this study supported the previous research result explaining that the compatible fungus for *A. coriophora* is *Ceratobasidium* (Kömpe and Mutlu 2021).

Fifty healthy and approximately equal-sized seedlings of the S4 stage were then planted directly in a natural area at a small distance from adult plants of *A. coriophora* in autumn (October - 2019) (Figure 1B) and the field was protected against potential animal destruction. The seedling's life cycle was followed until May 2020 without any interference. All the seedlings were removed in the spring, and the tuber formation was evaluated. It was determined that tubers of different sizes developed in 35 seedlings. After cleaning the soil residues from the surfaces of the tubers, their dimensions and weights were determined. The tubers were buried again in the soil, and the phenological process was followed up to the flowering stage. In the first year (T₁, Table.2), 35

seedlings produced only one tuber. During the summer, the tubers remained dormant in the soil, and in October 2020 the first leaves and roots developed. From October to June 2021, the vegetative phase continued, and flowering occurred for the first time in June 2021 (Figure 1C). All tuber-forming seedlings (35 seedlings) flowered. The flowering process continued for about 1 month, and as a result of natural pollination, seeds were formed. All individuals were removed, and tuber numbers and sizes were determined (Figure 1D).

Tubers that were formed in 35 of the 50 developed seedlings (T₀) were retransferred to nature to control its growth and development during the first and second year of growth. T₀ presented relatively low measurements; the weight was about 0.35g, the width was about 0.72cm, and the length was about 0.88cm. After one year, 35 adult orchid plant's tubers (T₁) developed and it was determined that presented relatively higher measurements than T₀; where the width attended 2.34cm and the weight was the highest (7.15g).

After two years, it was determined that 31 adult plants (from the 35 plants that formed first tuber during the first year) formed second tubers (T₂) with also high measurements and only 22 adult plants (from 31 plants that formed two tubers) formed the third tubers (T₃). These small tubers (T₃) presented the lowest

measurements in terms of weigh, width, and length. Accordingly, for the first time in two years, a small population was able to form under natural conditions. The acclimatization process from using *in vitro* asymptotic or symbiotic production methods, (Zhang et al., 2015; Fatahi et al., 2022) has not been applied before the seedlings are planted in nature. In this study, we have shown that new individuals can be obtained with a compatible fungus isolated from *A. coriophora* roots for the reintroduction of orchids. Only a few studies have been conducted on the *ex vitro* and *in situ* germination and reintroduction of both tropical and temperate orchids and their mass production for economic purposes (ornamental and medicinal) (Quay et al., 1995; Aewsakul et al., 2013; Khasim et al., 2020; Kömpe and Mutlu 2021). In a similar study, the reintroduction of *ex*

vitro seedlings of *A. sancta* with a compatible fungus was successful (Deniz et al., 2022). One of the most effective ways of protecting orchids is by ensuring that they can be produced in sufficient quantities to meet industrial demands. Because sustainable production will meet the demand, there will be no need to harvest naturally occurring orchids. In this context, the cultivation provided will bring about protection, because the application of this method for endemic, rare, and threatened species also possible to create a successful and self-sufficient population in the wild. Therefore, filling the gap between orchid conservation theory through practice with cultivation and reintroduction will provide significant benefits both for industrial production and for the reintroduction of threatened species into the wild (Wu et al., 2014; Deniz et al., 2022).

Table 2. Measurements of *Anacamptis coriophora* tubers.

Tubers	Tuber Width (cm)	Tuber Length (cm)	Tuber Weight (g)
T0 (N=35)	0.72 ± 0.28	0.88 ± 0.31	0.35 ± 0.27
T1 (N=35)	2.34 ± 0.64	2.70 ± 0.61	7.15 ± 4.06
T2 (N=31)	1.49 ± 0.44	1.76 ± 0.52	2.57 ± 1.86
T3 (N=22)	1.04 ± 0.20	1.30 ± 0.43	0.93 ± 0.59

T0= tubers formed 6 months after seedlings plantation, T1= first year’s biggest tubers of the adult plants, T2= second year’s medium sized tuber of the adult plants, T3= second year’s third smallest tubers. All values are reported as mean ± SD, N= number of adult orchid plants that formed tubers.

4. Conclusion

This report is the first study on the cultivation of *A. coriophora*, which is important as a food supplement and medicinal orchid. It is also a pioneering method of protection and reintroduction for temperate orchids, which are threatened with extinction. The seedlings easily adapted to nature, and flowering occurred in the second year. 2 and 3 tubers were formed from each *A. coriophora* plant individual, and the number of individuals increased by about 2.5 times in a year. With this method, it will be possible to protect endemic, rare, and threatened orchids in small populations, and mass production of medicinal and economic orchids will be made easily and at a low cost.

Author Contributions

The percentage of the author(s) contributions is presented below. All authors reviewed and approved the final version of the manuscript.

	I.H	Y. ÖK
C	50	50
D	50	50
S	50	50
L	70	30
W	60	40
CR	20	80
SR	80	20
PM	50	50
FA	40	60

C=Concept, D= design, S= supervision, L= literature search, W= writing, CR= critical review, SR= submission and revision, PM= project management, FA= funding acquisition.

Conflict of Interest

The authors declared that there is no conflict of interest.

Ethical Consideration

Ethics committee approval was not required for this study because of there was no study on animals or

humans.

References

- Aewsakul N, Maneesorn D, Serivichyaswat P, Taluengit AT, Nontachaiyapoom S. 2013. *Ex vitro* symbiotic seed germination of *Spathoglottis plicata* Blume on common orchid cultivation substrates. *Sci Horticultur*, 160: 238-242.
- Bektaş E, Cüce M, Sökmen A. 2013. *In vitro* germination protocorm formation and plantlet development of *Orchis coriophora* (Orchidaceae) a naturally growing orchid species in Turkey. *Turkish J Botany*, 37(2): 336-342. 10.3906/bot-1205-28.
- Clements MA, Muir H, Cribb PJ. 1986. A Preliminary report on the symbiotic Germination of European terrestrial orchids. *Kew Bulletin*, 41: 437-445.
- Coats DJ, Dixon KW. 2007. Current perspectives in plant conservation biology. *Aust J Bot*, 55: 187-93.
- Çiğ A, Demirel DE, İşler S. 2018. *In vitro* symbiotic germination potentials of some *Anacamptis Dactylorhiza* *Orchis* and *Ophrys* terrestrial orchid species. *Appl Ecol Environ Res*, 16(4): 5141-5155.
- Deniz IG, Kömpe YÖ, Harzli I, Aytar EC, Mutlu VA, Uysal Dİ. 2022. From seed to flowering tuberous orchid using *ex vitro* symbiotic seed germination: A breakthrough study with *Anacamptis sancta*. *Rhizosphere*, 24: 100597. <https://doi.org/10.1016/j.rhisph.2022.100597>.
- Eşitgen A, Ercişli S, Eken C. 2005. Effects of Mycorrhiza Isolates on Symbiotic Germination of Terrestrial Orchids (*Orchis palustris* Jacq. and *Serapias vomeracea* subsp. *vomeracea* (Burm.f.) Briq. in Turkey. *Symbiosis*, 38: 59-68.
- quFatahi M, Vafaee Y, Nazari F, Tahir N.A. 2022. *In vitro* asymbiotic germination protocorm formation and plantlet development of *Orchis simia* Lam.: Athreatened terrestrial orchid species. *South African J Botany*, 151: 156-165.
- Ghorbani A, Gravendeel B, Naghibi F de Boer H. 2014. Wild orchid tuber collection in Iran: a wake-up call for conservation. *Biodiver Conserv*, 23: 2749-2760.
- Govaerts R, Bernet P, Kratochvil K, Gerlach G, Carr G, Alrich P, Pridgeon AM, Pfahl J, Campacci MA, Baptista DH, Tigges H, Shaw J, Cribb P, George A, Kreuz K, Wood JJ. 2017. World checklist of Orchidaceae. Facilitated by the Royal Botanic Gardens Kew, URL: <https://www.scienceopen.com/document?vid=2e89a8a9-1cc4-49b5-b8fc-1a54fa2f9f48> (accessed date: April 16, 2023).
- Gümüş C, Ellialtıoğlu Ş. 2012. Seed Germination and Development of *Serapias vomeracea* (Burm.fil.) Briq. ssp. *orientalis* Greuter in Tissue Culture. *Res J Biotechnol*, 7(3): 4-8.
- Hopper SD. 2000. How well do phylogenetic studies inform the conservation of Australian plants? *Aust J Bot*, 48: 321-28.
- Joppa LN, Roberts DL, Myers N, Pimm SL. 2011a. Biodiversity hotspots house most undiscovered plant species. *Proceed National Acad Sci USA*, 108: 13171-13176.
- Joppa LN, Roberts DL, Pimm SL. 2011b. How many species of flowering plants are there? *Proceed Royal Soc B*, 278: 554-559.
- Khasim SM, Hedge SN, Arnao MTG, Thammasiri K. 2020. Orchid biology: Recent Trends and challenges. Springer, New York, USA, pp: 547.
- Kömpe YÖ, Mutlu VA. 2021. *Ex vitro* symbiotic germination of the seeds of *Anacamptis coriophora* (L.) R.M. Bateman Pridgeon and M.W. Chase and *Orchis anatolica* Boiss. *Biol Futur*, 72: 509-516. <https://doi.org/10.1007/s42977-021-00100-5>.
- Kömpe YÖ, Karakaya H, Mutlu VA. 2021. Symbiotic propagation of the wet meadow orchid *Anacamptis laxiflora* for conservation and reintroduction. *Fresenius Environ Bullet*, 30(9): 10535-10544.
- Kömpe YÖ, Mutlu VA, Özkoç İ, Demiray S, Bozkurt S. 2022. Fungal diversity and *ex vitro* symbiotic germination of *Serapias vomeracea* (Orchidaceae). *Acta Botan Croatica*, 81(1): 108-116. DOI: 10.37427/botcro-2022-008.
- Kreziou A, de Boer H, Gravendeel B. 2016. Harvesting of salep orchids in North-western Greece continues to threaten natural populations. *Oryx*, 50(3): 393-396. <https://doi.org/10.1017/S0030605315000265>.
- León-Yáñez S, Valencia R, Pitman N, Endara L, Ulloa Ulloa C, Navarette H. 2011. Red book of the endemic plants of Ecuador. Quito: Pontificia Universidad Católica del Ecuador, Quito, Ecuador, pp: 957.
- Löki V, Tökölyi J, Süveges K, Lovas-Kiss A, Hürkan K, Sramko G, Molnar AV. 2015. The orchid flora of Turkish graveyards: a comprehensive field survey. *Willdenowia*, 45(2): 231-243.
- Mutlu, V. A., & Kömpe, Y. O. (2020). Mycorrhizal fungi of some *Orchis* species of Turkey. *Pakistan Journal of Botany*, 52(2), 687-695.
- Oktalira FT, Whitehead MR, Linde CC. 2019. Mycorrhizal specificity in widespread and narrow-range distributed *Caladenia* orchid species. *Fungal Ecol*, 42: 100869.
- Pujasatria GC, Miura C, Kaminaka H. 2020. *In vitro* symbiotic germination: A revitalized heuristic approach for orchid species conservation. *Plants*, 9(12): 1742.
- Qin H, Yang Y, Dong S. 2017. Threatened species list of China's higher plants. *Biodiver Sci*, 25: 696-744.
- Quay L, McComb JA, Dixon KW. 1995. Methods for *ex vitro* germination of Australian terrestrial orchids. *Hortsci*, 30: 1445-1446. <https://doi.org/10.21273/HORTSCI.30.7.1445>
- Sezik E. 2002. Turkish orchids and salep. *Acta Pharm Turcica*, 44: 151-157
- Sosa V, Platas T. 1998. Extinction and persistence of rare orchids in Veracruz Mexico. - *Conservation Biology* 12: 451-455.
- Steinfurt U, Verdugo G, Besoain X, Cisternas MA. 2010. Mycorrhizal association and symbiotic germination of the terrestrial orchid *Bipinnula fimbriata* (Poepp.) Johnston (Orchidaceae). *Flora-Morphol Distrib Funct Ecol Plants*, 205: 811-817.
- Wang H, Fang H, Wang Y, Duan L, Guo S. 2011. In situ seed baiting techniques in *Dendrobium officinale* Kimura et Migo and *Dendrobium nobile* Lindl.: the endangered Chinese endemic *Dendrobium* (Orchidaceae). *World J Microbiol Biotechnol*, 27: 2051-2059.
- Wu K, Zeng S, Lin D, Da Silva T, Bu Z, Zhang J, Duan J. 2014. *In vitro* propagation and reintroduction of the endangered *Renanthera imschootiana* Rolfe. *PLoS ONE*, 9: e110033. doi: 10.1371/j.pone.0110033.
- Zhang YY, Wu KL, Zhang JX, Deng RF, Duan J, Da Silva T, Huang WC, Zeng SJ. 2015. Embryo development in association with asymbiotic seed germination *in vitro* *Paphiopedilum armeniacum* S.C. Chen et F.Y. Liu. *Scie Report*, 5: 16356.
- Zhang S, Yang Y, Li J, Qin J, Zhang W, Huang W, Hu H. 2018. Physiological diversity of orchids. *Plant Divers*, 40(4): 196-208. <https://doi.org/10.1016/j.pld.2018.06.003>.
- Zhang Y, Li YY, Chen XM, Guo SX, Li YI. 2020. Effect of different mycobionts on symbiotic germination and seedling growth of *Dendrobium officinale* an important medicinal orchid. *Botan Stud*, 61: 2.



DETECTION OF BACTERIAL DIVERSITY OF VARIOUS HABITATS IN ÇORUM PROVINCE AND ITS CRIMINALISTICS CONTRIBUTION TO POSSIBLE CRIME SCENE STUDIES

Esra BALCI¹, Demet TATAR^{2*}, Aysel VEYISOGLU³, Ali TOKATLI^{4,5}

¹Hitit University, Graduate Training Institute, Department of Forensic Sciences, 19500, Çorum, Türkiye

²Hitit University, Osmancık Ömer Derindere Vocational School, Department of Medical Services and Techniques, 19500, Çorum, Türkiye

³Sinop University, Vocational School of Health Services, Department of Medical Laboratory Techniques, 57000, Sinop, Türkiye

⁴Ondokuz Mayıs University, Faculty of Science, Department of Biology, 55139, Samsun, Türkiye


⁵Ondokuz Mayıs University, Faculty of Agriculture, Department of Soil Science and Plant Nutrition, 55139, Samsun, Türkiye


Abstract: Microorganisms are not homogeneously distributed in environments, soil systems are heterogeneous. Soil can be an important evidence value in forensic investigations. It is among the important evidences that contribute to the solution of forensic events in forensic sciences. *Bacteria* contained in the soil are microbiological evidences. Not all bacteria can be cultured by conventional methods and the amount of cultured bacteria remains limited. Metagenomic studies have been carried out for non-culturable *Bacteria*. The aim of this study is to perform DNA isolation from soil samples taken from Yeşil Lake (swamp), Faculty of Arts and Sciences garden, agricultural land, Sıklık (forest area) regions of Çorum Province in Türkiye and to determine bacterial diversity by metagenomic analysis of DNA isolated from soil samples. Density and differences of isolates according to habitats were determined. It is thought that the result of this study can shed light on previous crime scene studies in the determined habitats and will contribute to possible future crime scene studies and forensic science that may occur later.


Keywords: Habitat, DNA isolation, Bacterial diversity, Criminalistics


*Corresponding author: Hitit University, Osmancık Ömer Derindere Vocational School, Department of Medical Services and Techniques, 19500, Çorum, Türkiye

E mail: demettatar@hitit.edu.tr (D. TATAR)

Esra BALCI  <https://orcid.org/0000-0002-7708-1967>

Demet TATAR  <https://orcid.org/0000-0002-9317-3263>

Aysel VEYISOGLU  <https://orcid.org/0000-0002-1406-5513>

Ali TOKATLI  <https://orcid.org/0000-0002-7559-8882>

Received: December 31, 2023

Accepted: February 26, 2024

Published: March 15, 2024

Cite as: Balci E, Tatar D, Veyisoğlu A, Tokatlı A. 2024. Detection of bacterial diversity of various habitats in Çorum province and its criminalistics contribution to possible crime scene studies. *BSJ Eng Sci*, 7(2): 334-341.

1. Introduction

The most important time to find the evidence that guides the forensic events is when the crime scene investigation is done. Crime scene investigation and the evidence to be obtained are very important in terms of starting and ending the investigation in the best and correct way. All kinds of material are evidence. Evidence can be found at the macro or micro level, depending on the way the event occurred. There is evidence that can be obtained at the micro level in cases where the DNA is degraded and not sufficient at the crime scene. Soil is physical evidence that can be distinguished at a crime scene thanks to the variability of the microorganisms it contains. Since factors such as temperature, humidity, pH, climate, and topography affect the soil structure differently in each area, a result can be obtained by finding differences with comparison. Because of the complex structure of soils, the analysis of inorganic and organic components provides complementary independent information about the soil's geological origin, dominant vegetation, management and environment (Dawson and Hillier,

2010; Efeoğlu et al., 2022).

In forensic microbiology, it is important that many bacteria can be used as evidence. Bioterrorism makes a great contribution to forensic sciences to find the time and cause of death and to establish the plot in crime scene investigation studies. 16S rRNA gene sequence analyzes are performed to find the taxonomic connection of prokaryotes. The presence of 16S rRNA in all bacteria makes 16S rRNA gene sequencing a universal method. However, this method is not a perfect measure of gene sequence variation. 16S rRNA gene analysis is widely used to identify bacteria found in soil. Analysis is difficult due to the large number of bacterial species found in the soil. Scientists prefer to use 16S rRNA gene analysis to study bacteria (Carter et al., 2017).

In a study conducted by Efeoğlu et al., 2022 they aimed to evaluate the importance of identifying microorganisms in soil in terms of forensic science. The study covered 20 regions identified and marked outside the residential areas within the borders of Istanbul. 83% bacteria and 17% fungi were detected in soil samples and physical evidence samples (fabric, rubber, metal, and wood)



collected.

Demanèche et al. (2017) conducted a blind test to determine the origine of two samples (one from the mock crime scene and the other from a 50:50 mixture of the crime scene and the alibi area) compared to three control samples (soil samples from the crime scene, from a context site 25 m away from the crime scene and from the alibi site which was the suspect's home). Two biological methods, Ribosomal Intergenic Spacer Analysis (RISA) and 16S rRNA gene sequencing with Illumina Miseq, were used to evaluate the discriminatory power of soil bacterial communities. Promising results were already observed with molecular methods applied to soil extracted DNA under specific conditions, including T-RFLP, ARDRA, RISA and HTS (High-throughput sequencing) methods such as metagenomic and amplicon sequencing. As a results of this study, RISA or High-throughput sequencing (HTS) in soil DNA was able to identify single-origin soil samples, a combination of methods was required to accurately identify samples of mixed origin and soil DNA can be a useful tool for forensic science (Demanèche et al., 2017).

Although numerical estimation of prokaryotic cells was made, this result was reached as a result of culturing. However, contrary to what is known, the rate of non-culturable bacteria is much higher than that of bacteria that can be cultured and identified in this way. Metagenomic studies promise to reveal the gene sequence of the majority of microorganisms, which cannot be easily obtained by pure culture, by providing the confidence to clarify this situation. Thus, it is possible to reveal and identify the presence of unknown microorganisms (Kunin et al., 2008).

The aim of this study was to perform metagenomic analysis and genomic marking on soil samples collected from Yeşil Lake (swamp), Sıklık Nature Park (forest), agricultural land and the garden of the Faculty of Arts and Sciences of Çorum Province in Türkiye. As a result of the determination of the microbiological ratio by DNA analysis in the soil samples obtained, it is thought that it will guide the forensic sciences and investigation in terms of determining whether the incident took place in the visible place or in a different place.

2. Materials and Methods

2.1. Collection and Storage of Soil Samples

Soil samples were collected from Yeşil Lake (Latitude: 40.763084, Longitude: 34.863324), Faculty of Arts and Sciences' garden (Latitude: 40.566835, Longitude: 34.934049), Sıklık Nature Park (Latitude: 40.351975, Longitude: 35.023487) and an active cultivated agricultural land in Çorum Province (Latitude: 40.416385, Longitude: 35.034248). The distance between the fields is one of the reasons for their selection. The reason for choosing these areas is differences between forested area, inner city, aquatic environment and agricultural land also there are north-

south differences in distance from each other.

While collecting the soil samples, attention was paid to the small number of people and acted quickly. Considering the hot weather, immediately after sampling, the soil was placed in a hot and cold protected aluminum-coated bag with ice cubes inside and was stored in a refrigerator at -20 degrees Celsius without wasting time. The soil sample was collected from a depth of 15-20 cm. This 0-15 cm depth was chosen because microbial activity has been reported to occur in the upper 15 cm (Castañeda and Barbosa, 2017). The samples taken were labeled and stored individually in ziplock bags. Samples taken during the daytime were packed in heat insulated bags containing ice cubes without waiting. In order to minimize heat loss, it was packed in bags, styrofoam boxes and delivered to the company to be analyzed within 18 hours.

2.2. DNA Extraction and Sequencing

DNA extraction and purification was performed using the Qiagen DNeasy PowerSoil Pro Kit. After the isolation, DNA concentrations and purity values of the samples were measured with a spectrophotometer device (Table 1). In DNA quantification with this device, measurements were made according to the absorbance values measured at 260 nm wavelength. The ratio of absorption values of DNA at 260 and 280 nm wavelengths (A₂₆₀/A₂₈₀) was used for purity control. If this ratio is in the range of 1.8-2.0, the isolated DNA is considered pure, and if it is outside the value range, the DNA is considered impure (Matlock, 2015). The obtained DNA samples were used in metagenomic analysis.

Table.1. Concentration values of isolated DNAs

Sample	Concentration (ng/ µL)
Sıklık Natural Park (SP)	33.516
Agricultural Land (AL)	23.955
Faculty of Art and Sciences (FAS)	19.409
Yesil Lake (YL)	25.816

Qiagen brand DNeasy PowerSoil Pro Kit (Figure 1) was used as the kit of choice, as it is effective and sensitive in the purification of proteins and nucleic acids in molecular biology applications and in the isolation of DNA from difficult samples such as compost, soil fertilizer and similar. QIAGEN's the second generation Inhibitor Removal Technology allows us to obtain high quality DNA that can be used immediately in difficult soil types such as environmental compost. With this kit, cell lysis is carried out by mechanical and chemical methods. Total genomic DNA is obtained by trapping on a silica membrane in spin column format and then eluted from the membrane by washing. The working protocol steps of the kit are as follows;

250 mg of soil, 800 µl of CD1 solution included in the kit are added to the PowerBead Pro Tube and vortexed. The tube used contains a buffer that will help disperse the soil particles, begin to dissolve the humic acids, and also

protect the nucleic acids from degradation. With a short vortexing process, the components in the tube are mixed and the buffer begins to disperse into the sample. After vortexing for a minimum of 10 minutes and ensuring that the samples are thoroughly homogenized, the tube is centrifuged at 15,000 rpm for 1 minute. The supernatant is transferred to a new 2 ml microcentrifuge tube. Add 200 µl of CD2 solution and vortex for 5 seconds. CD2 solution contains a reagent that can precipitate non-DNA organic and inorganic material including cell debris, humic substances, and proteins. It is centrifuged at 15,000 rpm for 1 minute and 700 µl of supernatant is taken into a new 2 ml microcentrifuge tube, avoiding the pellet. At this point, the pellet contains non-DNA humic acids, cell debris and proteins. Therefore, for the best DNA yield and quality, there should be no contamination from the pellet while taking the supernatant. 600 µl of CD3 solution, a highly concentrated salt solution, is added and vortexed for 5 seconds. Since DNA binds tightly to silica at high salt concentrations, the content of this solution is adjusted to allow DNA to bind. DNA binds selectively to the silica membrane in the MB spin column in the presence of high salt solution. Contaminants pass through the filter membrane and only DNA remains attached to the membrane. Here, 650 µl of lysate is loaded and centrifuged at 15,000 rpm for 1 minute. Transfer the MB spin column to a new 2 ml collection tube. 500 µl of EA solution, which is a wash bag that removes proteins and other non-aqueous substances, is added and centrifuged at 15,000 rpm for 1 minute. The bottom is discarded and the MB spin column is placed in the same 2 ml collection tube. 500 µl of C5 solution, an ethanol-based wash solution used to further clean the DNA attached to the silica filter membrane in the MB spin column, is added and centrifuged for 1 minute at 15,000 rpm. This wash solution removes residual salt, humic acid and other contaminants while allowing the DNA to remain attached to the silica membrane. The bottom is discarded and the MB spin column is placed in a new 2 ml collection tube. It is centrifuged at 16,000 rpm for 2 minutes. This rotation is important to remove all traces of the C5 solution. The MB spin column is placed in a new 1.5 ml Elution Tube. Add 50-100 µl of C6 solution to the center of the white filter membrane. Placing this solution in the middle of the membrane ensures that the membrane is wet so that the DNA is released from the membrane more efficiently and completely. The C6 solution is a salt-free (10 mM Tris) solution. The DNA bound in the presence of high salt is selectively liberated with the C6 solution. Centrifuge at 15,000 rpm for 1 minute and discard the MB spin column. As a result of these processes, DNA is isolated for other applications. The isolated DNA is amplified by PCR and sent for analysis for sequencing (URL, 2022).

After DNA isolation, NGS (Next Generation Sequencing) library was prepared and the sequencing process was started. Bioinformatics analysis was performed after sequencing. According to the absorbance values

measured at 260 and 280 nm wavelengths of the initially isolated DNA, it was assumed to be pure between 1.8-2.0 values (Matlock, 2015), and the purity level was checked by reading with a spectrophotometer (Topal Sarıkaya, 2008).

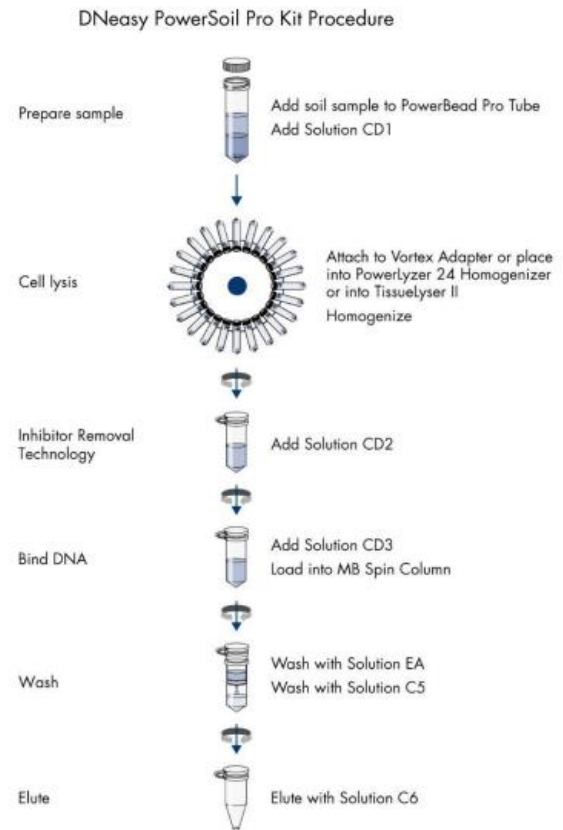


Figure 1. DNeasy powersoil pro kit procedure.

2.3. DNA Analyzing

When performing 16S amplicon sequencing and bioinformatics analysis, extracted DNA samples were subjected to amplicon sequencing library preparation using bacteria specific 341F (5'-CCTACGGGNGGCWGCAG-3') and 805R (5'- GACTACHVGGGTATCTAATCC-3') primers targeting V3-V4 region of the 16S rRNA gene. Prepared libraries were purified, quantified and further sequenced on MiSeq instrument (Illumina, USA) using 300bp paired-end chemistry. Demultiplexing and clipping of sequence adapters from raw sequences was performed by CASAVA data analysis software (Illumina, USA). The fragments with any mismatches to the barcodes or primers were excluded. PCR primers were removed from sequences using cutadapt (10.14806/ej.17.1.200) plugin within QIIME2 v2021.2 (10.1038/s41587-019-0209-9) as all amplicon sequencing workflow. Paired-end reads were joined (vsearch join-pairs) and quality filtered (quality-filter q-score-joined). Then, sequences were denoised using deblur (deblur denoise-16S) (10.1128/mSystems.00191-16). Taxonomy was assigned to each amplicon sequence variant (ASV) using 'feature-classifier classify-sklearn' plugin against the SILVA v138 database. Final ASV table was used to calculate alpha diversity metrics.

In the study, V3-V4 region was amplified based on Klindworth et al., 2013. The collected 4 metagenomic sequencing samples were sent to the USA through Artu Biotechnology. Since pure DNA was obtained, it was sent at room temperature. Sequencing of pure DNAs was performed using CASAVA software. As a result of the data obtained from the sequencing, alpha diversity metrics, taxonomic bar graphs and Krona pie chart graphs were created using DNA sequences, cleaned raw sequences, ASV (amplicon sequence variants) table.

3. Results

3.1. Phylum Level Distribution in the Soil

According to the results of metagenomic analysis, 1 kingdom, 26 phyla, 69 classes, 142 orders, 221 families, 382 genera and 658 species were identified in all samples. Bacterial branches in habitats are shown by a histogram graph (Figure 2).

In our study, the results of the analysis of the soil sample taken from the forest area (Sıklık Nature Park) showed that the bacterial distribution of this area is as follows: *Actinobacteriota* 64%, *Proteobacteria* 10%, *Chloroflexi* 10%, *Gemmatimonadota* 5%, *Acidobacteriota* 5%, *Planctomycetota* 5%, *Myxococcota* 0.8 %, *Firmicutes* 0.3% and *Methylomimirabilota* 0.2% (Figure 3). In a study by Lladó et al., 2017, it was determined that the acidic soils of coniferous forests mainly contain *Actinobacteriota*, *Proteobacteria* and *Acidobacteria*. Similarly, the presence of coniferous trees in the Sıklık Nature Park and the presence of more species of *Actinobacteriota* according to the analysis results of other soil samples support this information. At the same time, when all the analysis results are considered, the highest bacterial density was observed with 64% *Actinobacteriota* in the Sıklık Nature Park.

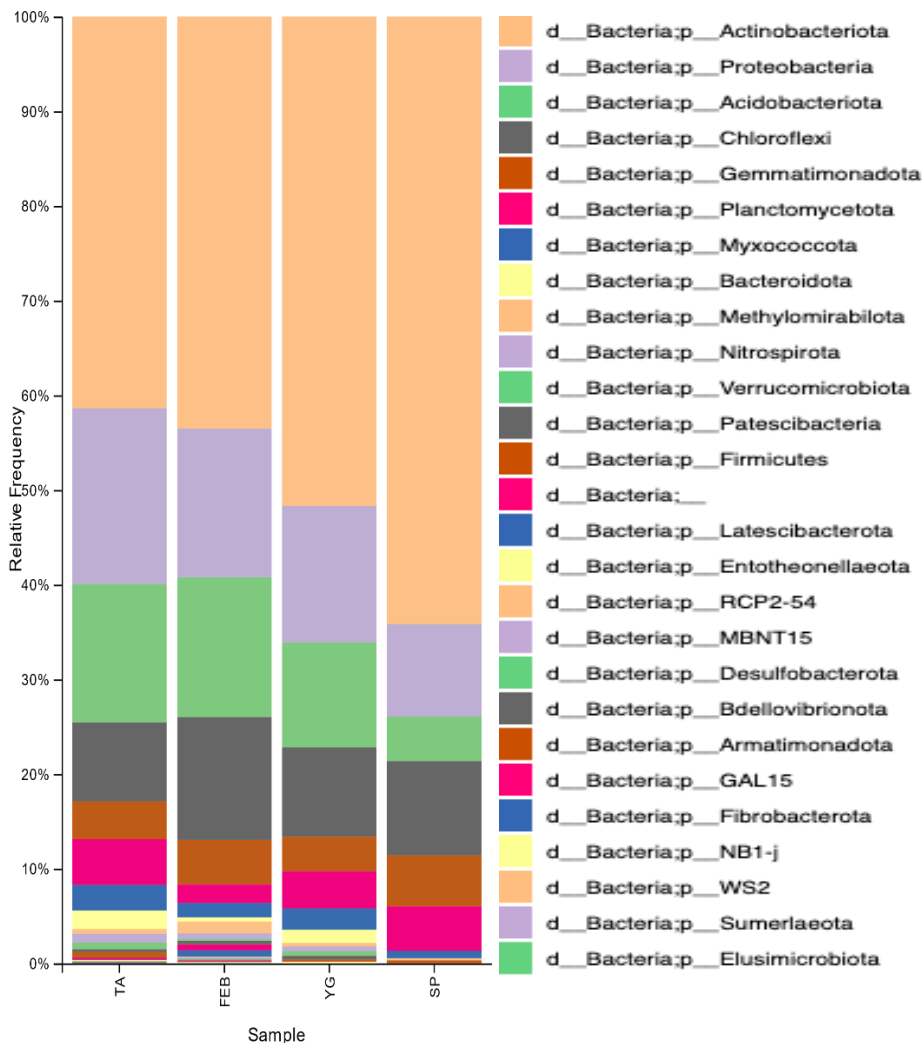


Figure 2. Representation of bacterial branches in habitats with histogram graph

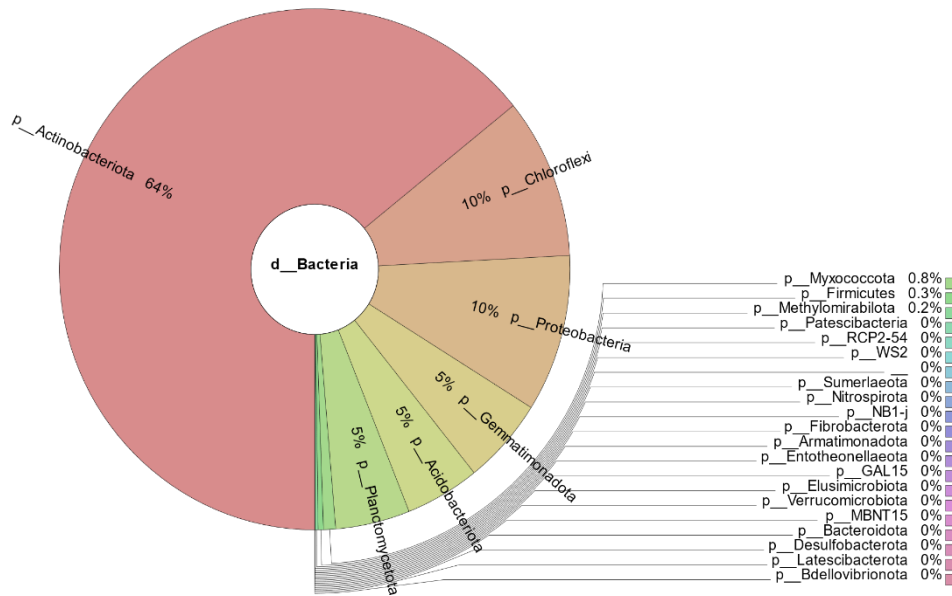


Figure 3. Representation of bacterial distribution in the soil sample taken from the Sıklık Nature Park on the Krona pie chart.

As a result of the analysis of the soil sample taken from the agricultural land, it was determined that while *Actinobacteriota* had the highest density with 41% followed by *Proteobacteria* 19%, *Acidobacteriota* 15%, *Chloroflexi* 8%, *Gemmatimonadota* 4%, *Planctomycetota* 5%, *Myxococcota* 3%, *Bacteroidota* 2%. 0.6% of *Firmicutes*, 0.5% of *Methylomirabilota*, 0.3% of *Patescibacteria*, but also the presence of 11 phyla less than 1% were determined (Figure 4).

As a result of the analysis of soil samples taken from the garden of Hitit University Faculty of Arts and Sciences, *Actinobacteriota* 44%, *Proteobacteria* 16%, *Acidobacteriota* 15%, *Chloroflexi* 13%, *Gemmatimonadota*

5%, *Planctomycetota* 2%, *Myxococcota* 2%, *Firmicutes* 0.03% and *Methylomirabilota* 1%, *Patescibacteria* was determined at a rate of 0.4% (Figure 5). At the same time, 14 different phyla were identified with percentages less than 1%. In the soil sample at the bottom of water we took from the Yeşil Lake as a swamp area, 52% *Actinobacteriota*, 14% *Proteobacteria*, 11% *Acidobacteriota* 9% *Chloroflexi*, 4% *Gemmatimonadota*, 4% *Planctomycetota*, 2% *Myxococcota*, 1% *Bacteroidota*, 0.2% *Firmicutes* and the presence of phyla such as 0.4% *Methylomirabilota* and 0.4% *Patescibacteria* were obtained (Figure 6).

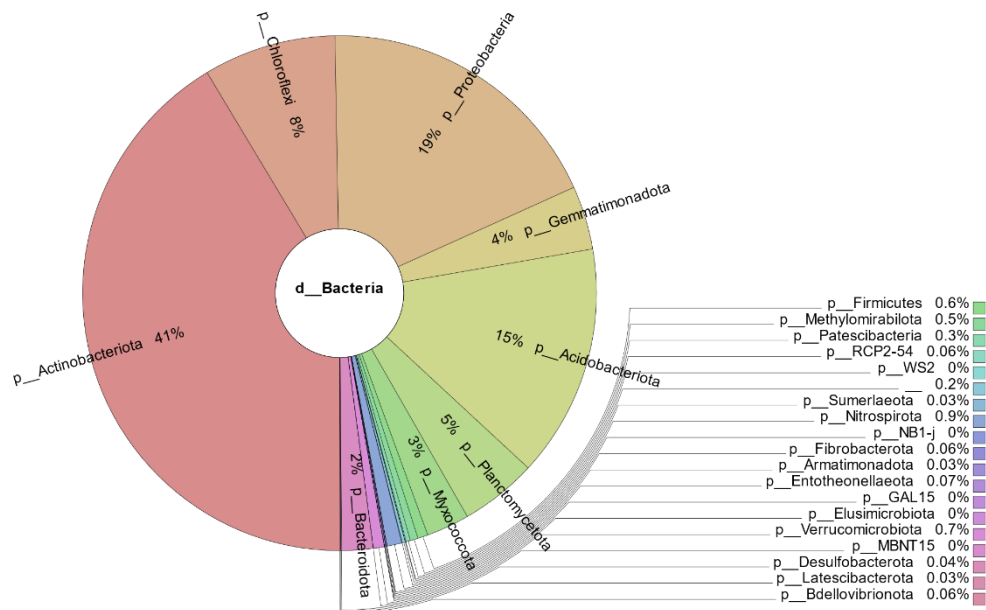


Figure 4. Demonstration of the bacterial distributions in the soil sample taken from the agricultural land on the Krona pie chart.

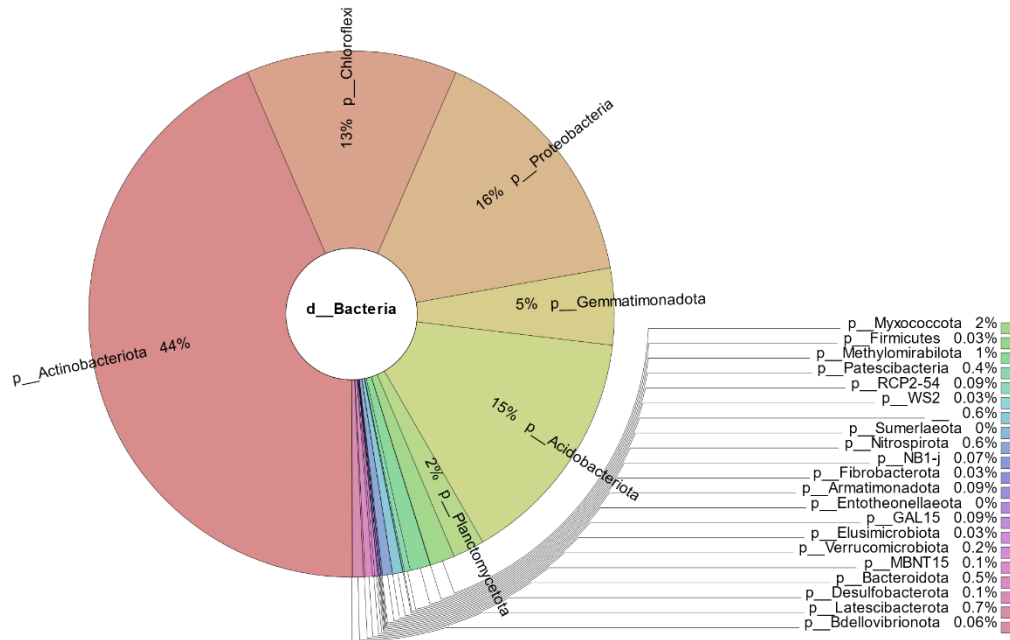


Figure 5. Demonstration of the bacterial distribution in the soil sample taken from the garden of the Faculty of Arts and Sciences on the Krona pie chart.

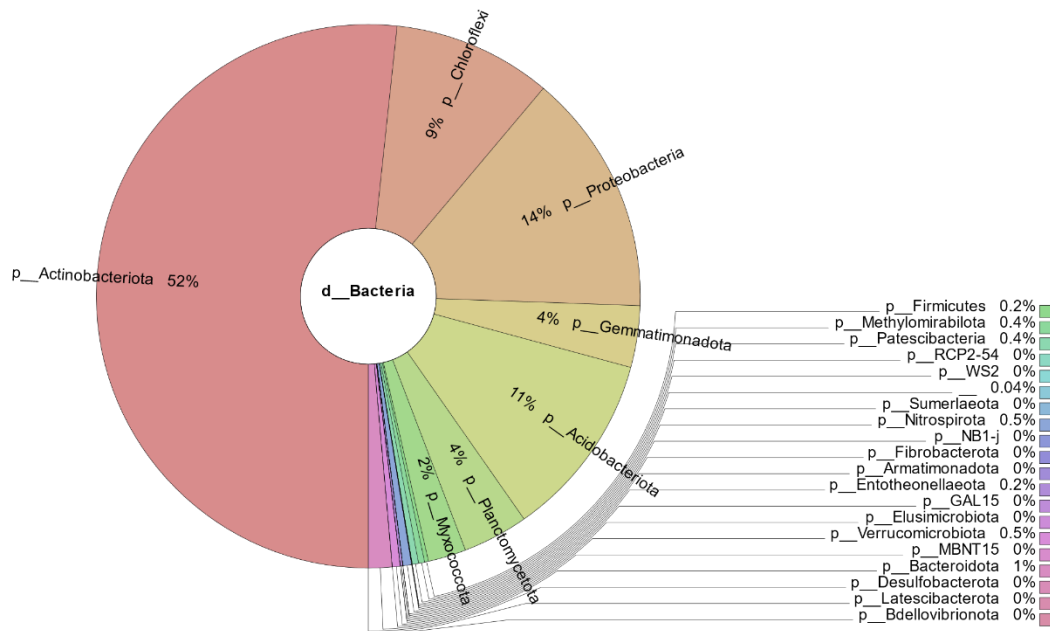


Figure 6. Demonstration of the bacterial distribution in the soil sample taken from the Green Lake on the Krona pie chart.

4. Discussion

It is present based on structures that geographical location is a more important factor than soil type in determining the microbial density in the soil (Habtom et al., 2019). In our study, the effective reason for determining the habitats was to take into account the areas with high crime rate and the potential to be a crime scene while selecting these areas, soil type was not taken into account and it was preferred that they were far from each other. It is also known that soil pH and C and N ratios in soil have an effect on the microbial community

(Lauber et al., 2009; Rasche et al., 2011). At the same time, it has been determined in some studies that the soil microbial activity decreases compared to the summer season, especially in the winter months when the temperature factor decreases (Guoju et al., 2012). Based on these researches, in our study, considering the temperature factor, sample collection was carried out in summer when the microbial activity was the highest, cold storage was carried out and the current soil microbial community was frozen.

The aim of this study is to isolate DNA from soil samples

collected from Yeşil Lake, the garden of the Faculty of Arts and Sciences, an agricultural land and the Sıklık Nature Park regions of Çorum Province in Türkiye and to perform metagenomic analysis with the isolated DNA. It is thought that the results obtained will reveal the bacterial diversity in the soil samples and the diversity of soil bacteria in the determined habitats will shed light on the events that have occurred before and may occur in the future.

Within the scope of this study, DNA analysis was performed on soil samples taken from four different areas (the garden of the Faculty of Arts and Sciences, the Sıklık Nature Park, the Green Lake and an agricultural land) considering the temperature factor. Then the bacterial rates were determined by metagenomic analysis through service procurement from Artı Biotechnology Company has been done. The 16S bacterial rRNA gene was amplified by polymerase chain reaction (PCR) and sequenced. The taxonomic classification of the product amplicon sequence variants obtained as a result of PCR was performed in the SILVA v138 database. Percentages of reads at each taxonomic level between samples were analyzed and data are at the species level. All of the obtained data could not be included in our study due to the large file size.

Lladó et al. (2017) determined that five phyla (*Acidobacteriota*, *Actinobacteriota*, *Proteobacteria*, *Bacteroidota* and *Firmicutes*) were abundant in most soils. Similarly, the graphs in this study show that all five phyla are proportionally higher. Recent studies have shown that surface and buried soil communities exhibit different behavior during the weathering process. While microbial communities in surface soil tend to decrease in taxon richness, diversity and equality; Microbial communities in close contact with buried cadavers show contrasting characteristics (e.g., increased taxon richness, consistent diversity, and decreased evenness). Furthermore, while *Proteobacteria* was cited as the most abundant phylum in burial soil samples, the relative abundance of *Acidobacteriota* decreased and *Firmicutes* increased in surface cadaver-soil communities, while microbial community composition remained fairly constant in buried soil communities (Finley et al. 2015, 2016; Oliveira and Amorim, 2018).

In the samples we took, while the density of *Actinobacteriota* was 64% in the Sıklık Nature Park, it was 52% in the Green Lake, 44% in the garden of the Faculty of Arts and Sciences, and 41% in the agricultural land. It is thought that the density difference determined in the Sıklık Nature Park and the agricultural land is due to the acidic feature of the coniferous trees mentioned in the study by Lladó et al. (2017). The fact that the samples taken from the Sıklık Nature Park were taken the lower part of the trees, the presence of pine forests around the Yeşil Lake, the growth of similar trees in the garden of the Faculty of Arts and Sciences, and the absence of similar trees near the agricultural land indicate that the rate decreases when the tree density decreases.

For the *Proteobacteria* group, results were close to each other with 19% in the agricultural land, 16% in the Faculty of Arts and Sciences, 14% in the Yeşil Lake and 10% in the Sıklık Nature Park. This situation supports the information that *Proteobacteria* are involved in the global carbon, nitrogen and sulphur cycle (Kerstens et al., 2006). In a study by Spain et al. (2009), it was stated that *Alphaproteobacteria* were the most abundant and diverse class in their study. Similarly, *Alphaproteobacteria* were found 10% in the Faculty of Science and Arts sample, 13% in the Agricultural Land, 11% in the Yeşil Lake and 6% in the Sıklık Nature Park, while *Gammaproteobacteria* was found 5% in the Faculty of Science and Arts and Agricultural Land samples, and 3% in Yeşil Lake and the Sıklık Nature Park. No data were available for the *Betaproteobacteria* class.

The *Acidobacteriota* group, which has the third largest ratio in terms of density, Kalam et al. (2020) stated that it is involved in the regulation of carbon, nitrogen and sulphur cycles. It is available in the literature that *Acidobacteriota* are dominant in microbial communities and also abundant in arable land (Kielak et al., 2009). According to the data obtained in our study, similarly, the presence of the *Acidobacterota* group was determined as 15% in the agricultural land and the garden of the Faculty of Arts and Sciences, 11% in the Yeşil Lake and 5% in the Sıklık Nature Park.

Even if our study was carried out to contribute to forensic science and to make microbial marking, the error rates of microorganism typing methods should be taken into account in a crime scene study, considering that there is a large amount of microorganisms in 1 gram of soil and the data we obtained belong to the sample area. Although we have come to a conclusion, it will be difficult to obtain data when there are incomparable samples due to the lack of a database with information on microorganisms found in Türkiye. Our study is a master's thesis, and with the increasing opportunities and technology in the future, another dimension can be added to metagenomic studies with more different examples.

5. Conclusion

Within the scope of this study, answers are sought to questions such as the relationship between the victim, the suspect and the crime scene at the crime scene, whether the soil samples found on the victim's soil or the suspect's belongings and the soil at the crime scene are similar and the extent of the microbial community. At the same time, our study can be considered as an important study in that it shows that phenotypic descriptions are not reliable and definitive results and that more reliable, inexpensive and short-term results can be obtained through metagenomic analysis.

Author Contributions

The percentage of the author(s) contributions is presented below. All authors reviewed and approved the final version of the manuscript.

	E.B.	D.T.	A.V.	A.T.
C	25	25	25	25
D	25	25	25	25
S		75	25	
DCP	25	25	25	25
DAI	25	25	25	25
L	25	25	25	25
W	75	25		
CR	25	25	25	25
SR	25	25	25	25
PM	25	25	25	25
FA	25	25	25	25

C=Concept, D= design, S= supervision, DCP= data collection and/or processing, DAI= data analysis and/or interpretation, L= literature search, W= writing, CR= critical review, SR= submission and revision, PM= project management, FA= funding acquisition.

Conflict of Interest

The authors declared that there is no conflict of interest.

Ethical Consideration

Ethics committee approval was not required for this study because of there was no study on animals or humans.

Acknowledgements

This research was supported by Hitit University (HITU; project no. ODMYO19004.22.001). This manuscript was produced from the master's thesis.

References

Carter DO, Tomberlin JK, Benbow ME, Metcalf JL. 2017. Forensic microbiology. John Wiley & Sons, Pondicherry, India, pp: 416.

Castañeda LE, Barbosa O. 2017. Metagenomic analysis exploring taxonomic and functional diversity of soil microbial communities in Chilean vineyards and surrounding native forests. PeerJ, 5: e3098.

Dawson LA, Hillier S. 2010. Measurement of soil characteristics for forensic applications. Surf Interface Anal, 42: 363-377. <https://doi.org/10.1002/sia.3315>.

Demanèche S, Schauser L, Dawson L, Franqueville, L, Simonet P. 2017. Microbial soil community analyses for forensic science: application to a blind test. Forensic Sci Int, 270: 153–158. doi: 10.1016/j.forsciint.2016.12.004.

Efeoğlu FG, Çakan H, Kara U, Daş T. 2022. Forensic microbiological analysis of soil and the physical evidence buried in soil obtained from several towns in Istanbul. Cureus, 14(2): e22329. doi: 10.7759/cureus.22329. PMID: 35317034; PMCID: PMC8934109.

Finley SJ, Benbow ME, Javan GT. 2015. Potential applications of soil microbial ecology and next-generation sequencing in

criminal investigations. Appl Soil Ecol, 88: 69–78. doi: 10.1016/j.apsoil.2015.01.001.

Finley SJ, Pechal JL, Benbow ME, Robertson B, Javan GT. 2016. Microbial signatures of cadaver gravesoil during decomposition. Microb Ecol, 71(3): 524–529. doi: 10.1007/s00248-015-0725-1.

Guoju X, Qiang Z, Jiangtao B, Fengju Z, Chengke L. 2012. The relationship between winter temperature rise and soil fertility properties. Air, Soil Water Res, 5: ASWR-S8599.

Habtom H, Pasternak Z, Matan O, Azulay C, Gafny R, Jurkevitch, E. 2019. Applying microbial biogeography in soil forensics. Forensic Sci Inter Genet, 38: 195-203.

Kalam S, Basu A, Ahmad I, Sayyed RZ, El-Enshasy HA, Dailin DJ, Suriani NL. 2020. Recent understanding of soil acidobacteria and their ecological significance: a critical review. Front Microbiol, 11: 580024.

Kerstens K, De Vos P, Gillis M, Swings J, Vandamme P, Stackebrandt E. 2006. Introduction to the Proteobacteria. In: Dworkin M, Falkow S, Rosenberg E, Schleifer KH, Stackebrandt E. The Prokaryotes. Springer, New York, USA, pp: 3-37.

Kielak A, Pijl AS, Van Veen JA, Kowalchuk GA. 2009. Phylogenetic diversity of Acidobacteria in a former agricultural soil. ISME J, 3(3): 378-382.

Klindworth A, Pruesse E, Schweer T, Peplies J, Quast C, Horn M, Glöckner FO. 2013. Evaluation of general 16S ribosomal RNA gene PCR primers for classical and next-generation sequencing-based diversity studies. Nucleic Acids Res, 41(1): e1-e1.

Kunin V, Copeland A, Lapidus A, Mavromatis K, Hugenholtz P. 2008. A bioinformatician's guide to metagenomics. Microbiol Molec Biol Rev, 72(4): 557-578.

Lauber CL, Hamady M, Knight R, Fierer N. 2009. Pyrosequencing-based assessment of soil pH as a predictor of soil bacterial community structure at the continental scale. Applied Environ Microbiol, 75(15): 5111-5120.

Lladó S, López-Mondéjar R, Baldrian P. 2017. Forest soil bacteria: diversity, involvement in ecosystem processes, and response to global change. Microbiol Molec Biol Rev, 81(2): e00063-16.

Matlock B. 2015. Assessment of nucleic acid purity. URL: <https://assets.thermofisher.com/TFSAssets/> (accessed date: March 21, 2022).

Oliveira M, Amorim A. 2018. Microbial forensics: new breakthroughs and future prospects. Appl Microbiol Biotechnol, 102(24): 10377-10391. doi: 10.1007/s00253-018-9414-6.

Rasche F, Knapp D, Kaiser C, Koranda M, Kitzler B, Zechmeister-Boltenstern S, Sessitsch A. 2011. Seasonality and resource availability control bacterial and archaeal communities in soils of a temperate beech forest. ISME J, 5(3): 389-402.

Spain AM, Krumholz LR, Elshahed MS. 2009. Abundance, composition, diversity and novelty of soil Proteobacteria. ISME J, 3(8): 992-1000.

Topal Sarıkaya A. 2008. DNA'nın izolasyonu ve analizi. Temizkan G, Arda N. Moleküler biyolojide kullanılan yöntemler. Nobel Tıp Kitabevleri, İstanbul, Türkiye, ss: 345.

URL. 2022. <https://www.qiagen.com/us/resources/resourcedetail?id=9bb59b74-e493-4aeb-b6c1-f660852e8d97&lang=en> (accessed date: March 21, 2022).



KATI YAĞ ALTERNATİFİ OLARAK ÇÖREKOTU YAĞI OLEOJELİNİN KRAKER YAPIMINDA KULLANIM POTANSİYELİNİN ARAŞTIRILMASI

Necla ÖZDEMİR ORHAN^{1*}, Zeynep EROĞLU²

¹Bitlis Eren University, Faculty of Health Sciences, Department of Nutrition and Dietetics, 13100, Bitlis, Türkiye

²Munzur University, Faculty of Health Sciences, Department of Nutrition and Dietetics, 62000, Tunceli, Türkiye

Özet: Günümüzde, gıdaların duyu kalite ve fonksiyonel özelliklerini geliştirmek için yoğun bir şekilde çalışılmaktadır. Katı yağlar, yapısında yüksek oranda doymuş yağ asitleri içermesi nedeniyle sağlık açısından sorun oluşturabilmektedir ve bu nedenle gıdalarda katı yağ yerine kullanılacak ikame maddeleri geliştirilmektedir. Bu çalışmada, kraker yapımında katı yağ ikame maddesi olarak çörekotu yağı oleojeli (ÇOYO) kullanılmış olup, krakerin fiziksel, duyu ve tekstürel özelliklerinde meydana gelen değişimler incelenmiştir. Kraker yapımında kullanılan shortening oranı % 0, % 50 ve % 100 olacak şekilde ÇOYO ile değiştirilerek, sırasıyla, Kontrol-kraker, % 50 ÇOYO-kraker ve %100 ÇOYO-kraker formülasyonları hazırlanmıştır. Kontrol-kraker, % 50 ÇOYO-kraker ve %100 ÇOYO-kraker örneklerinin nem değerleri sırası ile % 3.61, % 4.11 ve % 4.66 olarak bulunmuştur. En yüksek su aktivitesi değeri %100 ÇOYO-kraker (0,2315) ait olup bunu % 50 ÇOYO-kraker (0,1920) takip etmiştir. Bileşiminde ÇOYO bulunan krakerlerin L^* değerlerinin azaldığı ve a^* değerlerinin arttığı görülmüştür. En yüksek sertlik değeri (2396,90 g kuvvet) Kontrol-kraker için, en düşük sertlik değeri (1170,45 g kuvvet) %100 ÇOYO-kraker için (P<0,05). Formülasyonunda ÇOYO kullanılan krakerler duyu analizinde lezzet açısından daha çok beğenilmiştir (P<0,05). Genel beğeni açısından %100 ÇOYO-kraker örneği (7,18) en yüksek skoru alırken Kontrol-kraker örneği (6,55) en düşük skoru almıştır. Bu sonuçlar ÇOYO'nun kraker gibi ürünlerde kullanım potansiyelinin oldukça yüksek olduğunu göstermektedir.

Anahtar kelimeler: Çörek otu yağı, Oleojel, Katı yağ ikame maddesi, Kraker

Evaluation of the Potential Use of Black Cumin Oil Oleogel as a Fat Alternative in Cracker Production

Abstract: Nowadays, intensive studies have been carried out to improve the sensory, quality, and functional properties of foods. Fats raise question marks about health due to their high content of saturated fatty acids and therefore fat substitutes that can be used instead of fats have been developed. In this study, black cumin oil oleogel (BCOO) was used as a fat replacer in cracker production, and the changes in the physical, sensory, and textural properties of the cracker were investigated. The Control-cracker, 50%-cracker and 100%-cracker formulations were prepared by replacing shortening with BCOO at 0%, 50%, and 100% levels, respectively. The moisture content of the Control-cracker, 50% BCOO-cracker, and 100% BCOO-cracker was 3.61%, 4.11%, and 4.66%, respectively. The highest water activity belonged to the 100% BCOO-cracker (0.2315), followed by the 50% BCOO-cracker (0.1920). It was observed that L^* value decreased and a^* value increased in oleogel incorporated crackers (P<0.05). The highest hardness value (2396.90 g) belonged to the Control-cracker, the lowest (1170.45 g) belonged to the 100% BCOO-cracker (P<0.05). As for sensory analysis, the crackers incorporated with oleogels were shown to be the most preferable in terms of taste. The 100% BCOO-cracker had the highest score (7.18) while the Control-cracker had the lowest (6.55) for general acceptability. These results show that BCOO has a high potential for use in bakery products such as cracker.

Keywords: Black cumin oil, Oleogel, Fat replacer, Cracker

*Sorumlu yazar (Corresponding author): Bitlis Eren University, Faculty of Health Sciences, Department of Nutrition and Dietetics, 13100, Bitlis, Türkiye

E mail: ozdemirc@gmail.com (N. ÖZDEMİR ORHAN)

Necla ÖZDEMİR ORHAN <https://orcid.org/0000-0003-2581-1275>

Zeynep EROĞLU <https://orcid.org/0000-0002-6817-546X>

Gönderi: 03 Ocak 2024

Kabul: 27 Şubat 2024

Yayınlanma: 15 Mart 2024

Received: January 03, 2024

Accepted: February 27, 2024

Published: March 15, 2024

Cite as: Özdemir Orhan N, Eroğlu Z. 2024. Evaluation of the potential use of black cumin oil oleogel as a fat alternative in cracker production. BSJ Eng Sci, 7(2): 342-350.

1. Giriş

Son yıllarda tüketici davranışları sağlıklı atıştırmalıklardan yana hızla değişmektedir. Sağlığa faydalı bileşenler içeren yeni ürünlerin piyasaya sürülmesi önemli bir pazar eğilimi oluşturmaktadır. Özellikle tuzlu atıştırmalıklar (tuzlu krakerler) tatlı atıştırmalıklardan daha yaygın tüketilmektedir (Miller ve ark., 2017; Giannoutsos et al., 2023). Krakerler, özellikle ara öğünlerde tüketilen popüler bir atıştırmalık ürün

olarak karşımıza çıkmaktadır (Batista ve ark., 2019). Ülkemizde her yaş grubunun tükettiği ve sürekli pazarlanabilen atıştırmalıklardan biri olan kraker, tüketici taleplerine bağlı olarak çok farklı içeriklerle satılmaktadır (İzci ve Şengül, 2015). Ayrıca, fonksiyonel fırıncılık ürünleri içerisinde yeni ürün geliştirmeye fırsat sunan, en önemli ürün grubunu oluşturmaktadır (Toğrul, 2021; Bölükbaş, 2023). Kraker yapımında kullanılan yağ oranı, kraker çeşidine göre değişmekle birlikte genellikle



%10-15 civarındadır. Kraker yapımında istenilen yapısal özellikleri sağlamak amacıyla yüksek oranda doymuş yağ içeren katı yağlar kullanılmaktadır (Zhou ve ark., 2011). Bu durum da sağlıkla ilgili riskleri beraberinde getirmektedir. Doymuş ve trans yağ asidi içeriği yüksek gıdalarla beslenmenin kandaki düşük yoğunluklu lipoprotein (LDL) seviyesini olumsuz etkilediği ve kolesterol seviyesinin artmasına neden olduğu belirtilmiştir (Meng ve ark., 2018). Ayrıca, bu gıdaları fazla tüketen kişilerde kardiyovasküler hastalıklar, tip II diyabet ve obezite görülme sıklığı artmaktadır (Pehlivanoğlu ve ark., 2018). Son yıllarda yapılan çalışmalarda beslenme ile alınan doymuş yağ asidi miktarının azaltılması için; katı yağlar, oleojeller ile ikame edilmektedir. Doymamış yağ asidi içeriği yüksek sıvı yağların bir jelleştirme ajanı yardımı ile yapılandırılması sonucu elde edilen jel benzeri yapıları oleojel adı verilmektedir (Demirkesen ve Mert, 2019). Oleojeller, düşük doymuş yağ asidi içeriğine sahip olmalarının yanında, katı yağın ürün yapısına sağladığı olumlu katkıyı da sunmaktadır. Oleojel üretiminde ayçiçek yağı, zeytinyağı, balık yağı, fındık yağı ve soya fasulyesi yağının yaygın olarak kullanıldığı görülmektedir (Pehlivanoğlu ve ark., 2018; Kara, 2019; Swe ve Asavapichayont, 2018). Ayrıca, gıdalara farklı aroma ve fonksiyonel özellik kazandırmak amacıyla biyoaktif özelliklere sahip soğuk pres yağlar da oleojel üretiminde tercih edilmektedir. Flores-García ve ark. (2023) tarafından yapılan bir çalışmada soğuk pres keten tohumu yağı kullanılarak elde edilen oleojeller kurabiye yapımında kullanılmıştır. Formülasyonundaki shorteningin %70'i oleojel ile ikame edilen kurabiyelerin duyusal anlamda panelistler tarafından beğenildiği ve üründeki doymuş yağ miktarının önemli oranda azaldığı belirtilmiştir. Başka bir çalışmada balmumu ve pirinç kepeği mumu kullanılarak üretilen soğuk pres aspir yağı bazlı oleojellerin, kek endüstrisinde yaygın olarak kullanılan ticari katı yağların yerine kullanılabileceği belirtilmiştir (Badem ve Baştürk, 2023).

Çörekotu (*Nigella sativa* L.) tohumu ve soğuk pres çörekotu yağı Asya ve Afrika ülkelerinin beslenmesinde yer almaktadır. Bu ürünler sahip oldukları tokoferoller, steroller, fenolik bileşenler ve uçucu yağlar gibi biyoaktif maddeler ve yağ asidi dağılımı nedeniyle son zamanlarda Avrupa'da da tanınmaya ve giderek popüler hale gelmeye başlamıştır (Szydłowska-Czerniak ve ark., 2022). Bu nedenle, Avrupa Komisyonu'na göre çörekotu tohumu ve çörekotu yağı, Yeni Gıda Kataloğunda (Novel Food Catalogue) listelenen yeni gıdalar olarak kabul edilmektedir (Anonymous, 2023; Szydłowska-Czerniak ve ark., 2022). Yapılan çalışmalarda çörekotu tohumu veya yağından elde edilen ekstraktların üst solunum yolu şikayetlerini önemli ölçüde azalttığı, psikolojik ruh halini iyileştirdiği (Talbot ve Talbot, 2022) ve meme kanseri hastalarında akut radyodermatit insidansını azalttığı (Rafati ve ark., 2019) tespit edilmiştir. Çörekotu yağı sahip olduğu biyoaktif bileşenler nedeniyle oleojel üretiminde de kullanılmaktadır. Palamutoğlu (2021)

tarafından yapılan bir çalışmada; çörekotu ve ayçiçek yağları farklı oranlarda karıştırılmış ve oleojelatör olarak karnauba mumu kullanılarak farklı oleojeller elde edilmiştir. Elde edilen oleojeller köfte yapımında hayvansal yağ yerine kullanılmış olup çörekotu yağının köftede antioksidan aktivite sergilediği ve formülasyonundaki hayvansal yağın %25 oranında oleojel ile değiştirildiği köftelerin duyusal analizde panelistler tarafından daha çok beğenildiği ifade edilmiştir.

Bu çalışmanın amacı; katı yağ ikame maddesi olarak çörekotu yağı oleojeli (ÇOYO) kullanılmasının, krakerin kalite özellikleri üzerine olan etkisinin araştırılmasıdır. Literatürde ÇOYO'nun katı yağ ikame maddesi olarak herhangi bir unlu mamulde kullanımına rastlanmamış olup, bu çalışmanın literatüre ve gıda endüstrisine katkı sağlayacağı düşünülmektedir.

2. Materyal ve Yöntem

2.1. Materyal

Oleojel yapımında kullanılan soğuk pres çörekotu yağı ve shortening yerel firmalardan temin edilmiştir. Karnaubu mumu (carnauba, KahlWax 6642 Organik karnauba mumu, E903 kodlu gıda katkı maddesi, erime sıcaklığı 82-86 °C) IMCD Türkiye (İstanbul, Türkiye) firması tarafından ücretsiz olarak kullanımımıza sunulmuştur. Çalışmada kullanılan bütün kimyasallar analitik safliktadır ve analizler ise en az 2 tekerrür halinde yürütülmüştür.

2.2. Yağ Asidi Kompozisyonunun Belirlenmesi

Çörekotu yağının ve shorteningin yağ asidi metil esterleri IUPAC (1987)'a göre hazırlanmış olup, analiz; FID detektör ve TR-CN100 kapiler kolon (100 m, 0,25 mm iç çap, 0,20 µm film kalınlığı) (Teknokroma, Barselona, İspanya) ile entegre Gaz Kromatografisi (GC) (Shimadzu, Kyoto, Japan) cihazı kullanılarak yapılmıştır. Enjektör ve dedektör sıcaklıkları sırasıyla 230 ve 240 °C'dir. Fırın 140 °C sıcaklıkta 5 dk bekletilmiş olup, ardından 4 °C/dk sıcaklık artış hızı ile 240 °C'ye kadar ısıtılmış ve bu sıcaklıkta 20 dk bekletilmiştir. Helyum gazı 1 mL/dk lineer akış hızında taşıyıcı gaz olarak kullanılmış ve 1 µL örnek 1:100 split (bölme) oranı kullanılarak sisteme verilmiştir. Tanımlama işlemi için yağ asidi metil esterlerinin standartları kullanılmış ve çörekotu yağının ve shorteningin yağ asidi bileşimi yüzde (%) olarak verilmiştir.

2.3. Oleojel Üretimi

Çörekotu yağı oleojeli üretiminde, önceki çalışmamızda yer alan yöntem modifiye edilerek kullanılmıştır (Orhan ve Eroglu, 2022). Çörekotu yağı uygun bir kapta ısıtıcı kullanılarak 90 °C'ye ısıtılmış, üzerine karnauba mumu ilave edilmiş (çörekotu yağı:karnauba mumu, 93:7, w/w) ve karnauba mumunun yağ içerisinde tamamen erimesi için 5 dk boyunca manyetik karıştırıcı yardımıyla karıştırılmıştır. Ardından, çörekotu yağı-karnauba mumu karışımı su banyosuna (90 °C) alınarak 1 saat boyunca çalkalanmıştır (200 rpm). Çalkalama işleminin ardından, karışım oda sıcaklığında soğumaya bırakılmış ve böylece

çörekotu yağı oleojeli (ÇOYO) elde edilmiştir. Elde edilen oleojel buzdolabında (4 °C) saklanmış olup analizden 1 saat önce buzdolabından çıkarılmıştır.

2.4. Yağ Bağlama Kapasitesinin Belirlenmesi

ÇOYO 90 °C sıcaklıktaki su banyosunda eritilerek Eppendorf tüpüne aktarılmış (1 mL) ve ağırlığı kaydedilmiştir. Eppendorf tüpleri, oleojelin tekrar katılaşması için 24 saat boyunca buzdolabına bırakılmıştır. Ardından, tüpler buzdolabından alınarak oda sıcaklığında 1 saat bekletilmiş ve santrifüj edilmiştir (6000 rpm / 15 dk). Santrifüj işleminden sonra oleojelden ayrılan sıvı yağ alınmış ve ağırlığı ölçülmüştür (Choi ve ark., 2020). Oleojelden salınan yağ miktarı ve buna bağlı olarak da oleojelin yağ bağlama kapasitesi aşağıda verilen eşitlik 1 ve 2 yardımı ile hesaplanmıştır.

$$\text{Salınan yağ (\%)} = \frac{\text{Salınan yağ kütlesi (g)}}{\text{Numunenin toplam kütlesi (g)}} \times 100 \quad (1)$$

$$\text{Yağ bağlama kapasitesi (\%)} = 100 - \text{Salınan yağ (\%)} \quad (2)$$

2.5. Kraker Yapımı

Kraker yapımında 100 g un için; 60 mL su, 13 g shortening, 0,5 g sodyum bikarbonat, 2 g amonyum bikarbonat, 1,6 g tuz ve 0,5 g maya kullanılmıştır (Dülger-Altiner, 2015). Bu formülasyon Kontrol-kraker olarak adlandırılmıştır. Toplam shortening miktarının % 50'sinin ve tamamının yerine ÇOYO kullanılarak üretilen krakerler, sırasıyla, % 50 ÇOYO-kraker ve % 100 ÇOYO-kraker olarak adlandırılmıştır. Bu oranlar oleojellerin katı yağ ikame maddesi olarak kullanıldığı daha önce yapılan çalışmalar göz önünde bulundurularak belirlenmiştir (Adili ve ark., 2020; Kim ve ark., 2017). Maya dışındaki kuru malzemelerin tamamı yoğurma makinasının (Cookplus Promix Ef802, Karaca Züccaciye Tic. ve San. A.Ş., Türkiye) karıştırma kabına alınmıştır. Suyun bir kısmı kullanılarak maya aktive edilmiş ve kuru karışıma ilave edilmiştir. Daha sonra kalan su diğer malzemelere ilave edilip, önce düşük devirde (devir 2) 30 s ve ardından orta devirde (devir 4) 5 dk karıştırılmıştır. Elde edilen hamur merdane kullanılarak yaklaşık 2 mm kalınlığında açılmış ve kalıp yardımı ile kare parçalar (5x5 cm) halinde kesilmiştir. Kesilen parçalar yağlı kâğıt serili tepsilere alınmış ve laboratuvar tipi fırın kullanılarak 180 °C'de 20 dk pişirilmiştir. Pişirilen krakerler oda sıcaklığında soğumaya bırakılmış (1 saat) ve ardından analizler yapılmıştır.

2.6. Nem Analizi

Krakerler homojen olacak bir şekilde ufalanmış ve sabit ağırlığa getirilmiş örnek kaplarına yaklaşık 2 g olacak şekilde tartılmıştır. Ardından, 102 °C'de etüvde sabit ağırlığa gelinceye kadar bekletilmiştir ve ağırlık farkından yararlanılarak örneklerin nemi hesaplanmıştır (AOAC, 2000).

2.7. Su Aktivitesi

Kraker örneklerinin su aktivitesi, oda sıcaklığında su aktivitesi ölçüm cihazı (Novasina LabMaster, Novasina AG, Lachen, İsviçre) kullanılarak belirlenmiştir.

2.8. Renk Analizi

Kraker örneklerinin renk analizi Minolta CR-400 model

renk cihazı kullanılarak yapılmıştır (Konica Minolta CR-400, Tokyo, Japan). Ölçümlerden önce Minolta kalibrasyon plakası kullanılarak cihazın kalibrasyonu yapılmış olup sonuçlar L^* , a^* ve b^* değerleri şeklinde verilmiştir. L^* değeri 0 (siyah) ile 100 (beyaz) arasında değişen değerlerle koyuluğu ve parlaklığı; a^* değeri kırmızı (+a) ve yeşilliği (-a); b^* değeri ise sarılık (+b) ve maviliği (-b) ifade etmektedir.

2.9. Tekstür Analizi

Kraker örneklerinin tekstür analizinde sertlik (hardness) değerleri ölçülmüştür. Bu analiz için üç noktalı bükme probu (HDP/3PB) ve ağır yük platformu ile kombine edilmiş tekstür analiz cihazı kullanılmıştır (TA.XT2i, Stable Micro Systems, Surrey, İngiltere). Analizde kullanılan parametreler; ön test hızı: 1 mm/s, test hızı: 3 mm/s, test sonrası hız: 10 mm/s, uzaklık: 5 mm, tetikleme yükü: 50 g ve veri alma hızı: 500 pps olarak belirlenmiştir. Sertlik değerleri tekstür cihazının yazılımı kullanılarak hesaplanmıştır (Texture Exponent Software, ver: 6.1.18.0, Stable Micro System, Surrey, İngiltere). Analiz 25 °C'de yapılmıştır.

2.10. Duyusal Analiz

Örneklerin duyusal analizinde 9 puanlı hedonik skala (1 = çok kötü, 9 = çok iyi) kullanılmış olup, analize en az 10 adet eğitimli panelist katılmıştır. Örnekler görünüş, renk, koku, tat, tekstür ve genel kabul edilebilirlik kriterleri açısından değerlendirilmiştir. Krakerler 3 haneli rakamlar ile rastgele numaralandırılmış ve servis esnasında rastgele dizilmiştir. Panelistlerin tadım esnasında tat algısını yenilemeleri ve ağızlarını çalkalamaları için galeta ve su servis edilmiştir.

2.11. İstatistiksel Analiz

Verilerin istatistiksel olarak değerlendirilmesinde SPSS yazılımı (Windows, sürüm 16; IBM Corp., Armonk, NY, ABD) kullanılmış ve tek yönlü varyans analizi (ANOVA) uygulanmıştır. Değişkenler arasındaki anlamlı farkları saptamak için Duncan testi kullanılmıştır ($P < 0,05$).

3. Bulgular ve Tartışma

3.1. Yağ Asidi Dağılımı

Shortening ve çörekotu yağının yağ asidi dağılımları Tablo 1'de gösterilmiştir. Shorteningin temel yağ asidi bileşeni palmitik asit (% 41,39) olup bunu oleik asit (% 35,15) takip etmektedir. Çörekotu yağının temel yağ asidi bileşeni ise linoleik asit (% 55,88) olup bunu oleik asit (% 25,39) takip etmektedir. Shorteningin içeriğinde bulunan doymuş (% 49,24) ve doymamış yağ asitlerinin (% 49,23) toplamı neredeyse eşittir. Çörekotu yağının bileşimine bakıldığında ise doymuş yağ asitlerinin toplamı % 17,57 iken doymamış yağ asitlerinin toplamı % 82,08'lik bir orana ulaşmıştır. Ayyıldız ve ark. (2021) tarafından yapılan bir çalışmada; soğuk pres çörekotu yağının temel bileşenleri linoleik asit (% 54,80), oleik asit (% 24,90) ve palmitik asit (% 12,24) olarak belirtilmiş olup, bu yağ asitlerinin oranlarının bizim çalışmamızda elde edilen sonuçlara oldukça benzer olduğu görülmüştür. Albakry ve ark. (2022) tarafından yapılan çalışmada da benzer sonuçlar ortaya konulmuştur.

Shortening yağında % 1,16 oranında trans yağ asidi tespit edilmiş olup Türk Gıda Kodeksi gıda etiketleme kurallarına uygun olduğu görülmüştür. Türk Gıda Kodeksi Gıda Etiketleme ve Tüketicileri Bilgilendirme Yönetmeliği'ne göre; sürülebilir yağ/margarinler, yoğun yağlar, bitkisel yağlar ve bu yağları içeren gıdaların %2'den fazla trans yağ içermesi durumunda trans yağ miktarının belirtilmesi gerekir. Soğuk pres çörekotu yağında ise düşük miktarda (% 0,18) da olsa trans yağ asidi tespit edilmiştir. Bitkilerin yaprak ve tohumlarının trans yağ asitlerini içerebildiği ve buna bağlı olarak bitkisel ham yağlarda yaklaşık % 0,1 - % 0,3 oranında trans yağ asidi bulunabileceği literatürde belirtilmiştir

(Schwarz, 2000; Kahraman ve Küplülü, 2011). Ayyıldız ve ark. (2021) tarafından yapılan çalışmada, bizim çalışmamızdan farklı olarak çörekotu yağında trans yağ asidi tespit edilmemiştir. Ancak, çalışmada yer alan diğer soğuk pres yağlardan kabak çekirdeği yağı, ceviz yağı ve haşhaş yağının çeşitli oranlarda (% 0,11-% 0,40) trans yağ asidi içerdiği tespit edilmiştir. Fransa'da yapılmış olan bir çalışmada süpermarketlerden çeşitli bitkisel yağlar toplanmış ve yağ asidi bileşenleri incelenmiştir. Çalışma kapsamında analiz edilen soğuk pres avokado yağının trans yağ asidi içerdiği belirtilmiştir (Vingering ve ark., 2010).

Tablo 1. Shortening ve çörekotu yağının yağ asidi bileşimi (%)

Yağ Asitleri	Shortening	Çörekotu yağı
Miristik asit (C14:0)	1,64±0,02	0,15±0,00
Palmitik asit (C16:0)	41,39±0,44	11,73±0,04
Palmitoleik asit (C16:1)	0,18±0,00	0,16±0,01
Heptadekanoik asit (C17:0)	0,09±0,00	0,06±0,00
Stearik asit (C18:0)	5,69±0,15	3,07±0,00
Elaidik asit (C18:1 trans-9)	0,27±0,00	0,03±0,00
Oleik asit (C18:1)	35,15±0,41	25,39±0,16
Linolelaidik acid (C18:2 trans-9,12)	0,88±0,09	0,15±0,01
Linoleik asit (C18:2)	13,65±0,03	55,88±0,12
Araşidik asit (C20:0)	0,31±0,01	0,19±0,00
Eikosenoik asit (C20:1)	0,25±0,01	0,60±0,07
Heneikosanoik asit (C21:0)	-	2,34±0,00
Lignoserik asit (C24:0)	0,12±0,01	0,02±0,00
Nervonik asit (C24:1)	-	0,05±0,01
Doymuş Yağ Asitleri	49,24±0,29	17,57±0,05
Doymamış Yağ Asitleri	49,23±0,45	82,08±0,10
Trans Yağ Asitleri	1,16±0,09	0,18±0,01

3.2. Yağ Bağlama Kapasitesinin Belirlenmesi

ÇOYO'nun yağ bağlama kapasitesi % 98,93±0,35 olarak belirlenmiştir. Daha önce yapmış olduğumuz bir çalışmada da benzer bir üretim prosedürü uygulanarak çörekotu yağı-karnauba mumu oleojeli elde edilmiştir. Ancak, daha önce elde edilen oleojelde herhangi bir yağ kaybı gözlenmemiştir (Orhan ve Eroğlu, 2022). Bu durum çörekotu yağının ve karnauba mumunun bileşim farklılığından kaynaklanabilir. Her iki çalışmamızda da soğuk sıkım çörekotu yağı kullanılmış olup, bitkinin türü, yağ eldesinde kullanılan yöntemler, iklim ve coğrafya gibi faktörler yağın bileşimine etki edebilmektedir. Mumun yapısında bulunan minör bileşikler de jelatör-jelatör veya jelatör-çözücü interaksiyonlarını etkileyerek yağ fazı ile uyumsuzluğa neden olabilmektedir (Fayaz ve ark., 2020). Noonim ve ark. (2022) tarafından yapılan bir çalışmada palm yağı ve farklı oranlarda (% 5 ve % 10) karnauba mumu kullanılarak oleojel elde edilmiş olup, yeni üretilen oleojellerden olan yağ kaybının % 5'in altında olduğu ortaya konulmuştur. Öte yandan Li ve ark. (2022) tarafından yapılan çalışmada ise yüksek oleik asitli ayçiçek yağı ve karnauba mumu (% 5) kullanılmış olup, elde edilen oleojelin yağ bağlama kapasitesinin yaklaşık % 80 olduğu bulunmuştur. Bu durum yağların sahip olduğu farklı bileşim, polarite ve viskozite gibi

özelliklerin jelatör-yağ etkileşimlerini etkilemesinden ve buna bağlı olarak da farklı oleojel yapılarının ortaya çıkmasından kaynaklanabilmektedir (Fayaz ve ark., 2020).

3.3. Nem Analizi

Kraker örneklerinin nem içeriği değerleri Tablo 2'de gösterilmiştir. Kraker formülasyonu içerisindeki oleojel miktarı arttıkça örneklerin nem değerlerinin de arttığı görülmektedir. Bu durum oleojel içeren formülasyonlarda suyun daha iyi tutulmasından kaynaklanmaktadır (Giacomozzi ve ark., 2018). Gıda ürünlerinde oleojel kullanımı ısı direnci ve nem bariyeri sağlayabilmektedir (Demirkesen ve Mert, 2020). Naeli ve ark. (2023) yağ fazı olarak damıtılmış monoaçilgliserol ve oleojelatör olarak etil selüloz ve etil selüloz/hidroksipropil metil selüloz kullanarak oleojel elde etmiştir. Daha sonra bu oleojeller kek yapımında shortening yerine kullanılmış ve oleojel kullanılarak elde edilen keklerin nem değerlerinin kontrol örneğine göre daha yüksek olduğu görülmüştür. Brito ve ark. (2022) tarafından yapılan çalışmada da benzer sonuçlar elde edilmiş ve oleojel içeren kurabiyelerin nem içeriğinin shortening içeren örneklerle göre daha yüksek olduğu ifade edilmiştir.

Tablo 2. Kraker örneklerinin nem içeriği (%) ve su aktivitesi (a_w) değerleri

Örnek	Nem (%)	Su aktivitesi (a_w)
Kontrol-kraker	3,61±0,39 ^c	0,1320±0,0014 ^c
% 50 ÇOYO-kraker	4,11±0,16 ^b	0,1920±0,0071 ^b
% 100 ÇOYO-kraker	4,69±0,07 ^a	0,2315±0,0111 ^a

Aynı sütunda yer alan "a-c" harfleri örnek grupları arasındaki farkın istatistiki olarak önemli olduğunu ifade etmektedir ($P<0,05$)

3.4. Su Aktivitesi

Kraker örneklerinin su aktivitesi değerleri Tablo 2'de görülmektedir. En düşük a_w değeri Kontrol-kraker örneğine ait iken en yüksek a_w değeri % 100 ÇOYO-kraker örneğine aittir. Kraker formülasyonunda yer alan shorteningin ÇOYO ile değiştirilmesi a_w değerinin artmasına neden olmuştur. Oleojel içeren krakerlerde daha fazla su tutulmasının sonucu olarak örneklerin nem içeriği ve a_w değerleri artmıştır. Daha önce yapılan çalışmalarda unlu mamullerde yağ ikame maddesi olarak karbonhidrat ve protein kökenli ürünlerin kullanılması durumunda ürünlerin su aktivitesinin ve nem içeriğinin arttığı görülmüştür (Lee ve Inglett, 2006; Gallagher ve ark., 2003; Yashini ve ark., 2021). Çalışmamızdan elde edilen sonuçlara göre yağ ikame maddesi olarak oleojel kullanımı da nem ve su aktivitesi değerlerinin artmasına neden olmuştur. Nutter ve ark. (2023) tarafından yapılan çalışmada soya yağı ve pirinç kepeği mumu ile oleojel elde edilmiş olup, ardından sodyum aljinat ve κ -karreganan ile hazırlanan hidrojel ile karıştırılmış ve böylece bigel formülasyonu elde edilmiştir. Elde edilen bigel kurabiye yapımında kullanılmış ve ürünlerin su aktivitesi değerinde artışa neden olmuştur. Öte yandan, oleojel ilave edildiğinde ürünün su aktivitesinin düştüğünü belirten çalışmalar da mevcuttur (Yılmaz ve Ögütçü, 2015). Bu durumda, yağ ikame maddesi olarak

kullanılan materyalin kimyasal formülasyonu, kullanıldığı ürünün içeriği ve birbirleri ile olan etkileşimlerinin su aktivitesinin hareketini etkilediği söylenebilir.

3.5. Renk Analizi

Kraker örneklerinin renk analizi sonuçları Tablo 3'de verilmiştir. Kontrol-kraker örneği en yüksek L^* değerine sahip iken % 50 ÇOYO-kraker örneği en düşük L^* değerine sahiptir ($P<0,05$). Kraker formülasyonunda oleojel kullanımı; ÇOYO'nun parlaklık değerinin ($L^* = 27,98 \pm 0,76$) shorteninge göre ($L^* = 93,52 \pm 0,26$) daha düşük olması nedeniyle, örneklerin parlaklık değerinin azalmasına neden olmuştur (veri çizelgede gösterilmemiştir). En düşük a^* değerinin Kontrol-krakere ait olduğu ($P<0,05$) ve formülasyonda oleojel kullanıldığında a^* değerinin arttığı görülmektedir. Bu durum çörek otu yağının kırmızılık (+) ($a^* = 3,89 \pm 0,22$) değerinin shorteningin ise yeşillik değerinin (-) ($a^* = -2,33 \pm 0,07$) daha baskın olmasından kaynaklanmaktadır. Kraker yapımında oleojel kullanımının, örneklerin b^* değeri üzerinde istatistiksel olarak anlamlı bir etkisinin olmadığı görülmüştür (Tablo 3). Bu durum shorteningin b^* değeri ($14,66 \pm 0,34$) ile ÇOYO'nun ($13,15 \pm 0,34$) b^* değerinin birbirine yakın olmasından kaynaklanmaktadır.

Tablo 3. Kraker örneklerinin renk parametreleri ve tekstürel özellikleri

Örnek	L^*	a^*	b^*	Sertlik (g kuvvet)
Kontrol-kraker	64,04±2,40 ^a	1,31±0,12 ^c	27,89±1,24 ^a	2396,90±203,75 ^a
% 50 ÇOYO-kraker	57,03±1,94 ^c	3,02±0,26 ^a	27,38±1,58 ^a	1609,01±131,14 ^b
% 100 ÇOYO-kraker	61,63±2,63 ^b	2,46±0,22 ^b	26,21±1,15 ^b	1170,45±89,37 ^c

Aynı sütunda yer alan "a-c" harfleri örnek grupları arasındaki farkın istatistiki olarak önemli olduğunu ifade etmektedir ($P<0,05$).

Tang ve Gosh (2021) tarafından yapılan bir çalışmada da benzer sonuçlar elde edilmiştir. Kanola proteini izolatu kullanılarak kanola yağı emülsiyonları elde edilmiş ve bu emülsiyonlardan biri ısıl işleme tabi tutulmuştur. Ardından iki emülsiyon da vakum yardımı ile kurutulmuş ve homojen bir doku elde edilene kadar çırpılarak oleojel haline getirilmiştir. Oleojeller daha sonra kek yapımında kullanılmıştır. Oleojel kullanılarak hazırlanan hamurların L^* değerinin, shortening kullanılarak elde edilen kontrol örneğine göre daha düşük olduğu ifade edilmiştir. Isıl işlem görmüş oleojel içeren kek örneğinin L^* değerinin de protein denatürasyonuna bağlı olarak düştüğü

belirtilmiştir. Oleojel ile hazırlanan keklerin a^* ve b^* değerlerinin de kanola proteini içermeleri nedeniyle kontrol örneğine göre daha yüksek olduğu ifade edilmiştir. Barragán-Martínez (2022) tarafından yapılan başka bir çalışmada da kurabiye yapımında hibrid jel kullanılarak formülasyondaki shortening miktarı azaltılmaya çalışılmıştır. Çalışmada öncelikle kanola yağı ve kandelila mumu kullanılarak oleojel elde edilmiş ve ardından jelatinize nişasta hidrojel ile karıştırılarak hibrit jel elde edilmiştir. Elde edilen hibrit jel farklı oranlarda (% 0, 25, 50, 75 ve 100) shortening ile ikame edilerek kurabiye yapımında kullanılmıştır. Kurabiye

örneklerindeki hibrit jel miktarı arttıkça L^* değerinin arttığı, a^* değerinin azaldığı ve b^* değerinin arttığı görülmüştür. Bu değişimlere hibrit jel içerisinde bulunan nişastanın neden olduğu ifade edilmiştir. Yukarıda bahsedilen çalışmalardan da anlaşılacağı üzere, oleojeli oluşturan materyallerin renk değerlerine göre son ürünün renk değerlerinin değişmesi beklenen bir durumdur.

3.6. Tekstür Analizi

Kraker örneklerinin sertlik değerleri Tablo 3'de gösterilmiştir. Formülasyonunda oleojel bulunan krakerlerin sertlik değerlerinin kontrol örneğine göre daha düşük olduğu görülmektedir. Sertlik, kraker yeme kalitesini gösteren önemli parametrelerden biridir. Krakerde sertlik değerinin düşmesi yumuşak tekstüre ve buna bağlı olarak da üstün kaliteyi işaret etmektedir (Zhao ve ark., 2022). Duyusal analiz sonuçlarına bakıldığında ÇOYO kullanılarak hazırlanan krakerlerin yapı (tekstür) değerinin kontrol örneğinden daha yüksek olduğu görülmekte olup, bu durumu doğrulamaktadır. Öte yandan, sertlik değeri ve nem içeriği arasında zıt bir ilişki olduğu daha önce yapılan araştırmalar tarafından ortaya konulmuştur (Lee ve ark., 2022; Alamri ve ark., 2022). Bizim çalışmamızda elde edilen veriler de bu ilişkiyi doğrulamaktadır. Yüksek nem değerine sahip ÇOYO içerikli krakerlerin daha düşük sertlik değerine sahip olduğu görülmektedir.

Zhao ve ark. (2022) tarafından yapılan bir çalışmada yağ fazı olarak yüksek oleik asitli soya yağı ve oleojelatör olarak da monoasilgliserol ve pirinç kepeği mumu kullanılmış olup elde edilen oleojeller kraker yapımında kullanılmıştır. Oleojel kullanılarak elde edilen krakerlerin sertlik değerlerinin shortening kullanılarak elde edilen krakerlerin sertlik değerlerinden daha düşük olduğu görülmüştür. Krakerlerin düşük sertlik değerlerinin yüksek doymamış yağ asidi içeriği ile ilişkili olabileceği vurgulanmıştır. Tanislav ve ark. (2022) tarafından yapılan başka bir çalışmada ise çeşitli oleojelatörler (karnauba mumu, β -sitosterol:balmumu, β -sitosterol:lesitin, gliserol monostearat) kullanılarak

ayçiçek yağı oleojelleri elde edilmiştir. Elde edilen oleojeller bisküvi yapımında kullanılmış olup oleojel kullanılarak üretilen bisküvilerin hepsinin sertlik değerleri, margarin kullanılarak elde edilen kontrol örneğinin sertlik değerinden daha düşük bulunmuştur. Oleojel kullanılarak elde edilen bisküvilerin gevrek hamur ürünleri kategorisi için uygun olduğu belirtilmiştir. Jadhav ve ark. (2022) tarafından da oleojelin, kurabiye gibi unlu mamullerde doymuş yağın yerine uygun bir alternatif olduğu belirtilmiştir.

3.7. Duyusal Analiz

Kraker örneklerinin duyusal analiz sonuçları Tablo 4'de gösterilmiştir. Görünüş açısından en çok beğenilen örnek % 100 ÇOYO-kraker olmuştur. Kraker yapımında ÇOYO kullanılan örneklerin renk açısından daha çok beğenildiği görülmektedir. Renk analizi sonucunda ortaya konulan farklılıkların duyusal analize yansıdığı ancak aralarında istatistiksel olarak önemli bir farklılığın olmadığı anlaşılmaktadır ($P>0,05$). Koku açısından örnekler arasında herhangi bir farklılığa rastlanmamıştır ($P>0,05$). Bu durum; kraker yapımında ÇOYO kullanımının, ürün kokusuna olumsuz yansımadağını göstermesi açısından önemlidir. Örnekler lezzet açısından değerlendirildiğinde ise en yüksek puanı, yağ fazı olarak tamamen ÇOYO kullanılan örneğin aldığı görülmektedir ve bunu %50 ÇOYO-kraker örneği takip etmektedir ($P<0,05$). Lezzet açısından en düşük puanı ise Kontrol-kraker örneği almıştır. Yapı açısından da formülasyonunda ÇOYO barındıran örneklerin daha yüksek puanlar aldığı görülmektedir. Genel beğeni değerlendirmesinde ise en yüksek puanı % 100 ÇOYO-kraker örneği almış olup, en düşük puanı Kontrol-kraker örneği almıştır. Ancak, aralarındaki fark istatistiksel olarak anlamlı bulunmamıştır ($P>0,05$). Yapısında ÇOYO bulunduran krakerlerin görünüş dışındaki bütün değerlendirmelerde kontrol örneğinden daha yüksek puanlar aldığı görülmektedir. Elde edilen bu veriler, kraker yapımında yağ fazı olarak kullanılan shorteningin % 50 oranında ÇOYO ile ikame edilmesinin ve en önemlisi de shortening yerine tamamen ÇOYO kullanılmasının panelistler tarafından olumlu karşılandığını ortaya koymaktadır.

Tablo 4. Kraker örneklerinin duyusal değerlendirilmesi

Örnek	Görünüş	Renk	Koku	Lezzet	Yapı	Genel Beğeni
Kontrol-kraker	6,41±0,06 ^a	6,69±0,06 ^a	6,91±0,25 ^a	6,05±0,19 ^b	6,55±0,52 ^a	6,55±0,06 ^a
% 50 ÇOYO-kraker	6,32±0,33 ^a	7,37±0,39 ^a	6,96±0,19 ^a	6,50±0,20 ^{ab}	6,87±0,32 ^a	6,82±0,52 ^a
% 100 ÇOYO-kraker	6,82±0,13 ^a	6,96±0,06 ^a	6,91±0,00 ^a	7,09±0,25 ^a	6,82±0,00 ^a	7,18±0,00 ^a

Aynı sütunda yer alan "a-b" harfleri örnek grupları arasındaki farkın istatistiksel olarak önemli olduğunu ifade etmektedir ($P<0,05$).

Giacomozzi ve ark. (2022) tarafından yapılan çalışmada da benzer sonuçlar elde edilmiştir. Giacomozzi ve ark. (2022) yüksek oleik asitli ayçiçek yağı ve monoglisericit kullanarak oleojel elde etmiş ve bu oleojeli muffin yapımında kullanmıştır. Çalışmada kontrol olarak ticari margarin kullanılarak üretilen muffin kullanılmış ve örnekler duyusal özellikler açısından kıyaslanmıştır. Oleojel kullanılarak elde edilen muffinlerin genel kabul

edilebilirliği kontrol örneğinden daha yüksek bulunmuştur. Giacomozzi ve ark. (2022), geleneksel bir içeriğin değiştirilmesinin ürünün kabul edilebilirliğini etkilemesi nedeniyle bu sonuçların oldukça önemli olduğunu vurgulamıştır. Duyusal özellikler tüketicilerin satın alma eğilimlerini etkileyen en önemli parametrelerden biridir. Bu nedenle üreticiler, gıdaların duyusal özelliklerini geliştirmeyi ve tüketicinin

beğeneceği düzeye çekmeyi amaçlamaktadır (Ekin ve ark., 2021). Başka bir çalışmada ayçiçek yağı ve hidrosimetil selüloz kullanılarak oleojel elde edilmiş ve çeşitli oranlarda shortening ile karıştırılarak (oleojel: shortening; 0:100 50:50, 60:40, 70:30, 100:0) kruvasan yapımında kullanılmıştır. Katı yağ içeriği % 50 oranında oleojel ile ikame edilen örnek, kontrol örneğinden sonra duyuşal olarak en çok beğenilen ürün olmuştur (Espert ve ark., 2023).

4. Sonuç

Kraker yapımında ÇOYO kullanımı, örneklerde pişme esnasında suyun daha iyi tutulmasına neden olduğu için nem ve su aktivitesi değerlerinin artmasına neden olmuştur. Kraker formülasyonunda shortening miktarı azalıp ÇOYO miktarı arttıkça daha yumuşak ve daha üstün yeme kalitesine sahip krakerler üretilmiştir. Bu durum duyuşal analiz testindeki tekstür değerlendirmesine de yansımıştır. Kraker yapımında ÇOYO kullanımı, ürün lezzetinin panelistler tarafından daha çok beğenilmesine ($P<0,05$) ve genel beğeni açısından da ÇOYO ilaveli ürünlerin daha yüksek puan almasına neden olmuştur. Elde edilen veriler ışığında kraker yapımında ÇOYO kullanımının hem tekstürel hem de duyuşal açıdan başarılı sonuçlar verdiği ifade edilebilir. Ayrıca çörekotu yağının yüksek oranda doymamış yağ asidi içermesi nedeniyle ÇOYO içeren krakerlerin shortening içeren krakerlere göre daha sağlıklı olduğu söylenebilir. Bundan sonra yapılacak olan çalışmalarda; katı yağ ikame maddesi olarak ÇOYO kullanımının, ürüne fonksiyonel anlamda sağladığı katkı ve biyoyararlılık özellikleri araştırılmalıdır.

Katkı Oranı Beyanı

Yazar(lar)ın katkı yüzdesi aşağıda verilmiştir. Tüm yazarlar makaleyi incelemiş ve onaylamıştır.

	N.Ö.O.	Z.E.
K	50	50
T	50	50
Y	60	40
VTI	50	50
VAY	50	50
KT	60	40
YZ	60	40
KI	70	30
GR	70	30
PY	60	40

K= kavram, T= tasarım, Y= yönetim, VTI= veri toplama ve/veya işleme, VAY= veri analizi ve/veya yorumlama, KT= kaynak tarama, YZ= Yazım, KI= kritik inceleme, GR= gönderim ve revizyon, PY= proje yönetimi.

Çatışma Beyanı

Yazarlar bu çalışmada hiçbir çıkar ilişkisi olmadığını beyan etmektedirler.

Etik Onay Beyanı

Bu çalışmada hayvanlar ve insanlar üzerinde herhangi bir çalışma yapılmadığı için etik kurul onayı alınmamıştır.

Kaynaklar

- Adili L, Roufegarinejad L, Tabibiazar M, Hamishehkar H, Alizadeh A. 2020. Development and characterization of reinforced ethyl cellulose based oleogel with adipic acid: Its application in cake and beef burger. *Food Sci Technol*, 126: 109277. <https://doi.org/10.1016/j.lwt.2020.109277>.
- Alamri MS, Mohamed AA, Hussain S, Ibraheem MA, Qasem AAA, Shamlan G, Hakeem MJ, Ababtain IA. 2022. Functionality of cordia and ziziphus gums with respect to the dough properties and baking performance of stored pan bread and sponge cakes. *Foods*, 11(3): 466. <https://doi.org/10.3390/foods11030460>.
- Albakry Z, Karrar E, Ahmed IAM, Oz E, Proestos C, El Sheikh A, Oz F, Wu G, Wang X. 2022. Nutritional composition and volatile compounds of black cumin (*nigella sativa* L.) seed, fatty acid composition and tocopherols, polyphenols, and antioxidant activity of its essential oil. *Horticulturae*, 8(7): 575. <https://doi.org/10.3390/horticulturae8070575>.
- Anonymous. 2023. EU novel food status catalogue. URL: https://ec.europa.eu/food/safety/novel-food/novel-food-catalogue_en (accessed date: September 4, 2023).
- AOAC. 2000. Official methods of analysis of AOAC Inter (17 ed.). Method 935.36 Solid (total) in bread. AOAC Inter. Gaithersburg, MD, USA, pp: 143.
- Ayyıldız HF, Topkafa M, Sherazi STH, Mahesar SA, Kara H. 2021. Investigation of the chemical characteristics and oxidative stability of some commercial cold-pressed oils. *Konya J Engin Sci*, 9(4): 904-916. <https://doi.org/10.36306/konjes.913439>.
- Badem Ş, Baştürk, A. 2023. Oxidative stability and characterization of oleogels obtained from safflower oil-based beeswax and rice bran wax and their effect on the quality of cake samples. *J American Oil Chemists' Soc*, 2023: 1-15.
- Barragán-Martínez LP, Román-Guerrero A, Vernon-Carter EJ, Alvarez-Ramirez J. 2022. Impact of fat replacement by a hybrid gel (canola oil/candelilla wax oleogel and gelatinized corn starch hydrogel) on dough viscoelasticity, color, texture, structure, and starch digestibility of sugar-snap cookies. *Inter J Gastron Food Sci*, 29: 100563. <https://doi.org/10.1016/j.ijgfs.2022.100563>.
- Batista AP, Niccolai A, Bursic I, Sousa I, Raymundo A, Rodolfi L, Biondi N, Tredici MR. 2019. Microalgae as functional ingredients in savory food products: application to wheat crackers. *Foods*, 8: 611; doi:10.3390/foods8120611.
- Bölükbaş B. 2023. Ekşi hamur mikroorganizmaları kullanımının krakerin kalite ve biyoaktif özellikleri ile glisemik indeks üzerine etkisi, Yüksek Lisans Tezi, Yıldız Teknik Üniversitesi, Fen Bilimleri Enstitüsü, Gıda Mühendisliği A.B.D., İstanbul, Türkiye, ss: 55.
- Brito GB, Peixoto VODS, Martins MT, Rosário DKA, Ract JN, Conte-Júnior CA, Torres AG, Castelo-Branco VN. 2022. Development of chitosan-based oleogels via crosslinking with vanillin using an emulsion templated approach: Structural characterization and their application as fat-replacer. *Food Struct*, 32: 100264. <https://doi.org/10.1016/j.foostr.2022.100264>.
- Choi KO, Hwang HS, Jeong S, Kim S, Lee S. 2020. The thermal, rheological, and structural characterization of grapeseed oil oleogels structured with binary blends of oleogelator. *J Food*

- Sci, 85(10): 3432-3441. <https://doi.org/10.1111/1750-3841.15442>.
- Demirkesen I, Mert B. 2019. Utilization of beeswax oleogel-shortening mixtures in gluten-free bakery products. *J American Oil Chem Soc*, 96(5): 545-554. <https://doi.org/10.1002/aocs.12195>.
- Demirkesen I, Mert B. 2020. Recent developments of oleogel utilizations in bakery products. *Critical Rev Food Sci Nutri*, 60(14): 2460-2479. <https://doi.org/10.1080/10408398.2019.1649243>.
- Dülger-Altın D. 2015. Sağlıklı bir atıştırma: enerjisi azaltılmış kraker üretimi. Doktora Tezi, Uludağ Üniversitesi, Fen Bilimleri Enstitüsü, Gıda Mühendisliği A.B.D., Bursa, Türkiye, ss: 142.
- Ekin MM, Kutlu N, Meral R, Ceylan Z, Cavidoglu İ. 2021. A novel nanotechnological strategy for obtaining fat-reduced cookies in bakery industry: Revealing of sensory, physical properties, and fatty acid profile of cookies prepared with oil-based nanoemulsions. *Food BioSci*, 42: 101184. <https://doi.org/10.1016/j.fbio.2021.101184>.
- Espert M, Wang Q, Sanz T, Salvador A. 2023. Sunflower Oil-based Oleogel as Fat Replacer in Croissants: Textural and Sensory Characterisation. *Food Bioprocess Technol*, 16(9): 1943-1952. <https://doi.org/10.1007/s11947-023-03029-w>.
- Fayaz G, Polenghi O, Giardina A, Cerne V, Calligaris S. 2020. Structural and rheological properties of medium-chain triacylglyceride oleogels. *Inter J Food Sci Technol*, 56(2): 1040-1047. <https://doi.org/10.1111/ijfs.14757>.
- Flores-García CL, Medina-Herrera N, Rodríguez-Romero BA, Martínez-Avila GCG, Rojas R, Meza-Carranco Z. 2023. Impact of fat replacement by using organic-candelilla-wax-based oleogels on the physicochemical and sensorial properties of a model cookie. *Gels*, 9(8): 757. <https://doi.org/10.1111/ijfs.14757>.
- Gallagher E, O'Brien CM, Scannell AGM, Arendt EK. 2003. Use of response surface methodology to produce functional short dough biscuits. *J Food Engin*, 56: 269-271. [https://doi.org/10.1016/S0260-8774\(02\)00265-0](https://doi.org/10.1016/S0260-8774(02)00265-0).
- Giacomozzi AS, Carrin ME, Palla CA. 2018. Muffins elaborated with optimized monoglycerides oleogels: from solid fat replacer obtention to product quality evaluation. *J Food Sci*, 83(6): 1505-1515. <https://doi.org/10.1111/1750-3841.14174>.
- Giacomozzi AS, Carrin ME, Palla CA. 2022. Muffins made with monoglyceride oleogels: Impact of fat replacement on sensory properties and fatty acid profile. *JAACS*, 100(4): 343-349. <https://doi.org/10.1002/aocs.12674>.
- Giannoutsos K, Achilleas PZ, Koukoumaki DI, George M, Mourtzinos I, Sarris D, Gkatzionis K. 2023. Production of functional crackers based on non-conventional flours. Study of the physicochemical and sensory properties. *Food Chem Adv*, 2023(2): 100194. <https://doi.org/10.1016/j.focha.2023.100194>.
- IUPAC. 1987. Standard methods for analysis of oils, fats and derivatives. Blackwell Scientific Publications, IUPAC Method 2.301, Report of IUPAC Working Group WG 2/87, Network, USA, 7th ed., pp: 253.
- İzci L, Şengül B. 2015. Sensory acceptability and fatty acid profile of fish crackers made from carassius gibelio. *Food Sci Technol*, 35(4): 643-646. <https://doi.org/10.1590/1678-457X.6723>.
- Jadhav HB, Pratap AP, Gogate PR, Annapure US. 2022. Ultrasound-assisted synthesis of highly stable MCT based oleogel and evaluation of its baking performance. *Applied Food Res*, 2(2): 156. <https://doi.org/10.1016/j.afres.2022.100156>.
- Kahraman SD, Küplülü Ö. 2011. Trans yağ asitleri. *Vet Hekim Dern Derg*, 82(2): 15-24.
- Kara S. 2019. Karnaub ve balmumu vaksları ile hazırlanan oleojellerin dsc ve ft-ır spektroskopisi ile karakterizasyonu. Yüksek Lisans Tezi, İstanbul Sabahattin Zaim Üniversitesi Gıda Mühendisliği Anabilim Dalı, İstanbul, Türkiye, ss: 80.
- Kim JY, Lim J, Lee J, Hwang HS, Lee S. 2017. Utilization of oleogels as a replacement for solid fat in aerated baked goods: physicochemical, rheological, and tomographic characterization. *J Food Sci*, 82(2): 445-452. <https://doi.org/10.1111/1750-3841.13583>
- Lee JY, Lim T, Kim J, Hwang KT. 2022. Physicochemical characteristics and sensory acceptability of crackers containing red ginseng marc. *J Food Sci Technol*, 59(1): 212-219. <https://doi.org/10.1007/s13197-021-05002-x>.
- Lee S, Inglett GE. 2006. Rheological and physical evaluation of jet-cooked oat bran in low calorie cookies. *Inter J Food Sci Technol*, 41(5): 553-559. <https://doi.org/10.1111/j.1365-2621.2005.01105.x>.
- Li J, Guo R, Wang M, Bi Y, Zhang H, Xu X. 2022. Development and Characterization of Compound Oleogels Based on Monoglycerides and Edible Waxes. *ACS Food Sci Technol*, 2(2): 302-314. <https://doi.org/10.1021/acscfoodscitech.1c00390>.
- Meng Z, Guo Y, Wang Y, Liu Y. 2018. Oleogels from sodium stearyl lactylate-based lamellar crystals: structural characterization and bread application. *Food Chem*, 292: 134-142. <https://doi.org/10.1016/j.foodchem.2018.11.042>.
- Millar KA, Barry-Ryan C, Burke R, Hussey K, McCarthy S, Gallagher E. 2017. Effect of pulse flours on the physicochemical characteristics and sensory acceptance of baked crackers. *Inter J Food Sci Technol*, 52: 1155-1163. <https://doi.org/10.1111/ijfs.13388>.
- Naeli MH, Milani JM, Farmani J, Zargaraan A. 2023. Ethyl cellulose/hydroxypropyl methyl cellulose-based oleogel shortening: Effect on batter rheology and physical properties of sponge cake. *J American Oil Chem Soc*, 100(9): 743-755. <https://doi.org/10.1002/aocs.12695>.
- Noonim P, Rajasekaran B, Venkatachalam K. 2022. Structural characterization and peroxidation stability of palm oil-based oleogel made with different concentrations of carnauba wax and processed with ultrasonication. *Gels*, 8(12): 763. <https://doi.org/10.3390/gels8120763>.
- Nutter J, Shi X, Lamsal B, Acevedo NC. 2023. Plant-based bigels as a novel alternative to commercial solid fats in short dough products: Textural and structural properties of short dough and shortbread. *Food BioSci*, 54: 102865. <https://doi.org/10.1016/j.fbio.2023.102865>.
- Orhan NO, Eroglu Z. 2022. Structural characterization and oxidative stability of black cumin oil oleogels prepared with natural waxes. *J Food Process Preserv*, 46(12): 17211. <https://doi.org/10.1111/jfpp.17211>.
- Palamutoğlu R. 2021. Replacement of beef fat in meatball with oleogels (black cumin seed oil/sunflower oil). *J Hellenic Vet Med Soc*, 72(3): 3031-3040. <https://doi.org/10.12681/jhvms.28484>.
- Pehlivanoglu H, Ozulku G, Yildirim RM, Demirci M, Tokar OS, Sagdic O. 2018. Investigating the usage of unsaturated fatty acid-rich and low-calorie oleogels as a shortening mimetics in cake. *J Food Process Preserv*, 42(6): e13621. <https://doi.org/10.1111/jfpp.13621>.
- Rafati M, Ghasemi A, Saedi M, Habibi E, Salehifar E, Mosazadeh M, Maham M. 2019. Nigella sativa L. for prevention of acute radiation dermatitis in breast cancer: A randomized, double-blind, placebo-controlled, clinical trial. *Complement Ther Med*, 47: 102205. <https://doi.org/10.1016/j.ctim.2019.102205>.

- Schwarz W. 2000. Formation of trans polyalkenoic fatty acids during vegetable oil refining. *European J Lipid Sci Technol*, 102: 648-649. [https://doi.org/10.1002/1438-9312\(200010\)102:10<648:AID-EJLT648>3.0.CO;2-V](https://doi.org/10.1002/1438-9312(200010)102:10<648:AID-EJLT648>3.0.CO;2-V).
- Swe MTH, Asavapichayont P. 2018. Effect of silicone oil on the microstructure, gelation and rheological properties of sorbitan monostearate-sesame oil oleogels, *Asian J Pharmaceut Sci*, 13: 485-497, 2018. <https://doi.org/10.1016/j.ajps.2018.04.006>.
- Szydłowska-Czerniak A, Momot M, Stawicka B, Rabiej-Kozioł D, 2022. Effects of the chemical composition on the antioxidant and sensory characteristics and oxidative stability of cold-pressed black cumin oils, *Antioxidants*, 11: 1556. <https://doi.org/10.3390/antiox11081556>.
- Talbott SM, Talbott JA. 2022. Effect of thymoquin black cumin seed oil as a natural immune modulator of upper-respiratory tract complaints and psychological mood state. *Food Sci Nutri Res*, 5(1): 1-6.
- Tang YR, Ghosh S. 2021. Canola protein thermal denaturation improved emulsion-templated oleogelation and its cake-baking application. *Royal Soc Chem, RSC Adv*, 11(41): 25141-25157. <https://doi.org/10.1039/d1ra02250d>.
- Tanislav AE, Puscas A, Paucean A, Muresan AE, Semeniuc CA, Muresan V, Mudura E. 2022. Evaluation of structural behavior in the process dynamics of oleogel-based tender dough products. *Gels*, 8(5): 317. <https://doi.org/10.3390/gels8050317>.
- Toğrul İ. 2021. Gölevez (*Colocasia Esculenta* (L.) Schott) unu ilavesinin glutensiz krakerlerin besleyici ve duyuşal özelliklerine etkisi. Yüksek Lisans Tezi, Kocaeli Üniversitesi, Sosyal Bilimler Enstitüsü, Turizm İşletmeciliği A.B.D., Gastronomi ve Mutfak Sanatları A.B.D., Kocaeli, Türkiye, ss: 118.
- Vingering N, Oseredczuk M, du Chaffaut L, Ireland J, Ledoux M. 2010. Fatty acid composition of commercial vegetable oils from the French market analysed using a long highly polar column. *Oléagineux, Corps gras, Lipides*, 17(3): 185-192. <https://doi.org/10.1051/ocl.2010.0309>.
- Yashini M, Sahana S, Hemanth SD, Sunil CK. 2021. Partially defatted tomato seed flour as a fat replacer: effect on physicochemical and sensory characteristics of millet-based cookies. *J Food Sci Technol*, 58(12): 4530-4541. <https://doi.org/10.1007/s13197-020-04936-y>.
- Yılmaz E, Oğutcu M. 2015. The texture, sensory properties and stability of cookies prepared with wax oleogels. *Food Funct*, 6(4): 1194-1204. <https://doi.org/10.1039/c5fo00019j>.
- Zhao M, Rao J, Chen B. 2022. Effect of high oleic soybean oil oleogels on the properties of doughs and corresponding bakery products. *J American Oil Chem Soc*, 99(11): 1071-1083. <https://doi.org/10.1002/aocs.12594>.
- Zhou J, Faubion JM, Walker CE. 2011. Evaluation of different types of fats for use in high-ratio layer cakes. *LWT-Food Sci Technol*, 44(8): 1802-1808. <https://doi.org/10.1016/j.lwt.2011.03.013>.



ORMAN GÜLÜ (*Rhododendron ssp.*) ÇELİKLERİNİN KÖKLENMELERİ ÜZERİNE FARKLI UYGULAMALARIN ETKİLERİ

Bahadır ALTUN^{1*}, Hüseyin ÇELİK²

¹Kırşehir Ahi Evran University, Agricultural Faculty, Department of Horticulture, 40200, Kırşehir, Türkiye

²Ondokuz Mayıs University, Agricultural Faculty, Department of Horticulture, 55200, Samsun, Türkiye

Özet: Bu araştırma, Türkiye doğal orman gülü türlerinin (*Rhododendron ponticum* L., *R. luteum* Sweet, *R. caucasicum* Pallas, *R. simirnovii* Trautv ve *R. ungeronii* Trautv) çeliklerinin köklenme oranları (%) üzerine farklı çelik alma dönemi, farklı IBA dozlarının ve köklendirme ortamlarının etkilerini belirlemek amacıyla yürütülmüştür. Ağustos ayının sonu, Ekim ayının ilk yarısı ve Kasım ayının ikinci yarısında alınan tepe çelikleri, İndol-3-Bütirik Asit (IBA)'in 0, 2000 ppm, 4000 ppm ve 8000 ppm dozlarına tabi tutularak alttan ısıtmalı tavalarda ve mistleme sulama altında köklendirme ortamlarına dikilmiştir. Köklendirme ortamı olarak asidik torf+perlit (3:1) ve perlit ortamı kullanılmıştır. Araştırma sonucunda yıllara göre değişmekle beraber en yüksek köklenme oranları *R. ponticum*, *R. simirnovii* ve *R. ungeronii* türlerinde asidik torf+perlit (3:1) ortamında (sırasıyla % 75.83, %59.17 ve %25), *R. luteum* ve *R. caucasicum* türlerinde ise perlit ortamında (sırasıyla %64.17 ve %29.17) olduğu tespit edilmiştir. Orman gülü çeliklerinin köklenme seviyelerinin; türe, çelik alma dönemine, köklenme ortamına, kullanılan IBA dozuna ve yıllara bağlı olarak değişkenlik gösterdiği belirlenmiştir.

Anahtar kelimeler: *Rhododendron*, Çelik, Köklendirme ortamı, IBA


The Effect of Different Applications on Rooting of *Rhododendron spp* Cuttings


Abstract: This research was carried out to determine the effects of different cutting taking periods, IBA doses and different rooting environments on the rooting rates (%) of Turkish natural rhododendron species (*R. ponticum* L., *R. luteum* Sweet, *R. caucasicum* Pallas, *R. simirnovii* Trautv and *R. ungeronii* Trautv) cuttings. The shoot-tip-cuttings taken at the end of August, the first half of October and the second half of November were subjected to 0, 2000 ppm, 4000 ppm and 8000 ppm doses of Indole-3-Butyric Acid (IBA). They were then planted in rooting media in bottom heated pans and under misting irrigation. Acidic peat+perlite (3:1) and perlite medium were used as rooting media. As a result of the research, although it varies from year to year, the highest rooting rates were found in *R. ponticum*, *R. simirnovii* and *R. ungeronii* species in acidic peat + perlite (3:1) medium (75.83%, 59.17% and 25%, respectively). *R. luteum* and *R. caucasicum* species were found to be in perlite environment (64.17% and 29.17%, respectively). Rooting levels of rhododendron cuttings; It was determined that it varies depending on the species, cutting period, rooting environment, IBA dose used and years.

Keywords: *Rhododendron*, Cutting, Rooting medium, IBA

*Sorumlu yazar (Corresponding author): Kırşehir Ahi Evran University, Agricultural Faculty, Department of Horticulture, 40200, Kırşehir, Türkiye

E mail: bahaltun@gmail.com (B. ALTUN)

Bahadır ALTUN  <https://orcid.org/0000-0002-6503-7109>

Hüseyin ÇELİK  <https://orcid.org/0000-0003-1403-7464>

Gönderi: 01 Şubat 2024

Kabul: 01 Mart 2024

Yayınlanma: 15 Mart 2024

Received: February 01, 2024

Accepted: March 01, 2024

Published: March 15, 2024

Cite as: Altun B, Çelik H. 2024. The effect of different applications on rooting of *Rhododendron spp* cuttings. BSJ Eng Sci, 7(2): 351-358.

1. Giriş

Türkiye, biyoçeşitlilik yönünden dünyanın en önemli gen merkezlerinden biridir. Ülkenin sahip olduğu farklı ekolojiler ve topoğrafik yapılar birçok bitki türünün yetişmesine olanak sağlamaktadır. Zengin tür çeşitliliği içerisinde önemli bitkilerden biri de orman gülleridir. Bu bitkiler ülkemizde, Karadeniz kıyı şeridi boyunca, doğuda Artvin'den başlayarak, batıda Istranca Dağlarına kadar, dağların kuzeye bakan yamaçlarında doğal olarak yetişmektedir.

Günümüzde *Rhododendron* cinsi içerisinde yer alan bitkiler karakteristik özelliklerinden dolayı dış mekân düzenlemelerinde ve saksılı süs bitkisi olarak kullanım açısından son derece popüler bitkilerdir. Doğada yetişen orman güllerinin estetik güzelliği bu bitkilerin günümüz modern bahçelerindeki düzenlemelerde yaygın olarak kullanılmasını sağlamıştır. Kentsel peyzaj

planlamalarında kültüre alınmış doğal orman gülü türlerinin yanı sıra ıslah çalışmaları ile geliştirilmiş ve günümüzde sayıları binlerle ifade edilen orman gülü çeşitleri de sıkça kullanılmaktadır. Ülkemizde doğal olarak yayılış gösteren orman gülleri gösterişli süs bitkileri olmalarına rağmen yerli türler henüz kültüre alınmadığı için kentsel peyzaj uygulamalarında süs bitkisi olarak kullanılmamaktadır. Peyzaj planlamalarda kullanılan orman gülleri ise ithal edilerek, yüksek fiyatlarla tüketiciye sunulmaktadır.

Orman gülü fundagiller (*Ericaceae*) familyasındaki *Rhododendron* cinsi içinde yer alır. Doğal olarak yayılış gösteren orman güllerinin, doğal tür sayısı değişik kaynaklara göre değişmekle birlikte yaklaşık 1000 ile 1466 civarında olduğu bildirilmektedir (Rai ve ark., 2013; e-Floras, 2024). Herdemyeşil veya yaprağını döken çalı, nadiren de ağaç şeklinde bitkileri olan bir türdür



(Cullen, 2005). Yaprağını döken bazı orman gülü türlerinde yeşil olan yapraklar yeşilden sarıya sonra da kahverengi ve kızıla dönerek güzel bir sonbahar renk görünümü sergilemektedirler. Orman gülü çiçekleri sürgün uçlarında tek tek veya salkım halinde meydana gelip oldukça büyük ve çok farklı renktedirler. Gerek yaprak özellikleri gerekse çiçek renklerinden dolayı dünyada önemli bir süs bitkisi olan ormangülleri ülkemizde henüz süs bitkisi sektörüne kazandırılmamıştır (Altun, 2021).

Orman gülleri, alçak boylu yer örtücünden orta büyüklükteki çalı veya ağaca kadar oldukça farklı boyut ve şekillerde gelişen türleri içerir. Bazı çeşitler yuvarlak bir habitat oluştururken, diğerleri açık çalı veya dik büyüyen bir ağaç formunda olabilir (Cullen, 2005; Shen ve ark., 2015; Francon ve ark., 2017; Li ve ark., 2018). Bazı türler yaprak döken, diğerleri ise her dem yeşildir. *Rhododendron* türleri benzersiz özelliklerinden dolayı geniş bir kullanım alanına sahiptir. Bu bitkiler özellikle dış mekan peyzaj planlamalarında tek başına veya diğer çalılarla birlikte bordür bitkisi olarak, uzun boylu olanlar ise perde bitkisi veya vurgu bitkisi olarak kullanılabilir. Doğal ve kültürü yapılan *Rhododendron* türleri ve çeşitli ıslah yöntemleriyle elde edilen çeşitler, birçok ülkede bahçeleri gösterişli çiçekleriyle süslemektedir (Hay ve ark., 2006; Weia ve ark., 2018).

Değerli bir süs bitkisi olan ormangülü taksonu, diğer birçok kültür bitkisine benzer şekilde generatif veya vejetatif yöntemlerle çoğaltılabilmektedir. Dünyanın birçok ülkesinde kentsel peyzaj planlamalarında aranan ve istenen bitkiler olan orman gülleri ülkemizde henüz yeterince kullanılmamaktadır. Bunun başlıca nedenleri birçok bitki gibi kolay çoğaltılamaması ve yetiştirilmesi için asidik toprak ve nemli bir ortama ihtiyaç duymasıdır. Orman gülleri çoğaltım bakımından türler arasında oldukça farklı özellikler göstermekte ve her tür çoğaltma bakımından farklı koşullar istemektedir. Çelikle çoğaltmada başarıyı artırmak için çelik alma zamanı, çelik şekli (yeşil çeliklerde düz ve ökçeli kesim, odunsu çeliklerde düz kesim), sıcaklık uygulamaları, köklenmeyi teşvik edici madde uygulamaları (Hwang ve ark., 1998; Czekalski, 1988; Krzymin'ska ve Czekalski, 1998; Remotti, 2003; Ferriani ve ark., 2006) gibi bir çok yöntem ve vermikülit, hindistan cevizi lifi-torf-perlit- kum gibi farklı köklendirme ortamları köklendirmede ciddi oranda (%5-%95) farklılık yaratmaktadır (Matysiak ve Nowak, 2008; Pignatti ve ark., 2004). Bu çalışma ile düşük köklenme oranına sahip orman gülü türlerinin köklenme

yüzdelerinin artırılarak bu alandaki boşluğun doldurulması amaçlanmıştır.

2. Materyal ve Yöntem

2.1. Bitki Materyali

Araştırmanın bitki materyalini Artvin il ve ilçe sınırlarında doğal yayılış alanlarından alınan beş farklı *Rhododendron* türünün (*R. luteum* Sweet, *R. ponticum* L., *R. ungeronii* Trautv, *R. simirnowii* Trautv, *R. caucasicum* Pallas) çelikleri oluşturmuştur (Tablo 1).

2.2. Çeliklerin Alınması, Taşınması ve Köklendirme Ortamı

Seçilen ve teşhisleri yaptırılan 5 ormangülü türüne ait çelikler Ağustos ayının sonu, Ekim ayının ilk yarısı ve Kasım ayının ikinci yarısında olmak üzere 3 farklı dönemde yıllık sürgünlerden tepe çeliği olarak alınmıştır. Bu işlem 2 yıl tekrarlanmıştır. Tüm türlerden her dönemde 500'er adet çelik alınmıştır. Çeliklerde su kaybını minimuma indirmek amacıyla, tepe yaprağının yarısı bırakılarak diğer yaprakların tamamı çıkarılmıştır. Hazırlanan çelikler yirmişerli demetler halinde bağlanarak içerisine nemli gazete serili köpük kaplara konulmuş ve üzerlerine buz torbası konularak dikim zamanına kadar bu şekilde muhafaza edilmiştir. Araştırmada köklendirme ortamı olarak perlit ve asidik torf + perlit (3:1) karışımından oluşan iki farklı ortam kullanılmıştır. Köklendirme tavasına doldurulan bu karışım düz bir yüzey elde edilinceye kadar düzeltilmiştir. Her iki ortam dikimden önce sisleme ünitesinin çalıştırılmasıyla nemlendirilerek dikime hazır hale getirilmiştir.

2.3. Çeliklerin Dikimi

Deneme alanına getirilen çelikler, canlı dokuya ulaşmak için alt kesim dip boğumun hemen 0.5 cm altından düz olarak (Ağaoğlu ve ark., 2001) kesilmiştir. Hazırlanan çeliklerin dip kısımları 5 sn süre ile 0, 2000 ppm, 4000 ppm ve 8000 ppm dozlarında hazırlanan Indol Butrik Asit (IBA) çözeltisi içerisinde tutulmuştur. Daha sonra çelikler, sıcaklık (alttan ısıtmalı) ve nem kontrollü (sisleme altında) iki farklı köklendirme ortamına (perlit ve asidik torf+ perlit karışımı) tesadüf bloklarında bölünen bölünmüş parseller deneme desenine göre dikilmiştir. Her tekerrürde 20 adet çelik olacak şekilde 3 tekerrürlü olarak deneme kurulmuştur. Denemede homojeniteyi sağlamak için çelikler SÜ x SA: 4.5 x 3 cm aralıklarla dikilirken tekerrürler arasında 5.5 cm, türler arasında ise 10 cm aralık bırakılmıştır. Köklendirme ortamının sıcaklığı 24 °C (±1)'de sabit tutulmuştur.

Tablo 1. *Rhododendron* çeliklerinin alındıkları yerlere ait veriler

Türler	Rakım	Koordinat	Lokasyon
<i>R. ponticum</i> L.	1652 m	41°08'914 K / 41°46'205 D	Artvin
<i>R. luteum</i> Sweet	1671 m	41°10'424 K / 42°18'943 D	Şavşat
<i>R. simirnowii</i> Trautv.	1982 m	40°14'743 K / 41°35'699 D	Murgul
<i>R. ungeronii</i> Trautv.	1249 m	41°18'870 K / 41°53'495 D	Borçka
<i>R. caucasicum</i> Pallas	2289 m	41°43'450 K / 42°28'376 D	Şavşat

Köklendirme ortamının nemi ise çeliklerin yaprakları kurumayacak şekilde sisleme zamanı manuel olarak ayarlanarak sağlanmıştır. Çelikler 190 gün sonra köklendirme ortamlarından sökülerek değerlendirilmiştir. Köklendirme ortamından sökülen çeliklerde bir veya daha fazla adventif kök oluşturan çelik köklenmiş olarak kabul edilmiştir. Elde edilen sonuçlar % olarak hesaplanmış ve köklenme oranı belirlenmiştir.

İstatistik analizler

Denemelerden elde edilen 2 yıllık veriler birleştirilmiş ve analiz edilmeden önce Log(10) transformasyonuna tabii tutulmuştur. Elde edilen bulgulara tek yönlü varyans analizi (P<0.05) uygulanmıştır. Ele alınan konular arasındaki farklılıklar Duncan çoklu karşılaştırma testi ile gruplandırılmıştır. Çizelgedeki veriler orjinal değerlerdir ve harflendirmeler transforme edilmiş veriler üzerinden yapılmıştır. İstatistik Analizleri SPSS (v.29) Paket Programı kullanılarak yapılmıştır.

3. Bulgular

Türkiye’de doğal olarak yetişen *R. ponticum* L., *R. luteum* Sweet, *R. smirnovii* Trautv., *R. ungeronii* Trautv. ve *R. caucasicum* Pallas. orman gülü türlerinden farklı dönemlerde alınan tepe çeliklerine, farklı IBA dozları uygulanarak farklı ortamlarda köklendirilmiştir. İki yıl tekrarlanan çalışma sonucunda elde edilen bulgular türler bazında aşağıda değerlendirilmiştir.

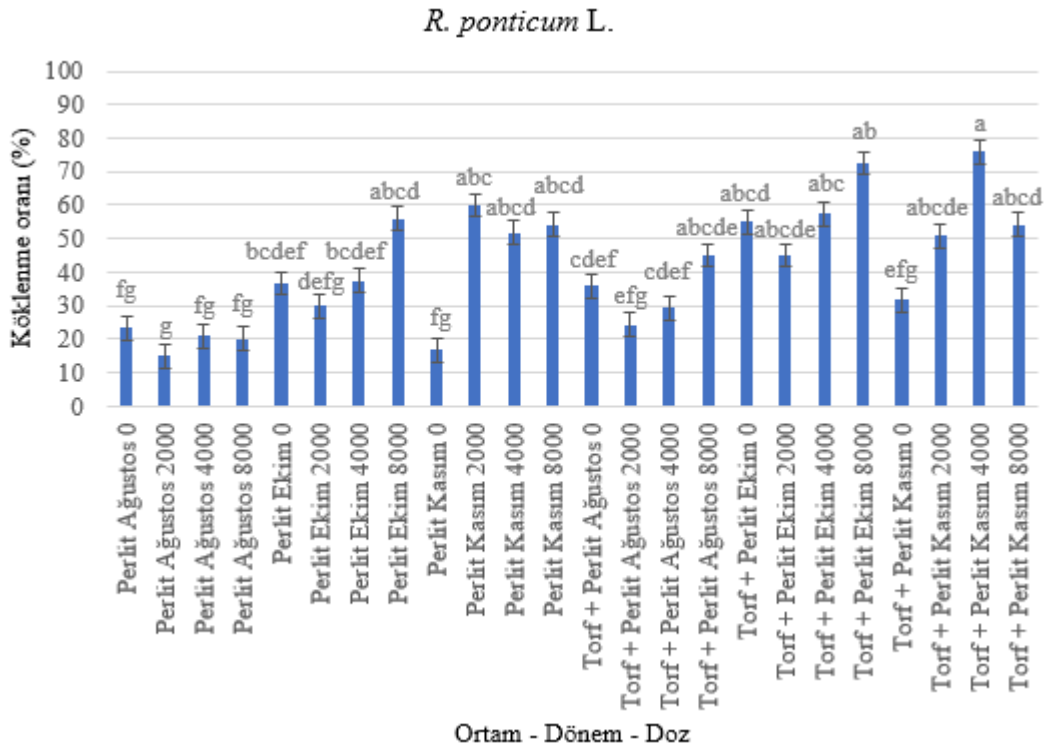
3.1. *Rhododendron ponticum* L.

R. ponticum L. orman gülü türünün tepe çeliklerinin köklenme oranları üzerine, köklendirme ortamlarının, çelik alma dönemlerinin, IBA dozlarının ve yılların etkileri Şekil 1’de verilmiştir. Elde edilen sonuçlar incelendiğinde perlit ortamı ile torf+perlit ortamı

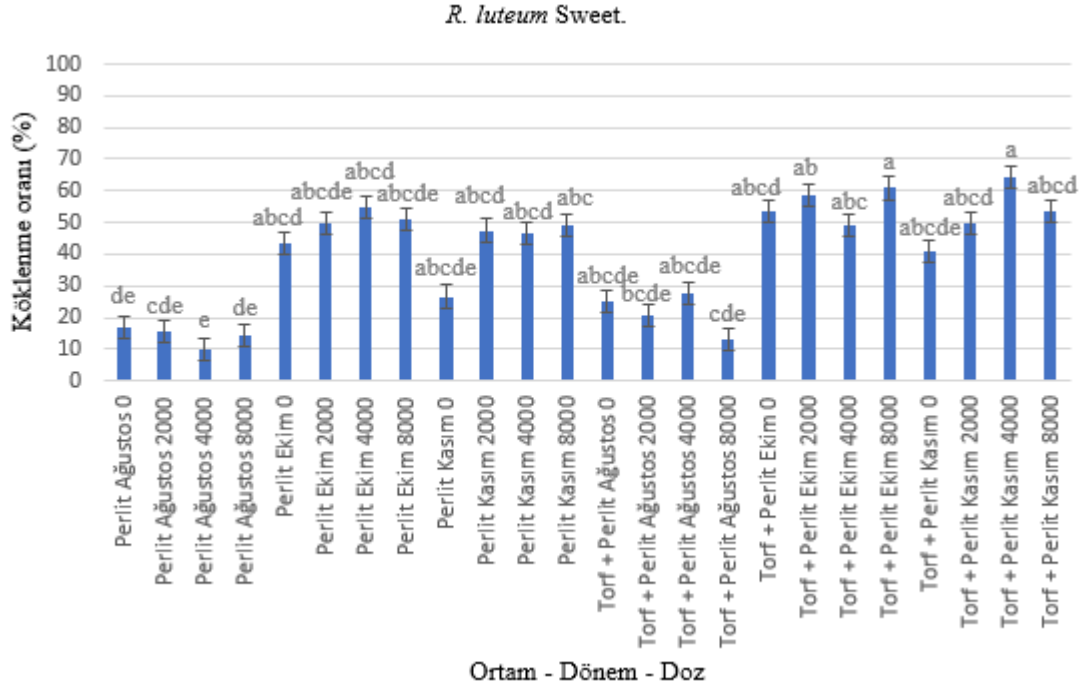
arasındaki farklılıkların istatistiki olarak önemli düzeyde (P<0,05) olduğu tespit edilmiştir (F(23,120)=4,98). Perlit ortamında en yüksek köklenme oranı %60 ile Kasım ayında alınan ve 2000 ppm IBA dozu uygulanan çeliklerden elde edilmiştir. Aynı ortamda en düşük değer (%15) ise Ağustos ayında alınarak 2000 ppm IBA uygulanan çeliklerden elde edilmiştir. Torf+perlit ortamında ise en yüksek köklenme oranı (%75,83) Kasım ayında alınan ve 4000 ppm IBA dozu uygulanan çeliklerden elde edilmiştir. Aynı ortamda Ekim ayında alınan ve 8000 ppm IBA uygulanan çeliklerden %72,5 oranında köklenme elde edilirken, bu ortamda en düşük köklenme oranı %24,17 olarak Ağustos ayında alınan ve 2000 ppm IBA uygulanan çeliklerde gerçekleşmiştir.

3.2. *Rhododendron luteum* Sweet.

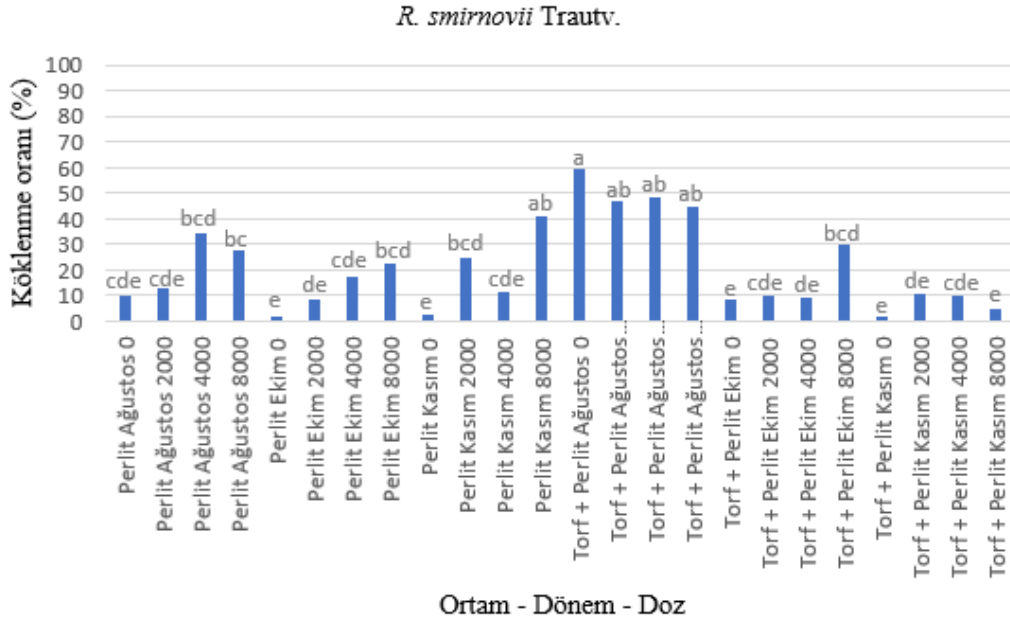
R. luteum Sweet. türünün tepe çeliklerinin köklenme oranları üzerine, köklendirme ortamlarının, çelik alma dönemlerinin, IBA dozlarının ve yılların etkileri Şekil 2’de verilmiştir. Elde edilen sonuçlar incelendiğinde perlit ortamı ile torf+perlit ortamı arasındaki farklılıkların istatistiki olarak önemli düzeyde (P<0,05) olduğu tespit edilmiştir (F(23,120)=2,24). Perlit ortamında en yüksek köklenme oranı %55 ile Ekim ayında alınan ve 4000 ppm IBA uygulanan çeliklerden elde edilmiştir. Aynı ortamda en düşük değer (%10) ise Ağustos ayında alınarak 4000 ppm IBA uygulanan çeliklerden elde edilmiştir. Torf+perlit ortamında ise en yüksek köklenme oranı %64,17 ile Kasım ayında alınan ve 4000 ppm IBA dozu uygulanan çeliklerden elde edilmiştir. Bu ortamda en düşük köklenme oranı %13,33 olarak Ağustos ayında alınan ve 8000 ppm IBA uygulanan çeliklerde gerçekleşmiştir.



Şekil 1. *R. ponticum* L. türü çeliklerinin köklenme oranları.



Şekil 2. *R. luteum* Sweet. türü çeliklerinin köklenme oranları.



Şekil 3. *R. smirnovii* Trautv. türü çeliklerinin köklenme oranları.

3.3. *Rhododendron smirnovii* Trautv.

R. smirnovii Trautv. türü tepe çeliklerinin köklenme oranları üzerine, köklendirme ortamlarının, çelik alma dönemlerinin, IBA dozlarının ve yılların etkileri Şekil 3'de verilmiştir. Elde edilen sonuçlar incelendiğinde perlit ortamı ile torf+perlit ortamı arasındaki farklılıkların istatistiki olarak önemli düzeyde ($P<0,05$) olduğu tespit edilmiştir ($F(23,120)=7,47$). Perlit ortamında en yüksek köklenme oranı %40,83 ile Kasım ayında alınan ve 8000 ppm IBA uygulanan çeliklerden elde edilmiştir. Torf+perlit ortamında ise en yüksek köklenme oranı ise

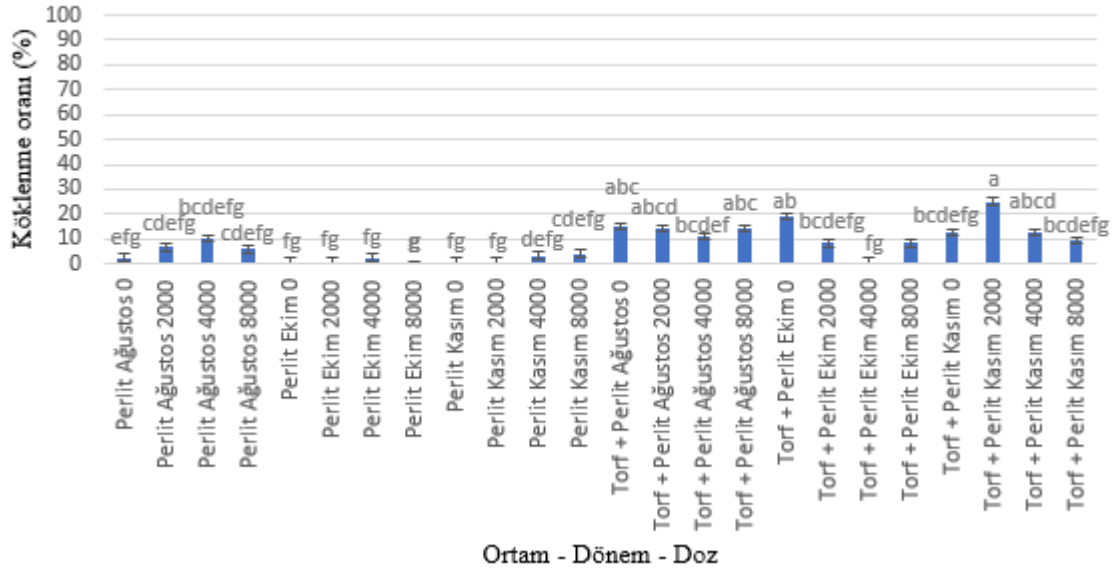
(%59,17) Ağustos ayında alınan ve IBA dozu uygulanmayan kontrol grubu çeliklerden elde edilmiştir.

3.4. *Rhododendron ungeronii* Trautv.

R. ungeronii Trautv. türü tepe çeliklerinin köklenme oranları üzerine, köklendirme ortamlarının, çelik alma dönemlerinin, IBA dozlarının ve yılların etkileri Şekil 4'de verilmiştir. Elde edilen sonuçlar incelendiğinde perlit ortamı ile torf+perlit ortamı arasındaki farklılıkların istatistiki olarak önemli düzeyde ($P<0,05$) olduğu tespit edilmiştir ($F(23,120)=4,29$). Perlit ortamında en yüksek köklenme oranı %10 ile Ağustos ayında alınan ve 4000

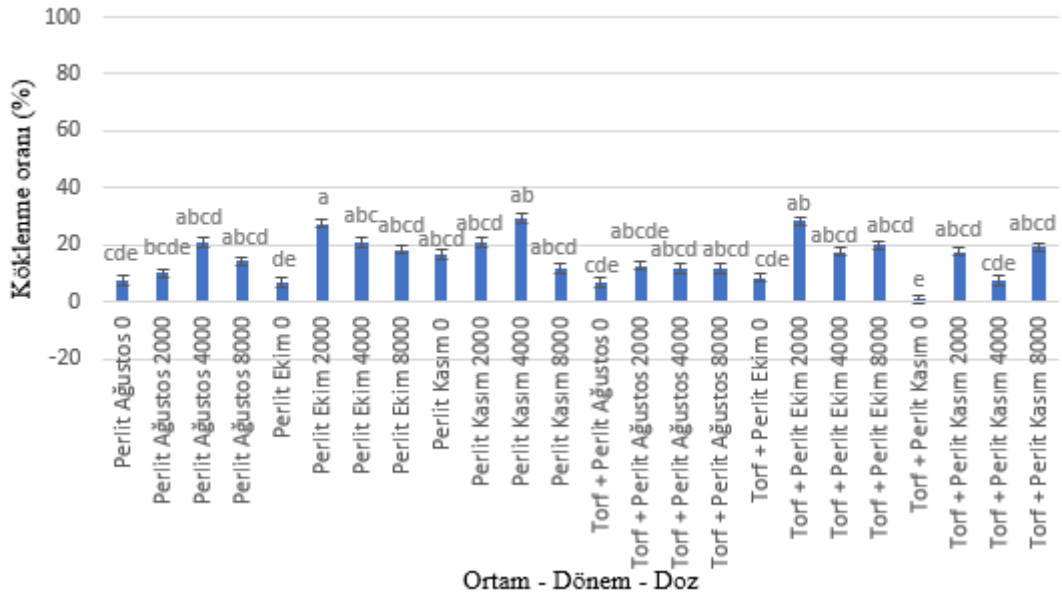
ppm IBA uygulanan çeliklerden elde edilmiştir. (%25) Kasım ayında alınan ve 2000 ppm IBA dozu Torf+perlit ortamında ise en yüksek köklenme oranı uygulanan çeliklerden elde edilmiştir.

R. ungeronii Trautv.



Şekil 4. *R. ungeronii* Trautv. türü çeliklerinin köklenme oranları.

R. caucasicum Pallas



Şekil 5. *R. caucasicum* Pallas. türü çeliklerinin köklenme oranları

3.5. *Rhododendron caucasicum* Pallas.

R. caucasicum Pallas türü tepe çeliklerinin köklenme oranları üzerine, köklendirme ortamlarının, çelik alma dönemlerinin, IBA dozlarının ve yılların etkileri Şekil 5'de verilmiştir. Elde edilen sonuçlar incelendiğinde perlit ortamı ile torf+perlit ortamı arasındaki farklılıkların istatistiki olarak önemli düzeyde ($P < 0,05$) olduğu tespit edilmiştir ($F(23,120)=2,51$). Perlit ortamında en yüksek köklenme oranı %29,17 ile Kasım ayında alınan ve 4000 ppm IBA uygulanan çeliklerden elde edilmiştir. Torf+perlit ortamında ise en yüksek köklenme oranı (%28,33) Ekim ayında alınan ve 2000 ppm IBA dozu uygulanan çeliklerden elde edilmiştir.

4. Tartışma

R. ponticum L. orman gülü türünün çeliklerinin köklenme oranları yıllar birleştirilerek incelendiğinde en yüksek köklenme oranını %75,83 ile Kasım ayında alınan ve 4000 ppm IBA dozu uygulanan ve Torf+perlit ortamında dikilen çeliklerden elde edilmiştir. Çeliklerin köklenme oranları üzerine birçok faktör etkilidir. Bu faktörlerin başında, bitkinin genetik yapısının yanında, çeliğin bünyesinde bulunan veya hazır olarak verilen büyüme düzenleyici maddeler gelmektedir. *R. ponticum* L. çeliklerinin anatomik yapısı ile yan kök oluşumu üzerine

bir araştırma yapan Strzelecka (2007), bitki büyümeyi düzenleyicisi uygulanan çeliklerde adventif kök oluşumlarının 3. haftadan sonra meydana geldiğini, uygulama yapılmayan kontrol çeliklerinde ise dikimden 6 hafta sonra bile köklenme olmadığı bildirmiştir. Almeida ve ark. (2003) ise *R. ponticum* subsp. *baeticum* türünün çelikleri ile yaptıkları çalışmada oksin (IBA ve NAA) uygulamalarının köklenme başarısını %91 ile %100'e çıkarabileceğini ifade etmektedirler. Lonca ve ark. (2004) Brilliant (*Rhododendron*) çeşidi çeliklerinde köklenme oranının torf + perlit ortamında %78,5, torf ortamında ise %69,5 olduğunu ve büyümeyi düzenleyici maddelerin köklenmeyi önemli düzeyde artırdığını bildirmişlerdir. Kondratovics ve Megre (2000) IBA uygulamasının köklenmeyi artırdığı gibi adventif kök oluşumunu da hızlandığını ortaya koymuşlardır. Zaharia ve ark. (2002), Apollo orman gülü çeşidinin çelikle çoğaltılması üzerine yaptıkları bir çalışmada büyümeyi düzenleyici madde uygulanmasıyla köklenme süresinin kıaldığını tespit etmişlerdir. Araştırmacıların bulguları ile elde mevcut çalışma sonucunda elde edilen bulgular paralellik arz etmekte ve *R. ponticum* çeliklerinin köklenebilmesi için büyümeyi düzenleyici madde kullanımının gerekli olduğunu ortaya koymaktadır. Ayrıca mevcut çalışma sırasında çeliklerin köklenmesi üzerine dönemlerin, köklendirme ortamlarının ve hatta yılların dahi etkisinin olduğu belirlenmiştir.

Köklendirme çalışmasının yapıldığı *R. luteum* türünün çeliklerinin yıllar birleştirilerek yapılan analiz sonucunda köklenme oranı bakımından en yüksek oran Kasım ayında alınan ve 4000 ppm IBA dozu uygulandıktan sonra Torf+perlit ortamına dikilen çeliklerde %64,17 olarak gerçekleşmiştir. Araştırmada ilk yıl %93'ler seviyesinde çok yüksek olan köklenme oranları, ikinci yıl %33'ler seviyesine düşmüştür. *R. luteum* türünde II. yıl külleme hastalığı gözlemlenmiştir. Bu hastalıkla düzenli olarak kültürel ve kimyasal mücadele yapılmasına rağmen köklü ve köksüz çeliklerin aşırı derecede külleme etkisinde kaldığı tespit edilmiştir. II. yıl köklenme oranında yaşanan düşüşün külleme hastalığından kaynaklanabileceği düşünülmektedir. Mevcut çalışmada yaprak döken tek tür olan *R. luteum* ilk yıl verileri dikkate alındığında en yüksek köklenme oranını veren tür olarak ortaya çıkmıştır. Aleksandrova ve Zarubenko (1991) tarafından yapılan bir çalışmada, yaprak döken 13 ve yarı herdemeyeşil olan 17 orman gülü türü ile hibrid çeşitlerin çelikle çoğaltılması denenmiştir. Araştırmacılar, büyümeyi düzenleyici madde uygulamalarıyla köklenmenin büyük oranda arttığını, en yüksek dozların en iyi sonucu verdiğini ve herdemeyeşil türlere göre yaprak döken türlerin daha kolay köklendiğini saptamışlardır. Araştırmacıların çalıştığı türler ile bu çalışmadaki orman gülü türleri farklı olsa da çoğaltma çalışmasından elde edilen sonuçlar araştırmacıların elde ettiği sonuçlarla paralellik göstermektedir.

R. smirnovii Trautv. orman gülü türüne ait çeliklerin köklenmesi üzerine araştırmanın her iki yılında Ağustos döneminde alınan ve kontrol dozu uygulanarak torf

ortamına dikilen çeliklerde I. yıl % 5,00, II. yıl ise %73,33 oranında köklenme elde edilmiştir (Altun, 2011). Ancak yıllar birleştirilerek yapılan analiz sonucunda en yüksek köklenme oranı (%59,17) Ağustos ayında alınan IBA uygulamadan Torf+perlit ortamına dikilen çeliklerden elde edilmiştir. Çalışmadaki bütün türlerde olduğu gibi yıllar arasında meydana gelen bu farkın alınan çeliklerin yıllar bazında maruz kaldığı iklim koşullarından kaynaklanabileceği düşünülmektedir. Ayrıca diğer bir faktör ise Hieke (1979) tarafından yapılan çalışma içerisinde saklıdır. Bu çalışmada araştırmacı 262 orman gülü çeşidinin yapraklarının ve çiçek tomurcuklarını soğuklara dayanımlarını araştırmış, en dayanıklı yaprak ve çiçeklerin *R. smirnovii* ile *R. catawbiense* türlerinde olduğunu bildirmiştir. Ayrıca çelikleri kolay köklenen çeşitlerin soğuklara dayanıklı olmadığını tespit etmiştir. Dolayısıyla soğuklara en dayanıklı tür olarak tespit edilen *R. smirnovii* türünün çelikleri zor köklenebilir. Ylatalo (1979) da yaptığı çalışmada *R. smirnovii*'nin en zor köklenen tür olduğunu bildirmektedir. Czekalski (1998) ise bu türün vejetatif olarak çoğaltılması üzerine çok az çalışıldığı ve genellikle vejetatif yolla çoğaltılmasının zor olduğunu bildirmektedir. Ancak bütün bu verilere rağmen mevcut çalışmada özellikle II. yıl elde edilen %73,33'lük köklenme oranının oldukça yüksek olduğu ve *R. smirnovii* türünün çelikle kolaylıkla çoğaltılabilmesinin mümkün olduğu düşünülmektedir.

R. ungerii Trautv. orman gülü türünde çeliklerin köklenme oranı üzerine uygulamaların etkisi incelendiğinde uygulamaların ve çelik alma zamanlarının köklenme üzerine istatistiki anlamda etkili olduğu tespit edilmiştir. Araştırma kapsamında *R. ungerii* çeliklerinin en zor ve en düşük oranda köklendikleri tespit edilmiştir. Köklendirme ortamında 220 gün tutulan çeliklerde kallus oluşumunun gerçekleştiği, çeliklerin hayatta kaldığı ancak köklenme oranlarının oldukça düşük olduğu belirlenmiştir. Benzer sonuçlara ulaşan Czekalski (1998) de bu türün vejetatif olarak çoğaltılmasının çok zor olduğunu bildirmektedir. Czekalski (1996) peyzaj bitkisi olarak kullanılan 4 kültür çeşidinin çelikleri ile yaptığı çalışmada çeliklerin düşük bir köklenme kabiliyeti ve canlılık sergilediğini ve 451 çelikten sadece 7 bitki elde edebildiğini bildirmiştir. Her bitki vejetatif veya generatif yöntemlerle çoğaltılabilir. Burada önemli olan bitki için uygun çoğaltma yönteminin tespit edilmesidir. Çeliklerinde köklenme oranları çok düşük olan bu tür de havai daldırma ile %100 oranında çok yüksek düzeyde bir köklenme gerçekleşmiştir (Altun, 2023). Dolayısıyla yapılan çalışmalar dikkate alındığında bu tür için çelikle çoğaltma yönteminin çok uygun bir yöntem olmadığı sonucuna varılabilir.

R. caucasicum Pallas çeliklerinin köklenme oranları üzerine ortam, dönem, doz ve yılların etkileri incelendiğinde en yüksek köklenme oranı %28,33 seviyesinde kaldığı tespit edilmiştir. Yukarıda *R. ungerii* türünde bahsedildiği gibi bu tür için de uygun çoğaltma yönteminin çelik değil havai daldırma olduğu söylenebilir. Altun (2023) yaptığı çalışmada havai

daldırma yöntemi ile *R. caucasicum* türünde %100 oranında köklenme meydana geldiğini bildirmiştir. Elde edilen verilere göre orman gülü çeliklerinin köklenmeleri üzerine türlerin, çelik alma dönemlerinin, köklenme ortamı özelliklerinin ve kullanılan büyümeyi düzenleyici madde dozlarının etkili olduğu ve her türün her uygulamaya farklı reaksiyon gösterdiği tespit edilmiştir. Her orman gülü türünün köklenme için farklı uygulamalara ihtiyaç duyduğu ortaya konulmuştur. Nitekim Remotti (2003), orman gülü çeliklerinin köklenme kabiliyetinin IBA uygulamasıyla arttığını ve türlere göre farklı IBA dozlarının daha etkili olduğunu saptamıştır. Çalışmamız sonucunda ortaya çıkan bulgular araştırmamızın bulgularıyla paralellik arz etmektedir.

5. Sonuç

Son yıllarda Karadeniz Bölgesinde süs bitkileri sektörü hızla gelişme göstermesine rağmen; gerek iklimsel koşullardan gerekse bölge üreticisinin ekonomik ve teknik altyapısının yetersizliğinden dolayı, süs bitkileri yetiştiriciliğinin yoğun olarak yapıldığı Ege, Akdeniz ve Marmara Bölgelerinin üreticileri ile rekabet edebilmesi mevcut türlerle mümkün görülmemektedir. Bu koşullar altında, bu çalışmayla ve devamında yapılacak çalışmalarla birlikte bölgenin doğal bitkisi olan orman güllerinin süs bitkileri sektörüne kazandırılmasıyla bölgemiz üreticileri avantajlı hale gelecektir. Orman güllerinde sera koşullarında çoğaltma sağlansa bile, köklü çeliklerin veya tohumdan elde edilen fidelerin saksılara şaşırtılmasından sonra dış koşullara adaptasyonlarının oldukça zor olduğu tespit edilmiştir. Bu durumun iklim, toprak ve sulama suyu ile yakından ilgili olduğu düşünülmektedir. Dolayısıyla bölgemiz, özellikle de Doğu Karadeniz bölgesi orman gülleri için ideal iklim koşullarına sahip olduğundan bölge üreticisi diğer bölge üreticilerine göre daha avantajlıdır. Ülkemizde özellikle süs bitkileri konusunda ıslah çalışmaları son derece yetersizdir. Son yıllarda doğal türlerle ivme kazanan ıslah çalışmalarına orman güllerinin de dahil edilmesi önemlidir.

Katkı Oranı Beyanı

Yazar(lar)ın katkı yüzdesi aşağıda verilmiştir. Tüm yazarlar makaleyi incelemiş ve onaylamıştır.

	B.A.	H.Ç.
K	100	
T	50	50
Y	50	50
VTI	100	
VAY	50	50
KT	100	
YZ	100	
KI		100
GR	50	50
PY	50	50
FA	100	

K= kavram, T= tasarım, Y= yönetim, VTI= veri toplama ve/veya

işleme, VAY= veri analizi ve/veya yorumlama, KT= kaynak tarama, YZ= Yazım, KI= kritik inceleme, GR= gönderim ve revizyon, PY= proje yönetimi, FA= fon alımı.

Çatışma Beyanı

Yazarlar bu çalışmada hiçbir çıkar ilişkisi olmadığını beyan etmektedirler.

Etik Onay Beyanı

Bu araştırmada hayvanlar ve insanlar üzerinde herhangi bir çalışma yapılmadığı için etik kurul onayı alınmamıştır.

Destek ve Teşekkür Beyanı

Bu makale Bahadır ALTUN'un Doktora Tezinden üretilmiştir. Doktora Tez çalışmasından üretilen bu araştırma TAGEM SBT I-ALTP 3 KRDZ kod numarası ile TAGEM tarafından desteklenmiştir. Verdiği destekten dolayı bu kuruma teşekkür ederim. Ayrıca bu araştırmamın sağlıklı bir şekilde yürüebilmesi için vermiş oldukları desteklerden dolayı T.C. Orman ve Su İşleri Bakanlığı il ve ilçe teşkilatı çalışanlarına da teşekkür ederim.

Kaynaklar

- Ağaoğlu S, Çelik H, Çelik M, Fidan Y, Gülsen Y, Günay A, Halloran N, Köksal D, Yanmaz R. 2001. Genel bahçe bitkileri, 2. Baskı. Ankara Üniversitesi Ziraat Fakültesi Eğitim, Araştırma ve Gelistirme Vakfı Yayınları, Ankara, Türkiye, pp: 369.
- Aleksandrova MS, Zarubenko AU. 1991. Rhododendron propagation by cuttings with the use of growth regulators. Byullet Glavnogo Botanicheskogo Sada, 159: 37-42.
- Almeida R, Gonçalves S, Romano A. 2003. Micropropagation of Iberian rose bay. Contribution to the conservation and reproduction of an endemic plant of Monchique mountain. Revista de Biologia, 21: 29-42.
- Altun B. 2011. Türkiye orman güllerinin toplanması ve kültüre alınması. Doktora Tezi, Ondokuz Mayıs Üniversitesi Fen Bilimleri Enstitüsü, Bahçe Bitkileri Bölümü, Samsun, Türkiye, pp: 247.
- Altun B. 2021. Orman gülü. Ed: Kazaz S, Yalçın Mendi Y, Süs Bitkileri Islahı (Türler), Gece Kitaplığı Yayınları, Ankara, Türkiye, pp: 415-442.
- Altun B. 2023. Effects of seasons and indole-3-butyric acid doses on the propagation of some native rhododendron species by air layering technique in their natural habitats. BioResources, 18(3): 5209-5221.
- Cullen J. 2005. Hardy Rhododendron species a guide to identification. Timber Press, New York, US, pp: 496.
- Czekalski M. 1996. Rhododendrons propagated from leaf cuttings. American Rhododendron Soc J, 50(3): 144-145.
- Czekalski M. 1998. Rhododendrons in the former Soviet Union Caucasian species. American Rhododendron Soc, 52(2): 81-89.
- e-Floras. 2024. Rhododendron. URL: http://www.efloras.org/browse.aspx?flora_id=0 &name_str=Rhododendron&btn_Search=Search. (erişim tarihi: 31 Ocak 2024).
- Ferriani AP, Bortolini MF, Zuffellato-Ribas KC, Koehler HS. 2006. Vegetative propagation of azaléia tree (Rhododendron thomsonii Hook. f.) from cuttings. Semina: Ciências Agrárias, 27(1): 35-42.
- Francon L, Corona C, Roussel E, Saez JL, Stoffel M. 2017. Warm

- summers and moderate winter precipitation boost *Rhododendron ferrugineum* L. growth in the Taillefer massif (French Alps). *Sci Tot Environ*, 586: 1020-1031.
- Hay F, Klin J, Probert R. 2006. Can a post-harvest ripening treatment extend the longevity of *Rhododendron* L. seeds? *Scientia Horticult*, 111: 80-83.
- Hieke K. 1979. Evaluation of frost resistance and capacity for propagation by cuttings in the Pruhonice collection of evergreen large-flowered rhododendron. *Casopis Slezskeho Muzea*, 28(1): 31-72.
- Hwang SK, Hwang HJ, Kim KS. 1998. Effect of cutting dates and rooting promoters on rooting of *Rhododendron mucronulatum* Turcz. *Korean J Horticult Sci Technol*, 16(1): 33-36.
- Kondratovics U, Megre D. 2000. Anatomical peculiarities of adventitious root formation of rhododendron cuttings during rooting. *Rhododendron Immergrüne Laubgehölze Jahrbuch*, 2000: 72-85.
- Krzymin'ska A, Czekalski M. 1998. Double utilization of medium for rooting rhododendron cuttings. *Roczniki Akademii Rolniczej w Poznaniu Ogrodnictwo*, 27: 171-176.
- Li S, Sun W Ma. 2018. Does the giant tree *Rhododendron* need conservation priority? *Global Ecol Conservat*, 15: e00421.
- Lonca C, Zaharia D, Bele C. 2004. Experimental results concerning the effect of the substrates and rhysogen substances by using cuttings in azalea. *Seria Horticult*, 61: 71-75.
- Matysiak, B., Nowak, J. 2008. Coir substrates for rooting of ornamental ericaceous plants. *Propagation of Ornamental Plants*. 8(2):76-80.
- Pignatti, G., Cason, M., Ducci, F., 2004. Vegetative propagation through cuttings of alpine shrubs for bio-engineering. *Sherwood - Foreste ed Alberi Oggi*. 10(6):11-16.
- Rai U, Lama D, Thapa N, Rai S. 2013. Diversity of *Rhododendron linnaeus* (Ericaceae) in Singalila National Park located in the Darjeeling part of the Himalaya. *Pleione*, 7(2): 424-440.
- Remotti D. 2003. Evaluation of the rooting capacity of nineteenth century rhododendrons. *Info Agrario*, 59(1): 51-53.
- Shen SK, Wu FQ, Yang GS, Wang YH, Sun WB. 2015. Seed germination and seedling emergence in the extremely endangered species *Rhododendron protistum* var. *giganteum*—the world's largest *Rhododendron*. *Flora*, 216: 65-70.
- Strzelecka K. 2007. Anatomical structure and adventitious root formation in *Rhododendron ponticum* L. cuttings. *Acta Sci Polonorum - Hortorum Cultus*, 6(2): 15-22.
- Weia X, Chenb J, Zhangc C, Wang Z. 2018. In vitro shoot culture of *Rhododendron fortunei*: An important plant for bioactive phytochemicals. *Indust Crops Products*, 126: 459-465.
- Ylatalo M. 1979. Factors affecting the rooting of rhododendron cuttings. *J Sci Agri Soc Finland*, 51(3): 163-171.
- Zaharia D, Dumitras A, Cantor M, Zaharia A. 2002. Studies on improving vegetative multiplication by using cuttings in *Azalea indica*. *Seria Horticultura*, 57: 262-265.



A NEW SPECTROPHOTOMETRIC METHOD FOR DETERMINATION OF CARVEDILOL FROM TABLET

Figen EREK^{1*}, Işıl AYDIN²

¹Dicle University, Faculty of Science, Department of Chemistry, Diyarbakır, 21280, Türkiye


²Dicle University, Faculty of Pharmacy, Department of Analytical Chemistry, Diyarbakır, 21280, Türkiye


Abstract: In this study, a new spectrophotometric method was developed for the quantitative analysis of Carvedilol and the method was validated. The method depends on the reaction between the carvedilol and 1,2,5,8-tetrahydroxyanthraquinone in methanol to yield colored charge transfer complex giving maximum absorbance at 560 nm. For optimization of the proposed method, several parameters were investigated such as solvent type, reaction time, and quinalizarin concentration. The stoichiometry of colored charge transfer complex was found to be 2:1 (reagent: drug) by Job's method. Beer's Law is obeyed in the concentration range of 0.5-60 µg/mL with 0.9986 correlation efficient. Limit of detection (LOD) and limit of quantification (LOQ) were found 0.147 µg/mL, 0.491 µg/mL, respectively. The proposed method can be successfully applied pharmaceutical formulation.

Keywords: Charge transfer complex, Job's method, Molecular absorption spectroscopy

*Corresponding author: Dicle University, Faculty of Science, Department of Chemistry, Diyarbakır, 21280, Türkiye

E mail: figen.erek@dicle.edu.tr (F. EREK)

Figen EREK  <https://orcid.org/0000-0002-2861-5504>

Işıl AYDIN  <https://orcid.org/0000-0001-6571-6032>

Received: February 13, 2024

Accepted: March 05, 2024

Published: March 15, 2024

Cite as: Erek F, Aydın I. 2024. A new spectrophotometric method for determination of carvedilol from tablet. *BSJ Eng Sci*, 7(2): 359-364.

1. Introduction

Beta-blockers, which reduce the activity of sympathetic nerves by blocking beta-adrenergic receptors, are in the cardiovascular drug class (Mutlu, 2010; Vale et al., 2019). β -blockers are divided into three groups as first generation non-selective group, second generation β_1 -selective group, third generation β_1 -high selective and vasodilator group (Mutlu, 2010).

Carvedilol (CRV), [(6)-1-(carbazole-4-yloxy)-3-((2-(o-methoxyphenoxy)ethyl)amino)-2-propanol], is a third-generation β -blocker agent having nonselective β_1 -adrenoreceptor blockade, vasodilation, antioxidant properties (Streim et al., 1987; Brian and William, 2004). CRV is a white powder, whose solubility is very good in dimethylsulfoxide; soluble in methylene chloride and methanol; slightly soluble in ethanol and isopropanol; insoluble in water. Its melting point is in the range of 114-115 °C (Moffat et al., 2004).

Several methods have been developed for analysis of carvedilol in the literature, such as chromatographic (Junwei et al., 2015), spectrophotometric (Verma and Syed, 2007, Rani et al., 2013), electroanalytic (Soleymanpour and Ghasemian, 2015) detections.

Spectrophotometric methods are, especially UV-Visible spectrophotometry, often preferred techniques due to its low cost and simplicity in the determination analysis of pharmaceutical preparations (Ragaa et al., 2013; Kirtimaya et al., 2016). Charge transfer reactions have been commonly studied by UV-Visible spectrophotometric

methods. The charge transfer complexes are formed by the molecular interaction of electron donors and acceptors. These colored complexes should absorb at a different wavelength from the donor and acceptor molecules at the UV-visible region (Ragaa et al. 2013). In this study, a new, simple, rapid, validated spectrophotometric method that does not interfere with the excipients has been developed for the determination of carvedilol (CRV) in pharmaceutical formulation. Direct analyzes of Carvedilol with UV-vis spectrophotometer cannot be performed because excipients interfere with pharmaceutical formulations. In this method, direct analysis was performed by extracting carvedilol from pharmaceutical tablet without applying any purification process. The method depends on the reaction between the CRV (π -acceptor group) and 1,2,5,8-tetrahydroxyanthraquinone (π -donor group) in the methanol to yield colored charge transfer complex that is measured at 560 nm. This colored complex made possible the quantitative determination of CRV, spectrophotometrically.

2. Materials and Methods

2.1. Apparatus and Reagents

The UV-VIS spectral measurements were made by using T80+ UV/VIS Spectrometer (PG Instruments Ltd), Varian Cary 100 Bio UV/VIS double beam UV-VIS spectrophotometers equipped with 1 cm matched quartz cells. All solvents (methanol, ethanol, 1-propanol, 2-



propanol, chloroform, N,N-dimethylformamide (DMF), acetone and acetonitrile) used in this work were of HPLC grade and Merck branded. CRV, which is certified to be 99.5% pure, was obtained from Bilim Drug Company, Istanbul, Türkiye. Coronis tablet (Bilim Drug Company) labeled to contain 25 mg CRV per tablet used in the proposed method on was received from in the local pharmacy. Quinalizarin, (1,2,5,8-tetrahydroxy-anthraquinone), was purchased from Sigma Aldrich company. Sucrose, Povidone K25, Magnesium stearate, Lactose monohydrate were purchased from Glentham Life Sciences Company.

The stock solutions 500 µg/mL of CRV and 3.10⁻³ mol/L of Quin were prepared with methanol in 50 mL flasks, daily.

2.2. Construction of Calibration Curves

The aliquots in the range of 0.01-1.2 mL CRV (500 µg/mL) solution were transferred to volumetric flasks (at 27 °C) to obtain concentrations in the range 0.5-60 µg/mL of CRV. Following this, 1.25 mL of 3.0 mmol/L Quin solution was added to these solutions and completed to 10 mL with methanol. These final mixtures were thoroughly mixed. Three replications were made for each solution. The absorbance of the prepared solutions was measured at 560 nm against Quin blanks. Finally, the measured absorbances versus the concentration of CRV were plotted.

2.3. Assay Procedure for Tablets

The average weight of a tablet containing 25 mg of CRV was calculated by weighing ten randomly tablets. The weighed ten tablets, then, were finely powdered in a dry and clean agate mortar. Afterwards, an accurately weighed quantity of the powder equivalent to 25 mg of CRV were transferred into the volumetric flask and dissolved in 25 mL methanol. The final mixture was both shaken and sonicated for 30 min, and then filtered by using quantitative filter paper. The volume of filtered solution was completed to the mark with methanol to prepare a stock solution of 250 µg/mL. Then, some working concentrations were prepared from the filtered solution. The proposed method was applied to the prepared solutions. The amount of CRV in the tablet was calculated according to the calibration curve.

3. Results and Discussion

3.1. The Effect of the Solvent Type

In the method based on the formation of colored charge

transfer complex, the optimum solvent is to facilitate the charge transfer (Gouda and Kassem, 2012; Mohammed et al., 2018). Therefore the effects of solvents such as Methanol, DMF, Ethanol, Acetonitrile, Chloroform, 1-propanol, 2 -propanol and Acetone, on the charge transfer reaction were investigated.

As seen in Table 1, Methanol, which gave the highest absorbance of the complex, was accepted as the optimum solvent. The charge transfer reaction is thought to proceed through the radical anion. It is thought that the capacity of methanol to form stable hydrogen bonds with the radical anion is higher than that of acetonitrile (Gouda and Kassem, 2012). While Quin gives maximum absorbance at 491 nm in methanol, CRV-Quin complex gives maximum absorbance at 560 nm. The fact that Quin and CRV-Quin charge transfer complex absorb at different wavelengths in the UV-visible region showed that CRV can be determined easily and precisely with Quin (Gouda and Kassem, 2012).

Table 1. The effect of solvents type

Solvents	Absorbance	±SD
Methanol	0.501	0.014
DMF	0.264	0.015
1-propanol	0.142	0.023
Acetonitrile	0.130	0.034
Ethanol	0.123	0.028
2-propanol	0.112	0.016
Acetone	0.061	0.004
Chloroform	0.041	0.002

SD= standard deviation

3.2. The Effect of the Reagent Concentration

The transformation of a very large part of the analyte in solution into the colored complex in a short time, that is, the rapid transfer of charge to equilibrium and achieving the maximum sensitivity of the complex also depends on the concentration of the reagent (Gouda and Kassem, 2012; Mohammed et al., 2018). To determine optimum concentration of reagent, 0.25-2.25 mL of 3.10⁻³ mol/L Quin was added into the CRV solutions. The solution was stirred for 2 min to complete the reaction. At the end of the study, the optimum volume of 3.10⁻³ mol/L Quin solution was found to be 1.25 mL. After this point, it was observed that the absorbance did not change much and reached the maximum density. The related results are shown in Figure 3.

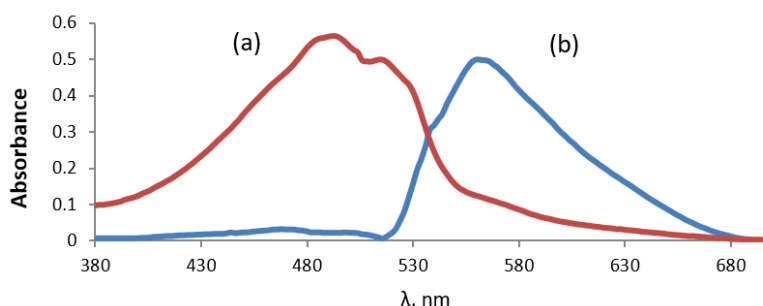


Figure 2. Spectra of Quin (a) and Quin-CRV complex (b) in methanol.

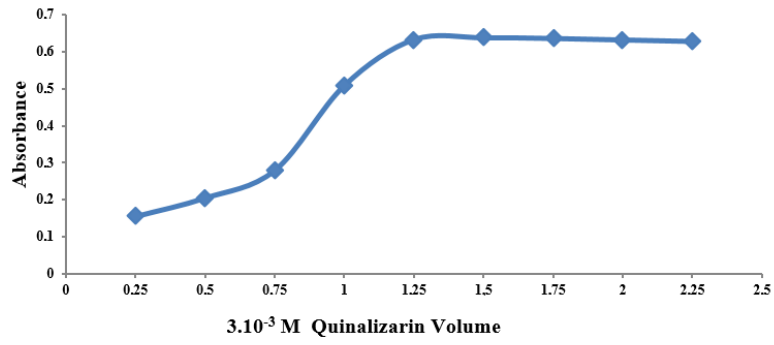


Figure 3. Effect of the quinalizarin concentration.

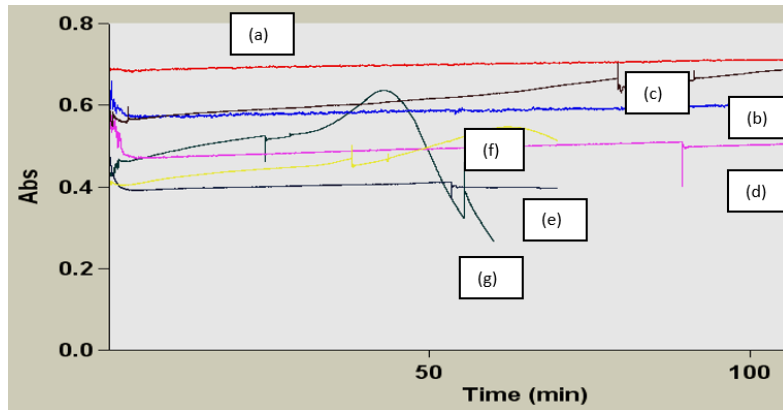


Figure 4. The reaction time and temperature CRV-Quin charge transfer complex (27 °C: (a), 35 °C: (b), 40 °C: (c), 45 °C: (d), 50 °C: (e), 55 °C: (f), 60 °C: (g)).

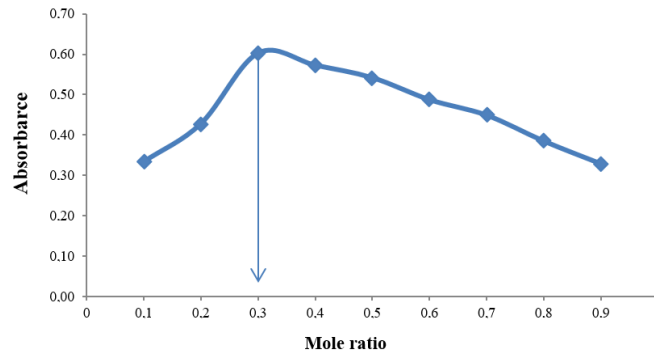


Figure 5. Job's method to the reaction between Quin and CRV ($\lambda = 560$ nm).

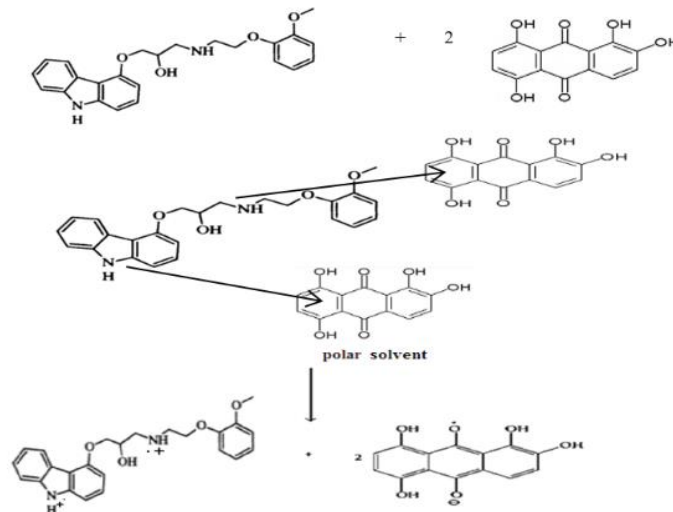


Figure 6. Possible mechanism of radical anion formation from Quin and CRV reaction.

3.3. The Effect of the Reaction Time and Temperature

It was observed that the absorbance of the colored complex was both the most stable and the maximum at 27±2 °C (laboratory temperature). For this reason, it was decided that the optimum temperature was 27±2 °C. The absorbance of the charge transfer complex remained unchanged from the beginning for 120 min at 27 °C. Therefore, the optimum reaction time was kept shorter than 1 min at 27 °C. The absorbance of the complex was immediately measured. As the temperature increased, the stability of the complex deteriorated (Figure 4).

3.4. Characterization of CRV-Quin Charge Transfer Complex

Job's continuous variation method (Kelani et al., 1997) was used to determine the stoichiometry of the charge transfer complex in methanol medium. As seen in Figure 5, it has been determined that CRV and Quin react at a rate of 1-2. The proposed mechanism for this reaction is shown in Figure 6. It was thought that the charge transfer complex (n-π) was formed by transferring the loads in the -NH and -OH groups of the drug to the center with load deficiency in Quin. According to the literature, the mechanism related to n-π type interaction has also been proposed (Gouda et al., 2012).

3.5 Validation

3.5.1. Analytical performance of developed method

Firstly, the linear working range was found that this range is 0.5-60 µg /mL. The equation of the calibration curve is $y = 0.0169x + 0.0778$ with 0.9981 correlation coefficient (y=Absorbance of complex, x=Concentration of CRV (µg/mL)). In this method, LOD and LOQ at 95 % confidence level were found to be 0.147 µg/mL, 0.491 µg/mL, respectively. LOQ and LOD were calculated according to the Equation 1:

$$LOD=3s/b, LOQ=10s/b \tag{1}$$

where *s*: standard deviation of absorbances of blank solution *b*: the slope of the calibration curve (URL1).

All parameters related to calibration are given in Table 2.

Accuracy: In the recovery study with pure CRV, values were obtained between 98.8 and 100.8% (Table 3). In the standard method of addition, recovery was obtained in the range of 98.4 to 99.4% (Table 4). In these two methods, RE % was lower than 1.6% and RSD % was lower than 1.5%. The high and good accuracy of the method depends on the low RSD % and RE %. RE % and RSD % were found to be low in the proposed method. At 95% confidence level and 4 degrees of freedom, the experimental *t* was calculated as 1.97 and the recovery was found to be 100.7%. The theoretical *t* value is taken

as 2.77. The experimental *t* value being less than the theoretical *t* value indicates that there is no systematic error in the method and it is applicable for the determination of CRV in tablets (URL1).

Precision: In the precision study, the solutions prepared at any concentration within the working range were analyzed at 3 different times within the same day (in 1 day) and on 3 different days, and the results were evaluated (Table 6). When the proposed method is applied to the solutions of CRV prepared in two different concentrations during the intraday and inter days, it is seen that the difference between absorbances is not much. RSD % is lower than 2% (URL1).

Stability: In the stability study, after applying the proposed method to 15 µg/ mL, 45 µg/mL solutions, and absorbance measurements of each solution were taken at 24 h intervals for 72 h. The low change in absorbance of the solutions for 72 h indicates that the complex is very stable (URL1).

Specificity: The effects of the excipients such as Lactosemonohydrate, Sucrose, Povidone K25, Magnesium stearate (Mg-St.) on the absorbance were investigated by applying proposed method to solution 45 µg/mL of CRV (Table 7) (Korkmaz et al., 2005). In this method, it has been observed that these excipients do not have a significant effect on absorbance.

Robutness: Small changes were made in the optimization parameters in the robustness study of the proposed method (URL1, Altunay et al., 2023). In the study, changes of ±0.05 mL in Quin volume and ±2°C in temperature were examined. In both parameters, recoveries were obtained in the range of 99.00-100.22 %. RSD % was lower than 1% and RE % was less than 1.05 % (Table 8). It was observed that the method was not affected by small changes in optimization parameters.

Table 2. Optimum conditions and analytical parameters

Parameters	Values
λ_{maks}	560
Linearity dynamic range (µg/mL)	0.5-60
Correlation coefficient (r ²)	0.9981
Regression equation	$y=0.0169x+0.0778$
Slope	0.0169
Interception	0.0778
LOD (µg/mL)	0.147
LOQ (µg/mL)	0.491
Molar Absorptivity (L.mol ⁻¹ .cm ⁻¹)	2737

Table 3. Recovery of CRV in proposed method

Taken (µg/mL)	Found Conc. (µg/mL)	Recovery%	SD	RSD%	RE%
15	14.82	98.83	0.07	0.46	1.17
30	29.79	99.32	0.4	1.35	0.68
45	44.57	99.04	0.43	0.96	0.96
60	59.87	99.79	0.84	0.84	0.21

Table 4. the standard addition technique for the determination of the CRV in pharmaceutical preparation

Taken	Added (µg/mL)	Recovery%	SD	RSD%	RE%
20µg/mL	8	98.6	0.19	0.69	1.41
	12	99.4	0.33	1.02	0.57
	16	99.1	0.39	1.11	0.93
	20	98.4	0.53	1.34	1.57
	24	99.0	0.39	0.89	0.97

Table 5. t-test for pharmaceutical preparation of CRV

Commercial Brand	Found Calculated ±SD	Recovery%	t test
Coronis (25 mg CRV)	25.17 ± 0.19	100.68	1.97

Table 6. Intra-day and inter-day precision of proposed method (Taken Concentration: 45 µg/mL and 15 µg/mL)

Found Conc. (µg/mL)	Intra-day		Found Conc. (µg/mL)	Inter-day	
	44.79	15.00		44.57	14.96
±SD	0.06	0.12	±SD	0.18	0.21
RSD%	0.14	0.83	RSD%	0.41	1.40

Table 7. Effect of interfer substances in proposed method

$\hat{I}_1:\hat{I}_2$ (µg/mL)	LMH Recovery%	Sucrose Recovery%	Povidon K25 Recovery%	Mg-St Recovery%
0:45	100	100	100	100
45:45	98.6	99.8	100.1	95.2
450:45	98.8	100	100.2	103.0
4500:45	100.6	99.8	96.6	103.2

\hat{I}_1 : interfere s. conc., \hat{I}_2 : CRV Conc.

Table 8. The effect of small change in Quin volume and reaction temperature on absorbance

		Recovery%	SD	RSD%	RE%
Quin Volume (mL)	1.25 + 0.05	99.00	0.36	0.80	1.05
	1.25 – 0.05	100.22	0.21	0.47	0.22
Temperature (°C)	27 + 2	99.04	0.37	0.83	0.96
	27 – 2	99.22	0.15	0.33	0.78

4. Conclusion

In this study, spectrophotometric method based on charge transfer reaction between CRV and Quin was developed for determination of CRV from tablet formulation. The analytical procedure of this study was applied by optimizing several parameters such as solvent type, reagent concentration, reaction temperature and time, stoichiometric ratio. Then the method was validated. The stoichiometry of colored charge transfer complex was found to be 2:1(reagent:drug) by Job's method. Beer's Law is obeyed in the concentration range of 0.5-60 mg/L with 0.9986 correlation efficient. LOD and LOQ were found 0.147 mg/L, 0.491 mg/L, respectively. The proposed method has some advantages such as being very simple and accurate, robust, without interference and economic. In addition, it does not require extra processes such as purification, heating, a buffer.

Author Contributions

The percentage of the author(s) contributions is presented below. All authors reviewed and approved the final version of the manuscript.

	F.E.	I.A.
C	90	10
D	100	
S	100	
DCP	90	10
DAI	80	20
L	90	10
W	70	30
CR	50	50
SR	100	
PM		100
FA		100

C=Concept, D= design, S= supervision, DCP= data collection and/or processing, DAI= data analysis and/or interpretation, L= literature search, W= writing, CR= critical review, SR= submission and revision, PM= project management, FA= funding acquisition.

Conflict of Interest

The authors declared that there is no conflict of interest.

Ethical Consideration

Ethics committee approval was not required for this study because of there was no study on animals or humans.

Acknowledgements

We would like to thank to Dicle University for supporting the subject scientific study (Project number: ECZ: 19.001).

References

Altunay N, Haq HU, Castro-Muñoz R. 2023. Optimization of vortex-assisted hydrophobic magnetic deep eutectic solvent-based dispersive liquid phase microextraction for quantification of niclosamide in real samples. *Food Chem*, 426: 136646.

Briann D, William TA. 2004. Pharmacology of carvedilol. *Am J Cardiol*, 93: 3B-6B.

Gouda AA, Kasssem M. 2012. Novel spectrophotometric methods for determination of desloratidine in pharmaceutical formulations based on charge transfer reaction. *Arabian J Chem*, 9: 1712-1720. <https://doi.org/10.1016/j.arabjc.2012.04.050>.

Junwei L, Wang L, Wang S, Chen M, Hu EG, Ge R. 2015. Simultaneous quantification of carvedilol and its metabolites in rat plasma by ultra-performance liquid chromatography tandem mass spectrometry and pharmacokinetic application. *J Chromatogr B*, 974: 138-146. <https://doi.org/10.1016/j.jchromb.2014.10.037>.

Kelani K, Bebawy LI, Abdel-Fattah L, Ahamad AS. 1997. Spectrophotometric determination of some n-donating drugs using DDQ. *Anal. Letters*, 10(30): 1843-1860.

Kirtimaya M, Kumar BK, Kumari MM, Subrahmanyam BSS. 2016. New analytical method development and validation of chlorpheniramine maleate by using UV-visible spectrophotometry. *Indo American J Pharmaceut Sci*, 7: 767-

772.

Korkmaz D, Demir C, Aydın F, Ataman OY. 2005. Cold vapour generation and on-line trapping of cadmium species on quartz surface prior to detection by atomic absorption spectrometry. *J Anal At Spectrom*, 20: 46-52.

Moffat AC, Osselton MD, Widdop B. 2004. Clarke's analysis of drugs and poisons. Pharmaceutical Press, London, UK, pp: 2736.

Mohamed EM, Frag YZ, Hathoot AA, Shalaby EA. 2018. Molecular and biomolecular spectroscopy. *Spectrochimica Acta Part A*: 189: 357-365. <https://doi.org/10.1016/j.saa.2017.08.027>.

Mutlu B. 2010. Vasodilator Beta blockers in cardiovascular disease. *Trakya Univ J Medic Fac*, 27: 26-30.

Ragaa El-S, Ayman AG, El-Azzazy R. 2013. Spectrophotometric Study on the charge transfer complex between sumatriptan succinate and some Π -acceptors and alizarin derivatives. *Chem Indust Chem Eng Quart*, 4: 529-540. <https://doi.org/10.2298/CICEQ1205133087E.96>.

Rani YN, Ravi BV, Kumar V, Smitapadma M. 2013. Development and validation of new analytical methods for the estimation of carvedilol in bulk and pharmaceutical dosage. *Asian J Pharmaceut Clin Res*, 6: 2.

Soleymanpour A, Ghasemian M. 2015. Chemically modified carbon paste sensor for the potentiometric determination of carvedilol in pharmaceutical and biological media. *Measurement*, 59: 14-20. <https://doi.org/10.1016/j.measurement.2014.09.046>.

Streim K, Spomer, G, MullerBeckmann, B, Bartsch, WJ. 1987. *Cardiovasc. Pharmacol*, 10: 33.

URL1: <https://database.ich.org/> (accessed date: November 12, 2023).

Vale GT, Ceron CS, Gonzaga NA, Simplicio JA, Padovan JC. 2019. Three Generations of β -blockers: History, class differences and clinical applicability. *Curr Hypertens Rev*, 15: 22. <https://doi.org/10.2174/1573402114666180918102735>.

Verma JK, Syed HA. 2007. Extractive spectrophotometric method for determination of carvedilol in tablets. *Indian J Pharm Sci*, 2: 303-304. <https://doi.org/10.4103/0250-474X.33166>.



THE EFFECTS OF DIFFERENT NITROGENOUS FERTILIZER SOURCES AND DOSES ON FOOTBALL FIELD GRASS PERFORMANCES

Merve MARANGOZ^{1*}, İbrahim HOSAFLIOĞLU¹


¹Iğdır University, Faculty of Agriculture, Department of Crop Science, 76000, Iğdır, Türkiye


Abstract: Nitrogen has a huge importance in terms of ensuring the development of roots and shoots in grass and giving plants resistance to diseases. Using the right fertilizer in appropriate doses in the maintenance and repair of football fields is one of the maintenance procedures that increase grass performance. This study was carried out on the football field grass established at Iğdır University Sehit Bulent Yurtseven Campus during the 2020 vegetation period in Iğdır conditions. The research aimed to determine the most suitable fertilizer type and dose for football fields. The experiment was designed with three replications according to the randomized blocks factorial trial design. In the application area, a grass mixture of *Festuca arundinacea* Jaguar 4G 30%, *Festuca arundinacea* Apache 20%, *Festuca arundinacea* Arid III 20%, *Lolium perenne* Belida 15% and *Lolium perenne* Esquire 15% was used. As nitrogenous fertilizer sources, 20-10-10 7S03, 15-5-20 + 2 CaO + MgO, ammonium sulfate (21% N) and urea (46% N) fertilizers are 0, 2, 4, 6 and 8 g/m²/ It was administered in monthly doses. In the study, the effects of nitrogen use in fertilization on grass plant height, quality, fresh grass amount, and leaf green tone and leaf texture were observed. As a result of the study, it was determined that the most ideal fertilizer type and dose were 6 and 8 g m⁻² doses of urea and ammonium sulfate fertilizers.

Keywords: Nitrogen fertilizer type, Grass plants, Grass quality, Football field, Fertilizer dose

*Corresponding author: Iğdır University, Faculty of Agriculture, Department of Crop Science, 76000, Iğdır, Türkiye

E mail: biomerve@gmail.com (M. MARANGOZ)

Merve MARANGOZ  <https://orcid.org/0009-0009-0143-1420>

İbrahim HOSAFLIOĞLU  <https://orcid.org/0000-0002-0455-0515>

Received: February 20, 2024

Accepted: March 10, 2024

Published: March 15, 2024

Cite as: Marangoz M, Hosaflioglu I. 2024. The effects of different nitrogenous fertilizer sources and doses on football field grass performances. BSJ Eng Sci, 7(2): 365-373.

1. Introduction

When grass fields are mentioned, football fields come to mind first. It is important to create a grass cover on football fields that allows the ball to move and prevents football players from getting injured by falling. Just as the types and mixtures of grass used in the football field facility are important, it is necessary to apply the correct fertilizers and doses to ensure continuity, in addition to periodic ventilation and irrigation. The lawns on sports fields require meticulous maintenance. When maintenance is disrupted, sports fields may lose their appearance in a short time and become unplayable (Orçun, 1979).

Nitrogen fertilization in lawns is very important. The formation of abundant green leaves on lawns is desirable due to forming intense cover. Therefore, the presence of nitrogen is important for vegetative green leaf development, and it is needed more than other nutritional elements (Orçun, 1979). Nitrogen has a positive effect on development by accelerating development and increasing the growth rate, especially in wheat crops (Kaçar, 1977). The selection of a durable and successful grass mixture for football fields is directly proportional to the strengths and weaknesses of the species and their ability to adapt to the environment. In

the study we conducted in Iğdır province, which shows a 'microclimate' feature in terms of climate, the selected plants are cool climate grass species. The grasses were selected from among the species that are resistant to stepping on, can grow quickly and are durable. *Festuca arundinacea* (reedy ball) has a deep root structure and is highly resistant to heat and drought, in addition to developing in the form of a ball and forming a frequent grass surface. *Lolium perenne* L. (*perennial English grass*), on the other hand, is a fast-growing species and is a species that is highly resistant to running over and wearing off (Anonymous, 2020a). In the study, the effect of different fertilizer forms used in different seasons on the grass quality criteria in a grass area established with a dual grass mixture under Iğdır conditions was examined.

2. Materials and Methods

2.1. Trial Area

The research was established at the Sehit Bulent Yurtseven Campus of Iğdır University in 16 May 2020 with three repetitions according to the factorial trial pattern in the coincidence blocks.



2.2. Climate Characteristics

The monthly average temperature (0 °C), monthly average relative humidity (%) and monthly total precipitation (mm: kg m⁻²) values for the period in which the experiment was conducted are given in Table 1 (Anonymous, 2020b). According to Table 1, the average total rainfall in Iğdır for many years during the period when the research was conducted was 168.7 mm, and in the year when the experiment was conducted, it was 153.3 mm, and 15.4 mm less precipitation was observed in 2020 compared to many years. According to the precipitation and temperature averages for many years, the average temperature in Iğdır during the research period was 19.4 °C, the average temperature during the research period of 2020, when the research was conducted, was 19.8 °C, and the temperature values are similar. While the average relative humidity was 53% compared to the average for many years, it reached 53.3% in 2020.

2.3. Soil Properties

Before October, by being taken a soil sample from a depth of 0-30 cm, physical and chemical analysis was performed, and the results are given in Table 2 (Anonymous, 2020c). When the soil sample taken from the trial area was examined, it was found that the soil had a medium lime content (10.57), slightly alkaline pH (8.38), good potassium level (73.27), phosphorus rich (13.76), medium organic matter levels (2.04%), unsalted total salt content (0.01%) and clay loam structure.

2.4. The Types of the Plants Used the Types and Doses of Fertilizers

In the study, *Festuca arundinacea* Jaguar 4 G 30%, *Festuca arundinacea* Apache 20%, *Festuca arundinacea* Arid III 20%, *Lolium perenne* Belida 15%, *Lolium perenne* Esquire 15% grass mixture was preferred. In the research, four different commercial fertilizers [20-10-10 + 7 SO₃; 15-5-20 + 2CaO + 2 MgO; Ammonium Sulfate (21% N) and Urea (46% N)] were applied as nitrogen fertilizer sources. Five different fertilizer doses (0, 2, 4, 6 and 8 g/m²/month) were used, one of which was a control.

2.5. Planting and Maintenance Operations

While the test area was being prepared at the Sehit Bulent Yurtseven Campus of Iğdır University, the existing foreign materials were firstly removed from the area, and fine leveling was carried out with the help of a rake after rough leveling of the area was carried out with agricultural machines. The parcel area was determined as 2 m x 1 m = 2 m² (Misia, 1991; Hunt and Dunn, 1993). The distance between the parcels is 0.5 m. Purity and germination rates were determined in the laboratory before planting, and the planting rates of grass species were determined (Oral and Açıköz, 1999). 8 g/m² of pure phosphorus (46% TSP) was given together with the planting process in order to develop the grass roots ideally. 80 g of grass seed mixture was planted by hand to each parcel. After the planting, cover soil (peat) was laid on the seed with a thickness of 1 cm and pressed with a cylinder. The irrigation process was carried out regularly every day in the morning and evening both during the germination and development and structuring stages depending on the varying weather conditions. The weeds in the parcels were removed by hand procedure and the grass was allowed to develop and cover the area. All maintenance operations in the area were carried out periodically and cleaning was carried out 3 weeks (21 days) before each measurement process.

2.6. Experimental Measurement and Research Methods

The plant height was measured with the help of a ruler at 10 separate points of each parcel (Mulvah, 1999). To determine the leaf width, 10 different leaves were measured and averaged with the help of a caliper in each parcel. A scale of 1-9 (1 yellow, 9 dark emerald green) was used to determine the green leaf color tones (Spanberk et al, 1986). The grass quality was determined according to the 1-9 scale (1 is the worst, 9 is the best grass quality) (Sills and Carrow, 1983; Mehall et al, 1983). The amount of wet grass was expressed as gram/m², which was weighed using sensitive measuring instruments.

Table 1. Iğdır province climate data

Months	Total monthly precipitation (mm)		Average temperature (°C)		Average relative humidity (%)	
	2020	Many years	2020	Many years	2020	Many years
May	76.1	50.7	18.6	18.0	55.0	52.8
June	15.7	34.0	23.9	22.9	44.7	47.0
July	30.2	14.9	26.7	26.3	48.4	44.3
August	15.3	9.9	24.2	26.3	47.6	45.7
September	1.4	10.1	23.5	21.3	47.7	50.2
October	7.3	28.7	14.5	14.7	62.9	63.9
November	7.3	20.4	7.2	6.0	67.0	67.4
Average	153.3	168.7	19.8	19.4	53.3	53.0

Table 2. The results of the analysis of the test soil

Depth	Lime Ratio (%)	pH	(K) (kg/da)	(P) (kg/da)	Organic Matter (%)	Total Salt (%)	Soil Structure
0-30 cm	10.57	8.38	73.27	13.76	2.04	0.01	Clay loam

Statistical Analysis

The statistical analysis of the experiment was performed using the statistical package program JMP 5.0.1. According to the results of the variance analysis, the differences between the averages of the statistically significant characteristics were compared with the LSD multiple comparison test (Steel and Torrie Dec, 1980).

3. Results and Discussion

The results of the variance analysis of the averages obtained in the research are given in Table 3. As it can be seen in Table 3, the effect of applications on all the studied features was found to be statistically significant.

3.1. Plant Height

When the plant sizes were examined during the summer period, the effects of fertilizer type, fertilizer dose and the interactions of these factors were found to be important at the level of 1%. (Table 3) Plant sizes obtained in different fertilizer types and doses in summer season are given in Table 4. In terms of plant height, 20-10-10 fertilizer was found in the lowest amount with 15.3 cm in the average fertilizer type, and urea fertilizer was found in the highest amount with 21.7 cm. On the other hand, the average fertilizer dose remained the highest with 24.3 cm at an 8 g m² fertilizer dose, and the control fertilizer dose remained the lowest with 10.4 cm. In the fertilizer variety and fertilizer dose interactions, the control fertilizer doses remained in the lowest amounts in the fertilizer varieties, while the urea fertilizer was found to be the highest with an 8 g m² fertilizer dose of 27.3 cm. Our study shows that the plant height values are like the values of Karakurt (2003).

The effects of fertilizer type, fertilizer dose and the interactions of these factors on plant height values were

found to be significant at the level of 1% in the autumn period. (Table 3) Plant sizes obtained from measurements made in the autumn period are given in Table 4. According to Table 5, urea gave the highest plant height values with 24.1 cm in the average fertilizer variety in the autumn period. The 20-10-10 fertilizer remained at the lowest plant height value with 16.6 cm. In the average fertilizer dose, the 8 g m² fertilizer dose reached the highest plant height with 27 cm, while the control fertilizer dose was found to be the lowest with 10.3 cm. In the fertilizer variety and dose interactions, 15-5-20 and urea fertilizers were found to have the lowest values with 9.7 cm, 9.7 cm, respectively, and reached the highest height value with 6 and 8 g m² doses of urea with 31.4 cm and 30.8 cm, respectively. The values of our study coincide with the values of Zengin (2019) and Gökçe (2019).

As our study has been evaluated in terms of plant height, monthly doses of 8 g m² of urea and ammonium sulfate fertilizers in summer and autumn periods has been very effective in the mixtures of *F. arundinacea*, and *L. perenne*. In grass species, plant sizes increased with urea fertilizer, which is used as a nitrogen source in both seasonal conditions and gave the highest values. Especially at a monthly dose of 8 g m² of urea, plant sizes showed quite high values.

The results of the study show that the ammonium sulfate and urea fertilizers used in the experiment dissolving quickly in the soil were quickly taken up by plants and stimulated growth. However, the 20-10-10 and 15-5-20 composite fertilizer varieties with controlled release had a slow effect on the lawn performance values.

Table 3. The results of the variance analysis of the research findings

Source of variation	The amount of age		Plant height		Tint		Grass quality	Leaf width
	F Value		F Value		F Value		F Value	F Value
	Y	S	Y	S	Y	S	Y	S
Type of fertilizer (TF)	76.6**	44.1**	91.0**	225.4**	45.5**	51.5**	3.2*	3.5*
Dosage of Fertilizer (DF)	230.4**	163.1**	223.6**	590.0**	101.5**	109.2**	63.5**	117.0**
TF x DF	7.8**	4.5*	8.7**	21.5**	2.5*	8.2**	NS	2.7*

**P<0.01 is important in probability limits, *P<0.05 is important in probability limits, NS= insignificant, Y= Summer, S= Autumn.

Table 4. Average plant sizes obtained in different fertilizer types and doses in summer season (cm)

Type of fertilizer	Dosage of fertilizer					Average
	0	2	4	6	8	
20-10-10	10.9 ^k	13.3 ^{ij}	14.3 ^{hi}	18.2 ^g	19.7 ^{fg}	15.3 ^d
15-5-20	9.9 ^k	11.6 ^{jk}	15.4 ^h	20.9 ^{ef}	23.5 ^{cd}	16.3 ^c
Ammonium sulfate	10.2 ^k	18.4 ^g	22.6 ^{de}	24.1 ^{cd}	26.5 ^{ab}	20.4 ^b
Urea	10.7 ^k	20.8 ^{ef}	24.3 ^{cd}	25.1 ^{bc}	27.3 ^a	21.7 ^a
Average	10.4 ^e	16.0 ^d	19.2 ^c	22.1 ^b	24.3 ^a	

Table 5. Plant sizes obtained in different types and doses of fertilizers in the autumn season (cm)

Type of fertilizer	Dosage of fertilizer					Average
	0	2	4	6	8	
20-10-10	11.2 ^{jk}	14.7 ⁱ	16.4 ^h	20.7 ^g	23.7 ^{ef}	16.6 ^d
15-5-20	9.7 ^k	12.0 ^j	16.4 ^h	19.8 ^g	25.3 ^{cd}	17.4 ^c
Ammonium sulfate	10.7 ^{jk}	20.3 ^g	24.2 ^{de}	26.0 ^c	28.1 ^b	21.9 ^b
Urea	9.7 ^k	22.3 ^f	26.5 ^c	31.4 ^a	30.8 ^a	24.1 ^a
Average	10.3 ^e	17.3 ^d	20.9 ^c	24.5 ^b	27.0 ^a	

While fertilizers that dissolve quickly in the soil had an immediate effect on the height of the grass, compound fertilizers provided slower growth. For all fertilizer types, as the doses increased, plant heights also increased. Nitrogen positively affected plant height and development in grass (Escapes, 1977).

3.2. Color

When the color shades obtained in the summer season were examined, it was determined that the fertilizer type and fertilizer dose were 1% important, and the interactions of these factors were 5% important (Table 3).

The color performances obtained in different fertilizer types and doses are given in Table 6. According to Table 7, urea and ammonium sulfate fertilizers showed the highest color performance with 8.20 and 8.13 points in the average fertilizer variety in terms of color tone on lawns in the summer season. 20-10-10 fertilizer remained the lowest color performance value with a score of 6.73. In terms of fertilizer dose averages, while the 8 g m² fertilizer dose had the highest value with 8.42 points, the control fertilizer dose had the lowest green color performance value with 5.42 points. The color values of our study are like the values of Yilmaz and Avcioglu (2002), Kesemen (2008), Salman and Avcioglu (2010), Türk and Sözüren (2016), Türk and Kılıç (2017), Abdelkader et al (2018), Köktaş (2019) studies.

The effects of fertilizer type, dose, and interactions on the color values of lawns in autumn were found to be significant at the level of 1% (Table 3). The obtained color tone performance values are given in Table 7.

According to Table 7, it has been found that ammonium sulfate and urea have the highest performances in the averages of fertilizer variety in terms of color shades. The 20-10-10 fertilizer exhibited the lowest performance with a score of 5.80. In terms of fertilizer dose averages, 6 and 8 g m² fertilizer doses reached the highest color tone values by receiving 8.25 and 8.08 points, respectively. In the fertilizer type and dose interactions, ammonium sulfate and urea exhibited high performance by receiving the highest score values at fertilizer doses of 2, 4, 6 and 8 g m². The control fertilizer dose, on the other hand, had the lowest scores in all fertilizer varieties. Our study values Aslan and Çakmakçı (2004), Zorer et al. (2004), Türk and Kılıç (2017), Abdelkader et al (2018), Zengin (2019), Gökçe (2019) are in line with their values.

When our research was examined in terms of color tone, it was observed that plant color performance has quite high values in areas where urea is applied in summer season and ammonium sulfate and urea are applied 8 g m² per month in autumn season. However, it has been found that monthly doses of 2 g m² and 4 g m² fertilizers show similar performance.

The results of our study show that increases in nitrogen doses have improved leaf color performance in lawns.

Table 6. Color shades obtained in different types and doses of fertilizers in the summer season (points)

Type of fertilizer	Dosage of fertilizer					Average
	0	2	4	6	8	
20-10-10	5.67 ^g	7.33 ^{cde}	7.00 ^{de}	7.67 ^{cd}	8.00 ^{bc}	6.73 ^c
15-5-20	4.67 ^h	7.00 ^{de}	6.67 ^{ef}	7.33 ^{cde}	8.00 ^{bc}	7.13 ^b
Ammonium sulfate	5.33 ^{gh}	8.67 ^{ab}	8.67 ^{ab}	9.00 ^a	9.00 ^a	8.13 ^a
Urea	6.00 ^{fg}	8.67 ^{ab}	8.67 ^{ab}	9.00 ^a	8.67 ^{ab}	8.20 ^a
Average	5.42 ^d	7.75 ^c	7.92 ^{bc}	8.25 ^{ab}	8.42 ^a	

Table 7. Color shades obtained in different types and doses of fertilizers in the summer season (points)

Type of fertilizer	Dosage of fertilizer					Average
	0	2	4	6	8	
20-10-10	4.00 ^c	6.00 ^b	5.67 ^b	8.67 ^a	8.67 ^a	5.80 ^c
15-5-20	4.33 ^c	6.00 ^b	6.33 ^b	6.33 ^b	6.00 ^b	6.60 ^b
Ammonium sulfate	4.00 ^c	8.67 ^a	8.67 ^a	9.00 ^a	8.67 ^a	7.80 ^a
Urea	4.33 ^c	8.67 ^a	8.67 ^a	9.00 ^a	9.00 ^a	7.93 ^a
Average	4.17 ^c	8.67 ^a	7.33 ^b	8.25 ^a	8.08 ^a	

Table 8. Grass qualities obtained in different types and doses of fertilizers in the summer season (points)

Type of fertilizer	Dosage of fertilizer					Average
	0	2	4	6	8	
20-10-10	7.00	7.33	8.33	8.67	8.67	7.53 ^b
15-5-20	6.67	7.00	8.00	8.67	9.00	7.67 ^{ab}
Ammonium sulfate	6.33	7.00	7.33	8.67	9.00	7.87 ^{ab}
Urea	5.67	7.33	7.00	8.67	9.00	8.00 ^a
Average	6.42 ^d	7.17 ^c	7.67 ^b	8.67 ^a	8.92 ^a	

Table 9. Grass qualities obtained in different types and doses of fertilizers in the autumn season (points)

Type of fertilizer	Dosage of fertilizer					Average
	0	2	4	6	8	
20-10-10	6.33 ^d	8.33 ^{abc}	8.00 ^{bc}	8.67 ^{ab}	9.00 ^a	8.07 ^a
15-5-20	5.33 ^e	8.33 ^{abc}	8.00 ^{bc}	8.67 ^{ab}	9.00 ^a	7.87 ^{ab}
Ammonium sulfate	5.00 ^{ef}	7.67 ^c	7.67 ^c	8.67 ^{ab}	9.00 ^a	7.60 ^b
Urea	4.33 ^f	7.67 ^c	8.67 ^{ab}	8.67 ^{ab}	8.67 ^{ab}	7.60 ^b
Average	5.25 ^c	8.00 ^b	8.08 ^b	8.67 ^{ab}	8.92 ^a	

The lowest color scores were obtained from the control groups in the summer season, and the highest values were taken from the 8 g m² N applications. When N, which forms the structure of chlorophyll in chloroplasts, increases, the number of chlorophylls also increases (Orçun, 1979). With the increase of N doses, darkening and increase in leaf color tones were observed.

3.3. Grass Quality

When the lawn quality data were examined in the summer season, as the fertilizer dose was found to be 1% and the fertilizer variety effects were found to be 5% significant, the interaction between the two was not found to be significant (Table 3). The grass quality performances obtained in different fertilizer types and doses are given in Table 8.

When Table 8 was examined, urea fertilizer reached the highest lawn quality performance with 8.0 points in terms of lawn quality in the averages of fertilizer types in summer season. It was found that the 20-10-10 fertilizer was the lowest performance value with a score of 7.53. In terms of fertilizer dose averages, while 6 and 8 g m² fertilizer doses showed the highest performance with 8.67 points and 8.92 points respectively, the control fertilizer dose exhibited the lowest performance with 6.42 points. In our study, the grass quality values were found similar study values of Zorer et al. (2004), Avcioglu and Geren (2012), Abdelkader et al. (2018), Köktaş (2019).

The effects of fertilizer dose on grass quality values in the autumn season were found to be significant at the level of 1%, the effects of fertilizer type and factor interactions were found to be significant at the level of 5% (Table 3). Lawn quality performances of different fertilizers and doses are given in Table 9. When Table 9 was examined, it was seen that 20-10-10 fertilizer showed the highest lawn quality performance with 8.07 points in the averages of fertilizer type. Ammonium sulfate and urea fertilizers had the lowest quality performance with a

score of 7.6. In the average fertilizer dose, 6 and 8 g m² fertilizer doses reached the highest values with 8.67 and 8.92 points respectively, and the control fertilizer dose had the lowest value with 5.25 points. While urea fertilizer showed the lowest performance with 4.33 points of the control dose in the fertilizer type and fertilizer dose interactions, 20-10-10, 15-5-20 and ammonium sulfate fertilizers exhibited the highest performance with 8 g m² fertilizer doses receiving 9.0 full points. The values of our study are compatible with the values of Abdelkader et al. (2018), Köktaş (2019), Zengin (2019), Gökçe (2019), Özaydın (2019).

Nitrogen has increased the color performance of plants, especially in grass fields, and enabled their rapid development. In terms of grass quality, it can be said that high doses of nitrogen sources increase performance values. It was found that the grass quality received high values in the plots where 6 g m² and 8 g m² urea and ammonium sulfate fertilizers were used monthly.

3.4. Leaf Width

When the leaf width data for the summer period were examined, the effects of fertilizer type, fertilizer dose and the interactions of these factors were found to be insignificant (Table 3). The most leaf values obtained in different fertilizer types and doses during the summer period are given in Table 10.

The leaf width values obtained in our study were insignificant in terms of all factors and were among the thin leaves according to the Beard (1973) classification. The values obtained were close to the values of Kesemen (2008), Türk and Sözüren (2016), Türk and Kılıç (2017), but were found to be slightly lower.

In the leaf width values obtained in the autumn season, the type of fertilizer was found to be 5%, the effects of fertilizer dose and interactions were found to be significant at the level of 1% (Table 3). Leaf width values obtained from different fertilizer types and doses are given in Table 11.

Table 10. Leaf width obtained in different types and doses of fertilizer in summer season (mm)

Type of fertilizer	Dosage of fertilizer					Average
	0	2	4	6	8	
20-10-10	0.84	0.73	1.23	1.08	1.11	1.00
15-5-20	0.99	0.94	1.32	1.37	1.33	1.19
Ammonium sulfate	1.43	1.48	1.34	1.42	1.44	1.42
Urea	1.51	1.41	1.41	1.40	1.42	1.43
Average	1.19	1.14	1.32	1.32	1.33	

Table 11. Leaf width obtained in different types and doses of fertilizers in the autumn season (mm)

Type of fertilizer	Dosage of fertilizer					Average
	0	2	4	6	8	
20-10-10	2.10 ⁱ	2.33 ^{fgh}	2.58 ^{cd}	2.49 ^{de}	2.43 ^{ef}	2.39 ^b
15-5-20	2.06 ⁱ	2.36 ^{fgh}	2.65 ^{bc}	2.51 ^{de}	2.73 ^{ab}	2.46 ^a
Ammonium sulfate	2.10 ⁱ	2.30 ^{gh}	2.40 ^{efg}	2.71 ^{ab}	2.77 ^{ab}	2.46 ^a
Urea	2.07 ⁱ	2.26 ^h	2.39 ^{efg}	2.75 ^{ab}	2.82 ^a	2.46 ^a
Average	2.08 ^e	2.31 ^d	2.51 ^c	2.61 ^b	2.69 ^a	

According to Table 11, the 15-5-20, ammonium sulfate and urea fertilizers reached the highest leaf width values with 2.46 mm in the average fertilizer variety in the autumn season. The 20-10-10 fertilizer had the lowest leaf width with 2.39 mm. In the average fertilizer dose, the 8 g m² fertilizer dose reached the highest leaf value with 2.69 mm, while the control fertilizer dose was found to be the lowest with 2.03 mm. In the fertilizer type and dose interactions, the urea 8 g m² fertilizer dose was found to be the highest with a leaf value of 2.82 mm, while the control doses of all fertilizer types were found to be at the lowest leaf width values. While the values of our study were consistent with the values of Türk and Sözüren (2016), they remained slightly below the values of Türk and Kılıç (2017).

In terms of leaf texture, summer season values were found to be lower than autumn values. Fungal disease has developed in *L.perenne* species due to the increase in temperature in the summer season and the humidity of the vegetation environment and losses have occurred in this species. *F. arundinacea* species, which has a wide leaf width, was dormant in vegetation, therefore leaf tissue values were determined to be higher in autumn than in summer. While the leaf tissue remained thin in the control groups, it was found that the leaf tissue was large in the parcels given nitrogen.

It is thought that the reason for the low values is that the leaves that germinated immediately after planting did not fully reach the inherited leaf tissue values.

It is thought that the reason why our values differ slightly is because the width of the leaf may vary depending on environmental factors. In our study, while *F. arundinacea* is included in the mixture, it was used as a plain in Kılıç and Türk's study. In addition, studies have recently been carried out on the *F. arundinacea* species to obtain a variety with small palms. The varieties used in our study should be evaluated as varieties that have been improved in terms of leaf blades.

3.5. The Amount of Fresh Grass

When the amounts of fresh grass were examined in the summer period, the effects of fertilizer type, fertilizer dose and the interactions of these factors were found to be significant at the level of 1% because of the variance analysis. The Duncan test was applied, and the differences were revealed (Table 3). The results of the analysis of the amount of plant fresh grass obtained in different types and doses of fertilizer in the summer season are given in Table 12.

According to Table 8.a, urea and ammonium sulfate fertilizer varieties were found in the highest amounts with 1045 g and 1011 g values in terms of fresh grass yields in the average fertilizer variety, while the 20-10-10 and the 15-5-20 fertilizer varieties remained in the lowest amounts with 679 g and 733 g values. In the average fertilizer dose, while 8 g m² fertilizer dose accounted for the highest fresh grass yield with a value of 1283 g, the control fertilizer dose remained at the lowest amount with a value of 328 g. In the fertilizer variety and fertilizer dose interactions, the urea was the highest with a dose of 8 g m², while the control fertilizer doses remained in the lowest amounts in all fertilizer varieties. The values of our study show similarities with the values of Hosaflioglu (2009), Kaş (2010), Ozaydin (2019), Koçak (2019).

When the fresh grass data in the autumn period were examined, the effects of fertilizer type and fertilizer dose were found to be significant at the level of 1% and the effects of their interactions were found to be significant at the level of 5% (Table 3). The amounts of fresh grass obtained in different fertilizer types and doses in the autumn season are given in Table 13.

According to Table 13, ammonium sulfate and urea fertilizers in lawns had the highest yield values with 771 g and 813 g in terms of fresh grass values in the autumn period. The 20-10-10 fertilizer gave the lowest fresh grass value with 506 g.

Table 12. The amount of fresh grass obtained in different types and doses of fertilizers in the summer season (g)

Type of fertilizer	Dosage of fertilizer					Average
	0	2	4	6	8	
20-10-10	310 ^j	517 ⁱ	600 ⁱ	750 ^h	1217 ^{cd}	679 ^b
15-5-20	347 ^j	517 ⁱ	767 ^h	933 ^{fg}	1100 ^{dc}	733 ^b
Ammonium sulfate	320 ^j	833 ^{gh}	1233 ^{cd}	1283 ^{bc}	1383 ^{ab}	1011 ^a
Urea	327 ^j	983 ^{ef}	1217 ^{cd}	1253 ^{bc}	1433 ^a	1045 ^a
Average	328 ^e	713 ^d	954 ^c	1055 ^b	1283 ^a	

Table 13. The amount of fresh grass obtained in different types and doses of fertilizers in the autumn season (g)

Type of fertilizer	Dosage of fertilizer					Average
	0	2	4	6	8	
20-10-10	227 ^k	257 ^{jk}	300 ^{jk}	697 ^{gh}	1050 ^{bc}	506 ^c
15-5-20	320 ^{jk}	383 ^j	533 ⁱ	767 ^{e-h}	983 ^{cd}	597 ^b
Ammonium sulfate	327 ^{jk}	727 ^{fgh}	810 ^{efg}	897 ^{de}	1127 ^{ab}	771 ^a
Urea	313 ^{jk}	633 ^{hi}	840 ^{ef}	1017 ^{bc}	1263 ^a	813 ^a
Average	297 ^e	500 ^d	621 ^c	837 ^b	1106 ^a	

In terms of fertilizer dose averages, the highest efficiency was achieved with 1106 g at an 8 g m² fertilizer dose, while the control fertilizer dose remained at the lowest level with 297 g. The urea fertilizer received the highest amount of fresh grass with 1263 g at a dose of 8 g m². While the values of our study were found to be like Gökçe (2019) values, they were found to be higher than Rich (2019) values.

The fresh grass values determined in our studies in terms of the amount of fresh grass, came out higher than the values of Zorer et al. (2004). One of the reasons for this is that the period from cleaning to evaluation methods in our study (three weeks) is longer than in the studies of Zorer et al (2004). Another reason is that the species used in the mixture are species with a fast-developing hereditary structure, the types used by Zorer et al. are that they have a slow-developing hereditary structure. Also, the high percentage of the fast-growing *F. arundinacea* species in the mixture (70%) is one of the reasons. Our study shows similarities with the values of Hosaflioglu (2009) study. In the study conducted by Akdeniz and Hosaflioglu (2016) under Iğdır conditions, the values of the amount of fresh grass found were found to be higher than the values of our study. It is thought that this difference is also caused by maintenance and environmental factors. While the summer values of our study are similar to the study values of Kaş (2010), Ozaydin (2019) and Koçak (2019), the autumn values correspond to the values of Gökçe (2019).

4. Conclusion

The highest performance values for football fields under Iğdır conditions were obtained in pure nitrogen of ammonium sulfate and urea fertilizer varieties in 6 and 8 g m² fertilizer doses. Football fields are areas that are often worn out and destroyed because of stepping over. Besides that, the deformation of the grass tissue in these areas is tolerated quickly, a rapid development of the

grass should be ensured again. In our study, monthly doses of 6-8 g m² of pure nitrogen of ammonium sulfate and urea fertilizers are recommended to ensure the rapid development of the grass and to cover the damages. Ammonium sulfate and urea fertilizers showed a faster effect in terms of nitrogen element compared to the composite fertilizer varieties included in the study. As a matter of fact, ammonium sulfate and urea fertilizers soon after application quickly came to the form that the plant will benefit from in the soil, became effective in the grass, and manifested itself in the strong development of vegetative structure such as trunk and leaves. As a matter of fact, shortly after the application of ammonium sulphate and urea fertilizers, vegetative revolutionary strong groups such as stems and leaves, which were effective in the separation of forms that would benefit from the beginning in the general soil, proved themselves. However, the effect of the 20-10-10, the 15-5-20 composite fertilizers on the development of vegetative structure has remained weak since it takes longer to reach the form that the plant will use in the soil, especially in terms of nitrogen element.

According to the data of this study, in the football grass fields where pressure and wearing off are intense, ammonium sulfate and urea fertilizer types of nitrogen which are quickly taken up by plants from the soil are needed for the species that are under heavy pressure to recover and for the vegetation to always remain uniformly green.

For football fields that are not under much pressure or worn out little under Iğdır conditions, it is recommended to apply a dose of pure nitrogen 2 g m² of ammonium sulfate and urea fertilizers to maintain a dark color tone and give the desired grass quality. A dose of 2 g m² of pure nitrogen of these fertilizers on football fields was especially sufficient to preserve the green color texture. It has already been concluded that a dose of 2 g m² of pure nitrogen will be sufficient in these fertilizer

varieties, since the wear and tear by pressure is also low. By applying fertilizer in lower doses, the amount of fresh grass and plant height values were lower, contributing to savings in labor, time, and other costs. It is very important to carry out fertilization as much as necessary to prevent environmental pollution in an ecological sense.

Author Contributions

The percentage of the author(s) contributions is presented below. All authors reviewed and approved the final version of the manuscript.

	M.M.	İ.H.
C	50	50
D	50	50
S	50	50
DCP	50	50
DAI	50	50
L	50	50
W	50	50
CR	50	50
SR	50	50
PM	50	50
FA	50	50

C=Concept, D= design, S= supervision, DCP= data collection and/or processing, DAI= data analysis and/or interpretation, L= literature search, W= writing, CR= critical review, SR= submission and revision, PM= project management, FA= funding acquisition.

Conflict of Interest

The authors declared that there is no conflict of interest.

Ethical Consideration

Ethics committee approval was not required for this study because of there was no study on animals or humans.

Acknowledgements

This article was prepared from the thesis at Iğdır University, The Institute of Graduate Studies, and the Department of Agricultural Sciences.

References

AbdelKader HH. 2018. Effect of different fertilization programs on the growth characteristics and chemical composition of turfgrasses of five established football fields. *Mansoura Univ J*, 9(4): 315-320.

Akdeniz H, Hosaflioglu I. 2016. Effects of nitrogen fertilization on some turfgrass characteristics of perennial ryegrass (*Lolium perenne* L.). *J Agri Sci Technol B*, 6: 226-237.

Anonymous. 2020a. Ankomer seed and agricultural industry trade limited company, URL: www.ankomer.com (cessed date: December 16, 2020).

Anonymous. 2020b. Iğdır Provincial Directorate of Meteorology Data. Iğdır, Türkiye.

Anonymous. 2020c. Iğdır University ALUM Soil Analysis Laboratory. Iğdır, Türkiye.

Arslan M, Çakmakçı S. 2004. Determination of adaptation

abilities and performances of different grass species and varieties in coastal conditions of Antalya province. *J Fac Agri Akdeniz Univ*, 17(1): 31-42.

Avcıoğlu R, Geren H. 2012. Research on the performance of some warm climate grass wheat plants in Mediterranean climate. *J Ege Univ Fac Agri*, 22(1): 1-17.

Beard JB. 1973. *Turfgrass. Science and Culture*, Prentice-Hall, Inc., New York, US, pp: 658.

Gökçe V. 2019. Reed ball (*Festuca arundinacea* L.) from grass plant plants under Iğdır ecological conditions. The effect of different nitrogen (N) doses on grass quality elements. Bachelor's Thesis, Iğdır University, Institute of Science, Iğdır, Türkiye, pp: 23.

Hosaflioglu İ. 2009. A research on the determination of wheat species and varieties that can be used in grass fields facility under Van conditions. PhD Thesis, Van Yüzüncü Yıl University, Institute of Natural Sciences, Van, Türkiye, pp: 52.

Kaçar B. 1977. Bitki besleme. Ankara Üniversitesi Ziraat Fakültesi Yayınları, No: 637, Ankara, Türkiye, pp: 318.

Karakurt E. 2003. Some morphological and phenological characters of green field grass species in Ankara/Haymana conditions. *J Agri Sci*, 10(3): 275-280.

Kaş G. 2010. The effect of different fertilizer application and form times on the development of subsoil and above-ground components in English grass. MSc Thesis, ordu University, Institute of Natural and Applied Sciences, Ordu, Türkiye, pp: 49.

Kesemen E. 2008. Evaluation of plant characteristics of red fescue (*Festuca rubra* L.) using various nitrogen doses. MSc Thesis, Institute of Natural Sciences, Department of Field Crops, Ankara, Türkiye, pp: 54.

Koçak M. 2019. Green field performances of some wheat grass plants planted lean and mixed: Tekirdağ/ Sultanköy example. MSc Thesis, Namık Kemal University, Institute of Natural and Applied Sciences, Tekirdağ, Türkiye, pp: 67.

Köktaş Z. 2019. Some cool climate of different nitrogen sources affects on the development of lawn plants and lawn quality. MSc thesis, Uludağ University, Institute of Natural Sciences Bursa, Türkiye, pp: 57.

Misia A. 1991. Effect of cool season turfgrass seed mixtures on lawn characteristics. *Bull Fac Agri Univ Cairo*, 42: 401-414.

Mulvalı B. 1999. Effects of different nitrogen fertilizer applications on the turf performances of some turfgrasses. MSc Thesis, Ege University, Institute of Natural Sciences, İzmir, Türkiye, pp: 75.

Oral N, Açıkgöz R. 1999. Research on seed mixtures, October rates and nitrogen fertilizer applications for grass fields to be established in Bursa region. Turkey 3. Proceedings of the Field Crops Congress, November 15-18, Adana, Türkiye, pp: 155-159.

Orçun E. 1979. Private garden architecture, lawn areas facility and maintenance technique. Ege University Faculty of Agriculture Publications, Publication No: 152, İzmir, Türkiye, pp: 106.

Özaydın E. 2019. Determination of adaptation and grass field characteristics of varieties belonging to some grass species in Şanlıurfa ecological conditions. MSc Thesis, Harran University, Institute of Science, Şanlıurfa, Türkiye, pp: 67.

Salman A, Avcıoğlu R. 2010. The green field performances of some cool climate lawn plants in different fertilizer doses. *J Ege Univ Fac Agri*, 47(3): 1018-8851.

Sills MJ, Carrow RN. 1983. Turfgrass growth, N use and water use under soil compaction and N fertilization. *Argon J*, 75: 488-492.

Spangenberg BG, Fermanian TW, Wehner DV. 1986. Evaluation

- of liquid-applied nitrogen fertilizers on Kentucky bluegrass Turf Argon J, 78: 1002-1006.
- Steel RGD, Torrie JH. 1980. Principles and procedures of statistics. A biometrical approach. 2nd edition, McGraw-Hill, New York, US, pp: 20-90.
- Türk M, Kılıç G. 2017. A reed ball of different nitrogen doses (Festuca arundinacea L.) the effects of varieties on grass field performance. J Suleyman Demirel Univ Inst Sci, 21(1): 31-37.
- Türk M, Sözüren K. 2016. Perennial Grass of different nitrogen doses (Lolium perenne L.) the effects of varieties on grass field performance. J Süleyman Demirel Univ Fac Agri, 11(2): 99-107.
- Zengin S. 2019. English grass (Lolium perenne L.) from Lawn plant plants under Iğdır ecological conditions. The effect of different nitrogen (N) doses on grass quality elements. MSc Thesis, Iğdır University, Institute of Science, Iğdır, Türkiye, pp: 31.
- Zorer Ş, Hosaflıoğlu İ, Yılmaz İH. 2004. Determination of appropriate nitrogen fertilizer application times in lawn areas. Yüzüncü Yıl Univ Fac Agri J, 14(1): 27-34.